

AD-A119 491

SOUTHWEST RESEARCH INST SAN ANTONIO TX  
DELINEATION OF CONSTRAINTS IMPOSED BY PROPAGATION FACTORS AT HF--ETC(U)  
APR 76 E C HAYDEN

F/S 17/4

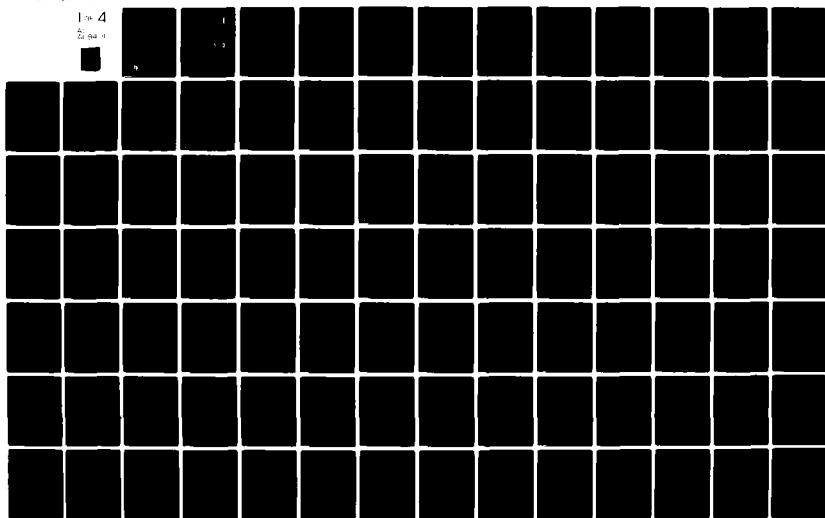
N00039-75-C-0481

NL

UNCLASSIFIED

1 of 4

5/84



**DELINEATION OF CONSTRAINTS IMPOSED  
BY PROPAGATION FACTORS AT HF  
ON JAMMING OF SHIPS COMMUNICATIONS**

by  
**E. C. Hayden, Ph.D.**

**FINAL TECHNICAL REPORT**  
**Contract N00039-75-C-0481**  
**Project 16-4312**

**Prepared for**  
**Department of the Navy**  
**Naval Electronic Systems Command**  
**Washington, DC 20360**

**April 1976**



**DISTRIBUTION STATEMENT A**  
**Approved for public release;**  
**Distribution Unlimited**

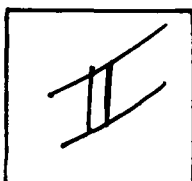
**SOUTHWEST RESEARCH INSTITUTE**  
**SAN ANTONIO      CORPUS CHRISTI      HOUSTON**

**AD A119491**

PHOTOGRAPH THIS SHEET

AD A119491

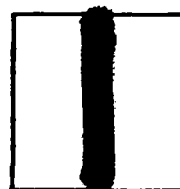
DTIC ACCESSION NUMBER



LEVEL

Southwest Research Inst.  
San Antonio, TX

Final Tech Rpt, Apr. 76



INVENTORY

Hayden, E.C.  
Contract N00039-75-C-0481

DOCUMENT IDENTIFICATION

DISTRIBUTION STATEMENT A

Approved for public release  
Distribution Unlimited

DISTRIBUTION STATEMENT

ACCESSION FOR	
NTIS	GRA&I <input checked="" type="checkbox"/>
DTIC	TAB <input type="checkbox"/>
UNANNOUNCED	<input type="checkbox"/>
JUSTIFICATION	
BY <i>Per Ltr (Aug 82-1503, dtd 6 July 82) on file</i>	
DISTRIBUTION / <i>6 July 82 on file</i>	
AVAILABILITY CODES <i>FL-88</i>	
DIST	AVAIL AND/OR SPECIAL
<i>A</i>	

DISTRIBUTION STAMP



**DTIC ELECTED**  
SEP 22 1982  
**S D**

DATE ACCESSIONED

82 09 21 036

DATE RECEIVED IN DTIC

PHOTOGRAPH THIS SHEET AND RETURN TO DTIC-DDA-2

**SOUTHWEST RESEARCH INSTITUTE**  
Post Office Drawer 28510, 8500 Culebra Road  
San Antonio, Texas 78284

**DELINEATION OF CONSTRAINTS IMPOSED  
BY PROPAGATION FACTORS AT HF  
ON JAMMING OF SHIPS COMMUNICATIONS**

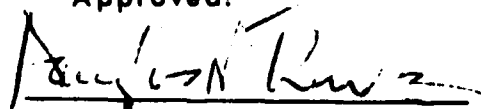
by  
**E. C. Hayden, Ph.D.**

**FINAL TECHNICAL REPORT**  
Contract N00039-75-C-0481  
Project 16-4312

Prepared for  
**Department of the Navy**  
**Naval Electronic Systems Command**  
**Washington, DC 20360**

**April 1976**

**Approved:**



**Douglas N. Travers**  
**Vice President**  
**Electromagnetics Division**



## PREFACE

The motivation for preparation of this document has its origin in frustration experienced in the planning and execution of jamming operations at HF. A major generator of frustration is the complexity of the wave propagation phenomena with which one must cope to maximize the probability of success in a venture. The purpose of this document is to enhance the ability to cope. To that end, a systematic basis is presented for understanding and, ultimately, for estimating the impact of HF propagation phenomena on the task of jamming signal delivery.

In the preparation of this document, it has been the intention of the author to provide both some of the features of an instructive text and some of the features of a design or operations handbook.

The functions of the textual material are twofold. One is to draw together from theory and practice instructive material to illuminate the character of wave propagation phenomena at HF and also to support the handbook material. Chapters 2.0 and 3.0 are devoted to this function. The other is to develop a formal statement of the jamming problem and to delineate a systematic procedure for its solution. In that procedure, the signal delivery function appears in explicit form, thereby giving guidance in application of the handbook material, either to system design or operational practice. This textual function is assigned to Chapter 1.0.

The handbook material is separated from the text and assembled in atlas form for convenient use. However, it is divided between Chapters 2.0 and 3.0 to afford close association with its supporting material. The function of the handbook material is to provide, under one cover, quantitative data--not otherwise easily accessible--sufficient to support limited problem solving. The author has attempted assiduously to format the handbook material so that role or influence of the several parameters is made evident. That is not always easy to do, especially for a quantity which is a function of five variables.

In Chapters 2.0 and 3.0, the salient features of transmission loss at HF are presented. For the sky wave (Chapter 2.0), the presentation is in terms of a selection of realistic--if not real--representative medium models. The ground wave (Chapter 3.0), being a simpler physical phenomenon and having a stable nature, admits a more nearly direct mode of presentation in terms of physical parameters.

Presentation of a complete technique for operational forecasting of sky wave properties is not contemplated for this document. However, the procedure used to produce the data which are presented in Chapter 2.0 would be amenable to expansion into a full forecast procedure. What would have to

added is the specific measurement, or forecast, of ionosphere morphology for each stated time and place. In this respect, the handbook material of Chapter 2.0 does not constitute a complete cookbook for an operational procedure. Some of the recipes are missing.

Operational application of the ground wave handbook material in Chapter 3.0 would require, at most, the addition of timely information on sea surface temperature and salinity and on refractivity of the lower atmosphere. As a matter of fact, it turns out that relatively little would be lost by assigning fixed values to these parameters, representative of marine conditions.

The problem of notation and nomenclature has been somewhat exasperating. Material has been drawn from a variety of sources, each of which has its own conventions. For help in sorting out the inevitable ambiguities, the attention of the reader is directed to the comprehensive Glossary of Symbols and Subscripts which has been provided.

## EXECUTIVE SUMMARY

### Motivation

The HF portion of the electromagnetic spectrum (2-32 MHz in this discourse) provides channels for a variety of useful communications services. The characteristics of communications systems in this range of frequencies are adaptable to provision of services from large moving platforms. Under favorable circumstances, terminal equipment requirements are modest and ranges from line-of-sight to several thousands of kilometers are possible.

The practice of jamming communications services in the HF part of the spectrum must cope with a complexity of wave propagation phenomena not experienced at higher frequencies.

This document is designed to illuminate both the nature of the wave propagation phenomena and their impact on planning and execution of a jamming operation. Its purpose is to enhance the ability to cope. A systematic basis is presented for understanding and, ultimately, for estimating the impact of HF wave propagation phenomena on jamming signal delivery. In addition to theoretical and explanatory material, handbook information is provided in detail adequate to support an appreciable degree of problem solving.

### Jamming

The function of communications jamming is to deny to the intended consumer access to communication services. Usually, the action is directed at a specific service, rendered at a specified time and place. Jamming of a radio communication system disrupts service without the necessity for direct physical intervention.

Jamming requires application onto a communication system of a spurious signal load. The spurious jamming signal contends with the authentic communication signal. The intended function of the spurious signal may be either to obscure the presence of the authentic signal, to obscure the meaning of the message carried by the authentic signal or to alter the meaning of the message carried by the authentic signal.

### Delivery

To be effective, the spurious signal load must be applied to a radio communication system at the point of reception of the authentic signal. Only at this point is efficacious contention feasible. It is characteristic of jamming ventures that the point of application of the jamming signal is remote from

the point of origin. At HF the distance may range from line-of-sight to several hundreds, or even a few thousands, of kilometers.

Thus, a crucial function in any jamming operation is delivery of the jamming signal from the point of its origin to the point of its application. The vehicles for delivery are the mechanisms of radio wave propagation. The delivered jamming signal must have strength adequate for effective contention at expected levels of communication signal strength.

### Attrition

In the delivery process, jamming signal power suffers attrition from a number of agencies. Agencies having effective influence at HF include:

- 1) divergence of the wavefront as it recedes from the source,
- 2) diffraction of the wavefront past the bulge of the curved earth,
- 3) refractive re-direction of the wavefront,
- 4) dissipative absorption of power from the wave.

The agencies of attrition depend on the delivery mode. The degree of attrition depends on the agency.

Capability to estimate the expected degree of jamming signal attrition is necessary:

- 1) to determine whether a specific operation, or class of operations, is inherently possible or impossible,
- 2) to estimate the required amount of a scarce, or limited, resource (in this case, jamming signal power), i. e., to estimate the "cost" of a venture.

The estimation of jamming signal attrition is the main thrust of this discourse. \*

### Modes

In the HF spectral region there are two principal modes of wave propagation by which jamming signal power can be delivered to a remote point.

\*There also are questions of jamming signal conformation to be addressed. They arise in optimizing jamming signal effectiveness and, hence, in minimizing requirement for the scarce resource. This topic is not treated here.

They are the sky wave and the ground wave. The characteristic properties of the two modes differ greatly. Both modes are of importance and, in some respects, they are complementary.

Of the two, only the sky wave offers the possibility of effective signal delivery at ranges greater than a few hundreds of kilometers. By contrast, the ground wave offers stability and total availability at ranges less than a few hundreds of kilometers. \* At intermediate ranges, the sky wave is susceptible to the lesser signal power attrition under best circumstances but its availability is limited.

The ability to estimate signal attrition in the delivery process requires understanding of the wave propagation mechanics supporting these two modes and the capability to evaluate the physical factors which influence their properties.

### Sky Wave

The sky wave is dependent on the presence and properties of the earth's ionized upper atmosphere--the ionosphere. The ionosphere serves as a refractive medium which, under favorable circumstances, can re-direct an outward traveling wavefront toward the surface of the earth. The properties of the ionosphere are subject to both temporal and spatial variation. Hence, this mode of signal delivery is subject to a widely varying degree of attrition of signal power.

The refractive capability of the ionosphere depends on the density of the electron distribution and on the frequency of the wave. It increases as the electron density increases and decreases as the frequency increases. Thus, at times of high electron density and with waves of low frequency, refractive capability is high. The potential then exists for signal delivery at short ranges--even to zero range. When the electron density is too low, or the frequency is too high, there is a lower limit to the range at which signal delivery potential exists. Then, an excluded zone--the "skip" zone--exists about the jamming source. This zone simply is not "illuminated" by the source via the sky wave delivery mode. Beyond the skip contour, the potential for signal delivery yet exists. If the frequency is much too high, the wave is not re-directed toward the earth. In essence, the skip contour recedes to infinity and the wavefront is lost in space.

Signal attrition in the sky wave mode arises from three of the four agencies:

\*The range is quite frequency dependent, decreasing as the frequency increases.

- 1) divergence of the wavefront as it recedes from the source,
- 2) refractive re-direction of the wavefront,
- 3) dissipative absorption of power from the wave.

It is easier to discuss the first two together and to break the aggregate apart in another way.

The first piece of the aggregate is initial loss, attributable to the radiative and receptive processes--the price of "going the first kilometer," so to speak. It is a stable quantity, a function only of frequency, and it ranges from about 38 dB at 2.0 MHz to 63 dB at 32 MHz.

The second piece (to be added to the first) has been called divergence loss. It depends only on the shape of ray trajectories between the jamming signal source location and the point of application of the jamming signal to the communications system. For one-hop ray trajectories, its normal range is from about 46 dB at zero range to about 70 dB at 3000 km. Its value at any particular range is subject to focusing and defocusing effects which depend on the specific electron density distribution and the wave frequency. Divergence loss is, thus, a time-varying function.

Loss by dissipative absorption of power from the wave is the real shocker. It can vary from less than 1 dB to values approaching 400 dB. It is a function of, at least:

- 1) solar zenith angle,
- 2) sunspot number,
- 3) electron gyrofrequency (proportional to the geomagnetic field at about 100 km altitude),
- 4) wave frequency,
- 5) ray trajectory elevation angle.

High values of absorption are associated with

low values of solar zenith angle,

high values of sunspot number,

low values of wave frequency (in the HF range),

low values of ray trajectory elevation angle.

During daytime hours, it generally is absorption which limits signal delivery capability in the lower portion of the HF range.

The probability of the existence of multiple time-varying ray paths to the delivery point is high. When this condition exists, interference among the multiple signals causes temporal and spatial signal fading patterns in the neighborhood of the delivery point. The time scale of the fading is on the order of a few seconds and the spatial scale is on the order of a few wavelengths. From moment to moment the effectiveness of a jamming signal can be enhanced or diminished, depending on the state of combination of the multiple rays.

The ionosphere is, above all, a part of the earth's atmosphere. It is a dynamic compressible fluid medium. It exhibits phenomena analogous to climate and weather. Its state is--as is weather--forecastable with limitations.

The temporal and spatial variability of the medium underscores the necessity to have knowledge of its state, concurrent in time and place with the scene of an operational venture. The ability to estimate signal power attrition depends on such knowledge. The knowledge can be had from extrapolation based on historical sequences of measurement, from concurrent local measurement or from a combination of the two. The last is, almost certainly, the most practicable.

#### Ground Wave

The ground wave is propagated past the bulge of the curved surface of the earth by the mechanism of diffraction. This mechanism is aided slightly by the small refractive effect of the lower (unionized) atmosphere. Propagation is influenced by the physical electrical properties of the earth (conductivity and permittivity), the refractivity profile of the atmosphere and the wave frequency.

The physical electrical properties of the earth are stable. Though the refractivity profile of the lower atmosphere generally is not stable, the refractive index exceeds unity only by 300 to 400 parts per million. The effect of the atmosphere at HF generally is minimal except near the limiting range. The consequence is that the ground wave is a stable mechanism for signal delivery.

Attrition of the ground wave signal is primarily attributable to three of the four agencies:

- 1) divergence of the wavefront as it recedes from the source,
- 2) diffraction of the wavefront past the bulge of the curved earth,
- 3) dissipative absorption of power from the wave.

Dissipative attrition is a consequence of the finite conductivity of the earth medium. Because, at HF, the conductivity of sea water is on the order of 500 times as great as that of land materials, the potential delivery range is much greater in a marine environment than it is in a terrestrial environment.

In a marine environment, the potential range of signal delivery is primarily a function of wave frequency. Because of the strong influence of the earth as a boundary for the ground wave, the decrement of signal intensity with distance is much less for a vertically polarized wave than for a horizontally polarized wave. For transmission between two small vertically polarized antennas, the range for a propagation loss of 120 dB\* varies from about 1000 km at 2 MHz to about 75 km at 32 MHz. For horizontally polarized antennas 15 meters above the water, the corresponding range is about 20 km at all frequencies in the range.

#### Application

The success of a communications jamming venture depends on the capability to deliver the jamming signal to the point of communication signal reception. Delivery must be accomplished on the wave frequency of the communication signal and during the time interval in which it is present. These two variables, frequency and time, are not under control of the jamming agent. They therefor act as constraints on the jamming operation.

In a tactical sense the power available for a jamming signal is very likely to be limited by the source equipment at hand. In a strategic sense, limited latitude may exist within which the jamming agent can exercise discretion over the amount of signal power resource to make available. The source power limit, determined by either of these criteria, becomes a third constraint on the jamming operation.

Given the three constraints, two steps in the decision procedure are yet at the discretion of the jamming agent:

---

\*This corresponds to a received signal level of 10  $\mu$ V in 100 $\Omega$  (1 picowatt) per watt radiated.



1. From the points of origin for the jamming signal available to the agent, select the one at which the probability of success is greatest.
2. On the basis of an estimate of probability of success, weighed against a criterion of operational value, decide to execute, or to not execute, the operation.

Whatever the scenario in the context of which these two steps must be carried out, the capability to estimate the degree of signal attrition in delivery is essential.

In a tactical scenario, the jamming agent may have little--or no--discretionary latitude about point of origin. If so, emphasis will be on the second of these steps. Nevertheless, an estimate of probability of success is needed, both to support the last step and, if the decision in that step is "go," to provide a basis for assessing the reliance to place on success of the operation. The basis for making these judgments is, fundamentally, the estimate of jamming signal attrition.

In a strategic scenario, the accent is on the first of the above steps, rather than the second. The task is to specify a suitable array of points of origin as a resource to be made available to the tactician. Again, the basis for judgment is the estimate of jamming signal attrition.

#### Conclusion

The point to the discussion above is that, whatever the scenario in the context of which a jamming operation is contemplated, provision is required for estimating signal attrition as the fundamental basis for assessment of the probability--or the possibility--of success.

In the HF spectral region that task is not trivial if any reliance is to be placed on the sky wave mode. The situation is not the counterpart of that at higher frequencies in which the procedure is simply to set a fixed maximum operational jamming range. There are too many possibilities at HF for occurrence of the "you can't get there from here" syndrome. The diurnal variation of absorption, alone, precludes the simple procedural approach.

If reliance is to be limited to the ground wave only, operational range between points of origin and delivery will be restricted, especially in the upper part of the HF band.

In a strategic scenario the signal loss estimation procedure is best based on a historical data base of information about temporal and spatial

properties of the ionosphere. Indeed, it must necessarily be so since real data are not available in advance.

In the context of a tactical scenario, initial reliance can well be placed on a historical data base for signal loss estimation. At least, a procedure so based certainly is better than going blind. At best, it offers a basis for judgment about best use of whatever latitude is available in point of origin. It might, for example, provide guidance for a get-in-position maneuver.

Final reliance, in a tactical scenario, is best placed on data acquired concurrently in time and place with the operation. This is especially important under marginal conditions. An example is delivery of a jamming signal to a point near the skip contour. The acquisition of such data from a ship platform is technologically feasible and, in fact, is not greatly more complex than HF communications practice.

## TABLE OF CONTENTS

	<u>Page</u>
LIST OF ILLUSTRATIONS	xiii
LIST OF TABLES	xvi
GUIDE TO ATLAS SECTIONS	xvi
GLOSSARY OF SYMBOLS AND SUBSCRIPTS	xvii
1.0 COMMUNICATIONS JAMMING AT HF	1
1.1 Formulation of the Problem	2
1.1.1 Background	2
1.1.2 Scope	5
1.1.3 Solution	9
1.2 Estimation of Power Attrition	13
1.2.1 Loss Definitions	13
1.2.2 Loss Calculations	19
2.0 THESKY WAVE	23
2.1 Definition of Sky Wave	24
2.2 Refractive Index Models	27
2.2.1 Complex Index of Refraction	27
2.2.2 Constraints on Modeling	36
2.2.3 Sources of Data for Profile Modeling	46
2.2.4 Electron Density Profile Models	51
2.3 Path Loss Concepts	68
2.3.1 Loss Mechanisms	68
2.3.2 Ray Path Properties	70
2.3.3 Divergence Loss	76
2.3.4 Application of Real Ionograms	87
2.3.5 Absorption Loss	97
2.3.6 Other Losses	102
2.3.7 The Polarization Problem	108

## TABLE OF CONTENTS (CONT)

	<u>Page</u>
2.4 Atlas of Electron Density Profile Models and Associated Transmission Diagrams	111
2.5 Atlas of Ionospheric Absorption Loss Tables	191
2.6 References for Sky Wave Mechanisms	242
 3.0 THE GROUND WAVE	 245
3.1 Definition of Ground Wave	246
3.2 Variable Quantities	250
3.2.1 Geophysical Property Variables	250
3.2.2 Path Terminal Disposition Variables	262
3.2.3 Source Property Variables	262
 3.3 Propagation Loss Concepts	 265
3.3.1 Definition of Propagation Loss	266
3.3.2 Calculation of Electromagnetic Fields	268
3.3.3 Application of Reciprocity Principles	269
3.3.4 Evaluation of Radiated and Available Power	271
3.3.5 Treatment of Antenna Gain	279
3.3.6 Wave and Antenna Polarization	282
 3.4 Atlas of Propagation Loss Charts	 284
3.5 References for Ground Wave Mechanisms	314

# LIST OF ILLUSTRATIONS

<u>Figure</u>	<u>Caption</u>	<u>Page</u>
1-1	Scenario panorama.	7
2-1	Complex index of refraction.	38
2-2	Ray plane and ray path parameters.	42
2-3	Alpha-Chapman layer parameters.	54
2-4a	Component layers and composite profile: 010WD/.	56
2-4b	Synthetic ionogram: 010WINDAY.	57
2-5a	Component layers and composite profile: 010SD/.	60
2-5b	Synthetic ionogram: 010SUMDAY.	61
2-6a	Component layers and composite profile: 200SD/.	62
2-6b	Synthetic ionogram: 200SUMDAY.	63
2-7a	Component layers and composite profile: 200WD/.	64
2-7b	Synthetic ionogram: 200WINDAY.	65
2-8	Transmission diagram with angle/range curve: 2.0 MHz.	71
2-9	Transmission diagram with angle/range curve: 4.0 MHz.	73
2-10	Transmission diagram with angle/range curve: 6.0 MHz.	75
2-11	Transmission diagram with multi-hop angle/range curves: 4.0 MHz.	77
2-12	Ray tube geometry.	79
2-13	Transmission diagram with angle/range and loss/ range curves: 2.0 MHz.	83

# LIST OF ILLUSTRATIONS (CONT)

<u>Figure</u>	<u>Caption</u>	<u>Page</u>
2-14	Transmission diagram with angle/range and loss/range curves: 4.0 MHz.	85
2-15	Transmission diagram with angle/range and loss/range curves: 6.0 MHz.	86
2-16	Real ionogram.	88
2-17	Transmission diagram derived from real ionogram: 2.4 MHz.	90
2-18	Transmission diagram derived from real ionogram: 3.3 MHz.	91
2-19	Transmission diagram derived from real ionogram: 4.0 MHz.	92
2-20	Transmission diagram derived from real ionogram: 5.0 MHz.	93
2-21	Transmission diagram derived from real ionogram: 6.0 MHz.	94
2-22	Transmission diagram derived from real ionogram: 7.0 MHz.	95
2-23	Transmission diagram derived from real ionogram: 10.0 MHz.	96
2-24	Chart system for estimating total ionospheric absorption loss.	101
3-1	The four regimes (wave paths numbered 1-4) to which propagation mechanisms are differentiated.	248
3-2	Geophysical factors related to the earth ( $\epsilon$ and $\sigma$ ) which affect ground wave propagation.	251
3-3	Conductivity ( $\sigma$ ) contour chart for sea water as a function of temperature (T) and salinity (S).	254

# LIST OF ILLUSTRATIONS (CONT)

<u>Figure</u>	<u>Caption</u>	<u>Page</u>
3-4	Geophysical factors related to the lower atmosphere ( $N_0$ , $N_s$ and $\Delta N/\Delta h$ ) which affect ground wave propagation.	255
3-5	Relative curvature of ray path and surface of the earth.	259
3-6	Earth radius factor ( $\alpha = a_e/a$ ) as a function of surface refractivity ( $N_s$ ).	261
3-7	Disposition of transmitter and receiver relative to the surface of the earth.	263
3-8	Path terminals (1 and 2) and their images (1' and 2') relative to the surface of the earth.	267
3-9	Coordinate structure showing values of three variables, conductivity ( $\sigma$ ), earth radius factor ( $\alpha$ ) and frequency ( $f$ ). The five stacks of "boxes" topped by a shaded area represent combinations of the three variables for which charts of propagation loss versus ground range are presented in the chart section.	285
3-10	Example of computer printout for a short range case. Range limit set at 90 km. Top: Vertical polarization. Bottom: Horizontal polarization.	286
3-11	Example of computer printout for a long range case. Propagation loss limit set at 200 dB. Top: Vertical polarization. Bottom: Horizontal polarization.	287

## LIST OF TABLES

<u>Table</u>	<u>Caption</u>	<u>Page</u>
2-1	Absorption coefficient formulas.	45
2-2	Layer parameter values for profile model examples.	66
2-3	Equivalent frequency.	104
2-4	Absorption index: solar variables (Parts a, b, c).	104
2-5	Absorption index: non-solar variables.	106
2-6	Total ionospheric loss: dissipative mechanisms.	107
2-7	Guide to atlas of electron density profiles and related transmission diagrams.	113
2-8	Guide to atlas of absorption loss tables.	193
3-1	Relationship between $N_g$ and $\alpha$ .	257
3-2	Directory to propagation loss charts.	289

## GUIDE TO ATLAS SECTIONS

<u>Section</u>	<u>Caption</u>	<u>Page</u>
2.4	Atlas of Electron Density Profile Models and of Associated Transmission Diagrams (69 Graphs and Diagrams) See Table 2-7 for directory.	114-190 113
2.5	Atlas of Ionospheric Absorption Loss (48 Tables) See Table 2-8 for directory.	194-241 193
3.4	Atlas of Propagation Loss Charts (24 Charts) See Table 3-2 for directory.	290-313 289



## GLOSSARY OF SYMBOLS AND SUBSCRIPTS

When material has been drawn from as many divergent sources as has that forming the basis for this document, conflicts in notation and nomenclature are inevitable. An author then is faced with a dilemma between (a) minimizing immediate confusion by developing an internally self-consistent and unambiguous notation and nomenclature, and (b) maintaining continuity in the ties to the basic sources by retaining notation and nomenclature used therein. In the main, the latter policy has been adopted. This document builds on those sources as external foundation, rather than absorbing them as internal structure. Changes have been made where necessary to avoid confusion within single expressions or topics. This glossary is provided to assist in sorting out the remaining ambiguities.

Certain quantities (e.g., loss, gain, attenuation) are variously expressed both in terms of basic electrical units (e.g., power or power ratio) and in decibel units. For use in this document the practice has been adopted of using upper case symbols to signify the quantities expressed in basic electrical units and the corresponding lower case symbols to signify the same quantities expressed in decibel units. This is contrary to practice in some areas of the literature and the reader should herewith be forewarned. However, it leads to better accord with preferred or recommended practice for symbolizing a number of the common electrical quantities. At this point it seems better to buck the former stream than to transgress the latter barrier.

Whenever multiple meanings are assigned to a symbol in the glossary, the one appropriate in a specific instance should be clear from the context in which the symbol is found. To determine the specific meaning of a subscripted symbol, first find the generic meaning of the basic symbol in the proper list (Roman or Greek), then find the specialization denoted by the subscript in the subscript list.

Units of all physical quantities are given in the rationalized MKSA system, with temperature in degrees Celsius ( $^{\circ}\text{C}$ ). Unless otherwise specifically indicated (e.g., by a subscript such as "kw" or "km" or by a qualifying notation with an equation), the basic unit, rather than a multiple or submultiple, is implied.

# SYMBOLS

<u>Entity Symbol</u>	<u>Entity Symbolized</u>	<u>Unit Symbol</u>
<u>Roman Symbols</u>		
A	Absorption aperture (of an antenna)	$m^2$
A	Amplitude of a complex exponential wave function	-
A	Area	$m^2$
A	Attenuation factor (loss ratio form)	-
A	Total absorption	np
$\Delta A$	Area increment (of a magnetic dipole)	$m^2$
a	Attenuation factor (decibel form)	dB
a	Radius of the earth: $6370 * 10^3$	m
B	Magnetic, geomagnetic, flux density Geomagnetic flux density in tables (CGS units)	$Wbm^{-2}$ , T $\Gamma$ (gauss)
C	Curvature, magnitude of curvature vector	$m^{-1}$
$\bar{C}$	Curvature vector	$m^{-1}$
$\Delta C$	Curvature difference or increment	$m^{-1}$
c	Velocity of light: $299.7925 * 10^6$	$ms^{-1}$
D	A region of the ionosphere below about 90 km	-
D	Distance: specifically, ground range or ground range equivalent	m
$\Delta D$	Increment of ground range	m
E	A region of the ionosphere between about 90 and 140 km	-
E	Electric field strength	$Vm^{-1}$
e	Electronic charge: $1.60210 * 10^{-19}$	C

Entity Symbol	Entity Symbolized	Unit Symbol
e/m	Electronic charge to mass ratio: $1.758796 * 10^{11}$	$\text{Ckg}^{-1}$
F	A region of the ionosphere above about 140 km	-
F1	A region of the ionosphere between about 140 and 200 km (a subdivision of F)	-
F2	A region of the ionosphere above about 200 km (a subdivision of F)	-
f	Cycle frequency: $f = \omega/2\pi$	$\text{Hz}, \text{s}^{-1}$
G	Gain of an antenna (power density ratio form)	-
g	Gain of an antenna (decibel form)	dB
H	Magnetic, geomagnetic, field intensity	$\text{Am}^{-1}$
H	Scale height in Chapman functions	m
h	Height above the surface of the earth	m
$\Delta h$	Height increment of one kilometer	km
I	Absorption index (not same as $\chi$ : see 2.3.5)	-
j	Square root of (-1)	-
K	Loss factor (see 2.3.5)	-
k	Propagation constant: $k = 2\pi/\lambda$	$\text{m}^{-1}$
L	Length	m
$\Delta L$	Length increment (of an electric dipole)	m
M	Dipole moment: electric magnetic	Am $\text{Am}^2$
m	Electronic mass: $9.1091 * 10^{-31}$	kg
N	Electron density of the ionosphere	$\text{m}^{-3}$

Entity Symbol	Entity Symbolized	Unit Symbol
N	Refractivity of the atmosphere	-
$\Delta N$	Refractivity increment in one kilometer	-
n	Complex index of refraction: $n^2 = (\mu - j\chi)^2$	-
n	Index of refraction, unspecialized (Ch. 2)	-
n	Refractive index of the atmosphere (Ch. 3)	-
P	Power	W
p	Power (decibel form)	dB
q	Electron production coefficient in Chapman functions	$m^{-3} s^{-1}$
R	Complex polarization ratio	-
R	Distance, radial, from a source	m
R	Resistance, radiation resistance	$\Omega$
R12	12-month running average sunspot number	-
r	Radial distance from center of earth: magnitude of position vector	m
r	Radial distance, spherical coordinate system	m
S	Salinity (parts per thousand)	‰
S	Magnitude of poynting vector; power density flux	$Wm^{-2}$
$\bar{S}$	Poynting vector	$Wm^{-2}$
s	Distance along ray trajectory	m
T	Cycle period of wave: $T = 1/f$	s
T	Temperature	°C
t	Time variable	s

Entity Symbol	Entity Symbolized	Unit Symbol
u	Velocity of an electron	$\text{m s}^{-1}$
v	Phase velocity of a wave	$\text{m s}^{-1}$
X	Plasma frequency variable: $X = \omega_N^2 / \omega^2$	-
x	Distance in wave function	m
x	Normalized height variable in Chapman functions	-
Y	Gyrofrequency variable: $Y = \omega_H / \omega$	-
Z	Collision frequency variable: $Z = \nu / \omega$	-
z	Normalized height variable in Chapman functions	-
<u>Greek Symbols</u>		
$\alpha$	Angle of ray trajectory relative to wavefront	-
$\alpha$	Earth radius ratio: $\alpha = a_e / a$	-
$\alpha$	Electron recombination coefficient in $\alpha$ -Chapman function	$\text{m}^3 \text{s}^{-1}$
$\beta$	Electron attachment coefficient in $\beta$ -Chapman function	$\text{s}^{-1}$
$\beta$	Elevation angle at ray trajectory ends	-
$\beta$	Local elevation angle of ray path	-
$\Delta\beta$	Increment of elevation angle	-
$\Gamma$	Loss (power ratio form)	-
$\gamma$	Loss (decibel form)	dB
$\Delta$	Increment of entity whose symbol follows	-
$\partial$	Partial differential	-
$\epsilon$	Permittivity, absolute, of a medium (Ch. 2)	$\text{Fm}^{-1}$

Entity Symbol	Entity Symbolized	Unit Symbol
$\epsilon$	Permittivity, relative, of a medium (Ch. 3)	-
$\epsilon_m$	Permittivity, absolute, of a medium (Ch. 3)	$\text{Fm}^{-1}$
$\epsilon_o$	Permittivity, absolute, of free space: $8.8542 * 10^{-12} \approx 1/(36\pi * 10^9)$	$\text{Fm}^{-1}$
$\epsilon_r$	Permittivity, relative, of a medium (Ch. 2)	-
$\eta$	Characteristic impedance of free space: $120\pi$	$\Omega$
$\theta$	Angle measured from dipole axis	-
$\theta$	Angle of wavefront normal relative to steady magnetic field (geomagnetic field)	-
$\theta$	Polar angle, spherical coordinate system	-
$\kappa$	Absorption coefficient	$\text{np m}^{-1}$
$\lambda$	Wavelength	m
$\lambda^{-1}$	Wave number	$\text{m}^{-1}$
$\mu$	Index of refraction: $n^2 = (\mu - j\chi)^2$	-
$\mu$	Permeability, absolute, of a medium (Ch. 2)	$\text{Hm}^{-1}$
$\mu_o$	Permeability, absolute, of free space (Ch. 2): $4\pi * 10^{-7}$	$\text{Hm}^{-1}$
$\mu_r$	Permeability, relative, of a medium (Ch. 2)	-
$\nu$	Electron collision (radian) frequency	$\text{s}^{-1}$
$\pi$	3.14159 26536	-
$\rho$	Radius of curvature	m
$\Sigma_i$	Summation operator, with index, i.	-
$\sigma$	Conductivity	$\text{mhom}^{-1}$

<u>Entity Symbol</u>	<u>Entity Symbolized</u>	<u>Unit Symbol</u>
$\phi$	Angle of ray incidence at 100 km height level	-
$\phi$	Angle of ray incidence on plane stratified ionosphere	-
$\phi$	Angle of ray trajectory relative to position vector, $r$	-
$\phi$	Azimuth angle, spherical coordinate system	-
$\phi$	Semi-apex angle of virtual ray trajectory	-
$\Delta\phi$	Increment of azimuth angle	-
$\chi$	Index of absorption: $n^2 = (\mu - j\chi)^2$	-
$\chi$	Solar zenith angle	-
$\omega$	Radian frequency: $\omega = 2\pi f$	$s^{-1}$

#### SUBSCRIPTS

<u>Subscr. Symbol</u>	<u>Subscript Signification</u>
$a$	Absorption (with $\Gamma, \gamma$ )
$b$	Basic, free-space (with $\Gamma, \gamma$ )
$d$	Divergence (with $\Gamma, \gamma$ )
$d$	Of an elemental dipole (with $G, g, A$ )
$,d$	From or by an elemental dipole (with $P, p$ )
$,d$	Relative to an elemental dipole (with $G, g$ )
$E$	Electric dipole (with radiation resistance)
$e$	Effective, modified (with $a$ -earth radius)
$eq$	Equivalent (with $f$ )

Subscr. Symbol	Subscript Signification
H	Total gyrofrequency (with $\omega, f$ )
h	Hearability (with $\Gamma, \gamma$ )
i	Initial (with $\Gamma, \gamma$ )
i	Summation index
, i	Relative to an isotropic element (with $G, g$ )
km	Kilometer units
kW	Kilowatt units
L	Longitudinal component (with $H, B, Y$ )
L	Longitudinal gyrofrequency (with $\omega, f$ )
M	Magnetic dipole (with radiation resistance)
m	Absolute, of a medium (with $\epsilon$ : alters units)
m	Position of maximum, $\chi \neq 0$ (with $h$ )
m	Value of maximum, $\chi \neq 0$ (with $N, q$ )
N	Plasma frequency (with $\omega, f$ )
o	Absolute, of free space (with $\epsilon, \mu$ : alters units)
o	Critical value (with $f, \omega, \phi$ )
o	Free space case (with $k, \lambda$ )
o	Position of maximum, $\chi = 0$ (with $h$ )
o	Sea level value (with $N$ -refractivity)
o	Value of maximum, $\chi = 0$ (with $N$ -electron density, $q$ )
oa	Overall, total (with $\Gamma, \gamma$ )



Subscr. Symbol	Subscript Signification
ph	Path (with $\Gamma, \gamma, G, g$ )
pn	Propagation (with $\Gamma, \gamma$ )
r	Real height (with h)
r	Received, available, absorbed (with P, p)
r	Receiver terminal, receiving antenna (with h)
r	Relative, of a medium (with $\epsilon, \mu$ : alters units)
r	Trajectory angle relative to position vector (with $\phi$ )
s	Source (with P, p)
s	Surface value (with N-refractivity)
T	Transverse component (with H, B, Y)
T	Transverse gyrofrequency (with $\omega, f$ )
t	Transmitted, radiated, emitted (with P, p)
t	Transmitter terminal, transmitting antenna (with h)
tn	Transmission (with $\Gamma, \gamma$ )
tt	Transmitting terminal (with $\Gamma, \gamma$ )
v	Virtual height (with h)
wm	Weighted mean
x	Unspecified function (with G, g)
1	Initial point, state, case
2	Final point, state, case
+	Ambiguous sign selection (with R)
-	Ambiguous sign selection (with R)

## 1.0 COMMUNICATIONS JAMMING AT HF

Jamming is a tactic used to disrupt the performance of a mechanism or system. It is characterized by the deliberate application of a spurious load which inhibits function.

The jamming load need not necessarily cause physical destruction of system mechanism -- though such may occur, either inadvertently or advertently. Thus, a printing press might be jammed destructively by insertion of a monkey wrench. A sewage disposal system might be jammed non-destructively by introduction of a large wad of paper. An electric power distribution system might be jammed -- either destructively or nondestructively, depending on the reaction of protective devices -- by application of a short-circuit load. It is worth noting that the degree to which system function is inhibited may depend on the point of application of the spurious load, as well as on the properties of the load.

In the context of this discourse, the systems of concern are radio communication systems, especially those operating between ships or between ship and land. More specifically, attention is to be focused on radio communication systems operating in the HF portion of the radio spectrum, at frequencies ranging from approximately 2-32 MHz.

## 1.1 FORMULATION OF THE PROBLEM

The salient feature of communication systems at HF is the possibility that signal power may be propagated via the earth's ionosphere, as well as along the surface of the earth.

Propagation along the surface of the earth at HF is similar in character to that which occurs at higher frequencies. However, because the wavelength is longer at HF than at higher frequencies, the wave dies out more slowly as it is propagated past the bulge of the curved earth. Over land, waves propagated in this mode die out very rapidly because of the lossy property of the earth. Over sea water, because of its high conductivity, the possibility exists that communication can be effected over a few hundreds of kilometers in the lower HF range.

Wave propagation via the earth's ionosphere has no counterpart at frequencies above the HF range. It is a striking phenomenon which, under favorable circumstances, affords communication over a very wide range of distance, from zero to several thousands of kilometers. The power attrition in this mode of propagation has wide variability. Even between a fixed pair of terminal points, loss may range from an amount somewhat less than the corresponding free space loss to a few hundreds of decibels.

Formulation of the jamming--or for that matter, the communications--problem at HF must take into account this striking mechanism for signal delivery.

### 1.1.1 Background

It will be convenient to establish a frame of reference in terms of which the detailed discussion is given context and proportion. Such is the intent of this subsection.

#### Objective: Deny Access

The objective of communications jamming (henceforth just "jamming") is to deny to the intended consumer access to specific radio communication services. In various situations, the goal may be either to render the presence of the signal undetectable or to render the original information content unintelligible.

### Principle: Spurious Signal

In communications jamming, the spurious load applied to the system is alternative signal power--a spurious signal. Evidently the spurious signal power must ultimately be delivered to the expected point of communication signal intercept or reception, not to the point of emission or transmission. Only at the former location is the spurious load effectively applied to the system.

The spurious signal--the jamming signal--may be designed either to obscure the communication signal energy--to overwhelm it--or to confound the signification of the message carried by the communication signal. The intended message may pass unobserved, may be rendered meaningless, or may acquire an altered meaning.

### Mechanism: Signal Delivery

The intent of a jamming operation may be to disrupt communications to a discrete signal intercept point or throughout a signal intercept area. If an area, it may be selected to include multiple discrete points or points of unknown or moving location. In any event, it is characteristic of the problem that the point of application of the jamming signal is remote--physically inaccessible--from the jammer.

Delivery of the jamming signal to the communication signal intercept area is a crucial function in any jamming operation. At HF it is a task of uncommon complexity. It is on this function that the thrust of this discourse is focused.

Delivery of a jamming signal to an intercept point or area is accomplished by invoking an appropriate wave propagation mechanism. Invariably, the mechanism selected will impose constraints on the positional relationship--e.g., distance and direction--between the receptor to be jammed and the jamming emitter. There exist conditions under which jamming is precluded by the positional situation. These present a sort of "you can't get there from here" dilemma. At HF these constraints are a bit unusual.

It is worth noting that ability to jam a receptor on a given frequency implies, at least, ability to communicate to the receptor location on that same frequency at that same time. This is an important concept, obvious as it may seem. The fact that a communication signal directed to a remote receptor can be heard at the jamming emitter location gives no positive assurance that the intended receptor of that signal can be jammed from the jamming emitter location.

### Optimization: Pseudo Message

As implied in the preceding discussion, the jamming power delivered to the communication signal intercept location is, itself, a signal. It may be--in fact, generally is--carrying "information," a pseudo message. Its effectiveness in jamming the receptor is a function not only of its intensity but also of the character of its pseudo message. Thus, synthesis of a configuration for the jamming signal, including both the character of the pseudo message and the method of its application to the jamming signal carrier, is a topic of significant importance.

The intent of such a signal synthesis procedure is to define an optimum signal configuration. At this level of the optimization process, optimability--or, perhaps, sub-optimability--may be defined as the best use of power, "best" in the sense of exhibiting the maximum jamming effectiveness for a given expenditure of signal power. The optimum configuration for the jamming signal is a function of the configuration of the communication signal with which it is expected to contend.

On another level of the optimization process, optimability may be defined as that state in the tradeoff between jamming effectiveness and signal power which exhibits a probability, considered acceptable for the purpose, that the jamming objective will be met. This state is equivalent to the minimum of an appropriate cost/benefit function.

### Specialization: Unique Factors

The behavior of radio systems operating in the HF portion of the electromagnetic spectrum is characterized by some unique properties. These properties are related to the properties of the medium--the ionosphere--which supports one of the mechanisms for signal delivery. The ionosphere is, above all, a portion of the earth's atmosphere. Its morphology is subject to variations in production by incident solar radiation on diurnal, seasonal and solar cyclic time scales, and to perturbation through redistribution by atmospheric motion. Within limits, morphology is forecastable, as is climate and weather. However, the degree of variability with geographic location, with phase of the controlling cyclic factors and from cycle to cycle of these factors, is great, as is that of climate and weather.

The gradual decrease of signal intensity with distance characteristic of VHF, UHF, and microwave signals is a familiar phenomenon with which one easily becomes comfortable. The situation is not so simple at HF.

Following an initial rapid decrease of intensity with distance, like that at higher frequencies, HF signals often exhibit a sudden, very large, increase in intensity. This is not a random but a regular--though not universal--phenomenon; it is called "skip." It is further discussed at a subsequent point under the topic of "hearability." This phenomenon materially complicates the task of delineating the constraints on position of the jamming emitter relative to the communications receptor.

#### 1.1.2 Scope

The number of factor combinations which can arise in postulating a jamming operation at HF is large. Thus, the number of situations which might, reasonably, be expected to require analysis is likewise large. It is unrealistic to expect simplistic universal solutions. The problem of designing or operating an HF communications jamming system can be reduced to manageable proportions by delineation of specific limited scenarios for which coverage is required.

The subject of communications jamming embraces a spectrum of disciplinary material which has substantial breadth. For the purpose of this discourse, attention is to be confined to a certain sub-field, taken from the total context, which is suggested by the document title.

The task of this subsection is to delineate the fundamental scenarios to be treated and the topical coverage which is intended.

#### Fundamental Scenarios

In the scenarios to be discussed, point coverage will be postulated. This may seem a restrictive condition, but is is amenable to easy relaxation at a later stage of the discussion.

Two fundamental scenarios will be postulated as the basis for signal delivery analysis. The first is jamming at a receptor point located on a ship at sea from an emitter point also located on a ship at sea. The distance between the ships would be limited to a few hundreds of kilometers, and the intervening surface would be restricted to seawater. The second scenario is jamming at a receptor point located on land from an emitter point located on a ship at sea. The limit on distance between the points would be greater--by, perhaps, an order of magnitude--than that in the first scenario. The location of the point on land would be in the interior, not adjacent to the shore.

### Scenario Elaboration

Analyses based on these two scenarios have a wider range of potential application than might be anticipated from their descriptions.

The first scenario is characterized by the probability that jamming signal delivery to the receptor point can be effected by the surface wave mode and by the possibility that delivery by the sky wave mode may be precluded by the skip phenomenon.

The second is characterized by positive exclusion of the possibility of delivery by the surface wave mode and by the possibility that delivery can be effected by the sky wave mode.

Thus, one scenario emphasizes signal delivery by ground wave and the other by sky wave. Note that the ground wave mode of propagation is ionosphere independent, while the sky wave mode is ionosphere dependent.

Two such scenarios are suggested in Figure 1-1. From Ship A, which is a jamming emitter platform, it is required to interdict communication signals shown incident on Ship C from an unspecified point of origin. Such signals may also be imagined to be incident on Ship B. Two possible modes of jamming signal delivery are portrayed, the ground wave and the sky wave. The sky wave is shown being reflected from the E and F regions of the ionosphere, unless launched at an elevation angle so high that complete penetration occurs. The role of the D region at HF is absorption of signal power, rather than reflection.

For delivery to Ship C, the sky wave is shown as a probability but--because of distance--the ground wave is shown as only a bare possibility. For delivery to Ship B, the ground wave is shown as a probability but the sky wave as an impossibility because of the skip phenomenon which can occur on ionospherically propagated signals.

The two fundamental scenarios may, thus, be superposed on other situations in which the same characteristic probabilities are exhibited. For example, the ship-to-ship scenario can be superposed on a ship-to-shore situation in which the sea surface is in the immediate foreground (within a few meters) of the shore point. The ship-to-land (interior) scenario can be superposed on a ship-to-ship situation in which the separation distance is large enough to ensure extinction of the ground wave, despite the high conductivity of sea water, or in which a substantial part of the intervening surface is land.\*

---

\*This comprises the so-called "mixed path" situation, which is difficult to treat mathematically.

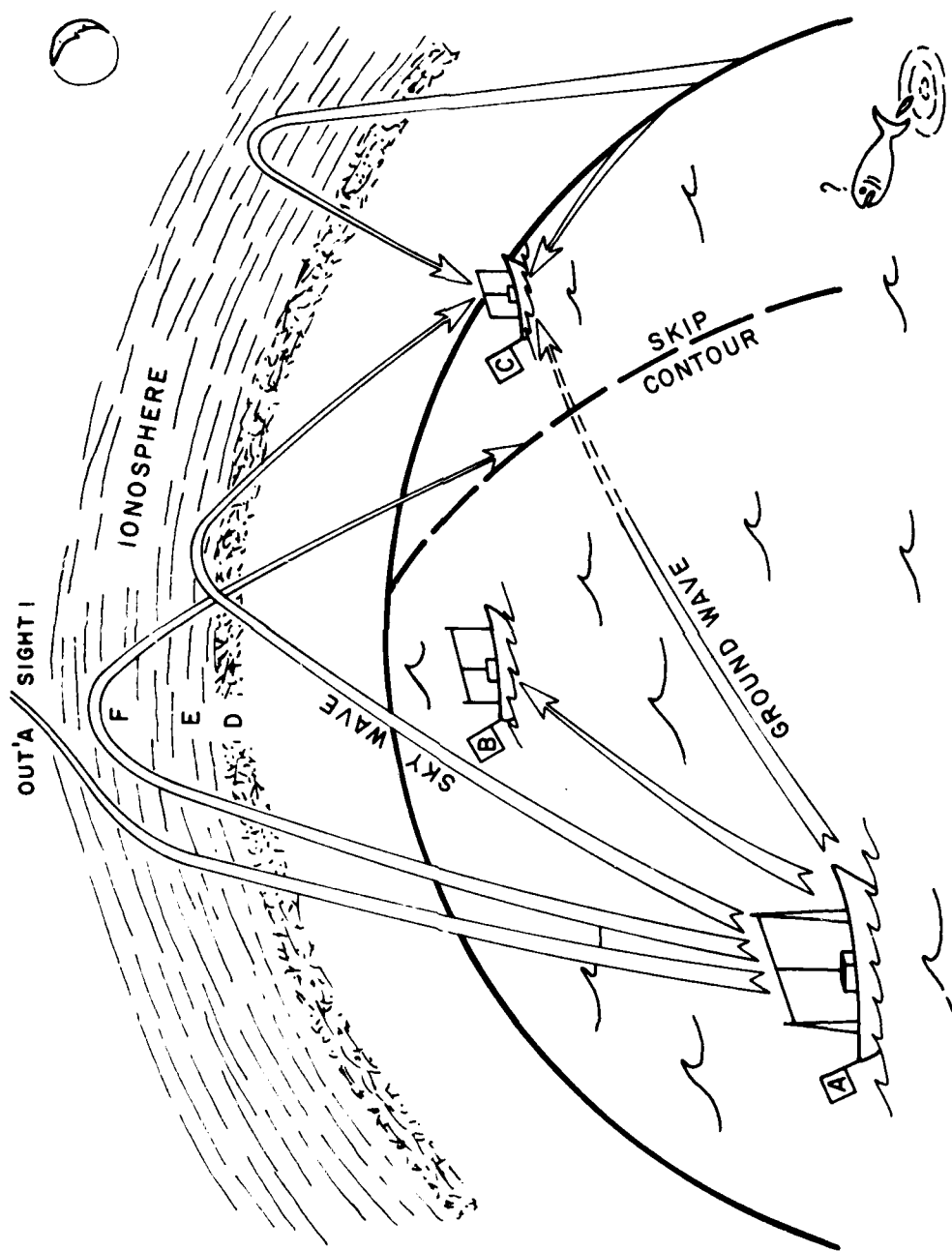


Figure 1-1. Scenario panorama.



In all situations the roles of the two points can be interchanged by invoking the appropriate reciprocity principles.

In the descriptions of the scenarios, point coverage was postulated. This is, fundamentally, the kind of result which calculation procedures produce. Field intensity or loss is determined on a point-to-point basis, and is a function of the relative locations of the points. However, antenna directivity at the jamming emitter will, in practice, be limited. Thus, a degree of area coverage is inevitable; in fact, it may be difficult to avoid coverage of a large area. Performance throughout any portion of such a coverage area can be evaluated by repeated exercise of the appropriate point analysis.

Thus, judiciously applied, the analyses of the two fundamental scenarios can be made to cover a large portion of the situations likely to be encountered by a shipboard jamming platform.

#### Topical Coverage

The specific technical topics to be treated are, generally, those which are related to delivery of the jamming signal to the communications signal intercept point. Topics specifically included are evaluation of transmission loss in the selected scenarios and the effect of antenna properties on delivered signal intensity. Topics specifically excluded are synthesis of optimal signal configurations and the estimation of the jamming signal power requirement.

It may seem strange to exclude the latter topic (power requirement) from a study of signal delivery mechanisms. The reason is that the power requirement depends on additional factors, namely: (a) the expected strength of the communication signal, (b) the required ratio of jamming to communication signal intensity (this latter is a measure of jamming effectiveness). When these additional factors are stated, estimation of the jamming signal power requirement is straightforward and simple.

The signal synthesis topic is logically separable from the signal delivery topic. It draws on a group of disciplines which differs from that on which delivery analysis is based. In the main, the effects are calculable independently. Other sources should be consulted for information on this topic. In lieu of specific information, one might--for discussion purposes--postulate a pseudo message which is random-noise-like and specify a required ratio of jamming noise power to communication signal power.

### 1.1.3 Solution

The communications jamming problem at HF has, so far, been delineated in a general broad-brush way. A prerequisite to formulation of a solution procedure is formulation of a specific question, the answer to which is identified as the required solution. In this instance it will be instructive to pose the question in two forms which are subtly, but significantly, different. One may be called the strategic form and the other the tactical form.

#### Strategic Form

Given a range of jamming scenarios for which coverage is required or desired:

- (a) What sub-range of the range, if any, is excluded by virtue of requiring a sensibly infinite resource?
- (b) Within the not-excluded sub-range, if any, what level of resource is required to assure (ie, to give acceptable probability of ) success?

It is in this form that the question might be posed by a strategist, requirement specifier, or systems designer. The essence of the question is, "Within the sub-range of the physically possible, what is the cost of the operation which I must, or wish to, execute?"

#### Tactical Form

Given a constraint on resources with which to conduct an operation:

- (a) What sub-range of the range of possible scenarios, if any, is precluded by the constraint?
- (b) Within the not-precluded sub-range, if any, what level of resource is required to assure (ie, to give acceptable probability of) success?

A tactician, mission manager or system operator would be likely to pose the question in this form. Formulated thus, the essence of the question is, "With the resource at hand, what is the sub-range of operations for which the probability of success is acceptable?" or "With the resource at hand, is the probability of success of this specific operation acceptable?"

### Common Element

The "not-excluded" and "not-precluded" scenario sub-ranges for the two questions are not congruent. That for the strategic form is scenario limited, but not specifically resource limited. By contrast, that for the tactical question is resource limited but not specifically scenario limited.

In the scenario-limited case, the locus to be determined in scenario space is the boundary between the sensibly impossible and the possible. On the "possible" side of the boundary, the required level of resource must be estimated. In the resource-limited case the locus to be determined in scenario space is the boundary between the impracticable and the practicable. On the "practicable" side of the boundary, estimation of the required level of resource may be of value.

Though the questions are not identical, there is a common element to the classification of points in the scenario space. It is the level of resource required. The difference between the cases is, simply, that resource level to which the specification "critical" is assigned. In both cases a quantitative estimate of resource requirement is essential. Indeed, a solution procedure can be constructed about an iterative estimation of the resource requirement property.

### Solution Procedure

The critical resource to be considered in this analysis is jamming signal power. Formulation of a solution procedure comprises specification of a definitive sequence of steps--an algorithm--by which the required level of jamming signal power can be estimated. A suitable sequence is the following:

- (1) Specify parameters of scenario.
  - (a) State operating frequency of communication signal to be jammed.
  - (b) State class of communication message to be interdicted.
  - (c) State time at which operation is to be conducted.
  - (d) Determine jamming signal delivery path (distance, direction, geographic location).

- (2) Assess potential signal delivery mechanisms.
  - (a) Estimate path\* or propagation\* loss on delivery path.
  - (b) Estimate influence of antenna characteristics on loss.
  - (c) Estimate transmission\* loss on delivery path.
  - (d) Estimate transmitting terminal\* loss.
  - (e) Estimate total\* or overall\* loss.
- (3) Optimize jamming signal configuration.
  - (a) Specify jamming signal pseudo message appropriate to communication signal message class.
  - (b) Specify method of application of pseudo message to jamming signal carrier.
  - (c) Specify required jamming/communication signal intensity ratio.
- (4) Estimate jamming signal source power requirement.
  - (a) Estimate communication signal intensity.
  - (b) Apply specified jamming/communication signal intensity ratio.
  - (c) Apply total loss estimate.
  - (d) Calculate estimated jamming signal source power requirement.
- (5) Determine solution status.
  - (a) Specify "critical" power level (e.g., "sensibly infinite" or "resource limit value").

---

\*These loss terms will be given precise definitions at a later stage in the discourse.

- (b) Compare estimated power requirement to assigned critical value.
- (c) If the estimated power requirement exceeds the critical value, declare the case "excluded" or "precluded."
- (d) If the estimated power requirement does not exceed the critical value, declare the case "not-excluded" or "not-precluded."

Note: If, rather than a single case, a sub-range boundary locus is to be defined, repeat the algorithm for additional scenarios until adequate locus definition is achieved.

The principal subject for this document, as its title suggests, is Step 2 of the solution algorithm. Section 1.2 of this chapter will be devoted to definition of the necessary signal power attrition concepts. The remaining two chapters will be devoted to exposition of methods for quantitative evaluation of power attrition in the two applicable mechanisms for signal delivery, the sky wave (Chapter 2.0), and the ground wave (Chapter 3.0).

## 1.2 ESTIMATION OF POWER ATTRITION

As the jamming signal proceeds from its source to the point of its application to the communication system, each mechanism along the way exacts a toll in power. Each of the several toll-exacting agencies must be identified, and the amount of its exaction must be evaluated or estimated. The function of this section is to make a gross identification of some toll-exacting agencies and to state the rules by which the tolls are to be determined.

### 1.2.1 Loss Definitions

Loss is defined to be the ratio of the power input to a transmission process,  $P_1$ , to the power available at the output of the process,  $P_2$ . The general symbol which will be used for loss is  $\Gamma$ . Thus,

$$\Gamma = P_1/P_2 \quad 1-1a$$

It is often convenient to express loss in decibel form, rather than power ratio form. For loss so expressed the symbol  $\gamma$  will be used. Thus,

$$\begin{aligned} \gamma &= 10 \text{ Log } \Gamma = 10 \text{ Log } (P_1/P_2) \\ &= 10 \text{ Log } P_1 - 10 \text{ Log } P_2 \end{aligned}$$

or

$$\gamma = P_1 - P_2 \quad 1-1b$$

Loss attributable to a specific agency or mechanism will be identified by a subscript on the generic loss symbol, e.g.,  $\Gamma_{tn}$  or  $\gamma_{tn}$  for "transmission" loss. A glossary of symbols and subscripts is given in the front of the document.

In describing the transmission of power from one point to another by means of radio waves, the concept of "transmission loss" often is a convenient fiction. Transmission loss,  $\Gamma_{tn}$ , is defined to be the ratio of power radiated from the transmitting antenna,  $P_t$ , to power available from the receiving antenna,  $P_r$ , considering the latter to be lossless.

$$\Gamma_{tn} = P_t/P_r \quad 1-2a$$

In decibel form,

$$10 \text{ Log } \Gamma_{tr} = 10 \text{ Log } P_t - 10 \text{ Log } P_r$$

or,

$$\gamma_{tr} = P_t - P_r \quad 1-2b$$

Thus, transmission loss includes the effects of the directive gains of antennas at both ends of the path. It excludes the efficiencies of both antennas and of the transmission facilities connecting the antennas to the terminal gear at both ends of the path.

Transmission loss is termed a "fiction" because it is not amenable to direct measurement, apart from the coordinated determination of efficiency of the terminal transmission facilities. Though it does include the antenna gains, it is not dependent on the specific means by which the gains are realized. Thus, apart from the directive gain values, transmission loss separates that system property which is a function of time and path location from the properties peculiar to the transmitting and receiving terminal facilities. This separation is convenient both in computation and in application of the loss data.

A "transmitting terminal" loss,  $\Gamma_{tt}$ , can be defined as the ratio of power,  $P_s$ , delivered by the source to the transmitting terminal transmission facilities to power,  $P_t$ , radiated from the transmitting antenna.

$$\Gamma_{tt} = P_s / P_t \quad 1-3a$$

In decibel form,

$$\gamma_{tt} = P_s - P_t \quad 1-3b$$

For this discussion it is not necessary to define a similar loss at the receiving terminal of the path. Only the ratio of available jamming signal power to available communication signal power will be of interest at the receiving end of the path. Both of these signals would experience the same receiving terminal transmission facility loss. Thus, it suffices to define these power levels without accounting for the terminal facility loss.\* This is in accord with the definition of transmission loss.

\*This would not be sufficient for a determination of receiving system sensitivity, but it does suffice for a determination of jamming susceptibility.

The total, or "overall," power loss,  $\Gamma_{oa}$ , can be defined, then, as the product of transmitting terminal loss and transmission loss.\*

$$\Gamma_{oa} = \Gamma_{tt} * \Gamma_{tn} \quad 1-4a$$

In decibel form,

$$\gamma_{oa} = \gamma_{tt} + \gamma_{tn} \quad 1-4b$$

Sometimes it is convenient to make complete the partial separation of "path" and "terminal" losses effected by the definition of transmission loss. This can be done by defining two additional loss concepts, "path loss" identified by the subscript ph and "propagation loss" identified by the subscript pn. In both cases the new definitions are effected by extraction of the antenna gains from transmission loss. In one case ( $\Gamma_{ph}$ ,  $\gamma_{ph}$ ) it is gain relative to an isotropic reference ( $G_{x,i}$ ) which is extracted.\*\* In the other case ( $\Gamma_{pn}$ ,  $\gamma_{pn}$ ) it is gain relative to an elemental dipole reference ( $G_{x,d}$ ) which is extracted.\*\*

Path loss ( $\Gamma_{ph}$ ) and path gain relative to an isotropic reference ( $G_{ph,i}$ ) are defined by the equation

$$\Gamma_{tn} = \Gamma_{ph} / G_{t,i} G_{r,i} = \Gamma_{ph} / G_{ph,i} \quad 1-5a$$

In decibel form

$$\gamma_{tn} = \gamma_{ph} - g_{t,i} - g_{r,i} = \gamma_{ph} - g_{ph,i} \quad 1-5b$$

---

\*The symbol \* in an equation denotes the multiplication operator.

\*\*The symbol  $G_{x,i}$  denotes power gain of an antenna (the type or function of which is indicated by x) relative to an isotropic reference. Except where explicit specification of the reference is either necessary to avoid ambiguity or desirable for expositional emphasis, the suffix subscript (, i) will ordinarily be omitted, but implied. A suffix subscript (, d) is similarly used to denote an elemental dipole reference. It must never be omitted. The symbol  $G_{d,i}$  denotes the gain of an elemental dipole relative to an isotropic reference. It has the value 3/2 (1.76 dB).



Propagation loss ( $\Gamma_{pn}$ ) and path gain relative to an elemental dipole reference ( $G_{ph,d}$ ) are defined similarly.\*

$$\Gamma_{tn} = \Gamma_{pn} / G_{t,d} G_{r,d} = \Gamma_{pn} / G_{ph,d} \quad 1-6a$$

In decibel form,

$$\gamma_{tn} = \gamma_{pn} - g_{t,d} - g_{r,d} = \gamma_{pn} - g_{ph,d} \quad 1-6b$$

Since  $G_{x,i} = G_{x,d} * G_{d,i}$  (see footnote reference just prior to Equations 1-5), it follows from Equations 1-5a and 1-6a that

$$\Gamma_{pn} = \Gamma_{ph} / (G_{d,i})^2 \quad 1-7$$

Some authors choose to go a step farther and break path loss down into two factors, a "path attenuation relative to free space" and a "free

---

\*In subsection 3.3.1 an alternate, but equivalent, definition of propagation loss is given. There, an analogy is drawn between propagation loss and transmission loss, rather than between propagation loss and path loss. In a sense, the propagation loss concept lies intermediate between the other two concepts. The alternate definition is used in Chapter 3.0 to facilitate discussion of the problem of determining power radiated and power received in the ground wave case. The equivalence is made evident from the following expansion of the transmission loss.

$$\Gamma_{tn} = \frac{P_t}{P_r} = \frac{P_{t,d} / G_{t,d}}{P_{r,d} * G_{r,d}} = \frac{P_{t,d}}{P_{r,d}} * \frac{1}{G_{t,d} G_{r,d}} = \Gamma_{pn} / G_{t,d} G_{r,d}$$

In this expression the final subscript (,d) signifies that the quantity is "radiated from" or "relative to" an elemental dipole. This expression appears explicitly in subsection 3.3.5. The reason for defining propagation loss in addition to path loss, to which it is quite similar, will there become evident. It is not commonly found in the literature.

space loss,  $\Gamma_b$ , for a distance equal to the real ground range,  $D$ . The path attenuation factor,  $A_{ph}$ , is defined by the following expression.

$$\Gamma_{ph} = A_{ph} \Gamma_b \quad 1-8a$$

In decibel form,

$$\gamma_{ph} = a_{ph} + \gamma_b \quad 1-8b$$

The free space loss ( $\Gamma_b, \gamma_b$ ) is considered a "basic loss" -- and is frequently so called. It is the loss in transmission between an isotropic transmitter and receiver separated a free-space equivalent distance equal to the ground range,  $D$ , of the path. Its value can easily be expressed in terms of  $D$ .

An isotropic source radiating a total power,  $P_t$  (watts), will produce a field intensity,  $S$  (watts/meter<sup>2</sup>), at a distance,  $D$  (meters), given by the following expression.

$$S = P_t / 4\pi D^2 \quad 1-9$$

The power,  $P_r$  (watts), available from an isotropic receiver in the incident field,  $S$ , is the product of  $S$  and the isotropic absorption area,  $A = \lambda^2 / 4\pi$  (meters<sup>2</sup>).

$$P_r = SA = (P_t / 4\pi D^2) (\lambda^2 / 4\pi) \quad 1-10$$

The basic or free space loss,  $\Gamma_b$ , is

$$\Gamma_b = P_t / P_r = (4\pi D / \lambda)^2 \quad 1-11a$$

In decibel form,

$$\begin{aligned} \gamma_b &= 20 \text{ Log } (4\pi D / \lambda) \\ &+ 21.98 + 20 \text{ Log } (D / \lambda) \quad (\text{dB}) \end{aligned} \quad 1-11b$$

It also is possible to define a counterpart to the path attenuation factor using  $\Gamma_{pn}$ , rather than  $\Gamma_{ph}$ , in Equations 1-8a,b. In doing so, two possibilities arise for definition of "basic loss." Each has its own justifying rationale.

One possibility is to define basic loss in terms of transmission between isotropic elements, just as was done in Equations 1-8a,b. Thus,

$$\Gamma_{pn} = A_{pn} \Gamma_b \quad 1-12$$

If this option is adopted, the quantity  $A_{pn}$  might be named "propagation attenuation factor" in analogy with the naming of "path attenuation factor."

Another possibility is to define basic loss for this case in terms of transmission between elemental dipole elements. Because this is in accord with the definition of propagation loss, it has a certain attractiveness. This new basic loss could be symbolized  $\Gamma_{b,d}$ .<sup>\*</sup> It is related to  $\Gamma_b$  (or  $\Gamma_{b,i}$ ) in the following way.

$$\Gamma_{b,d} = \Gamma_{b,i} / (G_{d,i})^2 = (4\pi D / \lambda G_{d,i})^2 \quad 1-13$$

From Equations 1-7, 1-8a, and 1-13, it follows that

$$\Gamma_{pn} = A_{ph} \Gamma_{b,d} \quad 1-14$$

From Equations 1-12, 1-14, and 1-13, it further follows that

$$A_{pn} = A_{ph} / (G_{d,i})^2 \quad 1-15$$

It will turn out to be more convenient to make use of the relationship given by Equation 1-14 than to use that given by Equation 1-12.

Before terminating this discussion of loss definitions, a caution ought to be issued. Implicit in the definition of transmission loss is the assumption that only one path between terminals exists. If, in fact, more than one exists the definition must be elaborated. The elaboration must specify a rule for combining the signal power arriving at the receiving terminal over the various paths. The two extreme cases would be deterministic phasor combination and random phasor combination. These are equivalent, respectively, to "voltage summing" and "power summing." Multiple path conditions will be encountered in discussion the sky wave.

---

<sup>\*</sup>That is to say, "basic loss between dipole elements." If it is necessary to make a positive distinction, the original basic loss could be symbolized  $\Gamma_{b,i}$ , ie, "basic loss between isotropic elements." Ordinarily the (,i) will be omitted, but implied.

### 1.2.2 Loss Calculations

In the preceding subsection, the total loss was successively subdivided into subordinate factors. The subdivision structure forms a five-level hierarchy.

$\Gamma_{oa} = \Gamma_{oa}$	Level 1	
$= \Gamma_{tt} \Gamma_{tn}$	Level 2	
$= \Gamma_{tt} \Gamma_{ph} / G_{ph}$	Level 3	
$= \Gamma_{tt} \Gamma_{ph} / G_t G_r$	Level 4a*	1-16a
$= \Gamma_{tt} A_{ph} \Gamma_b / G_{ph}$	Level 4b*	
$= \Gamma_{tt} A_{ph} \Gamma_b / G_t G_r$	Level 5	

In decibel form,

$\gamma_{oa} = \gamma_{oa}$	Level 1	
$= \gamma_{tt} + \gamma_{tn}$	Level 2	
$= \gamma_{tt} + \gamma_{ph} - g_{ph}$	Level 3	
$= \gamma_{tt} + \gamma_{ph} - g_t - g_r$	Level 4a*	1-16b
$= \gamma_{tt} + a_{ph} + \gamma_b - g_{ph}$	Level 4b*	
$= \gamma_{tt} + a_{ph} + \gamma_b - g_t - g_r$	Level 5	

An analogous structure based on  $\Gamma_{pn}$ , rather than  $\Gamma_{ph}$ , also was established.

---

\*Level 4a is formed from Level 3 by subdividing  $G_{ph}$  and Level 4b by subdividing  $\Gamma_{ph}$ .

$\Gamma_{oa} = \Gamma_{oa}$	Level 1	
$= \Gamma_{tt} \Gamma_{tn}$	Level 2	
$= \Gamma_{tt} \Gamma_{pn} / G_{ph,d}$	Level 3	1-17a
$= \Gamma_{tt} \Gamma_{pn} / G_{t,d} G_{r,d}$	Level 4a	
$= \Gamma_{tt} A_{ph} \Gamma_{b,d} / G_{ph,d}$	Level 4b	
$= \Gamma_{tt} A_{ph} \Gamma_{b,d} / G_{t,d} G_{r,d}$	Level 5	

In decibel form,

$\gamma_{oa} = \gamma_{oa}$	Level 1	
$= \gamma_{tt} + \gamma_{tn}$	Level 2	
$= \gamma_{tt} + \gamma_{pn} - g_{ph,d}$	Level 3	1-17b
$= \gamma_{tt} + \gamma_{pn} - g_{t,d} - g_{r,d}$	Level 4a	
$= \gamma_{tt} + a_{ph} + \gamma_{b,d} - g_{ph,d}$	Level 4b	
$= \gamma_{tt} + a_{ph} + \gamma_{b,d} - g_{t,d} - g_{r,d}$	Level 5	

For the purpose of this discourse, the total attrition of jamming signal power will be estimated by estimating the individual factors at Level 4a in the two hierarchies. This is the task delineated in Step 2 of the solution procedure formulated in subsection 1.1.3.

For reasons which will be made clear when the two delivery mechanisms are discussed, the path loss concept is convenient to use with the sky wave and the propagation loss concept is convenient to use with the ground wave.

The path attenuation factor concept will not be used explicitly in this discourse, but the basic loss concept defined in conjunction with it will appear, both in specialized form in connection with the sky wave and in the general form in connection with the ground wave.

The evaluation of path loss and transmission loss for the sky wave is the subject of Chapter 2.0. Chapter 3.0 is devoted to evaluation of propagation loss and transmission loss for the ground wave.

## 2.0 THE SKY WAVE

One of the two principal mechanisms for signal delivery in the HF portion of the radio spectrum is the sky wave. In this chapter its salient properties will be developed and displayed. The objective of the exposition is to elucidate principles by which transmission loss can be estimated for the sky wave case.

The concept of path loss is introduced as an intermediate stage in the estimation of transmission loss. It is convenient because it easily breaks apart into four factors, each of which can be evaluated separately.

At the end of the chapter information is provided in atlas form to display graphically the salient features of the sky wave and to provide data for problem solving.

PRECEDING PAGE BLANK-NOT FILMED

## 2.1 DEFINITION OF SKY WAVE

A compact radio emitter situated outside, but in the immediate neighborhood, of the surface of a very large spherical obstacle produces an electromagnetic wave which, eventually, will permeate--albeit not uniformly--the space in which the emitter/obstacle (source) system is embedded. Depending on the composition of the obstacle, the wave also may propagate, more or less, into its interior. In general, a portion of the power supplied to the emitter will be radiated from the source system, being propagated to the far reaches of the surrounding space, and will be lost to the source system. \*

Viewed as a whole, the configuration of the electromagnetic field in the space is, clearly, affected by the presence of the spherical obstacle. For example, the field beyond the obstacle on the side opposite the emitter will be lower than average. This region is said to be shadowed from the emitter by the obstacle. Viewed locally, from a small segment of a wavefront not too close to emitter or obstacle, the influence of the obstacle may be seen as completed rather than continuing.

The continuation of wavefront propagation by Huygenian wavelet construction principles makes evident the predominant importance of those areas of wavefront in the immediate neighborhood of a small wavefront segment to the propagation of that segment. Contributions from more distant portions of the wavefront are subordinate. A segment of wavefront,

---

\*If this approach to definition of the sky wave seems a bit esoteric, please bear with it. It is part of a strategy to unify the definition of the sky wave and that of the ground wave which will be treated in a subsequent chapter. The making of the distinction is not trivial. After all, both may arise from the same emitter under the same circumstances. More succinctly, the two are differing aspects of the same wave field.

In delimiting the extent of a "neighborhood," or the size of an "obstacle," or the degree of "closeness" of two locations, the unit of length to be used is the wavelength of the electromagnetic wave. In the HF portion of the radio spectrum (2 to 32 MHz for the purposes of this document), the wavelength ranges from 150 meters to 9.4 meters. In this frame of reference, the earth is a very large obstacle indeed. A critical dimension is the greatest linear extent of the emitter. It affects the distance at which the emitter is seen as "compact." An HF antenna which has a greatest linear dimension of one kilometer is a very large HF antenna; most would not exceed 150 meters. At a distance of 10 or more kilometers above the surface of the earth, almost any HF antenna system will be seen as compact.



far enough removed from emitter and obstacle, may begin to propagate as if the obstacle were not present. The power supporting such a segment of wavefront is lost to the source system; it is radiated.

Thereafter, propagation of the wavefront proceeds in accord with the principles of geometric optics. Ray concepts may be invoked. The obstacle itself--in this case the earth--exerts no continuing influence on the propagation of such portions of the wavefront. Its role is merely that of a launching platform which establishes the initial conditions of launch. The sky wave arises from such portions of the wavefront.

If the medium in which the source system is embedded is homogeneous in electromagnetic properties, rays will be straight lines. Power which once leaves the source system will be lost irretrievably.

The medium surrounding the earth is not electromagnetically homogeneous. Beginning at an altitude of 50 to 70 kilometers, the ionized upper atmosphere--the ionosphere--profoundly influences the propagation of electromagnetic waves in the HF portion of the spectrum. It provides a mechanism by which a portion of the electromagnetic energy incident on it can--under certain circumstances--be returned to earth.

Signal power from portions of the emitted wavefront which have progressed beyond the immediate influence of the earth, which is re-directed to the earth by the ionosphere, constitutes the sky wave.

The concern of this chapter is with the properties of the ionosphere as a medium for propagation of HF electromagnetic waves and with the influence of medium morphology on the transmission of signal power from point to point on the surface of the earth. In general, changes in medium properties in the ionosphere in a distance equal to the free-space wavelength at HF are small enough to justify application of the principles of ray optics. In any case, we shall assume that this is so and base our analysis on those principles.

The configuration of optical trajectories--or ray paths--in an optically inhomogeneous medium is a function of the refractive index, symbolized by  $n$ . We shall, therefor, be interested in the refractive index of the ionosphere. Explicitly, we shall require a refractive index model of the ionosphere--or a substitute therefor--valid in the 2 to 32 MHz range of frequency.

Before proceeding to an exploration of that topic, it is worth taking a moment to comment on the lower atmosphere. It is true, as we shall see in Chapter 3, that the refractive index of the lower atmosphere differs slightly

from that of free space, by about 300 parts in  $10^6$  at the surface of the earth. The refractive effects are so small in comparison with those of the ionosphere as to be totally negligible for sky wave propagation. The variation in refractive index in the lower atmosphere does become a factor in the propagation of energy by the ground wave mechanism. This effect will be treated in the chapter on the ground wave.

## 2.2 REFRACTIVE INDEX MODELS

The ionosphere and the geomagnetic field together form a medium in which the propagation of electromagnetic waves is extraordinarily complex. The phenomena are complex both because the properties of the medium are complex and because the morphology of the medium (the description of its form and structure) is complex. To develop a proper model for the medium, both of these characteristics must be treated.

Before proceeding to this task it seems prudent to make certain that the meanings of two frequently used descriptive terms are clear. The first, "isotropic," is used in describing the properties of a medium at a point. It means that the values of the characteristic parameters of the medium at a point do not depend on the orientation of the wave normal at that point. The antonym is "anisotropic." The second term, "homogeneous," is used in describing the morphology of a medium in a region. It means that the values of the characteristic parameters of the medium in a region do not depend on the position of a point in the region. The antonym is "inhomogeneous."

### 2.2.1 Complex Index of Refraction

Take a moment to review the meaning of the refractive index concept. In a medium characterized by scalar values of permeability,  $\mu$ , and permittivity,  $\epsilon$ , the square of the phase velocity,  $v$ , of a wave is given by

$$v^2 = 1/\mu\epsilon \quad 2-1$$

If the permeability and permittivity are each factored into a relative (non-dimensional) value representative of the medium ( $\mu_r, \epsilon_r$ ) and an absolute (dimensional) value for free space ( $\mu_0: \text{H/m}, \epsilon_0: \text{F/m}$ ), then the expression for the square of the phase velocity of a wave can be written

$$v^2 = 1/((\mu_r \epsilon_r)(\mu_0 \epsilon_0)) \quad 2-2$$

The quantity  $1/(\mu_0 \epsilon_0)$  is recognizable as the square of the velocity of light in free space,  $c^2$ . If the quantity  $(\mu_r \epsilon_r)$  is defined to be the square of the refractive index,  $n^2$ , then the expression above can be rewritten.

$$n^2 v^2 = c^2 \quad 2-3$$

So defined, the index of refraction is the factor by which the phase velocity in the medium must be multiplied to give the velocity of light in free space. If  $\mu_r = 1$ , then  $n^2$  is just the relative permittivity (or dielectric constant) of

the medium. \* For a common dielectric medium, polyethylene,  $n^2$  has a value of about 2.3. Furthermore, at HF the phase and group velocities in polyethylene are essentially equal so that a single refractive index concept (and value) suffices for both.

A simple wave with harmonic time variation, propagating in the positive direction along the x coordinate, may be expressed in the form

$$A \exp [j (\omega t - kx)] \quad 2-4$$

In this expression

$$\omega = 2\pi/T = 2\pi f \quad (\text{s}^{-1}) \quad 2-5$$

where T and f are, respectively, the temporal period and frequency, and

$$k = 2\pi/\lambda = 2\pi(\lambda^{-1}) \quad (\text{m}^{-1}) \quad 2-6$$

where  $\lambda$  and  $(\lambda^{-1})$  are, respectively, the wavelength and wave number (they may be thought of as a kind of spatial period and spatial frequency). The velocity of the wave, v, is given by the expression

$$v = \omega/k = \lambda/T \quad (\text{m/s}) \quad 2-7$$

If the wave is propagating in free space, the symbols for the parameters may be tagged to indicate the free space values; thus,

$$k_0 = 2\pi/\lambda_0 = 2\pi(\lambda_0^{-1}) \quad 2-8$$

Note that in this situation  $v = c$ , so that Equation 2-7 becomes

$$c = \omega/k_0 = \lambda_0/T$$

$$\text{or} \quad k_0 = \omega/c \quad 2-9$$

If the expression for wave velocity given by Equation 2-7 is substituted into the definition for refractive index given by Equation 2-3, the following relation is obtained after a slight rearrangement.

---

\*Hereafter, the relative permittivity,  $\mu_r$ , will always be assumed to have the value unity and the permeability will appear only in the form  $\mu_0$ , that of free space. Be hereby forewarned that a new use for the symbol  $\mu$  shortly will appear in connection with the refractive index.

$$k^2 = n^2 \frac{\omega^2}{c^2} \quad 2-10$$

With the aid of Equation 2-9, this relation can be re-expressed in the form

$$k^2 = n^2 k_0^2 \quad 2-11$$

Thus, another aspect of the index of refraction concept emerges. It is the factor by which the free space propagation constant,  $k_0$ , is multiplied to give the propagation constant in the medium,  $k$ . This value of  $k$  may be inserted into Equation 2-4 to give a modified description of a harmonic wave.

$$A \exp [j(\omega t - nk_0 x)] \quad 2-12$$

In this form the role of the index of refraction is made explicit.

In a simple low-loss dielectric like polyethylene, the index of refraction,  $n$ , is--for practical purposes--a real number. In a more general medium, it may be complex. It is convenient, in such cases, to write\*

$$n^2 = (\mu - j\chi)^2 \quad 2-13$$

At this point  $n$  is called the "complex index of refraction" (though the adjective "complex" is frequently omitted when the meaning is obvious from context or when the distinction is unnecessary),  $\mu$  is called the index of refraction and  $\chi$  is called the index of absorption. Using Equation 2-11, we may write

$$k^2 = (\mu - j\chi)^2 k_0^2 \quad 2-14$$

If this expression for  $k$  is inserted into Equation 2-4, the latter may be re-written in the form

$$A \exp [j(\omega t - \mu k_0 x) - \chi k_0 x] \quad 2-15$$

Note that  $\mu$ , the real part of the complex  $n$ , now assumes the role of the simpler  $n$  in Equation 2-4.

In this form (Equation 2-15) the reason for calling  $\chi$  an "index of absorption" is made apparent. The term  $\chi k_0 x$  produces an exponential

---

\*Don't be in too great a rush to do the "obvious," namely, to take the square root of both sides of this equation. It can get you into trouble with signs when expressions are derived for  $n^2$  in terms of the several physical quantities.

decrement of wave amplitude with distance,  $x$ . In fact, the product  $\chi k_0$  is given a name, "absorption coefficient," and a symbol,  $\kappa$ ; thus,

$$\kappa = \chi k_0 = \chi(\omega/c) \quad (\text{nepers/meter})$$

2-16

In comparison to the properties of a simple dielectric medium like polyethylene, those of a magneto-plasmic medium\* are significantly more complex in four important ways:

1. The magneto-plasmic medium is dispersive. Its index of refraction is a function of frequency. In general, the group velocity,  $\partial\omega/\partial k$ , is not equal to the phase velocity,  $\omega/k$ .
2. The magneto-plasmic medium is absorptive. Its index of refraction is complex. Both  $\mu$  and  $\chi$  are always positive and greater than zero. Under this circumstance, the absorption is dissipative; i. e., the absorption represents a conversion of wave energy into heat energy. The heat energy is manifest as an increase in the average random velocity of the particles constituting the gas.
3. The magneto-plasmic medium is birefringent. The index of refraction has two distinct values which, generally, differ significantly. Corresponding, respectively, to each of the two values of refractive index is a characteristic wave polarization.\*\* The birefringent property is a consequence of the presence of the steady uniform magnetic field and the mobility of the free electrons in the plasma. This property implies two different values of phase (and group) velocity and two possible ray paths arising from a single set of initial ray parameters.
4. The magneto-plasmic medium is anisotropic. Each of the two indices of refraction, and its corresponding characteristic polarization, are separate functions of the orientation of the wavefront normal with respect to the direction of the uniform steady magnetic field. The angle between these two directions

---

\*That is, a homogeneous gas, partially ionized, but, on a macroscopic scale, electrically neutral, together with a uniform steady magnetic field.

\*\*A "characteristic wave polarization" is one which will remain unchanged as a wave propagates through a homogeneous medium. For a simple dielectric medium this property is true for any state of polarization. Hence, there are no "characteristic" polarizations for such media.

is denoted by the symbol  $\theta$ . This property implies that phase velocity is direction dependent. As a consequence, in general, the direction of energy propagation (the ray direction) may differ from the direction of the wavefront normal. The angle between these two directions is denoted by the symbol  $\alpha$ .

These properties of a magneto-plasmic medium are expressed quantitatively by the Appleton-Hartree equations [1, 2, 3, 4]. The square of the complex refractive index is given by the Appleton-Hartree dispersion equation (Equation 4-49 of Kelso [1], for example).

$$n^2 = (\mu - j\chi)^2 \quad 2-17$$

$$= 1 - \frac{X}{(1 - jZ) - \frac{Y_T^2}{2(1-X-jZ)} \pm \left[ \frac{Y_T^4}{4(1-X-jZ)^2} + Y_L^2 \right]^{1/2}}$$

The complex polarization,\* R, is given by the Appleton-Hartree polarization equation (Equation 4-82 of Kelso [1], for example).

$$R = \frac{Y_T \pm \left[ Y_T^4 + 4(1-X-jZ)^2 Y_L^2 \right]^{1/2}}{2j(1-X-jZ)Y_L} \quad 2-18$$

Note that the two polarization states differentiated by the sign ambiguity in this equation have an interesting reciprocal property. If the values of R

\*The complex polarization, R, is defined to be the phasor ratio of a particular pair of orthogonal linearly polarized components of the magnetic field of the wave (this is not to be confused with the steady magnetic field). If, at a point, the wavefront normal is not parallel to the steady magnetic field, these two vector quantities define a plane which may be called the principal longitudinal plane. A plane perpendicular to the wavefront normal at the point is called the transverse plane. The magnetic field of the wave lies entirely in the transverse plane. The electric field of the wave may also have a third component in the direction of the wavefront normal. It is for this reason that the magnetic, rather than the electric, field of the wave is used in the definition of polarization. The principal longitudinal plane intersects the transverse plane in a line which may be used as a reference for direction in the transverse plane. The numerator of the polarization ratio is the component of the magnetic field of the wave which lies along this reference direction. The denominator is the component which is perpendicular to the principle longitudinal plane.

associated with the two signs are symbolized by  $R_+$  and  $R_-$ , a little algebra will suffice to show that the following relation holds for all values of the variables.

$$R_+ R_- = 1 \quad 2-19$$

The four variables,  $X$ ,  $Y_L$ ,  $Y_T$  and  $Z$ , appearing on the right-hand side of Equations 2-17 and 2-18 are normalized dimensionless quantities. They are convenient quantities because their use simplifies the formal appearance of a wide variety of relations which occur in the treatment of electromagnetic wave propagation in a magneto-plasmic\* medium. A part of the convenience arises from the fact that each bears information about a single physical property of the medium. These variables plus one additional,  $Y$ , are defined by the following five equations.

$$\begin{aligned} X &= \omega_N^2 / \omega^2 \\ &= (Ne^2 / \epsilon_0 m) / \omega^2 \end{aligned} \quad 2-20$$

$$\begin{aligned} Y &= \omega_H / \omega \\ &= [(\mu_0 H) |e| / m] / \omega \\ &= [B |e| / m] / \omega \end{aligned} \quad 2-21$$

$$\begin{aligned} Y_L &= \omega_L / \omega \\ &= [(-\mu_0 H \cos \theta) e / m] / \omega \\ &= [(-\mu_0 H_L) e / m] / \omega \\ &= [-B_L e / m] / \omega \end{aligned} \quad 2-22$$

$$\begin{aligned} Y_T &= \omega_T / \omega \\ &= [(-\mu_0 H \sin \theta) e / m] / \omega \\ &= [(-\mu_0 H_T) e / m] / \omega \\ &= [-B_T e / m] / \omega \end{aligned} \quad 2-23$$

---

\*Or, "magneto-ionic." There is a long history of use of the term "magneto-ionic" in connection with this topic. "Magneto-plasmic" has been used here to emphasize the plasma nature of the gaseous component of the medium. The effect of the heavy ions is ignored, at least in the sense that the assumption is made that their inertia prevents significant motion at the frequencies and field strength levels involved. Only the free electrons are assumed to move.



$$Z = \nu/\omega$$

2-24

The first four of these equations serve not only to define  $X$ ,  $Y$ ,  $Y_L$  and  $Y_T$ , but also to define four variables intermediate between them and the basic physical variables. The intermediate variables are the plasma radian frequency,  $\omega_N$ , and three electron gyro radian frequencies,  $\omega_H$  associated with the steady magnetic field ( $H$  or  $B$ ),  $\omega_L$  associated with the longitudinal component of the magnetic field ( $H_L$  or  $B_L$ ), and  $\omega_T$  associated with the transverse component of the magnetic field ( $H_T$  or  $B_T$ ).

Two variables appear which are associated with the electromagnetic wave. They are  $\theta$  which is the angle between the wavefront normal and the direction of the steady magnetic field, and  $\omega$  which is the wave radian frequency.

Three variables (not four, since  $B = \mu_0 H$ ) appear which are associated with the physical properties of the magneto-plasmic medium. They are (including both  $H$  and  $B$ ):

- N     The electron density (electrons/m<sup>3</sup>)
- H     The intensity of the steady magnetic field (amperes/m)
- B     The flux density of the steady magnetic field (webers/m<sup>2</sup> or teslas)
- $\nu$     The mean rate of electron-heavy particle collisions (the collision frequency) (collisions/s)

The remaining symbols stand for physical constants:

- $e$      The charge on an electron (coulombs)
- $m$      The mass of an electron (kilograms)
- $\epsilon_0$     The permittivity of free space (farads/m)
- $\mu_0$     The permeability of free space (henries/m)

Thus,  $n^2$ , the square of the complex index of refraction, and  $R$ , the characteristic wave polarization, are complex functions of five real physical variables. Of these, three ( $N$ ,  $H$  or  $B$ ,  $\nu$ ) are medium-related and two ( $\theta$ ,  $\omega$ ) are wave-related. The five physical variables are reduced to four formal mathematical variables ( $X$ ,  $Y$ ,  $Z$ ,  $\theta$  or  $X$ ,  $Y_L$ ,  $Y_T$ ,  $Z$ ) by assigning to the

wave radian frequency variable,  $\omega$ , the role of a normalizing factor or scaling unit.

Defined only through Equations 2-20 and 2-21, the plasma radian frequency,  $\omega_N$ , and the electron gyro radian frequency,  $\omega_H$ , seem to be just artificially contrived entities, called "radian frequencies" simply because they happen to have the appropriate dimensional property. However, each has an interesting physical significance.

If, in a plasma slab, the electrons are mechanically displaced en masse in a direction normal to the slab surface, an electrical restoring force will be produced between the electron body and the ion body. If the electron body is released, it will move under influence of the restoring force with an oscillatory motion. The radian frequency of natural mechanical oscillation will be just the plasma radian frequency in Equation 2-20. It is dependent only on the electron density,  $N$ , of the plasma.

An electron in uniform motion in a uniform steady magnetic field will experience a transverse force unless the direction of motion is parallel to the field. If the motion is in a plane transverse to the magnetic field, the electron will move in a circular orbit. If the motion is inclined to a transverse plane, the path will be a helix, the projection of which on a transverse plane is a circle. The radius of the orbital circle will depend on the kinetic energy of the electron and the inclination of the path to a transverse plane, as well as on the strength of the magnetic field. However, the angular velocity (radian frequency) with which the electron moves about the circular orbit (or path projection) will depend only on the strength of the magnetic field. It will be just the electron gyro radian frequency\* in Equation 2-21. The gyrofrequency, like the plasma frequency, is a frequency of natural mechanical oscillation.

If, then, the electron gas in a magneto-plasma is driven mechanically--as by a passing electromagnetic wave--one would expect the motional response of the electrons to maximize when the driving frequency equals one of the frequencies of natural oscillation. One would anticipate that at these frequencies wave/plasma interaction would exhibit exceptional behavior. Such is, indeed, the case. At these frequencies, the Appleton-Hartree equations exhibit critical properties.

In the ionosphere the plasma frequency (not radian frequency:  $f_N = \omega_N/2\pi$ ) ranges from essentially zero to, at times, as much as 10 MHz, or

---

\*Also called the "cyclotron radian frequency."

more. The electron gyrofrequency at ionosphere heights has a much more limited range, from about 0.7 to 1.8 MHz, with a most likely value in the neighborhood of 1.3 MHz. Thus, the plasma frequency range includes the lower half, more or less, of the HF range. The gyrofrequency is below the HF range. This latter is a fortunate circumstance because the complexity of wave behavior in the HF range is thereby kept down.

The quantity called "collision frequency,"  $\nu$ , appearing in Equation 2-24 is more nearly a contrived entity than are the plasma frequency and the gyrofrequency. An attempt to interpret it directly in physical terms is tenuous, at best.

In a plasma, electrons may be in motion, either by virtue of the plasma "temperature" or by virtue of excitation by a passing electromagnetic wave. The existence of electron motion raises the possibility of momentum transfer from electrons to heavy particles by interaction, i. e., by "collision." If an "electron momentum transfer unit" is defined as the product,  $\mu u$ , of electron mass ( $m$ ) and some sort of average electron velocity ( $u$ ), then the product  $\nu \mu u$  can represent a sort of average rate of electron momentum transfer. The quantity  $\nu$  is just a constant of proportionality which gives the number of momentum transfer units expended per unit time. It has the dimensional value  $s^{-1}$ , i. e., "frequency."

The quantity  $\nu \mu u$ , being a rate of change of momentum, is dimensionally equivalent to a force. It is used to account for an average viscous damping force on motion of the electron gas. This is a dissipative mechanism. If all electrons had the velocity  $u$ , and if all electron momentum were lost at each encounter, then  $\nu$  could be interpreted as the "collision frequency."\* The value of  $\nu$  is largest at the lowest levels in the ionosphere. It may there be of the order of  $10^4/s$ .

A full description of the properties of the Appleton-Hartree equations is a major undertaking in its own right. For further details the reader is urged to consult the references [1, 2, 3, 4]. To account for all of the phenomena observable in connection with electromagnetic waves at HF, incident on the ionosphere either vertically or obliquely, the full complexity of the Appleton-Hartree equations must be retained.

---

\*In Equation 2-24, it appears that  $\nu$  ought to be interpreted as a radian frequency. This is easily accomplished by setting  $\nu = 2\pi f_\nu$ . Then the momentum transfer unit is  $2\pi \mu u$  per cycle, or  $\mu u$  per radian, the "collision frequency" is  $f_\nu$  and the collision radian frequency is  $\nu$ .

Fortunately, the task at hand is not that all-encompassing. It is restricted to estimating the ratio of transmitted to delivered signal power. For this limited objective, it is practicable to work with reduced forms of the equations. The trick will be to find ways of reducing the complexity of the equations which do not simultaneously eliminate the essence of crucial phenomena. The admonition to take care not to dispose of the baby along with the bath water is to the point.

### 2. 2. 2 Constraints on Modeling

In the first section of this chapter, the need was established for a model of the refractive index of the ionosphere. It is a necessary basis for the calculation of ray paths, or trajectories, by the methods of geometrical optics. In the immediately preceding section, the nature of the index of refraction of a magneto-plasmic medium was introduced. It was found to be complex, both in the sense of the number system in terms of which it was represented and in the sense of the nature of its properties. The task at hand now is to effect some necessary and suitable simplifications in the description of medium properties and to relate model morphology to the real ionosphere.

In the process, it will be prudent to impose some constraints on the properties of the models to be considered. Without them the task becomes so complex that it is manageable only with great difficulty--a degree of difficulty well beyond the scope of this treatment. The task of this subsection is to explain and to justify the constraints to be imposed. The justification will be more heuristic than rigorous, arising from necessity and based in part on empiricism. The constraints imposed will be of two kinds:

1. Formula reductions which effect a simplification of medium properties.
2. Morphology restrictions which effect a simplification of wave trajectories.

The motivating factors for formula reduction and morphology restriction are essentially similar. They are the following:

1. To simplify the wave properties and trajectory configurations with which it is necessary to deal.
2. To simplify computational procedures to a level appropriate to the objectives of the operation and to a level commensurate with uncontrolled uncertainties in the process.

3. To make more clearly evident certain behavioral characteristics of waves in the medium.
4. To avoid or, at least, to minimize obstacles arising from lack of knowledge about some of the geophysical variables.

To this point, discussion of the complex index of refraction has been based on the assumption that the medium was homogeneous and static. The ionosphere is neither homogeneous nor static. To construct a model of the complex index of refraction in the ionosphere, then, it is necessary to have adequate knowledge of the spatial and temporal occurrences of three physical quantities:

1. The electron density,  $N$  (electrons/m<sup>3</sup>).
2. The geomagnetic field,  $H$  (amperes/m).  
or  $B$  (webers/m<sup>2</sup>). \*
- (Note that  $H$  and  $B$  are vector quantities and that both magnitude and direction are required.)
3. The electron collision frequency,  $\nu$  (collisions/s).

These physical quantities appear implicitly in Equations 2-17 and 2-18. Their involvement is shown explicitly in Equations 2-20 through 2-24.

There are two salient wave properties, the calculation of which is based directly on the refractive index model. The first is the configuration of the trajectory or ray path. It depends on  $\mu$ , the real part of the complex index of refraction--or, simply, the index of refraction. The second is absorption of energy from the wave by the medium. It depends on  $\chi$ , the negative of the imaginary part of the complex index of refraction--or the absorption index. A discussion of the two wave properties logically begins with  $\mu$  and the trajectory, since total absorption cannot be determined by the methods of geometrical optics without reference to the ray path.

The value of  $\mu$  derives, of course, from the Appleton-Hartree dispersion equation (Equation 2-17). The first step in deriving a reduced formula for  $\mu$  is to set  $Z = 0$  in Equation 2-17. Through Equation 2-24 it is implied that  $\nu = 0$ . With this simplification, Equation 2-17 reduces to

$$n^2 = (\mu - j\chi)^2 \quad \text{2-25}$$

$$= 1 - \frac{X}{1 - \frac{Y_T^2}{2(1-X)} \pm \left[ \frac{Y_T^4}{4(1-X)^2} + Y_L^2 \right]^{1/2}}$$

\*The "weber/m<sup>2</sup>" is also called the "tesla."

Under Equation 2-25, the value of  $n^2$  is real; the complex property has been lost. This is a substantial advantage and sufficient motivation for this particular move. The real property of Equation 2-25 does not imply that  $\chi = 0$ . However, it does eliminate the dissipative property of the medium.\* The justification for setting  $Z$  (and  $v$ ) equal to zero is that in the ionosphere the places where  $v$  is large are places where  $\mu$  differs little from unity. Under this circumstance ray bending is small, so  $v$  exerts little influence on trajectory shape.

The next simplifying step is to set  $Y = 0$ . Through Equation 2-21, this clearly implies that  $H$  (or  $B$ ) has been made zero. Of course, if  $Y = 0$ , then  $Y_L = Y_T = 0$  also. With this simplification, Equation 2-25 reduces to

$$\begin{aligned} n^2 &= (\mu - j\chi)^2 \\ &= 1 - X \end{aligned} \tag{2-26}$$

As in Equation 2-25,  $n^2$  is real but  $\chi$  is not necessarily zero, and the dilemma is still with us. The variation of  $n^2$  with  $X$  is shown in Figure 2-1.

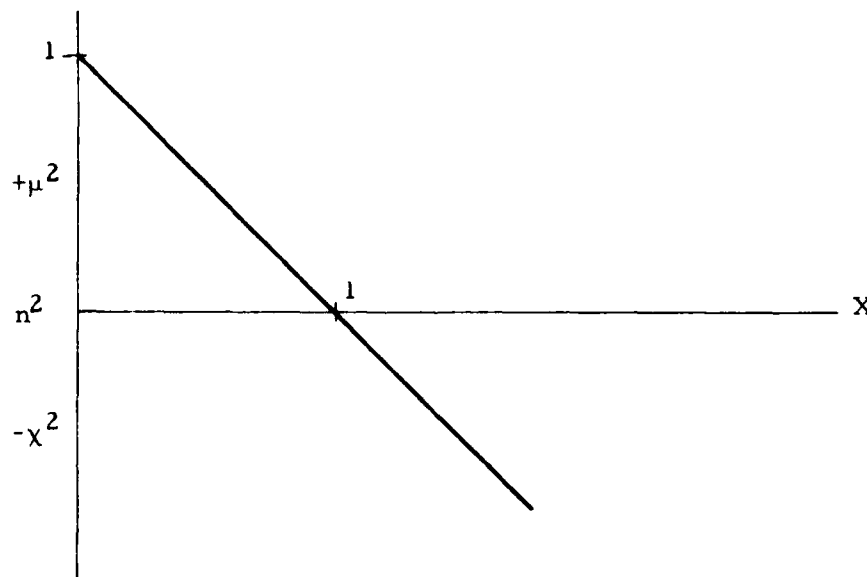


Figure 2-1. Complex index of refraction.

\*This apparent dilemma will be resolved shortly. Stay with it!

Setting  $Y$  equal to zero seems a drastic step and, in truth, it is. With it, two significant medium properties have been lost. The first is anisotropy. The dependence of  $n^2$  (and  $\mu^2$ ) on  $\theta$ , the angle between the wavefront normal and the geomagnetic field, has been lost. The second is birefringence. The square root factor with the ambiguous sign has been lost from the denominator.

Removal of the anisotropy property eliminates the ray path warpage-- at times very substantial--which occurs along the upper part of the trajectory, in the ionosphere, where ray bending is most severe. The justification for the simplification is that trajectory warpage on the entry part of the path is largely compensated by warpage on the exit part of the path. Our concern is for the terminal parameters\* of the trajectory, rather than for the details of its central portion.

Removal of the birefringence property reduces the number of ray paths possible in each case from two to one. The two possible ionospheric ray paths between two points differ significantly--even radically at times--in their central portions. Despite this, in most cases their terminal parameters are similar in value. At frequencies above the electron gyrofrequency (about 1.4 MHz) and for transmission over short to moderate distances (up to, say, 500 km), the ray called "extraordinary" may depart and arrive at a slightly higher angle of elevation than the one called "ordinary." When this is so, the ordinary ray is frequently the more important because it suffers less absorptive attenuation. \*\* The single trajectory calculated in the absence of the geomagnetic field approximates more closely the ordinary ray than it does the extraordinary ray. \*\*\* Frequently it falls between them. For the purpose of determining whether at least one ray path is possible between two points, the no-geomagnetic-field formulation serves except in marginal cases. In some marginal cases, an "extraordinary" ray path may be possible when no ordinary or no-field ray path is possible.

---

\*The ray path parameters which we require will be defined shortly in connection with Figure 2-2.

\*\*This will be made evident when approximations for  $\chi$  are discussed.

\*\*\*The reader should be aware that the ray called "ordinary" when the geomagnetic field is accounted for is not the same as the no-field ray except for the very restricted case in which the wavefront normal, everywhere along the ray path, is perpendicular to the geomagnetic field. In truth, neither of the characteristic waves possible in a magneto-plasma are, in that sense, ordinary. Both generally differ from the no-magnetic-field case. The birefringence property is more complicated in a magneto-plasma than it is in the optical materials in connection with which the terms "ordinary" and "extraordinary" originated.

Before leaving the discussion of index of refraction formulas, it is only fair to resolve the dilemma left hanging earlier. Equation 2-26 and Figure 2-1 show that for  $X < 1$ ,  $n^2$  is positive; for  $X > 1$ ,  $n^2$  is negative. If, in Equation 2-26, the complex representation for  $n^2$  is expanded, two expressions are obtained when real and imaginary terms across the equality are equated.

$$\begin{aligned} n^2 = \mu^2 - \chi^2 &= 1 - X \\ \mu\chi &= 0 \end{aligned} \quad 2-27$$

Thus, either  $\mu$  or  $\chi$  --or both--must be zero. The interpretation of Equation 2-27 is the following.

$$\begin{aligned} \chi &= 0; n^2 = \mu^2 = 1 - X \quad (X < 1) \\ \mu &= 0; n^2 = -\chi^2 = 1 - X \quad (X > 1) \end{aligned} \quad 2-28$$

Note that under this interpretation  $\chi^2$  is a positive number.

The significance of a non-zero, positive, value for  $\chi^2$  when  $\mu^2$  is zero can be deduced from Equation 2-15. When  $\mu = 0$  the "wave" property of the field is lost; the exchange of spatial and temporal phase variation expressed by the factor  $j(\omega t - \mu k_0 x)$  is destroyed. Only an amplitude decrement with the spatial variable,  $\chi k_0 x$ , remains. The field is said to be "evanescent." It is like the field in a waveguide at a frequency below the cutoff frequency. In a plasma, \* the condition  $X = 1$  is the boundary between the propagating and the evanescent states of the electromagnetic field. From Equation 2-20 it is clear that this condition corresponds to equality between the wave radian frequency and the natural plasma radian frequency.

The benefit gained by these two steps in formula reduction is great. The computation of  $n^2$ --and hence of  $\mu^2$ --is made very simple (Equation 2-26). The need for information about the collision frequency and for a detailed model of the geomagnetic field is eliminated from the calculation of  $\mu^2$ . \*\*

The value of  $n^2$  given by Equation 2-26 depends only on  $X$ . Through Equation 2-20, it is clear that of the geophysical quantities  $X$  depends only on  $N$ , the electron number density. Thus, the construction of refractive index models--models for  $\mu$ --has been reduced to the construction of electron number density models. This topic will be treated in the two following subsections (2.2.3 and 2.2.4).

---

\*We no longer have the right to say "magneto-plasma" because  $Y$  has been set to zero.

\*\*A need for some knowledge of the strength of the geomagnetic field still will exist in connection with evaluation of the index of absorption  $\chi$ .



In the construction of an index of refraction model of the ionosphere, it is expedient to impose a morphological constraint, in addition to the formula reduction already described. It is that spatial variation of the index of refraction be a function only of distance from the center of the earth, i.e., of height measured vertically above the surface of the earth. Under this constraint, the medium is said to be "spherically stratified." No variation with geographic coordinates (latitude and longitude) is permitted in the model. Thus, the electron number density model mentioned above becomes an electron density profile along a vertical locus.

In conjunction with the isotropy property, \* spherical stratification of the medium causes ray paths to lie in plane surfaces which contain the center of curvature of the spherically stratified structure--the center of the earth in this case. The ray plane will intersect the surface of the earth in a great circle curve. A portion of the great circle curve spanned by a ray trajectory which intersects it in two places is defined to be the sub-trajectory locus. The length of the sub-trajectory locus is the ground range. Figure 2-2 is an illustration of a ray in the ray plane. In the figure, the ray trajectory parameters (or, ray path parameters),  $\phi$ ,  $\beta$ ,  $h_v$ ,  $h_r$ , and  $D$  are defined.

The advantage of the spherical stratification constraint is that it permits ray paths to be calculated by a modification of Snell's law, called Bouguer's\*\* formula [ 5 ] (see Figure 2-2 for  $r$  and  $\phi_r$ ).

$$\mu r \sin \phi_r = \text{constant} \qquad 2-29$$

Seen on a global scale, the ionosphere certainly is not spherically stratified. For example, the day and night ionospheres on opposite sides of the earth differ greatly. Nevertheless, over limited regions spherical stratification is a tenable constraint if critical regions--such as the twilight zones--are avoided. Clearly, an electron density profile defining the spherical stratification of a model should be appropriate to the central portion of any associated path.

In concept, it is possible to take account of the variation of  $N$  with latitude and longitude, as well as with height. A price for so expanding the concept will be required in the form of added sophistication of the ray tracing procedure and, even worse, in construction of three dimensional electron density models. For the application to which this document is addressed,

---

\*Implied when  $Y$  was made zero.

\*\*Two spellings of this name are extant, Bouguer and Bouger.

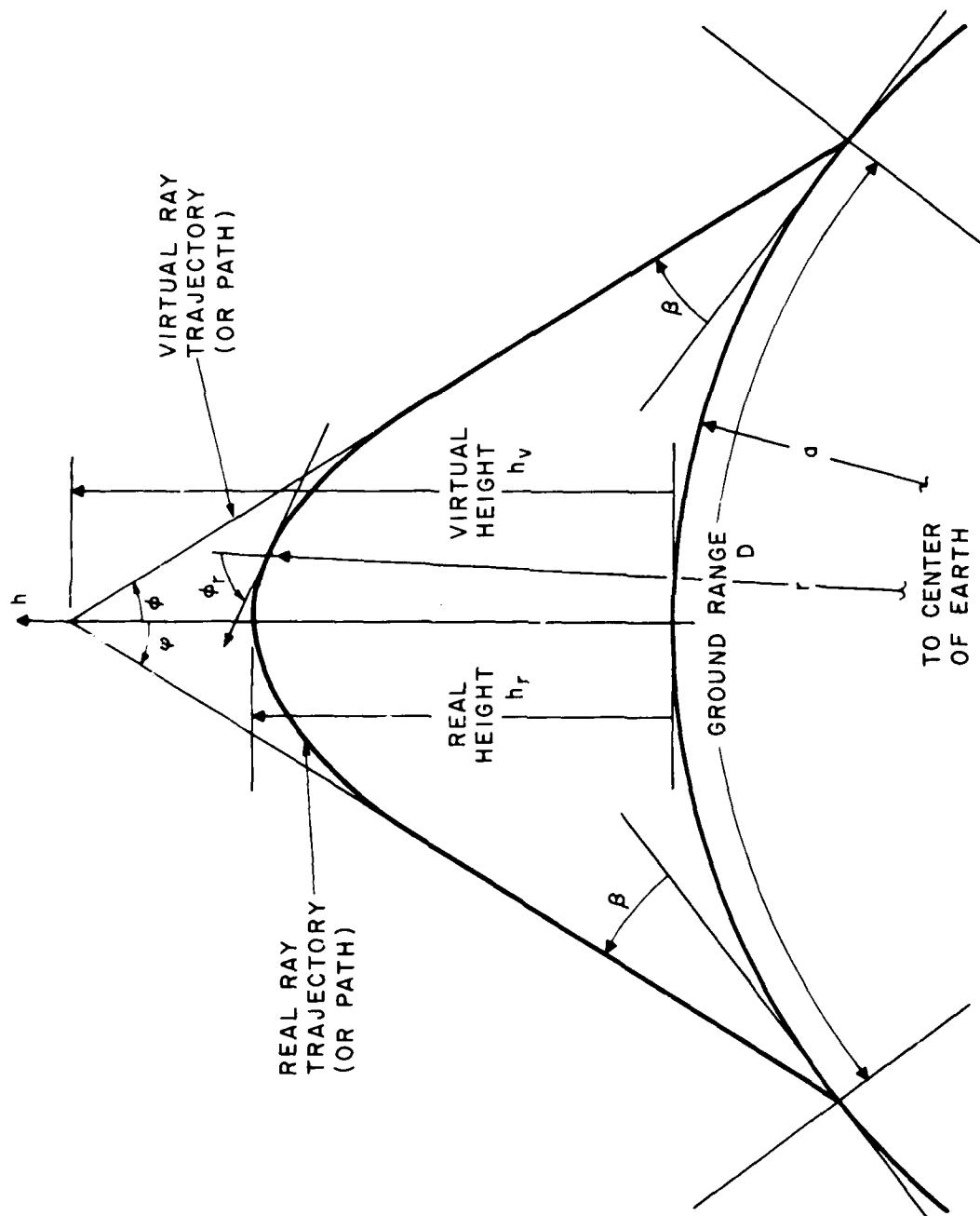


Figure 2-2. Ray plane and ray path parameters.

single-hop ray paths are the most probable configuration. Though error will certainly be experienced in some situations, it is not yet clear that the cost of so expanding the concept will be supported by commensurate benefit.

We leave, now, the discussion of index of refraction to take up a discussion of index of absorption,  $\chi$ . Like index of refraction, the value of index of absorption is obtained from Equation 2-17 for  $n^2 = (\mu - j\chi)^2$ . From the results obtained in the discussion of  $\mu$  (Equation 2-25), it is evident that  $Z$  cannot be made zero in discussing index of absorption. To do so would destroy the mechanism for absorption--throw the baby out with the bath, so to speak.

The inability to set  $Z$  to zero raises at least two problems. The first is that  $Z$  is proportional to electron collision frequency,  $\nu$  (Equation 2-24). Unfortunately, the spatial and temporal occurrence of  $\nu$  is not adequately known. Its distribution is not susceptible to direct measurement. Its physical interpretation is unclear. In fact, the collision frequency concept is one of the weak points of the Appleton-Hartree formulation. The second problem is that no single simplification of Equation 2-17 leads to an expression for  $\chi$ --or  $\kappa$ , the absorption coefficient (Equation 2-16)--satisfactory for use along an entire ray path. Use of the complete expression, or of several reduced expressions, each restricted to its particular realm of validity, would be required.

It will be useful--or, at least, informative--to examine a few of the possible reduced expression for  $\kappa$  (rather than  $\chi$ ). Before putting the expressions down, take a moment to note how  $\kappa$  (nepers/m) would be used to determine the total absorption,  $A$  (nepers), along a ray path. Since  $\kappa$  is the absorption coefficient measured in the direction of the wavefront normal ( $\alpha$  is the direction between the wavefront normal and the ray path),

$$A = \int_{\text{ray path}} \kappa \cos \alpha \, ds \quad (\text{nepers}) \quad 2-30$$

in which  $ds$  is an increment of ray path length.

Returning to expressions for  $\kappa$ , several examples are given in Table 2-1. In the table the symbols QL and QT stand, respectively, for

"quasi-longitudinal" and "quasi-transverse." \* Of the seven formulas given, only the first has general applicability along a ray path, and that only for the no-magnetic-field condition. The remaining six are divided into two classes called "non-deviative" and "deviative." Similarities within a class are notable.

The distinction between the non-deviative and deviative classes is easily illustrated with Formula 1 of Table 2-1. The value of  $\kappa$  can be large either because the product  $N\nu$  is large or because the factor  $\mu$  is small, or both (assume for the moment that  $\omega^2 \gg \nu^2$ , which is true for  $\omega$  in the HF range). The value of  $\nu$  is greatest near the lowest levels of the ionosphere. The value of  $N$  in this region tends to be low, but the value of the product  $N\nu$  tends to have its maximum value at a height of 100 km or less. \*\* The value of  $\mu$  depends on  $N$  and is small only when  $N$  is large ( $X \approx 1$ ). This condition occurs, generally, higher in the ionosphere. \*\*\* Thus, the conditions  $N\nu$  large and  $\mu$  small tend to occur in different regions of the ionosphere. Near the bottom of the ionosphere, where  $N\nu$  maximizes,  $N$  tends to be small and  $\mu$  near unity. Thus, little ray bending occurs in this region. Hence, absorption occurring because of a large value of  $N\nu$  is called "non-deviative." When  $\mu$  is low,  $N$  is likely to be a rapid function of distance along the trajectory. Hence, absorption occurring because  $\mu$  is small is called "deviative." Evidently, even deviative absorption does not occur if  $\nu = 0$ . It also is evident that the distinction between the two classes is not sharp. It is more a matter of circumstance than of principle.

---

\*The terms "quasi-longitudinal" and "quasi-transverse" refer to the direction of the wavefront normal (measured by the angle  $\theta$ ) relative to the direction of the steady magnetic field. They connote that propagation or absorption properties are "similar to" those which obtain when the wavefront normal (not the ray direction) is longitudinal or transverse with respect to the magnetic field direction. The implication is that the actual cases might be approximated by the appropriate extreme (longitudinal or transverse) case. The boundary separating QL and QT domains is given by a double inequality ( $\gtrless$ ) statement [3]. It is important to be aware of the fact that the values of variables other than  $\theta$  (e.g.,  $X$ ) influence the location of the boundary between the domains. It is not strictly sufficient that the wavefront normal be "nearly longitudinal" or "nearly transverse." For example, in the neighborhood of  $X = 1$ , all cases converge on the transverse case and there is, really, no applicability of the QL approximation. It also is not necessarily true that the QL and QT approximations are good over the entire domains defined by the inequality. There is a region astride the boundary within which neither is good. This is not really surprising since the approximations are derived from extreme cases.

\*\*The D and low E regions of the ionosphere.

\*\*\*The F and higher E regions of the ionosphere.

Table 2-1. Absorption coefficient formulas.

Conditions	Expression (Formula)	Restrictions	Class
No Magnetic Field			
1.	$\kappa = \frac{e^2}{2\epsilon_0 mc\mu} * \frac{N\nu}{\omega^2 + \nu^2}$		General
2. $\mu^2 \approx 1$	$\kappa = \frac{e^2}{2\epsilon_0 mc} * \frac{N\nu}{\omega^2 + \nu^2}$		Non-Deviative
3. $1 - \mu^2 \gg \chi^2$	$\kappa = \frac{\nu}{2c} (\frac{1}{\mu} - \mu)$		Deviative
With Magnetic Field			
4. QL*	$\kappa = \frac{e^2}{2\epsilon_0 mc\mu} * \frac{N\nu}{(\omega \pm  \omega_L )^2 + \nu^2}$	If +, $X < 1$ If -, $X \neq \pm Y$	Non-Deviative
5. QL*	$\kappa = \frac{\nu\omega}{2c(\omega \pm  \omega_L )} * (\frac{1}{\mu} - \mu)$	$X \approx 1 \pm Y$ x, z wave	Deviative
6. QT*	$\kappa = \frac{e^2}{2\epsilon_0 mc\mu} * \frac{N\nu \sin 2\theta}{\omega^2 + \nu^2}$	$X < 1$ o wave	Non-Deviative
7. QT*	$\kappa = \frac{\nu c \sin 2\theta}{2c} (\frac{1}{\mu} - \mu)$	$X \approx 1$ , $X \neq 1$ o wave	Deviative

\*QL = Quasi-Longitudinal, QT = Quasi-Transverse

Under the QL condition, the gyro radian frequency appears in the formulas. The + and - signs denote, respectively, the ordinary and extraordinary rays. Under this condition, the absorption coefficient for the extraordinary ray is greater than that for the ordinary ray. Since the gyrofrequency is near the lower limit of the HF range, its influence is significant in the lowest part of the range.

For wave frequencies well above the gyrofrequency and collision frequency, non-deviative absorption is inversely proportional to the square of the wave frequency. Deviative absorption is independent of wave frequency.

Because  $\kappa$  gives absorption per unit distance, total absorption along a trajectory (Equation 2-30) depends on the distance the ray travels in each of the absorptive regions. Thus, a ray path leaving (or returning to) the earth at a small angle of elevation ( $\beta$ ) would travel a large distance in the D region of the ionosphere and, thus, be subject to a maximum of non-deviative absorption. Because of the large angle of incidence on the ionosphere, ray reflection could occur at a value of  $\mu$  well above zero (the Bouguer formula, Equation 2-29). Thus, the ray might suffer little deviative absorption. For a steeper ray path, the circumstances could well be reversed.

We have not yet arrived at a satisfactory basis for constructing a model for  $\chi$  or  $\kappa$ . And, indeed, we shall not. Primarily for lack of knowledge about the morphology of electron collision frequency ( $\nu$ ) it will be necessary to fall back on empirical measurements of total path absorption. To such measurements a mathematical model can be fitted which will, thereafter, represent them. Such a model will be introduced in the discussion of absorption loss under the topic of path loss (2.3.5). In that expression, of the geophysical variables, only the gyrofrequency remains explicitly visible.

### 2.2.3 Sources of Data for Profile Modeling

In the subsection preceding this (2.2.2), it was shown how the problem of constructing a model of the index of refraction of the ionosphere, under certain constraints, can be reduced to that of specifying the spatial and temporal occurrence of electron number density,  $N$ , in the ionosphere. Under the radial variation constraint, spatial variation was limited to the radial coordinate, i. e., to height above the surface of the earth. The model resulting was called an "electron density profile." Such profiles are commonly referred to as  $N(h)$  curves ("N of h curves"). Note that no constraints or conditions have yet been placed on the temporal variation of  $N(h)$ . In this subsection sources of data for construction of a set of electron density profiles will be discussed.

It is well to retain in the conscious reaches of one's mind the fact that the ionosphere is, above all, a portion of the earth's atmosphere. It is a dynamic compressible fluid medium. It is subject to all of the physical influences which affect the unionized atmosphere. That is to say, it exhibits "climate" and "weather" phenomena. In addition, the ionosphere in motion is influenced by the geomagnetic field through dynamo and motor principles.

The production of ionization is a consequence of incidence on the earth's atmosphere of solar radiation, both electromagnetic radiation at short optical and ultra violet wavelengths arising from steady processes on the sun and irregular electromagnetic and particle radiation arising from traumatic events on the sun. The loss of ionization is governed by complex photochemical processes in the atmosphere. For a very lucid and highly instructive accounting of these phenomena, a small paperback book by one of the masters of the field, J. A. Ratcliffe, is recommended [6].

To simply represent fully the spatial and temporal occurrence of N, with no reference to causative agents, a variable system would be required having, at least, the structural complexity given in the following chart.

<u>Class: Subclass</u>	<u>Variable or Phenomenon</u>
Spatial	Height or altitude
	Latitude
	Longitude
Temporal: Cyclic or Quasi-cyclic	Diurnal phase (hour)
	Seasonal phase (month)
	Solar cycle phase ( $\approx$ 11 years)
Temporal: Irregular	Subsolar cycle dependence
	Sudden Ionospheric Disturbance (SID)
	Ionospheric Storm
	Traveling Ionospheric Disturbance (TID)

Spatial and temporal variations are not really independent. Many of the features of the N distribution are wave-like in character. There is, therefore, a degree of interchangeability between space and time.

If it is to be useful for estimation of signal delivery capability, an electron density model (or profile in the simple case) must have both spatial and temporal concurrence with the operational action contemplated. The problem is where to get data satisfying these conditions.

Three methodologies present themselves as candidates for sources of basic data from which to construct models of the spatial and temporal occurrence of N. They are:

1. Analysis based on theoretical principles.
2. Empirical determination concurrent in place and time with use.
3. Extrapolation (forecasting) based on a record of past empirical determinations.

None of these candidates offers full satisfaction of the requirement. However, each has something to contribute. The three will be discussed in turn.

It is not yet possible, even for a simple profile at a stated time, to set down a theoretical model representation strictly in terms of physical processes. We still are dependent on empirical data both for functional form of the model and for values of model parameters. This is especially true of the F region of the ionosphere. There are, however, two well-known model representations of ionospheric "layers" based on single simple physical process concepts. They are the Chapman functions,  $\alpha$ -Chapman and  $\beta$ -Chapman [1, 2, 4]. The functions are statements of the equilibrium condition between an electron production process and an electron loss process. The  $\alpha$ -Chapman function assumes a recombination loss process; the  $\beta$ -Chapman function assumes an attachment loss process. The parameters  $\alpha$  and  $\beta$  which characterize these functions are called, respectively, "recombination" and "attachment" coefficients.\* Theory does not yet yield adequate evaluations of these coefficients. Nor are real ionospheric processes as simple, even in a single layer or region, as those which are the basis of these models. Neither diffusion nor mass transport processes enter these models.

Neither function alone is suitable for representation of an entire ionosphere profile. However, the  $\alpha$ -Chapman function, especially, is useful as a component to supply functional form for the construction of composite models. We shall so use it, in association with empirically determined parameter values, in subsection 2.2.4.

For concurrent empirical determination of electron density profiles, three principal techniques are available. One is a direct method and two are indirect methods.

---

\*Both functions also involve a "production" coefficient,  $q$ , the same for both.



The direct method makes use of a rocket-borne Langmuir probe, data from which are telemetered back to a ground terminal. Generally, records are obtainable on both upgoing and downcoming portions of the trajectory (though these may not coincide). For reasons of practicability the method is limited to heights less than about 150 km. It also is expensive for regular or frequent use. It requires special facilities for rocket launch and provisions for safe rocket impact on return. The method has been useful for exploring the D and lower E regions of the ionosphere where the indirect methods do not perform well. It has produced interesting information about structural features which may be involved in "sporadic E" transmission. Other rocket-based techniques also have been used for more specialized purposes [4, 7, 8].

The two indirect methods both make use of radio techniques. Both depend on the return of radio signal energy from the electron gas structure in a radar-like mode. However, the two energy return mechanisms differ greatly.

One indirect method--the Thompson scatter, or incoherent scatter, method--operates at a frequency high enough for the wave to penetrate the ionosphere completely. The frequency, typically, would be in the VHF or UHF range. Energy in a high-power narrow beam, illuminating the ionosphere along a vertical boresight axis, is incoherently scattered by each of the very many individual electrons. The level of the scattered power received on the ground in a given range increment is proportional to the electron density in the corresponding height increment. The method is primarily applicable to regions having rather large values of electron density. Because most of the incident wave energy penetrates the ionosphere completely, the method is capable of acquiring electron density data from regions above the height at which the density is maximum. Thus it does not suffer from the "valley" problem inherent in the next method to be described. Principal disadvantages are inability to produce data when the electron density is low and the requirement for a large antenna structure and a high level of radiated power.

In contrast to the incoherent scatter method, the second indirect method makes use of frequencies below that at which the wave penetrates the entire ionosphere. Typically, this means frequencies from around 10 MHz down to some lower limit, ordinarily about 1 or 2 MHz. Return of wave energy is a consequence of "reflection" at a height where  $\mu$  is nearly zero ( $\mu = 0$  at reflection only if  $Z = 0$ ). A radar technique is used to measure the "effective range" of the ionosphere as a function of frequency. The process is called "ionosphere sounding," the device is called an "ionosonde," and the record which it produces is called an "ionogram." The ionogram is a graph of round-trip signal transit time, interpreted as an effective, or

"virtual," height, plotted as a function of sounding frequency. \* Since it is common to use the symbol  $h'$  (though we have used  $h_v$ ) for virtual height and  $f$  for frequency, the functional relationship which is graphed is  $h'(f)$ . The graphs (ionograms) are commonly called "h-prime (of) f curves." \*\*

As long as the electron density increases monotonically with height, the real height of reflection (but not necessarily the virtual height) will increase continuously with frequency. If the profile is not monotonic, but has a local maximum, the condition for reflection will not again be satisfied above the height of maximum unless at greater height the electron density again rises above its value at the maximum. As a consequence, the real height of reflection will jump discontinuously if a local (or global) maximum is encountered in the profile function.

Thus, it is characteristic of the method that any region having an electron density less than that in some lower region is obscured from view. As a result, returns cannot be obtained from regions above the major (global) maximum of electron density or from regions which represent a "valley" in the electron density profile. The first is no disadvantage (jamming and communication signals would not be returned to earth from that region anyway); the second may be because a relevant portion of the profile is passed over, not being sampled continuously in height.

The last described method does not give the electron density profile immediately. The signal is reflected at a "real height" where the value of  $\mu$  is, essentially, zero. The height measured, the virtual height, differs from the real height because the signal group velocity becomes low as the reflection height is approached. The height difference can be large, especially if the wave passes slowly through a region of small gradient of electron density just below the reflection level. To get the electron density profile, the virtual height curve must first be converted to a real height curve\*\*\* [1, 2, 4]. Then,

---

\*Examples of calculated ionograms will be given at a later stage in the discussion.

\*\*In British practice  $p$  (for "path") is generally used instead of  $h$  and the graph representing  $p'(f)$  becomes a "p-dash (of) f curve."

\*\*\*It is at this point that the "valley problem" arises. In the region where a valley exists, the real height of reflection is indeterminate. Because the valley region is not continuously scanned or sampled by the reflected wave, information about profile details in this region is lost; only an aggregate effect of the region is retained. The virtual height to real height conversion cannot be made in the valley and will be in error at heights greater than the upper edge of the valley. Ordinarily this is not a catastrophic failure (except for researchers who want to know what valley contours look like). The error frequently is small (because valley depth is shallow) and it generally diminishes rapidly with further increases in height.

using the reflection condition and Equations 2-26 and 2-20, the frequency scale of the ionogram can be converted to an electron density scale.

Because the "reflection" process is coherent and, indeed, quasi-specular the level of power required for this method is low--of the order of a few tens of watts average. It is feasible to use the method for empirical determination of ionospheric data concurrent with use. Evidently, it can only produce a profile over the position where the sounding equipment is located.

It is by the ionosonde method that the preponderance of information about the spatial and temporal morphology of the ionosphere has been obtained.

Basic data for model construction can be extrapolated from historical records of empirically determined information. This is possible because behavior patterns having a degree of regularity are discernible in the historical record sequence.

During the decades of the 1950s and 1960s, much effort was expended in collecting data about the ionosphere. Some of this data has been used to construct models which give synoptic representations of certain ionospheric parameters. A description of one such model is obtainable from the C. C. I. R.,\* an agency of the International Telecommunications Union [9]. Additional or later information may be available from contributing agencies. Representations of this sort, based on data acquired in historical sequence at a limited set of locations, provide a means for extrapolation in time and interpolation in location.

The C. C. I. R. model does not represent electron density profiles per se. From the ionospheric parameters which it does represent, profiles of limited form can be constructed. Since the model represents monthly median values of the parameter observations on which it is based, profiles constructed from it also will reflect that property. Access to major computing capability is required to exploit this model to best advantage. Data from this source and others have been used to determine parameter values for construction of a set of electron density profiles [4, 6, 7, 8, 9, 10].

#### 2.2.4 Electron Density Profile Models

The topic of this subsection is construction of a set of electron density profile models. Referring to them as "a set" implies some organizational

---

\*Initials for the French language version of International Radio Consultative Committee.

relationship among them. In this instance the organizing principle is sampling the range of regular temporal variation. It is intended that each member of the set be realistic, if not real. It further is intended that each member be "representative"\* of the temporal context from which it is drawn. The spatial context from which the set as a whole is drawn is the region of moderate geomagnetic latitude.

The intent is to show a method by which profile models can be constructed and to assemble a set with which to illustrate the principal phenomena related to sky wave mode of signal delivery. The set is not intended to be a comprehensive catalog of all significant cases, nor are the members intended to be relatable to specific time and place.

The  $\alpha$ -Chapman function\*\* has been selected as the basic building block for model construction. It is flexible, reasonably simple, and does have some relationship to physical process. It can provide a good representation of E and F1 region structures. It is less well suited to representation of the F2 region in which the physical processes are less  $\alpha$ -Chapman like, but it suffices.

Alternative choices for building block functions are available. One is the parabolic, or quasi-parabolic, layer. These nonphysical functions have the advantage that, properly formulated, analytic solutions for trajectory parameters are possible. This property obviates the necessity for using incremental ray tracing procedures. However, this advantage seems realizable only if the layers are kept discrete, i. e., nonoverlapping. The result is a somewhat unrealistic electron density profile. Nevertheless, parabolic and quasi-parabolic layer form functions have found application in some communication forecasting procedures [11].

---

\*Use of the adjective "typical" in this context has deliberately been avoided. A "typical" member of a class is one to which other members bear some evident similarity. When the details of class members vary widely, it may be hard to find one which can be called "typical." On the other hand, if pertinent characteristics of class members are each averaged over the class, a "representative" member description can be synthesized. The problem is a little like that of trying to specify the temperature of a man with his feet in a refrigerator and his head in an oven. It is hard to assign to him a "typical" temperature. He appears, at once, both to be hot headed and to have cold feet. Yet, an "average" temperature is definable which, in a limited sense, is representative of his condition.

\*\*Described in subsection 2. 2. 3.

The  $\alpha$ -Chapman function is given by the following expression, \*[ 1 ]

$$N(h) = N_0 \exp \left\{ \left( \frac{1}{2} \right) [ 1 - z - (\sec \chi) \exp (-z) ] \right\} \quad 2-31$$

in which

$$N_0 = (q_0/\alpha)^{1/2}, \quad z = (h - h_0)/H$$

When the function is expressed in this form the roles of several physical parameters are made evident. The parameters appearing are the electron production rate coefficient,  $q_0$ , the electron recombination coefficient,  $\alpha$ , the solar zenith angle,  $\chi$ , and the layer scale height (a measure of layer thickness),  $H$ . It is convenient to absorb  $q_0$  and  $\alpha$  into  $N_0$  because both of the former are difficult to evaluate, either theoretically or empirically, whereas  $N_0$  is subject to straightforward evaluation by empirical means.

When  $\chi = 0$ , the  $\alpha$ -Chapman function,  $N(h)$ , has a maximum at  $z = 0$  (i. e., at  $h = h_0$ ). The value,  $N(h_0)$ , at the maximum is  $N_0$ . Making use of Equation 2-20, Equation 2-26 and the concept that reflection of the wave occurs at a level where  $\mu = 0$ , the value of  $N_0$  can be related to a critical frequency,  $f_0$ , for which  $\mu = 0$  at  $h = h_0$ .

$$N_0 = f_0^2 \frac{4\pi^2 \epsilon_0 m}{e^2} \quad 2-32a$$

If  $f_0$  is in Hz and  $N_0$  is in electrons per cubic meter, then

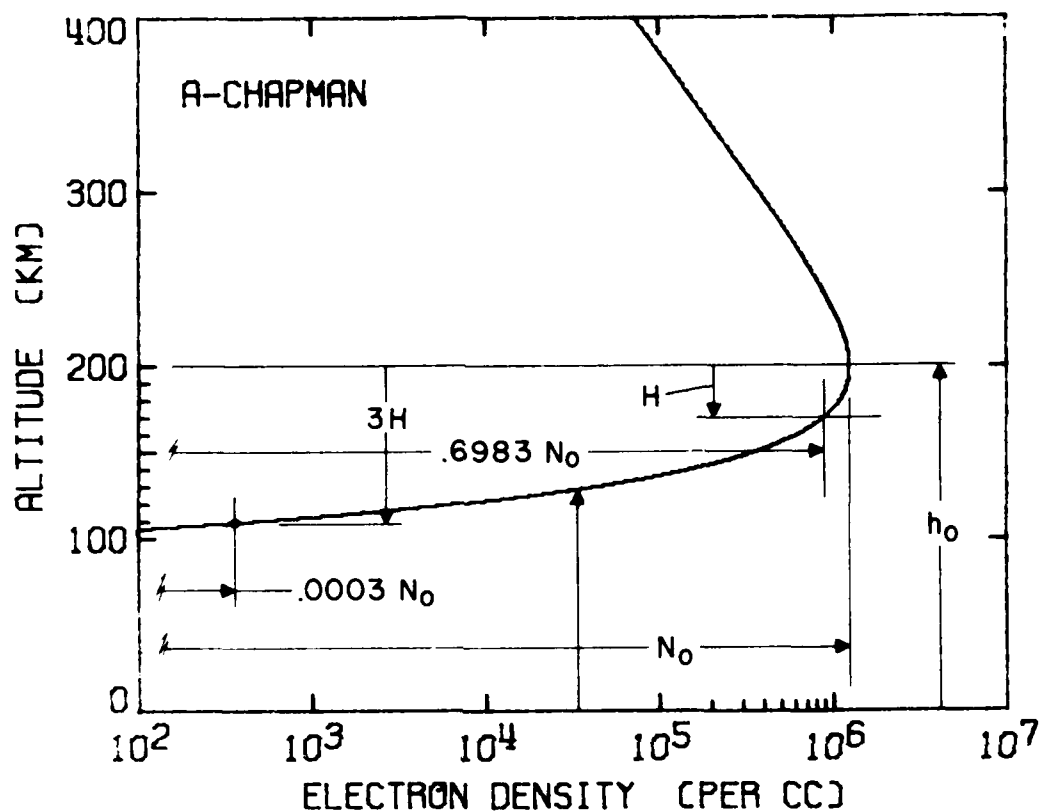
$$N_0 = f_0^2 / 80.6 \quad 2-32b$$

When the wave frequency equals the critical frequency, wave reflection occurs at  $h = h_0$ . At any higher frequency, the wave would penetrate past the layer maximum. An example of the  $\alpha$ -Chapman function is shown in Figure 2-3 for the case  $\chi = 0$ . \*\* The values of the parameters used are given given below the graph, and their meanings are noted on the graph.

By making two simple substitutions into Equation 2-31, it can be recast in a form which brings out some interesting properties of the function. If we set

Here  $\chi$  is the solar zenith angle, not the index of absorption.

It may seem strange to plot the independent variable,  $n$ , on the ordinate and the dependent variable,  $N(h)$ , on the abscissa. However, this is customary for the sake of the psychological value of having height on a "vertical" axis. It also is in accord with use of the ordinate for height in ionograms.



SOLAR ZENITH ANGLE -  $x$ :

0 deg

CRITICAL (PENETRATION) FREQUENCY -  $f_0$ : 10.0 MHz

$N_0 = f_0^2 / 80.6$  ( $f_0$  in Hz,  $N_0$  in  $m^{-3}$ )

VALUE OF MAXIMUM DENSITY -  $N_0$ :

$[1.24 \times 10^{12} / m^3$   
 $1.24 \times 10^6 / cm^3]$

HEIGHT OF MAXIMUM DENSITY -  $h_0$ :

200 km

SCALE HEIGHT OF LAYER -  $H$ :

30 km

Figure 2-3. Alpha-Chapman layer parameters.

$$N_0 = N_m (\sec \chi)^{1/2}, \quad z = x + \ln \sec \chi \quad 2-33a$$

then,

$$h_m = h_0 + H \ln \sec \chi, \quad x = (h - h_m)/H \quad 2-33b$$

and,

$$N(h) = N_m \exp \left\{ (1/2) [1 - x - \exp(-x)] \right\} \quad 2-34$$

Like Equation 2-31 when  $\chi = 0$  and  $z = 0$ , Equation 2-34 has a maximum for  $x = 0$  (i. e., for  $h = h_m$ ). The value,  $N(h_m)$ , at the maximum is  $N_m$ . Note that the shape of the exponential term in Equation 2-34 does not depend on  $\chi$  (as it does in Equation 2-31). Thus, changing the value of  $\chi$  moves the height of maximum from  $h_0$  at  $\chi = 0$  to  $h_m = h_0 + H \ln \sec \chi$  at nonzero values of  $\chi$ . The value of  $N_m$  changes from  $N_0$  at  $\chi = 0$  to  $N_0 (\cos \chi)^{1/2}$  for nonzero values of  $\chi$ . Changing  $\chi$  simply shifts the curve in  $h$  and scales the value of  $N(h_m)$ .

For purposes of model construction,  $\chi$  has been set to zero and layer configuration controlled by setting  $h_0$ ,  $N_0$  and  $H$ . This is a more tractable procedure than trying to retain  $\chi$  variation. Real ionospheric layers do not vary with solar zenith angle quite in the manner of the  $\alpha$ -Chapman function, especially in the F2 region and during the dark hours.

The construction of a composite profile model is illustrated in Figure 2-4. At the top of Figure 2-4a (left page) two  $\alpha$ -Chapman functions are shown, one at Level 1 representing an E region and another at Level 3 representing an F region. The Level 1 parameter values are:  $h_0 = 110$  km,  $H = 10$  km and  $f_0 = 2.4$  MHz. The Level 3 parameter values are:  $h_0 = 210$  km,  $H = 40$  km and  $f_0 = 5.4$  MHz. When these two functions are summed, the composite profile model at the bottom of Figure 2-4a is obtained. The profile represents ionization in the E region and in the undivided F region.

Given the expression for a profile such as that in Figure 2-4a, it is possible to compute the corresponding virtual height/frequency curve, i. e., to produce a "synthetic ionogram"--one which is calculated rather than measured. The first step is to find the real height of reflection as a function of frequency,  $h_f(f)$ . In truth, since the function  $N(h)$  is known, it is more expeditious to find the inverse function,  $f(N(h_f))$ , using Equations 2-20 and 2-26, than it is to find  $h_f(f)$ . The function  $f(N(h_f))$  is the frequency which would be

\*Level 2 will be used in later illustrations.

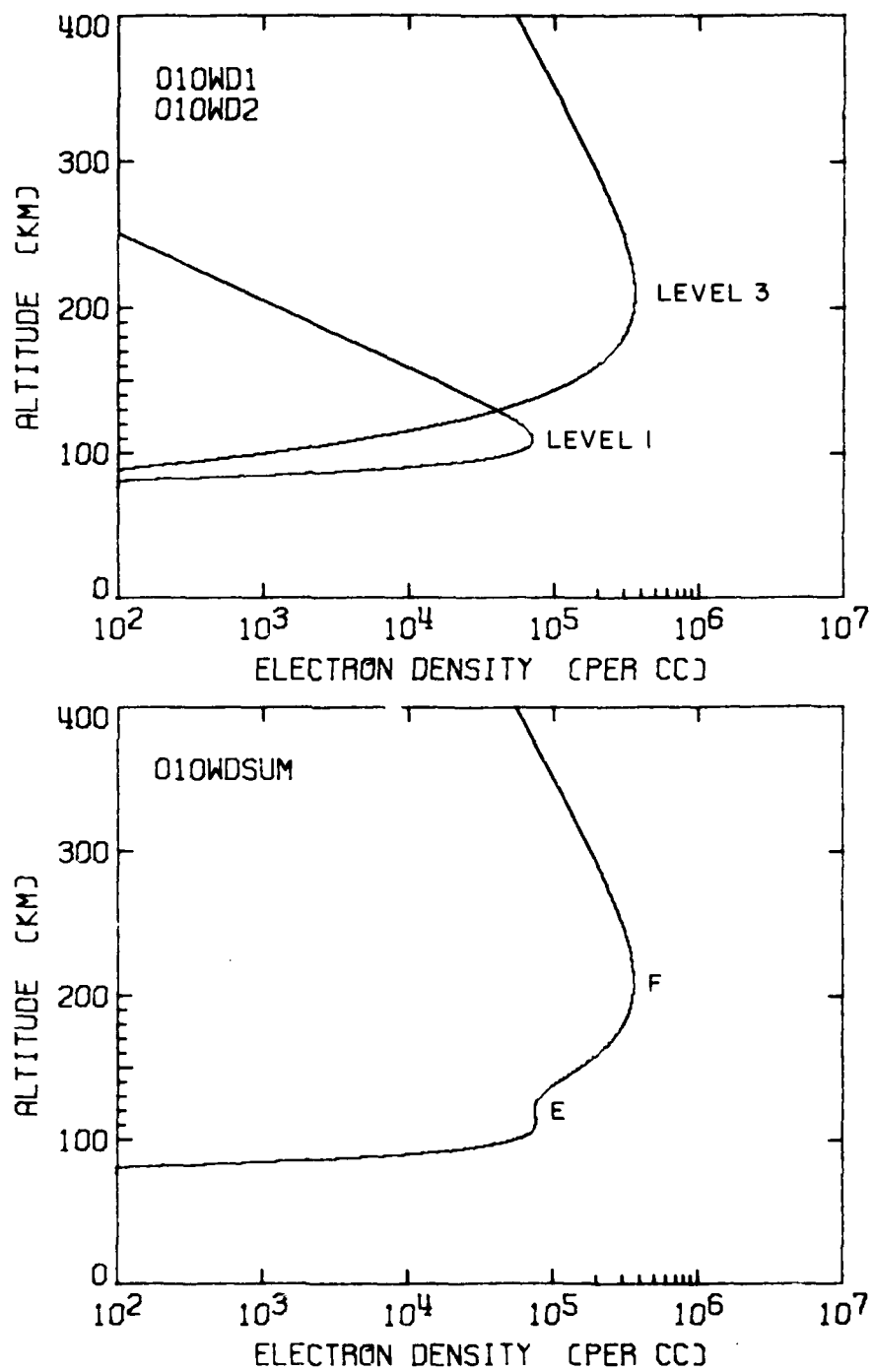


Figure 2-4a. Component layers and composite profile: 010WD/.



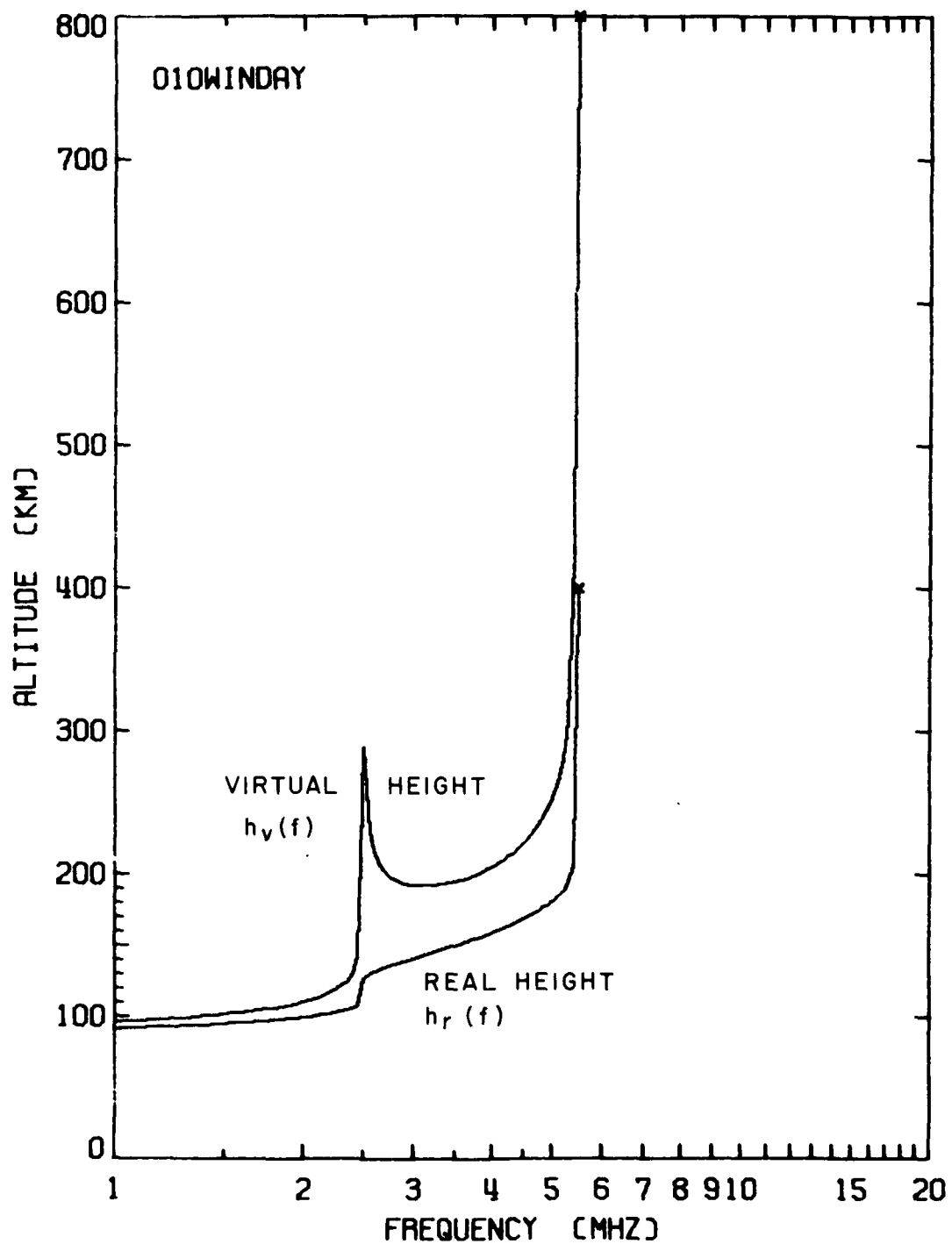


Figure 2-4b. Synthetic ionogram: 010WINDAY.

reflected at height  $h_r$  on account of the value  $N(h_r)$  of the electron density (compare Equations 2-32).

$$f(N(h_r)) = \left[ \frac{N(h_r) e^2}{4\pi^2 \epsilon_0 m} \right]^{1/2} = [80.6 N(h_r)]^{1/2} \quad 2-35$$

The real height curve corresponding to the profile model of Figure 2-4a is the lower curve in Figure 2-4b (right page). \* This curve, of course, would not appear on a real ionogram; it is not measurable.

The second step in production of a synthetic ionogram is to compute the virtual height,  $h_v$ , corresponding to the real height,  $h_r$ , at each synthetic sounding frequency. The virtual height is just the one-way group path for a vertical trajectory [1, 2, 4]. For the conditions  $Z = 0$  and  $Y = 0$ , the virtual height can be evaluated from the following expression.

$$h_v(f) = \int_0^{h_r} \frac{dh}{u(f, h)} \quad 2-36$$

This integral can be evaluated numerically, using Equations 2-26, 2-20, and 2-31 to evaluate  $u(f, h)$ . The virtual height curve--the  $h_v(f)$  curve--corresponding to the profile model of Figure 2-4a is the upper curve in Figure 2-4b. Note the significant difference in real and virtual heights, especially in the neighborhood of the frequency (2.5 MHz) at which the wave penetrates the E region and is reflected from the F region.

The level parameters chosen for the example in Figure 2-4 produce a profile representative of a winter day at a time of low sunspot number (010). Additional examples of the construction of composite profile models are shown in Figures 2-5, 2-6, and 2-7. Level parameter values for these figures (as well as for Figure 2-4) are given in Table 2-2.

Figure 2-5 differs from Figure 2-4 primarily by the addition of a third  $\alpha$ -Chapman function at an intermediate level (Level 2). The third function was added to represent an F1 region process which is a feature of summer profiles. The critical frequencies of the functions have been adjusted from the winter day values to represent summer day conditions. That of Level 1 has been raised slightly and that of Level 3 has been lowered slightly. The value of  $h_0$  for Level 3 has been raised somewhat. Note that the inflection in the profile between the F1 and F2 regions has caused a second cusp to appear in the synthetic ionogram (Figure 2-5b).

\*The "x" at the end of the curve signifies ray penetration of the model ionosphere.

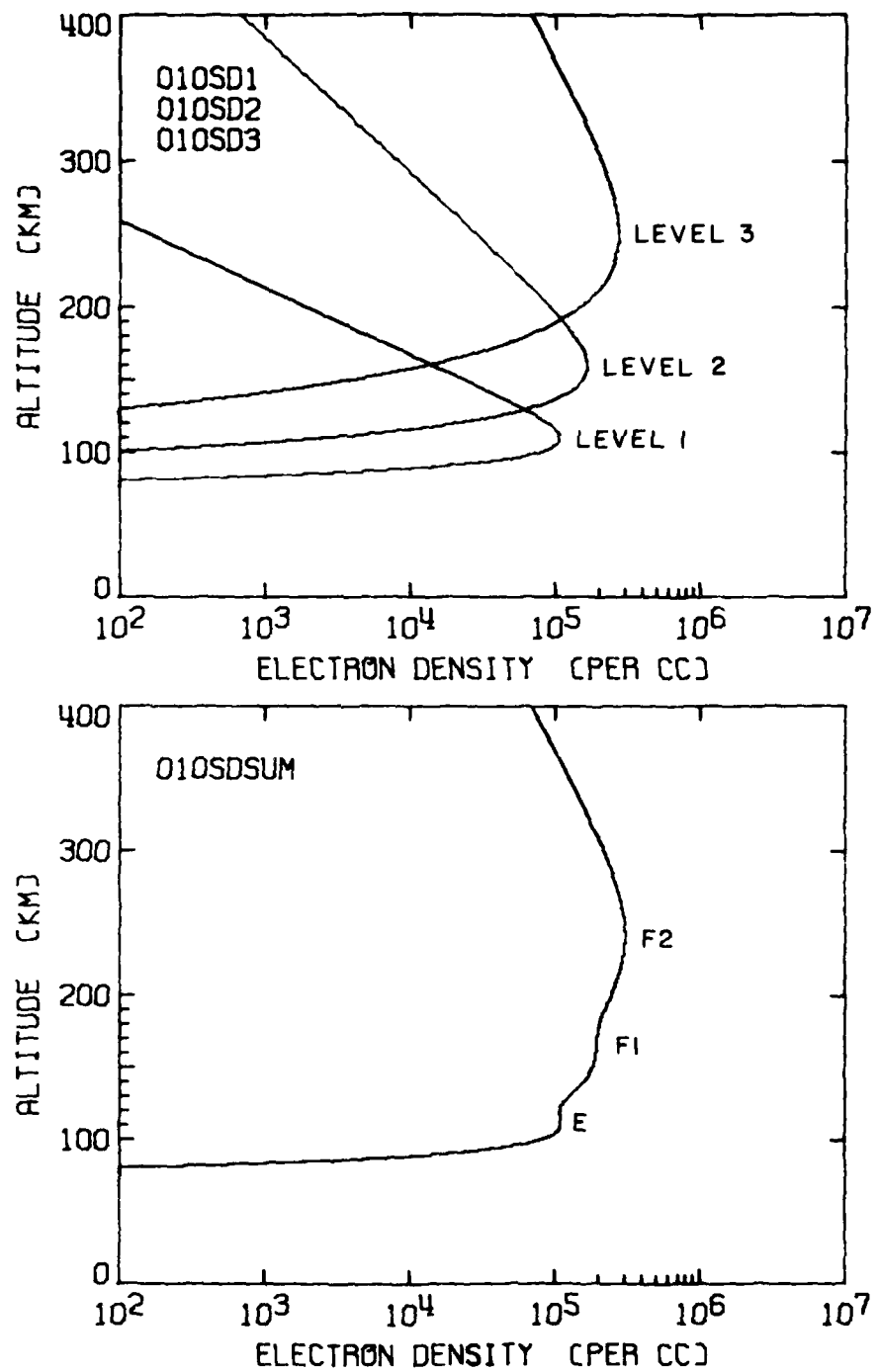


Figure 2-5a. Component layers and composite profile: 010SD/.

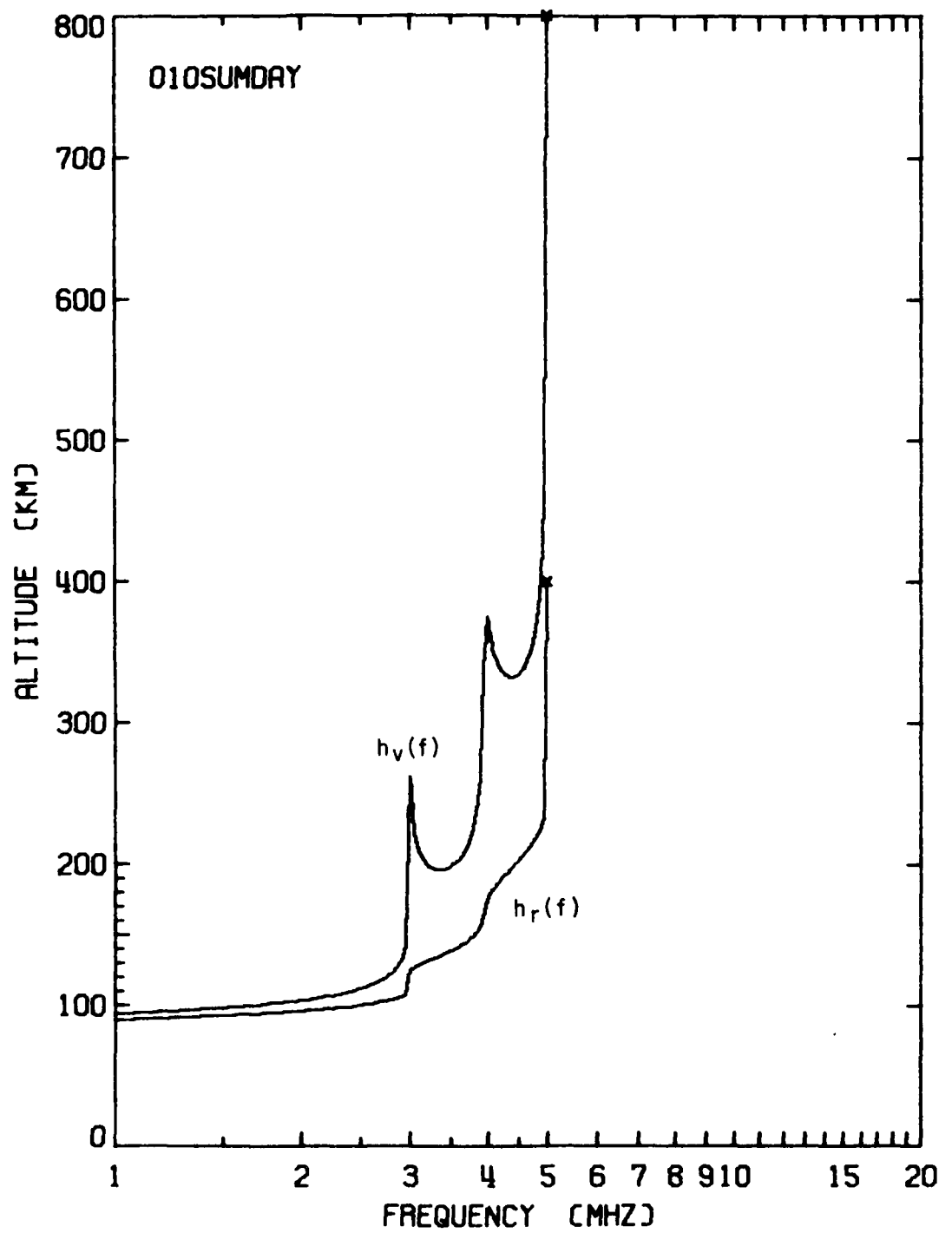


Figure 2-5b. Synthetic ionogram: 010SUMDAY.

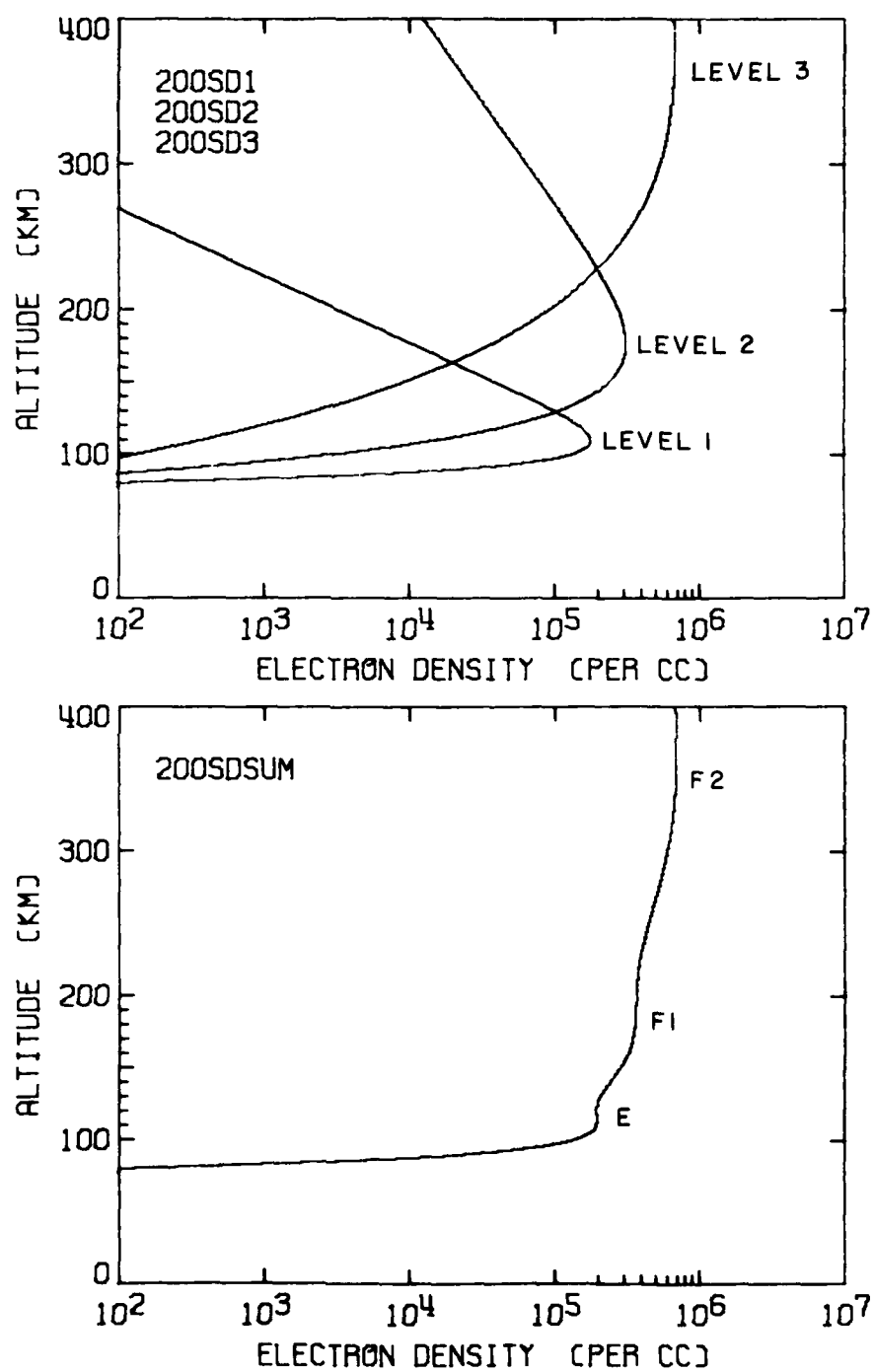


Figure 2-6a. Component layers and composite profile: 200SD/.

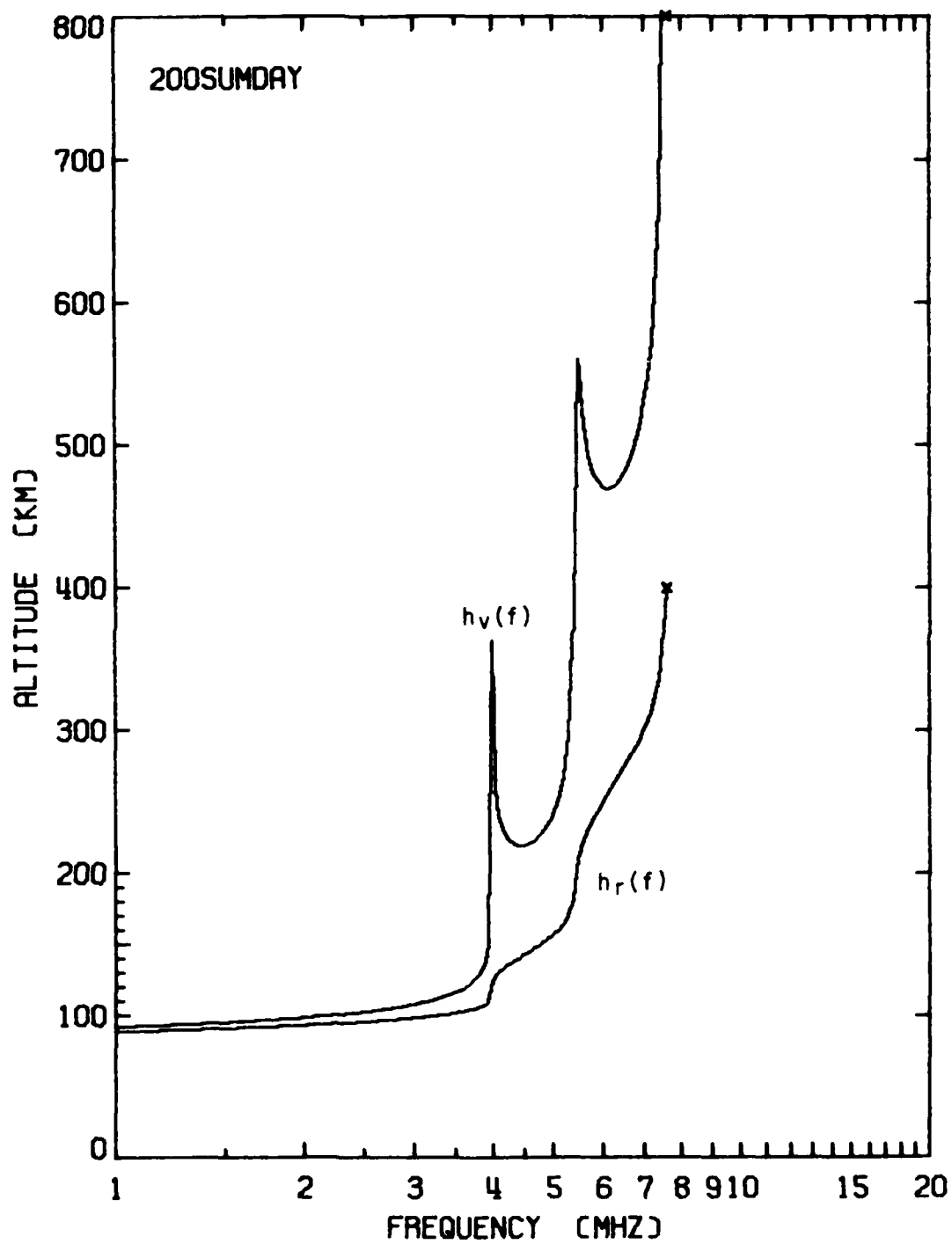


Figure 2-6b. Synthetic ionogram: 200SUMDAY.

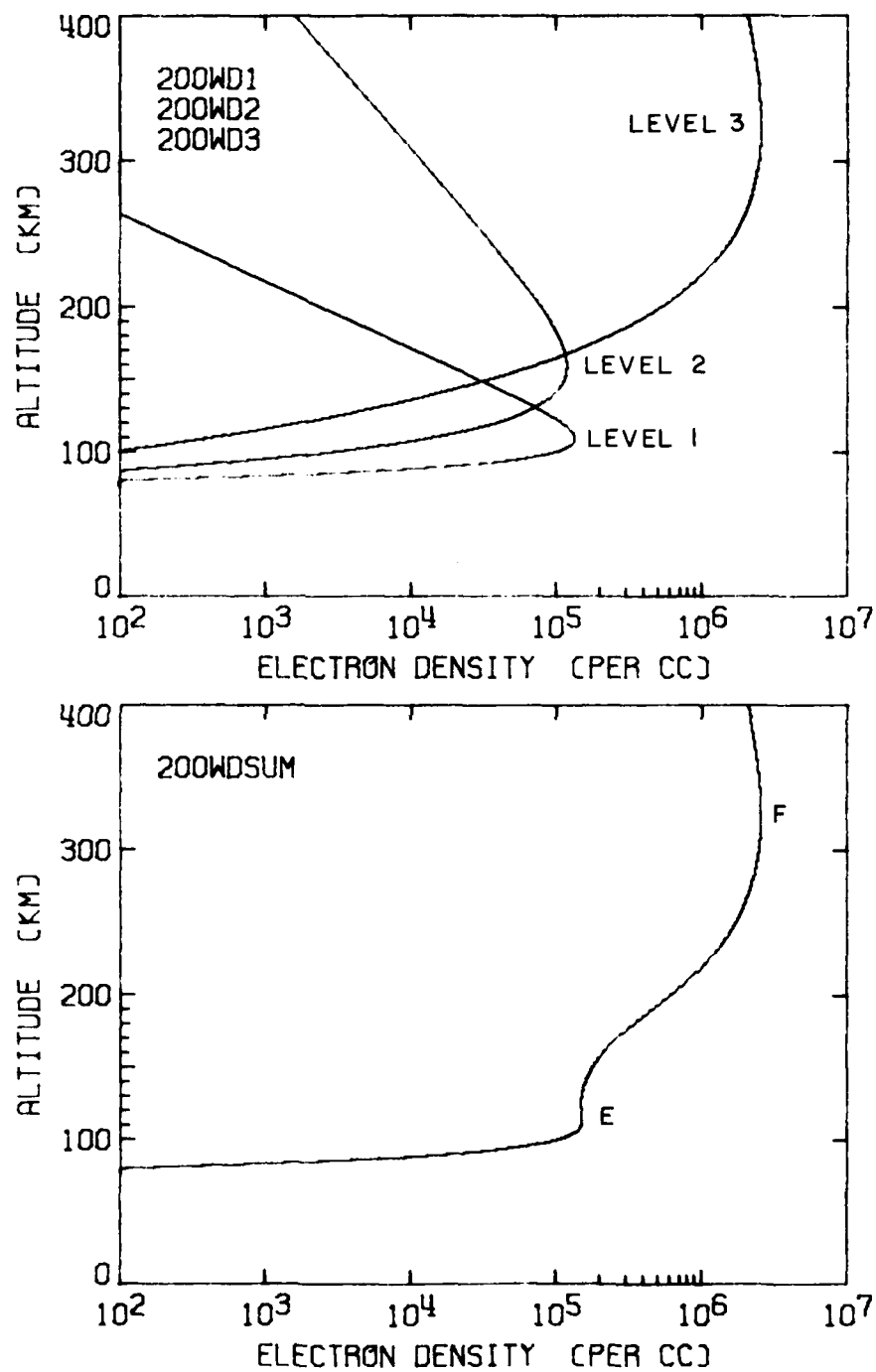


Figure 2-7a. Component layers and composite profile: 200WD/.

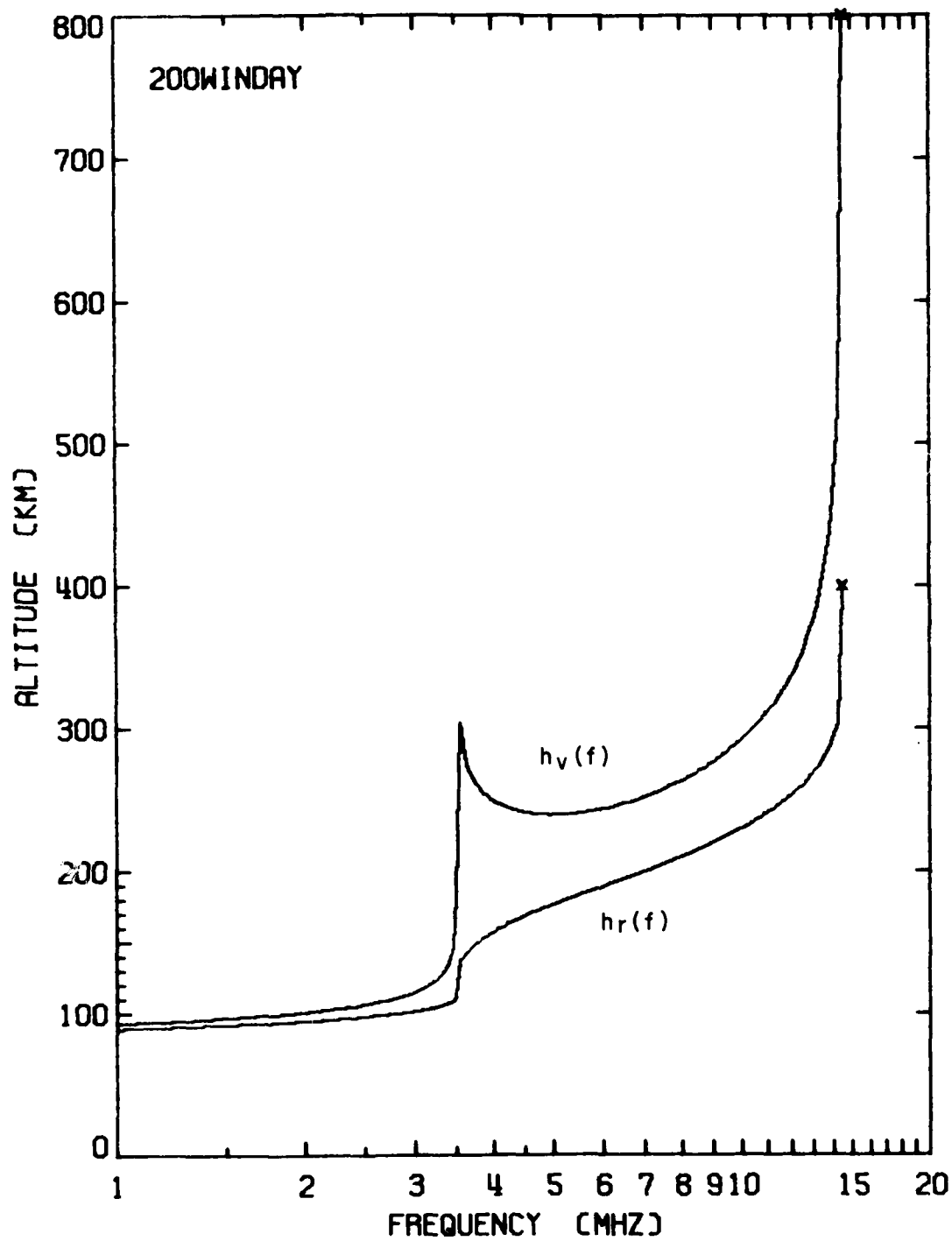


Figure 2-7b. Synthetic ionogram: 200WINDAY.



Table 2-2. Layer parameter values for profile model examples.

Figure 4                      Winter Day                      Low Sunspot Number (010)

Level 1:  $h_o = 110$  km,  $H = 10$  km,  $f_o = 2.4$  MHz  
 Level 2: Absent  
 Level 3:  $h_o = 210$  km,  $H = 40$  km,  $f_o = 5.4$  MHz

Figure 5                      Summer Day                      Low Sunspot Number (010)

Level 1:  $h_o = 110$  km,  $H = 10$  km,  $f_o = 2.95$  MHz  
 Level 2:  $h_o = 160$  km,  $H = 20$  km,  $f_o = 3.65$  MHz  
 Level 3:  $h_o = 250$  km,  $H = 40$  km,  $f_o = 4.70$  MHz

Figure 6                      Summer Day                      High Sunspot Number (200)

Level 1:  $h_o = 110$  km,  $H = 10$  km,  $f_o = 3.80$  MHz  
 Level 2:  $h_o = 177$  km,  $H = 30$  km,  $f_o = 5.00$  MHz  
 Level 3:  $h_o = 375$  km,  $H = 90$  km,  $f_o = 7.40$  MHz

Figure 7                      Winter Day                      High Sunspot Number (200)

Level 1:  $h_o = 110$  km,  $H = 10$  km,  $f_o = 3.30$  MHz  
 Level 2:  $h_o = 160$  km,  $H = 25$  km,  $f_o = 3.10$  MHz  
 Level 3:  $h_o = 325$  km,  $H = 70$  km,  $f_o = 14.40$  MHz

Figure 2-6, for a summer day at a time of high sunspot number (200), is similar to Figure 2-5 in character. However, the critical frequencies have been scaled up and the value of  $h_o$  for the F2 region has been raised.

Figure 2-7 illustrates a different application for a function at Level 2. It is used to nearly fill a potential deep valley, without producing an F1 region signature on the profile or in the synthetic ionogram. The F1 region signature is seldom a feature of winter profiles except at low values of sunspot number. An alternative method for filling the valley would be to increase the scale height (H) of the Level 3 function, omitting the Level 2 function. When this was attempted, it turned out that, by the time the Level 3 scale height was made large enough to control valley depth, the Level 3 function contributed too much to the electron density at heights on the low side of the Level 1 function. Note that the synthetic ionogram of Figure 2-7b shows no cusp corresponding to a transition from the Level 2 to the Level 3 function. That is because the profile of Figure 2-7a shows no maximum or inflection point related to the Level 2 function.

Using the principles just described, a set of twelve electron density profile models has been constructed. The models are presented in Section 2.4, in association with other types of diagram derived from them. Information has been drawn from a number of sources to guide selection of the functional forms and the parameter values used to construct the profile models [1, 4, 6, 7, 8, 9, 10].

## 2.3 PATH LOSS CONCEPTS

In Chapter 1.0, the concept of transmission loss was introduced in generalized form. At this point in Chapter 2.0 the necessary background has been established for application of wave propagation principles to the estimation of transmission loss in the sky wave case. The task of this section is to detail an estimation procedure.

### 2.3.1 Loss Mechanisms

In Chapter 1.0 the path loss,  $\Gamma_{ph}$ , was defined in terms of the transmission loss,  $\Gamma_{tn}$ , and the two antenna gains,  $G_t$  and  $G_r$ , through the following relation.

$$\Gamma_{tn} = \Gamma_{ph} / G_t G_r \quad 2-37$$

We shall assume for the moment that  $G_t$  and  $G_r$  are known and understood and shall concentrate on evaluating  $\Gamma_{ph}$ .

In the sky wave case, it is convenient to break  $\Gamma_{ph}$  down into four components, partly because differing mechanisms are at work and partly for convenience in calculation. Toward this end, the makeup of  $\Gamma_{ph}$  can be shown as the product of four factors.

$$\Gamma_{ph} = \Gamma_h * \Gamma_i * \Gamma_d * \Gamma_a \quad 2-38a$$

In decibel form,

$$\gamma_{ph} = \gamma_h + \gamma_i + \gamma_d + \gamma_a \quad 2-38b$$

The factor  $\Gamma_h$  signifies a quantity which we shall name "hearability." It is a discrete variable having only two values, unity and zero. It expresses the possibility--or the impossibility--that a ray trajectory can exist between the path terminal points. Evaluation of hearability will be discussed in subsection 2.3.2 under the heading Ray Path Properties. The initial loss,  $\Gamma_i$ , arises from the mechanics of radiating and receiving the wave. It is convenient to discuss it in conjunction with  $\Gamma_d$ . The divergence loss,  $\Gamma_d$ , is a consequence of the spreading of the wavefront as it recedes from the source. It is the subject of subsection 2.3.3. The final one of the four factors,  $\Gamma_a$ , accounts for power dissipated in the medium along the ray path which the wavefront traverses. It will be treated in subsection 2.3.5.

There is a theorem which it is convenient to introduce at this stage in the discussion. It is called the Secant Law and is a part of Martyn's equivalence theorem [1,2,4]. It can be stated as follows:

In a plane-stratified field-free collisionless ionosphere two rays, one incident normal to the stratification planes and the other incident obliquely to the stratification planes at an angle  $\phi$  to the normal, will have the same real level of reflection if the wave frequencies associated with the two rays satisfy the following relationship:

$$f_{\text{oblique}} = f_{\text{normal}} \sec \phi \quad 2-39$$

For a horizontally stratified structure, "normal" is "vertical."

One interpretation of equation 2-39 is that at a given real reflection height,  $h_r$ , for a value of electron density  $N(h_r)$ , oblique rays can have a higher frequency than can normal or vertical rays.

Another interpretation is obtained if the frequency associated with the vertical ray is a profile critical frequency,  $f_{o,\text{normal}}$ . Then the height of reflection,  $h_r$ , of the vertical ray will be  $h_o$  for the profile. For a given value of frequency associated with the oblique ray, a critical angle,  $\phi_o$ , is defined through Equation 2-39.

$$\sec \phi_o = \frac{f_{\text{oblique}}}{f_{o,\text{vertical}}} \quad 2-40$$

For a given frequency  $f_{\text{oblique}}$ , rays incident at angles greater than  $\phi_o$  will be reflected but rays incident at angles less than  $\phi_o$  will penetrate past the profile maximum at  $h_o$ . This critical angle phenomenon is a little like the critical angle for total internal reflection in optics. It is the basis for the so-called "iris effect." The critical angle,  $\phi_o$ , clearly depends on the value of electron density,  $N_o$ , at the height of maximum,  $h_o$ , and on the wave frequency,  $f_{\text{oblique}}$ .

The second part of Martyn's equivalence theorem states that:

Under the conditions for which the Secant Law is valid, the virtual (or apparent) height of reflection\* of an oblique ray is the same as the virtual height of reflection of the equivalent vertical ray. "Equivalence" means that both rays are reflected at the same real height.

\*See Figure 2-2 for the counterpart quantity in the spherically stratified geometry case.

In a spherically stratified profile model, the Secand Law as just stated does not hold precisely. Nevertheless, the concepts of real height equivalence between vertical and oblique rays and of a critical angle,  $\phi_0$ , are still valid. They are just harder to determine.

Since the second part of Martyn's theorem is based on the Secant Law, it too is not strictly valid in a spherically stratified medium. However, if the portion of a trajectory which is within the ionosphere does not subtend too great an angle at the center of the earth, so that the medium curvature which is spanned is not too great, then Martyn's theorem gives useful answers. If a plane stratified ionosphere, with its normal vertical at the center of a trajectory, is substituted for the spherically stratified ionosphere above a spherical earth surface, the combination may be called a "hybrid" model. Such a model permits simplified calculation of the portion of the trajectory internal to the ionosphere and avoids the errors engendered by assumption of a plane earth surface in calculation of the portion external to the ionosphere. Application of this hybrid ("H") model will be discussed in subsection 2.3.4.

#### 2.3.2 Ray Path Properties

Given an electron density profile model, the Bouguer formula (Equation 2-29) can be used to trace a ray through the medium specified by the model. The trajectory parameters (Figure 2-2) for the ray can, thereby, be determined. If the process is repeated for a number of rays launched at different values of elevation angle, an empirical functional relationship between ground range,  $D$ , and elevation angle,  $\beta$ , can be established. An example of such a relationship is given in Figure 2-8. To produce this figure, ray trajectories were calculated for 91 values of  $\beta$ , in one degree increments from  $\beta = 0^\circ$  to  $\beta = 90^\circ$ , using the profile structure given in Figure 2-4. It is convenient to call the graphical presentation of trajectory parameter data a "transmission diagram," in this case an angle/range transmission diagram.

In Figure 2-8 a ray launched at an elevation angle of  $30^\circ$  has been selected as an example. The diagram shows that this ray spans a ground range of about 320 km. Note that the angle/range curve is for the operating frequency of 2.0 MHz. From Figure 2-4b, it is evident that the operating frequency is lower than the E-region critical frequency, the first cusp on the virtual height curve of the synthetic

AD-A119 491

SOUTHWEST RESEARCH INST SAN ANTONIO TX

F/G 17/4

DELINEATION OF CONSTRAINTS IMPOSED BY PROPAGATION FACTORS AT HF--ETC(U)

APR 76 E C HAYDEN

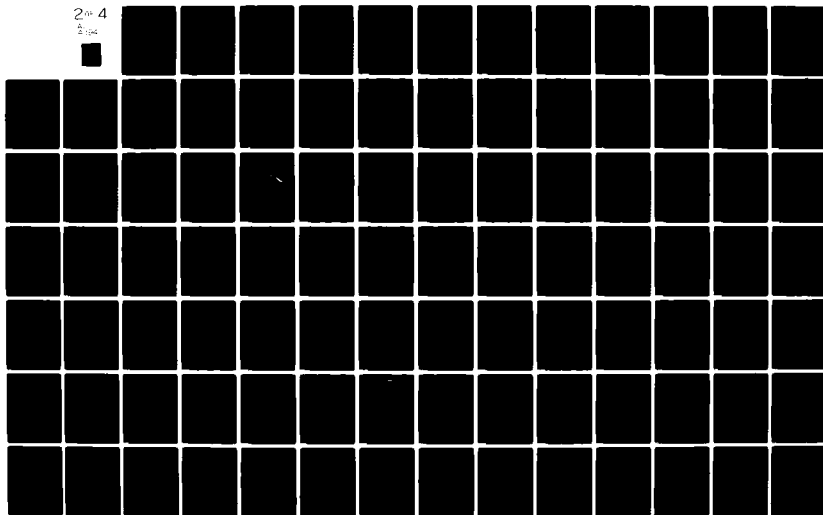
N00039-75-C-0481

NL

UNCLASSIFIED

2 of 4

8-104



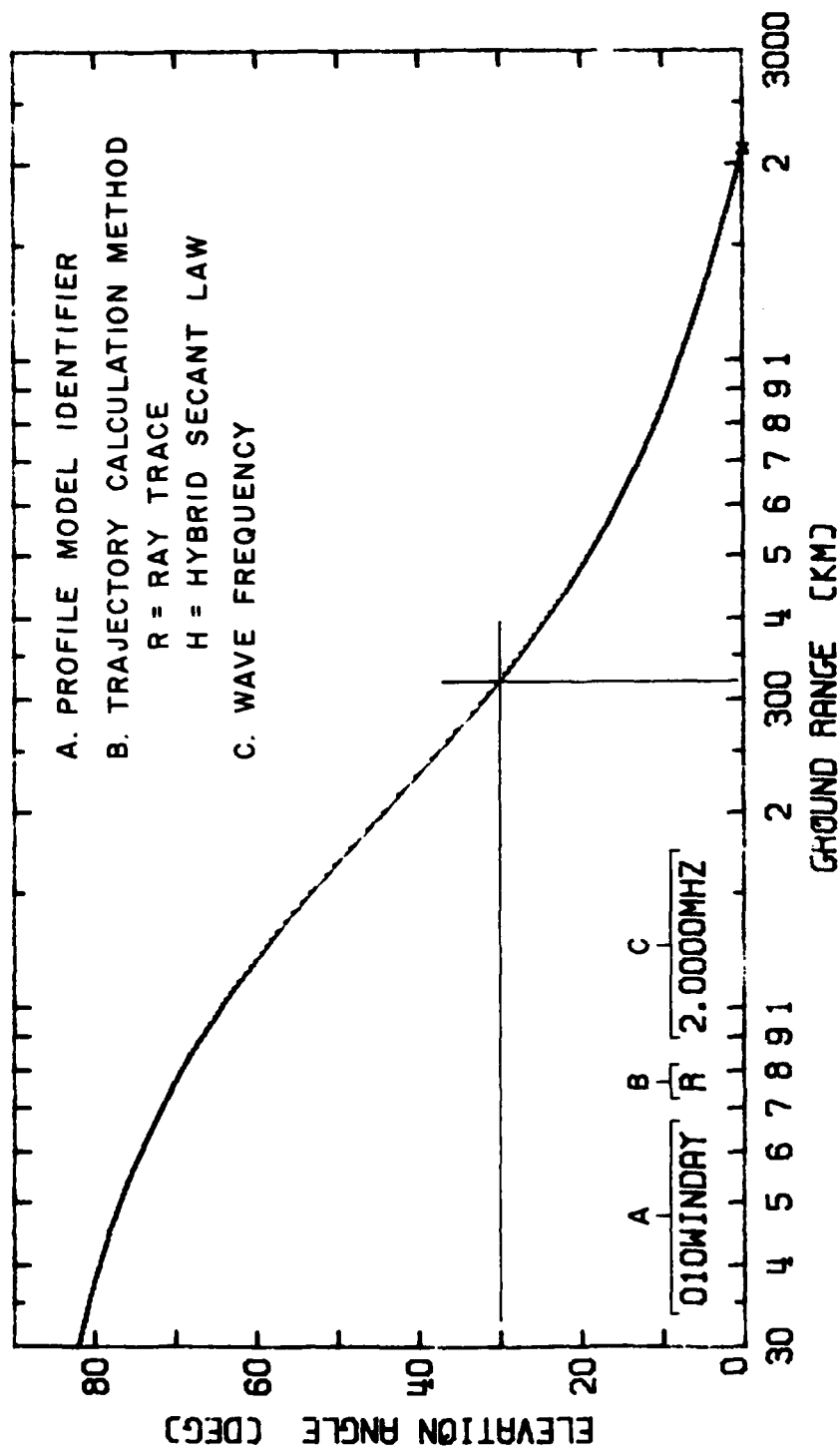


Figure 2-8. Transmission diagram with angle/range curve: 2.0 MHz.

The diagram of Figure 2-8 shows that a ray path is possible at all ground ranges between 30 km and about 2100 km.\* For this case the factor  $\Gamma_h$  has the following functional form.

$$\Gamma_h = 1 \quad 0 \leq D \leq 2100 \text{ km}$$

2-41

$$\Gamma_h = 0 \quad 2100 \text{ km} < D$$

The shape of the curve in Figure 2-8 is characteristic of cases in which the operating frequency falls below the lowest layer critical frequency in the model and, hence, below the lowest cusp in the virtual height curve. For this case, all transmission--the entire curve--involves reflection from E-region levels only. The operating frequency is too low for penetration to F-region levels, even for  $\beta = 90^\circ$ .

Figure 2-9 is an angle/range transmission diagram, using the same profile model as Figure 2-8, but for an operating frequency of 4.0 MHz. This frequency has been chosen to lie between the two critical frequencies of the profile model and, thus, between the cusp and final penetration frequencies of the virtual height curve. The functional form of  $\Gamma_h$  for this diagram is essentially that of Equation 2-41. However, the curve shows an interesting additional detail for ground ranges between about 350 and 600 km.

The cusp in the angle/range curve marks the elevation angle which separates ray reflection in the E-region from ray reflection in the F-region. At higher elevation angles, trajectory apogee\*\* is in the F-region; at lower, it is in the E-region. The critical elevation angle in the case depicted is about  $38^\circ$ .

This curve also exhibits an E-region "skip" range of about 350 km. This is the minimum ground range which can be spanned by a trajectory having its apogee in the E-region. At a ground range of 400 km, the

---

\*Actually, ray paths are also possible for ground ranges less than 30 km. Because the operating frequency, 2.0 MHz, is lower than the highest profile model critical frequency (5.4 MHz), ray paths are possible to zero range.

\*\*Apogee: The highest point on a ray trajectory.



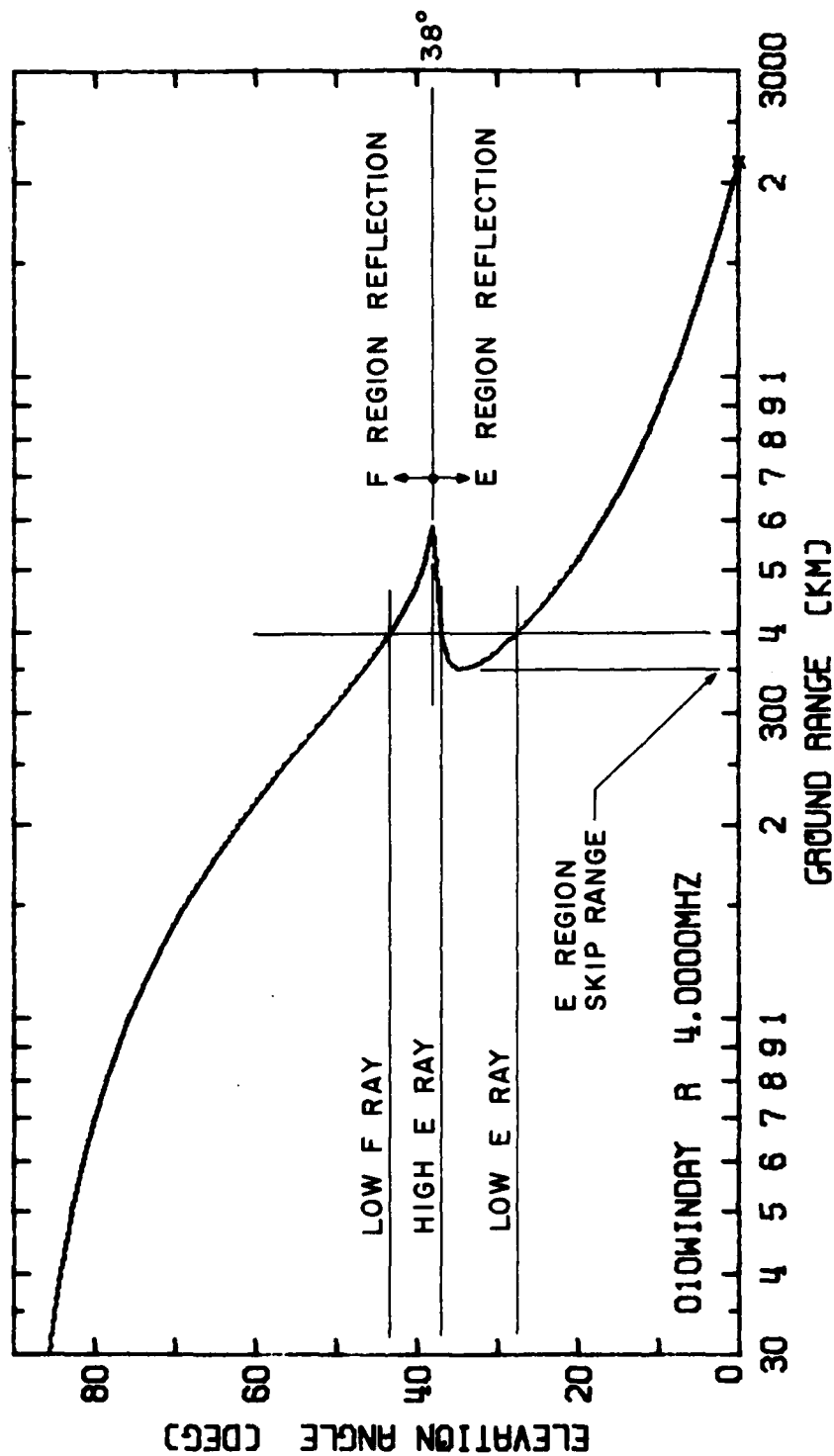


Figure 2-9. Transmission diagram with angle/range curve: 4.0 MHz.

diagram shows that three ray paths are possible at elevation angles of about  $28^\circ$ ,  $37^\circ$ , and  $43^\circ$ .\* There is a low E-ray and a low F-ray. These are the "normal" rays for the E- and F-regions. Also shown is a high E-ray. Rays of this latter sort are commonly called Pedersen rays. Even though three ray paths are possible at ground ranges between 350 and 600 km, the factor  $\Gamma_h$  is given the functional value unity in this range.\*\*

The shape of the curve in Figure 2-9 is characteristic of cases in which one profile model critical frequency and one cusp in the synthetic ionogram lie below the operating frequency.

Suppose, now, that an operating frequency is selected above the highest critical frequency of the profile model, i.e., above the penetration frequency shown in the synthetic ionogram. For the model of Figure 2-4, 6.0 MHz would be such a frequency. Figure 2-10 shows the transmission diagram produced for that frequency.

A new feature appears in this diagram. At elevation angles above about  $64^\circ$ , no rays return to earth. This is an example of the "iris effect" mentioned in discussing the Secant Law (subsection 2.3.1). The critical angle ( $\phi_0$  of Equation 2-40) is, in this case, approximately  $(90 - 64) = 26^\circ$ . There is exhibited an F-skip range at about 325 km as well as an E-skip range at about 610 km. No rays at all are returned to earth at a range less than about 325 km. No transmission is possible to points within this "skip zone" by normal sky wave means. Unless ground wave coverage extends to the F-skip distance, an annular zone will exist which is unreachable on this operating frequency.\*\*\* At a range of 350 km, two possible rays are

\*This is not a consequence of a birefringence property. It is purely geometrical in origin. If birefringence were added to the model, six trajectories would be possible.

\*\*In a more elaborate treatment,  $\Gamma_h$  might be allowed to assume a more complicated form to account for interference effects among multiple rays. Here it is used only to indicate "hearability," i.e., that "at least one ray is possible" or "no rays are possible."

\*\*\*The drop in signal amplitude as range decreases past the skip contour is truly dramatic. However, the signal strength within the skip zone is not strictly zero. The skip contour is a ray "caustic," on which signal amplitude cannot be computed on the basis of ray theory; the theory breaks down on such loci. Resort must be taken to diffraction principles. Some signal energy is diffracted within the skip contour. Other mechanisms, principally scattering from irregular structures, operate to "illuminate" the skip zone dimly. The illumination level is generally low and unpredictable.

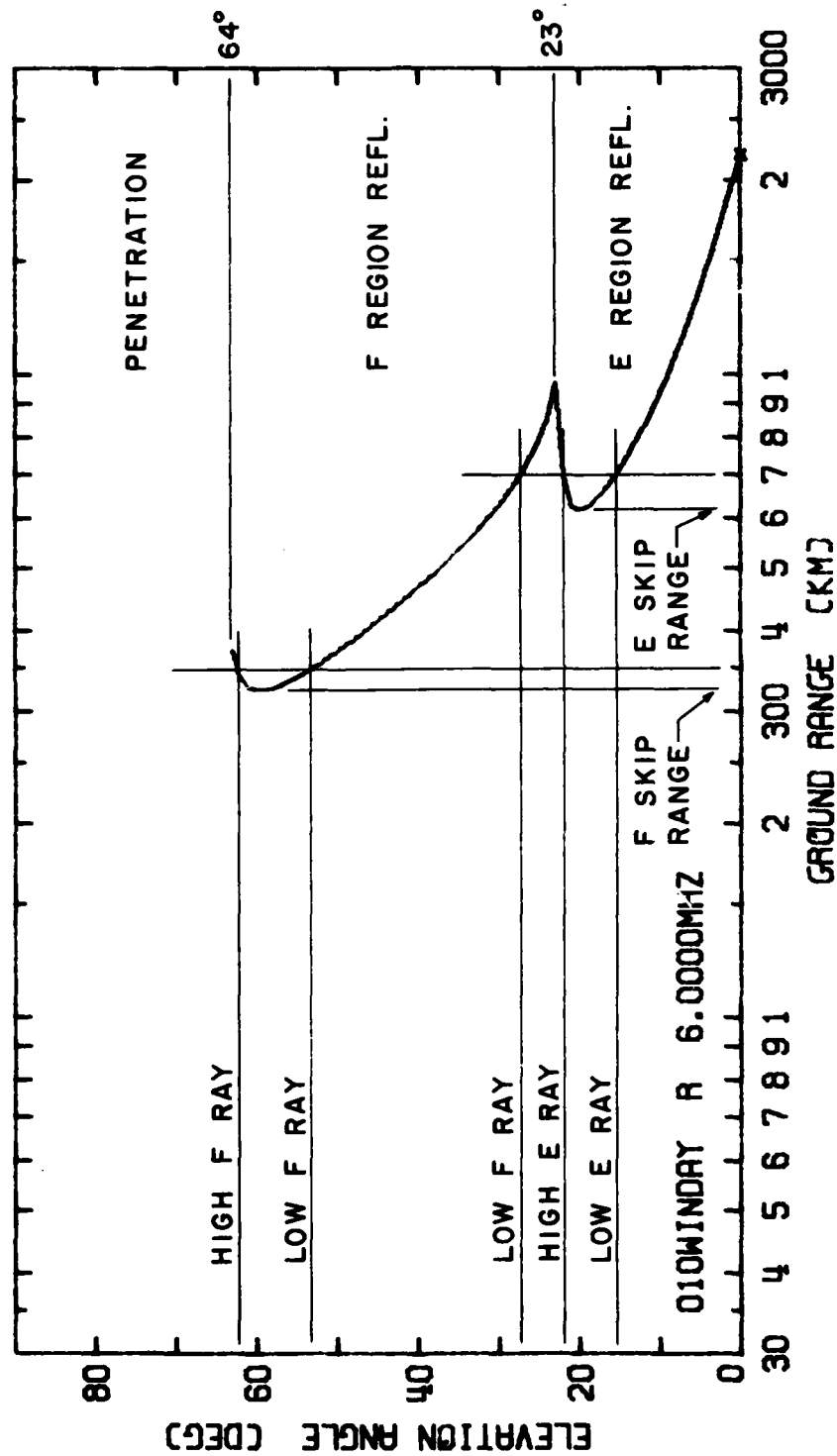


Figure 2-10. Transmission diagram with angle/range curve: 6.0 MHz.

shown, low and high F rays. At 700 km, three possible rays are shown as before. Actually, a high F ray also is possible at all ranges above 325 km. It does not show beyond 370 km on this diagram because, at an elevation angle  $1^\circ$  greater than that which gave the 370° range, the ray penetrated the ionosphere. The missing part of the curve beyond 370 km could be produced by tracing rays at much smaller elevation angle increments, perhaps  $0.1^\circ$ , above  $64^\circ$ .

Again, the shape of this curve is characteristic of cases in which the operating frequency is above the highest profile model critical frequency and in which a second critical frequency is present below the highest one. The radius of the skip zone is a function of the ratio of the operating frequency to the highest profile critical frequency, increasing with that ratio. The hearability factor,  $\Gamma_h$ , for this case would have the following functional form.

$$\begin{aligned} \Gamma_h &= 1 & 325 \text{ km} \leq D \leq 2200 \text{ km} \\ \Gamma_h &= 0 & D < 325 \text{ km}; 2200 \text{ km} < D \end{aligned} \quad 2-42$$

So far only the properties of single-hop trajectories have been considered. Multiple hop trajectories are possible. Each hop can separately be treated like a single-hop case. Two hops are coupled by assuming the same elevation angle for both (i. e., specular reflection) at the intermediate ground reflection region. It is possible, in concept, to use a different profile model for each hop. If the same profile model is appropriate in the apogee region of all hops, then the hops will be identical and, at 4.0 MHz, a diagram like that in Figure 2-11 will be produced from the model of Figure 2-4. Note that at a given angle ( $51^\circ$  in the example illustrated), the possible ranges are in the ratio 1:2:3 (in the example, 300, 600, and 900 km).

Along with the atlas of electron density profile models presented in section 2.4, there is presented an atlas of transmission diagrams associated with the profiles. For each profile, several angle/range curves have been derived at appropriate operating frequencies to illustrate behavior of the hearability function.

### 2.3.3 Divergence Loss

If a wave is launched into free space from a compact source, the ray trajectories associated with the wavefront are straight radial lines. If a

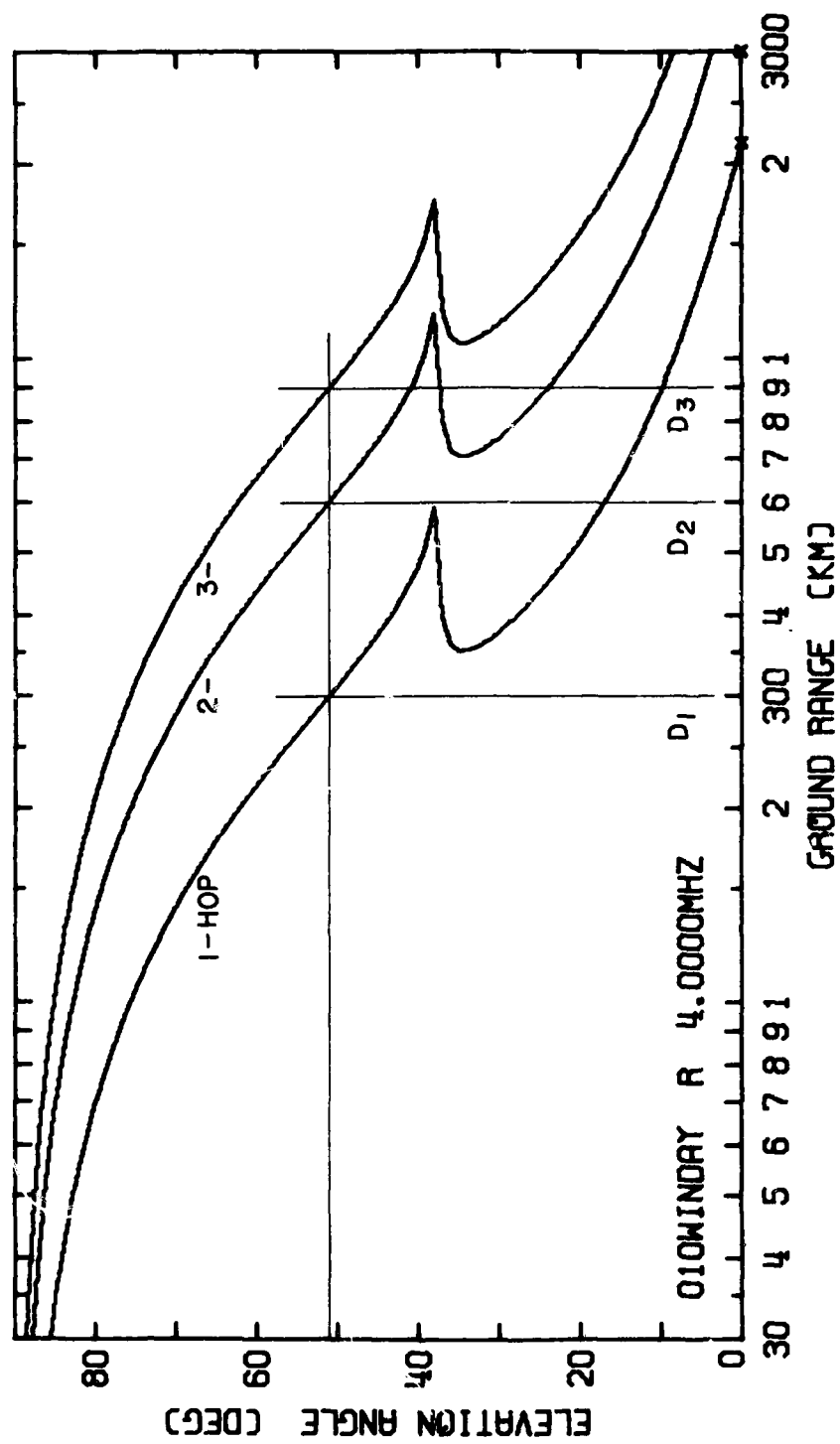


Figure 2-11. Transmission diagram with multi-hop angle/range curves: 4.0 MHz.

small closed curve lying in a wavefront is described, the rays passing through it define a conical increment of solid angle. If ray theory is, indeed, applicable, it follows that the power launched (radiated) within the cone stays within the cone. The area of wavefront intersected by the cone increases as the square of the distance of the wavefront from the source. Thus, the wave intensity (power density: watts/meter<sup>2</sup>) will diminish as the square of the distance.

Whenever ray (i.e., geometrical optical) theory is applicable, the same principles generally apply even though the rays are not straight. The difference is that the cross-sectional area of the "ray tube," and the wave intensity, no longer vary exactly as the square of the distance from the source. The "once in the tube, always in the tube" principle makes it possible to compare signal intensities at different points along a ray central to the tube simply by computing tube cross-sectional areas at the two points. Wave intensity is inversely proportional to tube cross-sectional area.

It is possible to get into trouble with this principle. If the ray tube should collapse so that its cross section becomes a line (like the fill end of a toothpaste tube), the tube cross-sectional area becomes zero. The same occurs if all the tube wall-defining rays should pass through the same point. The latter is familiar as the geometrical image of a point in a simple anastigmatic lens system. If the power density in the wavefront is non-zero at other tube cross sections, it would appear to go infinite at such zero-area cross sections. This "unreal" result occurs because ray theory is not applicable to the calculation of wave intensity at such points. Diffraction theory (physical optics) must be used. If we are careful to avoid such "crimped tube" situations,\* ray principles may be applied to the estimation of sky wave field intensity.

Figure 2-12 is an attempt to portray a bent ray tube such as might occur in sky wave cases. The surface of the earth is represented by a circle arc,  $E_1, E_2, E_3$ . On the surface at T is located a compact source. Through this location a radial line is passed from the center of the earth, C, to T'. Two planes, making an azimuth angle,  $\Delta\phi$ , with each other at T, are passed through the line CTT'. They are the planes CTT'A'AC and CTT'B'BC. The corner B' is beyond the corner A' in the sketch. The planes intersect the surface of the earth in great circle arcs, respectively, TA and TB. From the source four rays are launched, two in each plane.

---

\*The loci formed by such "crimps" are called ray "caustics."

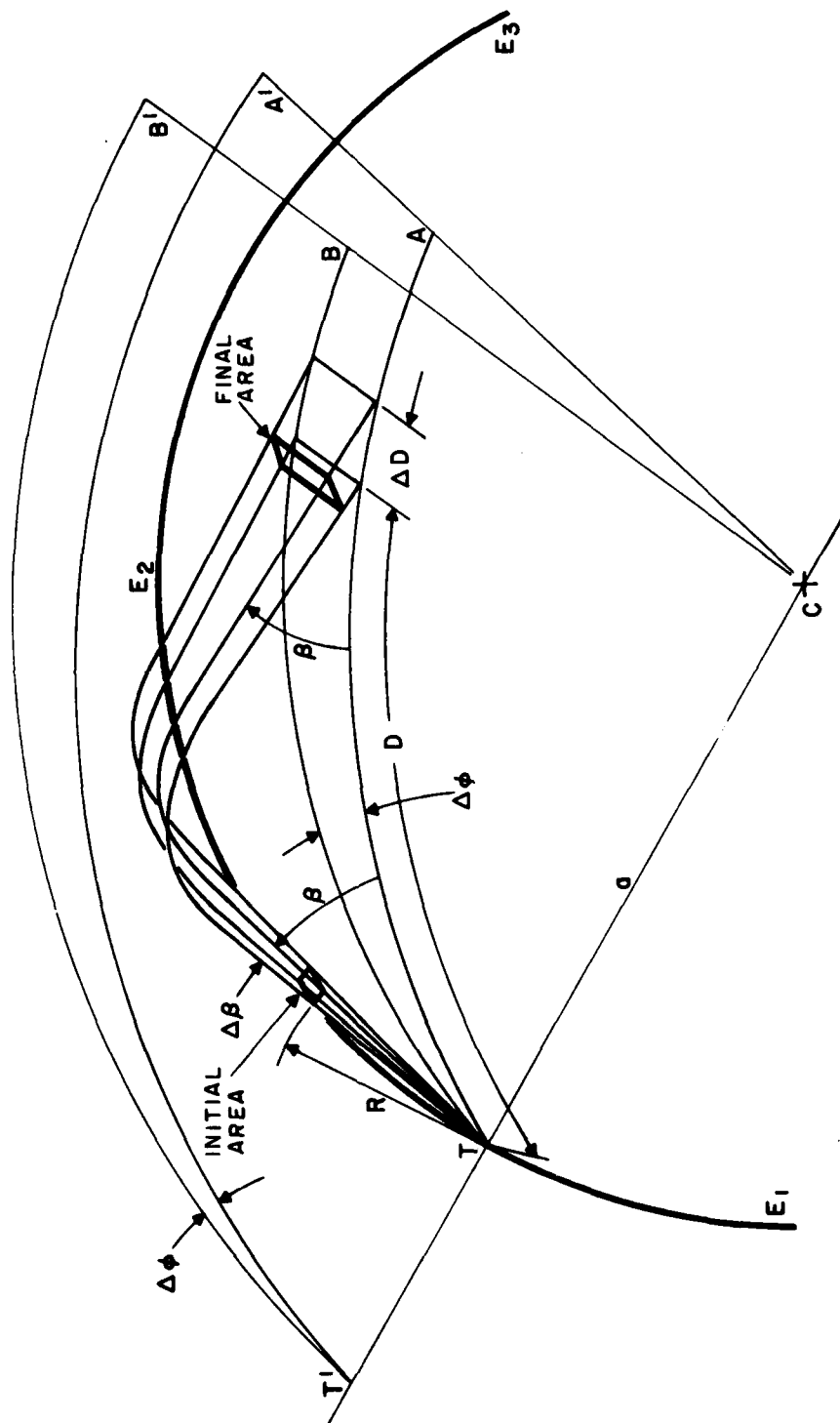


Figure 2-12. Ray tube geometry.

In each plane the rays are at elevation angles  $\beta$  and  $(\beta + \Delta\beta)$ . At a distance  $R$  along the rays, before they start bending on entry into the ionosphere, a tube cross-sectional area called "initial area" is defined. Just before the rays intersect the earth, a similar tube cross-sectional area called "final area" is defined. As the tube intersects the earth, a surface area is defined which is not normal to the central ray of the tube.

It will be convenient to assign the value 1 km to the radial distance,  $R$ , to the initial area. There is no special magic in the particular value, 1 km. It is, simply, large enough to avoid the pointed tube end at  $T$  and small enough to occur well before ray bending in the ionosphere sets in. The basis now has been established for computing  $\Gamma_i$ , the initial loss.

If the source at  $T$  radiates, in an isotropic pattern, an amount of power,  $P_t$  (watts), then the power density,  $S$  (watts/m<sup>2</sup>), at the initial area can be calculated. It is

$$S = \frac{P_t}{4\pi R^2} \quad 2-43$$

If an isotropic receiver were located at the initial area, the power available from it,  $P_r$ , would be ( $A$  is the isotropic absorption aperture)

$$P_r = AS = \frac{\lambda^2}{4\pi} * \frac{P_t}{4\pi R^2} = P_t \left( \frac{\lambda}{4\pi R} \right)^2 \quad 2-44$$

The initial loss,  $\Gamma_i$ , is defined as  $P_t/P_r$  for this case; thus,

$$\Gamma_i = \left( \frac{4\pi R}{\lambda} \right)^2 \quad 2-45$$

Thus,  $\Gamma_i$  is a special case of the free space transmission loss,  $\Gamma_b$ . It is a function only of the wavelength (or frequency). If  $R$  is re-expressed in kilometers,  $R = R_{km} * 10^3$ , and if  $R_{km} = 1$ , then

$$\Gamma_i = \left( \frac{4\pi}{\lambda} * 10^3 \right)^2 \quad 2-46a$$



The loss can also be expressed in decibel form,

$$\begin{aligned}\gamma_i &= 10 \log \Gamma_i = 10 \log \left( \frac{4\pi}{\lambda} * 10^3 \right)^2 \\ &= 20 [\log (4\pi * 10^3) - \log \lambda]\end{aligned}$$

$$\gamma_i = 81.98 - 20 \log \lambda \quad (\text{dB}) \quad 2-46b$$

It also is convenient to have  $\gamma_i$  expressed in terms of frequency, instead of wavelength.

$$\begin{aligned}\gamma_i &= 20 [\log (4\pi * 10^3) - \log (c/f)] \\ &= 20 [\log (4\pi * 10^3/c) + \log f] \\ &= 20 [\log (4\pi * 10^3/299.7925) + \log f_{\text{MHz}}]\end{aligned}$$

$$\gamma_i = 32.45 + 20 \log f_{\text{MHz}} \quad (\text{dB}) \quad 2-46c$$

At the limits of the HF range,  $\gamma_i$  has the values

$$\gamma_i|_{2.0 \text{ MHz}} = 32.45 + 6.02 = 38.47 \text{ dB}$$

$$\gamma_i|_{32.0 \text{ MHz}} = 32.45 + 30.10 = 62.55 \text{ dB}$$

It might be said that the initial loss ( $\Gamma_i, \gamma_i$ ) is the price for "going the first kilometer."

If, now, the isotropic receiver is moved to the final area, an additional loss occurs. This additional loss may be called the "divergence loss,"  $\Gamma_d$ . It is defined to be

$$\Gamma_d = \frac{\text{Wave Intensity at Initial Area}}{\text{Wave Intensity at Final Area}} \quad 2-47a$$

By the "once in the tube, always in the tube" principle,  $\Gamma_d$  can be expressed in terms of the initial and final areas.

$$\Gamma_d = \frac{\text{Final Area}}{\text{Initial Area}} \quad 2-47b$$

The problem now is to calculate the two areas.

Calculation of the initial area is straight forward. It is

$$\text{Initial Area} = R * \Delta\beta * R * \Delta\phi * \cos \beta \quad 2-48$$

Calculation of the final area is a little trickier. It can be found in terms of the surface area defined by the intersection of the ray tube with the earth. The longitudinal (in the ray plane) dimension of this area, is  $\Delta D$ . The transverse (between ray planes) dimension is  $\Delta\phi * a * \sin (D/a)$ , in which  $a$  is the radius of the earth. The final area is at an angle  $\beta$  to the surface area. Thus, the final area is

$$\text{Final Area} = \Delta D * \sin \beta * \Delta\phi * a * \sin (D/a) \quad 2-49$$

The divergence loss,  $\Gamma_d$ , is (via Equation 2-47b)

$$\Gamma_d = \frac{(\Delta D) a \sin \beta \sin (D/a)}{(\Delta\beta) R^2 \cos \beta} \quad 2-50$$

If  $D$  (and, of course,  $\Delta D$ ),  $a$  and  $R$  are re-expressed in kilometers and  $R_{km}$  is set equal to unity,

$$\Gamma_d = \frac{\Delta D_{km}}{\Delta\beta} * \frac{a_{km} \sin \beta \sin (D_{km}/a_{km})}{\cos \beta} \quad 2-51$$

If  $D$  could be expressed as a function of  $\beta$ , and if  $dD/d\beta$  could be found, this expression might be written just in terms of one of the variables, either  $\beta$  or  $D$ . There is, in general, no simple way to do this. The functional relationship depends on the details of profile shape and on the frequency. Fortunately, however, that functional relationship between  $\beta$  and  $D$  is just the one portrayed by the angle/range curve of the transmission diagram. All the data required to calculate  $\Gamma_d$  are contained in the ray parameter sets used to produce the angle/range curve of the transmission diagram.

It is convenient to express the divergence loss,  $\Gamma_d$ , as a function of the ground range,  $D_{km}$ , rather than the elevation angle,  $\beta$ . The procedure for accomplishing this is illustrated in Figure 2-13. For any given ray,  $D_{km}$  is given for a specified value of  $\beta$ . For two adjacent rays, the angle increment,  $\Delta\beta$ , is specified and the ground range increment,  $\Delta D_{km}$ , can be found. Starting at the left scale of Figure 2-13, an angle,  $\beta$ , and increment,  $\Delta\beta$ , are specified. Via the angle/range functional curve these define values of  $D_{km}$  and  $\Delta D_{km}$ . For these, a value of  $\Gamma_d$  is found by Equation 2-51

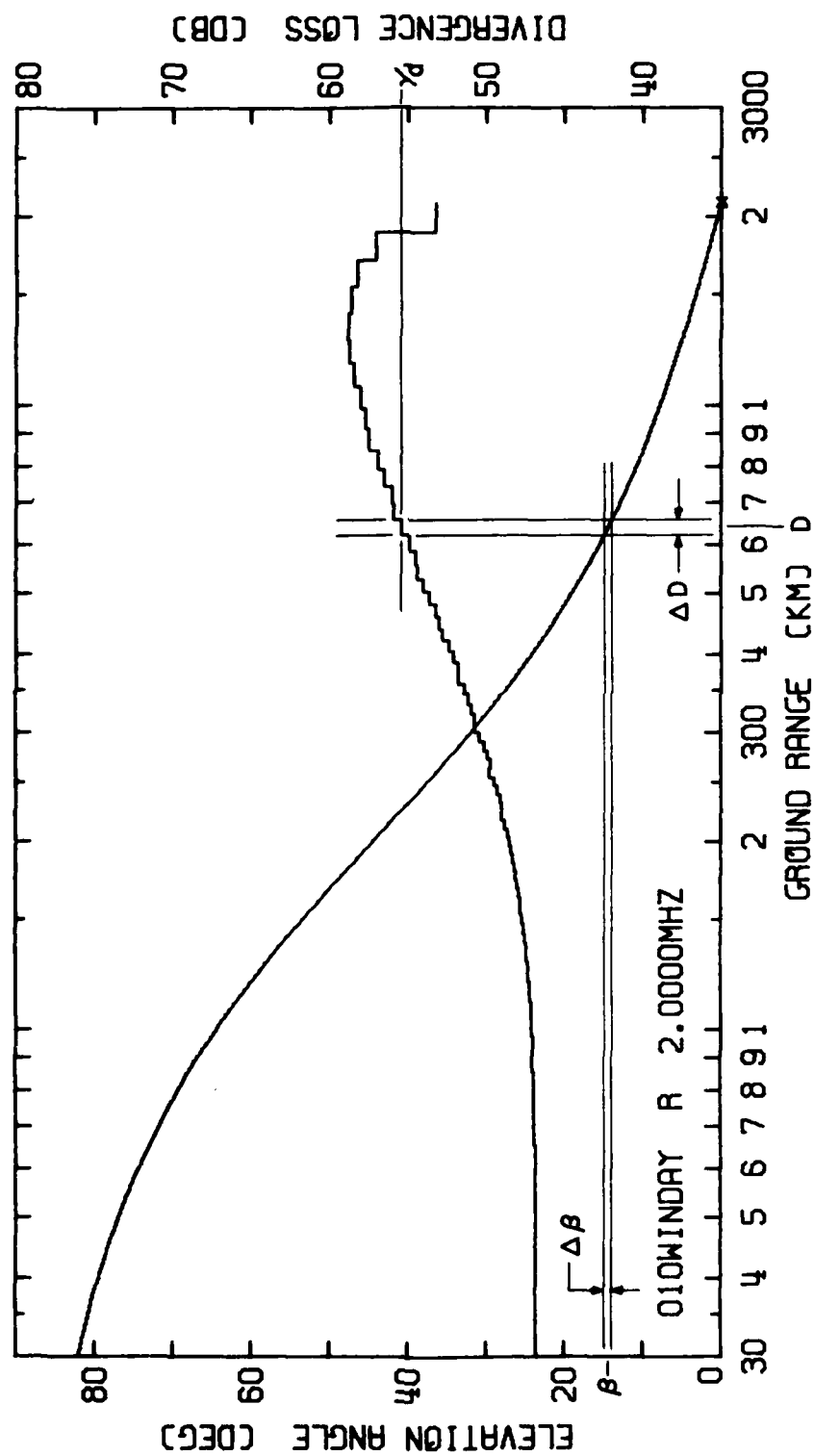


Figure 2-13. Transmission diagram with angle / range and loss / range curves: 2.0 MHz.

and plotted, against the right hand scale, to span the increment  $\Delta D$ . Thus, a loss/range curve having a staircase form is produced. The "treads" of the stairs give the loss values computed for the range increments which they span. The "risers" of the stairs serve only to show the order in which the treads are connected. Thus, Figure 2-13 shows a transmission diagram in which a loss/range curve has been added to the angle/range curve of Figure 2-8.

It is informative to compare the divergence loss shown in Figure 2-13 with free space values for corresponding distances. Recall that with this profile model, reflection was from the E-region of the ionosphere at 2.0 MHz. For very short ground ranges, the signal travels to the ionosphere and back, a distance of about 200 km for E-region reflection. The inverse square law divergence loss for that distance would be

$$\Gamma_d|_{200 \text{ km}} = 20 \text{ Log } (200/1) = 46.0 \text{ dB} \quad 2-52$$

In Figure 2-13 the value of  $\Gamma_d$  for  $D_{\text{km}} = 30$  is about 47 dB. At a ground range of 3000 km, the height of the ionosphere can be neglected and the ray path length assumed to be 3000 km. For inverse square law divergence loss at this distance, the value would be

$$\Gamma_d|_{3000 \text{ km}} = 20 \text{ Log } (3000/1) = 69.5 \text{ dB} \quad 2-53$$

If the loss curve given in Figure 2-13 continued its initial trend, it would be close to this value at 3000 km. However, the loss actually diminishes as the limiting range of 2100 km is approached. This is an example of a phenomenon called "horizon focusing." It is a geometrical phenomenon that does not depend on profile. It is a sort of "whispering gallery" effect that occurs when a source is inside of, but close to, a spherical reflecting shell.

Figures 2-14 and 2-15 are Figures 2-9 and 2-10 to which have been added, respectively, the corresponding loss/range curves for 4.0 MHz and 6.0 MHz. Examine Figure 2-14 for a moment. To help unravel the loss curve, it is useful to start at either the left or the right side and follow the angle/range and loss/range curves together, recalling how the latter was constructed from the former. Starting at the left, note the rapid increase in loss as the limiting low F ray angle is approached. Note the badly defocused condition of the high E ray. This is an indication that the high rays are likely to be unimportant as vehicles for signal delivery. Note the very sharp focusing at the E skip range, where the loss value drops

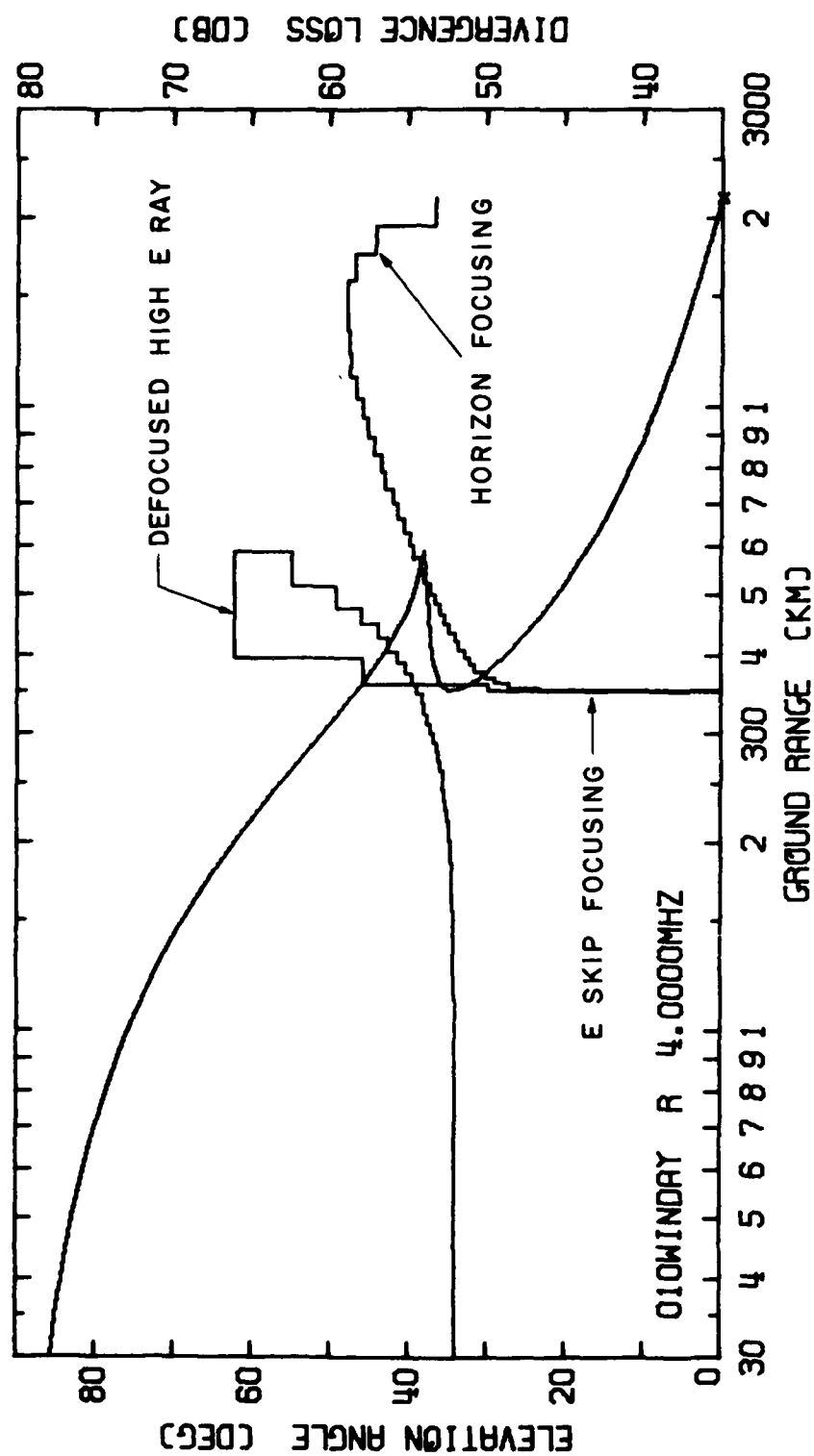


Figure 2-14. Transmission diagram with angle/range and loss/range curves: 4.0 MHz.

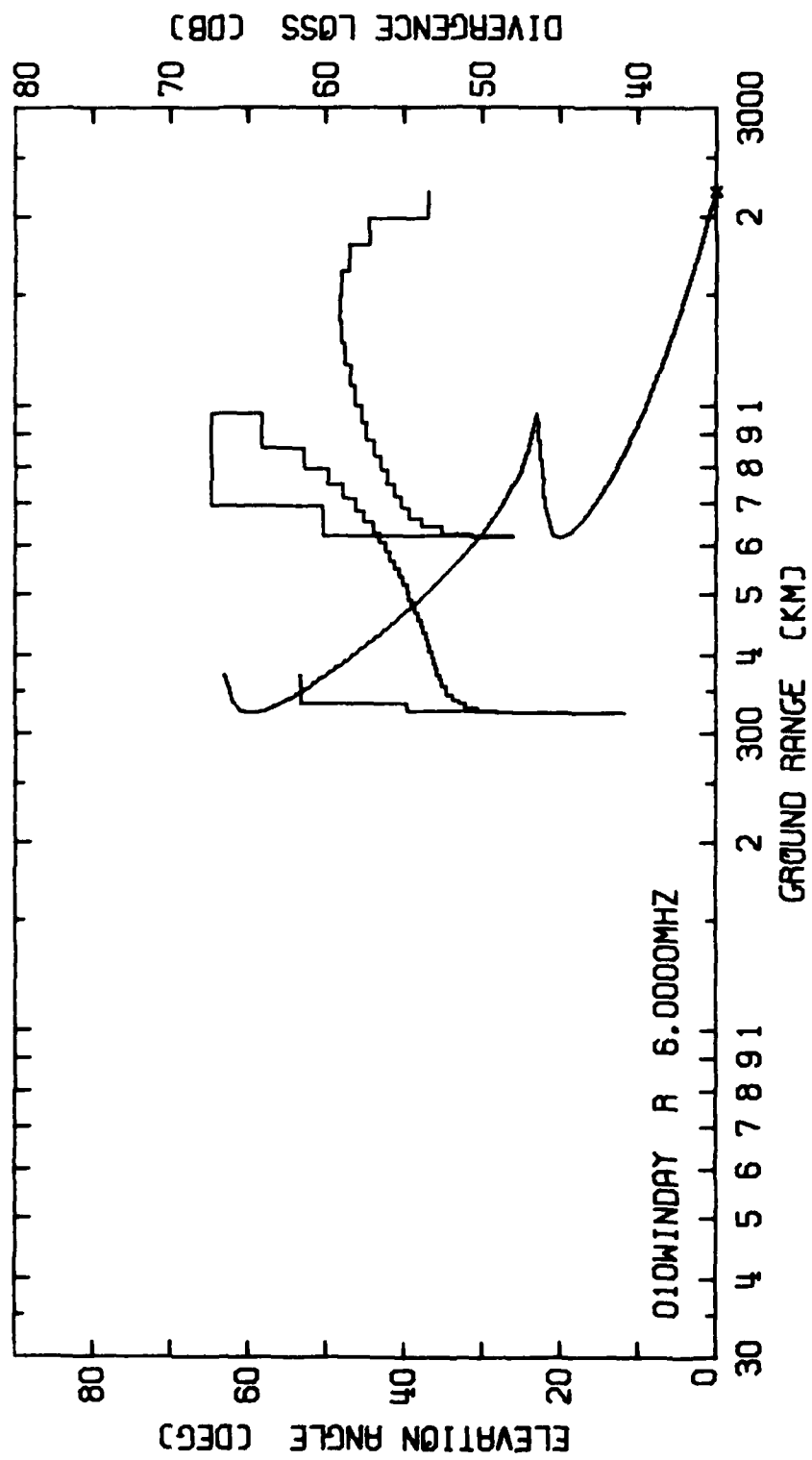


Figure 2-15. Transmission diagram with angle/range and loss/range curves: 6.0 MHz.

off scale at the bottom. At the E skip range, the "nose" of the angle/range curve has a vertical slope. This implies that all rays launched within a small range of angles (about  $42^{\circ}$ - $43^{\circ}$  in this case) are directed to the same ground range. Thus, the skip contour about a source is a ray caustic. Ray principles are not applicable to calculation of signal strength right on this locus. The loss value calculated is anomalously low.

The interpretation of Figure 2-15 proceeds in like manner, but the behavior is just a bit more complicated. The fact that in Figure 2-15 the skip focusing loss is greater than in Figure 2-14 is fortuitous. The minimum value calculated depends critically on the exact manner in which the selected elevation angle values happen to define the skip nose of the angle/range curve.

To recapitulate, divergence loss is not a dissipative loss. It is geometrical in origin. For one-hop trajectories, it will range between about 40 and 75 dB, except in cases of strong focusing or defocusing. An atlas of divergence loss/ground range curves is presented in section 2.4 in association with the related profile models and elevation angle/ground range curves.

#### 2.3.4 Application of Real Ionograms

In subsection 2.3.2 it was shown how angle/range transmission diagrams could be constructed from a profile model, given a specified operating frequency, by a ray tracing procedure. Suppose that, rather than a profile model, one has acquired a real concurrent ionogram. How can one then proceed?

One tack is to proceed to invert the ionogram into an electron density profile and, then, proceed as in subsection 2.3.2. There is another method which, though it has limitations, is quite practical in most instances. It is based on the Secant Law and Martyn's Theorem stated in subsection 2.3.1.

A sample of a real measured ionogram is given in Figure 2-16. This ionogram was produced on a digital ionosonde developed at Southwest Research Institute. Height/frequency pairs of values were listed to a line printer from the ionosonde store. These pairs were manually entered into a computer program which prepared a file compatible with the synthetic ionogram files used to plot Figures 2-4b through 2-7b. To prepare Figure 2-16, the real ionogram data were plotted on the same grid format--using the same plotting program--as the synthetic ionograms. In Figure 2-16 the curve is virtual height. No real height

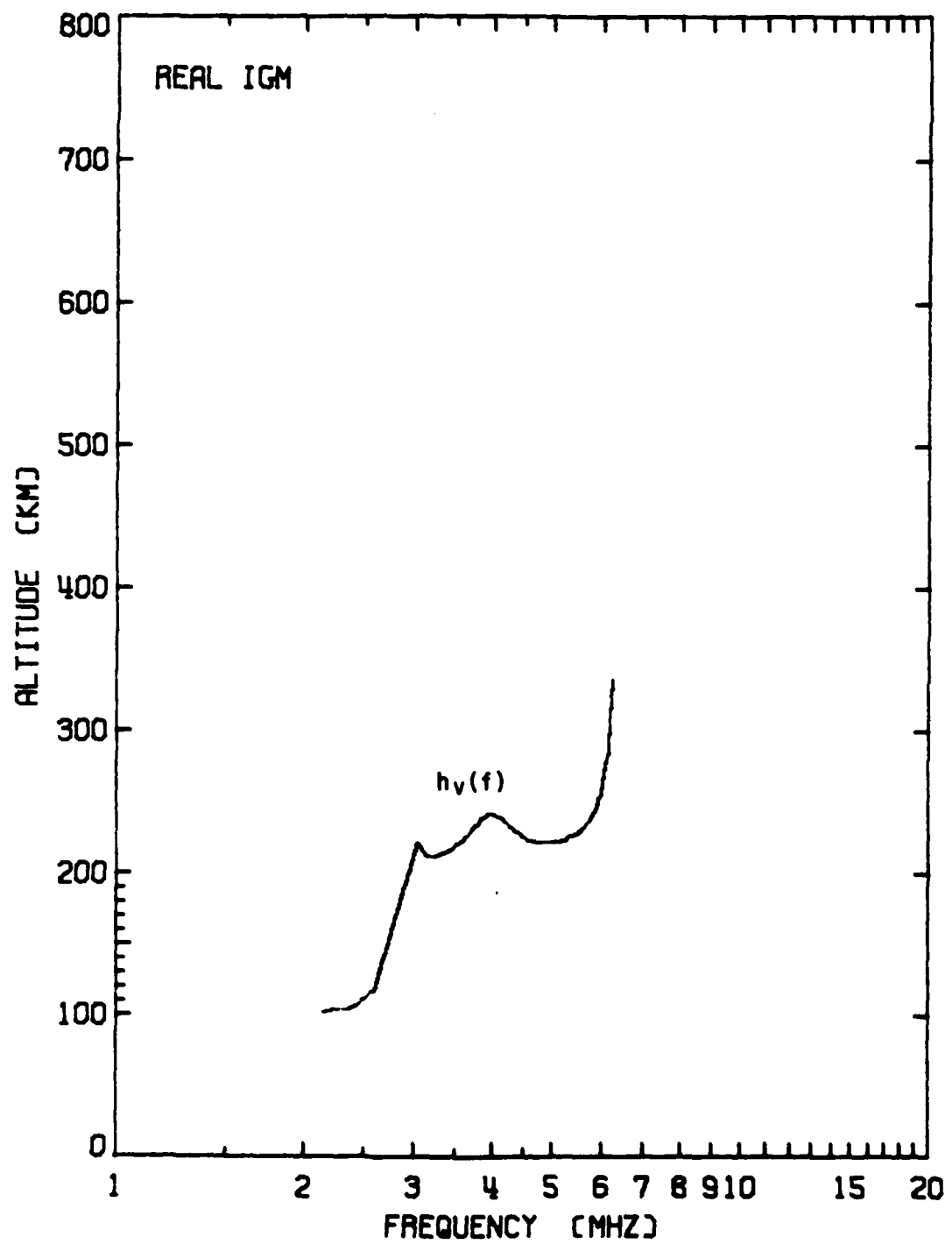


Figure 2-16. Real ionogram.



curve is available. The inclined straight segment of the virtual height curve (between about 2.6 MHz and 3.0 MHz) is a plotting artifact. No data were available in this frequency range. The reason is the high value of "deviative" absorption associated with ray penetration of the E-region.

Assume an operating frequency of 2.4 MHz. The virtual/height frequency pairs from the ionogram, at frequencies lower than 2.4 MHz, can be used to define an oblique virtual ray apex angle,  $\phi$ , (Equation 2-39) and to give an oblique virtual height,  $h_v$ . \* In Equation 2-39, the frequency  $f_{\text{oblique}}$  is the operating frequency and the frequency  $f_{\text{normal}}$  is the ionogram frequency. By Martyn's theorem the virtual height paired with  $f_{\text{normal}}$  in the ionogram can also be used as the height of the oblique virtual ray trajectory. From here it is a matter of simple trigonometry to calculate the ground range and elevation angle, assuming the hybrid model with a spherical earth surface. This calculation can be repeated for all available ionogram frequencies below the operating frequency. \*\*

In the ionogram shown in Figure 2-16, there are not many virtual height/frequency pairs available below 2.4 MHz. However, since reflection at the lowest available frequency is from E-region levels it is reasonably safe to extend the ionogram to lower frequencies at a height equal to that measured at the lowest available frequency. This has been done to produce Figure 2-17. The + sign on the curve at about 100 km ground range is where the procedure "ran out of ionogram." The part of the curve to the right of that point is extrapolated.

Figures 2-18 through 2-23 show transmission diagrams derived from the same ionogram for higher operating frequencies. In each case it is instructive to note where the operating frequency falls with respect to the various features of the ionogram. The short period fluctuation which occurs in the loss/range curves of some of the diagrams arises from the discrete nature of the height scale used in the digital ionosonde. Because of the missing data at the E/F transition in the ionogram, the E-skip phenomena are not as well defined in the angle/range curves as in those derived from the profile models. Nevertheless, it is possible satisfactorily to define the hearability function and to estimate the divergence loss.

\*Similar to  $\phi$  and  $h_v$  in the spherical model portrayed in Figure 2-2, but in a plane-stratified ionosphere.

\*\*Ionogram frequencies above the operating frequency would give a value of  $\sec \phi$  less than unity.

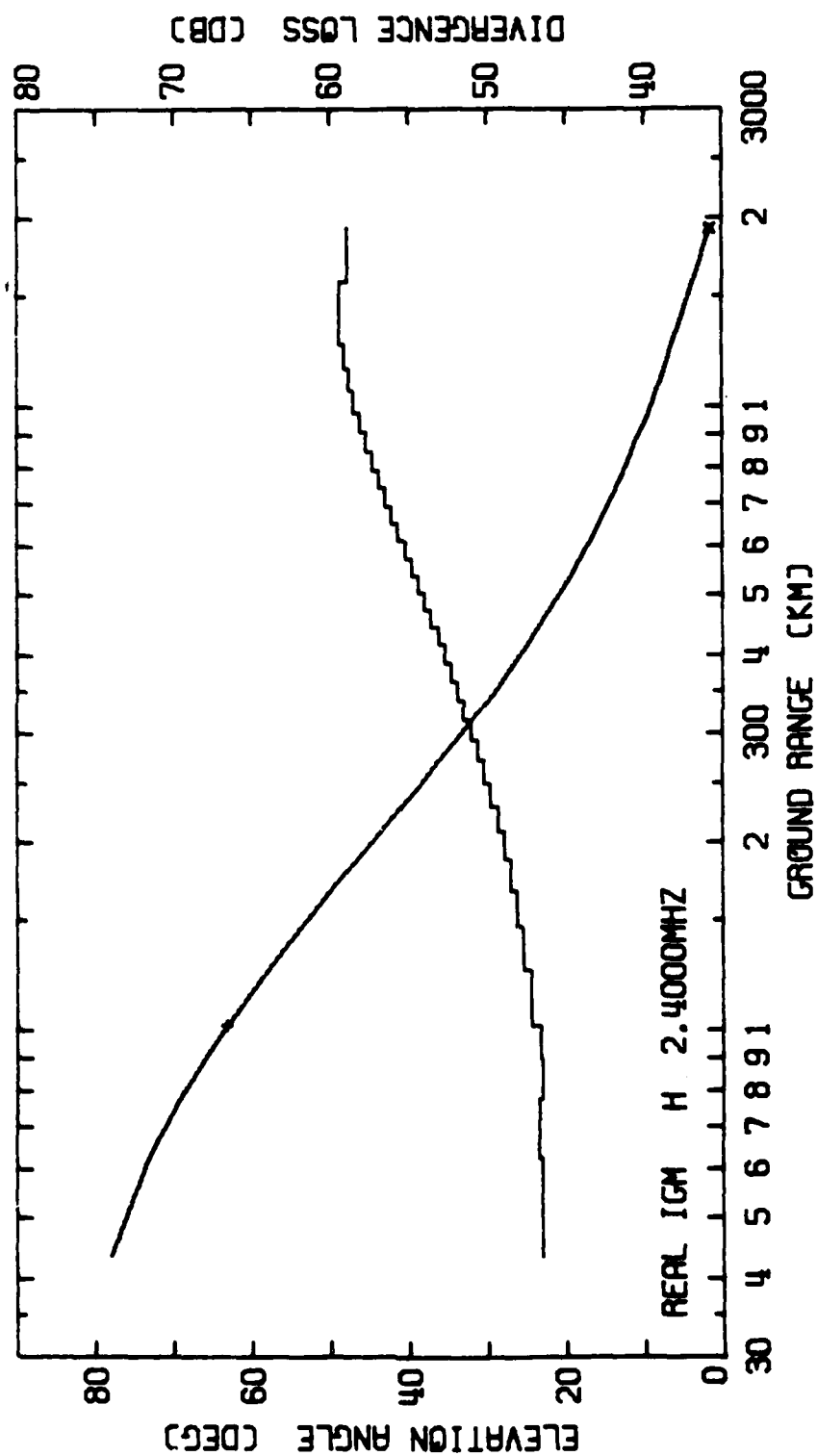


Figure 2-17. Transmission diagram derived from real ionogram: 2.4 MHz.

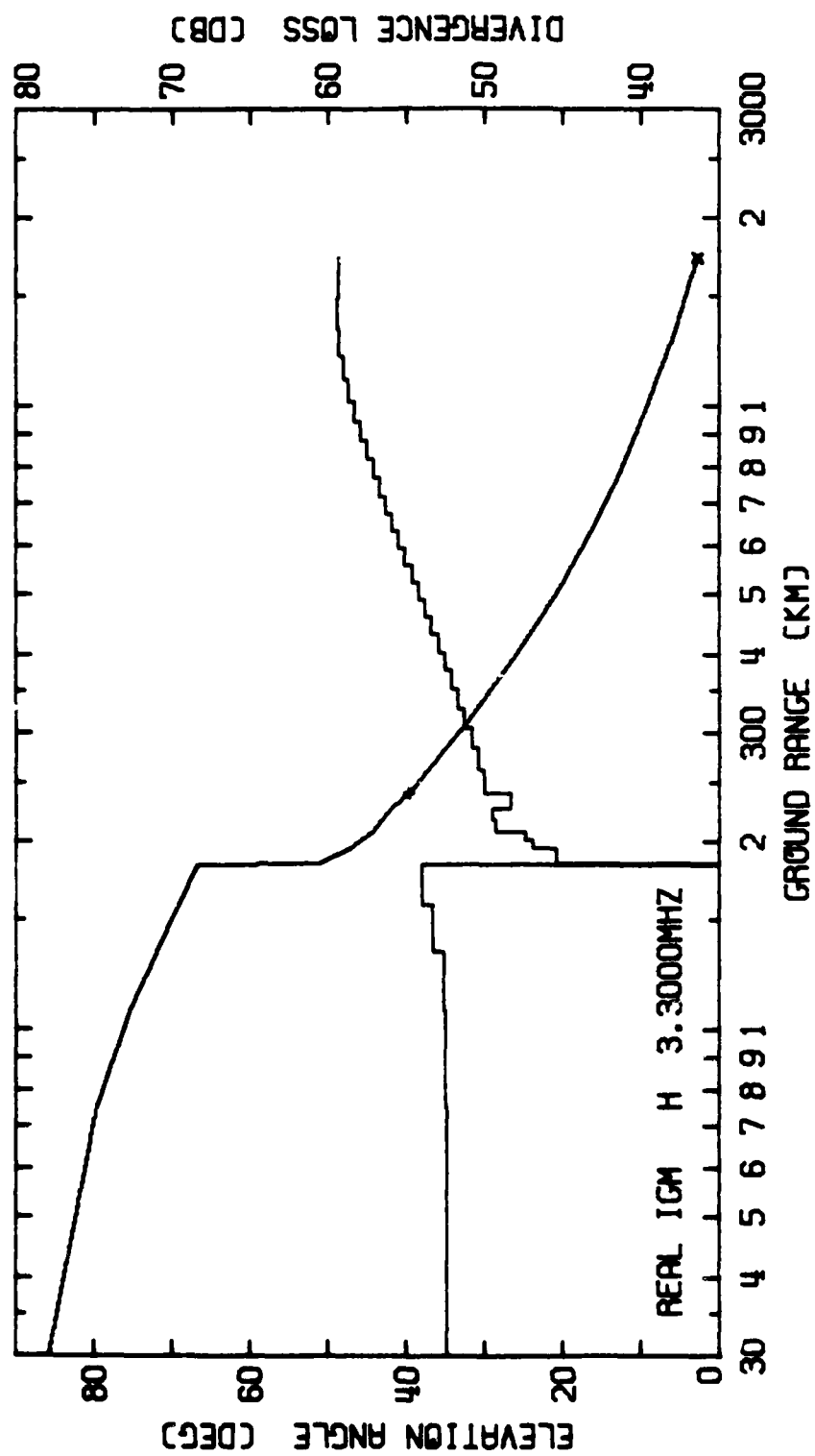


Figure 2-18. Transmission diagram derived from real ionogram: 3.3 MHz.

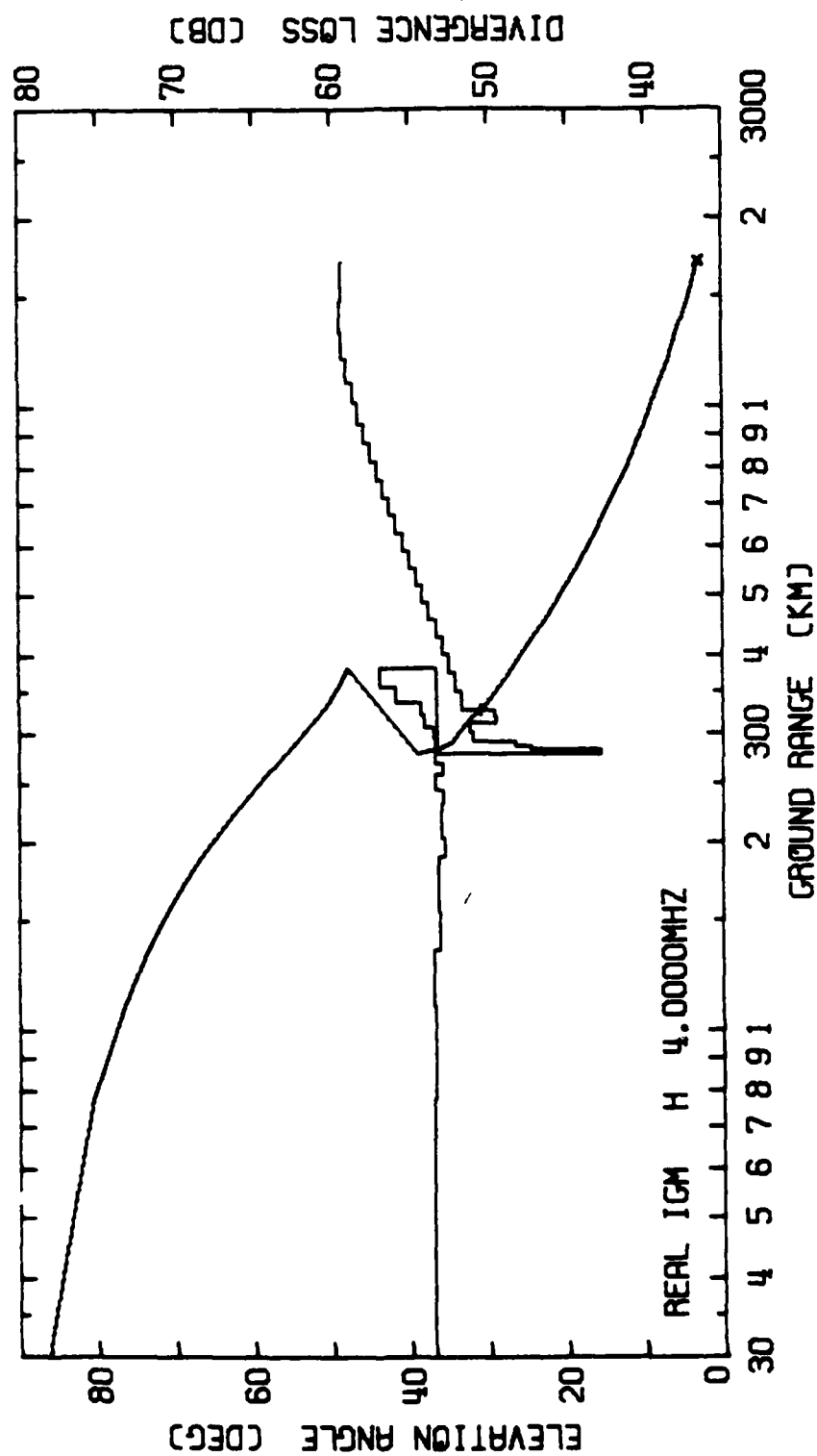


Figure 2-19. Transmission diagram derived from real ionogram: 4.0 MHz.

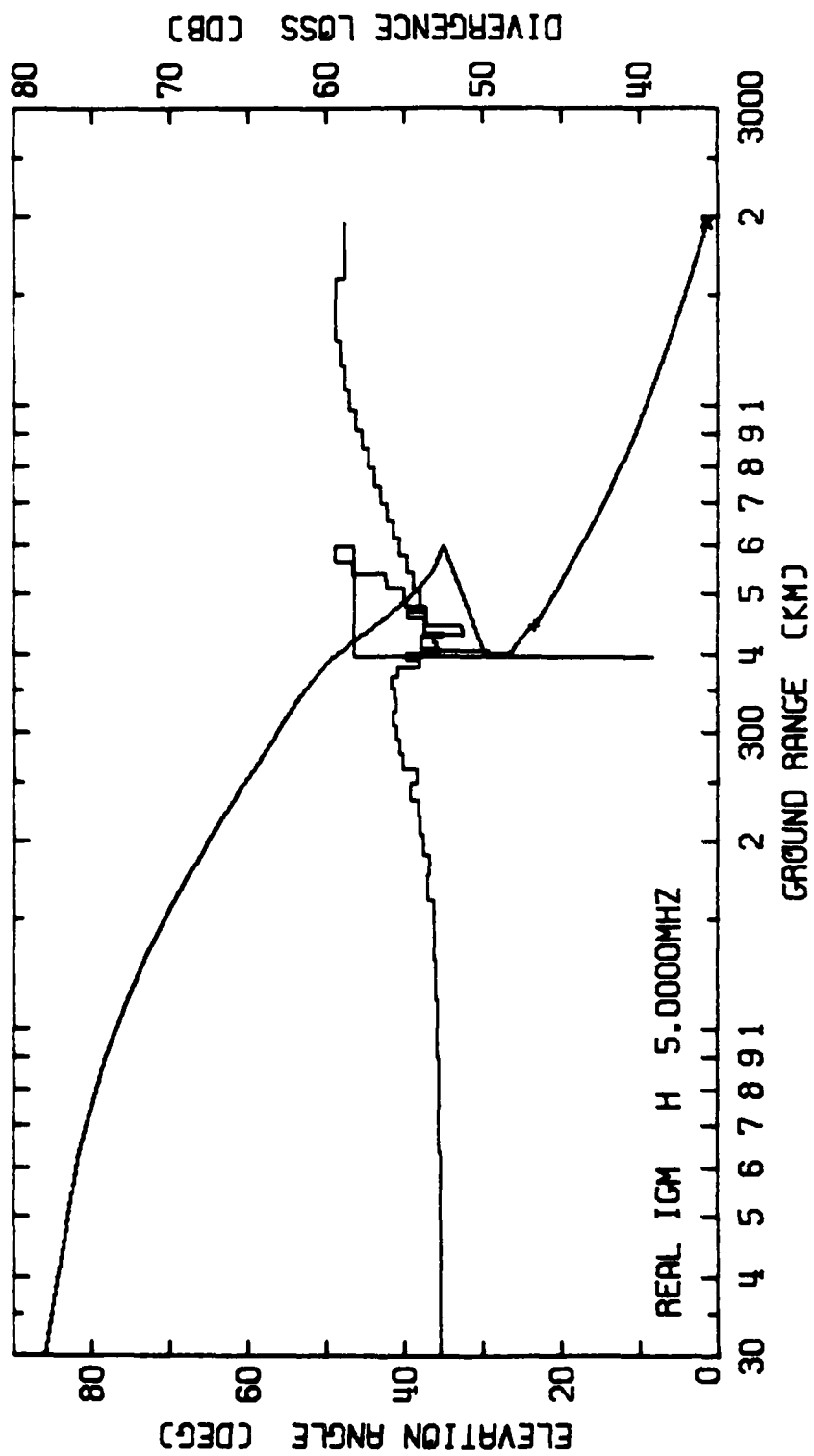


Figure 2-20. Transmission diagram derived from real ionogram: 5.0 MHz.

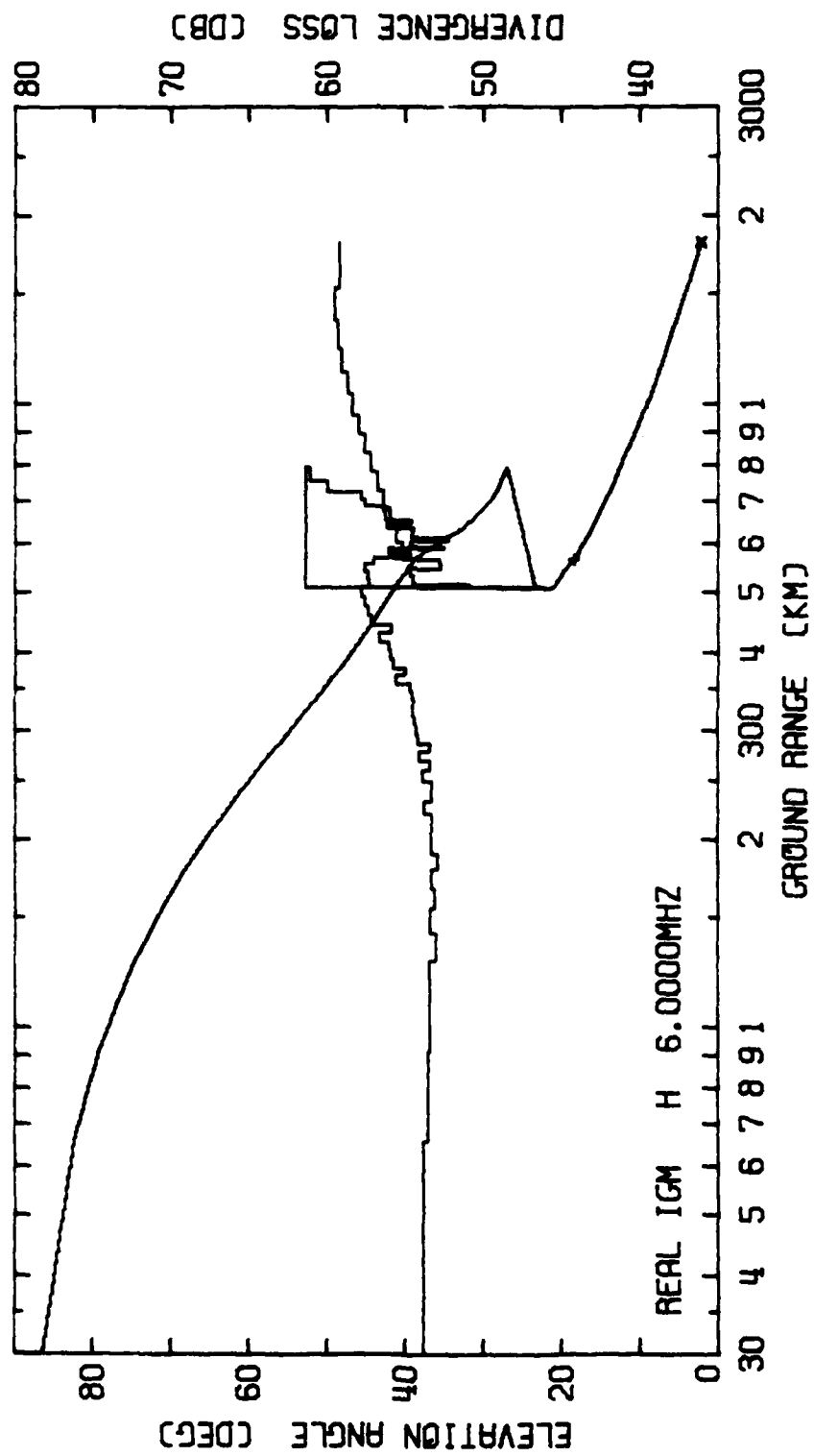


Figure 2-21. Transmission diagram derived from real ionogram: 6.0 MHz.

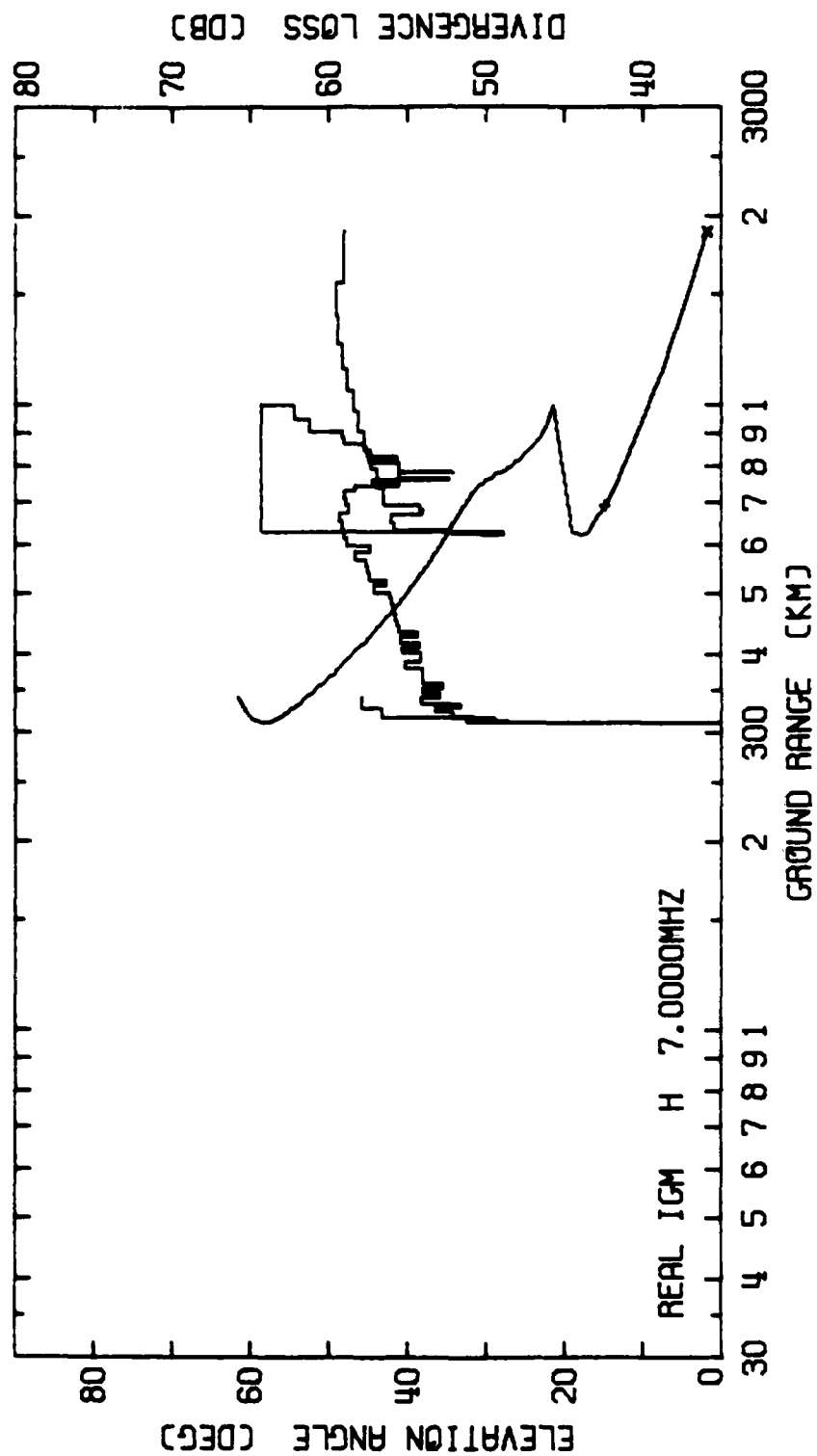


Figure 2-22. Transmission diagram derived from real ionogram: 7.0 MHz.





### 2.3.5 Absorption Loss

The difficulties involved in constructing a satisfactory model of the index of absorption,  $\chi$ , or the absorption coefficient,  $\kappa$ , were discussed in subsection 2.2.2. For lack of a model based on physical processes, it is necessary to fall back on an empirical model which is representative of measured absorption data. That is, the functional form of the model and its parameter values are chosen to fit adequately the measured data. In that sense the model represents the data.

The C.C.I.R. of the International Telecommunications Union has promulgated one such formula, suggested for general use [11]. There are others developed by agencies which have contributed to the work of the C.C.I.R. The C.C.I.R. formula is

$$\gamma_a = \frac{677.2 \sec \phi}{(f + f_H)^{1.98} + 10.2} * I \quad (\text{dB}) \quad 2-54a$$

$$I = \text{The larger of:} \quad 2-54b$$

$$(1 + 0.0037 (R12)) (\cos 0.881\chi)^{1.3}$$
$$0.1$$

In these equations the symbols have the following meanings:\*

$\gamma_a$  - Ionospheric absorption loss (dB).

$\phi$  - Angle of ray path incidence on the 100 km level.

\*At this point we run headlong into a morass of symbolic confusion. It is common practice in the literature of this subject to use the symbol  $\chi$  both for the index of absorption, which is part of the complex index of refraction, and for solar zenith angle on which absorption is dependent. The former use arose in subsection 2.2.1 and the latter in 2.2.4. The two uses for  $\chi$  should not occur in the same expression. However, both appear in the text of this subsection. Usually the context will make clear which entity is intended. To compound this particular confusion, the term "absorption index" is used in the literature to denote two different entities. The first is that symbolized above by  $\chi$ . The second is symbolized by  $I$  and defined by Equation 2-54b. The two entities are not the same. Neither should be confused with the absorption coefficient,  $\kappa$ , or the loss,  $K$ , defined later.

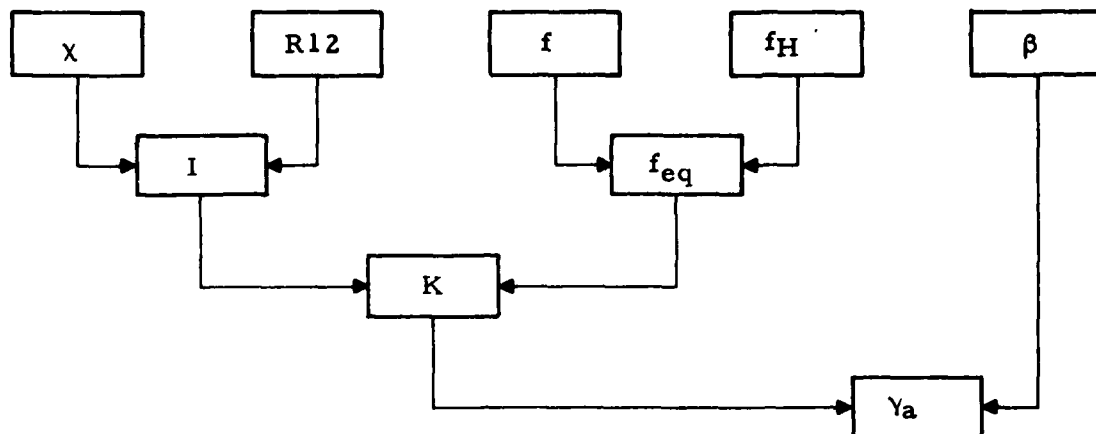
- $f$  = Wave frequency.
- $f_H$  = Gyrofrequency associated with the full geomagnetic field.
- $I$  = Absorption index (not to be confused with entity of the same name symbolized by  $\chi$ ).
- $R12$  = 12-month running average sunspot number.
- $\chi$  = Solar zenith angle (not absorption index).

Note that Equations 2-54 give the absorption loss directly in decibel form ( $\gamma_a$ ) rather than in power ratio form ( $\Gamma_a$ ).

For our purposes it is more convenient to specify  $\gamma_a$  in terms of the elevation angle of the ray at its ground intersection ( $\beta$ ) than in terms of  $\phi$  given above. This can be accomplished by replacing the factor  $\sec \phi$  in Equation 2-54a by an equivalent function of  $\beta$  ( $a_{km}$  is the radius of the earth in kilometers).

$$\sec \phi = 1/[1 - (a_{km} \cos \beta / (a_{km} + 100))^2]^{1/2} \quad 2-55$$

The absorption loss,  $\gamma_a$ , is a function of five variables:  $\beta$ ,  $f$ ,  $f_H$ ,  $\chi$ ,  $R12$ . To develop a graphical representation of loss data, it is necessary to break the calculation down into stages. Ordinary graphs are two-dimensional representations. Thus, two variables can be combined graphically to produce values of a single intermediate variable. The process can be continued with pairs of intermediate variables. The order in which the variables are entered into the process is important to the convenience of the procedure. The variables least likely to change in a given situation should be entered first, if possible. Thus, the variables most likely to change will require retracing of only the final portion of the procedure. The organization selected to solve the loss equation can be shown in flow chart form.



To handle the five independent variables, three intermediate variables and four graphical stages are required. The intermediate variables, absorption index (I), equivalent frequency ( $f_{eq}$ ) and loss factor (K) are defined by the following equations.

$$I = \text{The larger of:} \quad 2-56a$$

$$(1 + 0.0037 (R12)) (\cos 0.881 \chi)^{1.3}$$

$$0.1$$

$$f_{eq} = f + f_H \quad 2-56b$$

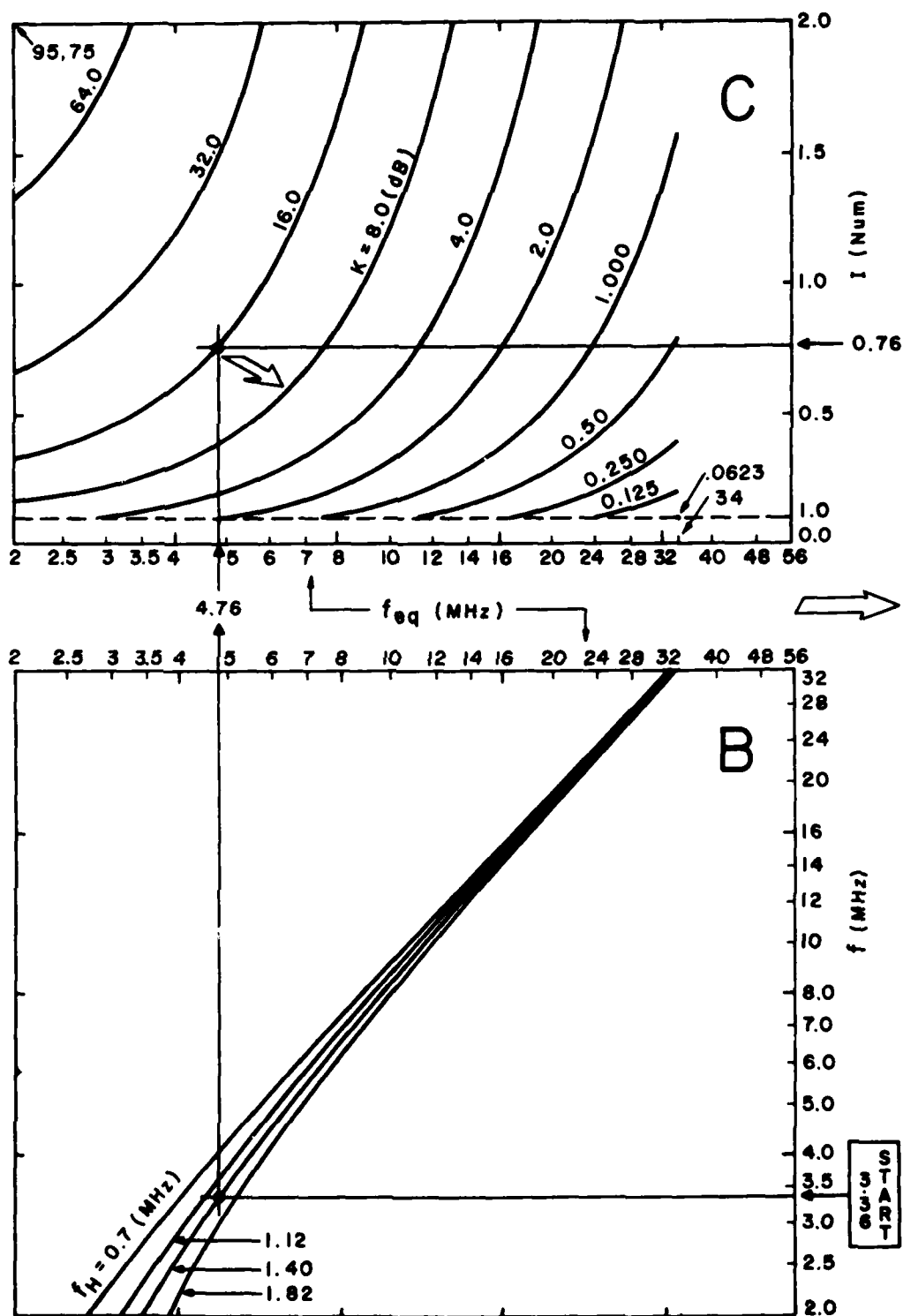
$$K = 677.2 I / (f_{eq}^{1.98} + 10.2) \quad 2-56c$$

Finally,

$$\gamma_a = K / [1 - (a_{km} \cos \beta / (a_{km} + 100))^2]^{1/2} \quad 2-57$$

The graph set to solve Equation 2-54 is given in Figure 2-24. An example of a solution is shown. The solution procedure is as follows:

- (1) On Graph A, start at  $\chi = 50^\circ$ . Let  $R12 = 45$ . Find  $I = 0.76$ .
- (2) On Graph B, start at  $f = 3.36$  MHz. Let  $f_H = 1.40$  MHz. Find  $f_{eq} = 4.76$  MHz.



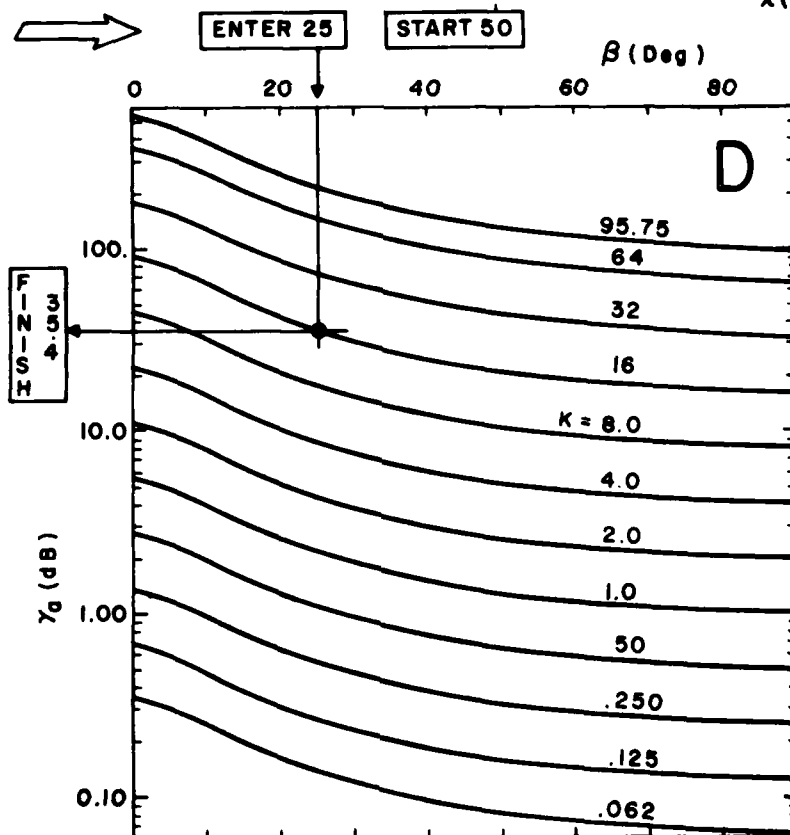
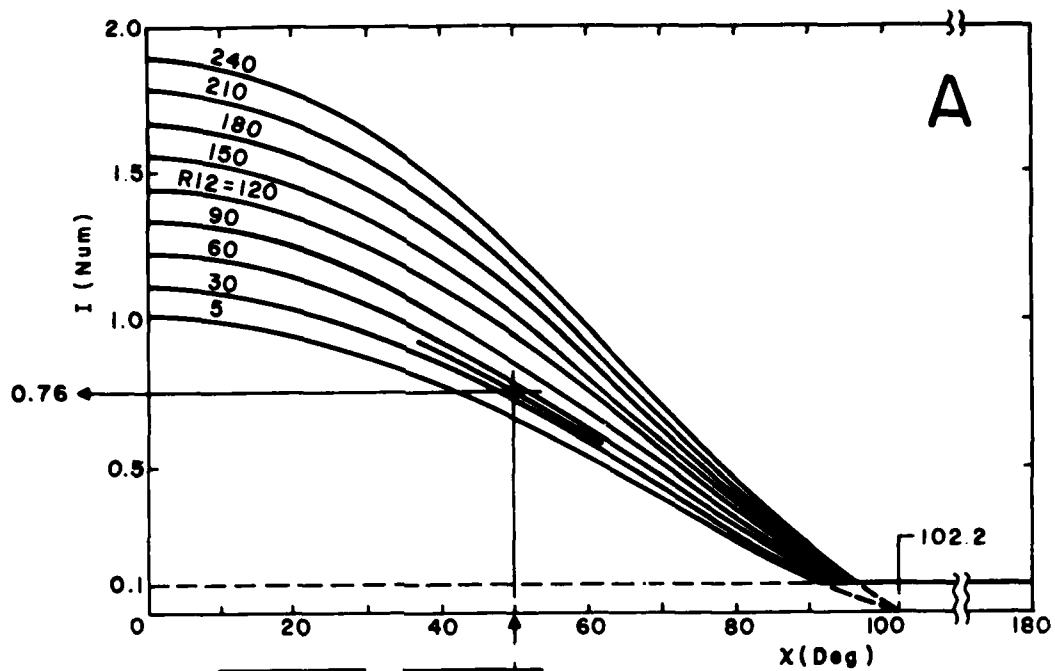


Figure 2-24. Chart system for estimating total ionospheric absorption loss.

- (3) On Graph C, enter values of  $I$  and  $f_{eq}$  from Graphs A and B. Find  $K = 16.0$ .
- (4) On Graph D, enter at  $\beta = 25^\circ$ . Intersect  $K = 16.0$  contour and find  $\gamma_a = 35.4$  dB.

To facilitate production of a set of working charts for estimation of  $\gamma_a$ , the data from which Figure 2-24 were prepared are given in Tables 2-3 through 2-6. These tables are not particularly convenient for direct use. They have been arranged to facilitate plotting. To this end, each of the parametric curves of Figure 2-24 is given as a function of the scale variables. An atlas of working tables of absorption loss, arranged for convenient use, is presented in section 2.5.

Estimation of absorption loss by means of this empirical model has some limitations. For a discussion of the limitations the reader is referred to the original sources [11]. This loss model represents monthly median data. There are daily variations about the monthly median. In addition, there are variations related to factors other than those explicitly accounted for in the model. Information about such "Expected Excess System Loss" is given in tabular form in one of the references [11]. Median values given for Expected Excess System Loss range from 9 dB to 29 dB. Spread about the median ranges from -18 dB to +31 dB. Other factors considered in the tables are time of day, season, geomagnetic latitude, and ground range.

A point to note in the atlas tables is the very wide range of absorption loss values which can be experienced. Absorption loss ranges from very low values (as low as 0.5 dB) for large values of solar zenith angle and high frequencies, to very high values (as high as 400 dB) for small values of solar zenith angle, large sunspot number and low frequencies. These are one-hop values.

It is absorption that limits signal delivery in the lower part of the HF range during daytime hours.

#### 2.3.6 Other Losses

If path loss is to be calculated for a multi-hop trajectory, at least two additions to the procedure already described must be made. The first is obvious. It is to combine the divergence and absorption loss estimates for the individual hops. The second is to take account of the ground reflection loss at hop juncture points. This loss can be approximated by the mean square combination of the standard Fresnel ground reflection coefficients for the two polarizations (parallel and perpendicular). The coefficients

Table 2-3. Equivalent frequency.

EQUIVALENT FREQUENCY, FFQ (MHZ), AS A FUNCTION  
OF GYRO-FREQUENCY, FH, AND WAVE-FREQUENCY, F

WAVE FREQUENCY* (MHZ)	FULL GYRO-FREQUENCY (MHZ)			
	0.70	1.12	1.40	1.82
2.00	2.70	3.12	3.40	3.82
2.83	3.53	3.95	4.23	4.65
4.00	4.70	5.12	5.40	5.82
5.66	6.36	6.78	7.06	7.48
8.00	8.70	9.12	9.40	9.82
11.31	12.01	12.43	12.71	13.13
16.00	16.70	17.12	17.40	17.82
21.63	23.33	23.75	24.03	24.45
32.00	32.70	33.12	33.40	33.82

Table 2-4. Absorption index: solar variables (Parts a,b,c).

ABSORPTION INDEX, I (NUMERIC), AS A FUNCTION  
OF SOLAR VARIABLES

SOLAR ZENITH ANGLE* (DEG)	TWELVE MONTH RUNNING AVERAGE SUNSPOT NUMBER (NUMERIC)			
	5.	15.	45.	135.
0.0	1.018	1.055	1.161	1.499
5.0	1.015	1.051	1.162	1.494
10.0	1.013	1.039	1.149	1.477
15.0	0.984	1.019	1.127	1.448
20.0	0.957	0.992	1.096	1.409
25.0	0.923	0.956	1.057	1.359
30.0	0.892	0.914	1.011	1.299
35.0	0.835	0.866	0.957	1.230
40.0	0.783	0.811	0.897	1.153
45.0	0.725	0.751	0.830	1.068
50.0	0.663	0.687	0.759	0.976
55.0	0.597	0.619	0.684	0.879
60.0	0.529	0.548	0.605	0.778
65.0	0.458	0.475	0.525	0.674
70.0	0.386	0.401	0.443	0.569
75.0	0.315	0.327	0.361	0.464
80.0	0.245	0.254	0.281	0.361
85.0	0.177	0.184	0.203	0.261
90.0	0.114	0.118	0.131	0.168
95.0	0.100	0.100	0.100	0.100
100.0	0.100	0.100	0.100	0.100

(Continued on following page.)

SOLAR ZENITH ANGLE (DEG)	TWELVE MONTH RUNNING AVERAGE SUNSPOT NUMBER (NUMERIC)			
	30.	60.	90.	120.
0.0	1.111	1.222	1.333	1.444
5.0	1.107	1.217	1.328	1.438
10.0	1.094	1.203	1.313	1.422
15.0	1.073	1.180	1.287	1.394
20.0	1.044	1.148	1.252	1.357
25.0	1.007	1.107	1.208	1.309
30.0	0.962	1.059	1.155	1.251
35.0	0.911	1.002	1.093	1.184
40.0	0.854	0.939	1.025	1.110
45.0	0.791	0.870	0.949	1.028
50.0	0.723	0.795	0.868	0.940
55.0	0.651	0.716	0.782	0.847
60.0	0.577	0.634	0.692	0.749
65.0	0.500	0.550	0.599	0.649
70.0	0.422	0.464	0.506	0.548
75.0	0.344	0.378	0.412	0.447
80.0	0.267	0.294	0.321	0.347
85.0	0.194	0.213	0.232	0.252
90.0	0.125	0.137	0.150	0.162
95.0	0.100	0.100	0.100	0.100
100.0	0.100	0.100	0.100	0.100

SOLAR ZENITH ANGLE (DEG)	TWELVE MONTH RUNNING AVERAGE SUNSPOT NUMBER (NUMERIC)			
	150.	180.	210.	240.
0.0	1.555	1.666	1.777	1.888
5.0	1.549	1.660	1.770	1.881
10.0	1.531	1.640	1.750	1.859
15.0	1.502	1.609	1.716	1.823
20.0	1.461	1.565	1.669	1.774
25.0	1.409	1.510	1.610	1.711
30.0	1.347	1.443	1.539	1.636
35.0	1.276	1.367	1.458	1.549
40.0	1.195	1.281	1.366	1.451
45.0	1.107	1.186	1.265	1.344
50.0	1.012	1.084	1.157	1.229
55.0	0.912	0.977	1.042	1.107
60.0	0.807	0.865	0.922	0.980
65.0	0.699	0.749	0.799	0.849
70.0	0.590	0.632	0.674	0.716
75.0	0.481	0.515	0.550	0.584
80.0	0.374	0.401	0.427	0.454
85.0	0.271	0.290	0.310	0.329
90.0	0.174	0.187	0.199	0.212
95.0	0.100	0.100	0.101	0.107
100.0	0.100	0.100	0.100	0.100



Table 2-5. Absorption index: non-solar variables.

ABSORPTION INDEX, I (NUMERIC), AS A FUNCTION OF LOSS FACTOR, K, AND EQUIVALENT FREQUENCY, FEQ		LOSS FACTOR (DECIBELS)											
EQUIV FREQ (MHZ)		0.125	0.250	0.500	1.000	2.000	4.000	8.000	16.000	32.000	64.000		
2.00	0.003	0.005	0.010	0.021	0.042	0.084	0.167	0.334	0.668	1.337			
2.38	0.003	0.006	0.012	0.023	0.047	0.093	0.186	0.372	0.745	1.489			
2.83	0.003	0.007	0.013	0.027	0.053	0.107	0.213	0.426	0.852	1.704			
3.36	0.004	0.008	0.016	0.031	0.063	0.125	0.251	0.502	1.004	2.008			
4.00	0.005	0.010	0.019	0.038	0.076	0.152	0.304	0.609	1.217	2.435			
4.76	0.006	0.012	0.024	0.047	0.095	0.190	0.380	0.759	1.518	3.037			
5.66	0.008	0.015	0.030	0.061	0.121	0.243	0.486	0.971	1.943	3.885			
6.73	0.011	0.020	0.040	0.079	0.159	0.318	0.635	1.270	2.540	5.081			
8.00	0.013	0.026	0.053	0.106	0.211	0.423	0.846	1.692	3.383	6.766			
9.51	0.018	0.036	0.071	0.143	0.286	0.571	1.143	2.285	4.570	9.141			
11.31	0.024	0.049	0.098	0.195	0.390	0.780	1.561	3.122	6.244	12.488			
13.45	0.034	0.067	0.134	0.269	0.538	1.075	2.151	4.301	8.602	17.205			
16.00	0.047	0.093	0.186	0.373	0.745	1.491	2.982	5.963	11.926	23.853			
19.03	0.065	0.130	0.260	0.519	1.038	2.076	4.153	8.305	16.611	33.221			
22.63	0.091	0.181	0.363	0.725	1.451	2.902	5.803	11.606	23.213	46.425			
26.91	0.127	0.254	0.508	1.016	2.032	4.065	8.129	16.258	32.517	65.034			
32.00	0.178	0.356	0.713	1.426	2.852	5.704	11.407	22.815	45.629	91.258			
34.00	0.201	0.401	0.803	1.606	3.212	6.423	12.847	25.694	51.387	102.774			

Table 2-6. Total ionospheric loss: dissipative mechanisms.

TOTAL IONOSPHERIC LOSS, GAMMA (DECIBELS), AS A FUNCTION OF LOSS FACTOR, K, AND ELEVATION ANGLE, BETA		LOSS FACTOR (DECIBELS)											
ELEV ANGLE (DEG)		0.062	0.125	0.250	0.500	1.000	2.000	4.000	8.000	16.000	32.000	64.000	71.814
0.0	0.36	0.71	1.43	2.85	5.71	11.42	22.84	45.68	91.36	182.71	365.43	410.04	
5.0	0.32	0.64	1.28	2.56	5.13	10.25	20.51	41.02	82.04	164.08	328.16	368.22	
10.0	0.25	0.51	1.02	2.04	4.09	8.17	16.34	32.69	65.37	130.75	261.49	293.42	
15.0	0.20	0.40	0.81	1.62	3.23	6.47	12.94	25.87	51.75	103.49	206.98	232.26	
20.0	0.16	0.33	0.66	1.32	2.63	5.27	10.54	21.08	42.15	84.31	168.62	189.20	
25.0	0.14	0.28	0.56	1.11	2.22	4.43	8.86	17.72	35.44	70.88	141.77	159.08	
30.0	0.12	0.24	0.48	0.96	1.91	3.83	7.66	15.31	30.62	61.24	122.49	137.44	
35.0	0.11	0.21	0.42	0.85	1.69	3.38	6.77	13.53	27.06	54.12	108.25	121.46	
40.0	0.09	0.19	0.38	0.76	1.52	3.05	6.09	12.18	24.37	48.73	97.47	109.37	
45.0	0.09	0.17	0.35	0.70	1.39	2.79	5.57	11.14	22.29	44.58	89.15	100.04	
50.0	0.08	0.16	0.32	0.65	1.29	2.58	5.17	10.35	20.66	41.33	82.66	92.75	
55.0	0.08	0.15	0.30	0.61	1.21	2.42	4.85	9.69	19.38	38.77	77.55	87.02	
60.0	0.07	0.14	0.29	0.57	1.15	2.30	4.60	9.19	18.38	36.76	73.53	82.50	
65.0	0.07	0.14	0.27	0.55	1.10	2.20	4.40	8.80	17.60	35.19	70.38	78.97	
70.0	0.07	0.13	0.27	0.53	1.06	2.12	4.25	8.50	16.99	33.98	67.97	76.27	
75.0	0.06	0.13	0.26	0.52	1.03	2.07	4.14	8.27	16.55	33.09	66.18	74.27	
80.0	0.06	0.13	0.25	0.51	1.01	2.03	4.06	8.12	16.24	32.48	64.96	72.89	
85.0	0.06	0.13	0.25	0.50	1.00	2.01	4.01	8.03	16.06	32.12	64.24	72.08	
90.0	0.06	0.13	0.25	0.50	1.00	2.00	4.00	8.00	16.00	32.00	64.00	71.81	

should be evaluated at the ray path elevation angle,  $\beta$ . Formulas for the reflection coefficients can be found in standard texts on electromagnetics.\*

Large and, generally, unforecastable anomalous increases in loss are associated with two types of solar event [6, 7, 8].

Solar flares release intense bursts of x-rays which cause "sudden ionospheric disturbances" (SID's). The consequence is a large increase in absorption loss on the entire sunlit side of the earth. The effects last up to an hour and can be catastrophic. It is, perhaps, some small consolation that if such a condition prevents delivery of a jamming signal it also probably prevents delivery of the communication signal.

Streams of charged particles emitted by the sun during solar flares are, at times, intercepted by the earth. The particles are guided by the geomagnetic field toward the auroral zones. Absorption is increased, especially in the neighborhood of the auroral and polar regions. Over much of the earth F-region critical frequencies may be reduced. In some cases a 27-day recurrence period is evident as solar rotation brings storm centers having extended life into view repeatedly.

#### 2.3.7 The Polarization Problem

In discussing the complex index of refraction of a magneto-plasma (subsection 2.2.1), the birefringent property of the medium was pointed out. It is manifest in the sign ambiguity which appears in both the Appleton-Hartree equations, the dispersion equation and the polarization equation. The concept of a characteristic wave polarization was introduced. Some justification was given for ignoring this property in the calculation of ray path parameters. It is not possible to ignore it in a discussion of the polarization of sky waves. Sky wave polarization is important because of its role in wave interaction with the antennas at the path terminals.

When a wave of arbitrary polarization is present at some point in the ionosphere it can be decomposed into two components, each of which is one of the characteristic waves. Because the index of refraction of the two components (characteristic waves) is not the same, each wave goes its own way, so to speak. The two trajectories can diverge significantly. At every point along its trajectory each characteristic wave adjusts its

---

\*E.g., Jordan, E. C., Electromagnetic Waves and Radiating Systems, Prentice-Hall, 1950; 5.07-5.13.

polarization state to that required by the medium parameter values and wavefront direction at that point. The characteristic polarization depends only on the values of the medium parameters and the wavefront direction at a point and not at all on how the wave got to that point. If the amount which medium parameter values change in a free space wavelength is not too great, and if losses are not too great, the characteristic waves travel with a high degree of independence.

Consider what happens along a pair of characteristic wave trajectories, both of which span the same two terminal points. Suppose that the polarization of the wave radiated by the source is arbitrary.

As the wave from the source enters the ionosphere, its power density is divided into two parts, each of which contributes to the establishment of one of the characteristic waves appropriate to the point and direction of entry. Without additional information, the splitting ratio cannot be determined. The splitting principle is that at some stage in the entry process,\* the two characteristic waves must exist in such amounts that their sum matches the incident wave. Depending on the polarization of the incident wave, the split may range from 100% one way to 100% the other way. If, for the incident wave, all polarization states are equally probable, there is analytical justification for asserting that, "on the average," the split is 50/50. Thus, on the average, each of the characteristic waves established is likely to have an intensity 3 dB below that of the wave incident from the source.

As the characteristic waves leave the ionosphere toward the other end of the trajectory, the birefringent property vanishes. The two waves become a single composite wave.\*\* In a manner like to that on entry, the strength and polarization state of the exiting wave must, at some stage in the exit process, match the sum of the characteristic waves from which it is composed. The relative phase of the two characteristic waves on exit depends on the difference between the phase path lengths of the two characteristic wave trajectories. Because the trajectories are long (measured in wavelength units), the difference may have any value. If the two characteristic waves suffer the same loss, then, on average, they will combine to form an exiting wave with arbitrary polarization.

---

\*The details of the splitting process are still a matter for some conjecture [2].

\*\*Single because all components travel at the same velocity. Composite because the two characteristic waves may not be moving in the same direction on exit.

The pot is further stirred by the dynamic time-varying character of the medium. The phase path lengths of the two characteristic wave trajectories, and their difference, vary with time.\* Thus, without specific situational details, the polarization of the exiting wave cannot be determined. On the average, the state of wave polarization on exit bears no deterministic relationship to that on entry. All states of exit polarization must be considered equally probable. On the average, the ionosphere must be considered a perfect random depolarizer.\*\*

The power which an antenna can extract from a wave incident at a specified wavefront normal direction depends on the polarization state of the wave relative to that polarization state which is characteristic of the antenna for that direction of wavefront normal. If all states of wave polarization are equally probable, then, on the average, an antenna characterized by any fixed single state of polarization will extract one half of the power which could be extracted from a wave of the same power density having a polarization which matched that characteristic of the antenna.

The simplest procedure for handling the polarization problem is to reduce the receiving antenna power gain,  $G_r$ , by the factor 2.0 (subtract 3 dB from  $g_r$ ). It must be kept in mind that the factor 2.0 is correct only "on the average." The true factor can range from 1.0 to  $\infty$  (subtract 0.0 dB to  $\infty$  dB), and is a time-varying quantity on a scale of seconds.

Note that the gain of the antennas ( $G, g$ ) is a function of the elevation angle,  $\beta$ .\*\*\* Thus, the gain values to use in Equation 2-37 are those for the ray trajectory elevation angle,  $\beta$ .

---

\*Interference of this sort among waves having time-varying phase properties is the major cause of the rapid forms of sky wave intensity fading.

\*\*In a more elaborate analysis, specific situations can be defined in which the exit polarization can be specified (it still bears no relationship to the entry polarization). For example, such cases can arise from differential absorption between characteristic waves (note the  $\pm$  in the factor  $\omega \pm |\omega_L|$  in some formulas given in Table 2-1) or from selective elimination of one of the characteristic waves near the skip contour (subsection 2.2.2). If, however, geomagnetic orientation and geographic location of the trajectory and the operating frequency are not specified and fixed, the stated conclusion is justified.

\*\*\*It is also, of course, a function of azimuthal orientation.

## 2.4 ATLAS OF ELECTRON DENSITY PROFILE MODELS AND ASSOCIATED TRANSMISSION DIAGRAMS

There is presented in this section an atlas of material which is associated with the geometrical properties of ray trajectories.

There is a set of twelve electron density profile models. The electron density profile determines the refractive index profile. In concert with the ray elevation angle,  $\beta$ , and the operating frequency  $f$ , it determines trajectory shape. With each profile there is given the synthetic ionogram derived from it. Curves are shown on the ionogram for both real and virtual height of reflection.

From each profile model several transmission diagrams have been derived. Each shows both the angle/range curve from which the hearability function,  $\Gamma_h$ , is evaluated and the loss/range curve which is the evaluation of the divergence loss,  $\gamma_d$ . The operating frequencies used for deriving transmission diagrams have been selected after inspection of the synthetic ionogram. Usually, the frequency sequence includes a member representative of each regime or region exhibited in the ionogram. In one case (Ident. Symb. 010WINDAY) additional frequencies have been included in the sequence to illustrate behavior at or near critical points of the ionogram.

Table 2-7 is a guide to the atlas. It defines the twelve cases presented, gives the symbols by which graphs related to each can be identified, gives profile model parameters, and lists the frequency sequences for which transmission diagrams have been derived. In the first column of the table, under model parameters, the parameters for the  $\alpha$ -Chapman function representing each level are identified. Then, for the sum of the functions, the resulting critical frequencies are identified. The latter are not quite the same as the individual level critical frequencies because of function overlap.

The graphs are arranged in the atlas in the order given by the columns in the table. They are not assigned individual figure numbers, but can be identified by the symbol (e.g., 100WINNIT) appearing on each. See, for example, the legend data in Figure 2-8.

The purpose of the atlas is to illustrate the salient regular phenomena which are exhibited by the sky wave. Enough range of variation is included to illustrate day/night, summer/winter, and solar activity differences.

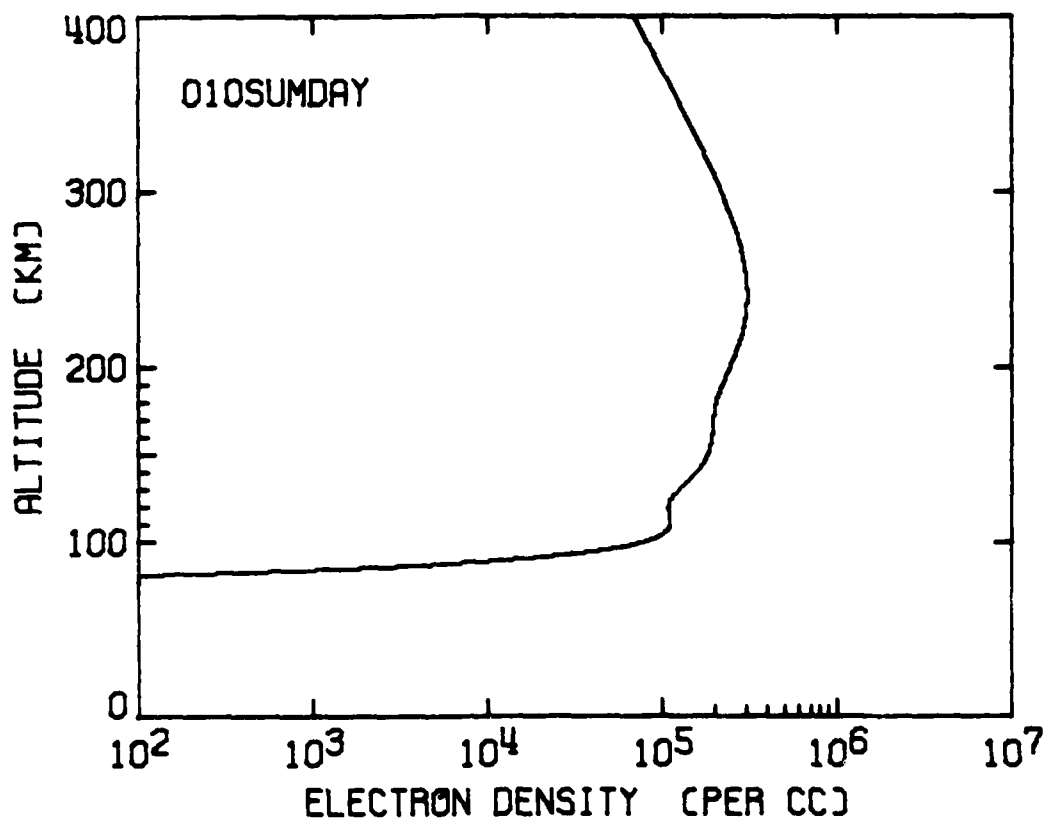
The atlas does not constitute a complete forecasting system for  $\Gamma_h$  and  $\gamma_d$ . For example, it does not show behavior for enough hours in the day, nor months in the year. It shows nothing of the geographic variability which exists. However, given an adequate data base of ionospheric characteristics, the principles used to produce the atlas could be developed into a forecast estimation system. Alternatively, given concurrent local empirical ionospheric data, the same principles could be developed into a real-time estimation system.

Table 2-7. Guide to atlas of electron density profiles and related transmission diagrams.

CASE →	R12=010				R12=100				R12=200			
	SUMMER		WINTER		SUMMER		WINTER		SUMMER		WINTER	
	DAY	NITE	DAY	NITE	DAY	NITE	DAY	NITE	DAY	NITE	DAY	NITE
Ident.	010	010	010	010	100	100	100	100	200	200	200	200
Symb.	SUM	SUM	WIN	WIN	SUM	SUM	WIN	WIN	SUM	SUM	WIN	WIN
	DAY	NIT	DAY	NIT	DAY	NIT	DAY	NIT	DAY	NIT	DAY	NIT
Ionosphere Profile Model Parameters												
Level 1.												
$h_o$	110	150	110	150	110	150	110	150	110	150	110	150
H	10	15	10	15	10	15	10	15	10	15	10	15
$f_o$	2.95	0.30	2.40	0.30	3.30	0.40	2.80	0.40	3.80	0.50	3.30	0.50
Level 2.												
$h_o$	160				167				177		160	
H	20				25				30		25	
$f_o$	3.65				4.40				5.00		3.10	
Level 3.												
$h_o$	250	325	210	275	300	350	250	300	375	400	325	350
H	40	55	40	40	60	65	55	50	90	85	70	65
$f_o$	4.70	4.00	5.40	3.00	6.00	5.25	9.90	4.00	7.40	6.50	14.40	5.00
Sum												
$f_o1$	3.0		2.5		3.5		3.0		4.0		3.5	
$f_o2$	4.0				4.75				5.5			
$f_o3$	5.0	4.0	5.5	3.0	6.25	5.25	10.0	4.0	7.5	6.5	14.5	5.0
Transmission Diagrams (Operating Frequency)												
1	2.0	2.0	2.0	2.0	2.5	2.5	2.25	2.5	3.0	3.0	2.5	3.0
2	3.5	3.5	2.3	3.5	4.0	4.25	5.5	5.0	4.5	5.0	7.0	6.5
3	4.5	5.0	2.5	6.0	5.5	7.0	11.0	9.0	6.5	9.0	16.0	12.0
4	6.0		2.7		7.5							
5			4.0									
6			5.0									
7			5.5									
8			6.0									
9			10.0									

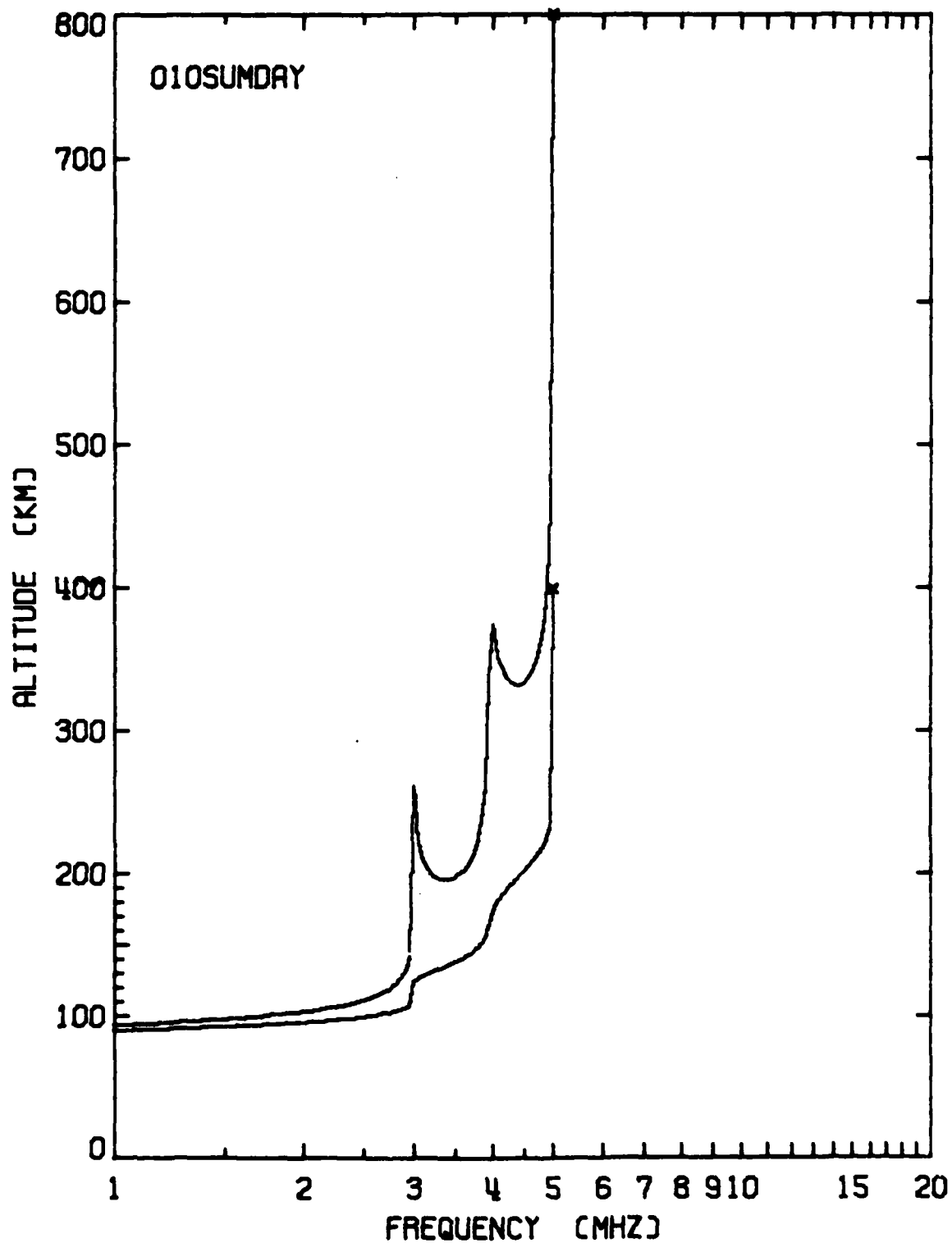
Note on units:  
 $h_o$  - km, H - km,  $f_o$  - MHz  
 Operating Frequency - MHz



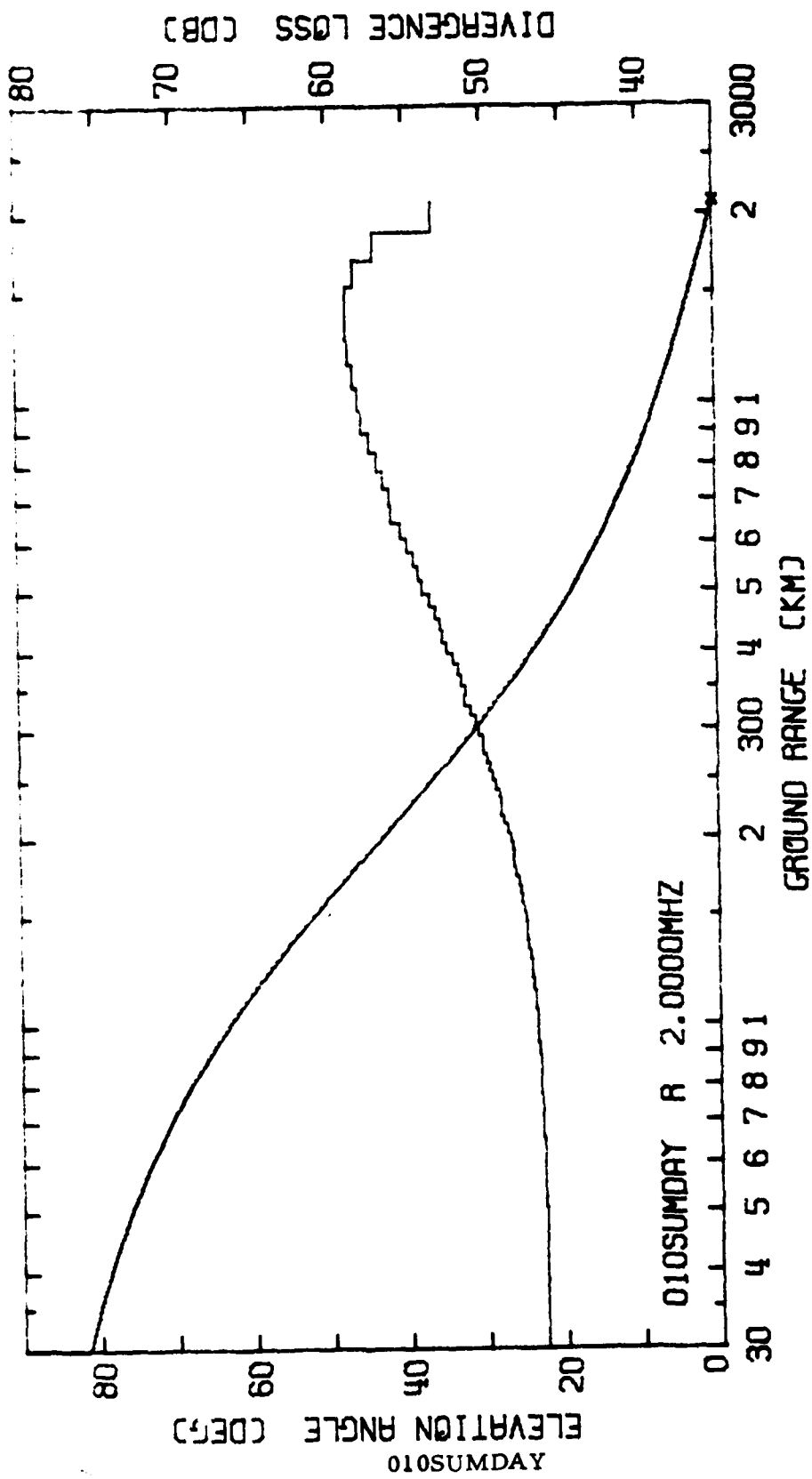


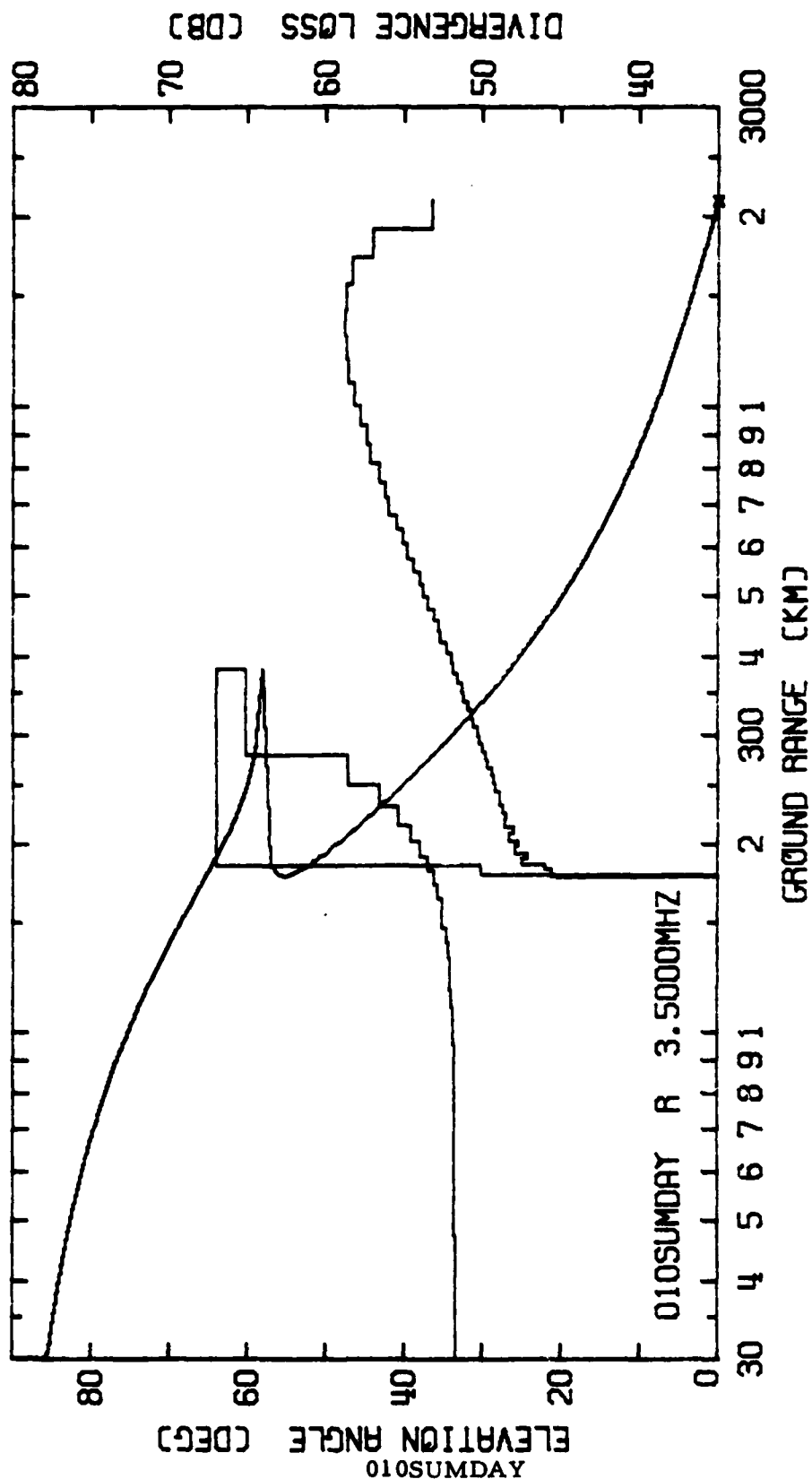
	<u>Level 1</u>	<u>Level 2</u>	<u>Level 3</u>
$h_o$ (km)	110	160	250
H (km)	10	20	40
$f_o$ (MHz)	2.95	3.65	4.70

010SUMDAY

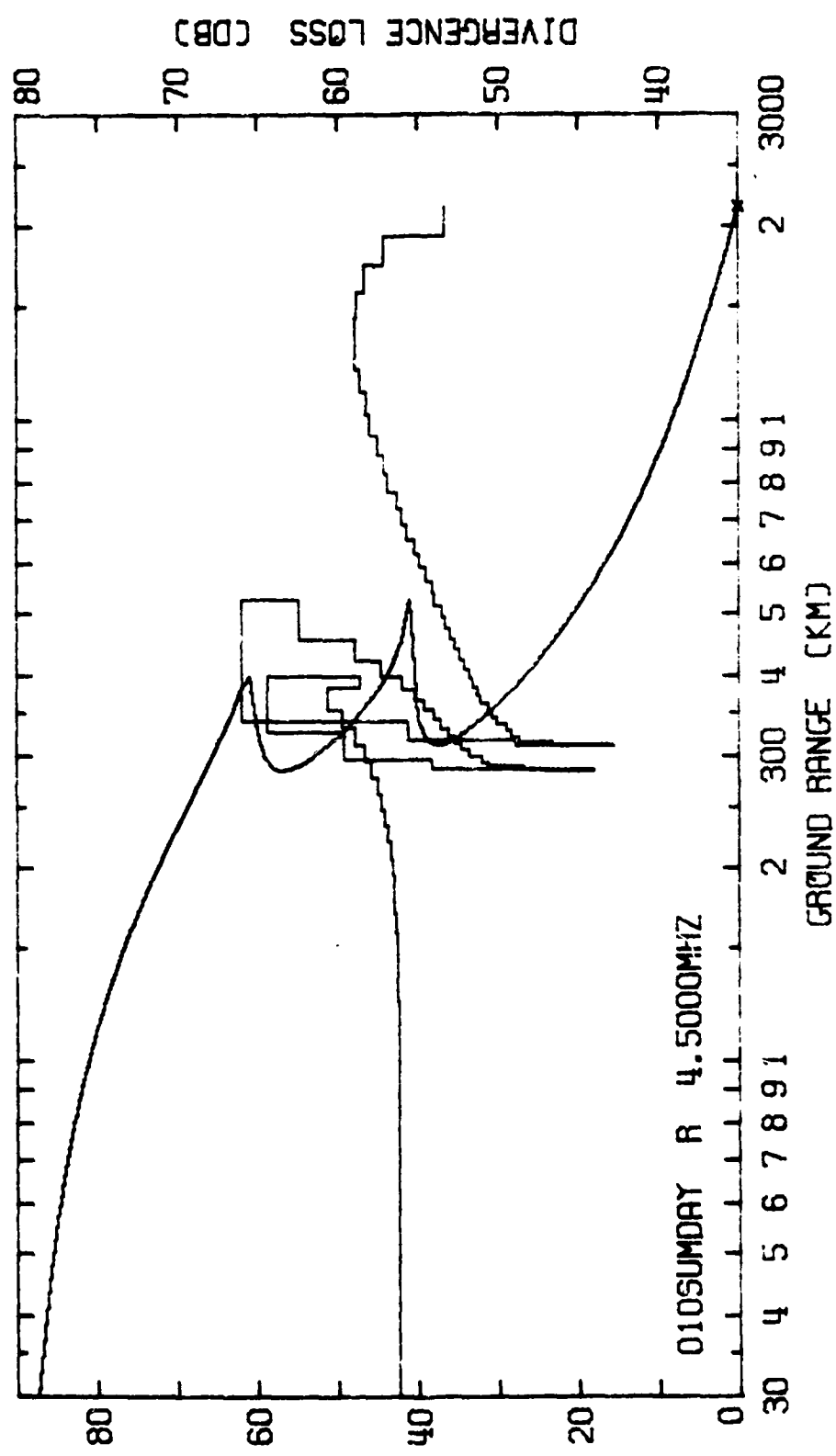


0105 SUNDAY





118  
YADSO10



ELEVATION ANGLE (DEG)

010SUMDAY

119

010SUMDAY R 6.0000MHZ

30 4 5 6 7 8 9 1

2

300

4

5

6

7

8

9

1

2

3000

GROUND RANGE (KM)

DIVERGENCE LOSS (DB)

80

70

60

50

40

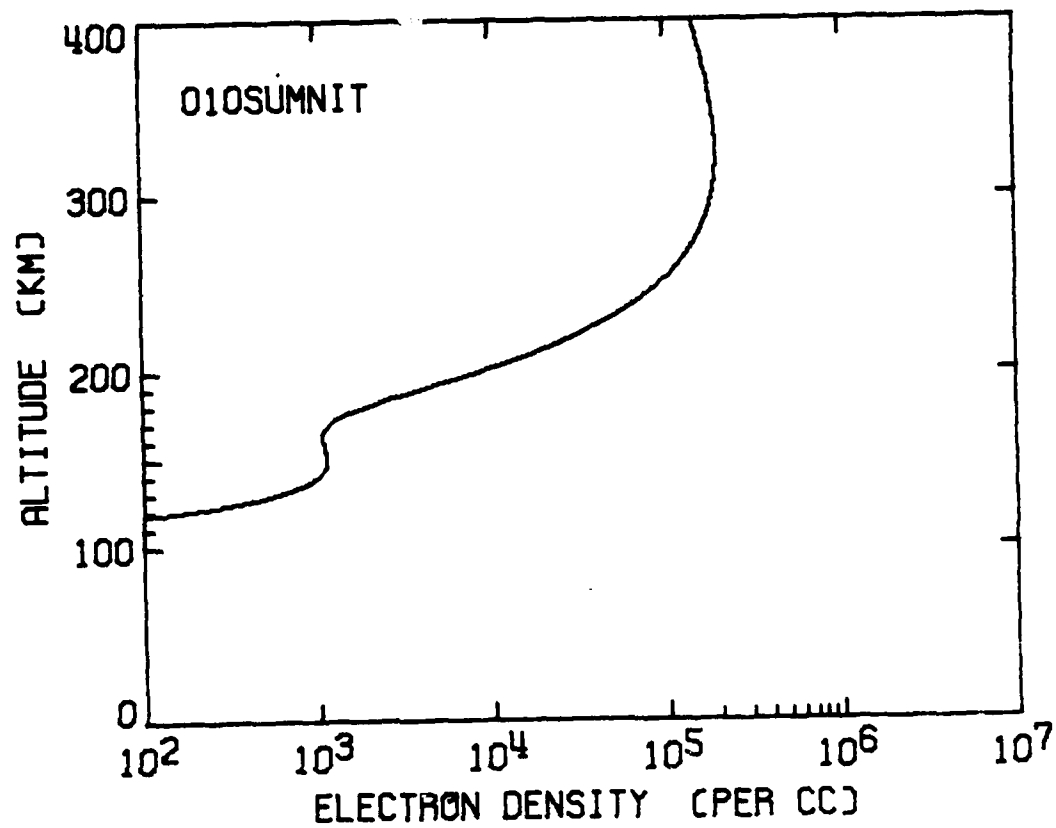
80

60

40

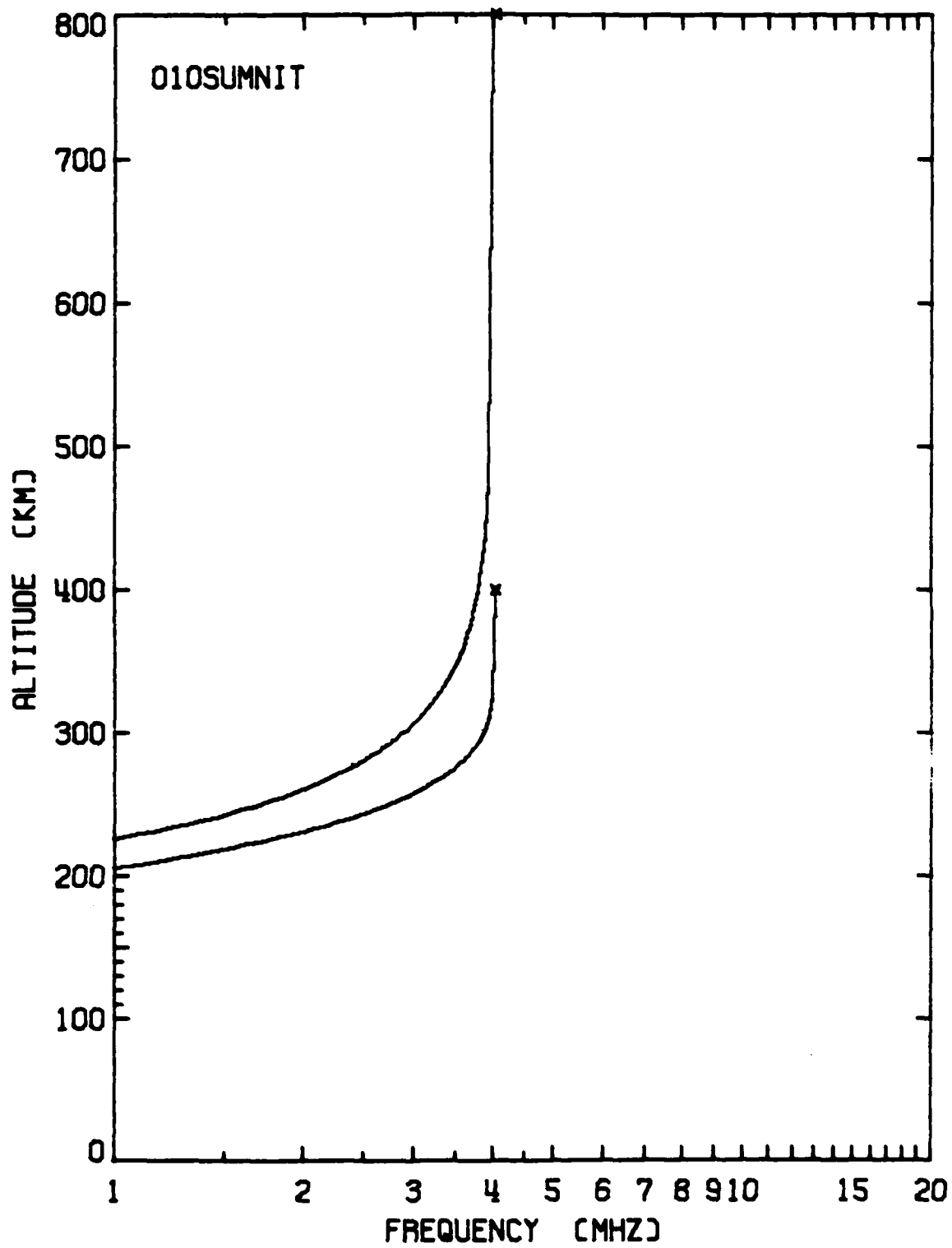
20

0



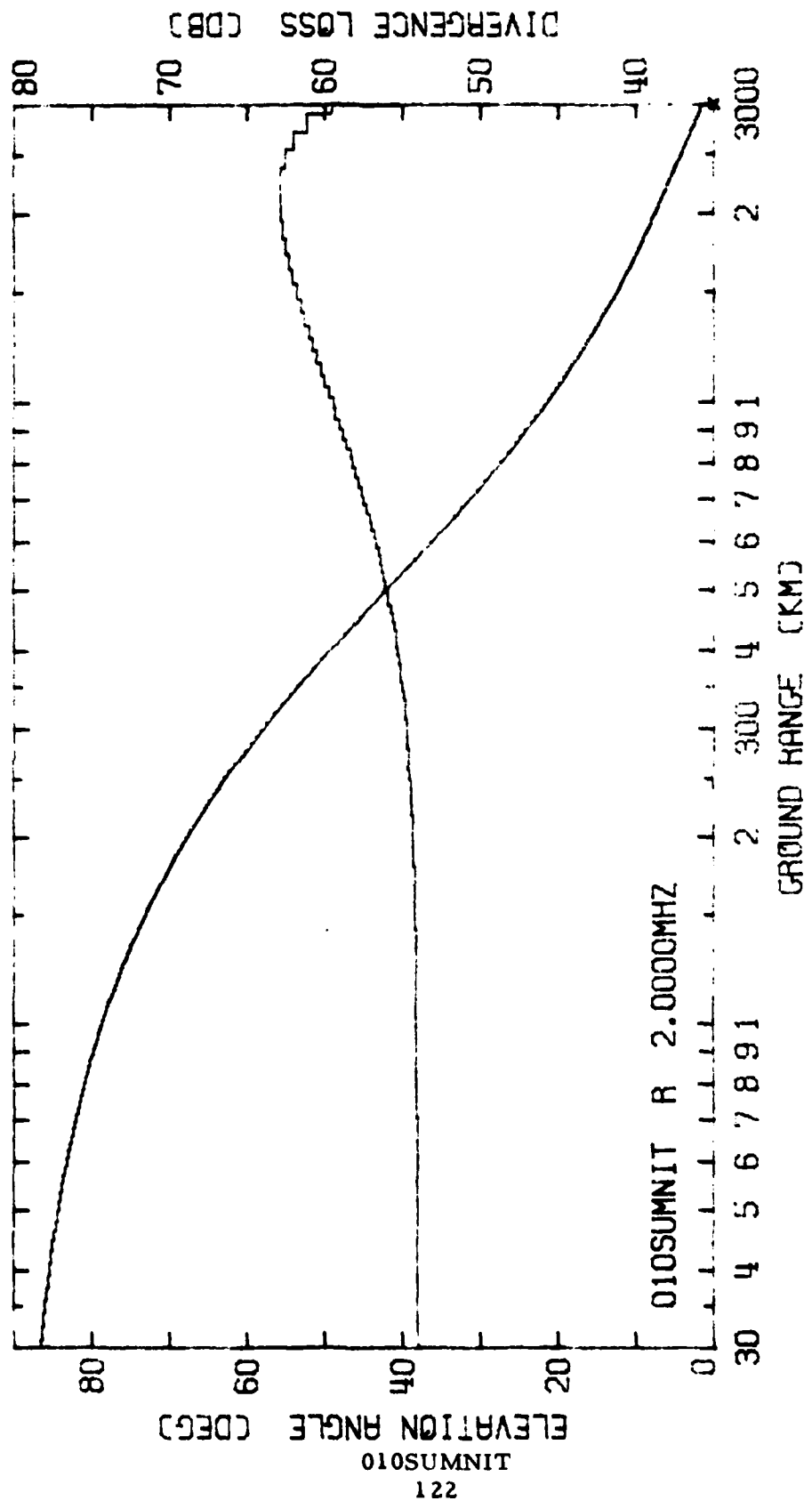
	<u>Level 1</u>	<u>Level 2</u>	<u>Level 3</u>
$h_o$ (km)	150	Absent	325
H (km)	15	Absent	55
$f_o$ (MHz)	0.30	Absent	4.00

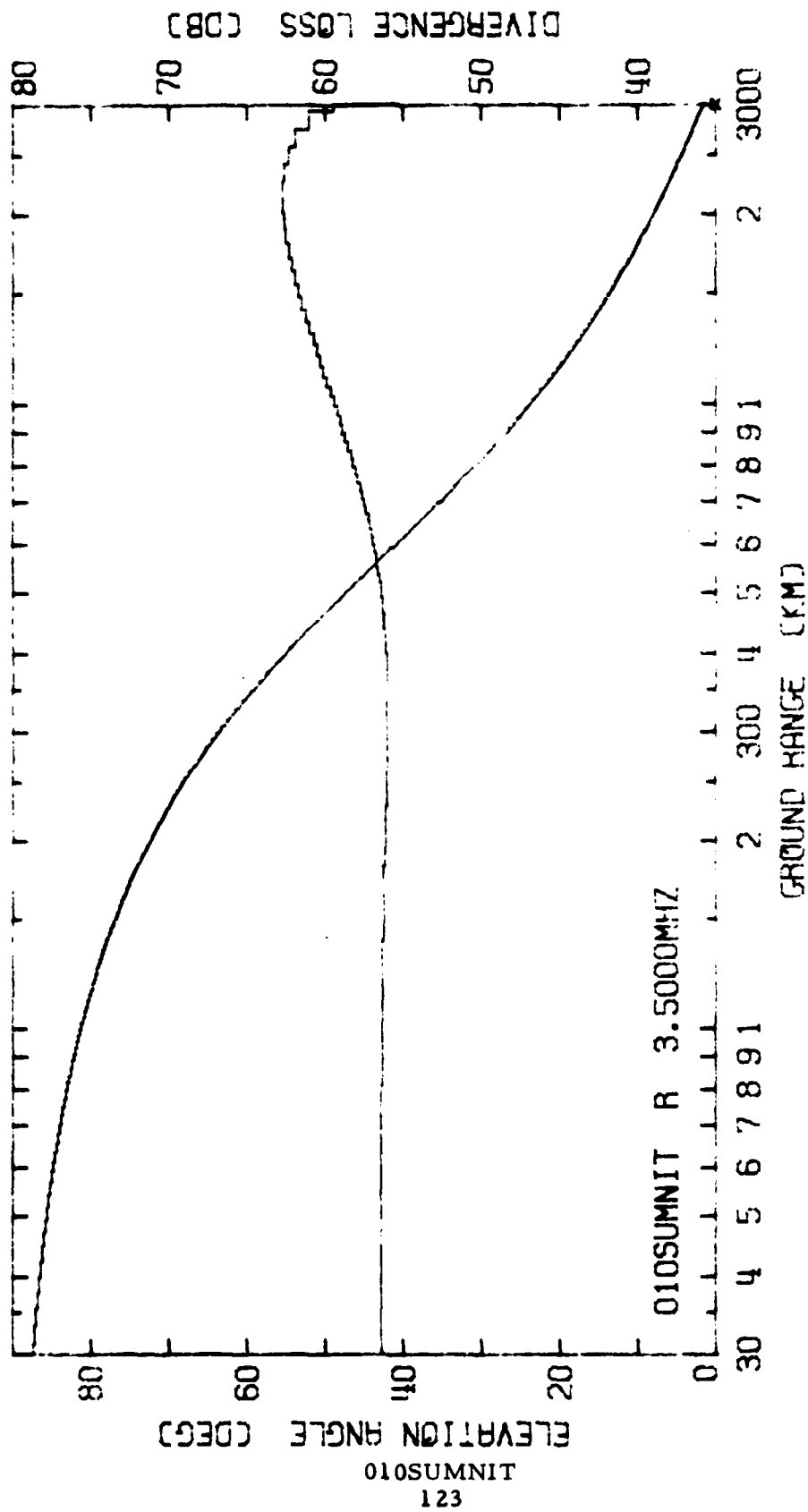
010SUMNIT

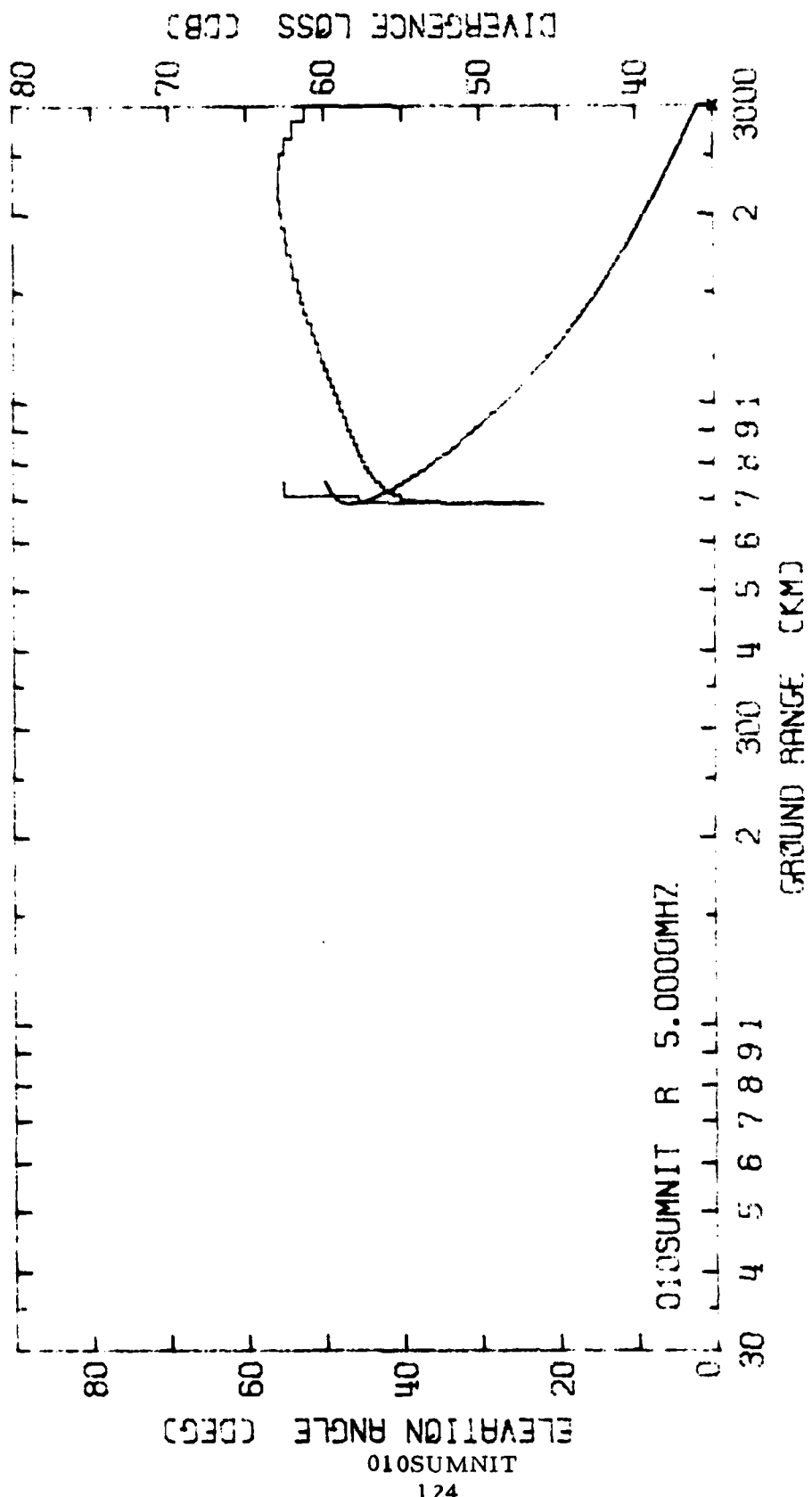


010SUMNIT  
121

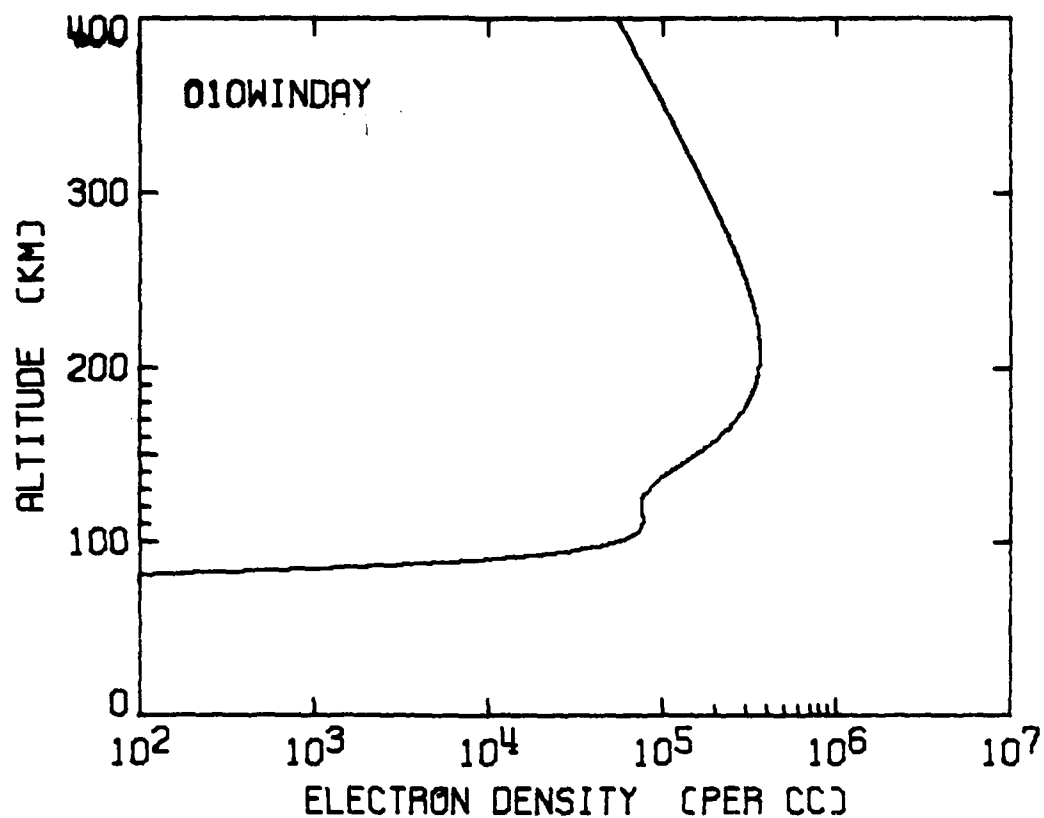




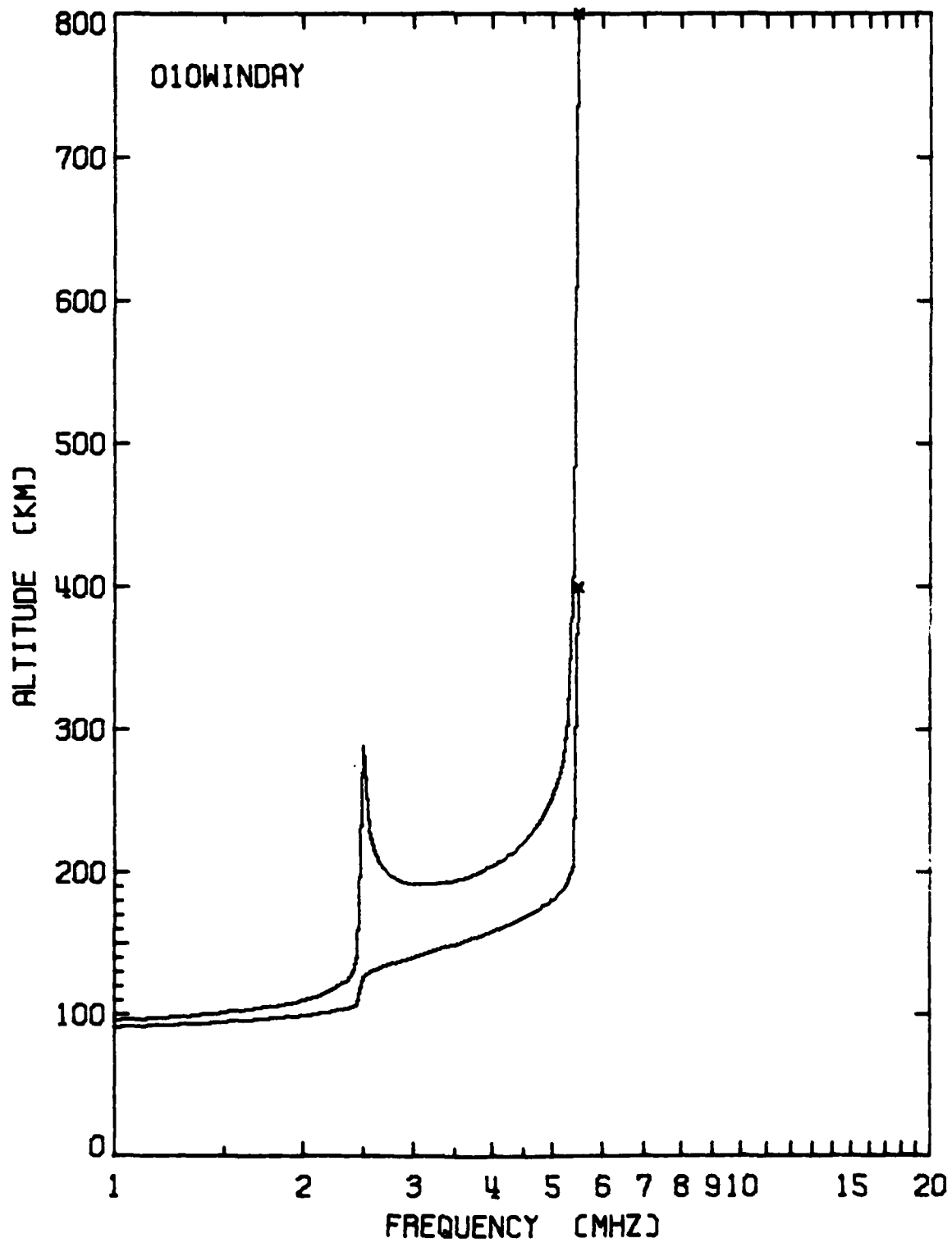




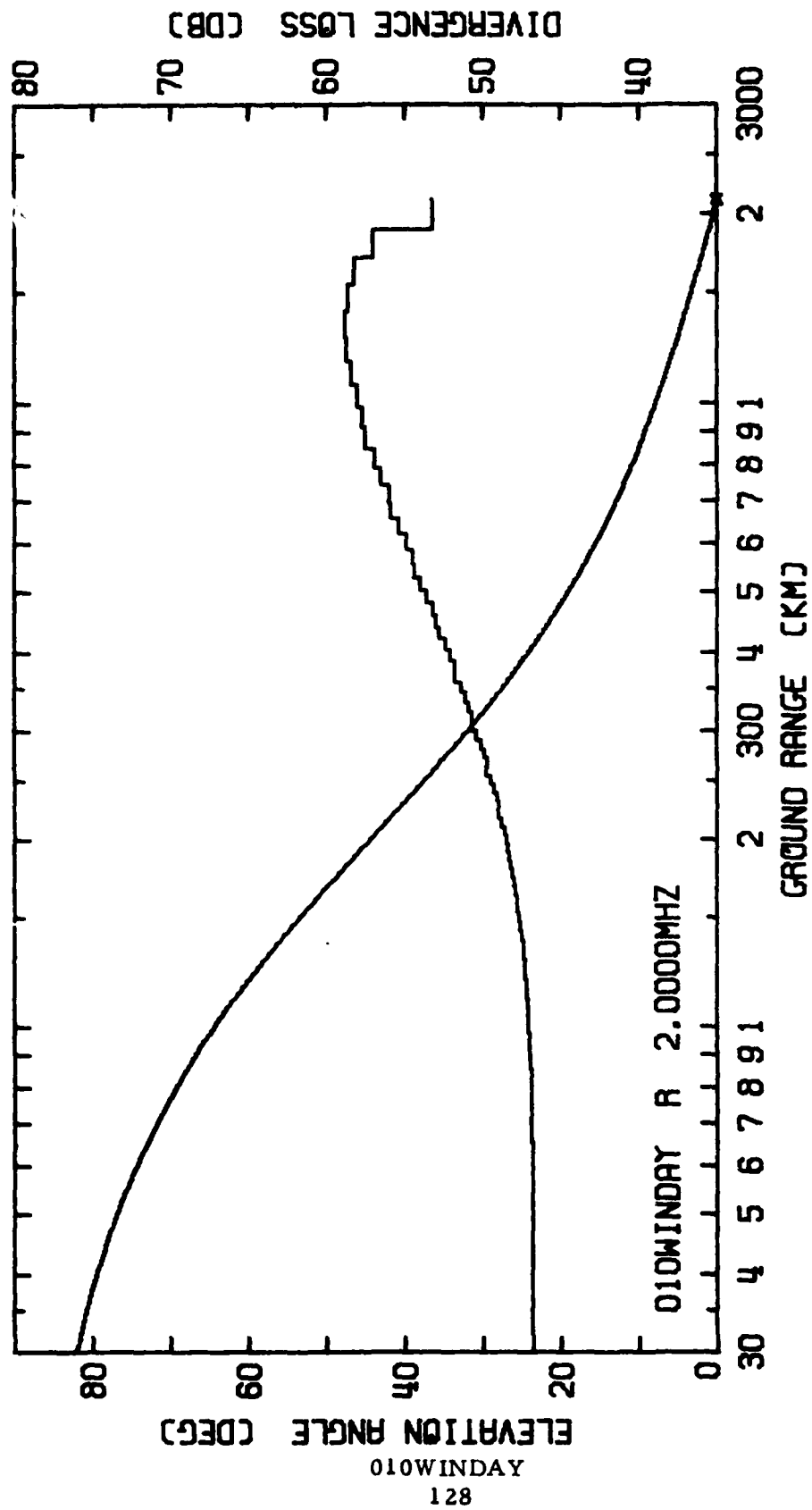
010SUMNIT  
124

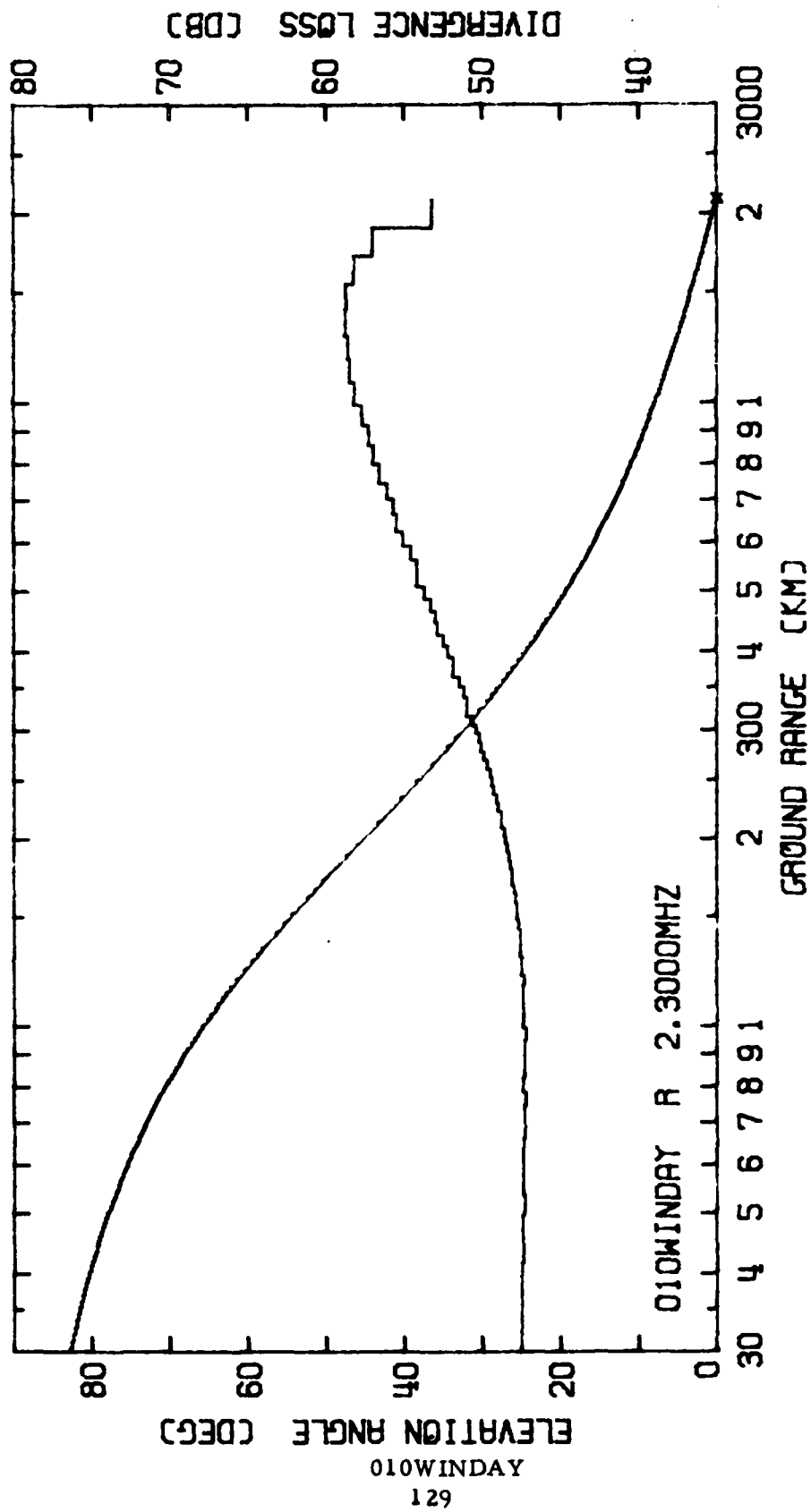


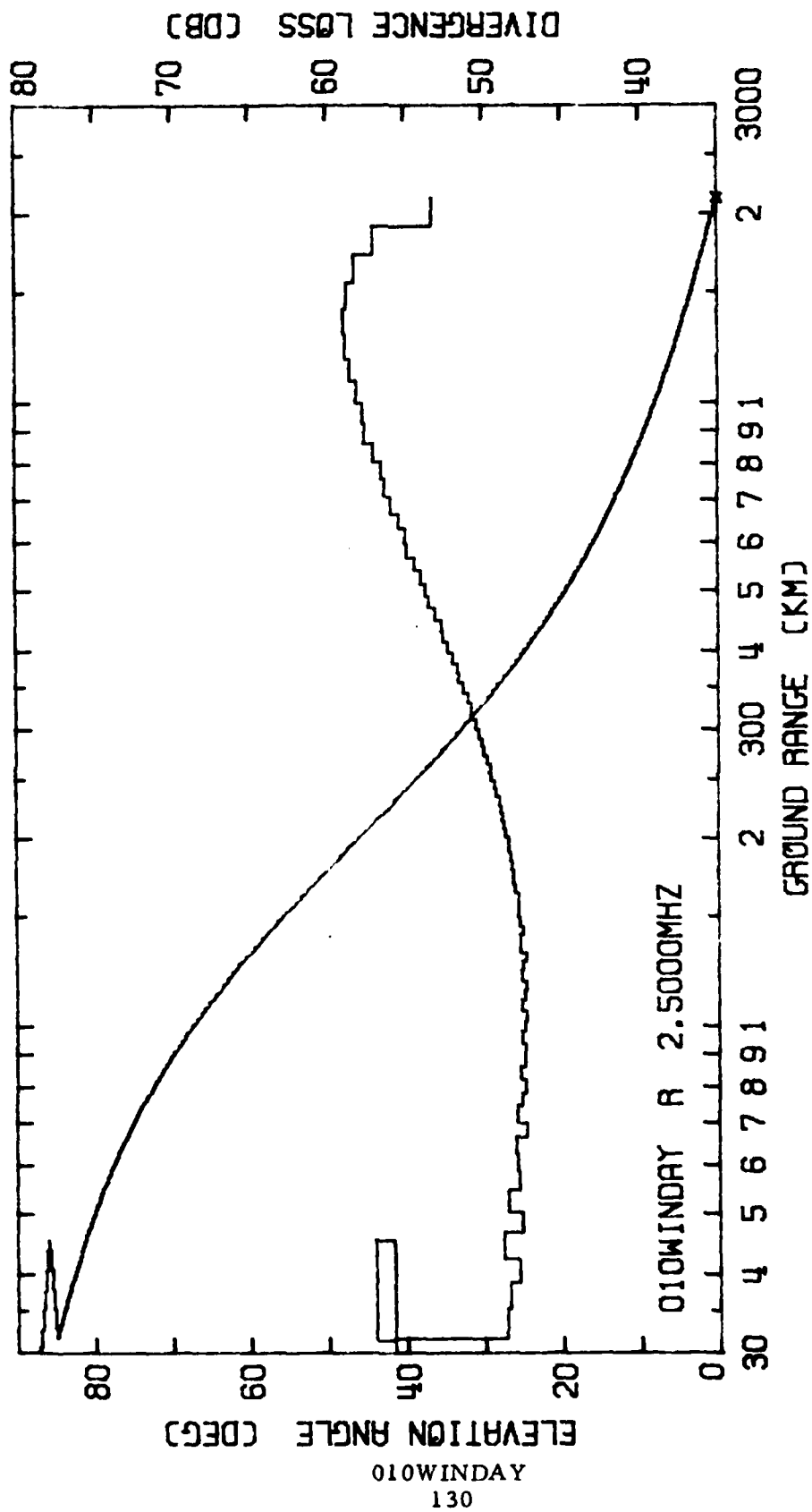
	<u>Level 1</u>	<u>Level 2</u>	<u>Level 3</u>
$h_o$ (km)	110	Absent	210
H (km)	10	Absent	40
$f_o$ (MHz)	2.40	Absent	5.40



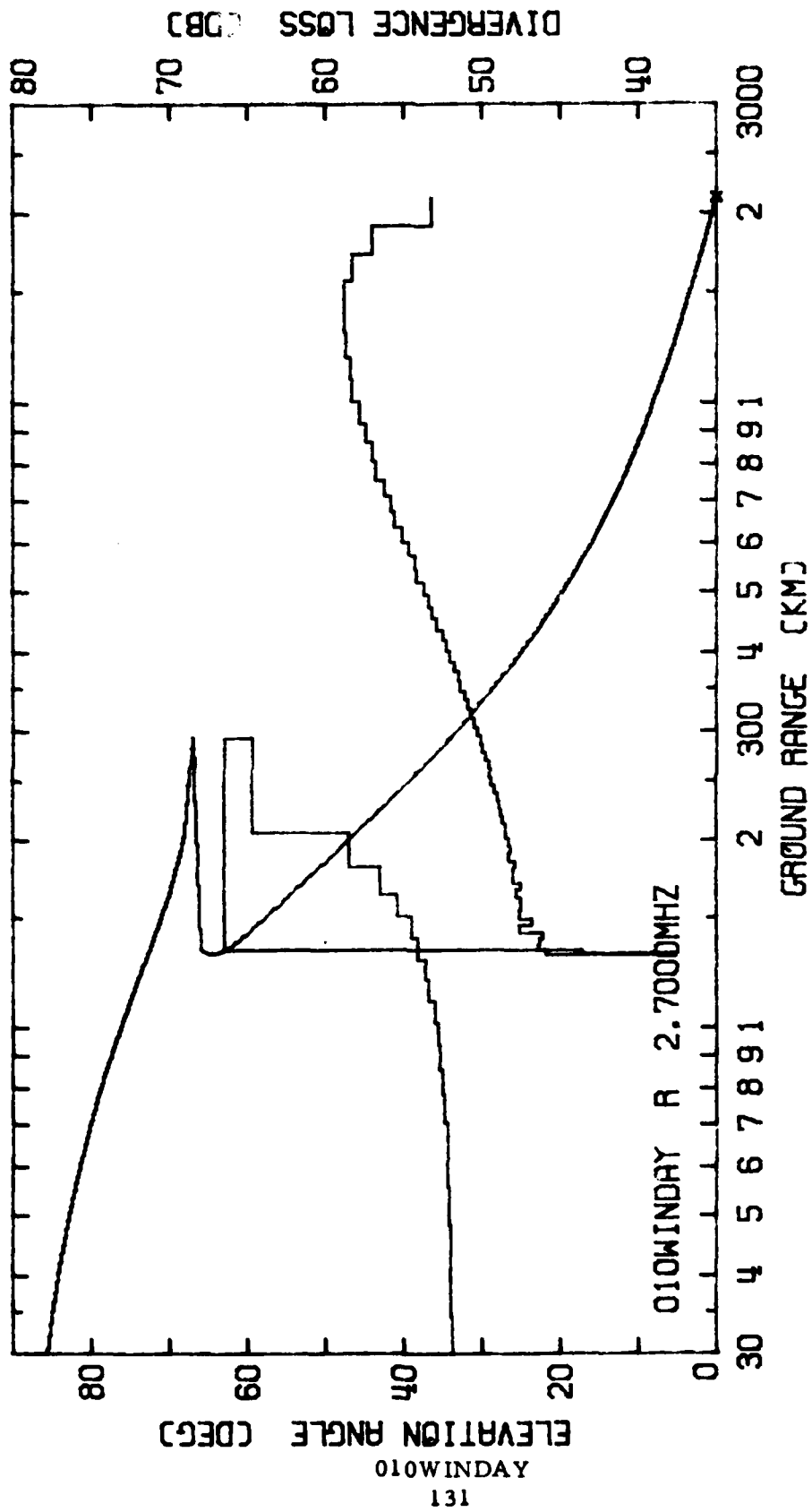
010WINDAY

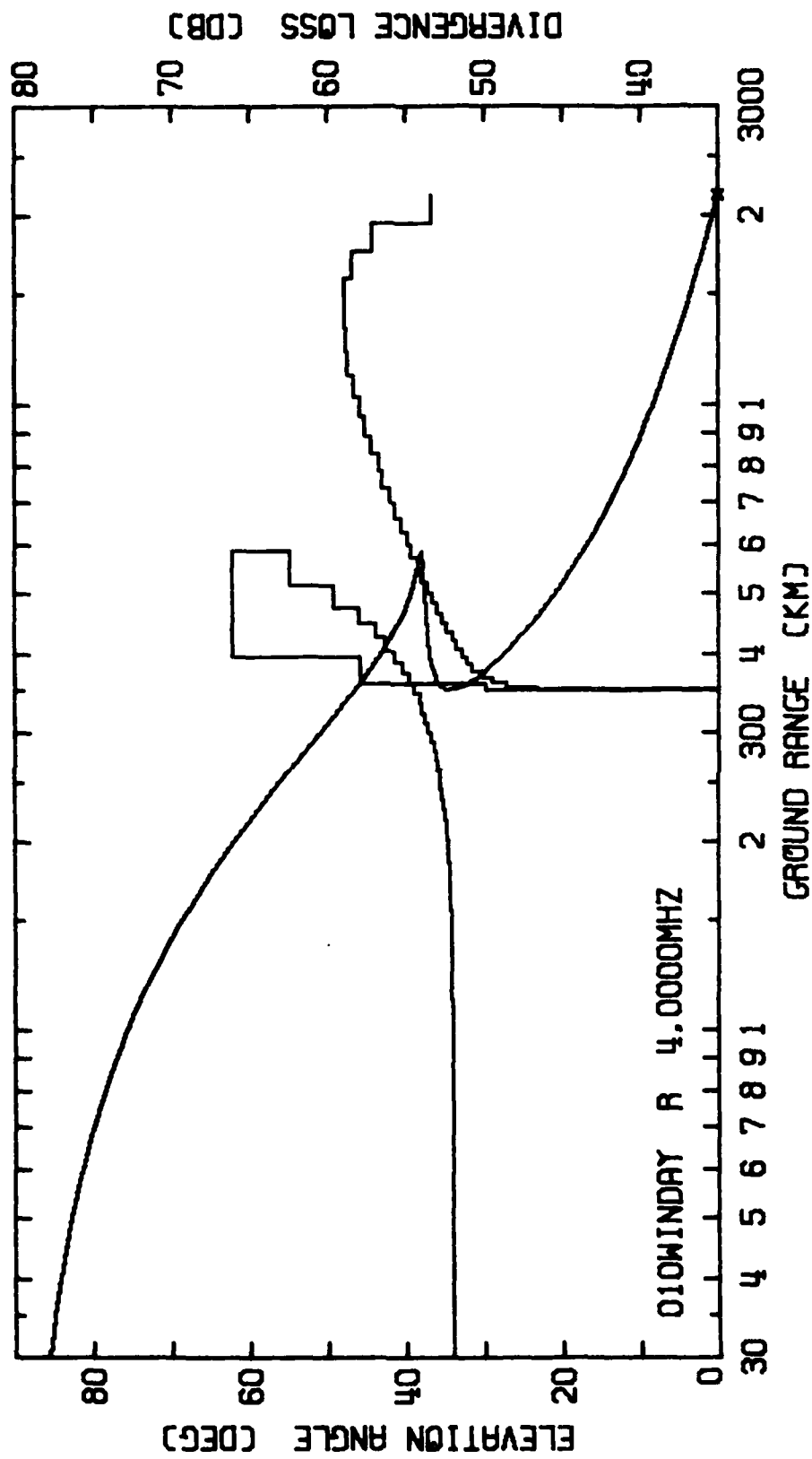




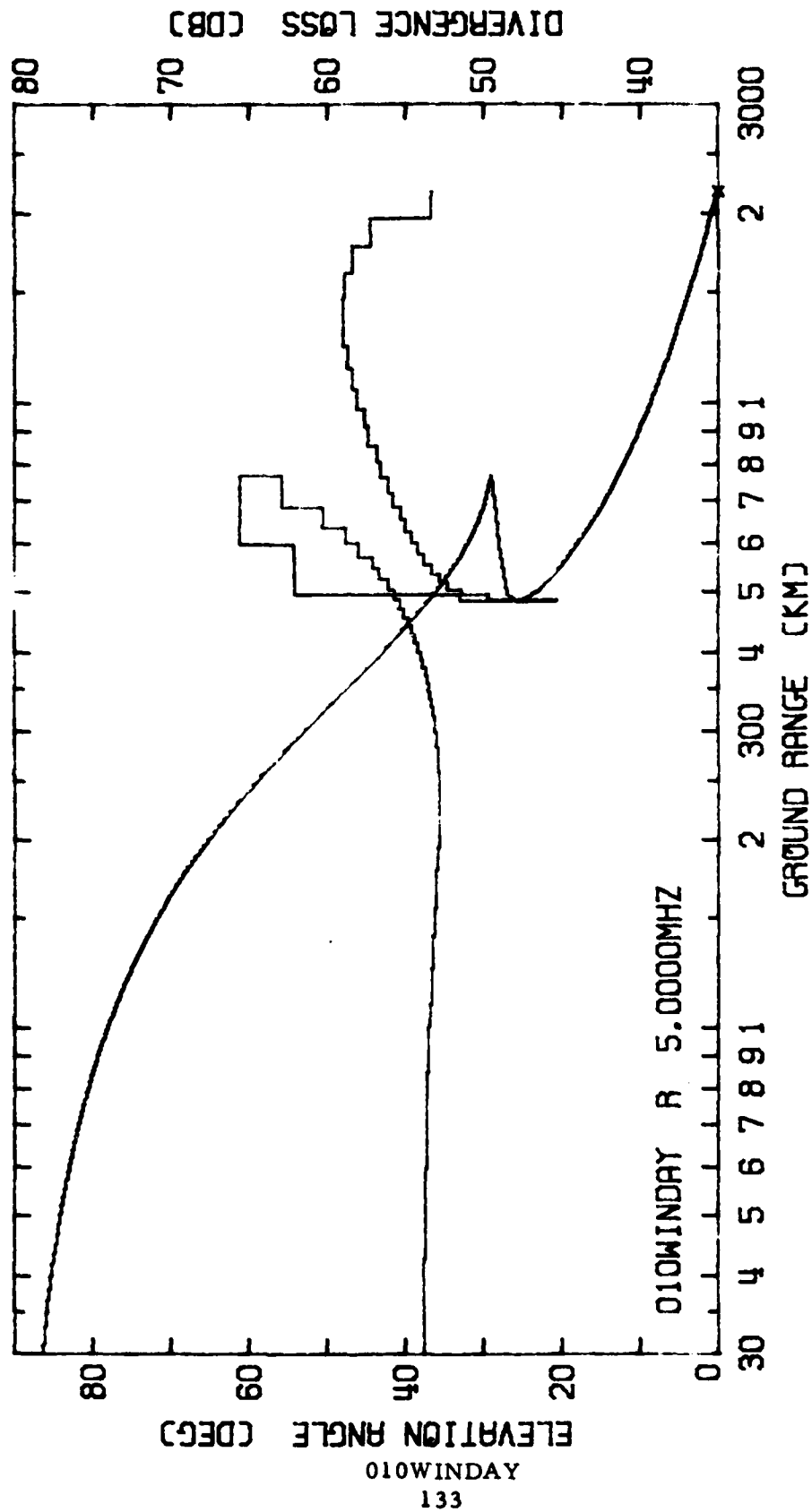


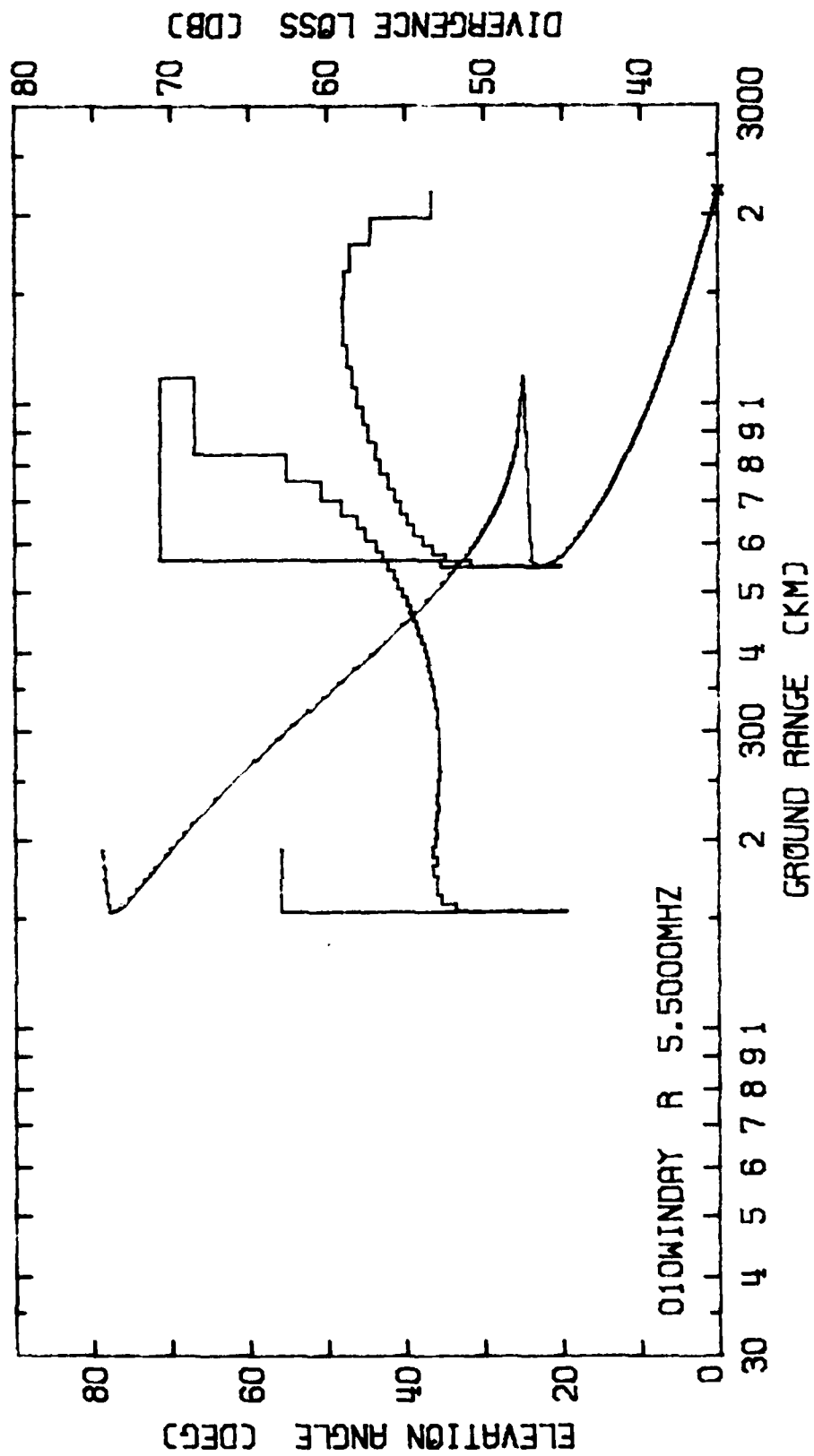




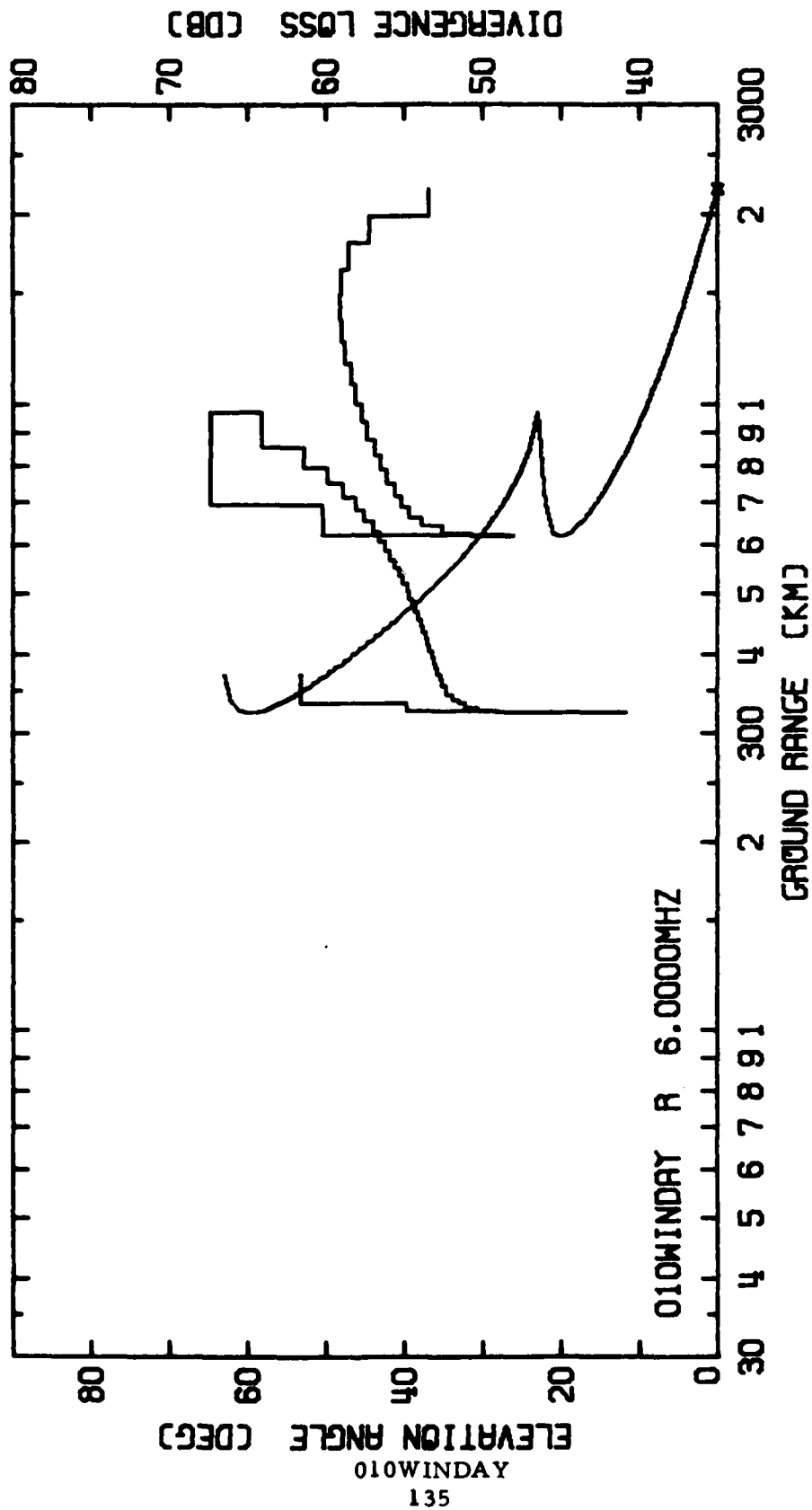


010WINDAY  
132

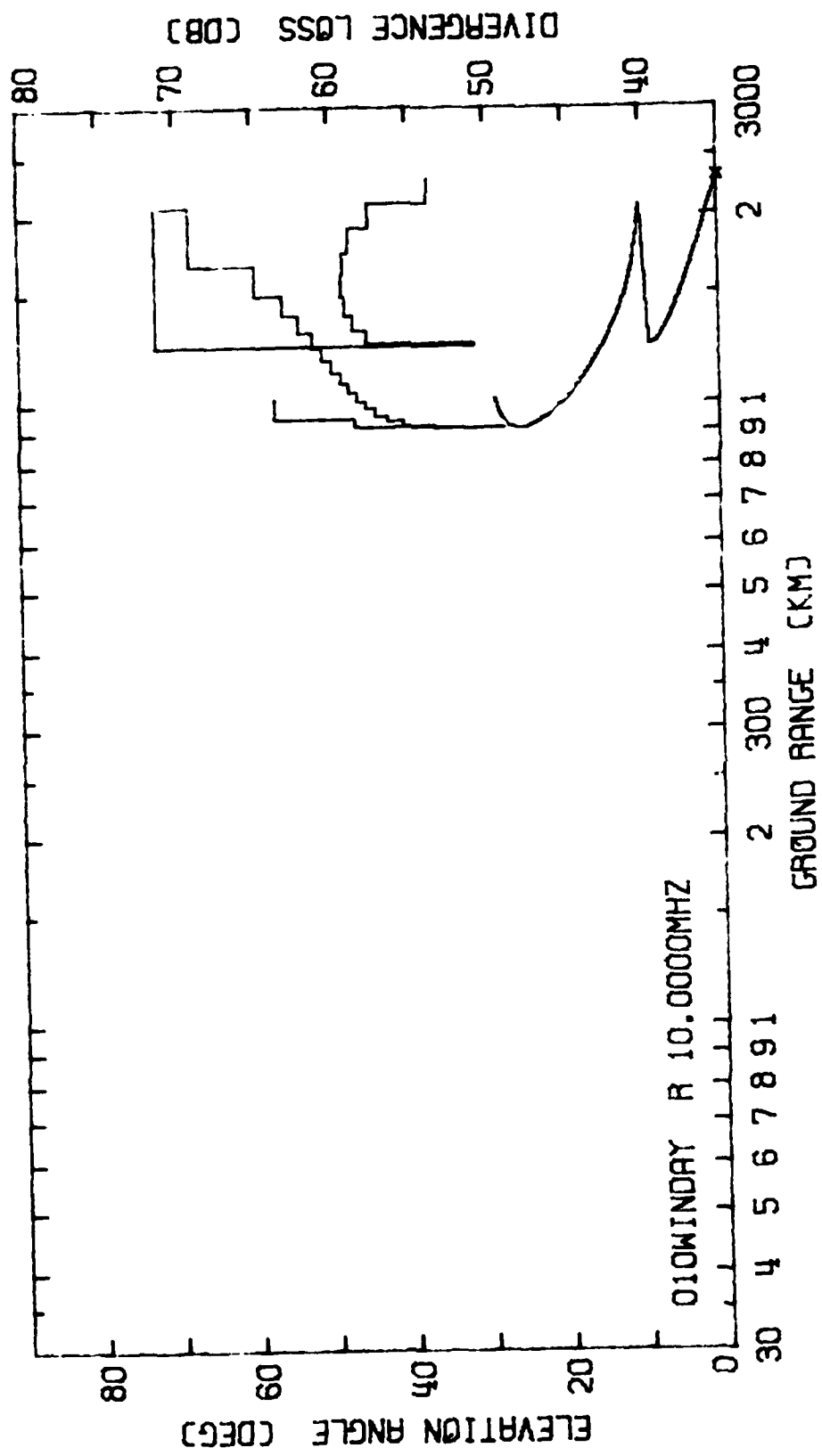


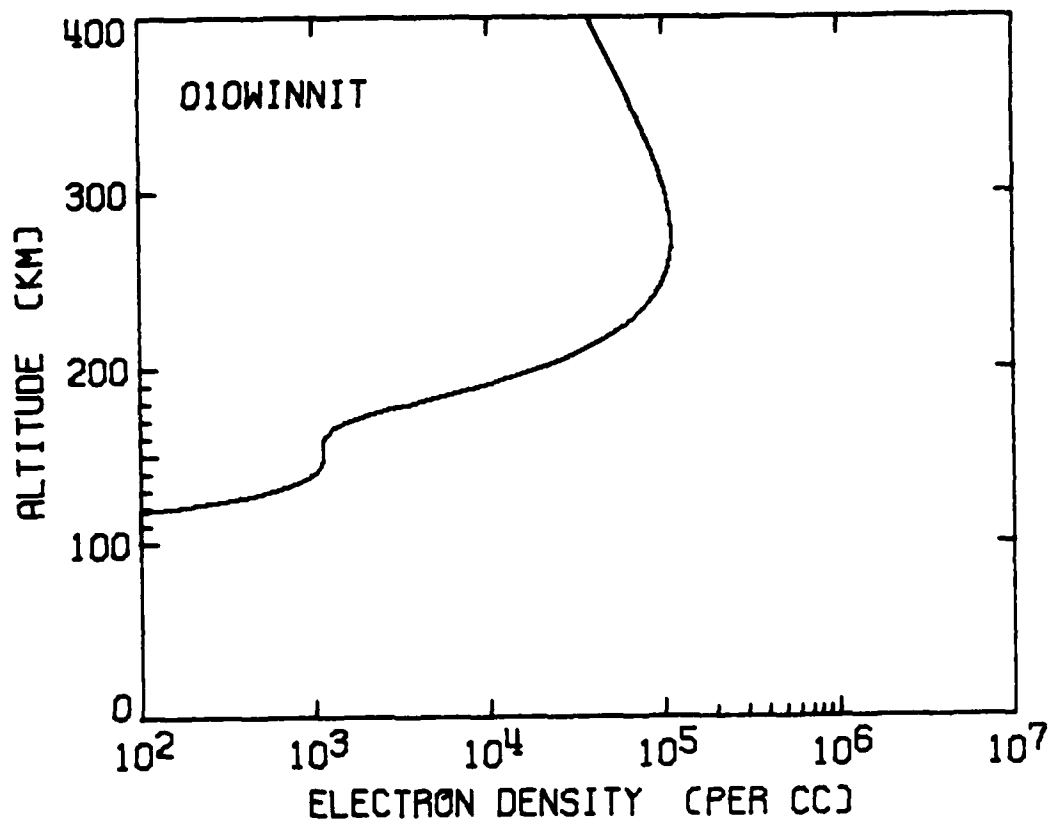


010WINDAY  
134



010WINDAY  
135

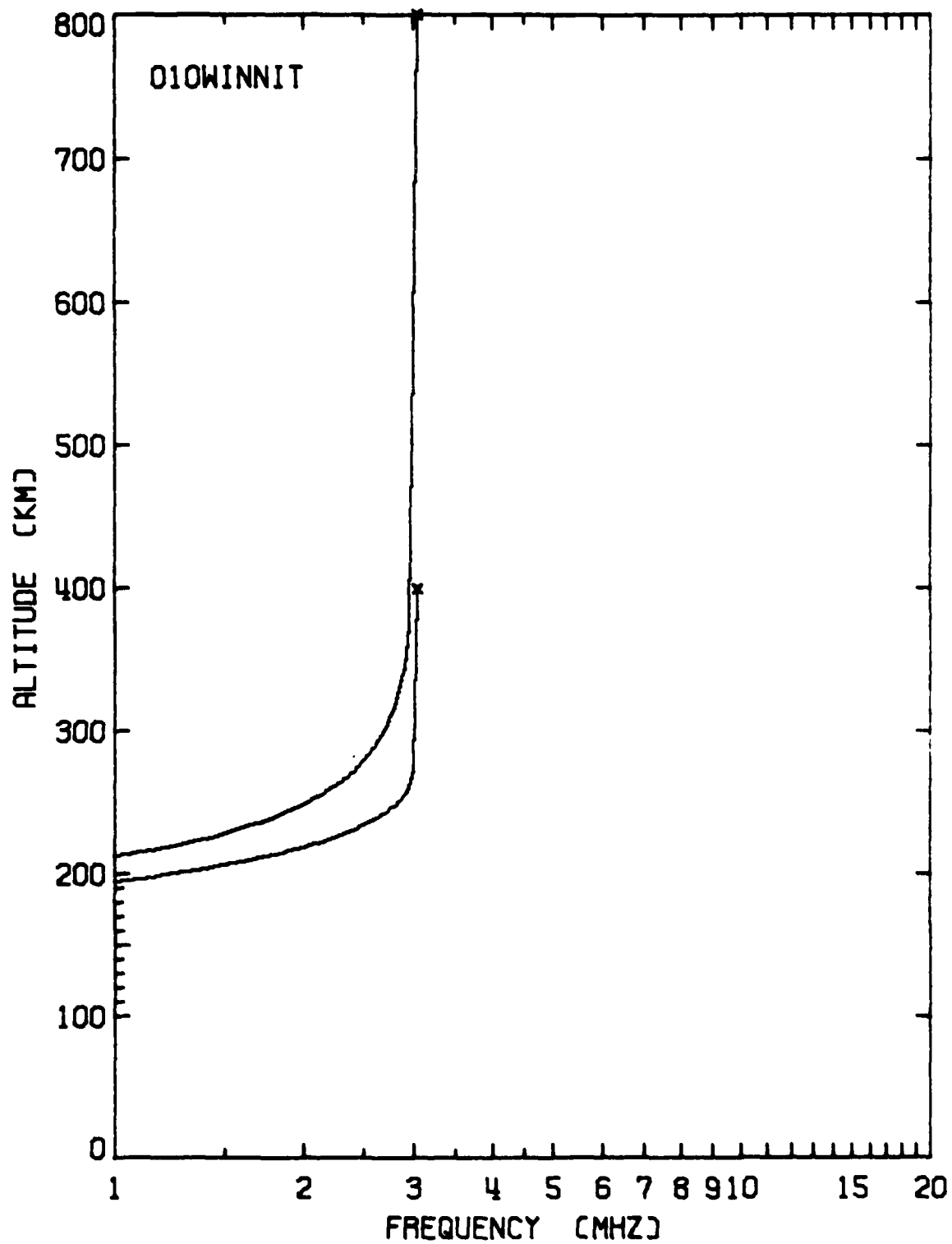




	<u>Level 1</u>	<u>Level 2</u>	<u>Level 3</u>
$h_o$ (km)	150	Absent	275
H (km)	15	Absent	40
$f_o$ (MHz)	0.30	Absent	3.00

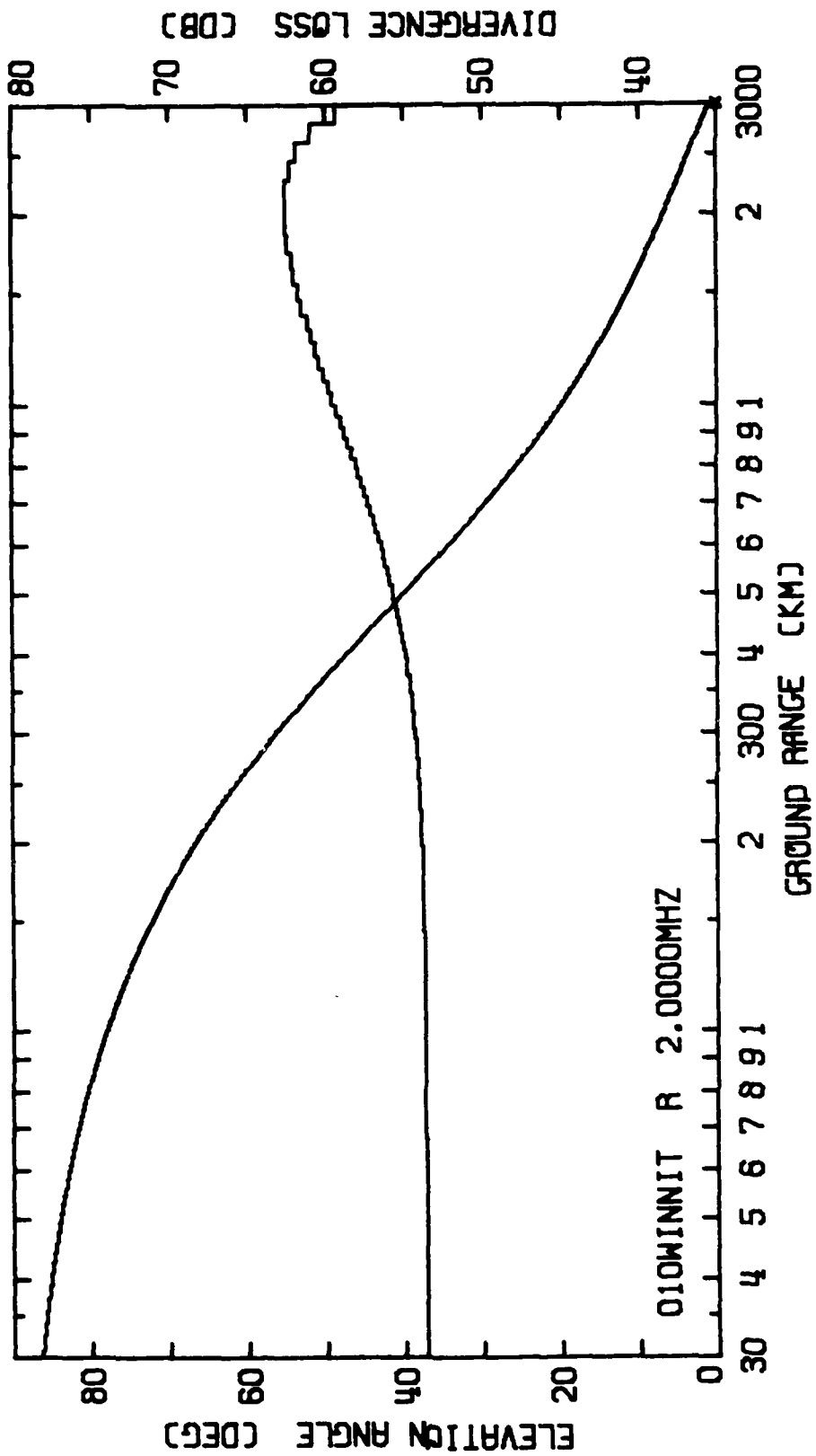
010WINNIT  
138

PROCESSING PAGE BLANK-NOT FILMED

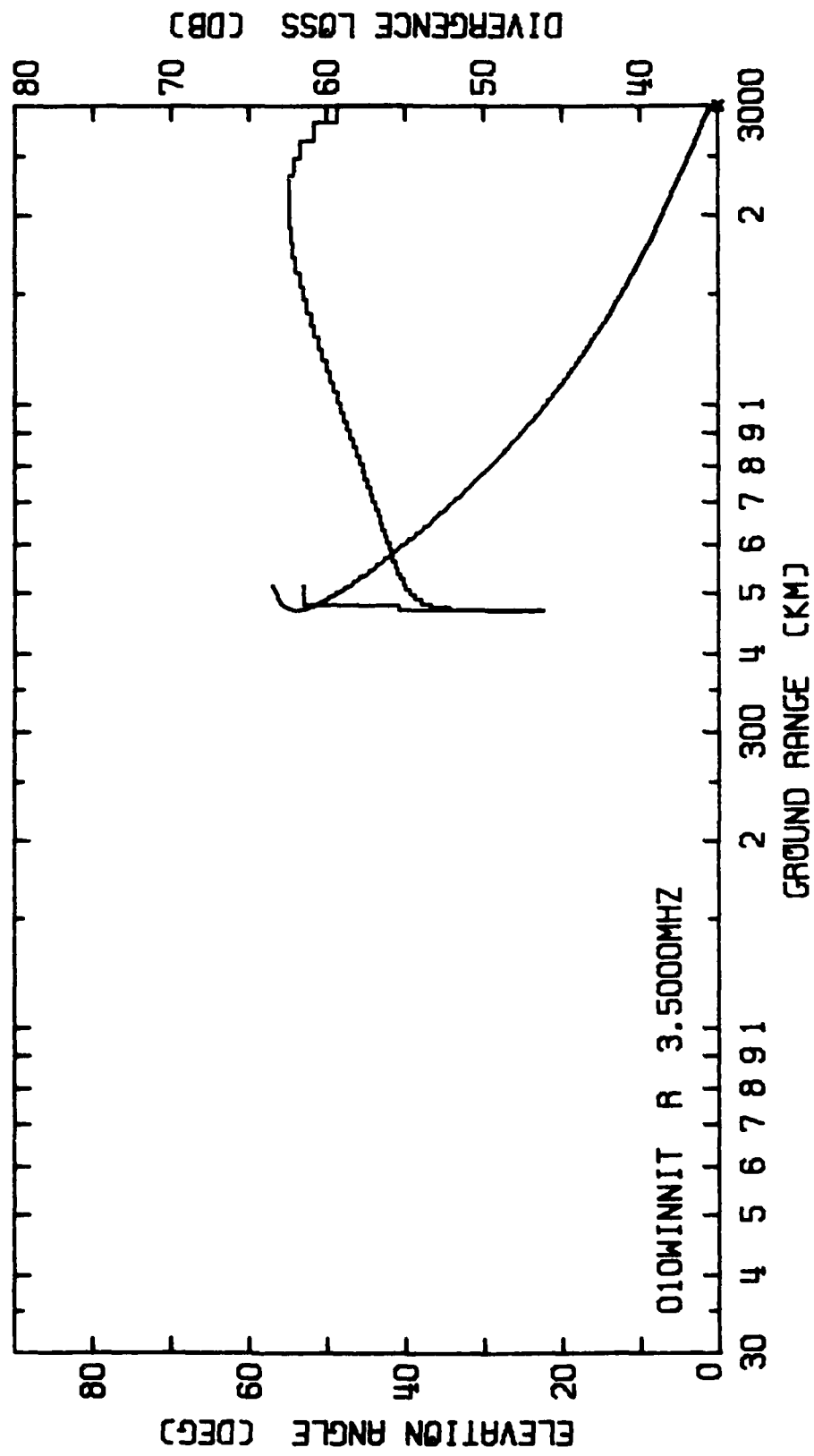


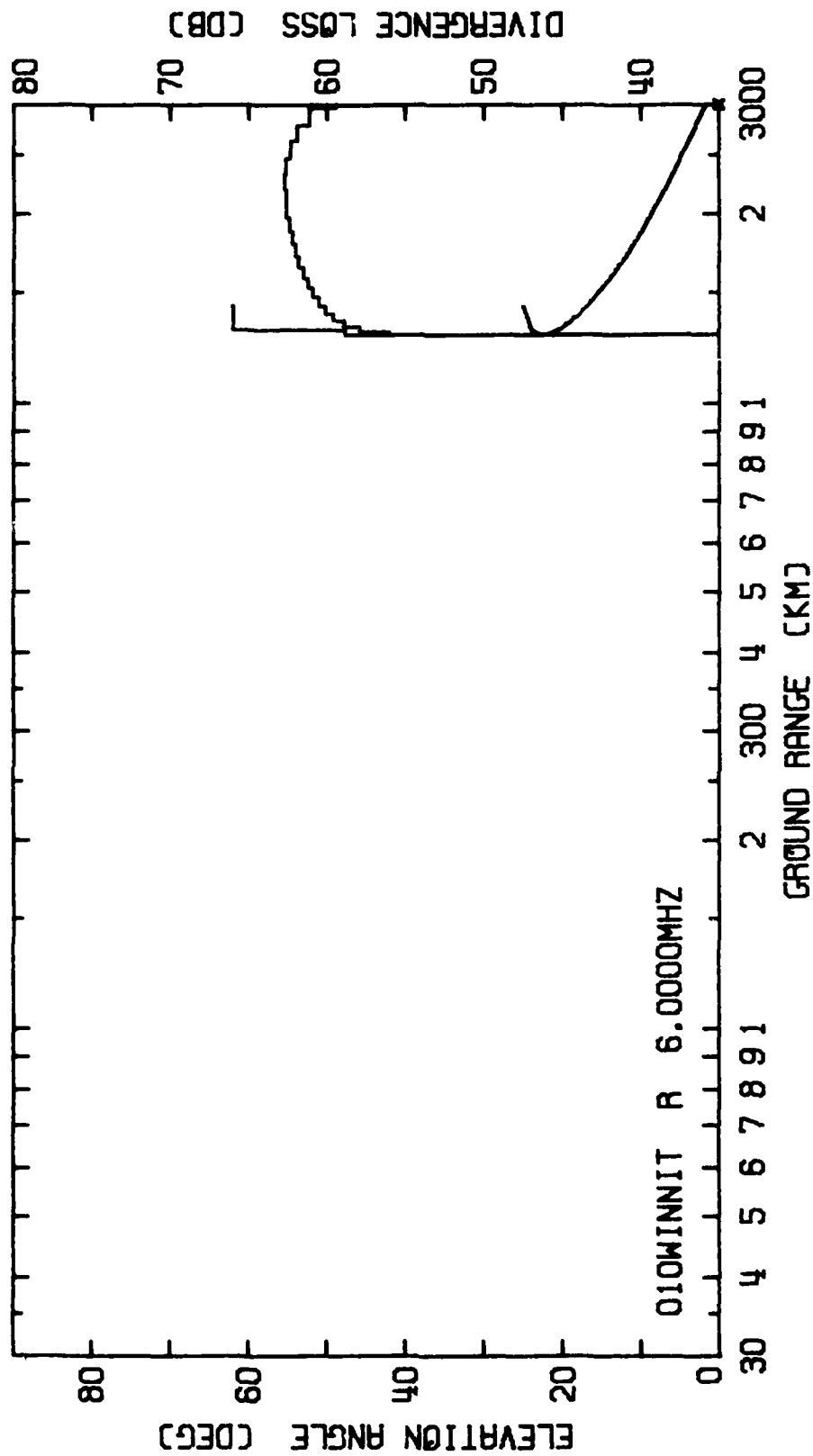
010WINNIT  
139

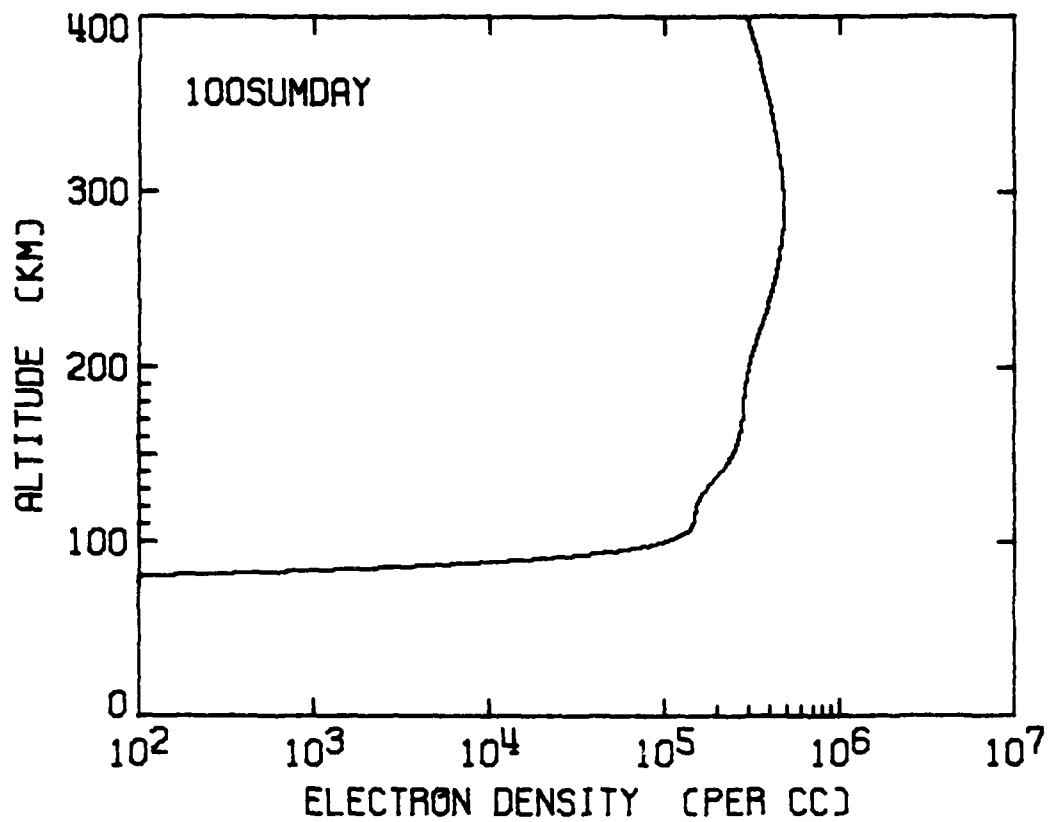




010WINNIT

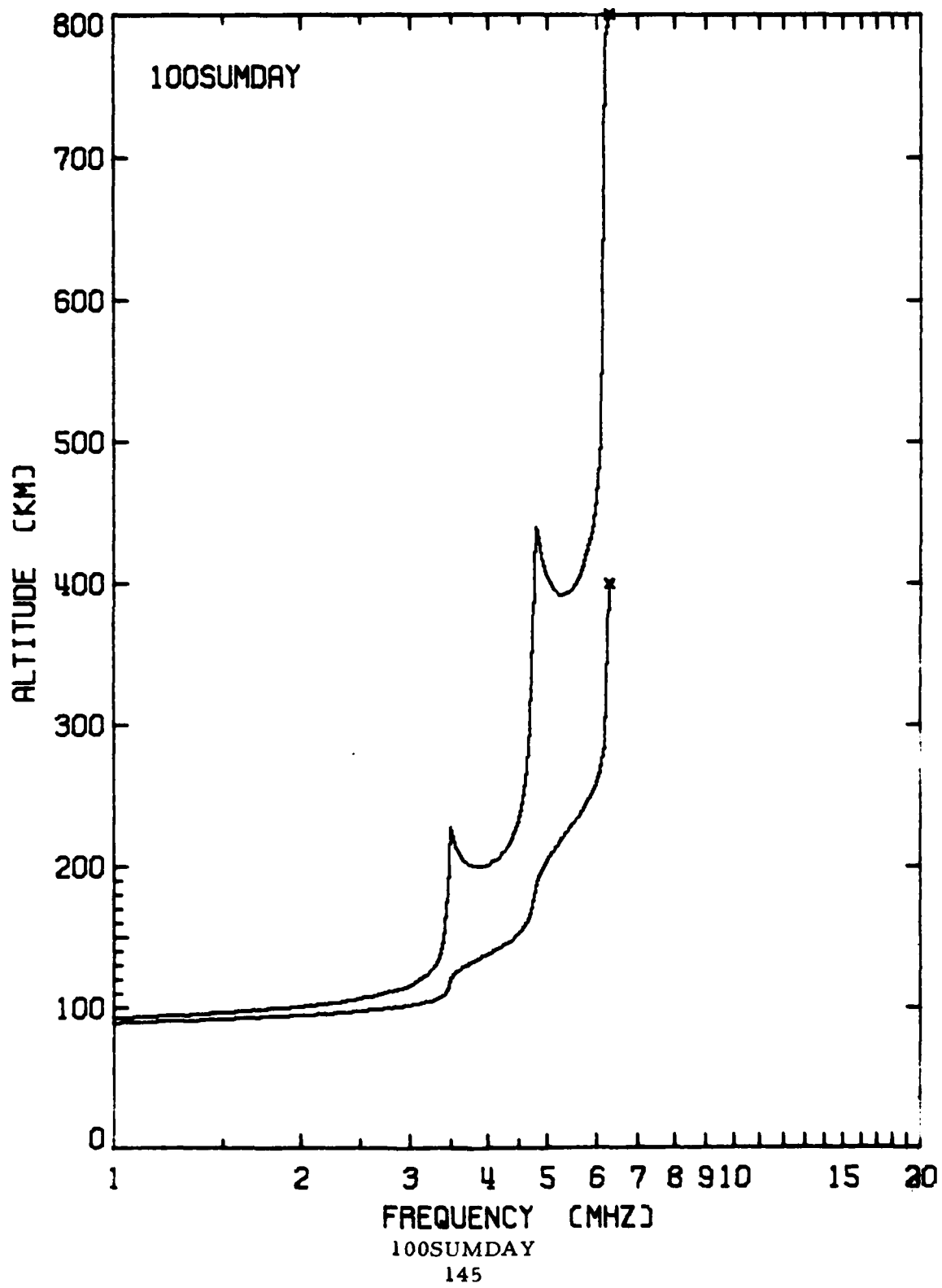


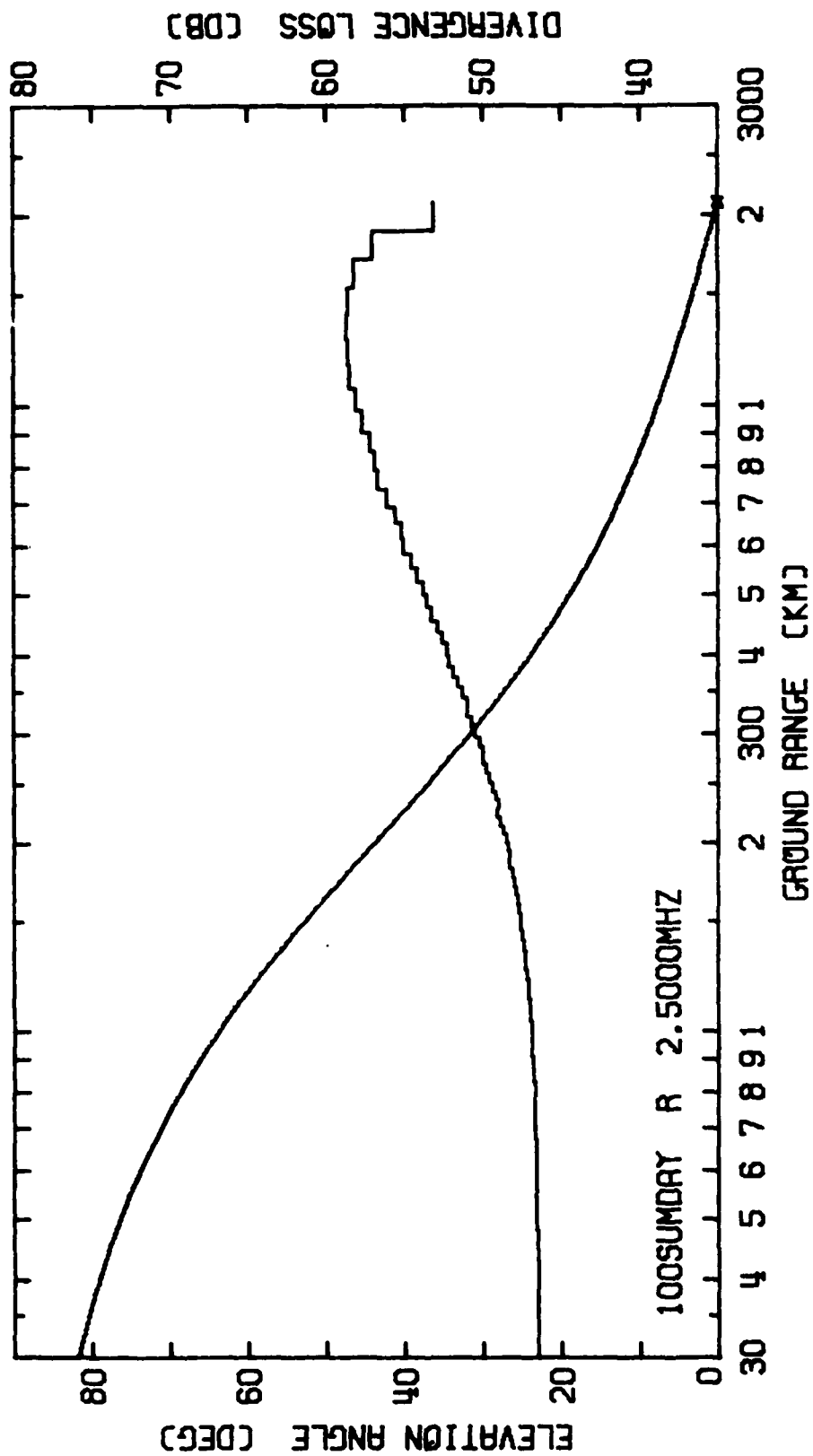




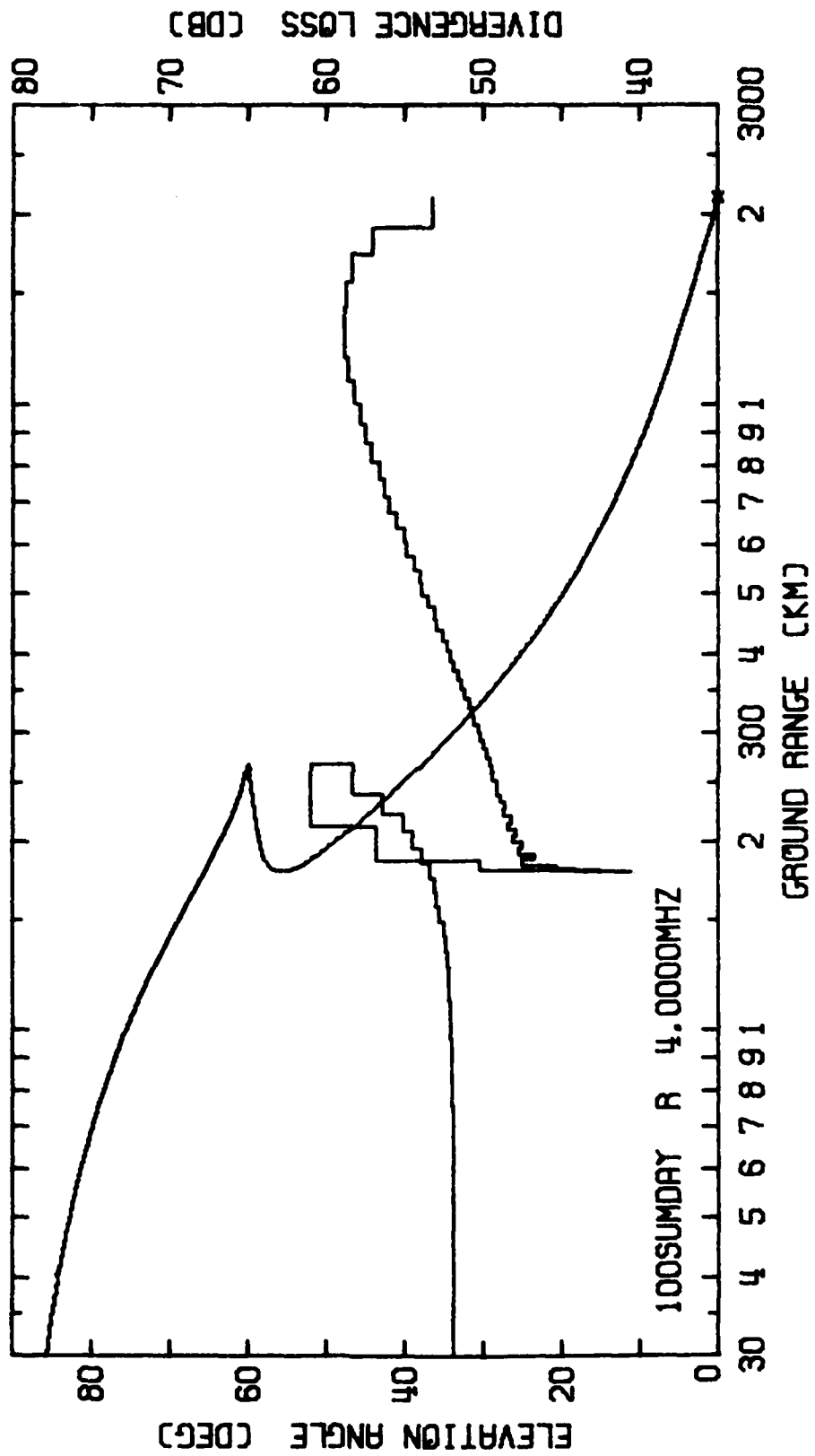
	<u>Level 1</u>	<u>Level 2</u>	<u>Level 3</u>
$h_o$ (km)	110	167	300
H (km)	10	25	60
$f_o$ (MHz)	3.30	4.40	6.00

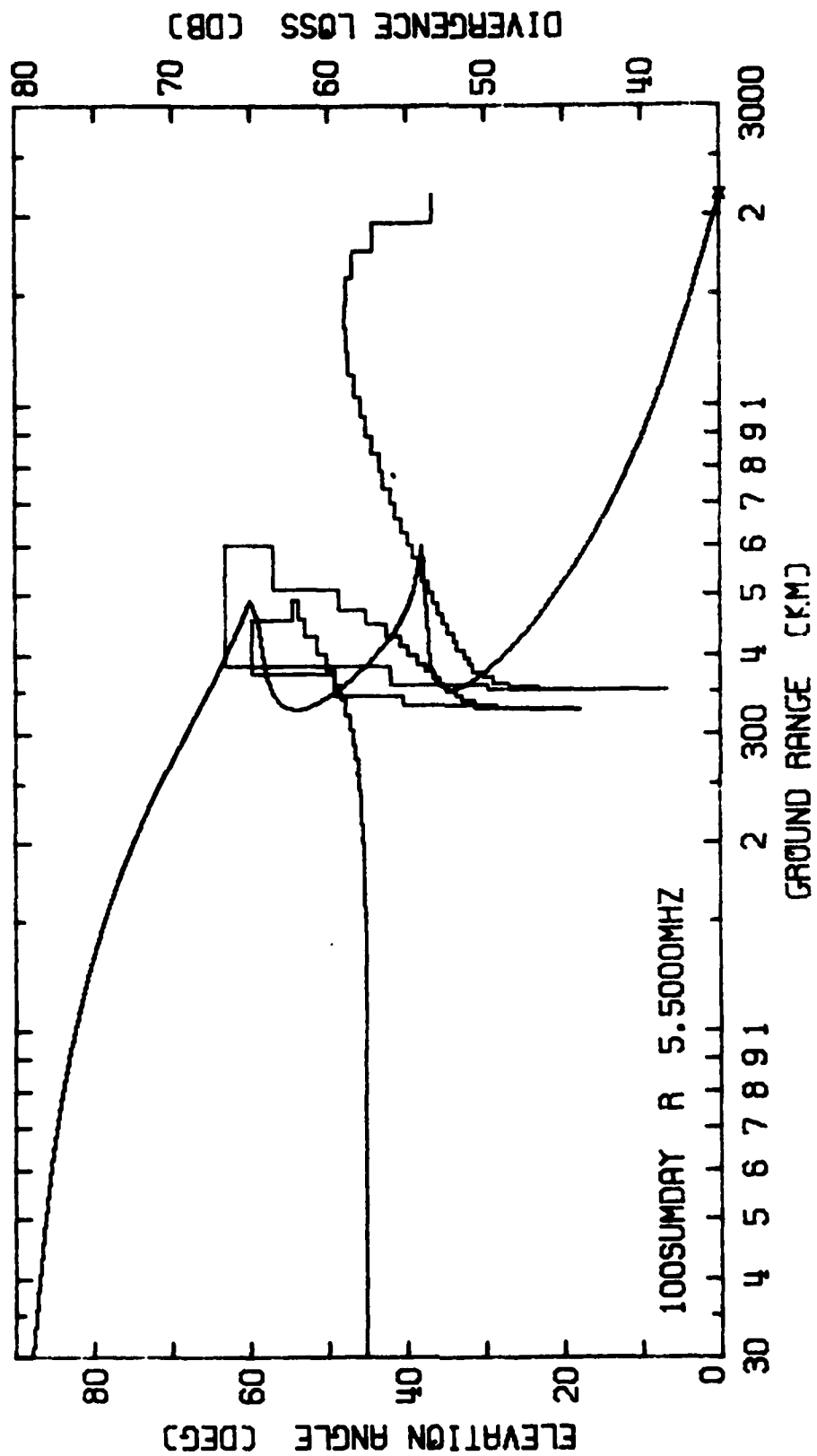
PRECEDING PAGE BLANK-NOT FILMED





100SUMDAY

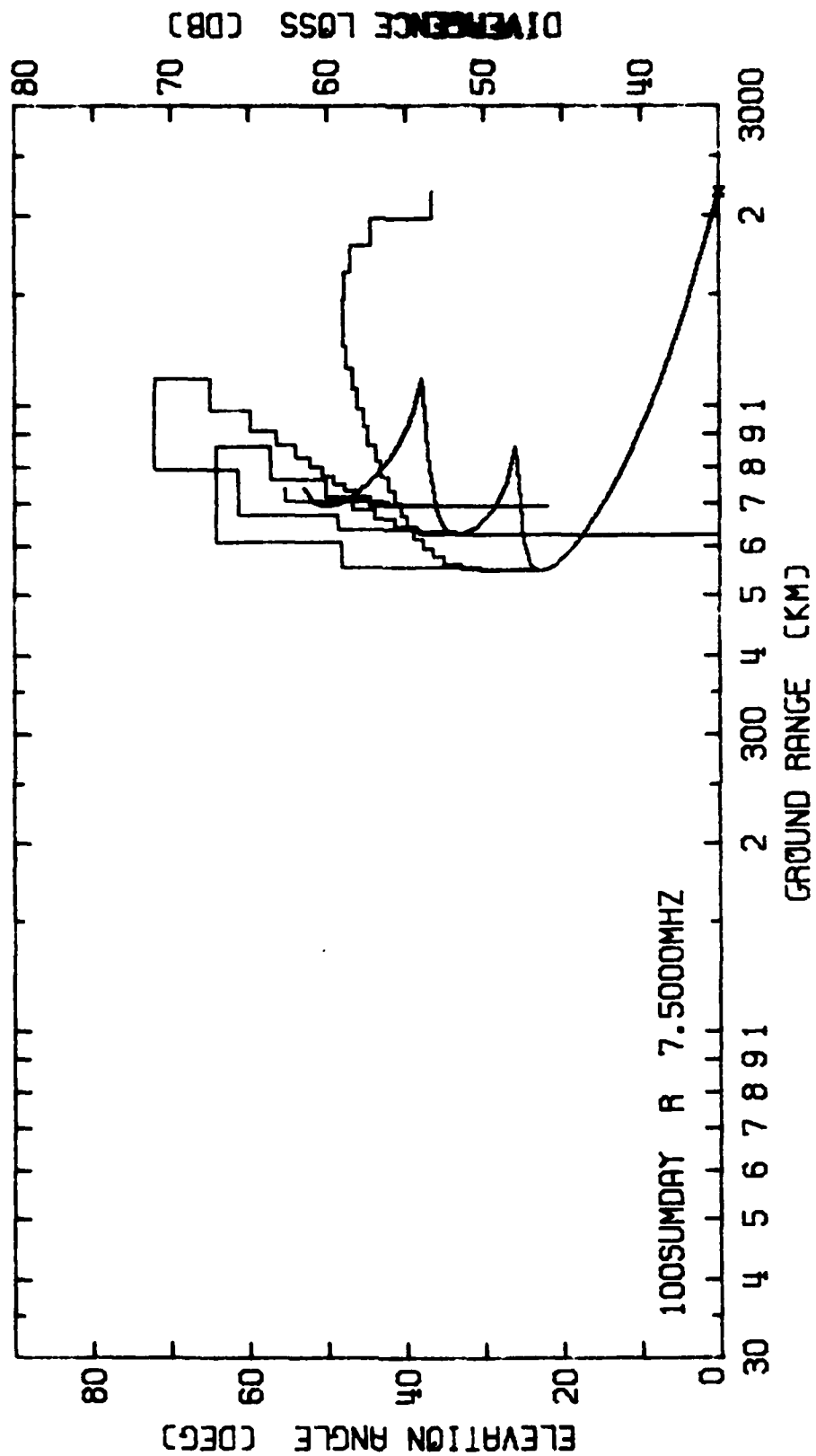




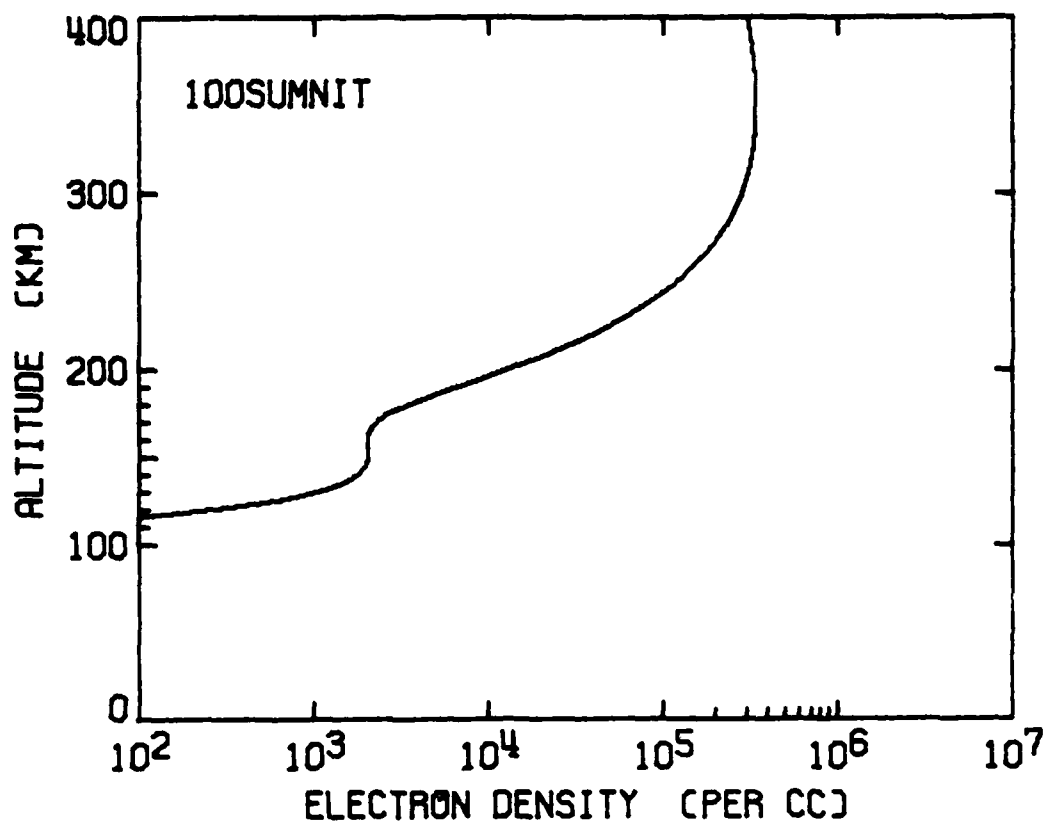
100SUMDAY

148



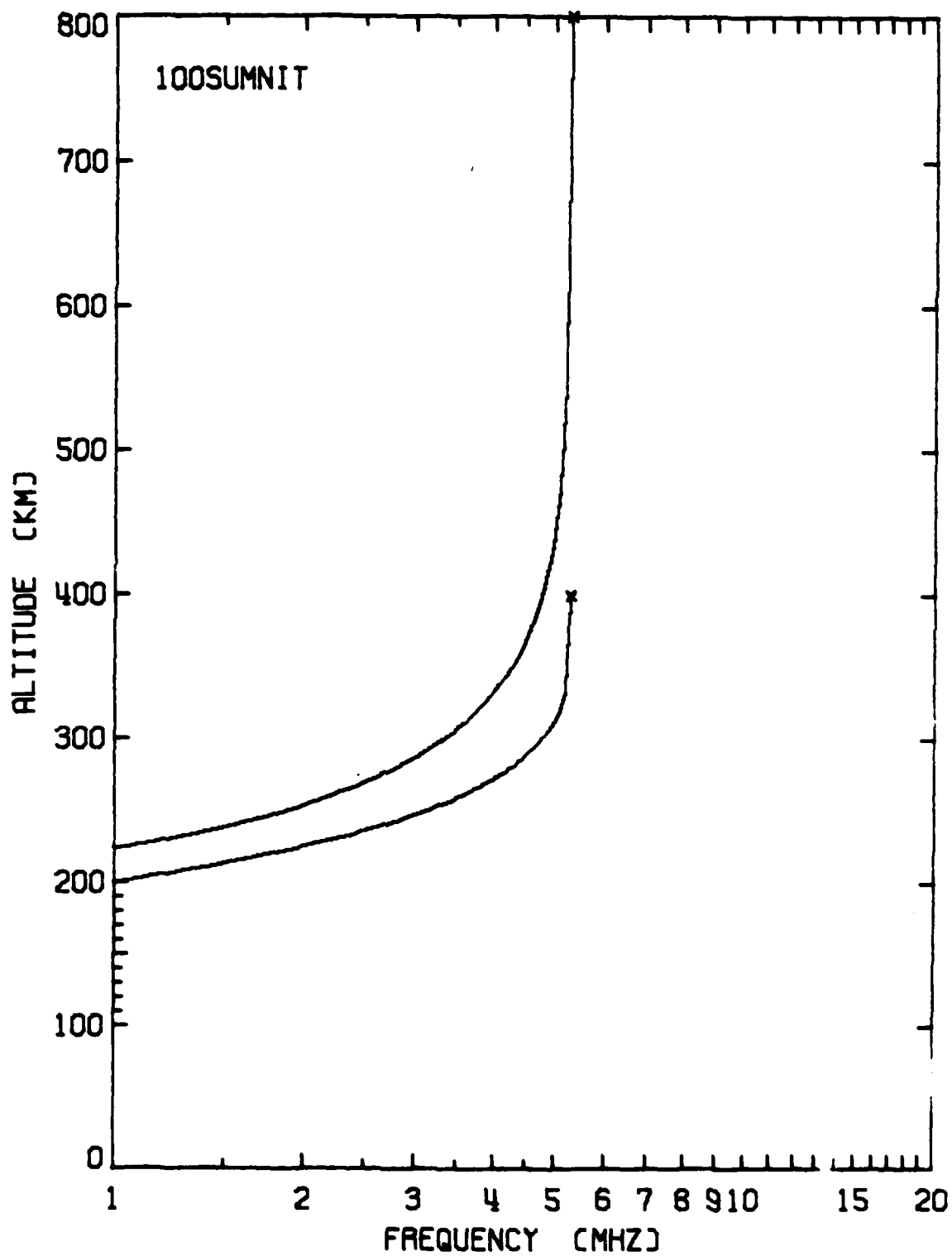


100SUMDAY  
149

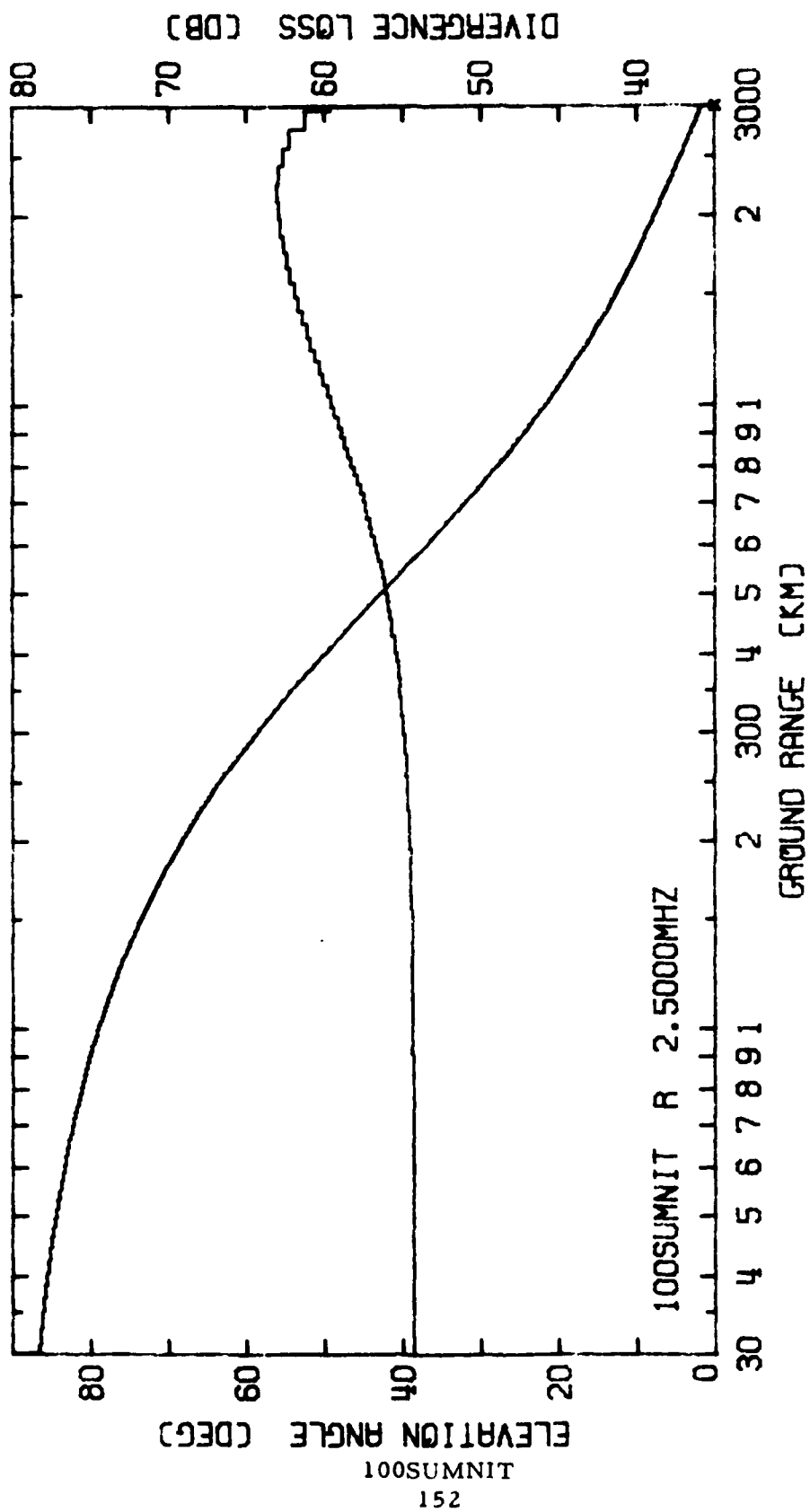


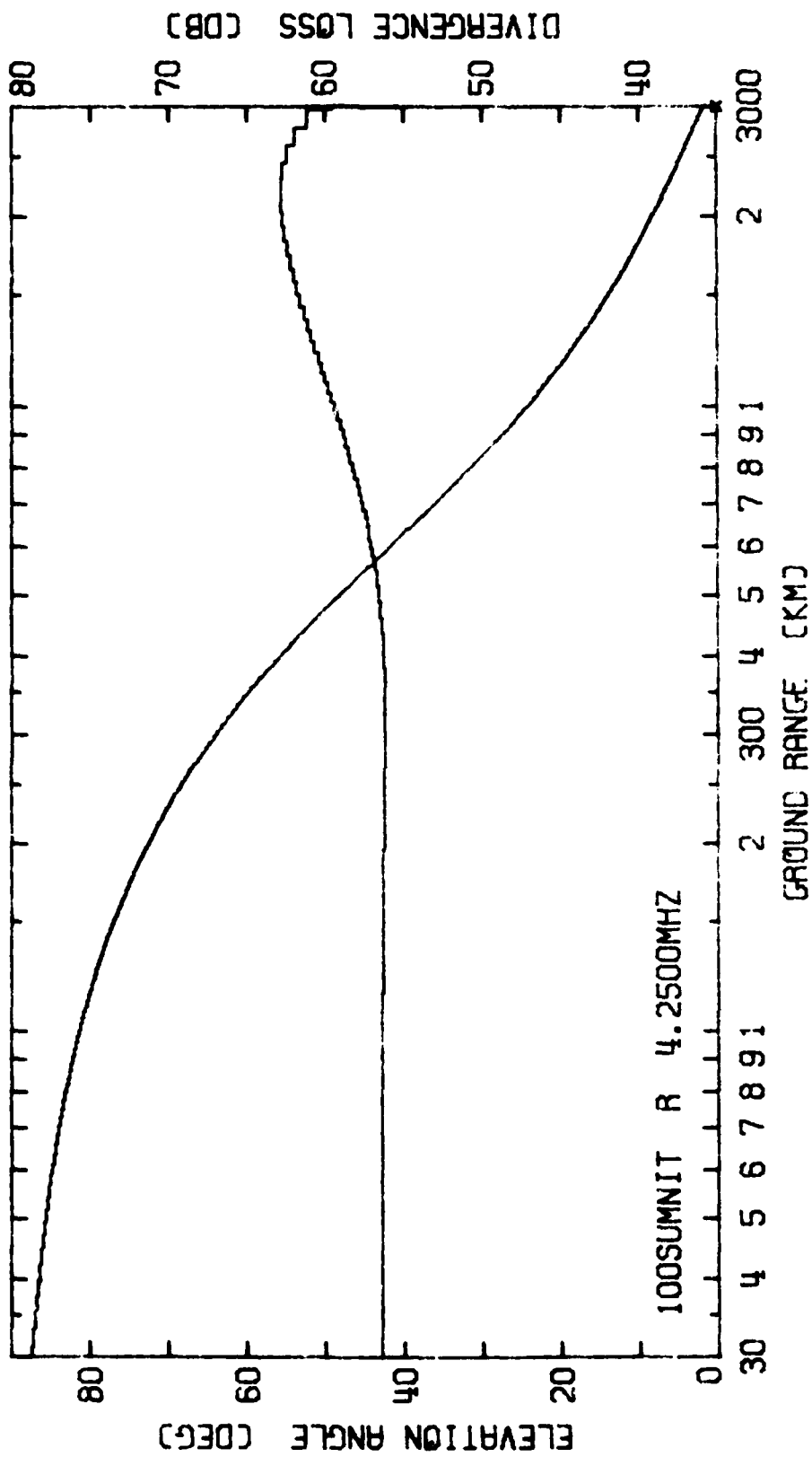
	<u>Level 1</u>	<u>Level 2</u>	<u>Level 3</u>
$h_o$ (km)	150	Absent	350
$H$ (km)	15	Absent	65
$f_o$ (MHz)	0.40	Absent	5.25

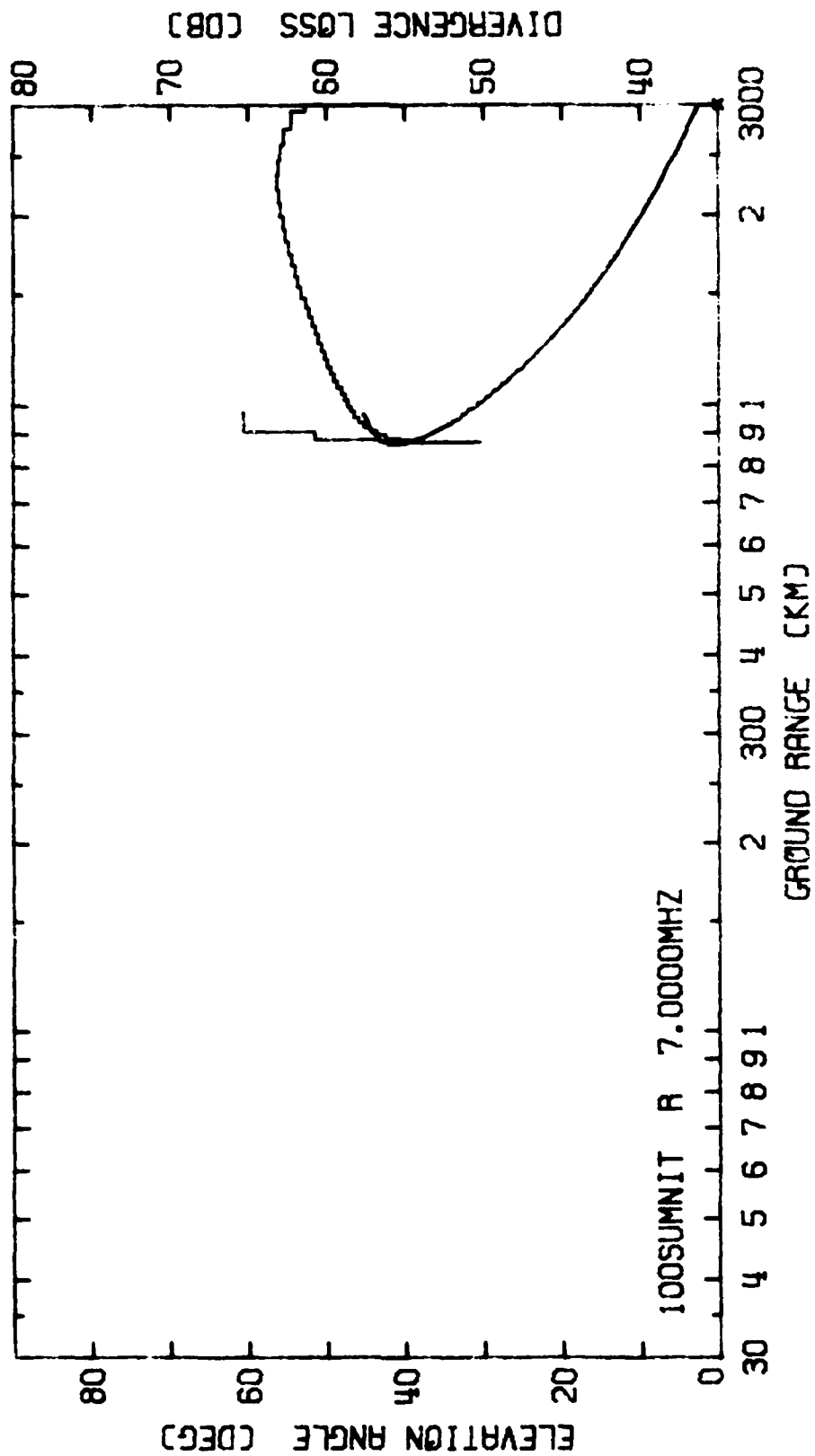
100SUMNIT  
150

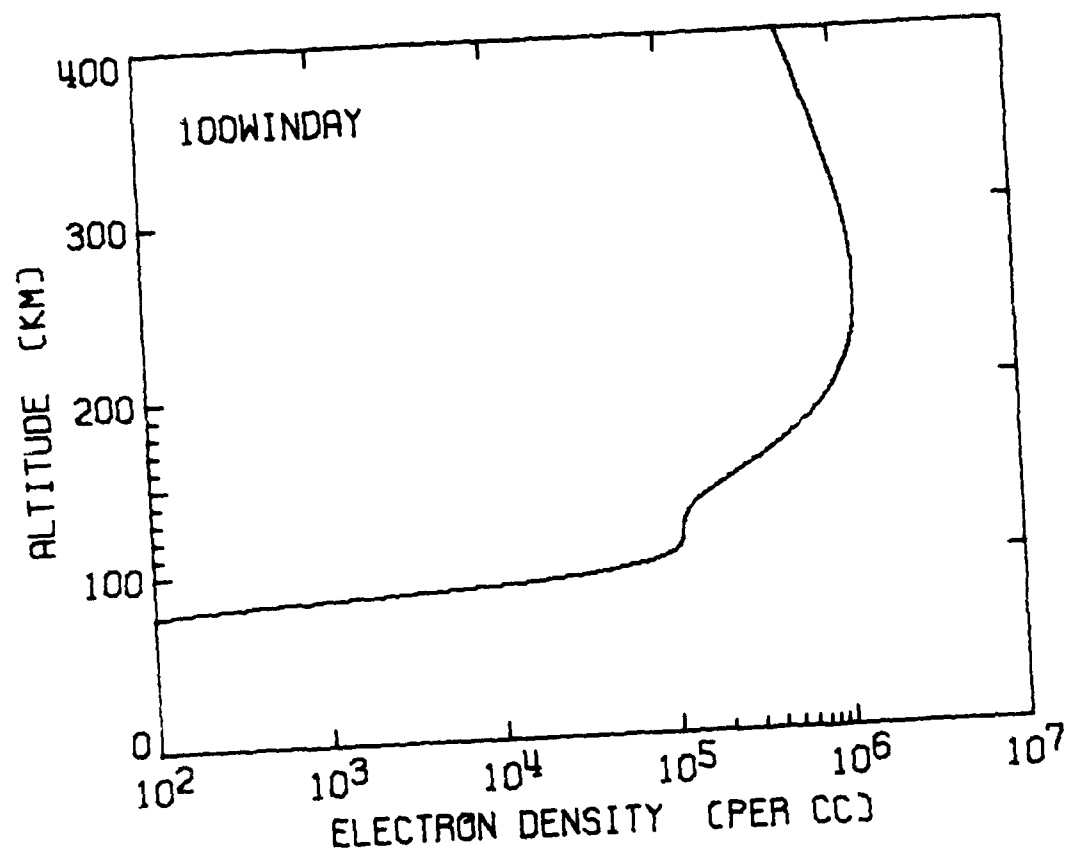


100SUMNIT



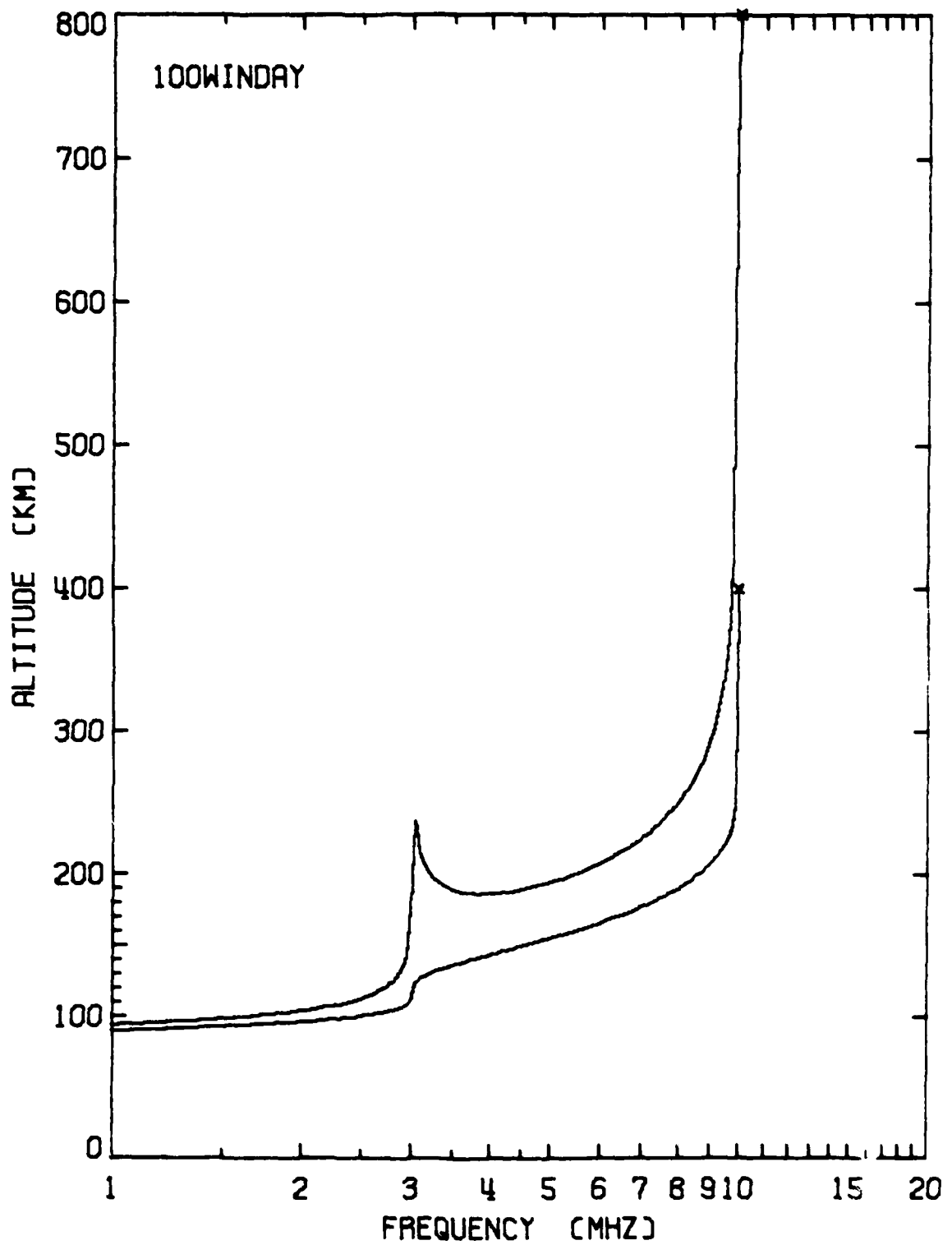






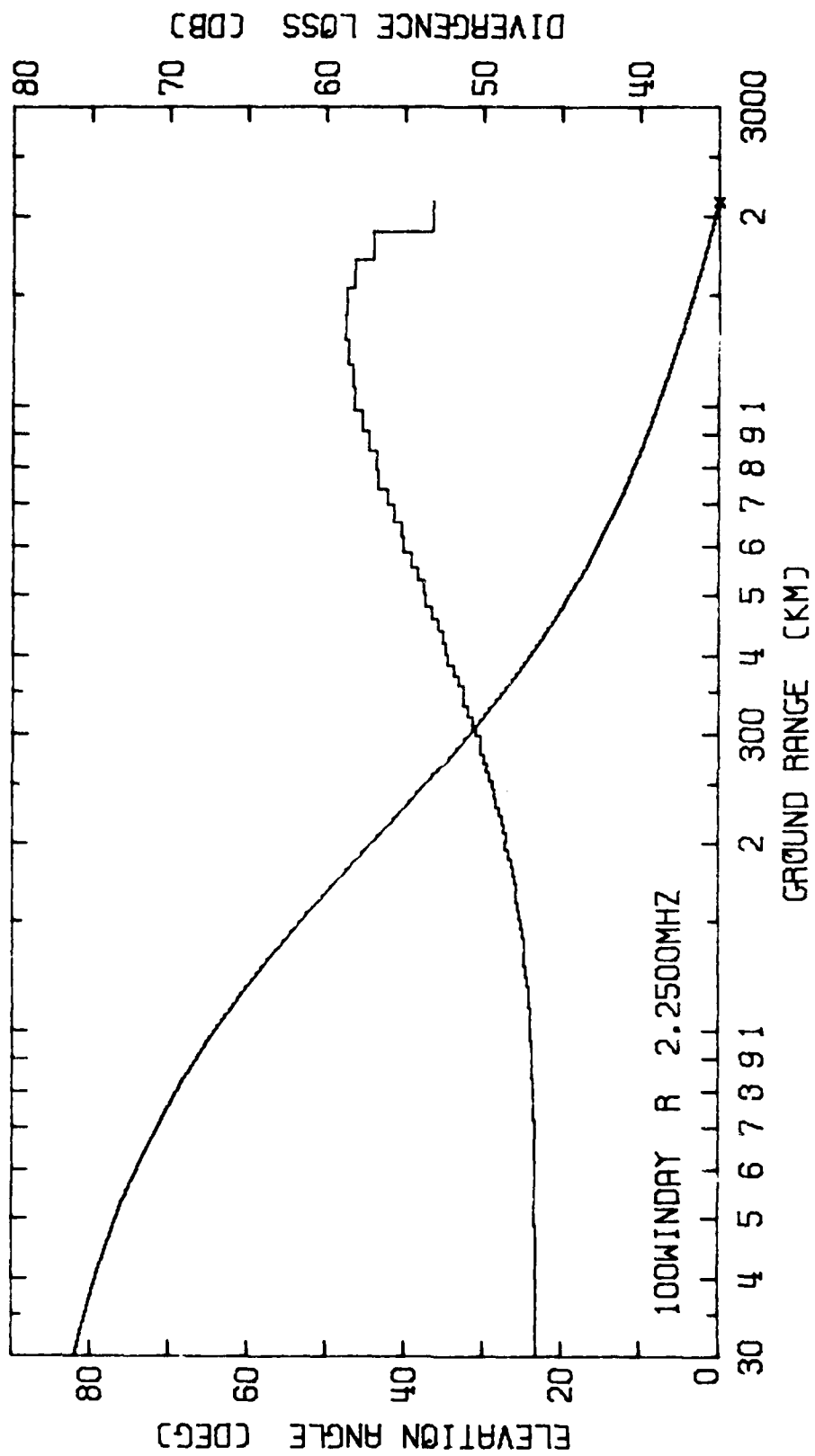
	<u>Level 1</u>	<u>Level 2</u>	<u>Level 3</u>
$h_o$ (km)	110	Absent	250
$H$ (km)	10	Absent	55
$f_o$ (MHz)	2.80	Absent	9.90

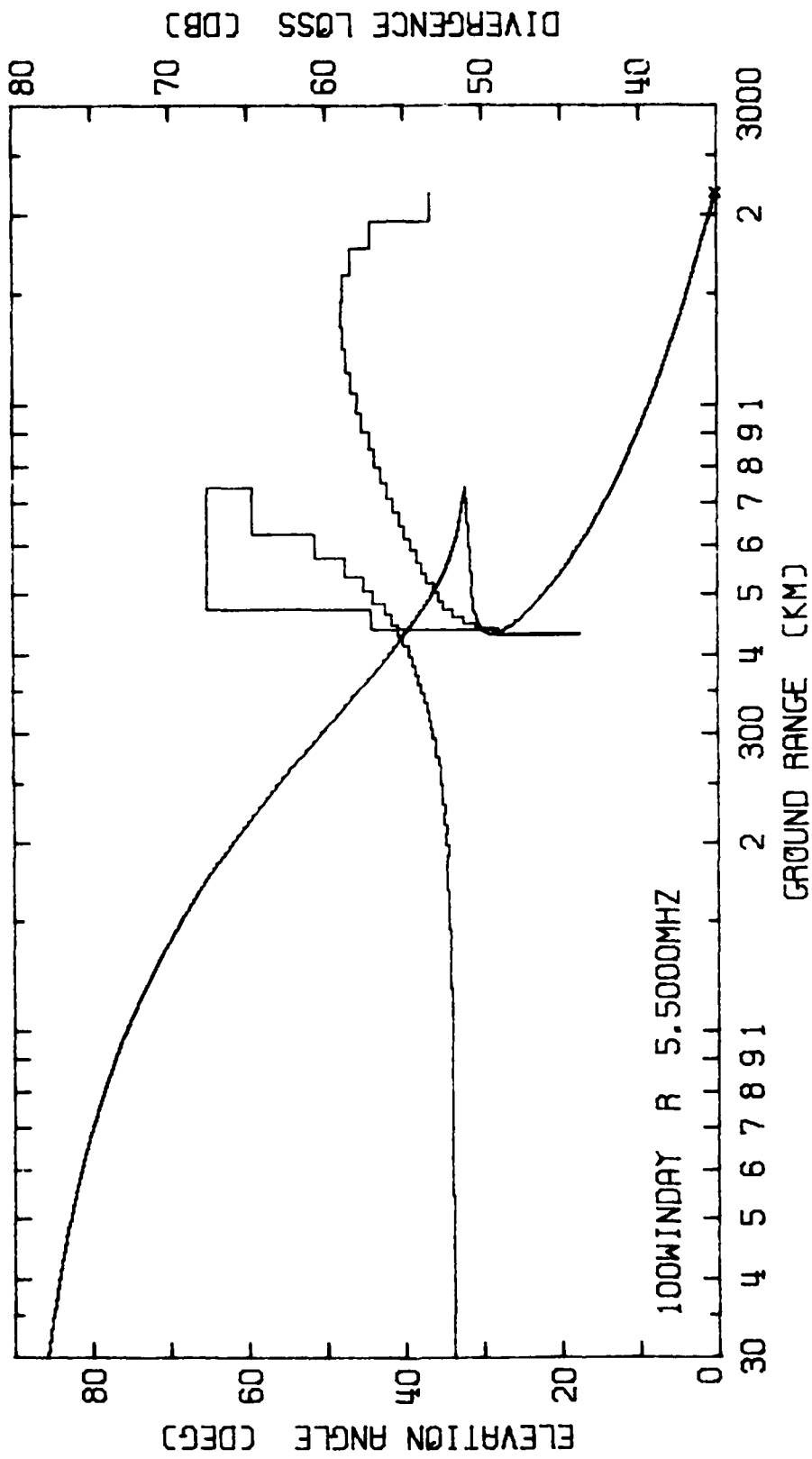
PRECEDING PAGE BLANK-NOT FILMED



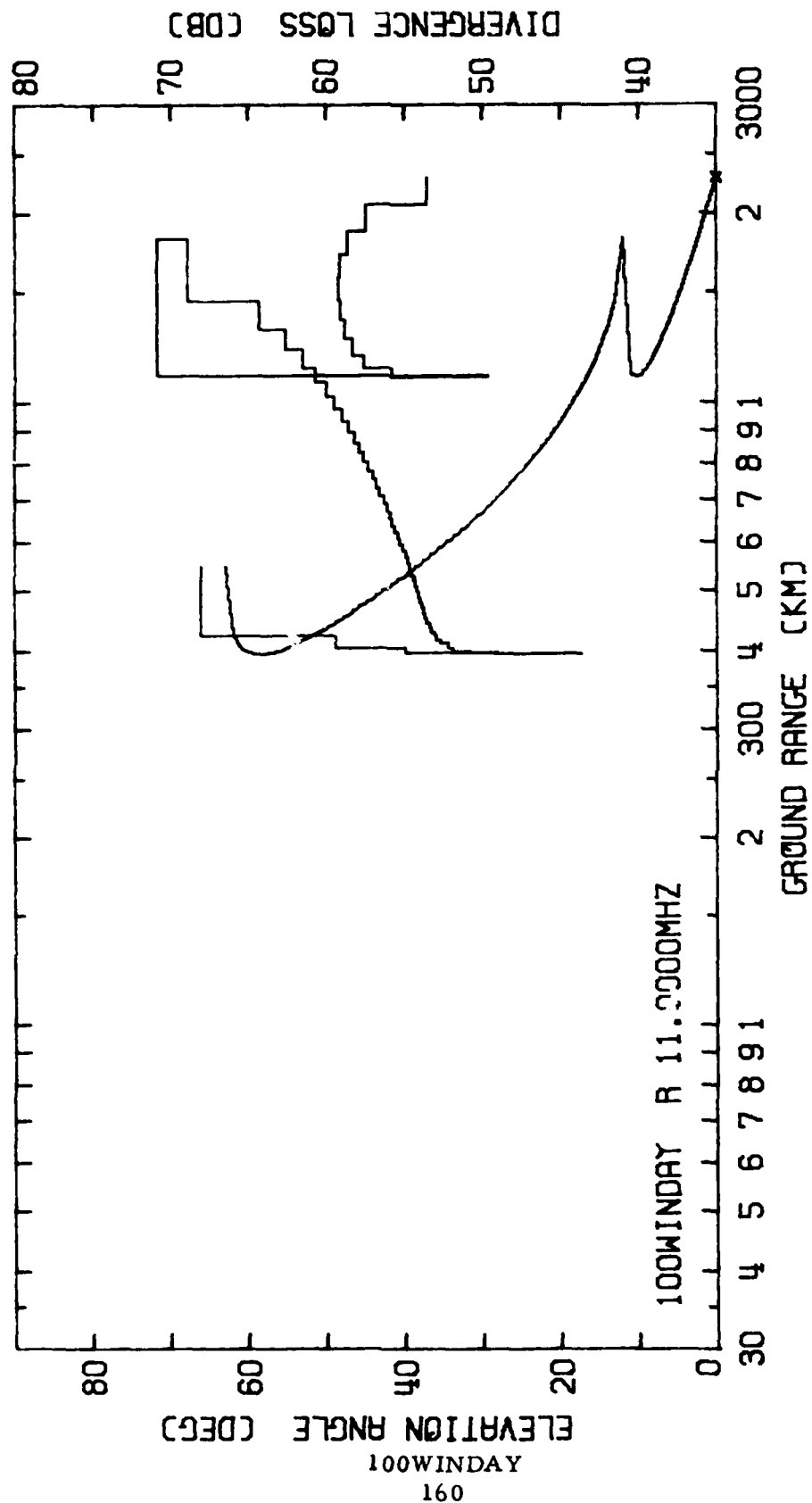
100WINDAY  
157

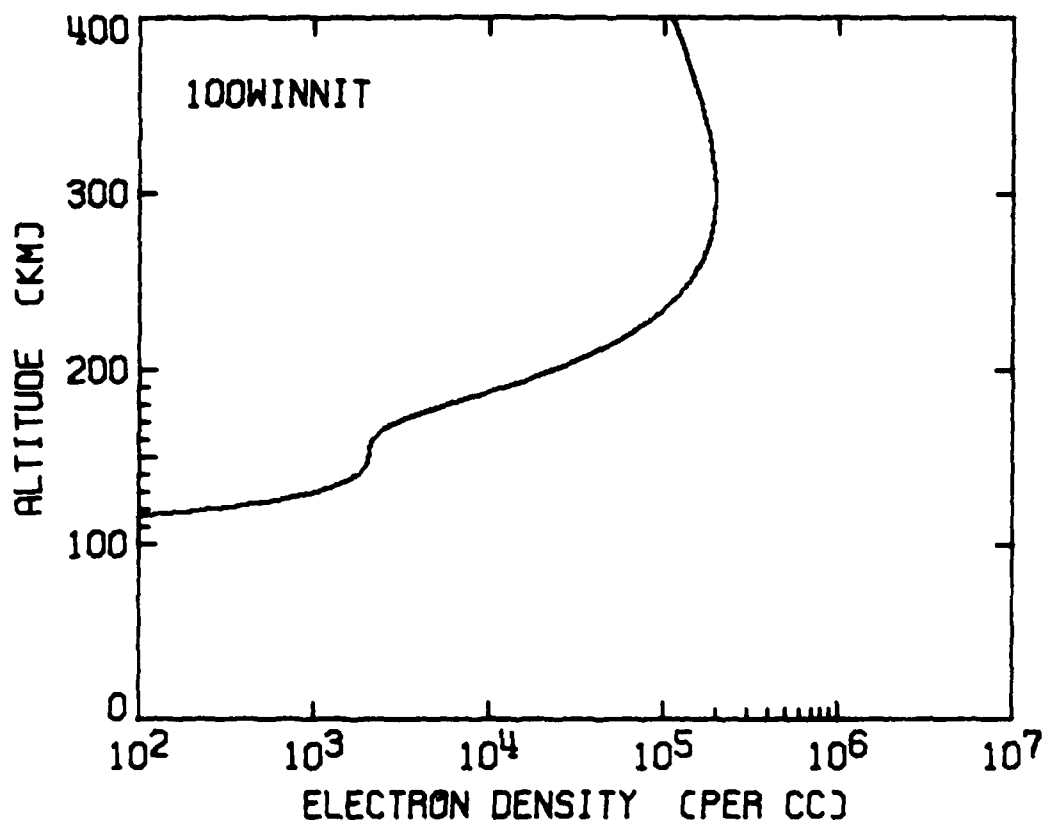






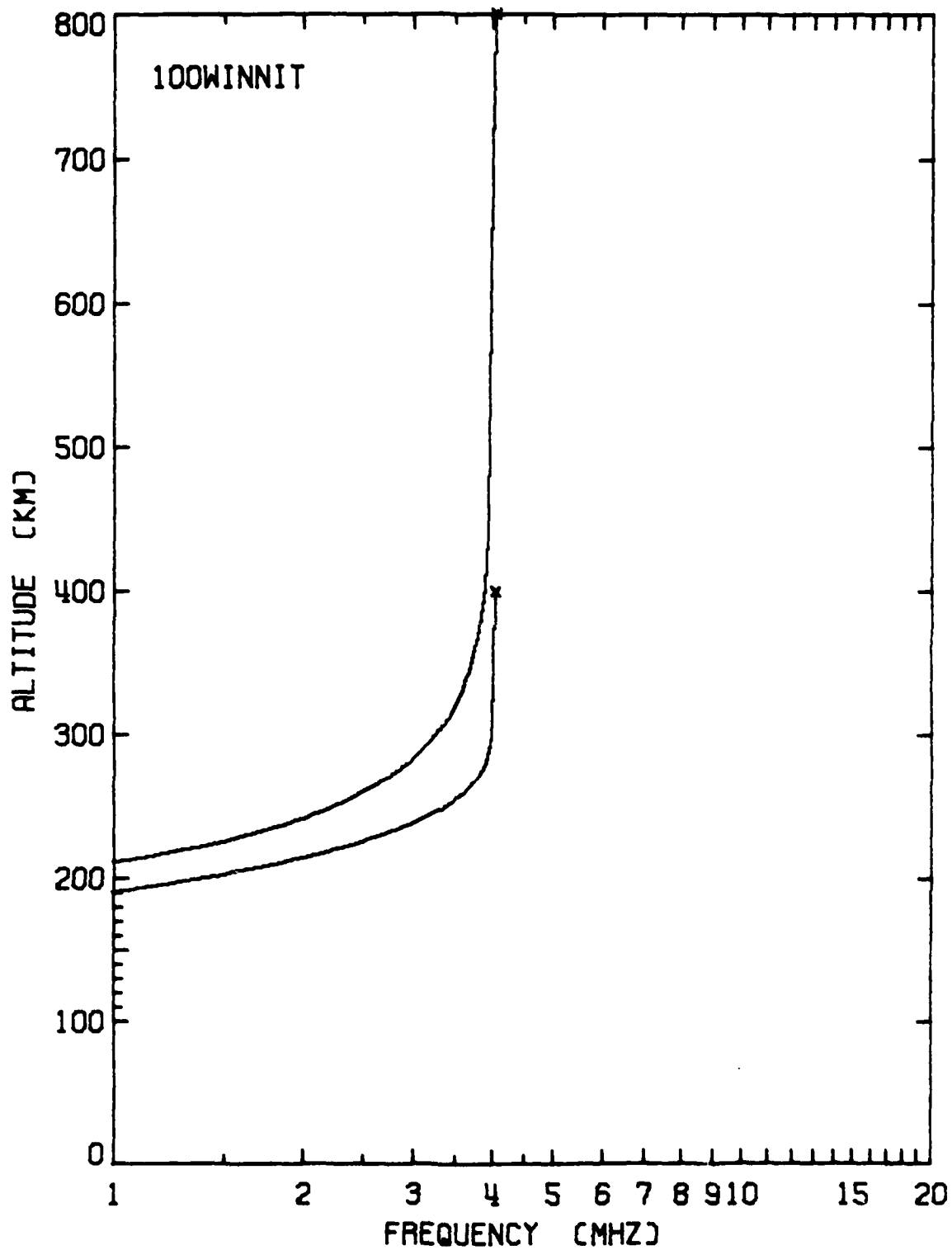
100WINDAY



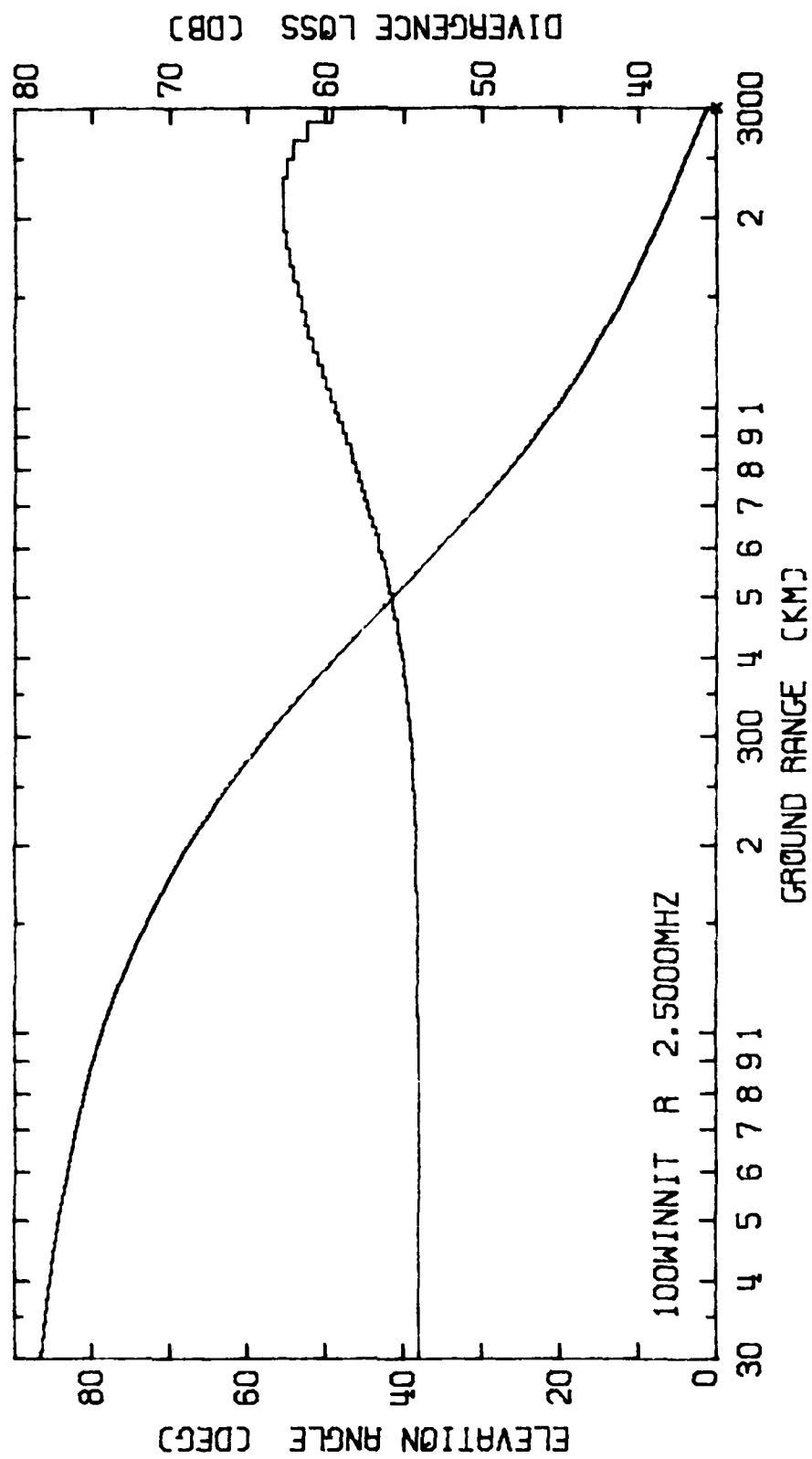


	<u>Level 1</u>	<u>Level 2</u>	<u>Level 3</u>
$h_o$ (km)	150	Absent	300
H (km)	15	Absent	50
$f_o$ (MHz)	0.40	Absent	4.00

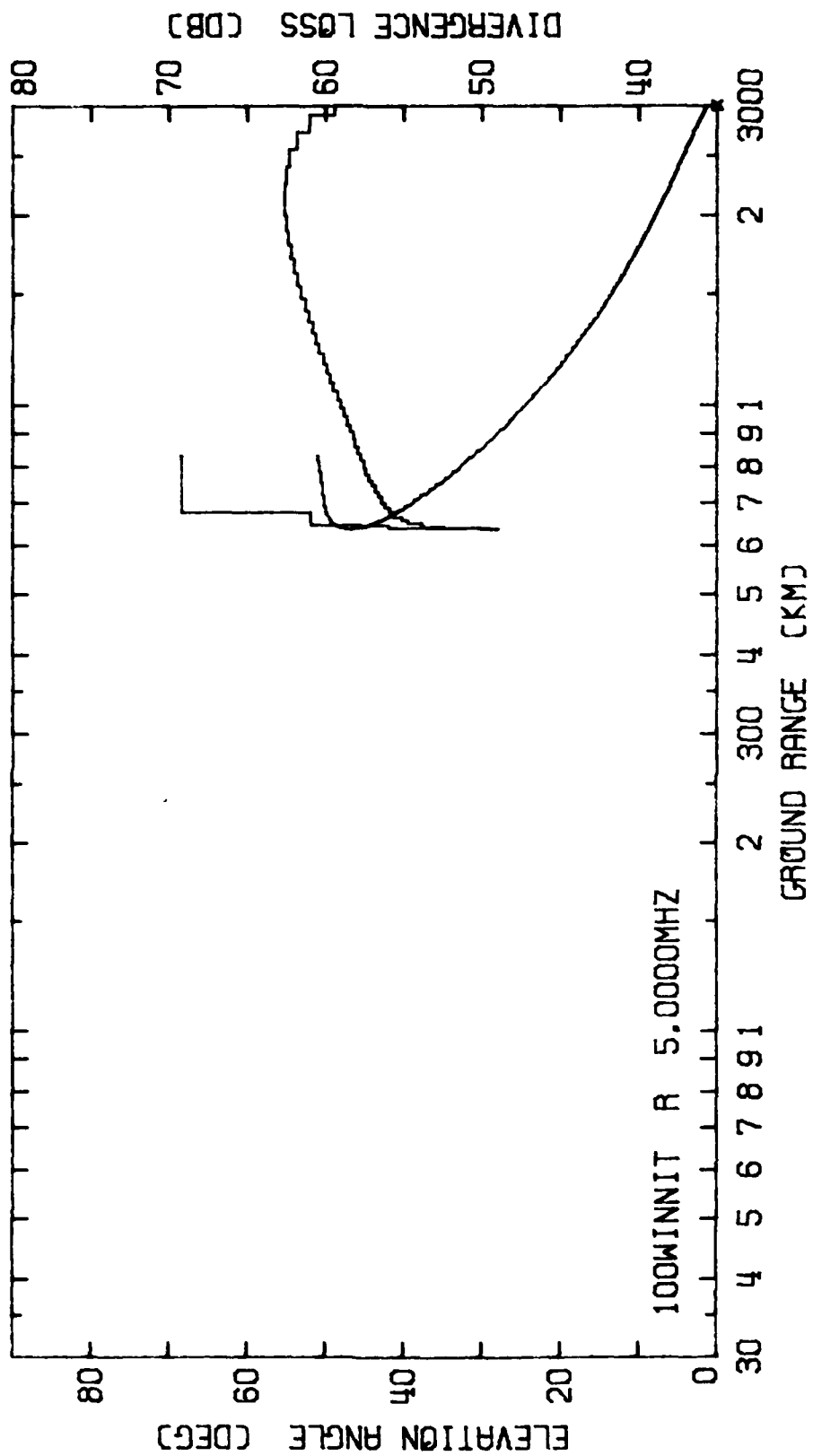
PRECEDING PAGE BLANK-NOT FILMED

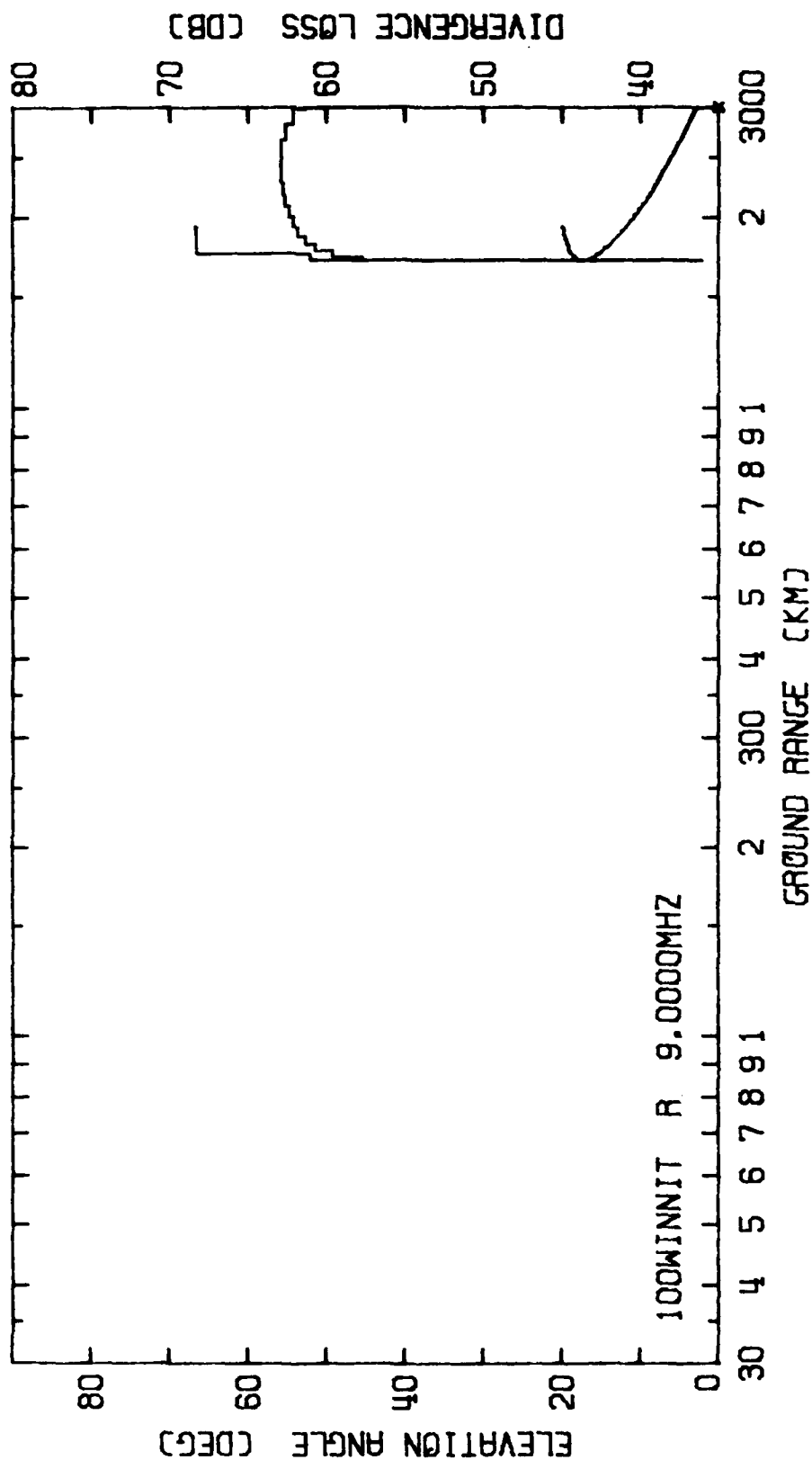


100WINNIT

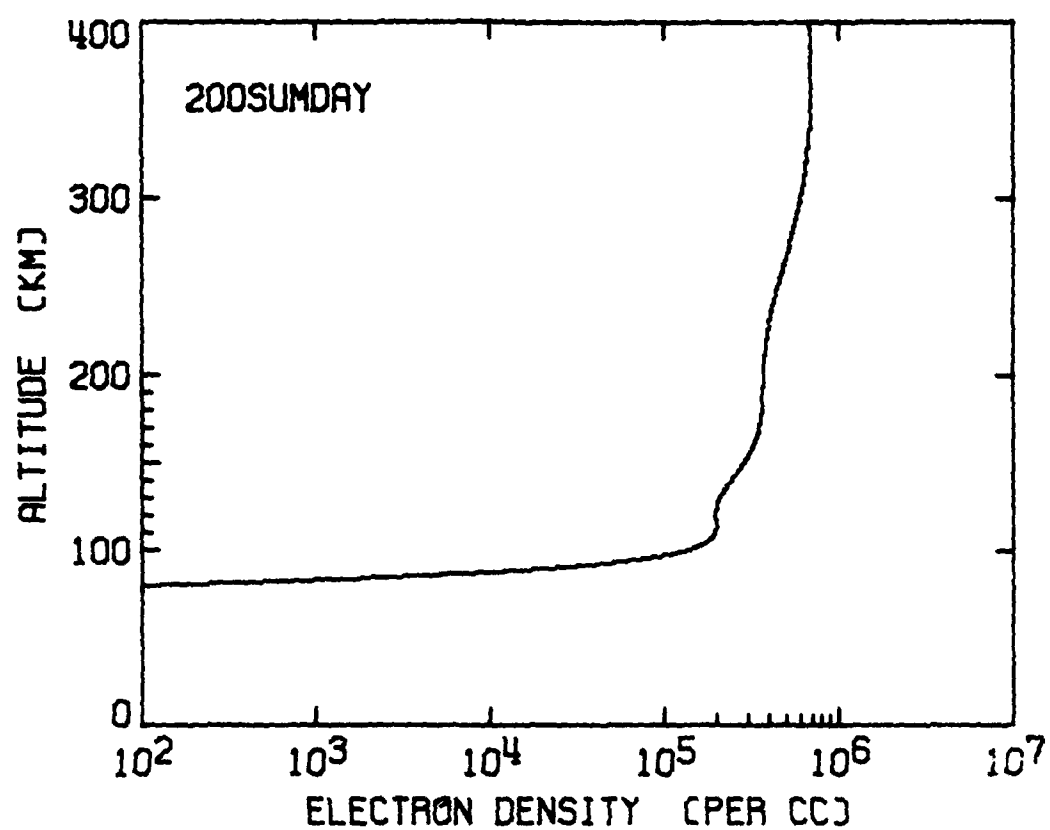


100WINNIT

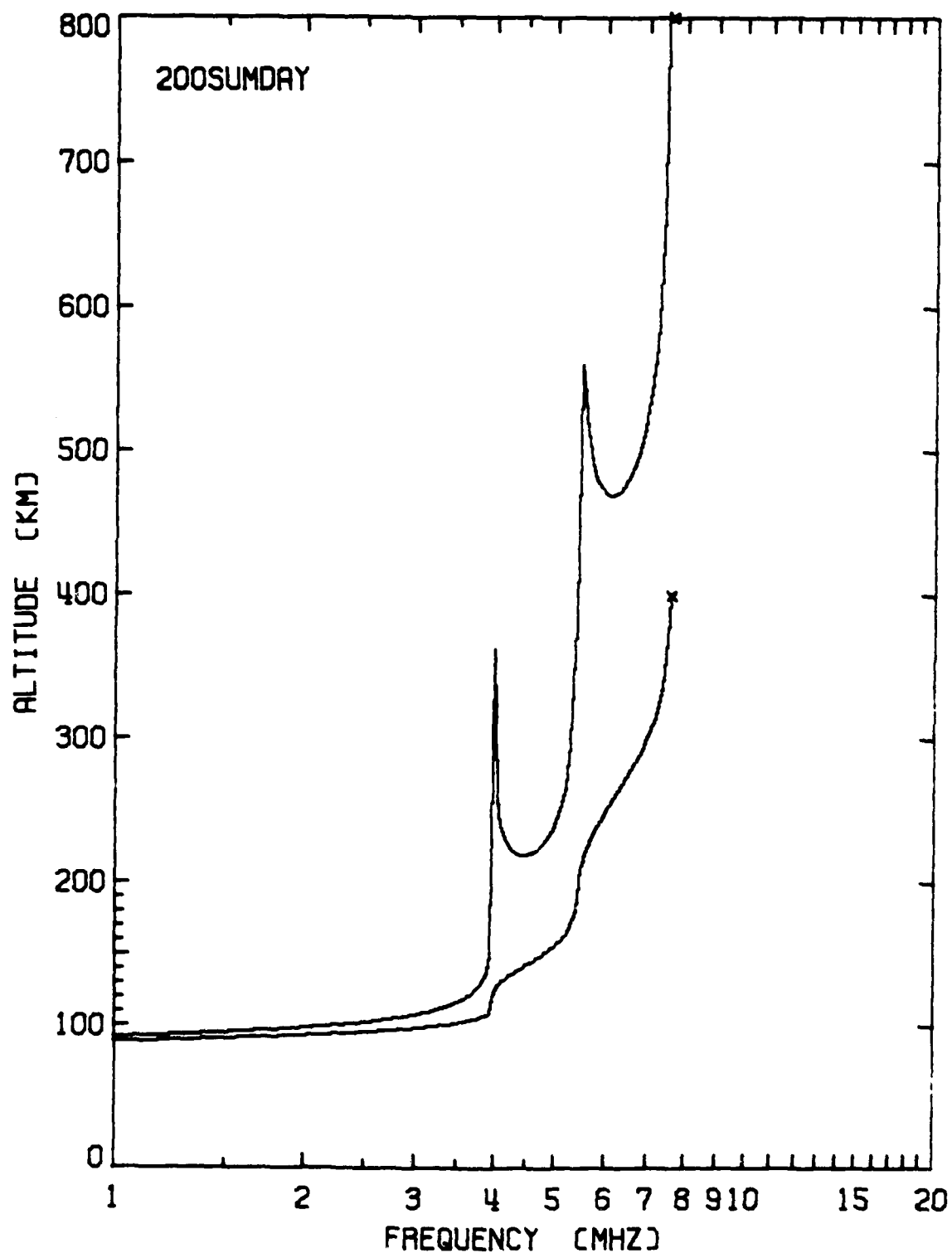




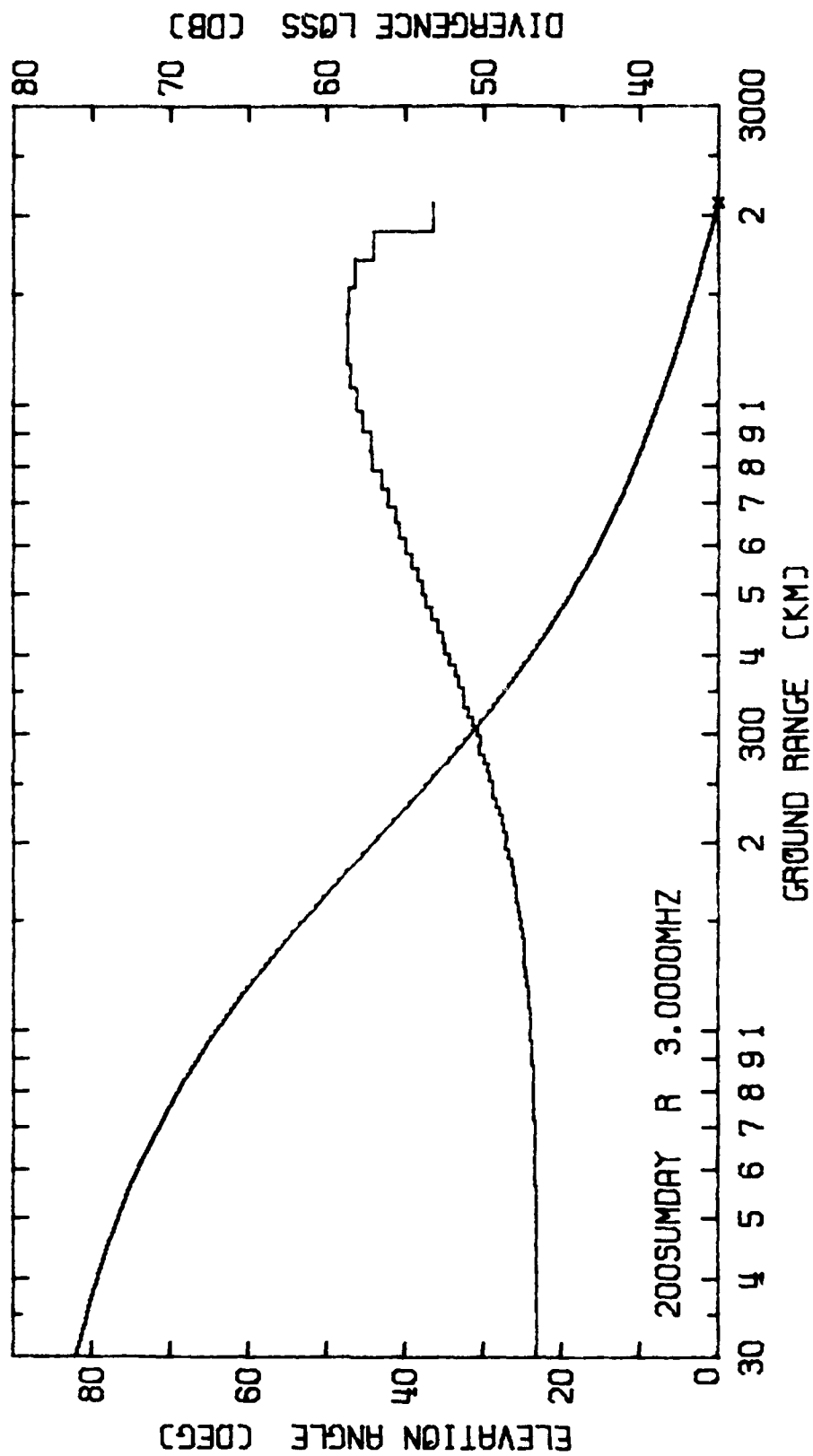




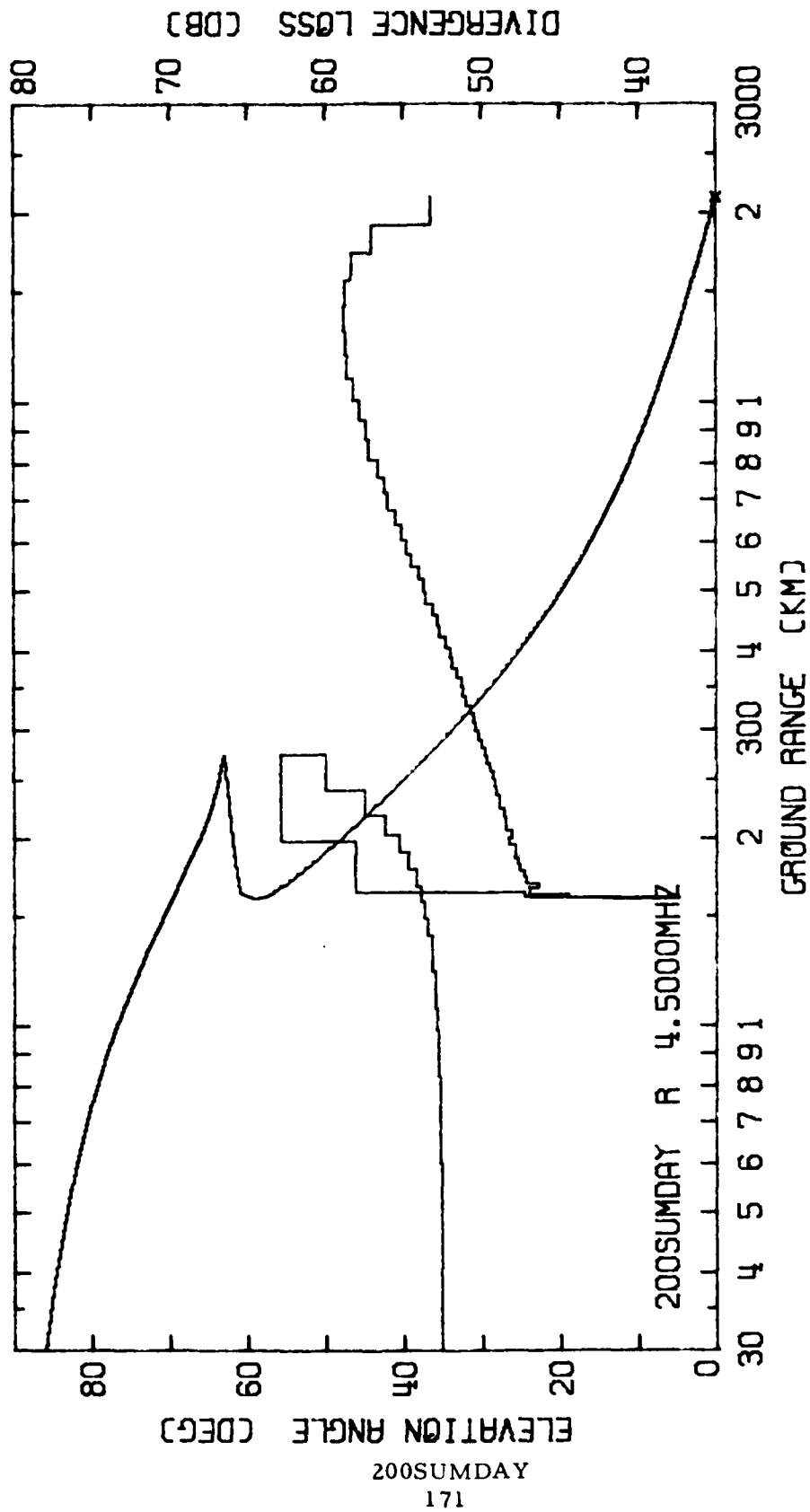
	<u>Level 1</u>	<u>Level 2</u>	<u>Level 3</u>
$h_o$ (km)	110	177	375
H (km)	10	30	90
$f_o$ (MHz)	3.80	5.00	7.40

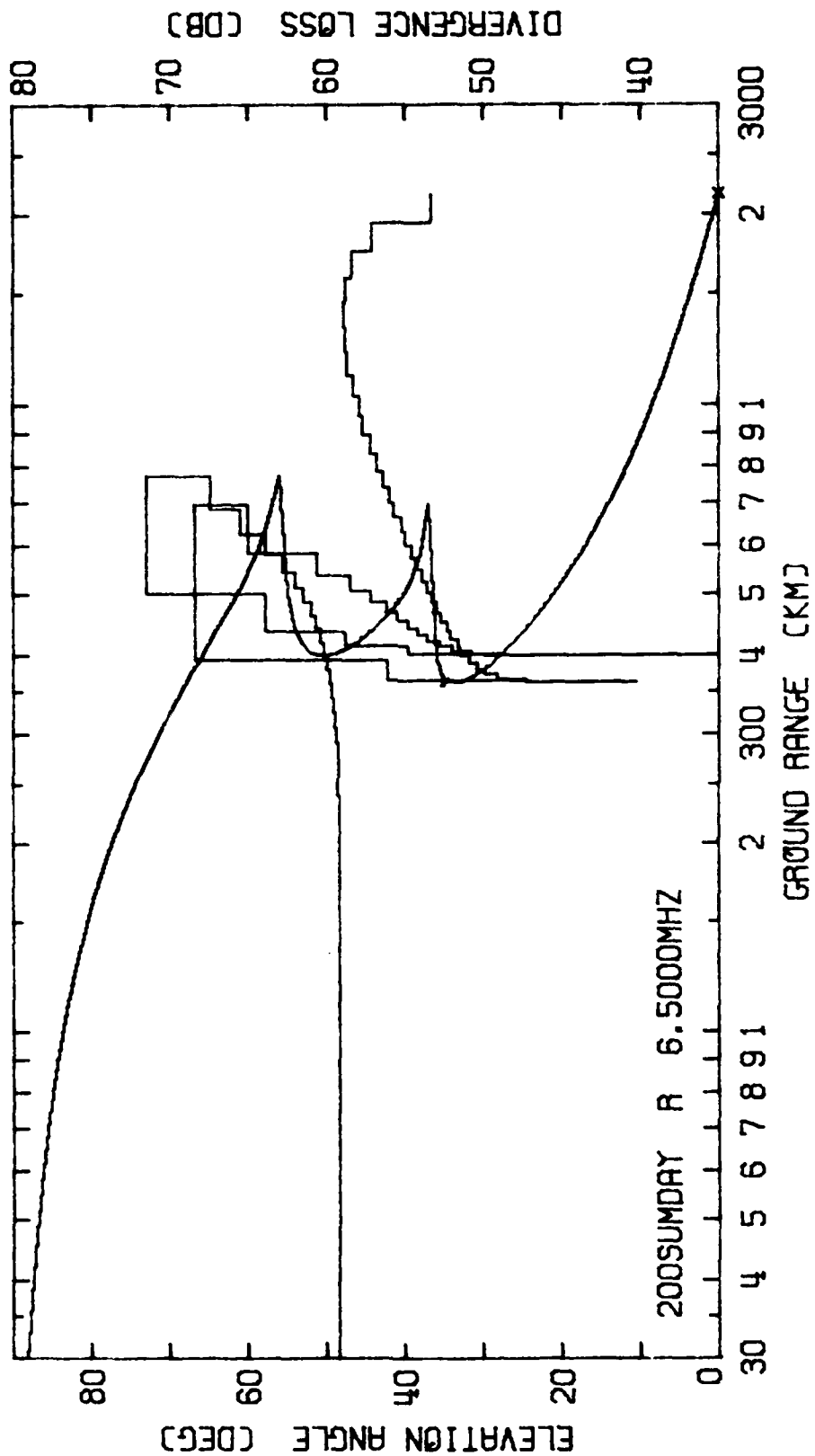


200SUMDAY

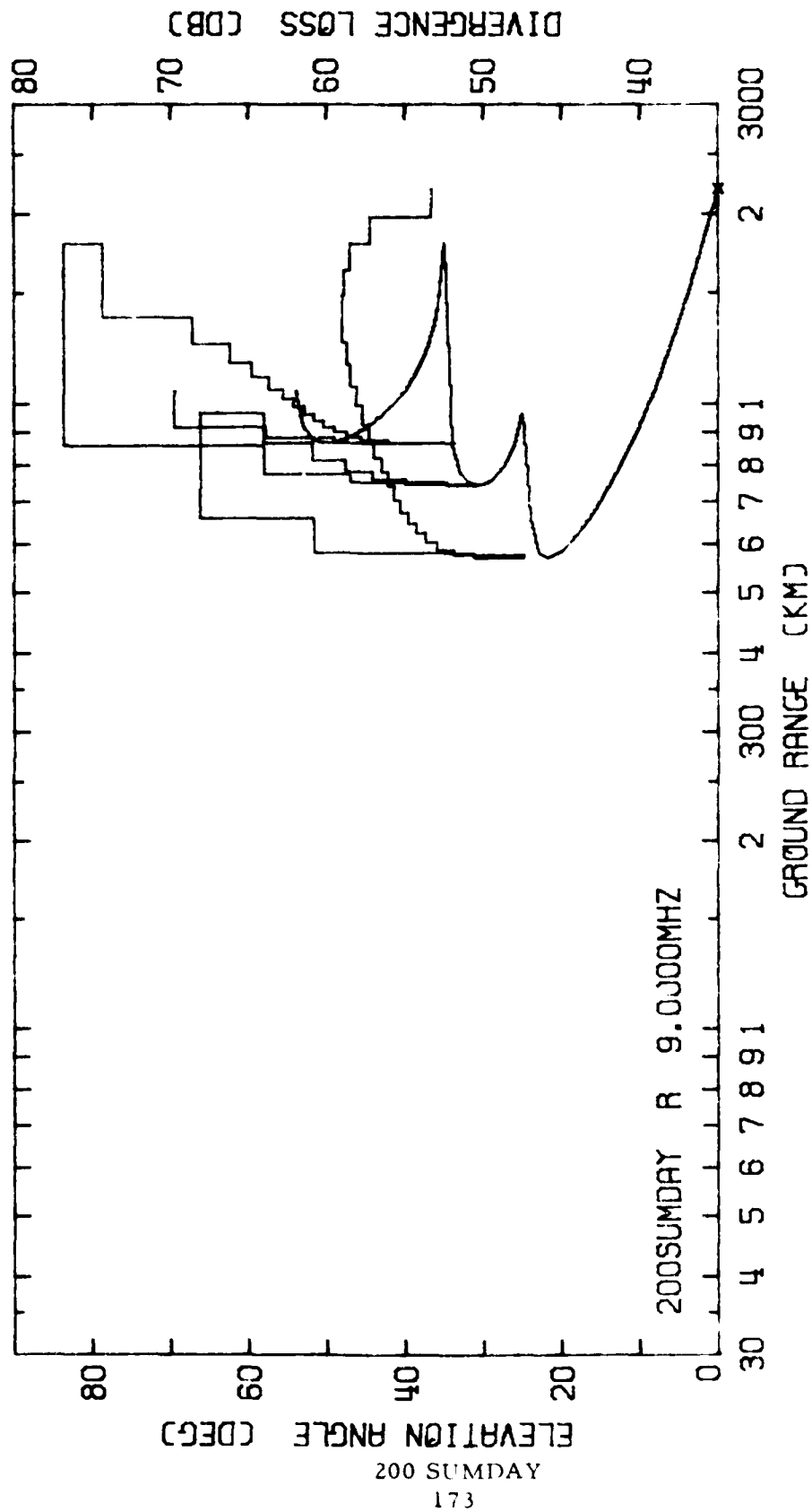


200SUMDAY





200SUMDAY  
172



AD-A119 491

SOUTHWEST RESEARCH INST SAN ANTONIO TX

F/G 17/4

DELINEATION OF CONSTRAINTS IMPOSED BY PROPAGATION FACTORS AT HF--ETC(U)

APR 76 E C HAYDEN

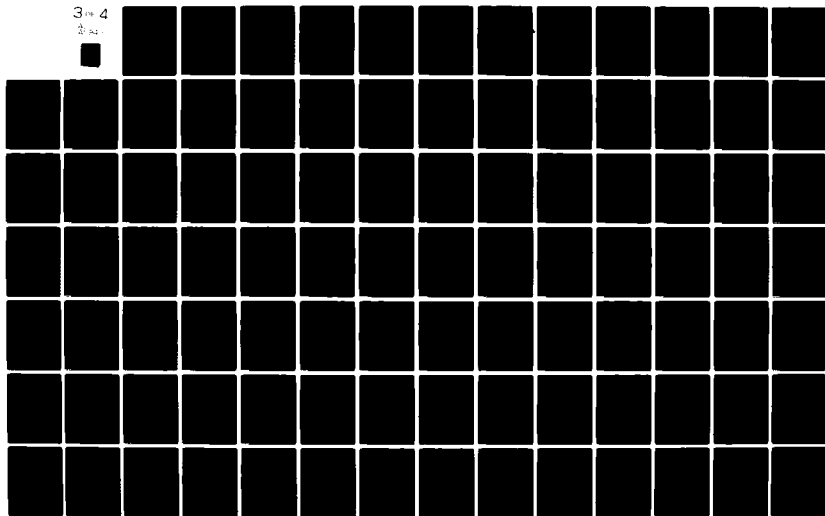
N00039-75-C-0481

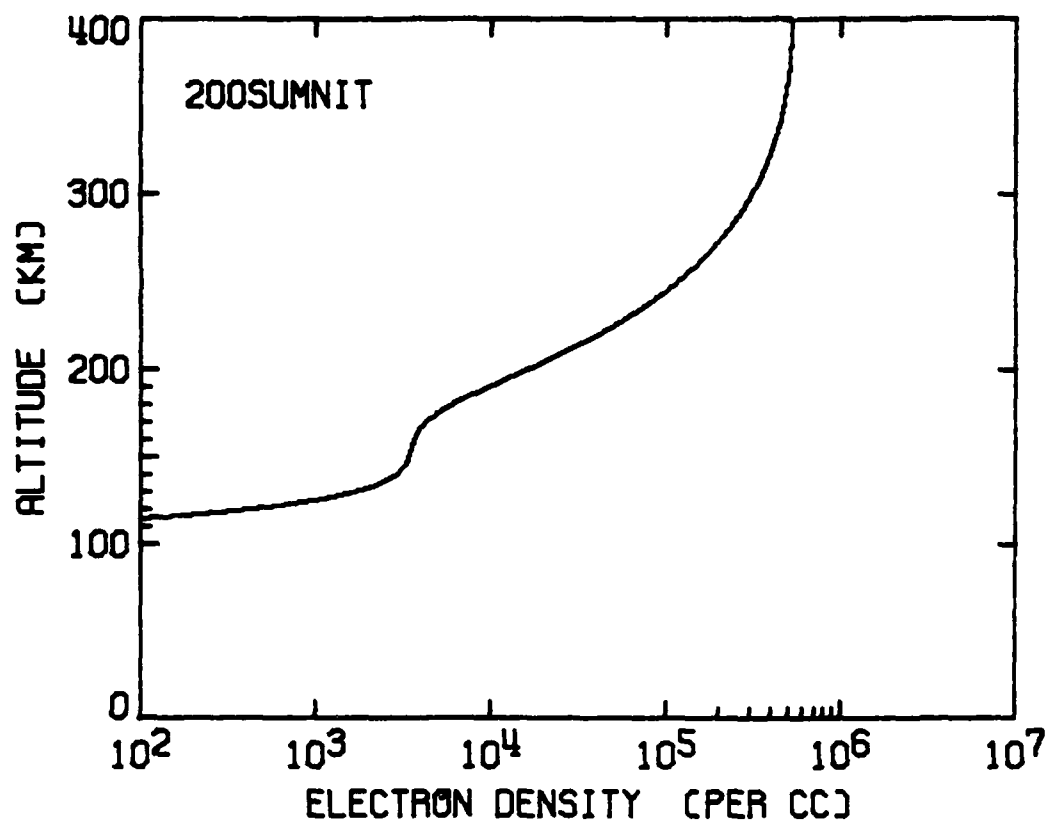
NL

UNCLASSIFIED

3 of 4

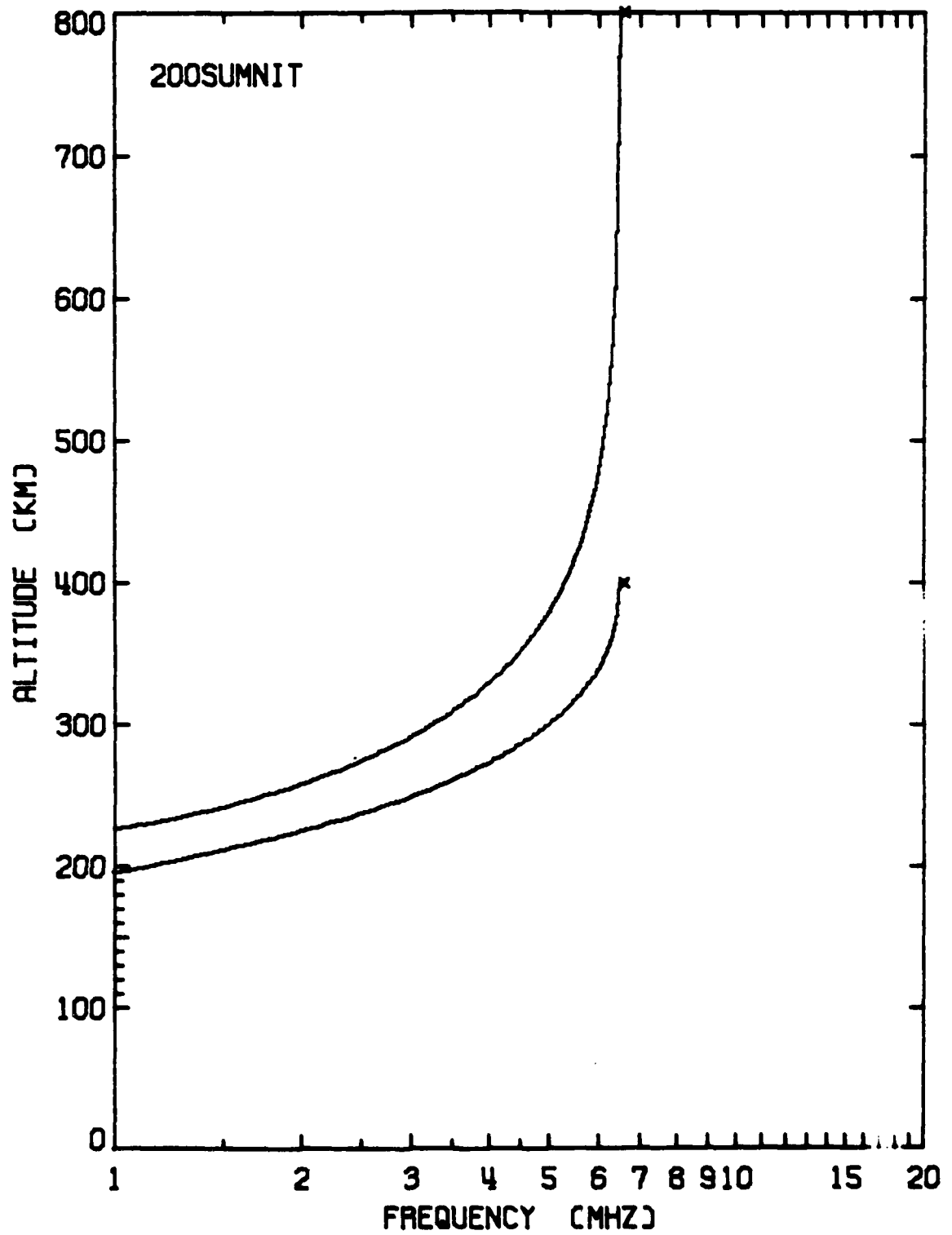
2 of 4



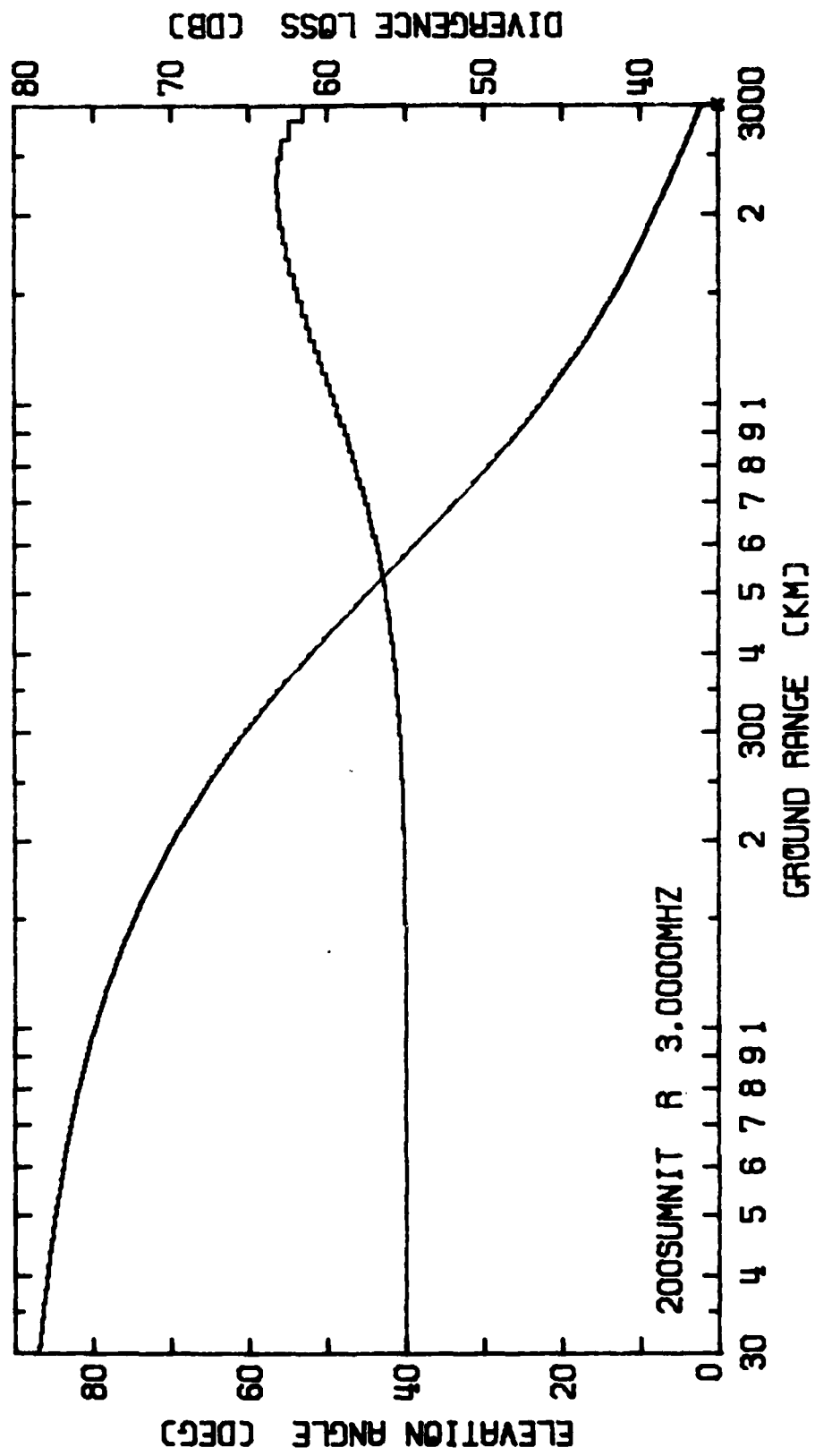


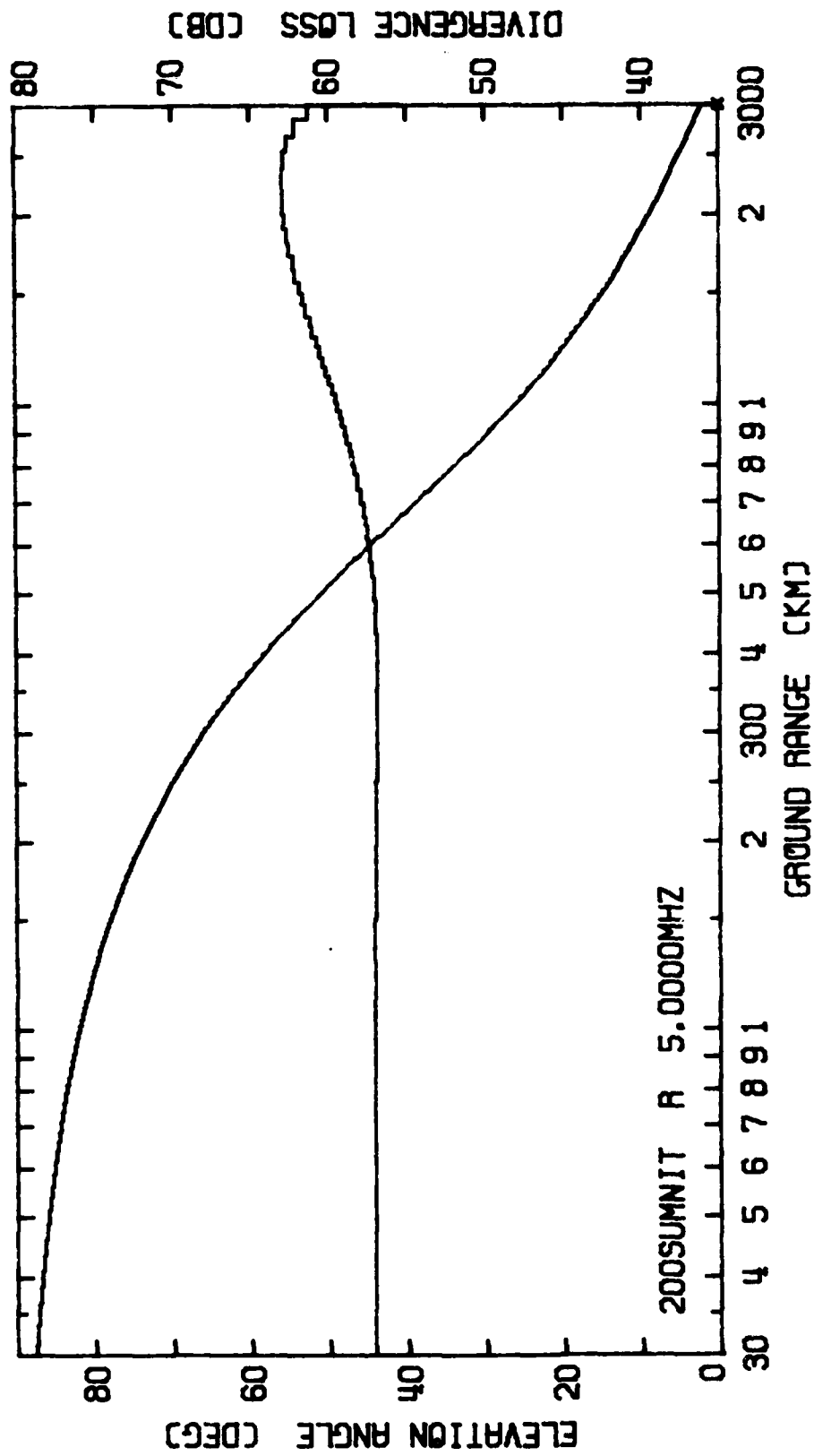
	<u>Level 1</u>	<u>Level 2</u>	<u>Level 3</u>
$h_o$ (km)	150	Absent	400
H (km)	15	Absent	85
$f_o$ (MHz)	0.50	Absent	6.50



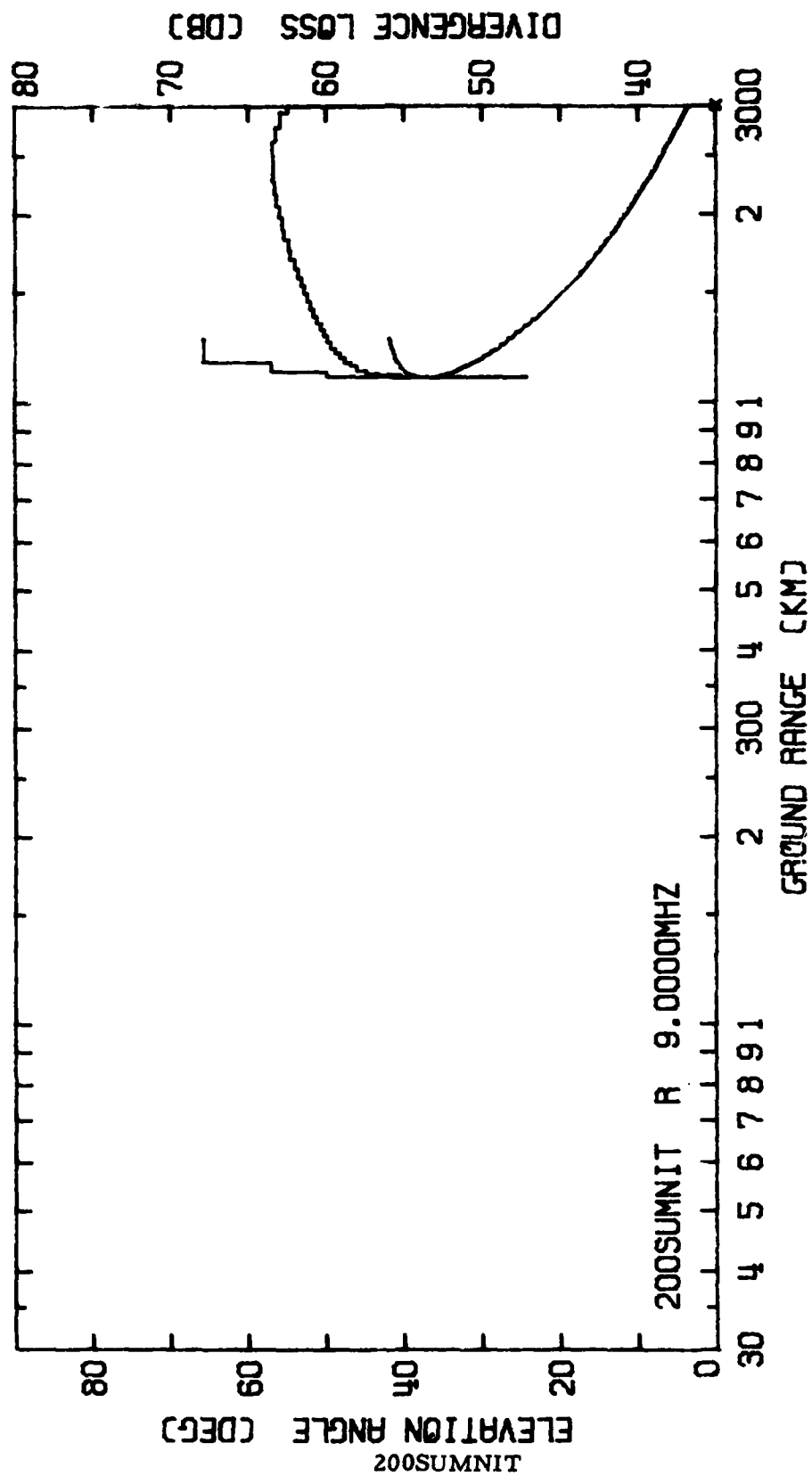


200SUMNIT  
175

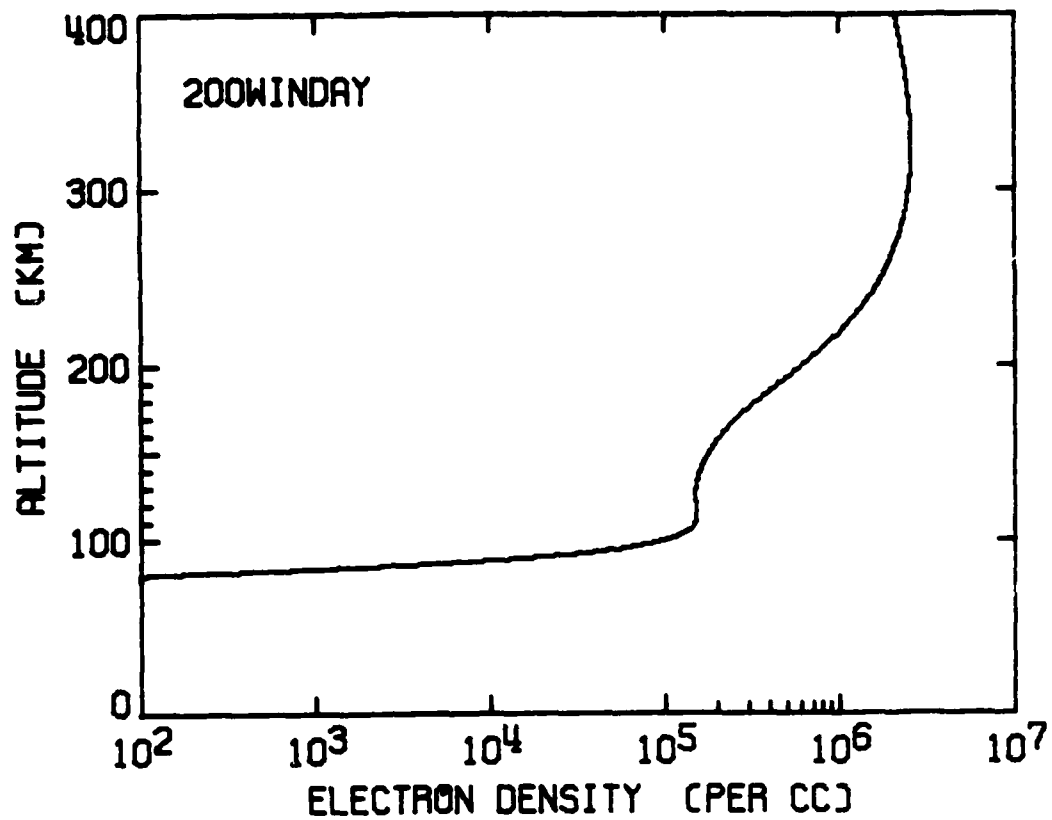




200SUMNIT  
177

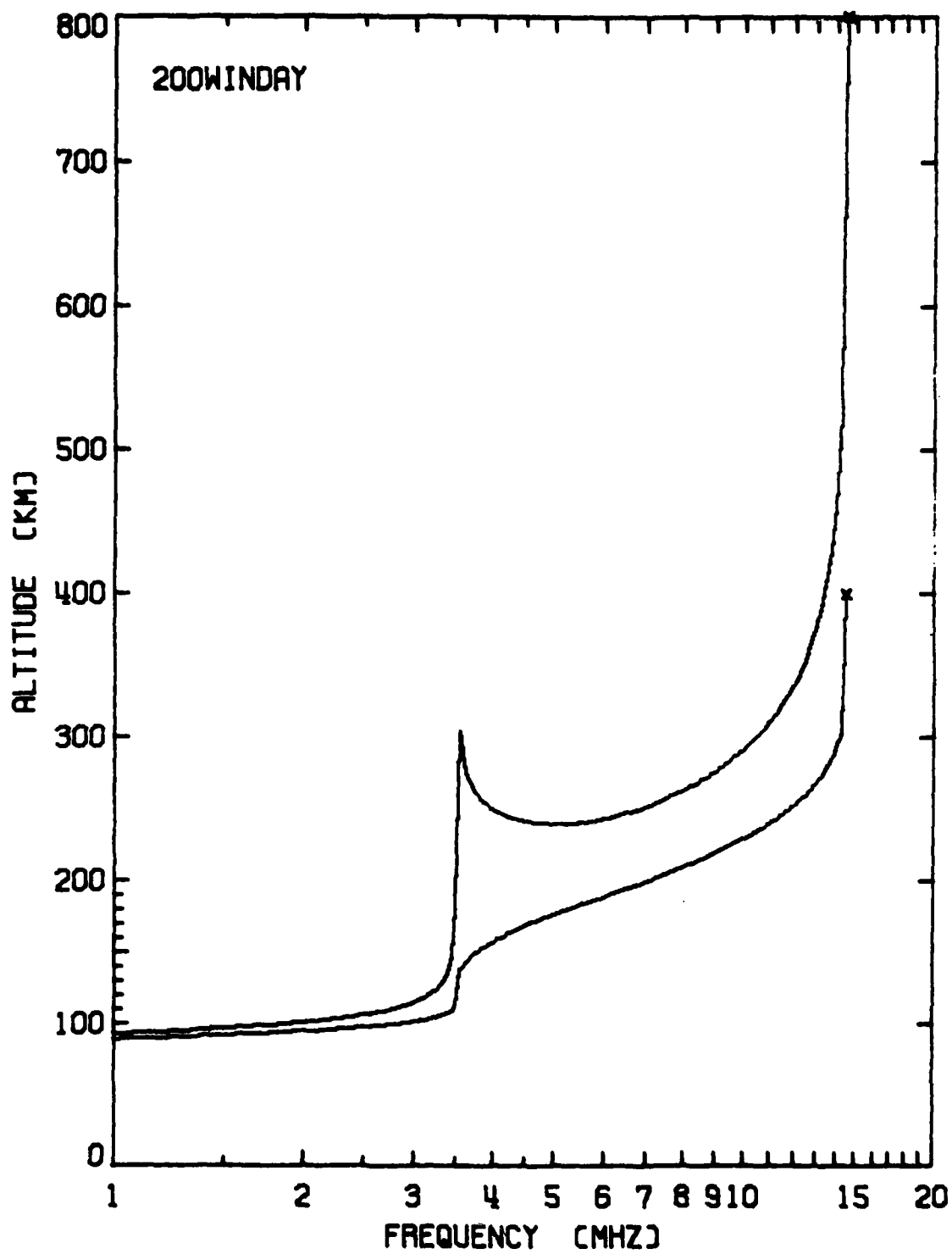


200SUMNIT

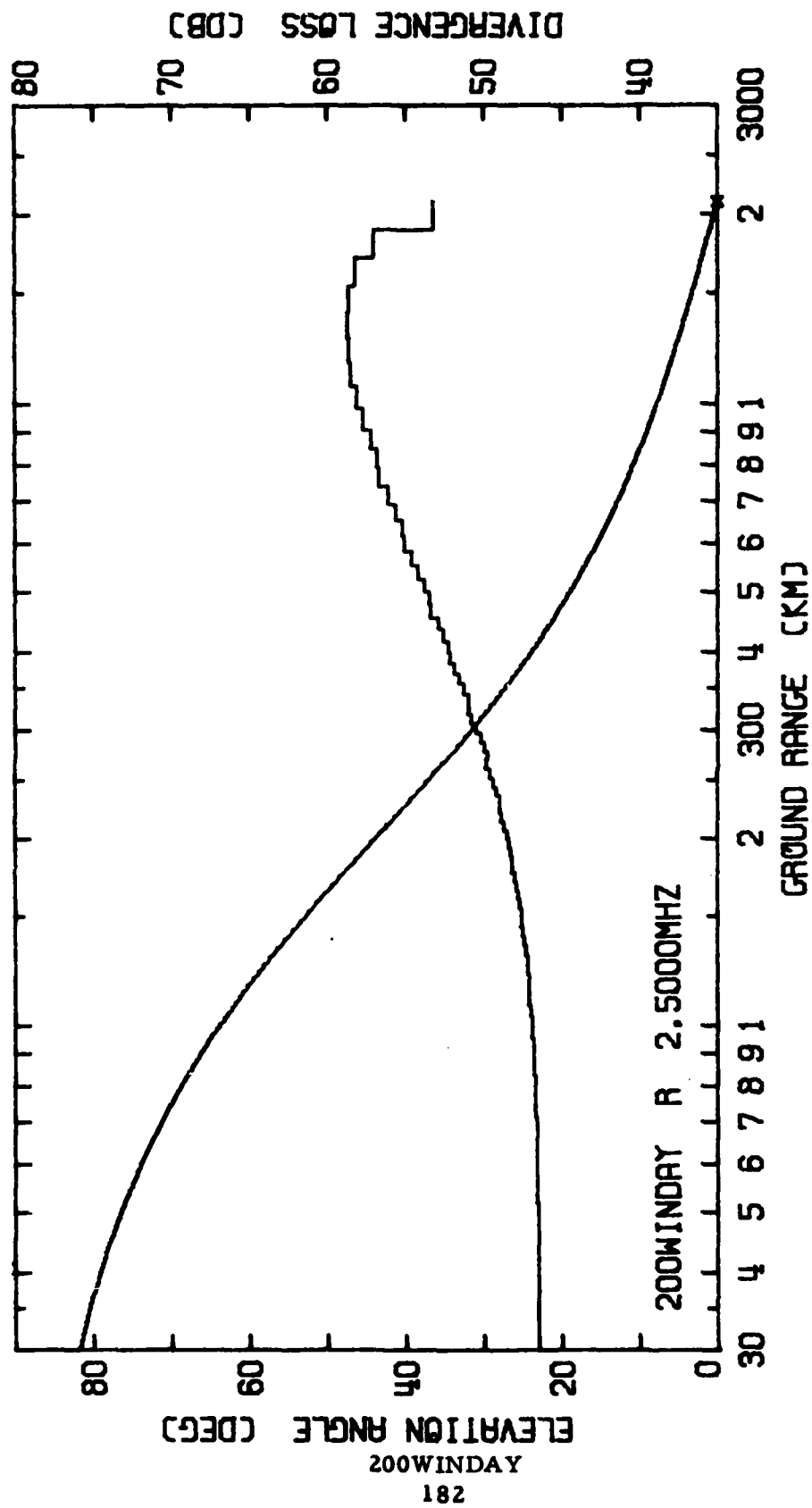


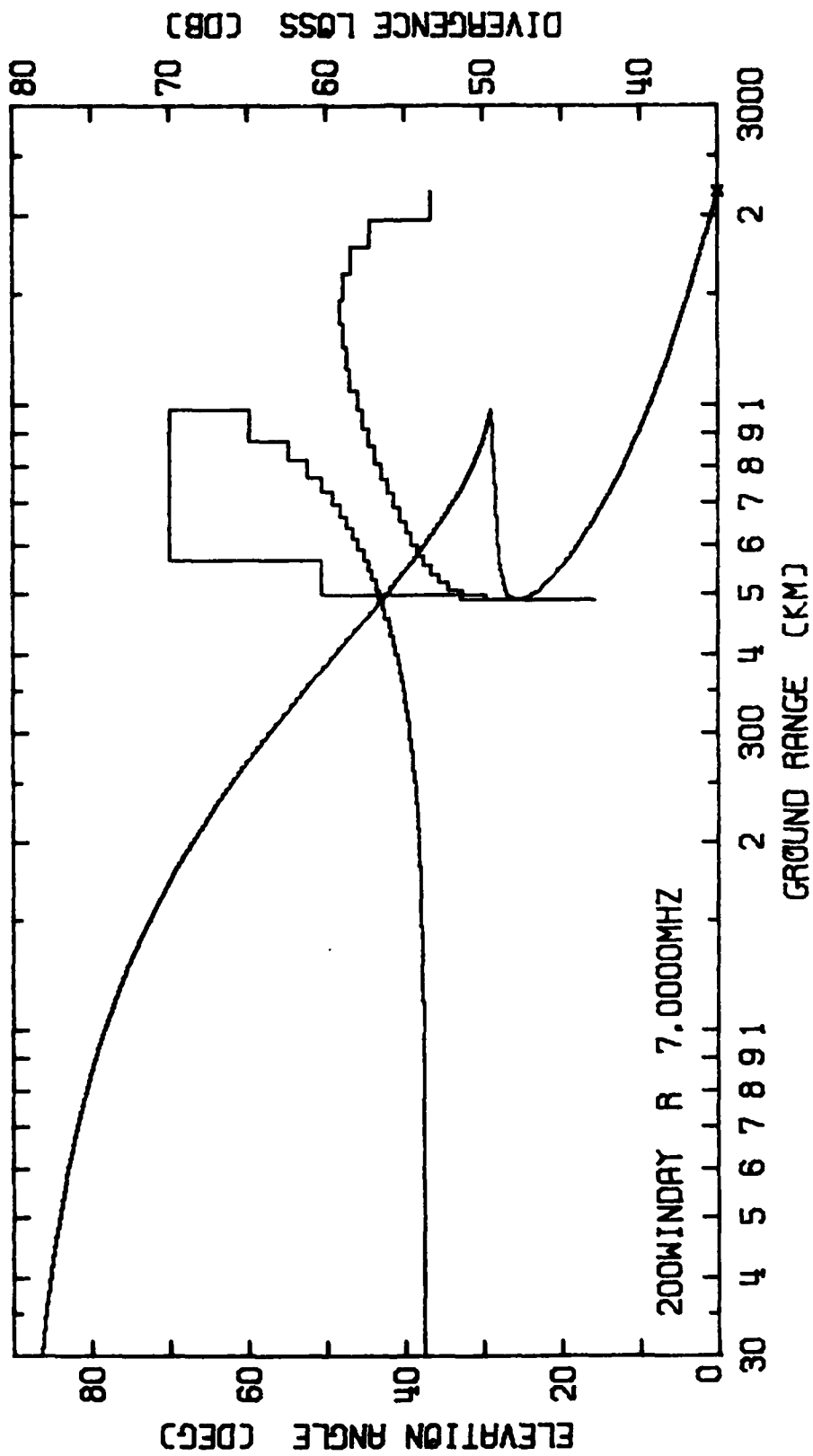
	<u>Level 1</u>	<u>Level 2</u>	<u>Level 3</u>
$h_o$ (km)	110	160	325
$H$ (km)	10	25	70
$f_o$ (MHz)	3.30	3.10	14.40

RECEIVED PAGE BLANK-NOT FILMED

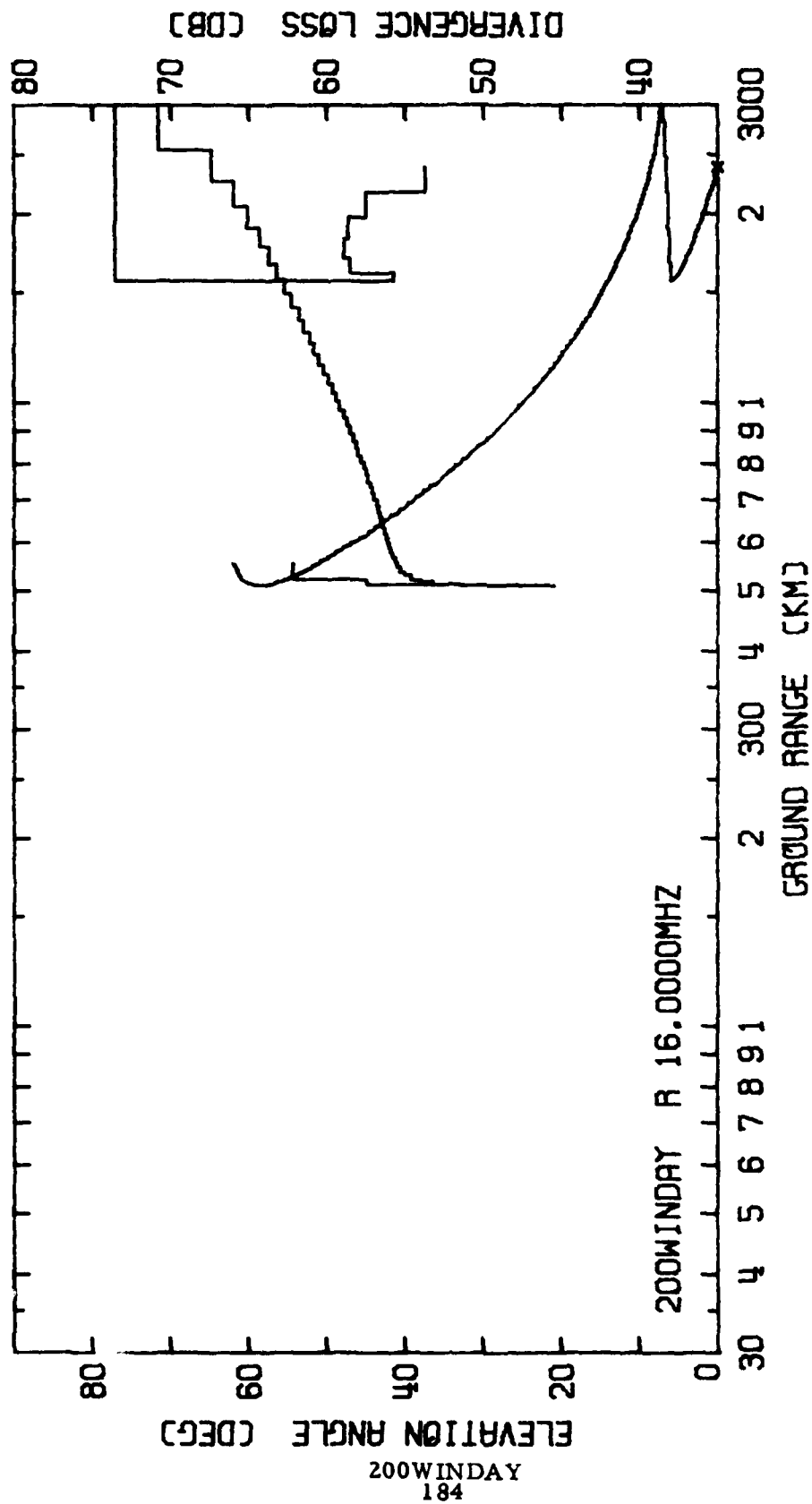


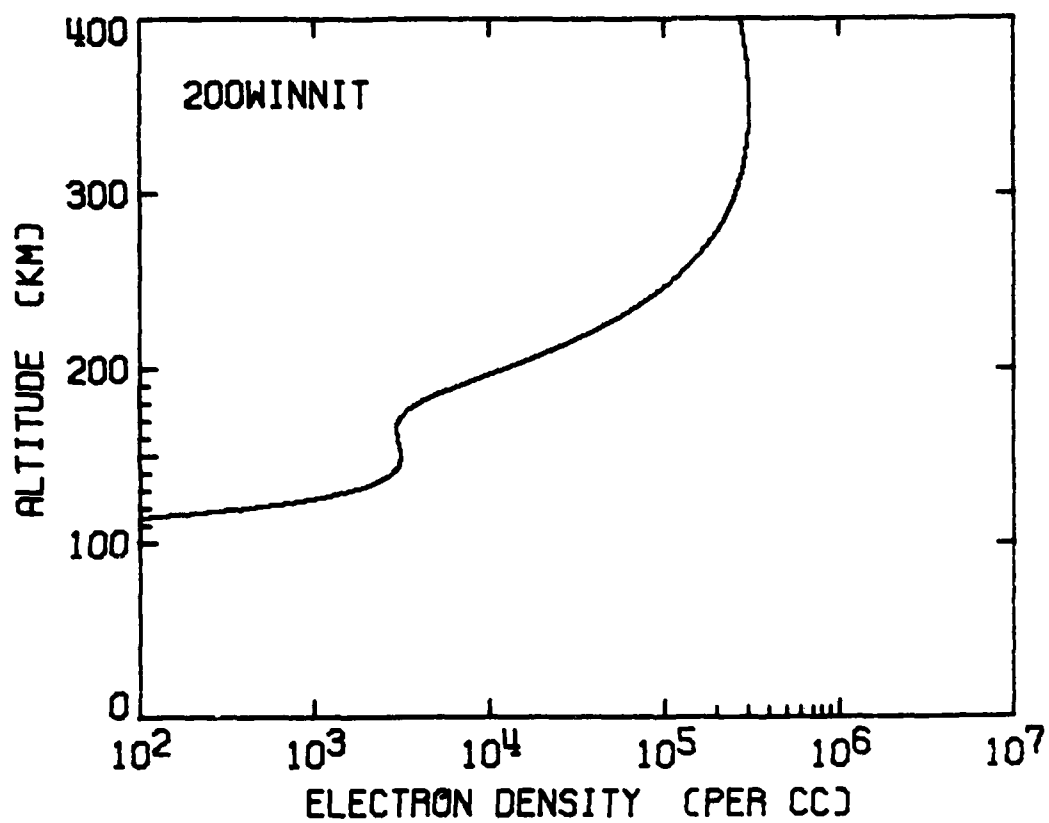
200WINDAY





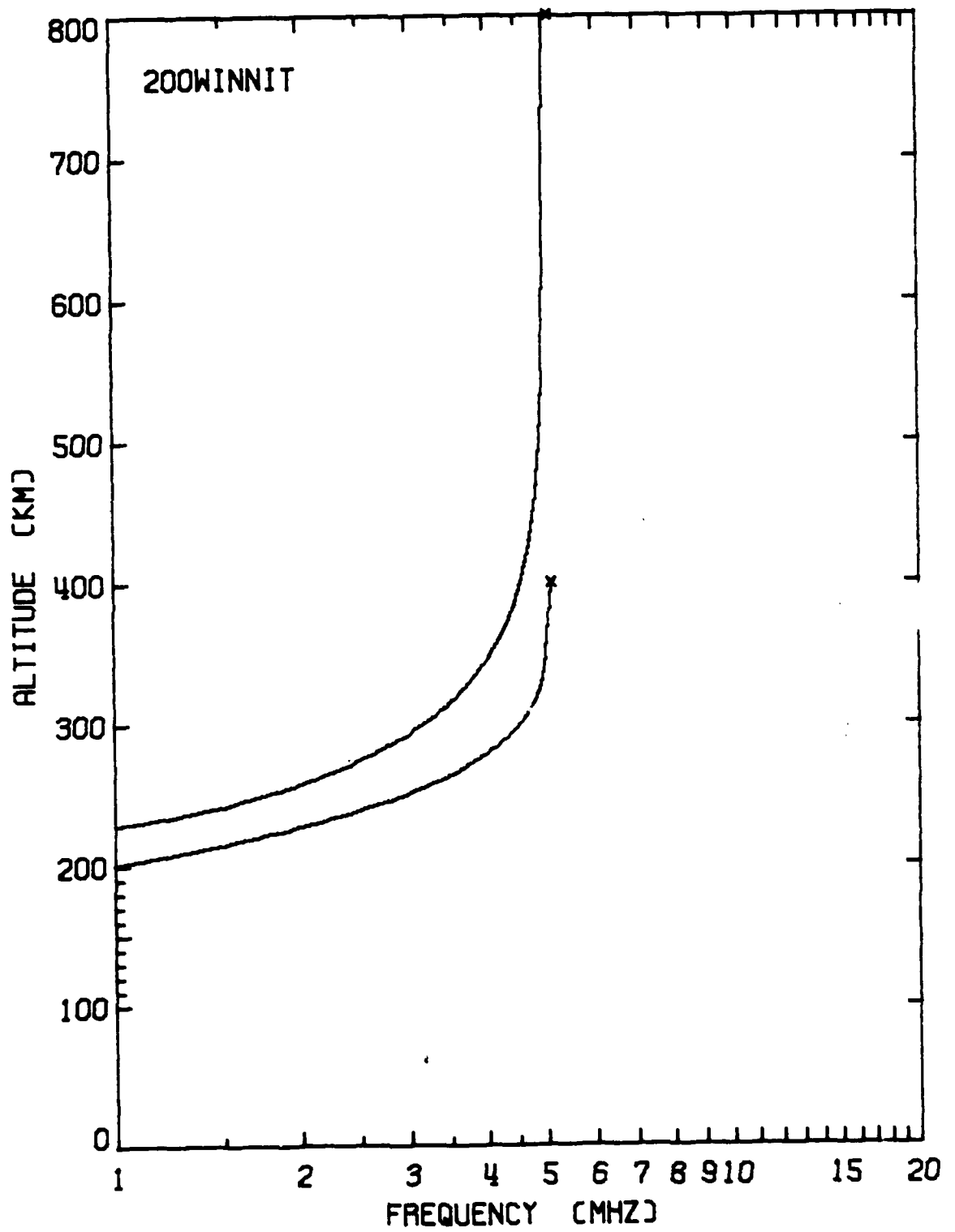




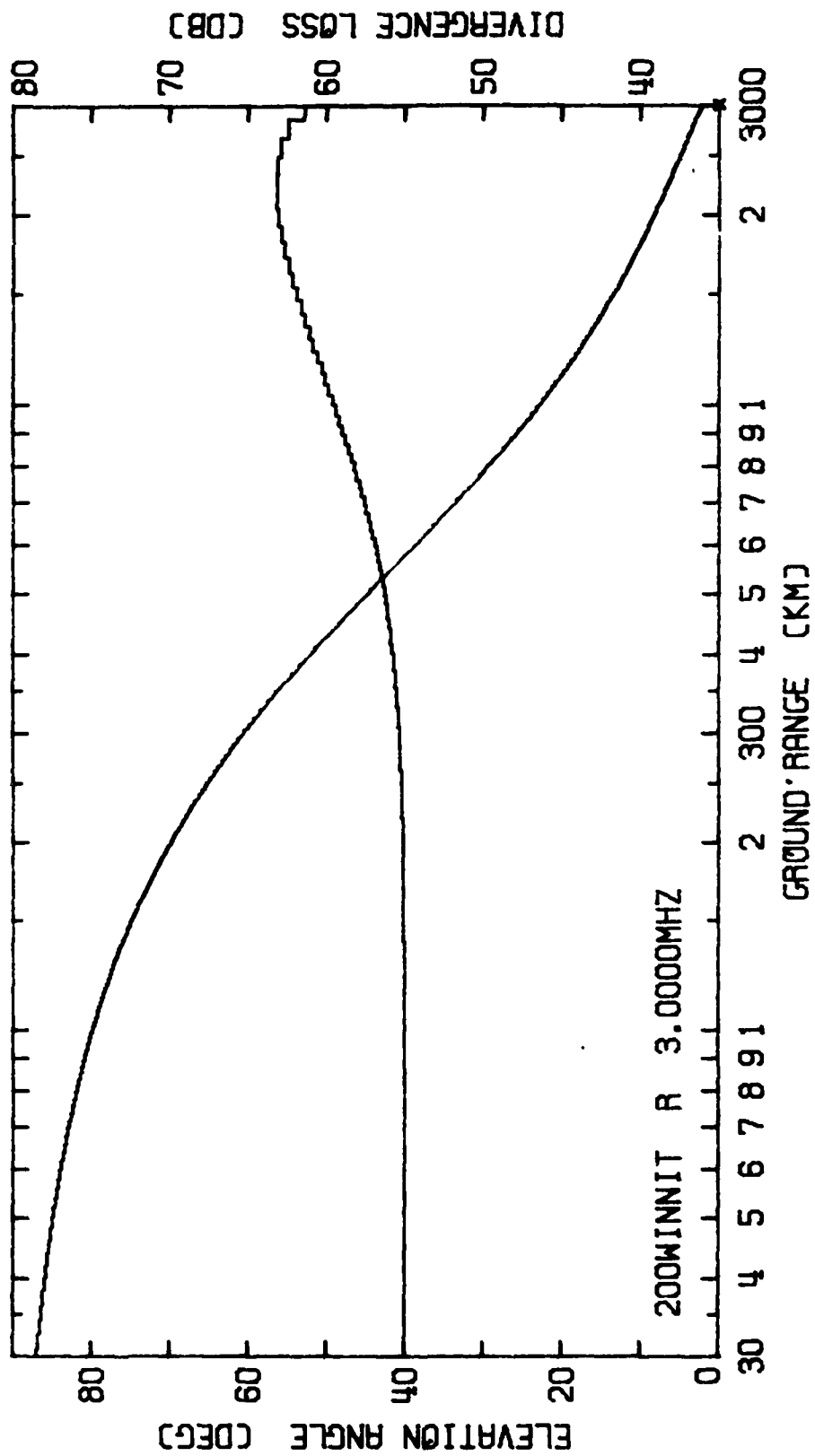


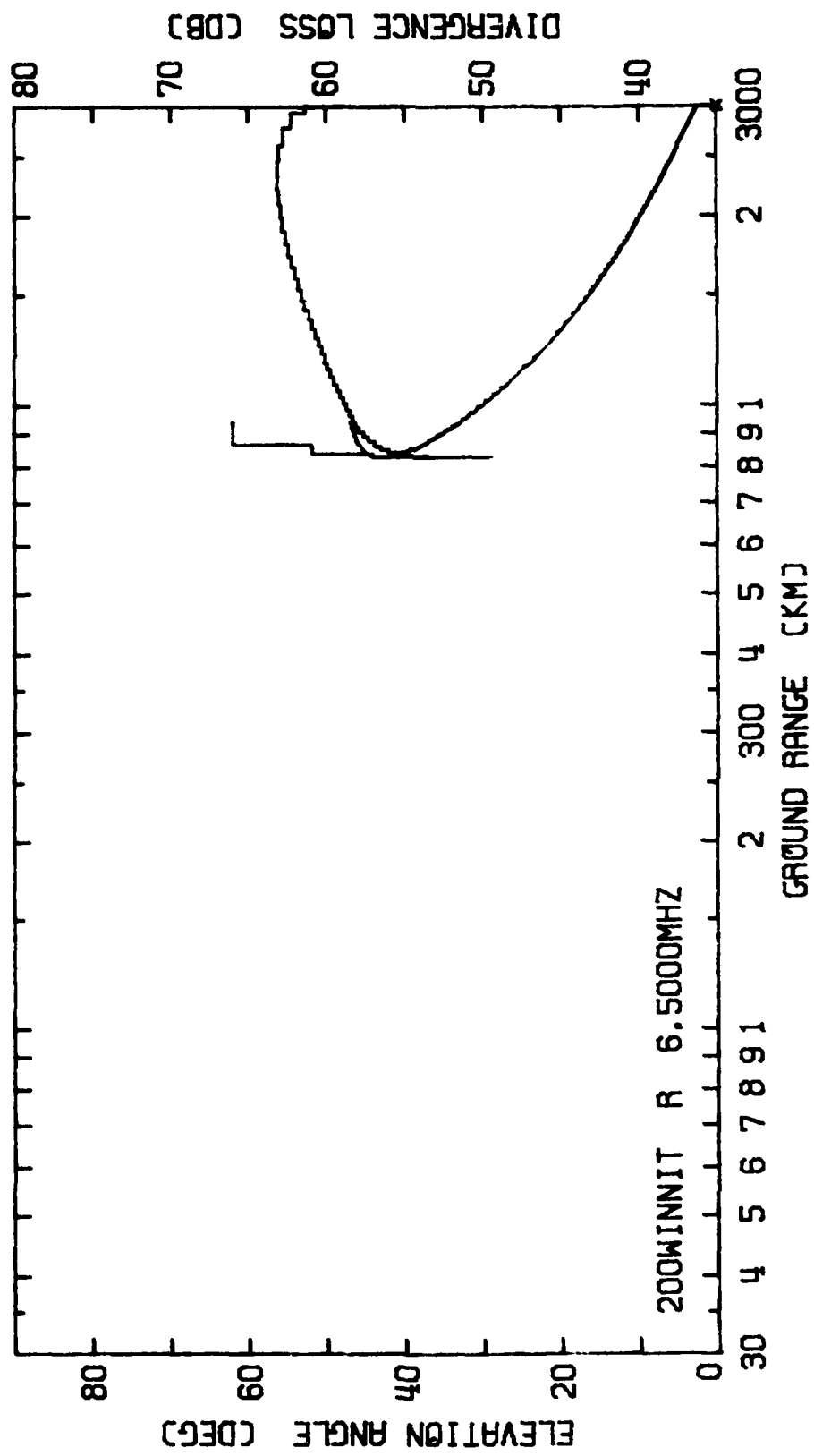
	<u>Level 1</u>	<u>Level 2</u>	<u>Level 3</u>
$h_o$ (km)	150	Absent	350
$H$ (km)	15	Absent	65
$f_o$ (MHz)	0.50	Absent	5.00

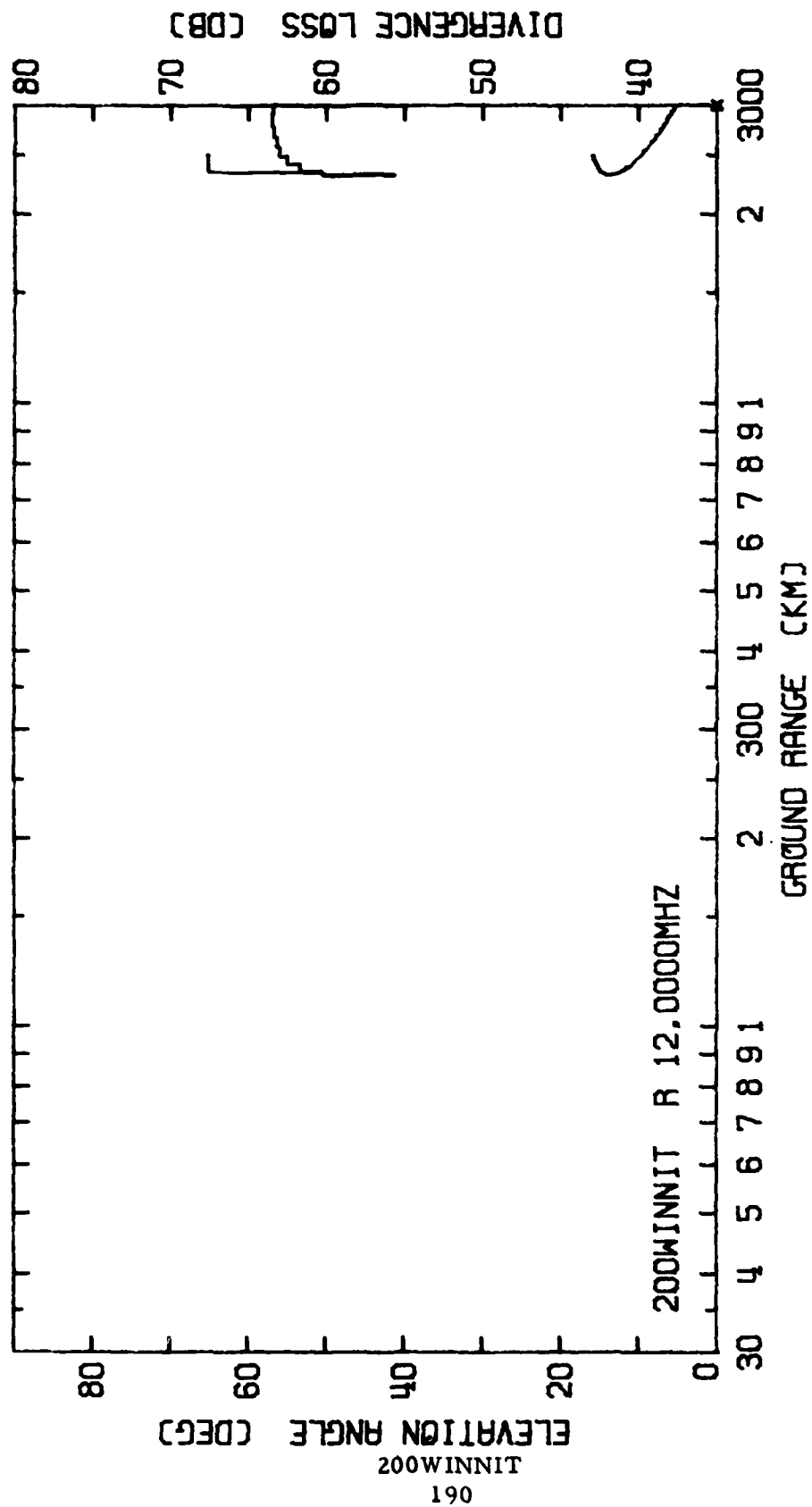
INFORMATION PAGE BLANK-NOT FILMED



200WINNIT  
187







## 2.5 ATLAS OF IONOSPHERIC ABSORPTION LOSS TABLES

The model used to estimate absorption loss is described in subsection 2.3.5. The tables in this atlas supplement the graphical solution of the model equation given in Figure 2-24. They are arranged to be more convenient in use than are the tables from which Figure 2-24 was constructed.

Table 2-8 is a guide to the atlas of absorption loss tables.\* Tables are arranged in the atlas in the order of the rows (lines) of Table 2-8. Each absorption loss table is assigned an identification symbol (eg, 045/112) which is given in the body of Table 2-8. The first half of the symbol is the 12-month running average sunspot number ( $R_{12}$ ). The second half is the electron gyrofrequency in hundredths of a MHz ( $f_H \times 10^{-4}$ ). The symbol will be found at the bottom of each table.

The tables in the atlas are divided into two groups, Basic Tables and Supplementary Tables. The tables in the basic group are for values of sunspot number:  $R_{12} = 5, 15, 45, 135$ . This sequence covers the range anticipated for the next solar cycle (Cycle 21, 1975-1985, approximately). In the supplementary group, tables are given for a sequence of sunspot number values which both interlaces the basic sequence and extends the basic sequence to the higher values which have been recorded in earlier solar cycles (e.g., in the second half of the 1950s decade).

To use the atlas, first select a value of sunspot number from either the basic or supplementary sequence. Using the first half of the identification symbol, locate the group of four tables for that value of  $R_{12}$ . Select the desired value of gyrofrequency from the sequence of four values. Using the last half of the identification symbol, locate the specific table within the group of four. In the specific table locate the section for the value of solar zenith angle nearest the desired value (the

---

\*In the headings of Table 2-8 and of the atlas tables a value of geomagnetic flux density is given in association with each value of electron gyrofrequency. The value is given in the gauss unit (CGS system),  $\Gamma$ , because it frequently is so found in the literature [10]. A sub-unit, the "gamma" ( $\gamma$ ) ( $1\gamma = 10^{-5}\Gamma$ ) also is frequently used. In recent literature the MKSA unit, weber/meter<sup>2</sup> ( $\text{Wb}/\text{m}^2$ ), or the tesla (T), appears [12]. The gauss and tesla have the relationship,  $1\Gamma = 10^{-4}\text{T}$ . Thus, the "gamma" ( $\gamma$ ) is equivalent to the nanotesla (nT).

column headed "SOLAR ANGLE"). Then read from the body of the table absorption loss in dB as a function of elevation angle (the column headed "SIGNAL ANGLE)--line--and operating frequency--column.



Table 2-8. Guide to atlas of absorption loss tables.

Running Average Sunspot Number	Electron Gyro-Frequency (MHz) Total Geomagnetic Field (Gauss)			
	0. 700	1. 120	1. 400	1. 820
	<u>0. 250</u>	<u>0. 400</u>	<u>0. 500</u>	<u>0. 650</u>
Basic Tables				
5	005/070	005/112	005/140	005/182
15	015/070	015/112	015/140	015/182
45	045/070	045/112	045/140	045/182
135	135/070	135/112	135/140	135/182
Supplementary Tables				
30	030/070	030/112	030/140	030/182
60	060/070	060/112	060/140	060/182
90	090/070	090/112	090/140	090/182
120	120/070	120/112	120/140	120/182
150	150/070	150/112	150/140	150/182
180	180/070	180/112	180/140	180/182
210	210/070	210/112	210/140	210/182
240	240/070	240/112	240/140	240/182

S S *		TOTAL IONOSPHERIC ABSORPTION LOSS (DECIBELS)									
O A I A *		*****									
L M G N *		AVERAGE SUNSPOT NUMBER (R12) 5.									
A G H G *		ELECTRON GYRO-FREQUENCY (MHZ) 0.700									
P L A L *		TOTAL GEOMAGNETIC FIELD (GAUSS) 0.250									
E L E *		*****									
		* SIGNAL FREQUENCY (MHZ)									
(DEG)	(DEG)	*	2.00	3.00	4.00	6.00	8.00	12.00	16.00	24.00	32.00
*****											
0	0	*	227.	167.	125.	74.	48.	24.	14.	7.	4.
	10	*	162.	120.	89.	53.	34.	17.	10.	5.	3.
	20	*	105.	77.	57.	34.	22.	11.	7.	3.	2.
	30	*	76.	56.	42.	25.	16.	8.	5.	2.	1.
	45	*	55.	41.	30.	18.	12.	6.	4.	2.	1.
	65	*	44.	32.	24.	14.	9.	5.	3.	1.	1.
90	*	40.	29.	22.	13.	8.	4.	3.	1.	1.	
*****											
20	0	*	213.	157.	117.	69.	45.	23.	14.	6.	4.
	10	*	153.	112.	84.	50.	32.	16.	10.	5.	3.
	20	*	98.	73.	54.	32.	21.	10.	6.	3.	2.
	30	*	71.	53.	39.	23.	15.	8.	5.	2.	1.
	45	*	52.	38.	29.	17.	11.	6.	3.	2.	1.
	65	*	41.	30.	23.	13.	9.	4.	3.	1.	1.
90	*	37.	28.	20.	12.	8.	4.	2.	1.	1.	
*****											
40	0	*	175.	129.	96.	57.	37.	19.	11.	5.	3.
	10	*	125.	92.	69.	41.	26.	13.	8.	4.	2.
	20	*	81.	59.	44.	26.	17.	9.	5.	2.	1.
	30	*	58.	43.	32.	19.	12.	6.	4.	2.	1.
	45	*	43.	31.	23.	14.	9.	5.	3.	1.	1.
	65	*	34.	25.	18.	11.	7.	4.	2.	1.	1.
90	*	31.	23.	17.	10.	6.	3.	2.	1.	1.	
*****											
60	0	*	118.	87.	65.	38.	25.	13.	7.	4.	2.
	10	*	84.	62.	46.	27.	18.	9.	5.	3.	1.
	20	*	54.	40.	30.	18.	11.	6.	3.	2.	1.
	30	*	39.	29.	22.	13.	8.	4.	3.	1.	1.
	45	*	29.	21.	16.	9.	6.	3.	2.	1.	0.
	65	*	23.	17.	12.	7.	5.	2.	1.	1.	0.
90	*	21.	15.	11.	7.	4.	2.	1.	1.	0.	
*****											
80	0	*	55.	40.	30.	18.	11.	6.	3.	2.	1.
	10	*	39.	29.	21.	13.	8.	4.	2.	1.	1.
	20	*	25.	19.	14.	8.	5.	3.	2.	1.	0.
	30	*	18.	13.	10.	6.	4.	2.	1.	1.	0.
	45	*	13.	10.	7.	4.	3.	1.	1.	0.	0.
	65	*	11.	8.	6.	3.	2.	1.	1.	0.	0.
90	*	10.	7.	5.	3.	2.	1.	1.	0.	0.	
*****											
100	0	*	3.	2.	1.	1.	1.	0.	0.	0.	0.
	10	*	2.	1.	1.	1.	0.	0.	0.	0.	0.
	20	*	1.	1.	1.	0.	0.	0.	0.	0.	0.
	30	*	1.	1.	0.	0.	0.	0.	0.	0.	0.
	45	*	1.	0.	0.	0.	0.	0.	0.	0.	0.
	65	*	1.	0.	0.	0.	0.	0.	0.	0.	0.
90	*	0.	0.	0.	0.	0.	0.	0.	0.	0.	
*****											
180	0	*	3.	2.	1.	1.	1.	0.	0.	0.	0.
	10	*	2.	1.	1.	1.	0.	0.	0.	0.	0.
	20	*	1.	1.	1.	0.	0.	0.	0.	0.	0.
	30	*	1.	1.	0.	0.	0.	0.	0.	0.	0.
	45	*	1.	0.	0.	0.	0.	0.	0.	0.	0.
	65	*	1.	0.	0.	0.	0.	0.	0.	0.	0.
90	*	0.	0.	0.	0.	0.	0.	0.	0.	0.	

005/070

S		TOTAL IONOSPHERIC ABSORPTION LOSS (DECIBELS)									
O A	I A	*****									
L N	G N	AVERAGE SUNSPOT NUMBER (R12) 5.									
A G	N G	ELECTRON GYRO-FREQUENCY (MHZ) 1.120									
R L	A L	TOTAL GEOMAGNETIC FIELD (GAUSS) 0.400									
E	L E	*****									
		* SIGNAL FREQUENCY (MHZ)									
(DEG)	(DEG)	2.00	3.00	4.00	6.00	8.00	12.00	16.00	24.00	32.00	
*****											
0	0	200.	147.	111.	67.	44.	23.	14.	7.	4.	
	10	143.	106.	79.	48.	31.	16.	10.	5.	3.	
	20	92.	68.	51.	31.	20.	10.	6.	3.	2.	
	30	67.	49.	37.	22.	15.	8.	5.	2.	1.	
	45	49.	36.	27.	16.	11.	6.	3.	2.	1.	
	65	38.	28.	21.	13.	8.	4.	3.	1.	1.	
	90	35.	26.	19.	12.	8.	4.	2.	1.	1.	
*****											
20	0	188.	139.	104.	63.	41.	21.	13.	6.	4.	
	10	134.	90.	74.	45.	29.	15.	9.	4.	3.	
	20	87.	64.	48.	29.	19.	10.	6.	3.	2.	
	30	63.	46.	35.	21.	14.	7.	4.	2.	1.	
	45	46.	34.	25.	15.	10.	5.	3.	1.	1.	
	65	36.	27.	20.	12.	8.	4.	2.	1.	1.	
	90	33.	24.	18.	11.	7.	4.	2.	1.	1.	
*****											
40	0	154.	113.	85.	51.	34.	17.	11.	5.	3.	
	10	110.	81.	61.	37.	24.	12.	8.	4.	2.	
	20	71.	52.	39.	24.	16.	8.	5.	2.	1.	
	30	51.	38.	29.	17.	11.	6.	4.	2.	1.	
	45	37.	28.	21.	13.	8.	4.	3.	1.	1.	
	65	30.	22.	16.	10.	6.	3.	2.	1.	1.	
	90	27.	20.	15.	9.	6.	3.	2.	1.	1.	
*****											
60	0	104.	77.	57.	35.	23.	12.	7.	3.	2.	
	10	74.	55.	41.	25.	16.	8.	5.	2.	1.	
	20	48.	35.	27.	16.	11.	5.	3.	2.	1.	
	30	35.	26.	19.	12.	8.	4.	2.	1.	1.	
	45	25.	19.	14.	8.	6.	3.	2.	1.	0.	
	65	20.	15.	11.	7.	4.	2.	1.	1.	0.	
	90	18.	13.	10.	6.	4.	2.	1.	1.	0.	
*****											
80	0	48.	35.	27.	16.	11.	5.	3.	2.	1.	
	10	34.	25.	19.	11.	8.	4.	2.	1.	1.	
	20	22.	16.	12.	7.	5.	3.	2.	1.	0.	
	30	16.	12.	9.	5.	4.	2.	1.	1.	0.	
	45	12.	9.	6.	4.	3.	1.	1.	0.	0.	
	65	9.	7.	5.	3.	2.	1.	1.	0.	0.	
	90	8.	6.	5.	3.	2.	1.	1.	0.	0.	
*****											
100	0	2.	2.	1.	1.	1.	0.	0.	0.	0.	
70	10	2.	1.	1.	1.	0.	0.	0.	0.	0.	
180	20	1.	1.	1.	0.	0.	0.	0.	0.	0.	
	30	1.	1.	0.	0.	0.	0.	0.	0.	0.	
	45	1.	0.	0.	0.	0.	0.	0.	0.	0.	
	65	0.	0.	0.	0.	0.	0.	0.	0.	0.	
	90	0.	0.	0.	0.	0.	0.	0.	0.	0.	

S S \* TOTAL IONOSPHERIC ABSORPTION LOSS (DECIBELS)  
 O A I A \*\*\*\*\*  
 L N G N \* AVERAGE SUNSPOT NUMBER (R12) 5.  
 A G N G \* ELECTRON GYRO-FREQUENCY (MHZ) 1.400  
 R L A L \* TOTAL GEOMAGNETIC FIELD (GAUSS) 0.500  
 F L F \*\*\*\*\*

		* SIGNAL FREQUENCY (MHZ)								
(DEG)	(DEG)	* 2.00	3.00	4.00	6.00	8.00	12.00	16.00	24.00	32.00
*****										
0	0	*	183.	136.	103.	63.	42.	22.	13.	6.
	10	*	131.	97.	73.	45.	30.	16.	10.	5.
	20	*	85.	63.	47.	29.	19.	10.	6.	3.
	30	*	61.	46.	34.	21.	14.	7.	4.	2.
	45	*	45.	33.	25.	15.	10.	5.	3.	2.
	65	*	35.	26.	20.	12.	8.	4.	3.	1.
20	90	*	32.	24.	18.	11.	7.	4.	2.	1.
	0	*	172.	128.	96.	59.	39.	20.	12.	6.
	10	*	123.	91.	69.	42.	28.	15.	9.	4.
	20	*	79.	54.	44.	27.	18.	9.	6.	3.
	30	*	58.	43.	32.	20.	13.	7.	4.	2.
	45	*	42.	31.	24.	14.	10.	5.	3.	1.
40	65	*	34.	25.	19.	11.	8.	4.	2.	1.
	90	*	30.	22.	17.	10.	7.	4.	2.	1.
	0	*	141.	104.	79.	48.	32.	17.	10.	5.
	10	*	101.	75.	56.	34.	23.	12.	7.	4.
	20	*	65.	48.	36.	22.	15.	8.	5.	2.
	30	*	47.	35.	26.	16.	11.	6.	3.	2.
60	45	*	34.	25.	19.	12.	8.	4.	2.	1.
	65	*	27.	20.	15.	9.	6.	3.	2.	1.
	90	*	25.	18.	14.	8.	6.	3.	2.	1.
	0	*	95.	70.	53.	33.	22.	11.	7.	3.
	10	*	68.	50.	38.	23.	15.	8.	5.	2.
	20	*	44.	33.	25.	15.	10.	5.	3.	2.
80	30	*	32.	24.	18.	11.	7.	4.	2.	1.
	45	*	23.	17.	13.	8.	5.	3.	2.	1.
	65	*	18.	14.	10.	6.	4.	2.	1.	1.
	90	*	17.	12.	9.	6.	4.	2.	1.	0.
	0	*	44.	33.	25.	15.	10.	5.	3.	2.
	10	*	32.	23.	18.	11.	7.	4.	2.	1.
100	20	*	20.	15.	11.	7.	5.	2.	1.	1.
	30	*	15.	11.	8.	5.	3.	2.	1.	0.
	45	*	11.	8.	6.	4.	2.	1.	1.	0.
	65	*	8.	6.	5.	3.	2.	1.	1.	0.
	90	*	8.	6.	4.	3.	2.	1.	1.	0.
	0	*	2.	2.	1.	1.	0.	0.	0.	0.
120	10	*	2.	1.	1.	1.	0.	0.	0.	0.
	20	*	1.	1.	1.	0.	0.	0.	0.	0.
	30	*	1.	1.	0.	0.	0.	0.	0.	0.
	45	*	1.	0.	0.	0.	0.	0.	0.	0.
	65	*	0.	0.	0.	0.	0.	0.	0.	0.
	90	*	0.	0.	0.	0.	0.	0.	0.	0.

005/140

S S \* TOTAL IONOSPHERIC ABSORPTION LOSS (DECIBELS)  
 O A I A \*  
 L N G N \* AVERAGE SUNSPOT NUMBER (R12) 5.  
 A G N G \* ELECTRON GYRO-FREQUENCY (MHZ) 1.820  
 R L A L \* TOTAL GEOMAGNETIC FIELD (GAUSS) 0.650  
 E L E \*

		* SIGNAL FREQUENCY (MHZ)									
(DEG)	(DEG)	* 2.00	* 3.00	* 4.00	* 6.00	* 8.00	* 12.00	* 16.00	* 24.00	* 32.00	
*****											
0	0	* 161.	120.	92.	57.	38.	21.	13.	6.	4.	
	10	* 115.	86.	66.	41.	28.	15.	9.	4.	3.	
	20	* 74.	56.	42.	26.	18.	9.	6.	3.	2.	
	30	* 54.	40.	31.	19.	13.	7.	4.	2.	1.	
	45	* 39.	29.	22.	14.	9.	5.	3.	2.	1.	
	65	* 31.	23.	18.	11.	7.	4.	2.	1.	1.	
20	90	* 28.	21.	16.	10.	7.	4.	2.	1.	1.	
	0	* 152.	113.	86.	54.	36.	19.	12.	6.	3.	
	10	* 108.	81.	62.	38.	26.	14.	9.	4.	2.	
	20	* 70.	52.	40.	25.	17.	9.	6.	3.	2.	
	30	* 51.	38.	29.	18.	12.	6.	4.	2.	1.	
	45	* 37.	28.	21.	13.	9.	5.	3.	1.	1.	
40	65	* 29.	22.	17.	10.	7.	4.	2.	1.	1.	
	90	* 27.	20.	15.	9.	6.	3.	2.	1.	1.	
	0	* 124.	93.	71.	44.	30.	16.	10.	5.	3.	
	10	* 89.	66.	50.	31.	21.	11.	7.	3.	2.	
	20	* 57.	43.	33.	20.	14.	7.	5.	2.	1.	
	30	* 42.	31.	24.	15.	10.	5.	3.	2.	1.	
60	45	* 30.	23.	17.	11.	7.	4.	2.	1.	1.	
	65	* 24.	18.	14.	8.	6.	3.	2.	1.	1.	
	90	* 21.	16.	12.	8.	5.	3.	2.	1.	0.	
	0	* 84.	62.	48.	30.	20.	11.	7.	3.	2.	
	10	* 60.	45.	34.	21.	14.	8.	5.	2.	1.	
	20	* 39.	29.	22.	14.	9.	5.	3.	1.	1.	
80	30	* 28.	21.	16.	10.	7.	4.	2.	1.	1.	
	45	* 20.	15.	12.	7.	5.	3.	2.	1.	0.	
	65	* 16.	12.	9.	6.	4.	2.	1.	1.	0.	
	90	* 15.	11.	8.	5.	3.	2.	1.	1.	0.	
	0	* 39.	29.	22.	14.	9.	5.	3.	1.	1.	
	10	* 28.	21.	16.	10.	7.	4.	2.	1.	1.	
100	20	* 18.	13.	10.	6.	4.	2.	1.	1.	0.	
	30	* 13.	10.	7.	5.	3.	2.	1.	1.	0.	
	45	* 9.	7.	5.	3.	2.	1.	1.	0.	0.	
	65	* 7.	6.	4.	3.	2.	1.	1.	0.	0.	
	90	* 7.	5.	4.	2.	2.	1.	1.	0.	0.	
	0	* 2.	1.	1.	1.	0.	0.	0.	0.	0.	
180	10	* 1.	1.	1.	0.	0.	0.	0.	0.	0.	
	20	* 1.	1.	1.	0.	0.	0.	0.	0.	0.	
	30	* 1.	0.	0.	0.	0.	0.	0.	0.	0.	
	45	* 0.	0.	0.	0.	0.	0.	0.	0.	0.	
	65	* 0.	0.	0.	0.	0.	0.	0.	0.	0.	
	90	* 0.	0.	0.	0.	0.	0.	0.	0.	0.	

005/182

S	S	*	TOTAL IONOSPHERIC ABSORPTION LOSS (DECIBELS)								
O A	I A	*****									
L N	G N	*	AVERAGE SUNSPOT NUMBER (R12) 15.								
A G	H G	*	ELECTRON GYRO-FREQUENCY (MHZ) 0.700								
R L	A L	*	TOTAL GEOMAGNETIC FIELD (GAUSS) 0.250								
E	L E	*****									
		*	SIGNAL FREQUENCY (MHZ)								
(DFG)	(DFG)	*	2.00	3.00	4.00	6.00	8.00	12.00	16.00	24.00	32.00
*****											
0	0	*	235.	173.	129.	76.	49.	25.	15.	7.	4.
	10	*	168.	124.	92.	55.	35.	18.	11.	5.	3.
	20	*	109.	80.	60.	35.	23.	12.	7.	3.	2.
	30	*	79.	58.	43.	26.	17.	8.	5.	2.	1.
	45	*	57.	42.	31.	19.	12.	6.	4.	2.	1.
	65	*	45.	33.	25.	15.	10.	5.	3.	1.	1.
	90	*	41.	30.	23.	13.	9.	4.	3.	1.	1.
*****											
20	0	*	221.	163.	121.	72.	46.	23.	14.	7.	4.
	10	*	158.	117.	87.	51.	33.	17.	10.	5.	3.
	20	*	102.	75.	56.	33.	21.	11.	6.	3.	2.
	30	*	74.	55.	41.	24.	16.	8.	5.	2.	1.
	45	*	54.	40.	30.	18.	11.	6.	3.	2.	1.
	65	*	43.	31.	23.	14.	9.	5.	3.	1.	1.
	90	*	39.	29.	21.	13.	8.	4.	2.	1.	1.
*****											
40	0	*	181.	133.	94.	59.	38.	19.	11.	5.	3.
	10	*	129.	95.	71.	42.	27.	14.	8.	4.	2.
	20	*	83.	61.	46.	27.	18.	9.	5.	2.	1.
	30	*	61.	45.	33.	20.	13.	6.	4.	2.	1.
	45	*	44.	33.	24.	14.	9.	5.	3.	1.	1.
	65	*	35.	26.	19.	11.	7.	4.	2.	1.	1.
	90	*	32.	23.	17.	10.	7.	3.	2.	1.	1.
*****											
60	0	*	122.	90.	67.	40.	26.	13.	8.	4.	2.
	10	*	87.	64.	48.	28.	18.	9.	6.	3.	2.
	20	*	56.	42.	31.	18.	12.	6.	4.	2.	1.
	30	*	41.	30.	22.	13.	9.	4.	3.	1.	1.
	45	*	30.	22.	16.	10.	6.	3.	2.	1.	1.
	65	*	24.	17.	13.	8.	5.	2.	1.	1.	0.
	90	*	21.	16.	12.	7.	4.	2.	1.	1.	0.
*****											
80	0	*	57.	42.	31.	18.	12.	6.	4.	2.	1.
	10	*	40.	30.	22.	13.	8.	4.	3.	1.	1.
	20	*	26.	19.	14.	8.	5.	3.	2.	1.	0.
	30	*	19.	14.	10.	6.	4.	2.	1.	1.	0.
	45	*	14.	10.	8.	4.	3.	1.	1.	0.	0.
	65	*	11.	8.	6.	4.	2.	1.	1.	0.	0.
	90	*	10.	7.	5.	3.	2.	1.	1.	0.	0.
*****											
100	0	*	3.	2.	2.	1.	1.	0.	0.	0.	0.
120	10	*	2.	1.	1.	1.	0.	0.	0.	0.	0.
140	20	*	1.	1.	1.	0.	0.	0.	0.	0.	0.
	30	*	1.	1.	1.	0.	0.	0.	0.	0.	0.
	45	*	1.	1.	0.	0.	0.	0.	0.	0.	0.
	65	*	1.	0.	0.	0.	0.	0.	0.	0.	0.
	90	*	0.	0.	0.	0.	0.	0.	0.	0.	0.

015/070

S S \* TOTAL IONOSPHERIC ABSORPTION LOSS (DECIBELS)  
 O A I A \*\*\*\*\*  
 L N G N \* AVERAGE SUNSPOT NUMBER (R12) 15.  
 A G N G \* ELECTRON GYRO-FREQUENCY (MHZ) 1.120  
 R L A L \* TOTAL GEOMAGNETIC FIELD (GAUSS) 0.400  
 E L E \*\*\*\*\*

		* SIGNAL FREQUENCY (MHZ)									
(DEG)	(DEG)	*	2.00	3.00	4.00	6.00	8.00	12.00	16.00	24.00	32.00
*****											
0	0	*	207.	153.	115.	69.	45.	23.	14.	7.	4.
	10	*	148.	109.	82.	50.	33.	17.	10.	5.	3.
	20	*	96.	71.	53.	32.	21.	11.	7.	3.	2.
	30	*	69.	51.	38.	23.	15.	8.	5.	2.	1.
	45	*	51.	37.	28.	17.	11.	6.	3.	2.	1.
	65	*	40.	29.	22.	13.	9.	5.	3.	1.	1.
20	90	*	36.	27.	20.	12.	8.	4.	2.	1.	1.
	0	*	194.	144.	108.	65.	43.	22.	13.	6.	4.
	10	*	139.	103.	77.	47.	31.	16.	10.	5.	3.
	20	*	90.	66.	50.	30.	20.	10.	6.	3.	2.
	30	*	65.	48.	36.	22.	14.	7.	4.	2.	1.
	45	*	47.	35.	26.	16.	10.	5.	3.	2.	1.
40	65	*	37.	28.	21.	13.	8.	4.	3.	1.	1.
	90	*	34.	25.	19.	11.	7.	4.	2.	1.	1.
	0	*	159.	117.	88.	53.	35.	18.	11.	5.	3.
	10	*	114.	84.	63.	38.	25.	13.	8.	4.	2.
	20	*	73.	54.	41.	25.	16.	8.	5.	2.	1.
	30	*	53.	39.	30.	18.	12.	6.	4.	2.	1.
60	45	*	39.	29.	22.	13.	9.	4.	3.	1.	1.
	65	*	31.	23.	17.	10.	7.	3.	2.	1.	1.
	90	*	28.	21.	15.	9.	6.	3.	2.	1.	1.
	0	*	107.	79.	60.	36.	24.	12.	7.	4.	2.
	10	*	77.	57.	43.	26.	17.	9.	5.	3.	1.
	20	*	50.	37.	27.	17.	11.	6.	3.	2.	1.
80	30	*	36.	27.	20.	12.	8.	4.	2.	1.	1.
	45	*	26.	19.	15.	9.	6.	3.	2.	1.	1.
	65	*	21.	15.	11.	7.	5.	2.	1.	1.	0.
	90	*	19.	14.	10.	6.	4.	2.	1.	1.	0.
	0	*	50.	37.	28.	17.	11.	6.	3.	2.	1.
	10	*	36.	26.	20.	12.	8.	4.	2.	1.	1.
100	20	*	23.	17.	13.	8.	5.	3.	2.	1.	0.
	30	*	17.	12.	9.	6.	4.	2.	1.	1.	0.
	45	*	12.	9.	7.	4.	3.	1.	1.	0.	0.
	65	*	10.	7.	5.	3.	2.	1.	1.	0.	0.
	90	*	9.	6.	5.	3.	2.	1.	1.	0.	0.
	0	*	2.	2.	1.	1.	1.	0.	0.	0.	0.
TO	10	*	2.	1.	1.	1.	0.	0.	0.	0.	0.
	20	*	1.	1.	1.	0.	0.	0.	0.	0.	0.
	30	*	1.	1.	0.	0.	0.	0.	0.	0.	0.
	45	*	1.	0.	0.	0.	0.	0.	0.	0.	0.
	65	*	0.	0.	0.	0.	0.	0.	0.	0.	0.
	90	*	0.	0.	0.	0.	0.	0.	0.	0.	0.

015/112

S S *		TOTAL IONOSPHERIC ABSORPTION LOSS (DECIBELS)									
O A I A *		*****									
L N G N *		AVERAGE SUNSPOT NUMBER (R12) 15.									
A G H G *		ELECTRON GYRO-FREQUENCY (MHZ) 1.400									
R L A I *		TOTAL GEOMAGNETIC FIELD (GAUSS) 0.500									
F L F *		*****									
		* SIGNAL FREQUENCY (MHZ)									
(DEG)	(DEG) *	2.00	3.00	4.00	6.00	8.00	12.00	16.00	24.00	32.00	
*****											
0	0 *	190.	141.	106.	65.	43.	23.	14.	7.	4.	
	10 *	136.	101.	76.	46.	31.	16.	10.	5.	3.	
	20 *	88.	65.	49.	30.	20.	10.	6.	3.	2.	
	30 *	64.	47.	36.	22.	14.	8.	5.	2.	1.	
	45 *	46.	34.	26.	16.	11.	6.	3.	2.	1.	
	65 *	37.	27.	20.	13.	8.	4.	3.	1.	1.	
90 *	33.	25.	19.	11.	8.	4.	2.	1.	1.		
*****											
20	0 *	178.	132.	100.	61.	40.	21.	13.	6.	4.	
	10 *	128.	95.	71.	44.	29.	15.	9.	4.	3.	
	20 *	82.	61.	46.	28.	19.	10.	6.	3.	2.	
	30 *	60.	44.	33.	20.	14.	7.	4.	2.	1.	
	45 *	44.	32.	24.	15.	10.	5.	3.	2.	1.	
	65 *	34.	25.	19.	12.	8.	4.	2.	1.	1.	
90 *	31.	23.	17.	11.	7.	4.	2.	1.	1.		
*****											
40	0 *	146.	108.	82.	50.	33.	17.	11.	5.	3.	
	10 *	105.	77.	58.	36.	24.	12.	8.	4.	2.	
	20 *	67.	50.	38.	23.	15.	8.	5.	2.	1.	
	30 *	49.	36.	27.	17.	11.	6.	4.	2.	1.	
	45 *	36.	26.	20.	12.	8.	4.	3.	1.	1.	
	65 *	28.	21.	16.	10.	6.	3.	2.	1.	1.	
90 *	26.	19.	14.	9.	6.	3.	2.	1.	1.		
*****											
60	0 *	99.	73.	55.	34.	22.	12.	7.	3.	2.	
	10 *	71.	52.	39.	24.	16.	8.	5.	2.	1.	
	20 *	45.	34.	25.	16.	10.	5.	3.	2.	1.	
	30 *	33.	24.	18.	11.	7.	4.	2.	1.	1.	
	45 *	24.	18.	13.	8.	5.	3.	2.	1.	0.	
	65 *	19.	14.	11.	6.	4.	2.	1.	1.	0.	
90 *	17.	13.	10.	6.	4.	2.	1.	1.	0.		
*****											
80	0 *	46.	34.	26.	16.	10.	5.	3.	2.	1.	
	10 *	33.	24.	18.	11.	7.	4.	2.	1.	1.	
	20 *	21.	16.	12.	7.	5.	3.	2.	1.	0.	
	30 *	15.	11.	9.	5.	3.	2.	1.	1.	0.	
	45 *	11.	8.	6.	4.	3.	1.	1.	0.	0.	
	65 *	9.	7.	5.	3.	2.	1.	1.	0.	0.	
90 *	8.	6.	4.	3.	2.	1.	1.	0.	0.		
*****											
100	0 *	2.	2.	1.	1.	1.	0.	0.	0.	0.	
70	10 *	2.	1.	1.	1.	0.	0.	0.	0.	0.	
180	20 *	1.	1.	1.	0.	0.	0.	0.	0.	0.	
	30 *	1.	1.	0.	0.	0.	0.	0.	0.	0.	
	45 *	1.	0.	0.	0.	0.	0.	0.	0.	0.	
	65 *	0.	0.	0.	0.	0.	0.	0.	0.	0.	
	90 *	0.	0.	0.	0.	0.	0.	0.	0.	0.	



		TOTAL IONOSPHERIC ABSORPTION LOSS (DECIBELS)									
S O A I A		*****									
L N G N		AVERAGE SUNSPOT NUMBER (R12) 15.									
A G N G		ELECTRON GYRO-FREQUENCY (MHZ) 1.820									
R L A L		TOTAL GEOMAGNETIC FIELD (GAUSS) 0.650									
E L E		*****									
		* SIGNAL FREQUENCY (MHZ)									
(DEG)	(DEG)	*	2.00	3.00	4.00	6.00	8.00	12.00	16.00	24.00	32.00
*****											
0	0	*	167.	125.	95.	59.	40.	21.	13.	6.	4.
	10	*	120.	89.	68.	42.	29.	15.	9.	5.	3.
	20	*	77.	58.	44.	27.	18.	10.	6.	3.	2.
	30	*	56.	42.	32.	20.	13.	7.	4.	2.	1.
	45	*	41.	30.	23.	14.	10.	5.	3.	2.	1.
	65	*	32.	24.	18.	11.	8.	4.	3.	1.	1.
90	*	29.	22.	17.	10.	7.	4.	2.	1.	1.	
*****											
20	0	*	157.	117.	89.	56.	37.	20.	12.	6.	4.
	10	*	112.	84.	64.	40.	27.	14.	9.	4.	3.
	20	*	72.	54.	41.	26.	17.	9.	6.	3.	2.
	30	*	53.	39.	30.	19.	13.	7.	4.	2.	1.
	45	*	38.	29.	22.	14.	9.	5.	3.	1.	1.
	65	*	30.	23.	17.	11.	7.	4.	2.	1.	1.
90	*	28.	21.	16.	10.	7.	4.	2.	1.	1.	
*****											
40	0	*	129.	96.	73.	46.	31.	16.	10.	5.	3.
	10	*	92.	69.	52.	33.	22.	12.	7.	4.	2.
	20	*	59.	44.	34.	21.	14.	8.	5.	2.	1.
	30	*	43.	32.	25.	15.	10.	5.	3.	2.	1.
	45	*	31.	23.	18.	11.	7.	4.	2.	1.	1.
	65	*	25.	18.	14.	9.	6.	3.	2.	1.	1.
90	*	23.	17.	13.	8.	5.	3.	2.	1.	1.	
*****											
60	0	*	87.	65.	49.	31.	21.	11.	7.	3.	2.
	10	*	62.	46.	35.	22.	15.	8.	5.	2.	1.
	20	*	40.	30.	23.	14.	10.	5.	3.	2.	1.
	30	*	29.	22.	17.	10.	7.	4.	2.	1.	1.
	45	*	21.	16.	12.	8.	5.	3.	2.	1.	0.
	65	*	17.	12.	10.	6.	4.	2.	1.	1.	0.
90	*	15.	11.	9.	5.	4.	2.	1.	1.	0.	
*****											
80	0	*	40.	30.	23.	14.	10.	5.	3.	2.	1.
	10	*	29.	21.	16.	10.	7.	4.	2.	1.	1.
	20	*	19.	14.	11.	7.	4.	2.	1.	1.	0.
	30	*	13.	10.	8.	5.	3.	2.	1.	1.	0.
	45	*	10.	7.	6.	3.	2.	1.	1.	0.	0.
	65	*	8.	6.	4.	3.	2.	1.	1.	0.	0.
90	*	7.	5.	4.	2.	2.	1.	1.	0.	0.	
*****											
100	0	*	2.	1.	1.	1.	0.	0.	0.	0.	0.
	10	*	1.	1.	1.	1.	0.	0.	0.	0.	0.
	20	*	1.	1.	1.	0.	0.	0.	0.	0.	0.
	30	*	1.	0.	0.	0.	0.	0.	0.	0.	0.
	45	*	0.	0.	0.	0.	0.	0.	0.	0.	0.
	65	*	0.	0.	0.	0.	0.	0.	0.	0.	0.
90	*	0.	0.	0.	0.	0.	0.	0.	0.	0.	
*****											
TO 180	0	*	2.	1.	1.	1.	0.	0.	0.	0.	0.
	10	*	1.	1.	1.	1.	0.	0.	0.	0.	0.
	20	*	1.	1.	1.	0.	0.	0.	0.	0.	0.
	30	*	1.	0.	0.	0.	0.	0.	0.	0.	0.
	45	*	0.	0.	0.	0.	0.	0.	0.	0.	0.
	65	*	0.	0.	0.	0.	0.	0.	0.	0.	0.
90	*	0.	0.	0.	0.	0.	0.	0.	0.	0.	

		TOTAL IONOSPHERIC ABSORPTION LOSS (DECIBELS)								
S S *		*****								
O A I A *		AVERAGE SUNSPOT NUMBER (R12) 45.								
L N G N *		ELECTRON GYRO-FREQUENCY (MHZ) 0.700								
A G N G *		TOTAL GEOMAGNETIC FIELD (GAUSS) 0.250								
R L A L *		*****								
E L E *		*****								
		* SIGNAL FREQUENCY (MHZ)								
(DEG)	(DEG)	* 2.00	3.00	4.00	6.00	8.00	12.00	16.00	24.00	32.00
*****										
0	0	* 260.	192.	143.	84.	55.	28.	16.	8.	4.
	10	* 186.	137.	102.	60.	39.	20.	12.	6.	3.
	20	* 120.	88.	66.	39.	25.	13.	8.	4.	2.
	30	* 87.	64.	48.	28.	18.	9.	6.	3.	2.
	45	* 63.	47.	35.	21.	13.	7.	4.	2.	1.
	65	* 50.	37.	27.	16.	11.	5.	3.	1.	1.
	90	* 46.	34.	25.	15.	10.	5.	3.	1.	1.
*****										
20	0	* 244.	180.	134.	79.	51.	26.	15.	7.	4.
	10	* 175.	129.	96.	57.	37.	19.	11.	5.	3.
	20	* 113.	83.	62.	37.	24.	12.	7.	3.	2.
	30	* 82.	60.	45.	27.	17.	9.	5.	2.	1.
	45	* 60.	44.	33.	19.	13.	6.	4.	2.	1.
	65	* 47.	35.	26.	15.	10.	5.	3.	1.	1.
	90	* 43.	32.	23.	14.	9.	5.	3.	1.	1.
*****										
40	0	* 200.	147.	110.	65.	42.	21.	13.	6.	3.
	10	* 143.	105.	78.	46.	30.	15.	9.	4.	2.
	20	* 92.	68.	51.	30.	19.	10.	6.	3.	2.
	30	* 67.	49.	37.	22.	14.	7.	4.	2.	1.
	45	* 49.	36.	27.	16.	10.	5.	3.	1.	1.
	65	* 38.	28.	21.	13.	8.	4.	2.	1.	1.
	90	* 35.	26.	19.	11.	7.	4.	2.	1.	1.
*****										
60	0	* 135.	99.	74.	44.	28.	14.	9.	4.	2.
	10	* 97.	71.	53.	31.	20.	10.	6.	3.	2.
	20	* 62.	46.	34.	20.	13.	7.	4.	2.	1.
	30	* 45.	33.	25.	15.	9.	5.	3.	1.	1.
	45	* 33.	24.	18.	11.	7.	3.	2.	1.	1.
	65	* 26.	19.	14.	8.	5.	3.	2.	1.	0.
	90	* 24.	17.	13.	8.	5.	3.	1.	1.	0.
*****										
80	0	* 63.	46.	34.	20.	13.	7.	4.	2.	1.
	10	* 45.	33.	25.	15.	9.	5.	3.	1.	1.
	20	* 29.	21.	16.	9.	6.	3.	2.	1.	0.
	30	* 21.	15.	12.	7.	4.	2.	1.	1.	0.
	45	* 15.	11.	8.	5.	3.	2.	1.	0.	0.
	65	* 12.	9.	7.	4.	3.	1.	1.	0.	0.
	90	* 11.	8.	6.	4.	2.	1.	1.	0.	0.
*****										
100	0	* 3.	2.	2.	1.	1.	0.	0.	0.	0.
TO	10	* 2.	2.	1.	1.	0.	0.	0.	0.	0.
180	20	* 1.	1.	1.	0.	0.	0.	0.	0.	0.
	30	* 1.	1.	1.	0.	0.	0.	0.	0.	0.
	45	* 1.	1.	0.	0.	0.	0.	0.	0.	0.
	65	* 1.	0.	0.	0.	0.	0.	0.	0.	0.
	90	* 1.	0.	0.	0.	0.	0.	0.	0.	0.

045/070

S S \* TOTAL IONOSPHERIC ABSORPTION LOSS (DECIBELS)  
 O A I A \*\*\*\*\*  
 L N G N \* AVERAGE SUNSPOT NUMBER (R12) 45.  
 A G N G \* ELECTRON CYRO-FREQUENCY (MHZ) 1.120  
 R L A L \* TOTAL GEOMAGNETIC FIELD (GAUSS) 0.400  
 E L E \*\*\*\*\*

		* SIGNAL FREQUENCY (MHZ)								
(DEG)	(DEG)	* 2.00	* 3.00	* 4.00	* 6.00	* 8.00	* 12.00	* 16.00	* 24.00	* 32.00
*****										
0	0	* 224.	169.	127.	77.	50.	26.	16.	7.	4.
	10	* 164.	121.	91.	55.	36.	19.	11.	5.	3.
	20	* 106.	78.	59.	35.	23.	12.	7.	3.	2.
	30	* 77.	57.	43.	26.	17.	9.	5.	3.	1.
	45	* 56.	41.	31.	19.	12.	6.	4.	2.	1.
	65	* 44.	33.	24.	15.	10.	5.	3.	1.	1.
20	90	* 40.	30.	22.	13.	9.	5.	3.	1.	1.
	0	* 215.	159.	119.	72.	47.	24.	15.	7.	4.
	10	* 154.	114.	85.	51.	34.	17.	11.	5.	3.
	20	* 99.	73.	55.	33.	22.	11.	7.	3.	2.
	30	* 72.	53.	40.	24.	16.	8.	5.	2.	1.
	45	* 52.	39.	29.	18.	12.	6.	4.	2.	1.
40	65	* 41.	31.	23.	14.	9.	5.	3.	1.	1.
	90	* 38.	28.	21.	13.	8.	4.	3.	1.	1.
	0	* 176.	130.	97.	59.	39.	20.	12.	6.	3.
	10	* 126.	93.	70.	42.	28.	14.	9.	4.	2.
	20	* 81.	60.	45.	27.	18.	9.	6.	3.	2.
	30	* 59.	44.	33.	20.	13.	7.	4.	2.	1.
60	45	* 43.	32.	24.	14.	9.	5.	3.	1.	1.
	65	* 34.	25.	19.	11.	7.	4.	2.	1.	1.
	90	* 31.	23.	17.	10.	7.	3.	2.	1.	1.
	0	* 119.	88.	66.	40.	26.	13.	8.	4.	2.
	10	* 85.	63.	47.	28.	19.	10.	6.	3.	2.
	20	* 55.	40.	30.	18.	12.	6.	4.	2.	1.
80	30	* 40.	29.	22.	13.	9.	5.	3.	1.	1.
	45	* 29.	21.	16.	10.	6.	3.	2.	1.	1.
	65	* 23.	17.	13.	8.	5.	3.	2.	1.	0.
	90	* 21.	15.	12.	7.	5.	2.	1.	1.	0.
	0	* 55.	41.	30.	18.	12.	6.	4.	2.	1.
	10	* 39.	29.	22.	13.	9.	4.	3.	1.	1.
100	20	* 25.	19.	14.	8.	6.	3.	2.	1.	0.
	30	* 18.	14.	10.	6.	4.	2.	1.	1.	0.
	45	* 13.	10.	7.	4.	3.	2.	1.	0.	0.
	65	* 11.	8.	6.	4.	2.	1.	1.	0.	0.
	90	* 10.	7.	5.	3.	2.	1.	1.	0.	0.
	0	* 3.	2.	2.	1.	1.	0.	0.	0.	0.
180	10	* 2.	1.	1.	1.	0.	0.	0.	0.	0.
	20	* 1.	1.	1.	0.	0.	0.	0.	0.	0.
	30	* 1.	1.	1.	0.	0.	0.	0.	0.	0.
	45	* 1.	0.	0.	0.	0.	0.	0.	0.	0.
	65	* 1.	0.	0.	0.	0.	0.	0.	0.	0.
	90	* 0.	0.	0.	0.	0.	0.	0.	0.	0.

045/112

S S \* TOTAL IONOSPHERIC ABSORPTION LOSS (DECIBELS)  
 O A I A \*\*\*\*\*  
 L N G N \* AVERAGE SUNSPOT NUMBER (R12) 45.  
 A G N G \* ELECTRON GYRO-FREQUENCY (MHZ) 1.400  
 R L A L \* TOTAL GEOMAGNETIC FIELD (GAUSS) 0.500  
 F L E \*\*\*\*\*

		* SIGNAL FREQUENCY (MHZ)									
(DEG)	(DEG)	*	2.00	3.00	4.00	6.00	8.00	12.00	16.00	24.00	32.00
*****											
0	0	*	210.	156.	117.	72.	48.	25.	15.	7.	4.
	10	*	150.	111.	84.	51.	34.	18.	11.	5.	3.
	20	*	97.	72.	54.	33.	22.	12.	7.	3.	2.
	30	*	70.	52.	39.	24.	16.	8.	5.	2.	1.
	45	*	51.	38.	29.	18.	12.	6.	4.	2.	1.
	65	*	40.	30.	23.	14.	9.	5.	3.	1.	1.
20	90	*	37.	27.	21.	13.	8.	4.	3.	1.	1.
	0	*	197.	146.	110.	67.	45.	23.	14.	7.	4.
	10	*	141.	105.	79.	48.	32.	17.	10.	5.	3.
	20	*	91.	67.	51.	31.	21.	11.	7.	3.	2.
	30	*	66.	49.	37.	23.	15.	8.	5.	2.	1.
	45	*	48.	36.	27.	16.	11.	6.	3.	2.	1.
40	65	*	38.	28.	21.	13.	9.	5.	3.	1.	1.
	90	*	35.	26.	19.	12.	8.	4.	3.	1.	1.
	0	*	161.	120.	90.	55.	37.	19.	12.	6.	3.
	10	*	115.	86.	65.	39.	26.	14.	8.	4.	2.
	20	*	74.	55.	42.	25.	17.	9.	5.	3.	2.
	30	*	54.	40.	30.	19.	12.	6.	4.	2.	1.
60	45	*	39.	29.	22.	13.	9.	5.	3.	1.	1.
	65	*	31.	23.	17.	11.	7.	4.	2.	1.	1.
	90	*	28.	21.	16.	10.	6.	3.	2.	1.	1.
	0	*	109.	81.	61.	37.	25.	13.	8.	4.	2.
	10	*	78.	58.	44.	27.	18.	9.	6.	3.	2.
	20	*	50.	37.	28.	17.	11.	6.	4.	2.	1.
80	30	*	37.	27.	20.	12.	8.	4.	3.	1.	1.
	45	*	27.	20.	15.	9.	6.	3.	2.	1.	1.
	65	*	21.	16.	12.	7.	5.	2.	2.	1.	0.
	90	*	19.	14.	11.	7.	4.	2.	1.	1.	0.
	0	*	50.	37.	28.	17.	11.	6.	4.	2.	1.
	10	*	36.	27.	20.	12.	8.	4.	3.	1.	1.
100	20	*	23.	17.	13.	8.	5.	3.	2.	1.	0.
	30	*	17.	13.	9.	6.	4.	2.	1.	1.	0.
	45	*	12.	9.	7.	4.	3.	1.	1.	0.	0.
	65	*	10.	7.	5.	3.	2.	1.	1.	0.	0.
	90	*	9.	7.	5.	3.	2.	1.	1.	0.	0.
	0	*	3.	2.	1.	1.	1.	0.	0.	0.	0.
180	10	*	2.	1.	1.	1.	0.	0.	0.	0.	0.
	20	*	1.	1.	1.	0.	0.	0.	0.	0.	0.
	30	*	1.	1.	0.	0.	0.	0.	0.	0.	0.
	45	*	1.	0.	0.	0.	0.	0.	0.	0.	0.
	65	*	0.	0.	0.	0.	0.	0.	0.	0.	0.
	90	*	0.	0.	0.	0.	0.	0.	0.	0.	0.

045/140

S S \* TOTAL IONOSPHERIC ABSORPTION LOSS (DECIBELS)  
 O A I A \*\*\*\*\*  
 L N G N \* AVERAGE SUNSPOT NUMBER (R12) 45.  
 A G N G \* ELECTRON GYRO-FREQUENCY (MHZ) 1.820  
 R L A L \* TOTAL GEOMAGNETIC FIELD (GAUSS) 0.650  
 E L E \*\*\*\*\*  
 \* SIGNAL FREQUENCY (MHZ)

(DEG)	(DEG)	* 2.00	* 3.00	* 4.00	* 6.00	* 8.00	* 12.00	* 16.00	* 24.00	* 32.00
*****										
0	0	* 185.	138.	105.	65.	44.	24.	15.	7.	4.
	10	* 132.	99.	75.	47.	32.	17.	10.	5.	3.
	20	* 85.	64.	49.	30.	20.	11.	7.	3.	2.
	30	* 62.	46.	35.	22.	15.	8.	5.	2.	1.
	45	* 45.	34.	26.	16.	11.	6.	4.	2.	1.
	65	* 36.	27.	20.	13.	8.	5.	3.	1.	1.
20	90	* 32.	24.	18.	11.	8.	4.	3.	1.	1.
	0	* 174.	130.	99.	62.	41.	22.	14.	7.	4.
	10	* 124.	93.	71.	44.	30.	16.	10.	5.	3.
	20	* 80.	60.	46.	28.	19.	10.	6.	3.	2.
	30	* 58.	43.	33.	21.	14.	7.	5.	2.	1.
	45	* 42.	32.	24.	15.	10.	5.	3.	2.	1.
40	65	* 33.	25.	19.	12.	8.	4.	3.	1.	1.
	90	* 30.	23.	17.	11.	7.	4.	2.	1.	1.
	0	* 142.	106.	81.	50.	34.	18.	11.	5.	3.
	10	* 102.	76.	58.	36.	24.	13.	8.	4.	2.
	20	* 66.	49.	37.	23.	16.	8.	5.	3.	1.
	30	* 48.	36.	27.	17.	11.	6.	4.	2.	1.
60	45	* 35.	26.	20.	12.	8.	4.	3.	1.	1.
	65	* 27.	20.	16.	10.	7.	3.	2.	1.	1.
	90	* 25.	19.	14.	9.	6.	3.	2.	1.	1.
	0	* 96.	72.	55.	34.	23.	12.	8.	4.	2.
	10	* 69.	51.	39.	24.	16.	9.	5.	3.	2.
	20	* 44.	33.	25.	16.	11.	6.	3.	2.	1.
80	30	* 32.	24.	18.	11.	8.	4.	3.	1.	1.
	45	* 23.	17.	13.	8.	6.	3.	2.	1.	1.
	65	* 18.	14.	11.	7.	4.	2.	1.	1.	0.
	90	* 17.	13.	10.	6.	4.	2.	1.	1.	0.
	0	* 44.	33.	25.	16.	11.	6.	3.	2.	1.
	10	* 32.	24.	18.	11.	8.	4.	3.	1.	1.
100	20	* 21.	15.	12.	7.	5.	3.	2.	1.	0.
	30	* 15.	11.	8.	5.	4.	2.	1.	1.	0.
	45	* 11.	8.	6.	4.	3.	1.	1.	0.	0.
	65	* 9.	6.	5.	3.	2.	1.	1.	0.	0.
	90	* 8.	6.	4.	3.	2.	1.	1.	0.	0.
	0	* 2.	2.	1.	1.	1.	0.	0.	0.	0.
180	10	* 2.	1.	1.	1.	0.	0.	0.	0.	0.
	20	* 1.	1.	1.	0.	0.	0.	0.	0.	0.
	30	* 1.	1.	0.	0.	0.	0.	0.	0.	0.
	45	* 1.	0.	0.	0.	0.	0.	0.	0.	0.
	65	* 0.	0.	0.	0.	0.	0.	0.	0.	0.
	90	* 0.	0.	0.	0.	0.	0.	0.	0.	0.

S S *		TOTAL IONOSPHERIC ABSORPTION LOSS (DECIBELS)									
O A I A *		*****									
L N G N *		AVERAGE SUNSPOT NUMBER (R12) 135.									
A G H G *		ELECTRON GYRO-FREQUENCY (MHZ) 0.700									
R L A L *		TOTAL GEOMAGNETIC FIELD (GAUSS) 0.250									
E L F *		*****									
		* SIGNAL FREQUENCY (MHZ)									
(DFG)	(DEG)	*	2.00	3.00	4.00	6.00	8.00	12.00	16.00	24.00	32.00
0	0	*	334.	246.	183.	109.	70.	35.	21.	10.	6.
	10	*	239.	176.	131.	78.	50.	25.	15.	7.	4.
	20	*	154.	114.	85.	50.	32.	16.	10.	5.	3.
	30	*	112.	83.	61.	36.	24.	12.	7.	3.	2.
	45	*	82.	60.	45.	26.	17.	9.	5.	2.	1.
	65	*	64.	47.	35.	21.	14.	7.	4.	2.	1.
20	0	*	314.	231.	172.	102.	66.	33.	20.	9.	5.
	10	*	225.	166.	123.	73.	47.	24.	14.	7.	4.
	20	*	145.	107.	79.	47.	30.	15.	9.	4.	2.
	30	*	105.	78.	58.	34.	22.	11.	7.	3.	2.
	45	*	77.	56.	42.	25.	16.	8.	5.	2.	1.
	65	*	60.	45.	33.	20.	13.	6.	4.	2.	1.
40	0	*	257.	189.	141.	83.	54.	27.	16.	8.	4.
	10	*	184.	135.	101.	60.	39.	20.	12.	5.	3.
	20	*	119.	87.	65.	38.	25.	13.	8.	4.	2.
	30	*	86.	63.	47.	28.	18.	9.	5.	3.	1.
	45	*	63.	46.	34.	20.	13.	7.	4.	2.	1.
	65	*	49.	36.	27.	16.	10.	5.	3.	1.	1.
60	0	*	173.	128.	95.	56.	36.	18.	11.	5.	3.
	10	*	124.	91.	68.	40.	26.	13.	8.	4.	2.
	20	*	80.	59.	44.	26.	17.	8.	5.	2.	1.
	30	*	58.	43.	32.	19.	12.	6.	4.	2.	1.
	45	*	42.	31.	23.	14.	9.	4.	3.	1.	1.
	65	*	33.	25.	18.	11.	7.	4.	2.	1.	1.
80	0	*	80.	59.	44.	26.	17.	9.	5.	2.	1.
	10	*	58.	42.	32.	19.	12.	6.	4.	2.	1.
	20	*	37.	27.	20.	12.	8.	4.	2.	1.	1.
	30	*	27.	20.	15.	9.	6.	3.	2.	1.	0.
	45	*	20.	14.	11.	6.	4.	2.	1.	1.	0.
	65	*	15.	11.	8.	5.	3.	2.	1.	0.	0.
100	0	*	4.	3.	2.	1.	1.	0.	0.	0.	0.
	10	*	3.	2.	2.	1.	1.	0.	0.	0.	0.
	20	*	2.	1.	1.	1.	0.	0.	0.	0.	0.
	30	*	1.	1.	1.	0.	0.	0.	0.	0.	0.
	45	*	1.	1.	1.	0.	0.	0.	0.	0.	0.
	65	*	1.	1.	0.	0.	0.	0.	0.	0.	0.
180	0	*	1.	1.	0.	0.	0.	0.	0.	0.	0.
	90	*	1.	1.	0.	0.	0.	0.	0.	0.	0.

135/070

S S \* TOTAL IONOSPHERIC ABSORPTION LOSS (DECIBELS)  
 O A I A \*\*\*\*\*  
 L N G N \* AVERAGE SUNSPOT NUMBER (R12) 135.  
 A G N G \* ELECTRON GYRO-FREQUENCY (MHZ) 1.120  
 R L A L \* TOTAL GEOMAGNETIC FIELD (GAUSS) 0.400  
 E L E \*\*\*\*\*

		* SIGNAL FREQUENCY (MHZ)									
(DEG)	(DEG)	* 2.00	* 3.00	* 4.00	* 6.00	* 8.00	* 12.00	* 16.00	* 24.00	* 32.00	
0	0	* 294.	217.	163.	98.	65.	33.	20.	10.	6.	
	10	* 210.	155.	117.	70.	46.	24.	14.	7.	4.	
	20	* 136.	100.	75.	45.	30.	15.	9.	4.	3.	
	30	* 94.	73.	55.	33.	22.	11.	7.	3.	2.	
	45	* 72.	53.	40.	24.	16.	8.	5.	2.	1.	
	65	* 57.	42.	31.	19.	12.	6.	4.	2.	1.	
20	0	* 52.	38.	29.	17.	11.	6.	4.	2.	1.	
	10	* 276.	204.	153.	92.	61.	31.	19.	9.	5.	
	10	* 198.	146.	110.	66.	43.	22.	14.	6.	4.	
	20	* 127.	94.	71.	43.	28.	14.	9.	4.	2.	
	30	* 93.	68.	51.	31.	20.	11.	6.	3.	2.	
	45	* 67.	50.	37.	23.	15.	8.	5.	2.	1.	
40	65	* 53.	39.	29.	18.	12.	6.	4.	2.	1.	
	90	* 48.	36.	27.	16.	11.	5.	3.	2.	1.	
	0	* 226.	167.	125.	76.	50.	26.	16.	7.	4.	
	10	* 162.	119.	90.	54.	36.	18.	11.	5.	3.	
	20	* 104.	77.	58.	35.	23.	12.	7.	3.	2.	
	30	* 76.	56.	42.	25.	17.	9.	5.	2.	1.	
60	45	* 55.	41.	31.	18.	12.	6.	4.	2.	1.	
	65	* 44.	32.	24.	15.	10.	5.	3.	1.	1.	
	90	* 40.	29.	22.	13.	9.	4.	3.	1.	1.	
	0	* 153.	113.	85.	51.	34.	17.	10.	5.	3.	
	10	* 109.	81.	61.	37.	24.	12.	7.	4.	2.	
	20	* 70.	52.	39.	24.	15.	8.	5.	2.	1.	
80	30	* 51.	38.	28.	17.	11.	6.	4.	2.	1.	
	45	* 37.	27.	21.	12.	8.	4.	3.	1.	1.	
	65	* 29.	22.	16.	10.	6.	3.	2.	1.	1.	
	90	* 27.	20.	15.	9.	6.	3.	2.	1.	1.	
	0	* 71.	52.	39.	24.	16.	8.	5.	2.	1.	
	10	* 51.	37.	28.	17.	11.	6.	3.	2.	1.	
100	20	* 33.	24.	18.	11.	7.	4.	2.	1.	1.	
	30	* 24.	18.	13.	8.	5.	3.	2.	1.	0.	
	45	* 17.	13.	10.	6.	4.	2.	1.	1.	0.	
	65	* 14.	10.	8.	5.	3.	2.	1.	0.	0.	
	90	* 12.	9.	7.	4.	3.	1.	1.	0.	0.	
	0	* 4.	3.	2.	1.	1.	0.	0.	0.	0.	
TO	10	* 3.	2.	1.	1.	1.	0.	0.	0.	0.	
	20	* 2.	1.	1.	1.	0.	0.	0.	0.	0.	
	30	* 1.	1.	1.	0.	0.	0.	0.	0.	0.	
	45	* 1.	1.	0.	0.	0.	0.	0.	0.	0.	
	65	* 1.	0.	0.	0.	0.	0.	0.	0.	0.	
	90	* 1.	0.	0.	0.	0.	0.	0.	0.	0.	

S S \* TOTAL IONOSPHERIC ABSORPTION LOSS (DECIBELS)  
 O A I A \*\*\*\*\*  
 L N G N \* AVERAGE SUNSPOT NUMBER (R12) 135.  
 A G H G \* ELECTRON GYRO-FREQUENCY (MHZ) 1.400  
 R L A L \* TOTAL GEOMAGNETIC FIELD (GAUSS) 0.500  
 E L E \*\*\*\*\*

		* SIGNAL FREQUENCY (MHZ)								
(DEG)	(DEG)	* 2.00	* 3.00	* 4.00	* 6.00	* 8.00	* 12.00	* 16.00	* 24.00	* 32.00
*****										
0	0	* 270.	200.	151.	92.	61.	32.	20.	9.	6.
	10	* 193.	143.	108.	66.	44.	23.	14.	7.	4.
	20	* 125.	92.	70.	43.	28.	15.	9.	4.	3.
	30	* 90.	67.	51.	31.	21.	11.	7.	3.	2.
	45	* 66.	49.	37.	23.	15.	8.	5.	2.	1.
	65	* 52.	39.	29.	18.	12.	6.	4.	2.	1.
20	90	* 47.	35.	26.	16.	11.	6.	3.	2.	1.
	0	* 254.	188.	142.	87.	58.	30.	18.	9.	5.
	10	* 181.	134.	102.	62.	41.	22.	13.	6.	4.
	20	* 117.	87.	65.	40.	27.	14.	8.	4.	2.
	30	* 85.	63.	48.	29.	19.	10.	6.	3.	2.
	45	* 62.	46.	35.	21.	14.	7.	4.	2.	1.
40	65	* 49.	36.	27.	17.	11.	6.	4.	2.	1.
	90	* 44.	33.	25.	15.	10.	5.	3.	2.	1.
	0	* 207.	154.	116.	71.	47.	25.	15.	7.	4.
	10	* 148.	110.	83.	51.	34.	18.	11.	5.	3.
	20	* 96.	71.	54.	33.	22.	11.	7.	3.	2.
	30	* 70.	52.	39.	24.	16.	8.	5.	2.	1.
60	45	* 51.	37.	28.	17.	11.	6.	4.	2.	1.
	65	* 40.	30.	22.	14.	9.	5.	3.	1.	1.
	90	* 36.	27.	20.	12.	8.	4.	3.	1.	1.
	0	* 140.	104.	78.	48.	32.	17.	10.	5.	3.
	10	* 100.	74.	56.	34.	23.	12.	7.	4.	2.
	20	* 65.	48.	36.	22.	15.	8.	5.	2.	1.
80	30	* 47.	35.	26.	16.	11.	6.	3.	2.	1.
	45	* 34.	25.	19.	12.	8.	4.	2.	1.	1.
	65	* 27.	20.	15.	9.	6.	3.	2.	1.	1.
	90	* 25.	18.	14.	8.	6.	3.	2.	1.	1.
	0	* 65.	48.	36.	22.	15.	8.	5.	2.	1.
	10	* 46.	34.	26.	16.	11.	6.	3.	2.	1.
100	20	* 30.	22.	17.	10.	7.	4.	2.	1.	1.
	30	* 22.	16.	12.	7.	5.	3.	2.	1.	0.
	45	* 16.	12.	9.	5.	4.	2.	1.	1.	0.
	65	* 13.	9.	7.	4.	3.	1.	1.	0.	0.
	90	* 11.	8.	6.	4.	3.	1.	1.	0.	0.
	0	* 3.	2.	2.	1.	1.	0.	0.	0.	0.
180	10	* 2.	2.	1.	1.	1.	0.	0.	0.	0.
	20	* 1.	1.	1.	1.	0.	0.	0.	0.	0.
	30	* 1.	1.	1.	0.	0.	0.	0.	0.	0.
	45	* 1.	1.	0.	0.	0.	0.	0.	0.	0.
	65	* 1.	0.	0.	0.	0.	0.	0.	0.	0.
	90	* 1.	0.	0.	0.	0.	0.	0.	0.	0.

135/140



S S \* TOTAL IONOSPHERIC ABSORPTION LOSS (DECIRELS)  
 O A I A \*\*\*\*\*  
 L N G N \* AVERAGE SUNSPOT NUMBER (R12) 135.  
 A G N G \* ELECTRON GYRO-FREQUENCY (MHZ) 1.820  
 R L A L \* TOTAL GEOMAGNETIC FIELD (GAUSS) 0.650  
 E L E \*\*\*\*\*

		* SIGNAL FREQUENCY (MHZ)									
(DEG)	(DEG)	*	2.00	3.00	4.00	6.00	8.00	12.00	16.00	24.00	32.00
*****											
0	0	*	238.	177.	135.	84.	57.	30.	19.	9.	5.
	10	*	170.	127.	97.	60.	41.	22.	13.	7.	4.
	20	*	110.	82.	62.	39.	26.	14.	9.	4.	2.
	30	*	80.	59.	45.	28.	19.	10.	6.	3.	2.
	45	*	58.	43.	33.	21.	14.	7.	5.	2.	1.
	65	*	46.	34.	26.	16.	11.	6.	4.	2.	1.
20	0	*	42.	31.	24.	15.	10.	5.	3.	2.	1.
	10	*	223.	167.	127.	79.	53.	28.	18.	9.	5.
	20	*	160.	119.	91.	57.	38.	20.	13.	6.	4.
	30	*	103.	77.	59.	36.	25.	13.	8.	4.	2.
	45	*	75.	56.	43.	27.	18.	10.	6.	3.	2.
	65	*	54.	41.	31.	19.	13.	7.	4.	2.	1.
40	0	*	43.	32.	24.	15.	10.	5.	3.	2.	1.
	10	*	39.	29.	22.	14.	9.	5.	3.	2.	1.
	20	*	183.	136.	104.	65.	44.	23.	14.	7.	4.
	30	*	131.	97.	74.	46.	31.	17.	10.	5.	3.
	45	*	84.	63.	48.	30.	20.	11.	7.	3.	2.
	65	*	61.	46.	35.	22.	15.	8.	5.	2.	1.
60	0	*	45.	33.	25.	16.	11.	6.	4.	2.	1.
	10	*	35.	26.	20.	12.	8.	4.	3.	1.	1.
	20	*	32.	24.	18.	11.	8.	4.	3.	1.	1.
	30	*	123.	92.	70.	44.	29.	16.	10.	5.	3.
	45	*	88.	66.	50.	31.	21.	11.	7.	3.	2.
	65	*	57.	42.	32.	20.	14.	7.	4.	2.	1.
80	0	*	41.	31.	24.	15.	10.	5.	3.	2.	1.
	10	*	30.	22.	17.	11.	7.	4.	2.	1.	1.
	20	*	24.	18.	14.	8.	6.	3.	2.	1.	1.
	30	*	22.	16.	12.	8.	5.	3.	2.	1.	0.
	45	*	57.	43.	33.	20.	14.	7.	4.	2.	1.
	65	*	41.	31.	23.	14.	10.	5.	3.	2.	1.
100	0	*	26.	20.	15.	9.	6.	3.	2.	1.	1.
	10	*	19.	14.	11.	7.	5.	2.	2.	1.	0.
	20	*	14.	10.	8.	5.	3.	2.	1.	1.	0.
	30	*	11.	8.	6.	4.	3.	1.	1.	0.	0.
	45	*	10.	7.	6.	4.	2.	1.	1.	0.	0.
	65	*	3.	2.	2.	1.	1.	0.	0.	0.	0.
180	0	*	2.	2.	1.	1.	0.	0.	0.	0.	0.
	10	*	1.	1.	1.	0.	0.	0.	0.	0.	0.
	20	*	1.	1.	1.	0.	0.	0.	0.	0.	0.
	30	*	1.	1.	0.	0.	0.	0.	0.	0.	0.
	45	*	1.	1.	0.	0.	0.	0.	0.	0.	0.
	65	*	1.	0.	0.	0.	0.	0.	0.	0.	0.
	90	*	0.	0.	0.	0.	0.	0.	0.	0.	0.

		TOTAL IONOSPHERIC ABSORPTION LOSS (DECIBELS)								
		*****								
		AVERAGE SUNSPOT NUMBER (R12) 30.								
		ELECTRON GYRO-FREQUENCY (MHZ) 0.700								
		TOTAL GEOMAGNETIC FIELD (GAUSS) 0.250								
		*****								
		* SIGNAL FREQUENCY (MHZ)								
(DEG)	(DEG)	* 2.00	* 3.00	* 4.00	* 6.00	* 8.00	* 12.00	* 16.00	* 24.00	* 32.00
*****										
0	0	* 248.	183.	136.	80.	52.	26.	16.	7.	4.
	10	* 177.	131.	97.	58.	37.	19.	11.	5.	3.
	20	* 114.	84.	63.	37.	24.	12.	7.	3.	2.
	30	* 83.	61.	46.	27.	17.	9.	5.	2.	1.
	45	* 60.	45.	33.	20.	13.	6.	4.	2.	1.
	65	* 48.	35.	26.	15.	10.	5.	3.	1.	1.
90	* 43.	32.	24.	14.	9.	5.	3.	1.	1.	
*****										
20	0	* 233.	171.	128.	76.	49.	25.	15.	7.	4.
	10	* 166.	123.	91.	54.	35.	18.	11.	5.	3.
	20	* 107.	79.	59.	35.	23.	11.	7.	3.	2.
	30	* 78.	57.	43.	25.	16.	8.	5.	2.	1.
	45	* 57.	42.	31.	18.	12.	6.	4.	2.	1.
	65	* 45.	33.	25.	15.	9.	5.	3.	1.	1.
90	* 41.	30.	22.	13.	9.	4.	3.	1.	1.	
*****										
40	0	* 190.	140.	104.	62.	40.	20.	12.	6.	3.
	10	* 136.	100.	75.	44.	29.	14.	9.	4.	2.
	20	* 88.	65.	48.	29.	18.	9.	6.	3.	2.
	30	* 64.	47.	35.	21.	13.	7.	4.	2.	1.
	45	* 46.	34.	25.	15.	10.	5.	3.	1.	1.
	65	* 37.	27.	20.	12.	8.	4.	2.	1.	1.
90	* 33.	25.	18.	11.	7.	4.	2.	1.	1.	
*****										
60	0	* 129.	95.	71.	42.	27.	14.	8.	4.	2.
	10	* 92.	68.	50.	30.	19.	10.	6.	3.	2.
	20	* 59.	44.	33.	19.	12.	6.	4.	2.	1.
	30	* 43.	32.	24.	14.	9.	5.	3.	1.	1.
	45	* 31.	23.	17.	10.	7.	3.	2.	1.	1.
	65	* 25.	18.	14.	8.	5.	3.	2.	1.	0.
90	* 23.	17.	12.	7.	5.	2.	1.	1.	0.	
*****										
80	0	* 60.	44.	33.	19.	12.	6.	4.	2.	1.
	10	* 43.	31.	23.	14.	9.	5.	3.	1.	1.
	20	* 27.	20.	15.	9.	6.	3.	2.	1.	0.
	30	* 20.	15.	11.	6.	4.	2.	1.	1.	0.
	45	* 15.	11.	8.	5.	3.	2.	1.	0.	0.
	65	* 11.	8.	6.	4.	2.	1.	1.	0.	0.
90	* 10.	8.	6.	3.	2.	1.	1.	0.	0.	
*****										
100	0	* 3.	2.	2.	1.	1.	0.	0.	0.	0.
	10	* 2.	2.	1.	1.	0.	0.	0.	0.	0.
	20	* 1.	1.	1.	0.	0.	0.	0.	0.	0.
	30	* 1.	1.	1.	0.	0.	0.	0.	0.	0.
	45	* 1.	1.	0.	0.	0.	0.	0.	0.	0.
	65	* 1.	0.	0.	0.	0.	0.	0.	0.	0.
90	* 1.	0.	0.	0.	0.	0.	0.	0.	0.	
*****										
180	0	* 3.	2.	2.	1.	1.	0.	0.	0.	0.
	10	* 2.	2.	1.	1.	0.	0.	0.	0.	0.
	20	* 1.	1.	1.	0.	0.	0.	0.	0.	0.
	30	* 1.	1.	1.	0.	0.	0.	0.	0.	0.
	45	* 1.	1.	0.	0.	0.	0.	0.	0.	0.
	65	* 1.	0.	0.	0.	0.	0.	0.	0.	0.
90	* 1.	0.	0.	0.	0.	0.	0.	0.	0.	

030/070

S	S	*	TOTAL IONOSPHERIC ABSORPTION LOSS (DECIBELS)									
O A	I A	*	*****									
L N	G N	*	AVERAGE SUNSPOT NUMBER (R12) 30.									
A G	N G	*	ELECTRON GYRO-FREQUENCY (MHZ) 1.120									
R L	A L	*	TOTAL GEOMAGNETIC FIELD (GAUSS) 0.400									
E	L E	*	*****									
		*	* SIGNAL FREQUENCY (MHZ)									
(DEG)	(DEG)	*	2.00	3.00	4.00	6.00	8.00	12.00	16.00	24.00	32.00	
*****												
0	0	*	218.	161.	121.	73.	48.	25.	15.	7.	4.	
	10	*	156.	115.	86.	52.	34.	18.	11.	5.	3.	
	20	*	101.	74.	56.	34.	22.	11.	7.	3.	2.	
	30	*	73.	54.	40.	24.	16.	8.	5.	2.	1.	
	45	*	53.	39.	29.	18.	12.	6.	4.	2.	1.	
	65	*	42.	31.	23.	14.	9.	5.	3.	1.	1.	
	90	*	38.	28.	21.	13.	8.	4.	3.	1.	1.	
*****												
20	0	*	205.	151.	113.	68.	45.	23.	14.	7.	4.	
	10	*	146.	108.	81.	49.	32.	17.	10.	5.	3.	
	20	*	94.	70.	52.	32.	21.	11.	6.	3.	2.	
	30	*	69.	51.	38.	23.	15.	8.	5.	2.	1.	
	45	*	50.	37.	28.	17.	11.	6.	3.	2.	1.	
	65	*	39.	29.	22.	13.	9.	4.	3.	1.	1.	
	90	*	36.	26.	20.	12.	8.	4.	2.	1.	1.	
*****												
40	0	*	167.	124.	93.	56.	37.	19.	12.	5.	3.	
	10	*	120.	88.	66.	40.	26.	14.	8.	4.	2.	
	20	*	77.	57.	43.	26.	17.	9.	5.	3.	1.	
	30	*	56.	41.	31.	19.	12.	6.	4.	2.	1.	
	45	*	41.	30.	23.	14.	9.	5.	3.	1.	1.	
	65	*	32.	24.	18.	11.	7.	4.	2.	1.	1.	
	90	*	29.	22.	16.	10.	6.	3.	2.	1.	1.	
*****												
60	0	*	113.	83.	63.	38.	25.	13.	8.	4.	2.	
	10	*	81.	60.	45.	27.	18.	9.	6.	3.	2.	
	20	*	52.	39.	29.	17.	11.	6.	4.	2.	1.	
	30	*	38.	28.	21.	13.	8.	4.	3.	1.	1.	
	45	*	28.	20.	15.	9.	6.	3.	2.	1.	1.	
	65	*	22.	16.	12.	7.	5.	2.	1.	1.	0.	
	90	*	20.	15.	11.	7.	4.	2.	1.	1.	0.	
*****												
80	0	*	52.	39.	29.	18.	12.	6.	4.	2.	1.	
	10	*	37.	28.	21.	13.	8.	4.	3.	1.	1.	
	20	*	24.	18.	13.	8.	5.	3.	2.	1.	0.	
	30	*	18.	13.	10.	6.	4.	2.	1.	1.	0.	
	45	*	13.	9.	7.	4.	3.	1.	1.	0.	0.	
	65	*	10.	7.	6.	3.	2.	1.	1.	0.	0.	
	90	*	9.	7.	5.	3.	2.	1.	1.	0.	0.	
*****												
100	0	*	3.	2.	1.	1.	1.	0.	0.	0.	0.	
TO	10	*	2.	1.	1.	1.	0.	0.	0.	0.	0.	
180	20	*	1.	1.	1.	0.	0.	0.	0.	0.	0.	
	30	*	1.	1.	0.	0.	0.	0.	0.	0.	0.	
	45	*	1.	0.	0.	0.	0.	0.	0.	0.	0.	
	65	*	1.	0.	0.	0.	0.	0.	0.	0.	0.	
	90	*	0.	0.	0.	0.	0.	0.	0.	0.	0.	

030/112

211

		TOTAL IONOSPHERIC ABSORPTION LOSS (DECIBELS)								
S S *		*****								
O A I A *		*****								
L N G N *		AVERAGE SUNSPOT NUMBER (R12) 30.								
A G N G *		ELECTRON GYRO-FREQUENCY (MHZ) 1.400								
R L A L *		TOTAL GEOMAGNETIC FIELD (GAUSS) 0.500								
E L E *		*****								
		* SIGNAL FREQUENCY (MHZ)								
(DEG)	(DEG)	2.00	3.00	4.00	6.00	8.00	12.00	16.00	24.00	32.00
*****										
0	0 *	200.	148.	112.	68.	45.	24.	15.	7.	4.
	10 *	143.	106.	80.	49.	32.	17.	10.	5.	3.
	20 *	92.	68.	52.	32.	21.	11.	7.	3.	2.
	30 *	67.	50.	38.	23.	15.	8.	5.	2.	1.
	45 *	49.	36.	27.	17.	11.	6.	4.	2.	1.
	65 *	39.	29.	22.	13.	9.	5.	3.	1.	1.
90 *	35.	26.	20.	12.	8.	4.	3.	1.	1.	
*****										
20	0 *	188.	139.	105.	64.	43.	22.	14.	7.	4.
	10 *	134.	100.	75.	46.	30.	16.	10.	5.	3.
	20 *	87.	64.	49.	30.	20.	10.	6.	3.	2.
	30 *	63.	47.	35.	22.	14.	7.	5.	2.	1.
	45 *	46.	34.	26.	16.	10.	5.	3.	2.	1.
	65 *	36.	27.	20.	12.	8.	4.	3.	1.	1.
90 *	33.	24.	18.	11.	7.	4.	2.	1.	1.	
*****										
40	0 *	154.	114.	86.	53.	35.	18.	11.	5.	3.
	10 *	110.	81.	62.	38.	25.	13.	8.	4.	2.
	20 *	71.	53.	40.	24.	16.	8.	5.	2.	1.
	30 *	52.	38.	29.	18.	12.	6.	4.	2.	1.
	45 *	38.	28.	21.	13.	9.	4.	3.	1.	1.
	65 *	30.	22.	17.	10.	7.	4.	2.	1.	1.
90 *	27.	20.	15.	9.	6.	3.	2.	1.	1.	
*****										
60	0 *	104.	77.	58.	35.	24.	12.	8.	4.	2.
	10 *	74.	55.	42.	25.	17.	9.	5.	3.	2.
	20 *	48.	35.	27.	16.	11.	6.	3.	2.	1.
	30 *	35.	26.	19.	12.	8.	4.	3.	1.	1.
	45 *	25.	19.	14.	9.	6.	3.	2.	1.	1.
	65 *	20.	15.	11.	7.	5.	2.	1.	1.	0.
90 *	18.	13.	10.	6.	4.	2.	1.	1.	0.	
*****										
80	0 *	48.	36.	27.	16.	11.	6.	3.	2.	1.
	10 *	34.	25.	19.	12.	8.	4.	2.	1.	1.
	20 *	22.	16.	12.	8.	5.	3.	2.	1.	0.
	30 *	16.	12.	9.	6.	4.	2.	1.	1.	0.
	45 *	12.	9.	7.	4.	3.	1.	1.	0.	0.
	65 *	9.	7.	5.	3.	2.	1.	1.	0.	0.
90 *	8.	6.	5.	3.	2.	1.	1.	0.	0.	
*****										
100	0 *	2.	2.	1.	1.	1.	0.	0.	0.	0.
	TO 10 *	2.	1.	1.	1.	0.	0.	0.	0.	0.
	180 20 *	1.	1.	1.	0.	0.	0.	0.	0.	0.
	30 *	1.	1.	0.	0.	0.	0.	0.	0.	0.
	45 *	1.	0.	0.	0.	0.	0.	0.	0.	0.
	65 *	0.	0.	0.	0.	0.	0.	0.	0.	0.
90 *	0.	0.	0.	0.	0.	0.	0.	0.	0.	

S S \* TOTAL IONOSPHERIC ABSORPTION LOSS (DECIBELS)  
 O A I A \*\*\*\*\*  
 L N G N \* AVERAGE SUNSPOT NUMBER (R12) 30.  
 A G N G \* ELECTRON GYRO-FREQUENCY (MHZ) 1.820  
 R L A L \* TOTAL GEOMAGNETIC FIELD (GAUSS) 0.650  
 E L E \*\*\*\*\*

		* SIGNAL FREQUENCY (MHZ)									
(DEG)	(DEG)	* 2.00	* 3.00	* 4.00	* 6.00	* 8.00	* 12.00	* 16.00	* 24.00	* 32.00	
*****											
0	0	* 176.	131.	100.	62.	42.	22.	14.	7.	4.	
	10	* 126.	94.	72.	45.	30.	16.	10.	5.	3.	
	20	* 81.	61.	46.	29.	19.	10.	6.	3.	2.	
	30	* 59.	44.	34.	21.	14.	8.	5.	2.	1.	
	45	* 43.	32.	24.	15.	10.	5.	3.	2.	1.	
	65	* 34.	25.	19.	12.	8.	4.	3.	1.	1.	
20	90	* 31.	23.	18.	11.	7.	4.	2.	1.	1.	
	0	* 165.	123.	94.	59.	39.	21.	13.	6.	4.	
	10	* 118.	88.	67.	42.	28.	15.	9.	5.	3.	
	20	* 76.	57.	43.	27.	18.	10.	6.	3.	2.	
	30	* 55.	41.	32.	20.	13.	7.	4.	2.	1.	
	45	* 40.	30.	23.	14.	10.	5.	3.	2.	1.	
40	65	* 32.	24.	18.	11.	8.	4.	3.	1.	1.	
	90	* 29.	22.	16.	10.	7.	4.	2.	1.	1.	
	0	* 135.	101.	77.	48.	32.	17.	11.	5.	3.	
	10	* 97.	72.	55.	34.	23.	12.	8.	4.	2.	
	20	* 62.	47.	36.	22.	15.	8.	5.	2.	1.	
	30	* 45.	34.	26.	16.	11.	6.	4.	2.	1.	
60	45	* 33.	25.	19.	12.	8.	4.	3.	1.	1.	
	65	* 26.	19.	15.	9.	6.	3.	2.	1.	1.	
	90	* 24.	18.	13.	8.	6.	3.	2.	1.	1.	
	0	* 91.	68.	52.	32.	22.	12.	7.	4.	2.	
	10	* 65.	49.	37.	23.	16.	8.	5.	3.	1.	
	20	* 42.	31.	24.	15.	10.	5.	3.	2.	1.	
80	30	* 31.	23.	17.	11.	7.	4.	2.	1.	1.	
	45	* 22.	17.	13.	8.	5.	3.	2.	1.	1.	
	65	* 18.	13.	10.	6.	4.	2.	1.	1.	0.	
	90	* 16.	12.	9.	6.	4.	2.	1.	1.	0.	
	0	* 42.	32.	24.	15.	10.	5.	3.	2.	1.	
	10	* 30.	23.	17.	11.	7.	4.	2.	1.	1.	
100	20	* 20.	15.	11.	7.	5.	2.	2.	1.	0.	
	30	* 14.	11.	8.	5.	3.	2.	1.	1.	0.	
	45	* 10.	8.	6.	4.	2.	1.	1.	0.	0.	
	65	* 8.	6.	5.	3.	2.	1.	1.	0.	0.	
	90	* 7.	6.	4.	3.	2.	1.	1.	0.	0.	
	0	* 2.	2.	1.	1.	1.	0.	0.	0.	0.	
180	10	* 2.	1.	1.	1.	0.	0.	0.	0.	0.	
	20	* 1.	1.	1.	0.	0.	0.	0.	0.	0.	
	30	* 1.	1.	0.	0.	0.	0.	0.	0.	0.	
	45	* 1.	0.	0.	0.	0.	0.	0.	0.	0.	
	65	* 0.	0.	0.	0.	0.	0.	0.	0.	0.	
	90	* 0.	0.	0.	0.	0.	0.	0.	0.	0.	

S S *		TOTAL IONOSPHERIC ABSORPTION LOSS (DECIBELS)									
O A I A *		*****									
L N G H *		AVERAGE SUNSPOT NUMBER (R12) 60.									
A G N G *		ELECTRON GYRO-FREQUENCY (MHZ) 0.700									
R L A L *		TOTAL GEOMAGNETIC FIELD (GAUSS) 0.250									
F L F *		*****									
		* SIGNAL FREQUENCY (MHZ)									
(DEG)	(DEG)	*	2.00	3.00	4.00	6.00	8.00	12.00	16.00	24.00	32.00
*****											
0	0	*	272.	201.	149.	88.	57.	29.	17.	8.	5.
	10	*	195.	144.	107.	63.	41.	21.	12.	6.	3.
	20	*	126.	93.	69.	41.	26.	13.	8.	4.	2.
	30	*	91.	67.	50.	30.	19.	10.	6.	3.	2.
	45	*	66.	49.	36.	22.	14.	7.	4.	2.	1.
	65	*	52.	39.	29.	17.	11.	6.	3.	2.	1.
90	*	48.	35.	26.	15.	10.	5.	3.	1.	1.	
*****											
20	0	*	256.	189.	140.	83.	54.	27.	16.	8.	4.
	10	*	183.	135.	100.	59.	38.	19.	12.	5.	3.
	20	*	118.	87.	65.	38.	25.	13.	7.	4.	2.
	30	*	86.	63.	47.	28.	18.	9.	5.	3.	1.
	45	*	62.	46.	34.	20.	13.	7.	4.	2.	1.
	65	*	49.	36.	27.	16.	10.	5.	3.	1.	1.
90	*	45.	33.	25.	15.	9.	5.	3.	1.	1.	
*****											
40	0	*	209.	154.	115.	68.	44.	22.	13.	6.	4.
	10	*	150.	110.	82.	49.	31.	16.	9.	4.	3.
	20	*	97.	71.	53.	31.	20.	10.	6.	3.	2.
	30	*	70.	52.	39.	23.	15.	7.	4.	2.	1.
	45	*	51.	38.	28.	17.	11.	5.	3.	2.	1.
	65	*	40.	30.	22.	13.	8.	4.	3.	1.	1.
90	*	37.	27.	20.	12.	8.	4.	2.	1.	1.	
*****											
60	0	*	141.	104.	78.	46.	30.	15.	9.	4.	2.
	10	*	101.	75.	55.	33.	21.	11.	6.	3.	2.
	20	*	65.	48.	36.	21.	14.	7.	4.	2.	1.
	30	*	47.	35.	26.	15.	10.	5.	3.	1.	1.
	45	*	34.	25.	19.	11.	7.	4.	2.	1.	1.
	65	*	27.	20.	15.	9.	6.	3.	2.	1.	0.
90	*	25.	18.	14.	8.	5.	3.	2.	1.	0.	
*****											
80	0	*	66.	48.	36.	21.	14.	7.	4.	2.	1.
	10	*	47.	35.	26.	15.	10.	5.	3.	1.	1.
	20	*	30.	22.	17.	10.	6.	3.	2.	1.	1.
	30	*	22.	16.	12.	7.	5.	2.	1.	1.	0.
	45	*	16.	12.	9.	5.	3.	2.	1.	0.	0.
	65	*	13.	9.	7.	4.	3.	1.	1.	0.	0.
90	*	11.	8.	6.	4.	2.	1.	1.	0.	0.	
*****											
100	0	*	3.	2.	2.	1.	1.	0.	0.	0.	0.
70	10	*	2.	2.	1.	1.	0.	0.	0.	0.	0.
180	20	*	1.	1.	1.	0.	0.	0.	0.	0.	0.
	30	*	1.	1.	1.	0.	0.	0.	0.	0.	0.
	45	*	1.	1.	0.	0.	0.	0.	0.	0.	0.
	65	*	1.	0.	0.	0.	0.	0.	0.	0.	0.
90	*	1.	0.	0.	0.	0.	0.	0.	0.	0.	

060/070

S S \* TOTAL IONOSPHERIC ABSORPTION LOSS (DECIBELS)  
 O A I A \*\*\*\*\*  
 L N G N \* AVERAGE SUNSPOT NUMBER (R12) 60.  
 A G N G \* ELECTRON GYRO-FREQUENCY (MHZ) 1.120  
 R L A L \* TOTAL GEOMAGNETIC FIELD (GAUSS) 0.400  
 E L F \*\*\*\*\*

		* SIGNAL FREQUENCY (MHZ)									
(DEG)	(DEG)	* 2.00	3.00	4.00	6.00	8.00	12.00	16.00	24.00	32.00	
*****											
0	0	*	240.	177.	133.	80.	53.	27.	16.	8.	5.
	10	*	171.	127.	95.	57.	38.	19.	12.	6.	3.
	20	*	111.	82.	61.	37.	24.	13.	8.	4.	2.
	30	*	80.	59.	45.	27.	18.	9.	6.	3.	2.
	45	*	58.	43.	32.	20.	13.	7.	4.	2.	1.
	65	*	46.	34.	26.	15.	10.	5.	3.	2.	1.
20	90	*	42.	31.	23.	14.	9.	5.	3.	1.	1.
	0	*	225.	166.	125.	75.	49.	26.	15.	7.	4.
	10	*	161.	119.	89.	54.	35.	18.	11.	5.	3.
	20	*	104.	77.	58.	35.	23.	12.	7.	3.	2.
	30	*	75.	56.	42.	25.	17.	9.	5.	2.	1.
	45	*	55.	41.	30.	18.	12.	6.	4.	2.	1.
40	65	*	43.	32.	24.	15.	10.	5.	3.	1.	1.
	90	*	39.	29.	22.	13.	9.	4.	3.	1.	1.
	0	*	184.	136.	102.	62.	40.	21.	13.	6.	4.
	10	*	132.	97.	73.	44.	29.	15.	9.	4.	3.
	20	*	85.	63.	47.	28.	19.	10.	6.	3.	2.
	30	*	62.	46.	34.	21.	14.	7.	4.	2.	1.
60	45	*	45.	33.	25.	15.	10.	5.	3.	1.	1.
	65	*	35.	26.	20.	12.	8.	4.	2.	1.	1.
	90	*	32.	24.	18.	11.	7.	4.	2.	1.	1.
	0	*	124.	92.	69.	42.	27.	14.	9.	4.	2.
	10	*	89.	66.	49.	30.	20.	10.	6.	3.	2.
	20	*	57.	42.	32.	19.	13.	7.	4.	2.	1.
80	30	*	42.	31.	23.	14.	9.	5.	3.	1.	1.
	45	*	30.	22.	17.	10.	7.	3.	2.	1.	1.
	65	*	24.	18.	13.	8.	5.	3.	2.	1.	0.
	90	*	22.	16.	12.	7.	5.	2.	1.	1.	0.
	0	*	58.	43.	32.	19.	13.	7.	4.	2.	1.
	10	*	41.	30.	23.	14.	9.	5.	3.	1.	1.
100	20	*	27.	20.	15.	9.	6.	3.	2.	1.	1.
	30	*	19.	14.	11.	6.	4.	2.	1.	1.	0.
	45	*	14.	10.	8.	5.	3.	2.	1.	0.	0.
	65	*	11.	8.	6.	4.	2.	1.	1.	0.	0.
	90	*	10.	7.	6.	3.	2.	1.	1.	0.	0.
	0	*	3.	2.	2.	1.	1.	0.	0.	0.	0.
180	TO	*	2.	2.	1.	1.	0.	0.	0.	0.	0.
	20	*	1.	1.	1.	0.	0.	0.	0.	0.	0.
	30	*	1.	1.	1.	0.	0.	0.	0.	0.	0.
	45	*	1.	1.	0.	0.	0.	0.	0.	0.	0.
	65	*	1.	0.	0.	0.	0.	0.	0.	0.	0.
	90	*	1.	0.	0.	0.	0.	0.	0.	0.	0.

060/112

S S \* TOTAL IONOSPHERIC ABSORPTION LOSS (DECIRELS)  
 O A I A \*\*\*\*\*  
 L N G N \* AVERAGE SUNSPOT NUMBER (R12) 60.  
 A G N G \* ELECTRON GYRO-FREQUENCY (MHZ) 1.400  
 R L A L \* TOTAL GEOMAGNETIC FIELD (GAUSS) 0.500  
 F L E \*\*\*\*\*

		* SIGNAL FREQUENCY (MHZ)									
(DEG)	(DEG)	* 2.00	* 3.00	* 4.00	* 6.00	* 8.00	* 12.00	* 16.00	* 24.00	* 32.00	
*****											
0	0	* 220.	163.	123.	75.	50.	26.	16.	8.	4.	
	10	* 157.	117.	88.	54.	36.	19.	11.	5.	3.	
	20	* 102.	75.	57.	35.	23.	12.	7.	4.	2.	
	30	* 74.	55.	41.	25.	17.	9.	5.	3.	2.	
	45	* 54.	40.	30.	18.	12.	6.	4.	2.	1.	
	65	* 42.	31.	24.	14.	10.	5.	3.	1.	1.	
	90	* 39.	29.	22.	53.	9.	5.	3.	1.	1.	
*****											
20	0	* 207.	153.	116.	71.	47.	25.	15.	7.	4.	
	10	* 148.	110.	83.	51.	34.	18.	11.	5.	3.	
	20	* 95.	71.	53.	33.	22.	11.	7.	3.	2.	
	30	* 69.	51.	39.	24.	16.	8.	5.	2.	1.	
	45	* 50.	37.	28.	17.	11.	6.	4.	2.	1.	
	65	* 40.	29.	22.	14.	9.	5.	3.	1.	1.	
	90	* 36.	27.	20.	12.	8.	4.	3.	1.	1.	
*****											
40	0	* 169.	125.	95.	58.	38.	20.	12.	6.	3.	
	10	* 121.	90.	68.	41.	27.	14.	9.	4.	2.	
	20	* 78.	58.	40.	27.	18.	9.	6.	3.	2.	
	30	* 57.	42.	32.	19.	13.	7.	4.	2.	1.	
	45	* 41.	31.	23.	14.	9.	5.	3.	1.	1.	
	65	* 33.	24.	18.	11.	7.	4.	2.	1.	1.	
	90	* 30.	22.	17.	10.	7.	4.	2.	1.	1.	
*****											
60	0	* 114.	85.	64.	39.	26.	14.	8.	4.	2.	
	10	* 82.	61.	46.	28.	19.	10.	6.	3.	2.	
	20	* 53.	39.	29.	18.	12.	6.	4.	2.	1.	
	30	* 38.	28.	21.	13.	9.	5.	3.	1.	1.	
	45	* 28.	21.	16.	10.	6.	3.	2.	1.	1.	
	65	* 22.	16.	12.	8.	5.	3.	2.	1.	0.	
	90	* 20.	15.	11.	7.	5.	2.	1.	1.	0.	
*****											
80	0	* 53.	39.	30.	18.	12.	6.	4.	2.	1.	
	10	* 38.	28.	21.	13.	9.	5.	3.	1.	1.	
	20	* 24.	18.	14.	8.	6.	3.	2.	1.	0.	
	30	* 18.	13.	10.	6.	4.	2.	1.	1.	0.	
	45	* 13.	10.	7.	4.	3.	2.	1.	0.	0.	
	65	* 10.	8.	6.	3.	2.	1.	1.	0.	0.	
	90	* 9.	7.	5.	3.	2.	1.	1.	0.	0.	
*****											
100	0	* 3.	2.	1.	1.	1.	0.	0.	0.	0.	
70	10	* 2.	1.	1.	1.	0.	0.	0.	0.	0.	
180	20	* 1.	1.	1.	0.	0.	0.	0.	0.	0.	
	30	* 1.	1.	0.	0.	0.	0.	0.	0.	0.	
	45	* 1.	0.	0.	0.	0.	0.	0.	0.	0.	
	65	* 1.	0.	0.	0.	0.	0.	0.	0.	0.	
	90	* 0.	0.	0.	0.	0.	0.	0.	0.	0.	



S S \* TOTAL IONOSPHERIC ABSORPTION LOSS (DECIBELS)  
 O A I A \*\*\*\*\*  
 L N G N \* AVERAGE SUNSPOT NUMBER (R12) 60.  
 A G N G \* ELECTRON GYRO-FREQUENCY (MHZ) 1.820  
 R L A L \* TOTAL GEOMAGNETIC FIELD (GAUSS) 0.650  
 E L E \*\*\*\*\*

		* SIGNAL FREQUENCY (MHZ)									
(DEG)	(DEG)	* 2.00	* 3.00	* 4.00	* 6.00	* 8.00	* 12.00	* 16.00	* 24.00	* 32.00	
*****											
0	0	* 194.	144.	110.	69.	46.	25.	15.	7.	4.	
	10	* 139.	103.	79.	49.	33.	18.	11.	5.	3.	
	20	* 89.	67.	51.	32.	21.	11.	7.	3.	2.	
	30	* 65.	48.	37.	23.	15.	8.	5.	2.	1.	
	45	* 47.	35.	27.	17.	11.	6.	4.	2.	1.	
	65	* 37.	28.	21.	13.	9.	5.	3.	1.	1.	
	90	* 34.	25.	19.	12.	8.	4.	3.	1.	1.	
*****											
20	0	* 182.	136.	103.	64.	43.	23.	14.	7.	4.	
	10	* 130.	97.	74.	46.	31.	17.	10.	5.	3.	
	20	* 84.	63.	48.	30.	20.	11.	7.	3.	2.	
	30	* 61.	45.	35.	22.	15.	8.	5.	2.	1.	
	45	* 44.	33.	25.	16.	11.	6.	3.	2.	1.	
	65	* 35.	26.	20.	12.	8.	4.	3.	1.	1.	
	90	* 32.	24.	18.	11.	8.	4.	3.	1.	1.	
*****											
40	0	* 149.	111.	85.	53.	35.	19.	12.	6.	3.	
	10	* 106.	79.	61.	38.	25.	14.	8.	4.	2.	
	20	* 69.	51.	39.	24.	16.	9.	5.	3.	2.	
	30	* 50.	37.	28.	18.	12.	6.	4.	2.	1.	
	45	* 36.	27.	21.	13.	9.	5.	3.	1.	1.	
	65	* 29.	21.	16.	10.	7.	4.	2.	1.	1.	
	90	* 26.	19.	15.	9.	6.	3.	2.	1.	1.	
*****											
60	0	* 100.	75.	57.	36.	24.	13.	8.	4.	2.	
	10	* 72.	54.	41.	25.	17.	9.	6.	3.	2.	
	20	* 46.	35.	26.	16.	11.	6.	4.	2.	1.	
	30	* 34.	25.	19.	12.	8.	4.	3.	1.	1.	
	45	* 25.	18.	14.	9.	6.	3.	2.	1.	1.	
	65	* 19.	14.	11.	7.	5.	2.	2.	1.	0.	
	90	* 18.	13.	10.	6.	4.	2.	1.	1.	0.	
*****											
80	0	* 47.	35.	26.	16.	11.	6.	4.	2.	1.	
	10	* 33.	25.	19.	12.	8.	4.	3.	1.	1.	
	20	* 21.	16.	12.	8.	5.	3.	2.	1.	0.	
	30	* 16.	12.	9.	6.	4.	2.	1.	1.	0.	
	45	* 11.	8.	6.	4.	3.	1.	1.	0.	0.	
	65	* 9.	7.	5.	3.	2.	1.	1.	0.	0.	
	90	* 8.	6.	5.	3.	2.	1.	1.	0.	0.	
*****											
100	0	* 2.	2.	1.	1.	1.	0.	0.	0.	0.	
TO	10	* 2.	1.	1.	1.	0.	0.	0.	0.	0.	
180	20	* 1.	1.	1.	0.	0.	0.	0.	0.	0.	
	30	* 1.	1.	0.	0.	0.	0.	0.	0.	0.	
	45	* 1.	0.	0.	0.	0.	0.	0.	0.	0.	
	65	* 0.	0.	0.	0.	0.	0.	0.	0.	0.	
	90	* 0.	0.	0.	0.	0.	0.	0.	0.	0.	

060/182

S S \* TOTAL IONOSPHERIC ABSORPTION LOSS (DECIBELS)  
 O A I A \*\*\*\*\*  
 L N G M \* AVERAGE SUNSPOT NUMBER (R12) 90.  
 A G N G \* ELECTRON GYRO-FREQUENCY (MHZ) 0.700  
 R L A L \* TOTAL GEOMAGNETIC FIELD (GAUSS) 0.250  
 E L F \*\*\*\*\*

		* SIGNAL FREQUENCY (MHZ)									
(DEG)	(DEG)	* 2.00	3.00	4.00	6.00	8.00	12.00	16.00	24.00	32.00	
*****											
0	0	*	297.	219.	163.	96.	62.	32.	19.	9.	5.
	10	*	213.	157.	117.	69.	45.	23.	13.	6.	4.
	20	*	137.	101.	75.	45.	29.	15.	9.	4.	2.
	30	*	100.	73.	55.	32.	21.	11.	6.	3.	2.
	45	*	72.	53.	40.	24.	15.	8.	5.	2.	1.
	65	*	57.	42.	31.	19.	12.	6.	4.	2.	1.
20	90	*	52.	38.	29.	17.	11.	6.	3.	2.	1.
	0	*	279.	206.	153.	91.	59.	30.	18.	8.	5.
	10	*	200.	147.	110.	65.	42.	21.	13.	6.	3.
	20	*	129.	95.	71.	42.	27.	14.	8.	4.	2.
	30	*	94.	69.	51.	30.	20.	10.	6.	3.	2.
	45	*	68.	50.	37.	22.	14.	7.	4.	2.	1.
40	65	*	54.	40.	29.	17.	11.	6.	3.	2.	1.
	90	*	49.	36.	27.	16.	10.	5.	3.	1.	1.
	0	*	228.	168.	125.	74.	48.	24.	14.	7.	4.
	10	*	163.	120.	90.	53.	34.	17.	10.	5.	3.
	20	*	105.	78.	58.	34.	22.	11.	7.	3.	2.
	30	*	77.	56.	42.	25.	16.	8.	5.	2.	1.
60	45	*	56.	41.	31.	18.	12.	6.	4.	2.	1.
	65	*	44.	32.	24.	14.	9.	5.	3.	1.	1.
	90	*	40.	29.	22.	13.	8.	4.	3.	1.	1.
	0	*	154.	114.	85.	50.	32.	16.	10.	5.	3.
	10	*	110.	81.	61.	36.	23.	12.	7.	3.	2.
	20	*	71.	52.	39.	23.	15.	8.	5.	2.	1.
80	30	*	52.	38.	28.	17.	11.	5.	3.	2.	1.
	45	*	38.	28.	21.	12.	8.	4.	2.	1.	1.
	65	*	30.	22.	16.	10.	6.	3.	2.	1.	1.
	90	*	27.	20.	15.	9.	6.	3.	2.	1.	0.
	0	*	71.	53.	39.	23.	15.	8.	5.	2.	1.
	10	*	51.	38.	28.	17.	11.	5.	3.	2.	1.
100	20	*	33.	24.	18.	11.	7.	3.	2.	1.	1.
	30	*	24.	18.	13.	8.	5.	3.	2.	1.	0.
	45	*	17.	13.	10.	6.	4.	2.	1.	1.	0.
	65	*	14.	10.	8.	4.	3.	1.	1.	0.	0.
	90	*	13.	9.	7.	4.	3.	1.	1.	0.	0.
	0	*	4.	3.	2.	1.	1.	0.	0.	0.	0.
180	10	*	3.	2.	1.	1.	1.	0.	0.	0.	0.
	20	*	2.	1.	1.	1.	0.	0.	0.	0.	0.
	30	*	1.	1.	1.	0.	0.	0.	0.	0.	0.
	45	*	1.	1.	0.	0.	0.	0.	0.	0.	0.
	65	*	1.	1.	0.	0.	0.	0.	0.	0.	0.
	90	*	1.	0.	0.	0.	0.	0.	0.	0.	0.

S S \* TOTAL IONOSPHERIC ABSORPTION LOSS (DECIBELS)  
 O A I A \*\*\*\*\*  
 L N G N \* AVERAGE SUNSPOT NUMBER (R12) 90.  
 A G N G \* ELECTRON GYRO-FREQUENCY (MHZ) 1.120  
 R L A L \* TOTAL GEOMAGNETIC FIELD (GAUSS) 0.400  
 E L E \*\*\*\*\*

		* SIGNAL FREQUENCY (MHZ)									
(DEG)	(DEG)	* 2.00	* 3.00	* 4.00	* 6.00	* 8.00	* 12.00	* 16.00	* 24.00	* 32.00	
*****											
0	0	* 261.	193.	145.	87.	57.	30.	18.	9.	5.	
	10	* 187.	138.	104.	63.	41.	21.	13.	6.	4.	
	20	* 121.	89.	67.	40.	26.	14.	8.	4.	2.	
	30	* 88.	65.	49.	29.	19.	10.	6.	3.	2.	
	45	* 64.	47.	35.	21.	14.	7.	4.	2.	1.	
	65	* 50.	37.	28.	17.	11.	6.	3.	2.	1.	
20	90	* 46.	34.	25.	15.	10.	5.	3.	1.	1.	
	0	* 246.	181.	136.	82.	54.	28.	17.	8.	5.	
	10	* 176.	130.	97.	59.	39.	20.	12.	6.	3.	
	20	* 113.	84.	63.	38.	25.	13.	8.	4.	2.	
	30	* 82.	61.	46.	28.	18.	9.	6.	3.	2.	
	45	* 60.	44.	33.	20.	13.	7.	4.	2.	1.	
40	65	* 47.	35.	26.	16.	10.	5.	3.	2.	1.	
	90	* 43.	32.	24.	14.	9.	5.	3.	1.	1.	
	0	* 201.	148.	111.	67.	44.	23.	14.	7.	4.	
	10	* 144.	106.	80.	48.	32.	16.	10.	5.	3.	
	20	* 93.	68.	51.	31.	20.	11.	6.	3.	2.	
	30	* 67.	50.	37.	23.	15.	8.	5.	2.	1.	
60	45	* 49.	36.	27.	16.	11.	6.	3.	2.	1.	
	65	* 39.	29.	21.	13.	8.	4.	3.	1.	1.	
	90	* 35.	26.	20.	12.	8.	4.	2.	1.	1.	
	0	* 136.	100.	75.	45.	30.	15.	9.	4.	3.	
	10	* 97.	72.	54.	32.	21.	11.	7.	3.	2.	
	20	* 63.	46.	35.	21.	14.	7.	4.	2.	1.	
80	30	* 45.	34.	25.	15.	10.	5.	3.	1.	1.	
	45	* 33.	24.	18.	11.	7.	4.	2.	1.	1.	
	65	* 26.	19.	14.	9.	6.	3.	2.	1.	0.	
	90	* 24.	18.	13.	8.	5.	3.	2.	1.	0.	
	0	* 63.	46.	35.	21.	14.	7.	4.	2.	1.	
	10	* 45.	33.	25.	15.	10.	5.	3.	1.	1.	
100	20	* 29.	21.	16.	10.	6.	3.	2.	1.	1.	
	30	* 21.	16.	12.	7.	5.	2.	1.	1.	0.	
	45	* 15.	11.	9.	5.	3.	2.	1.	1.	0.	
	65	* 12.	9.	7.	4.	3.	1.	1.	0.	0.	
	90	* 11.	8.	6.	4.	2.	1.	1.	0.	0.	
	0	* 3.	2.	2.	1.	1.	0.	0.	0.	0.	
180	10	* 2.	2.	1.	1.	0.	0.	0.	0.	0.	
	20	* 1.	1.	1.	0.	0.	0.	0.	0.	0.	
	30	* 1.	1.	1.	0.	0.	0.	0.	0.	0.	
	45	* 1.	1.	0.	0.	0.	0.	0.	0.	0.	
	65	* 1.	0.	0.	0.	0.	0.	0.	0.	0.	
	90	* 1.	0.	0.	0.	0.	0.	0.	0.	0.	

S S *		TOTAL IONOSPHERIC ABSORPTION LOSS (DECIBELS)									
O A I A *		*****									
L N G N *		AVERAGE SUNSPOT NUMBER (R12) 90.									
A G N G *		ELECTRON GYRO-FREQUENCY (MHZ) 1.400									
R L A L *		TOTAL GEOMAGNETIC FIELD (GAUSS) 0.500									
E L E *		*****									
		* SIGNAL FREQUENCY (MHZ)									
(DFG)	(DEG)	*	2.00	3.00	4.00	6.00	8.00	12.00	16.00	24.00	32.00
*****											
0	0	*	240.	178.	134.	82.	54.	29.	17.	8.	5.
	10	*	172.	127.	96.	59.	39.	20.	12.	6.	4.
	20	*	111.	82.	62.	38.	25.	13.	8.	4.	2.
	30	*	80.	60.	45.	28.	18.	10.	6.	3.	2.
	45	*	59.	43.	33.	20.	13.	7.	4.	2.	1.
	65	*	46.	34.	26.	16.	10.	5.	3.	2.	1.
	90	*	42.	31.	24.	14.	10.	5.	3.	1.	1.
*****											
20	0	*	225.	167.	126.	77.	51.	27.	16.	8.	5.
	10	*	161.	120.	90.	55.	37.	19.	12.	6.	3.
	20	*	104.	77.	58.	36.	24.	12.	8.	4.	2.
	30	*	76.	56.	42.	26.	17.	9.	5.	3.	2.
	45	*	55.	41.	31.	19.	12.	7.	4.	2.	1.
	65	*	43.	32.	24.	15.	10.	5.	3.	2.	1.
	90	*	39.	29.	22.	14.	9.	5.	3.	1.	1.
*****											
40	0	*	184.	137.	103.	63.	42.	22.	13.	6.	4.
	10	*	132.	98.	74.	45.	30.	16.	10.	5.	3.
	20	*	85.	63.	48.	29.	19.	10.	6.	3.	2.
	30	*	62.	46.	35.	21.	14.	7.	4.	2.	1.
	45	*	45.	33.	25.	15.	10.	5.	3.	2.	1.
	65	*	36.	26.	20.	12.	8.	4.	3.	1.	1.
	90	*	32.	24.	18.	11.	7.	4.	2.	1.	1.
*****											
60	0	*	125.	92.	70.	43.	28.	15.	9.	4.	3.
	10	*	89.	66.	50.	30.	20.	11.	6.	3.	2.
	20	*	57.	43.	32.	20.	13.	7.	4.	2.	1.
	30	*	42.	31.	23.	14.	9.	5.	3.	1.	1.
	45	*	30.	23.	17.	10.	7.	4.	2.	1.	1.
	65	*	24.	18.	13.	8.	5.	3.	2.	1.	0.
	90	*	22.	16.	12.	7.	5.	3.	2.	1.	0.
*****											
80	0	*	58.	43.	32.	20.	13.	7.	4.	2.	1.
	10	*	41.	31.	23.	14.	9.	5.	3.	1.	1.
	20	*	27.	20.	15.	9.	6.	3.	2.	1.	1.
	30	*	19.	14.	11.	7.	4.	2.	1.	1.	0.
	45	*	14.	10.	8.	5.	3.	2.	1.	0.	0.
	65	*	11.	8.	6.	4.	3.	1.	1.	0.	0.
	90	*	10.	7.	6.	3.	2.	1.	1.	0.	0.
*****											
100	0	*	3.	2.	2.	1.	1.	0.	0.	0.	0.
TO	10	*	2.	2.	1.	1.	0.	0.	0.	0.	0.
180	20	*	1.	1.	1.	0.	0.	0.	0.	0.	0.
	30	*	1.	1.	1.	0.	0.	0.	0.	0.	0.
	45	*	1.	1.	0.	0.	0.	0.	0.	0.	0.
	65	*	1.	0.	0.	0.	0.	0.	0.	0.	0.
	90	*	1.	0.	0.	0.	0.	0.	0.	0.	0.

090/140

220

S S \* TOTAL IONOSPHERIC ABSORPTION LOSS (DECIBELS)  
 O A I A \*\*\*\*\*  
 L N G N \* AVERAGE SUNSPOT NUMBER (R12) 90.  
 A G N G \* ELECTRON GYRO-FREQUENCY (MHZ) 1.820  
 R L A L \* TOTAL GEOMAGNETIC FIELD (GAUSS) 0.650  
 E L E \*\*\*\*\*

		* SIGNAL FREQUENCY (MHZ)									
(DEG)	(DEG)	* 2.00	3.00	4.00	6.00	8.00	12.00	16.00	24.00	32.00	
*****											
0	0	*	211.	158.	120.	75.	50.	27.	17.	8.	5.
	10	*	151.	113.	86.	54.	36.	19.	12.	6.	3.
	20	*	97.	73.	55.	35.	23.	12.	8.	4.	2.
	30	*	71.	53.	40.	25.	17.	9.	6.	3.	2.
	45	*	52.	38.	29.	18.	12.	7.	4.	2.	1.
	65	*	41.	30.	23.	14.	10.	5.	3.	2.	1.
	90	*	37.	28.	21.	13.	9.	5.	3.	1.	1.
*****											
20	0	*	198.	148.	113.	70.	47.	25.	16.	8.	4.
	10	*	142.	106.	81.	50.	34.	18.	11.	5.	3.
	20	*	92.	68.	52.	32.	22.	12.	7.	4.	2.
	30	*	67.	50.	38.	24.	16.	8.	5.	3.	2.
	45	*	48.	36.	28.	17.	12.	6.	4.	2.	1.
	65	*	38.	29.	22.	14.	9.	5.	3.	1.	1.
	90	*	35.	26.	20.	12.	8.	4.	3.	1.	1.
*****											
40	0	*	162.	121.	92.	58.	39.	21.	13.	6.	4.
	10	*	116.	87.	66.	41.	28.	15.	9.	4.	3.
	20	*	75.	56.	43.	27.	18.	10.	6.	3.	2.
	30	*	54.	41.	31.	19.	13.	7.	4.	2.	1.
	45	*	40.	30.	23.	14.	9.	5.	3.	2.	1.
	65	*	31.	23.	18.	11.	7.	4.	2.	1.	1.
	90	*	28.	21.	16.	10.	7.	4.	2.	1.	1.
*****											
60	0	*	110.	82.	62.	39.	26.	14.	9.	4.	2.
	10	*	78.	59.	45.	28.	19.	10.	6.	3.	2.
	20	*	51.	38.	29.	18.	12.	6.	4.	2.	1.
	30	*	37.	27.	21.	13.	9.	5.	3.	1.	1.
	45	*	27.	20.	15.	9.	6.	3.	2.	1.	1.
	65	*	21.	16.	12.	7.	5.	3.	2.	1.	0.
	90	*	19.	14.	11.	7.	5.	2.	2.	1.	0.
*****											
80	0	*	51.	38.	29.	18.	12.	6.	4.	2.	1.
	10	*	36.	27.	21.	13.	9.	5.	3.	1.	1.
	20	*	23.	17.	13.	8.	6.	3.	2.	1.	1.
	30	*	17.	13.	10.	6.	4.	2.	1.	1.	0.
	45	*	12.	9.	7.	4.	3.	2.	1.	0.	0.
	65	*	10.	7.	6.	3.	2.	1.	1.	0.	0.
	90	*	9.	7.	5.	3.	2.	1.	1.	0.	0.
*****											
100	0	*	3.	2.	1.	1.	1.	0.	0.	0.	0.
TO	10	*	2.	1.	1.	1.	0.	0.	0.	0.	0.
180	20	*	1.	1.	1.	0.	0.	0.	0.	0.	0.
	30	*	1.	1.	0.	0.	0.	0.	0.	0.	0.
	45	*	1.	0.	0.	0.	0.	0.	0.	0.	0.
	65	*	0.	0.	0.	0.	0.	0.	0.	0.	0.
	90	*	0.	0.	0.	0.	0.	0.	0.	0.	0.

090/182

S S *		TOTAL IONOSPHERIC ABSORPTION LOSS (DECIBELS)									
O A I A *		*****									
L N G N *		AVERAGE SUNSPOT NUMBER (R12) 120.									
A G N G *		ELECTRON GYRO-FREQUENCY (MHZ) 0.700									
R L A L *		TOTAL GEOMAGNETIC FIELD (GAUSS) 0.240									
E L F *		*****									
		* SIGNAL FREQUENCY (MHZ)									
(DEG)	(DEG)	*	2.00	3.00	4.00	6.00	8.00	12.00	16.00	24.00	32.00
*****											
0	0	*	322.	237.	177.	105.	68.	34.	20.	10.	6.
	10	*	230.	170.	126.	75.	48.	24.	15.	7.	4.
	20	*	149.	109.	81.	48.	31.	16.	9.	4.	3.
	30	*	108.	80.	59.	35.	23.	11.	7.	3.	2.
	45	*	79.	58.	43.	26.	16.	8.	5.	2.	1.
	65	*	62.	46.	34.	20.	13.	7.	4.	2.	1.
	90	*	56.	42.	31.	18.	12.	6.	4.	2.	1.
*****											
20	0	*	302.	223.	166.	98.	63.	32.	19.	9.	5.
	10	*	216.	159.	119.	70.	45.	23.	14.	6.	4.
	20	*	140.	103.	77.	45.	29.	15.	9.	4.	2.
	30	*	101.	75.	56.	33.	21.	11.	6.	3.	2.
	45	*	74.	54.	40.	24.	15.	8.	5.	2.	1.
	65	*	58.	43.	32.	19.	12.	6.	4.	2.	1.
	90	*	53.	39.	29.	17.	11.	6.	3.	2.	1.
*****											
40	0	*	247.	182.	136.	80.	52.	26.	16.	7.	4.
	10	*	177.	130.	97.	57.	37.	19.	11.	5.	3.
	20	*	114.	84.	63.	37.	24.	12.	7.	3.	2.
	30	*	83.	61.	45.	27.	17.	9.	5.	2.	1.
	45	*	60.	44.	33.	20.	13.	6.	4.	2.	1.
	65	*	48.	35.	26.	15.	10.	5.	3.	1.	1.
	90	*	43.	32.	24.	14.	9.	5.	3.	1.	1.
*****											
60	0	*	167.	123.	92.	54.	35.	18.	11.	5.	3.
	10	*	120.	88.	66.	39.	25.	13.	8.	4.	2.
	20	*	77.	57.	42.	25.	16.	8.	5.	2.	1.
	30	*	56.	41.	31.	18.	12.	6.	4.	2.	1.
	45	*	41.	30.	22.	13.	9.	4.	3.	1.	1.
	65	*	32.	24.	18.	10.	7.	3.	2.	1.	1.
	90	*	29.	22.	16.	10.	6.	3.	2.	1.	1.
*****											
80	0	*	77.	57.	42.	25.	16.	8.	5.	2.	1.
	10	*	55.	41.	30.	18.	12.	6.	4.	2.	1.
	20	*	36.	26.	20.	12.	7.	4.	2.	1.	1.
	30	*	26.	19.	14.	8.	5.	3.	2.	1.	0.
	45	*	19.	14.	10.	6.	4.	2.	1.	1.	0.
	65	*	15.	11.	8.	5.	3.	2.	1.	0.	0.
	90	*	14.	10.	7.	4.	3.	1.	1.	0.	0.
*****											
100	0	*	4.	3.	2.	1.	1.	0.	0.	0.	0.
TO	10	*	3.	2.	2.	1.	1.	0.	0.	0.	0.
180	20	*	2.	1.	1.	1.	0.	0.	0.	0.	0.
	30	*	1.	1.	1.	0.	0.	0.	0.	0.	0.
	45	*	1.	1.	1.	0.	0.	0.	0.	0.	0.
	65	*	1.	1.	0.	0.	0.	0.	0.	0.	0.
	90	*	1.	0.	0.	0.	0.	0.	0.	0.	0.

120/070

S S \* TOTAL IONOSPHERIC ABSORPTION LOSS (DECIBELS)  
 O A I A \*\*\*\*\*  
 L N G N \* AVERAGE SUNSPOT NUMBER (R12) 120.  
 A G N G \* ELECTRON GYRO-FREQUENCY (MHZ) 1.120  
 R L A L \* TOTAL GEOMAGNETIC FIELD (GAUSS) 0.400  
 E L F \*\*\*\*\*

		* SIGNAL FREQUENCY (MHZ)								
(DEG)	(DEG)	* 2.00	3.00	4.00	6.00	8.00	12.00	16.00	24.00	32.00
*****										
0	0	* 283.	209.	157.	95.	62.	32.	19.	9.	5.
	10	* 203.	150.	112.	68.	45.	23.	14.	7.	4.
	20	* 131.	96.	72.	44.	29.	15.	9.	4.	2.
	30	* 95.	70.	53.	32.	21.	11.	7.	3.	2.
	45	* 69.	51.	38.	23.	15.	8.	5.	2.	1.
	65	* 54.	40.	30.	18.	12.	6.	4.	2.	1.
20	90	* 50.	37.	27.	17.	11.	6.	3.	2.	1.
	0	* 266.	196.	147.	89.	58.	30.	18.	9.	5.
	10	* 190.	141.	106.	64.	42.	22.	13.	6.	4.
	20	* 123.	91.	68.	41.	27.	14.	8.	4.	2.
	30	* 89.	66.	49.	30.	20.	10.	6.	3.	2.
	45	* 65.	48.	36.	22.	14.	7.	4.	2.	1.
40	65	* 51.	38.	28.	17.	11.	6.	4.	2.	1.
	90	* 47.	34.	26.	16.	10.	5.	3.	2.	1.
	0	* 218.	161.	121.	73.	48.	25.	15.	7.	4.
	10	* 156.	115.	86.	52.	34.	18.	11.	5.	3.
	20	* 100.	74.	56.	34.	22.	11.	7.	3.	2.
	30	* 73.	54.	40.	24.	16.	8.	5.	2.	1.
60	45	* 53.	39.	29.	18.	12.	6.	4.	2.	1.
	65	* 42.	31.	23.	14.	9.	5.	3.	1.	1.
	90	* 38.	28.	21.	13.	8.	4.	3.	1.	1.
	0	* 147.	109.	81.	49.	32.	17.	10.	5.	3.
	10	* 105.	78.	58.	35.	23.	12.	7.	3.	2.
	20	* 68.	50.	38.	23.	15.	8.	5.	2.	1.
80	30	* 49.	36.	27.	16.	11.	6.	3.	2.	1.
	45	* 36.	26.	20.	12.	8.	4.	2.	1.	1.
	65	* 28.	21.	16.	9.	6.	3.	2.	1.	1.
	90	* 26.	19.	14.	9.	6.	3.	2.	1.	0.
	0	* 68.	50.	38.	23.	15.	8.	5.	2.	1.
	10	* 49.	36.	27.	16.	11.	6.	3.	2.	1.
100	20	* 31.	23.	17.	11.	7.	4.	2.	1.	1.
	30	* 23.	17.	13.	8.	5.	3.	2.	1.	0.
	45	* 17.	12.	9.	6.	4.	2.	1.	1.	0.
	65	* 13.	10.	7.	4.	3.	1.	1.	0.	0.
	90	* 12.	9.	7.	4.	3.	1.	1.	0.	0.
	0	* 3.	2.	2.	1.	1.	0.	0.	0.	0.
180	10	* 2.	2.	1.	1.	1.	0.	0.	0.	0.
	20	* 2.	1.	1.	1.	0.	0.	0.	0.	0.
	30	* 1.	1.	1.	0.	0.	0.	0.	0.	0.
	45	* 1.	1.	0.	0.	0.	0.	0.	0.	0.
	65	* 1.	0.	0.	0.	0.	0.	0.	0.	0.
	90	* 1.	0.	0.	0.	0.	0.	0.	0.	0.

S S \* TOTAL IONOSPHERIC ABSORPTION LOSS (DECIBELS)  
 O A I A \*\*\*\*\*  
 L N G N \* AVERAGE SUNSPOT NUMBER (R12) 120.  
 A G N G \* ELECTRON GYRO-FREQUENCY (MHZ) 1.400  
 R L A L \* TOTAL GEOMAGNETIC FIELD (GAUSS) 0.500  
 E L F \*\*\*\*\*

		* SIGNAL FREQUENCY (MHZ)								
(DEG)	(DEG)	* 2.00	* 3.00	* 4.00	* 6.00	* 8.00	* 12.00	* 16.00	* 24.00	* 32.00
*****										
0	0	* 260.	193.	145.	89.	59.	31.	19.	9.	5.
	10	* 186.	138.	104.	64.	42.	22.	13.	6.	4.
	20	* 120.	89.	67.	41.	27.	14.	9.	4.	2.
	30	* 87.	65.	49.	30.	20.	10.	6.	3.	2.
	45	* 63.	47.	35.	22.	14.	8.	5.	2.	1.
	65	* 50.	37.	28.	17.	11.	6.	4.	2.	1.
20	90	* 46.	34.	25.	16.	10.	5.	3.	2.	1.
	0	* 244.	181.	137.	84.	55.	29.	18.	9.	5.
	10	* 175.	129.	98.	60.	40.	21.	13.	6.	4.
	20	* 113.	83.	63.	39.	26.	13.	8.	4.	2.
	30	* 82.	61.	46.	28.	19.	10.	6.	3.	2.
	45	* 60.	44.	33.	20.	14.	7.	4.	2.	1.
40	65	* 47.	35.	26.	16.	11.	6.	3.	2.	1.
	90	* 43.	32.	24.	15.	10.	5.	3.	1.	1.
	0	* 200.	148.	112.	68.	45.	24.	14.	7.	4.
	10	* 143.	106.	80.	49.	32.	17.	10.	5.	3.
	20	* 92.	68.	52.	32.	21.	11.	7.	3.	2.
	30	* 67.	50.	37.	23.	15.	8.	5.	2.	1.
60	45	* 49.	36.	27.	17.	11.	6.	4.	2.	1.
	65	* 38.	29.	22.	13.	9.	5.	3.	1.	1.
	90	* 35.	26.	20.	12.	8.	4.	3.	1.	1.
	0	* 135.	100.	75.	46.	31.	16.	10.	5.	3.
	10	* 97.	72.	54.	33.	22.	11.	7.	3.	2.
	20	* 62.	46.	35.	21.	14.	7.	5.	2.	1.
80	30	* 45.	33.	25.	15.	10.	5.	3.	2.	1.
	45	* 35.	24.	18.	11.	7.	4.	2.	1.	1.
	65	* 26.	19.	15.	9.	6.	3.	2.	1.	1.
	90	* 24.	18.	13.	8.	5.	3.	2.	1.	0.
	0	* 63.	46.	35.	21.	14.	7.	5.	2.	1.
	10	* 45.	33.	25.	15.	10.	5.	3.	2.	1.
100	20	* 29.	21.	16.	10.	7.	3.	2.	1.	1.
	30	* 21.	16.	12.	7.	5.	2.	2.	1.	0.
	45	* 15.	11.	9.	5.	3.	2.	1.	1.	0.
	65	* 12.	9.	7.	4.	3.	1.	1.	0.	0.
	90	* 11.	8.	6.	4.	2.	1.	1.	0.	0.
	0	* 3.	2.	2.	1.	1.	0.	0.	0.	0.
120	10	* 2.	2.	1.	1.	1.	0.	0.	0.	0.
	20	* 1.	1.	1.	0.	0.	0.	0.	0.	0.
	30	* 1.	1.	1.	0.	0.	0.	0.	0.	0.
	45	* 1.	1.	0.	0.	0.	0.	0.	0.	0.
	65	* 1.	0.	0.	0.	0.	0.	0.	0.	0.
140	90	* 1.	0.	0.	0.	0.	0.	0.	0.	0.
	0	* 1.	0.	0.	0.	0.	0.	0.	0.	0.



S	S	*	TOTAL IONOSPHERIC ABSORPTION LOSS (DECIRELS)								
O A	I A	*****									
L N	G N	*	AVERAGE SUNSPOT NUMBER (R12) 120.								
A G	N G	*	ELECTRON GYRO-FREQUENCY (MHZ) 1.820								
R L	A L	*	TOTAL GEOMAGNETIC FIELD (GAUSS) 0.650								
E	L E	*****									
		*	SIGNAL FREQUENCY (MHZ)								
(DEG)	(DEG)	*	2.00	3.00	4.00	6.00	8.00	12.00	16.00	24.00	32.00
*****											
0	0	*	229.	171.	130.	81.	55.	29.	18.	9.	5.
	10	*	164.	122.	93.	58.	39.	21.	13.	6.	4.
	20	*	106.	79.	60.	37.	25.	13.	8.	4.	2.
	30	*	77.	57.	44.	27.	18.	10.	6.	3.	2.
	45	*	56.	42.	32.	20.	13.	7.	4.	2.	1.
	65	*	44.	33.	25.	16.	11.	6.	3.	2.	1.
	90	*	40.	30.	23.	14.	10.	5.	3.	2.	1.
*****											
20	0	*	215.	160.	122.	76.	51.	27.	17.	8.	5.
	10	*	154.	115.	87.	54.	37.	20.	12.	6.	3.
	20	*	99.	74.	56.	35.	24.	13.	8.	4.	2.
	30	*	72.	54.	41.	26.	17.	9.	6.	3.	2.
	45	*	52.	39.	30.	19.	13.	7.	4.	2.	1.
	65	*	41.	31.	24.	15.	10.	5.	3.	2.	1.
	90	*	38.	28.	21.	13.	9.	5.	3.	1.	1.
*****											
40	0	*	176.	131.	100.	62.	42.	22.	14.	7.	4.
	10	*	126.	94.	72.	45.	30.	16.	10.	5.	3.
	20	*	81.	61.	46.	29.	19.	10.	6.	3.	2.
	30	*	59.	44.	34.	21.	14.	8.	5.	2.	1.
	45	*	43.	32.	24.	15.	10.	5.	3.	2.	1.
	65	*	34.	25.	19.	12.	8.	4.	3.	1.	1.
	90	*	31.	23.	18.	11.	7.	4.	2.	1.	1.
*****											
60	0	*	119.	89.	68.	42.	28.	15.	9.	5.	3.
	10	*	85.	63.	48.	30.	20.	11.	7.	3.	2.
	20	*	55.	41.	31.	19.	13.	7.	4.	2.	1.
	30	*	40.	30.	23.	14.	9.	5.	3.	2.	1.
	45	*	29.	22.	16.	10.	7.	4.	2.	1.	1.
	65	*	23.	17.	13.	8.	5.	3.	2.	1.	1.
	90	*	21.	16.	12.	7.	5.	3.	2.	1.	0.
*****											
80	0	*	55.	41.	31.	19.	13.	7.	4.	2.	1.
	10	*	39.	29.	22.	14.	9.	5.	3.	2.	1.
	20	*	25.	19.	14.	9.	6.	3.	2.	1.	1.
	30	*	18.	14.	10.	7.	4.	2.	1.	1.	0.
	45	*	13.	10.	8.	5.	3.	2.	1.	1.	0.
	65	*	11.	8.	6.	4.	3.	1.	1.	0.	0.
	90	*	10.	7.	5.	3.	2.	1.	1.	0.	0.
*****											
100	0	*	3.	2.	2.	1.	1.	0.	0.	0.	0.
TO	10	*	2.	1.	1.	1.	0.	0.	0.	0.	0.
180	20	*	1.	1.	1.	0.	0.	0.	0.	0.	0.
	30	*	1.	1.	1.	0.	0.	0.	0.	0.	0.
	45	*	1.	0.	0.	0.	0.	0.	0.	0.	0.
	65	*	1.	0.	0.	0.	0.	0.	0.	0.	0.
	90	*	0.	0.	0.	0.	0.	0.	0.	0.	0.

S S \* TOTAL IONOSPHERIC ABSORPTION LOSS (DECIBELS)  
 O A I A \*  
 L N G M \* AVERAGE SUNSPOT NUMBER (R12) 150.  
 A G M G \* ELECTRON CYCLO-FREQUENCY (MHZ) 0.700  
 R L A L \* TOTAL GEOMAGNETIC FIELD (GAUSS) 0.250  
 F L F \*

\* SIGNAL FREQUENCY (MHZ)

(DEG)	(DEG) *	2.00	3.00	4.00	6.00	8.00	12.00	16.00	24.00	32.00
0	0 *	347.	255.	190.	113.	73.	37.	20.	10.	6.
	10 *	248.	183.	136.	81.	52.	26.	16.	7.	4.
	20 *	169.	118.	86.	52.	34.	17.	10.	5.	3.
	30 *	116.	86.	64.	38.	24.	12.	7.	3.	2.
	45 *	85.	62.	46.	27.	18.	9.	5.	3.	1.
	65 *	67.	49.	37.	22.	14.	7.	4.	2.	1.
	90 *	61.	45.	33.	20.	13.	6.	4.	2.	1.
20	0 *	326.	240.	179.	106.	68.	35.	21.	10.	6.
	10 *	233.	172.	128.	76.	49.	25.	15.	7.	4.
	20 *	159.	111.	82.	49.	32.	16.	10.	4.	3.
	30 *	109.	80.	60.	35.	23.	12.	7.	3.	2.
	45 *	79.	59.	43.	26.	17.	8.	5.	2.	1.
	65 *	63.	46.	34.	20.	13.	7.	4.	2.	1.
	90 *	57.	42.	31.	19.	12.	6.	4.	2.	1.
40	0 *	265.	196.	146.	87.	56.	28.	17.	8.	5.
	10 *	191.	141.	105.	62.	40.	20.	12.	6.	3.
	20 *	123.	91.	67.	40.	26.	13.	8.	4.	2.
	30 *	89.	61.	49.	29.	19.	9.	6.	3.	2.
	45 *	65.	48.	36.	21.	14.	7.	4.	2.	1.
	65 *	51.	38.	28.	17.	11.	5.	3.	2.	1.
	90 *	47.	34.	26.	15.	10.	5.	3.	1.	1.
60	0 *	180.	135.	98.	58.	38.	19.	11.	5.	3.
	10 *	129.	95.	71.	42.	27.	14.	8.	4.	2.
	20 *	83.	61.	46.	27.	17.	9.	5.	2.	1.
	30 *	60.	43.	33.	20.	13.	6.	4.	2.	1.
	45 *	45.	32.	24.	14.	9.	5.	3.	1.	1.
	65 *	35.	26.	19.	11.	7.	4.	2.	1.	1.
	90 *	32.	23.	17.	10.	7.	3.	2.	1.	1.
80	0 *	113.	83.	61.	46.	27.	17.	9.	5.	2.
	10 *	60.	43.	33.	19.	13.	6.	4.	2.	1.
	20 *	38.	28.	21.	12.	8.	4.	2.	1.	1.
	30 *	28.	21.	15.	9.	6.	3.	2.	1.	0.
	45 *	20.	15.	11.	7.	4.	2.	1.	1.	0.
	65 *	16.	12.	9.	5.	3.	2.	1.	0.	0.
	90 *	15.	11.	8.	5.	3.	2.	1.	0.	0.
100	0 *	4.	3.	2.	1.	1.	0.	0.	0.	0.
120	10 *	3.	2.	2.	1.	1.	0.	0.	0.	0.
140	20 *	2.	1.	1.	1.	0.	0.	0.	0.	0.
	30 *	1.	1.	1.	0.	0.	0.	0.	0.	0.
	45 *	1.	1.	1.	0.	0.	0.	0.	0.	0.
	65 *	1.	1.	0.	0.	0.	0.	0.	0.	0.
	90 *	1.	1.	0.	0.	0.	0.	0.	0.	0.

150/070

S	S	*	TOTAL IONOSPHERIC ABSORPTION LOSS (DECIBELS)							
O A	I A	*****								
I H	G H	*	AVERAGE SUNSPOT NUMBER (R12) 150.							
A G	H G	*	ELECTRON GYRO-FREQUENCY (MHZ) 1.120							
P L	A L	*	TOTAL GEOMAGNETIC FIELD (GAUSS) 0.400							
E	L E	*****								
			* SIGNAL FREQUENCY (MHZ)							
(DEG)	(DEG)	*	2.00	3.00	4.00	6.00	8.00	12.00	16.00	24.00 32.00
			*****							
0	0	*	305.	225.	169.	102.	67.	35.	21.	10. 6.
	10	*	218.	161.	121.	73.	48.	25.	15.	7. 4.
	20	*	141.	104.	78.	47.	31.	16.	10.	5. 3.
	30	*	102.	75.	57.	34.	22.	12.	7.	3. 2.
	45	*	74.	55.	41.	25.	16.	8.	5.	2. 1.
	65	*	59.	43.	33.	20.	13.	7.	4.	2. 1.
	90	*	53.	39.	30.	18.	12.	6.	4.	2. 1.
			*****							
20	0	*	287.	217.	159.	96.	63.	33.	20.	9. 5.
	10	*	205.	151.	114.	69.	45.	23.	14.	7. 4.
	20	*	132.	98.	73.	45.	29.	15.	9.	4. 3.
	30	*	96.	71.	53.	32.	21.	11.	7.	3. 2.
	45	*	70.	52.	39.	23.	15.	8.	5.	2. 1.
	65	*	55.	41.	31.	18.	12.	6.	4.	2. 1.
	90	*	50.	37.	28.	17.	11.	6.	3.	2. 1.
			*****							
40	0	*	234.	173.	130.	78.	51.	27.	16.	8. 4.
	10	*	168.	124.	93.	56.	37.	19.	12.	5. 3.
	20	*	108.	80.	60.	36.	24.	12.	7.	4. 2.
	30	*	79.	58.	45.	26.	17.	9.	5.	3. 1.
	45	*	57.	42.	32.	19.	13.	6.	4.	2. 1.
	65	*	45.	33.	25.	15.	10.	5.	3.	1. 1.
	90	*	41.	30.	23.	14.	9.	5.	3.	1. 1.
			*****							
60	0	*	158.	117.	88.	53.	35.	18.	11.	5. 3.
	10	*	113.	84.	63.	38.	25.	13.	8.	4. 2.
	20	*	73.	54.	40.	24.	16.	8.	5.	2. 1.
	30	*	53.	39.	29.	18.	12.	6.	4.	2. 1.
	45	*	39.	29.	21.	13.	8.	4.	3.	1. 1.
	65	*	30.	23.	17.	10.	7.	3.	2.	1. 1.
	90	*	28.	20.	15.	9.	6.	3.	2.	1. 1.
			*****							
80	0	*	73.	54.	41.	25.	16.	8.	5.	2. 1.
	10	*	52.	39.	29.	18.	12.	6.	4.	2. 1.
	20	*	34.	25.	19.	11.	7.	4.	2.	1. 1.
	30	*	25.	18.	14.	8.	5.	3.	2.	1. 0.
	45	*	18.	13.	10.	6.	4.	2.	1.	1. 0.
	65	*	14.	10.	8.	5.	3.	2.	1.	0. 0.
	90	*	13.	9.	7.	4.	3.	1.	1.	0. 0.
			*****							
100	0	*	4.	3.	2.	1.	1.	0.	0.	0. 0.
TO	10	*	3.	2.	1.	1.	1.	0.	0.	0. 0.
180	20	*	2.	1.	1.	1.	0.	0.	0.	0. 0.
	30	*	1.	1.	1.	0.	0.	0.	0.	0. 0.
	45	*	1.	1.	0.	0.	0.	0.	0.	0. 0.
	65	*	1.	1.	0.	0.	0.	0.	0.	0. 0.
	90	*	1.	0.	0.	0.	0.	0.	0.	0. 0.

S S \* TOTAL IONOSPHERIC ABSORPTION LOSS (DECIBELS)  
 O A I A \*  
 I M G M \* AVERAGE SUNSPOT NUMBER (R12) 150.  
 A G M G \* ELECTRON GYRO-FREQUENCY (MHZ) 1.400  
 P L A L \* TOTAL GEOMAGNETIC FIELD (GAUSS) 0.500  
 F L F \*

\* SIGNAL FREQUENCY (MHZ)

(DEG)	(DEG)	* 2.00	3.00	4.00	6.00	8.00	12.00	16.00	24.00	32.00
*****										
0	0	*	280.	207.	157.	96.	64.	33.	20.	10.
	10	*	200.	148.	112.	68.	45.	24.	15.	7.
	20	*	129.	96.	72.	47.	29.	15.	9.	5.
	30	*	94.	70.	52.	32.	21.	11.	7.	3.
	45	*	68.	51.	38.	23.	15.	7.	5.	2.
	65	*	54.	40.	30.	18.	12.	6.	4.	2.
20	0	*	49.	36.	27.	17.	11.	6.	4.	2.
	10	*	263.	195.	147.	90.	60.	31.	19.	9.
	20	*	189.	139.	105.	64.	43.	22.	14.	7.
	30	*	121.	90.	68.	41.	28.	14.	9.	4.
	45	*	88.	65.	49.	30.	20.	10.	6.	3.
	65	*	64.	48.	36.	22.	15.	8.	5.	2.
40	0	*	51.	38.	28.	17.	11.	6.	4.	2.
	10	*	46.	34.	26.	16.	10.	5.	3.	2.
	20	*	215.	159.	120.	74.	49.	26.	16.	8.
	30	*	154.	114.	86.	53.	35.	18.	11.	5.
	45	*	99.	74.	56.	34.	23.	12.	7.	3.
	65	*	72.	53.	40.	25.	16.	9.	5.	3.
60	0	*	52.	39.	29.	18.	12.	6.	4.	2.
	10	*	41.	31.	23.	14.	9.	5.	3.	1.
	20	*	38.	28.	21.	13.	9.	4.	3.	1.
	30	*	145.	108.	81.	50.	33.	17.	11.	5.
	45	*	104.	77.	58.	36.	24.	12.	8.	4.
	65	*	67.	50.	38.	23.	15.	8.	5.	2.
80	0	*	49.	36.	27.	17.	11.	6.	4.	2.
	10	*	44.	33.	25.	16.	10.	5.	3.	2.
	20	*	35.	26.	20.	12.	8.	4.	3.	1.
	30	*	28.	21.	16.	10.	6.	3.	2.	1.
	45	*	25.	19.	14.	9.	6.	3.	2.	1.
	65	*	25.	19.	14.	9.	6.	3.	2.	1.
100	0	*	67.	50.	38.	23.	15.	8.	5.	2.
	10	*	48.	36.	27.	16.	11.	6.	3.	2.
	20	*	31.	23.	17.	11.	7.	4.	2.	1.
	30	*	23.	17.	13.	8.	5.	3.	2.	1.
	45	*	16.	12.	9.	6.	4.	2.	1.	0.
	65	*	13.	10.	7.	4.	3.	2.	1.	0.
120	0	*	12.	9.	7.	4.	3.	1.	1.	0.
	10	*	3.	2.	2.	1.	1.	0.	0.	0.
	20	*	2.	1.	1.	1.	0.	0.	0.	0.
	30	*	1.	1.	1.	0.	0.	0.	0.	0.
	45	*	1.	1.	0.	0.	0.	0.	0.	0.
	65	*	1.	0.	0.	0.	0.	0.	0.	0.
180	0	*	1.	0.	0.	0.	0.	0.	0.	0.
	90	*	1.	0.	0.	0.	0.	0.	0.	0.

S	S	*	TOTAL IONOSPHERIC ABSORPTION LOSS (DECIBELS)								
O A	I A	*	AVERAGE SUNSPOT NUMBER (R12) 150.								
E N	G M	*	ELECTRON GYRO-FREQUENCY (MHZ) 1.820								
A G	H G	*	TOTAL GEOMAGNETIC FIELD (GAUSS) 0.650								
P L	A L	*	* SIGNAL FREQUENCY (MHZ)								
F	L E	*									
(DEG)	(DEG)	*	2.00	3.00	4.00	6.00	8.00	12.00	16.00	24.00	32.00
*****											
0	0	*	246.	184.	140.	87.	59.	31.	19.	9.	6.
	10	*	176.	132.	100.	62.	42.	22.	14.	7.	4.
	20	*	114.	85.	65.	40.	27.	14.	9.	4.	3.
	30	*	83.	62.	47.	29.	20.	11.	7.	3.	2.
	45	*	60.	45.	34.	21.	14.	8.	5.	2.	1.
	65	*	47.	35.	27.	17.	11.	6.	4.	2.	1.
	90	*	43.	32.	25.	15.	10.	6.	3.	2.	1.
*****											
20	0	*	231.	173.	132.	82.	55.	30.	18.	9.	5.
	10	*	165.	124.	94.	59.	40.	21.	13.	6.	4.
	20	*	107.	80.	61.	38.	25.	14.	8.	4.	2.
	30	*	78.	58.	44.	27.	19.	10.	6.	3.	2.
	45	*	56.	42.	32.	20.	13.	7.	4.	2.	1.
	65	*	45.	33.	25.	16.	11.	6.	4.	2.	1.
	90	*	41.	30.	23.	14.	10.	5.	3.	2.	1.
*****											
40	0	*	189.	141.	108.	67.	45.	24.	15.	7.	4.
	10	*	135.	101.	77.	48.	32.	17.	11.	5.	3.
	20	*	87.	65.	50.	31.	21.	11.	7.	3.	2.
	30	*	63.	47.	36.	22.	15.	8.	5.	2.	1.
	45	*	46.	34.	26.	16.	11.	6.	4.	2.	1.
	65	*	36.	27.	21.	13.	9.	5.	3.	1.	1.
	90	*	33.	25.	19.	12.	8.	4.	3.	1.	1.
*****											
60	0	*	128.	95.	73.	45.	30.	16.	10.	5.	3.
	10	*	91.	68.	52.	32.	21.	12.	7.	4.	2.
	20	*	59.	44.	34.	21.	14.	8.	5.	2.	1.
	30	*	43.	32.	24.	15.	10.	5.	3.	2.	1.
	45	*	31.	23.	18.	11.	7.	4.	2.	1.	1.
	65	*	25.	18.	14.	9.	6.	3.	2.	1.	1.
	90	*	22.	17.	13.	8.	5.	3.	2.	1.	1.
*****											
80	0	*	59.	44.	34.	21.	14.	8.	5.	2.	1.
	10	*	42.	32.	24.	15.	10.	5.	3.	2.	1.
	20	*	27.	20.	16.	10.	7.	3.	2.	1.	1.
	30	*	20.	15.	11.	7.	5.	3.	2.	1.	0.
	45	*	14.	11.	8.	5.	3.	2.	1.	1.	0.
	65	*	11.	9.	6.	4.	3.	1.	1.	0.	0.
	90	*	10.	8.	6.	4.	2.	1.	1.	0.	0.
*****											
100	0	*	3.	2.	2.	1.	1.	0.	0.	0.	0.
TO	10	*	2.	2.	1.	1.	1.	0.	0.	0.	0.
180	20	*	1.	1.	1.	0.	0.	0.	0.	0.	0.
	30	*	1.	1.	1.	0.	0.	0.	0.	0.	0.
	45	*	1.	1.	0.	0.	0.	0.	0.	0.	0.
	65	*	1.	0.	0.	0.	0.	0.	0.	0.	0.
	90	*	1.	0.	0.	0.	0.	0.	0.	0.	0.

S S \* TOTAL IONOSPHERIC ABSORPTION LOSS (DECIBELS)  
 O A I A \*  
 L N G H \* AVERAGE SUNSPOT NUMBER (R12) 180.  
 A G N G \* ELECTRON GYRO-FREQUENCY (MHZ) 0.700  
 R L A L \* TOTAL GEOMAGNETIC FIELD (GAUSS) 0.250  
 E L E \*

		* SIGNAL FREQUENCY (MHZ)									
(DEG)	(DEG)	* 2.00	3.00	4.00	6.00	8.00	12.00	16.00	24.00	32.00	
*****											
0	0	*	371.	274.	204.	121.	78.	39.	24.	11.	6.
	10	*	266.	196.	146.	86.	56.	28.	17.	8.	5.
	20	*	171.	126.	94.	56.	36.	18.	11.	5.	3.
	30	*	124.	92.	68.	40.	26.	13.	8.	4.	2.
	45	*	91.	67.	50.	29.	19.	10.	6.	3.	2.
	65	*	72.	53.	39.	23.	15.	8.	5.	2.	1.
20	0	*	65.	48.	36.	21.	14.	7.	4.	2.	1.
	10	*	349.	257.	191.	113.	73.	37.	22.	10.	6.
	20	*	250.	184.	137.	81.	52.	26.	16.	7.	4.
	30	*	161.	119.	88.	52.	34.	17.	10.	5.	3.
	45	*	117.	86.	64.	38.	25.	12.	7.	3.	2.
	65	*	85.	63.	47.	28.	18.	9.	5.	3.	1.
40	0	*	67.	50.	37.	22.	14.	7.	4.	2.	1.
	10	*	61.	45.	34.	20.	13.	6.	4.	2.	1.
	20	*	285.	210.	157.	93.	60.	30.	18.	9.	5.
	30	*	204.	151.	112.	66.	43.	22.	13.	6.	4.
	45	*	132.	97.	72.	43.	28.	14.	8.	4.	2.
	65	*	96.	71.	52.	31.	20.	10.	6.	3.	2.
60	0	*	70.	51.	38.	23.	15.	7.	4.	2.	1.
	10	*	55.	41.	30.	18.	12.	6.	3.	2.	1.
	20	*	50.	37.	27.	16.	10.	5.	3.	1.	1.
	30	*	103.	142.	106.	63.	40.	20.	12.	6.	3.
	45	*	138.	102.	76.	45.	29.	15.	9.	4.	2.
	65	*	89.	65.	49.	29.	19.	9.	6.	3.	2.
80	0	*	89.	65.	49.	29.	19.	9.	6.	3.	2.
	10	*	64.	47.	35.	21.	13.	7.	4.	2.	1.
	20	*	41.	30.	23.	13.	9.	4.	3.	1.	1.
	30	*	30.	22.	16.	10.	6.	3.	2.	1.	1.
	45	*	22.	16.	12.	7.	5.	2.	1.	1.	0.
	65	*	17.	13.	9.	6.	4.	2.	1.	1.	0.
100	0	*	16.	12.	9.	5.	3.	2.	1.	0.	0.
	10	*	4.	3.	2.	1.	1.	0.	0.	0.	0.
	20	*	3.	2.	2.	1.	1.	0.	0.	0.	0.
	30	*	2.	2.	1.	1.	0.	0.	0.	0.	0.
	45	*	1.	1.	1.	0.	0.	0.	0.	0.	0.
	65	*	1.	1.	0.	0.	0.	0.	0.	0.	0.
180	0	*	1.	1.	0.	0.	0.	0.	0.	0.	0.
	10	*	1.	1.	0.	0.	0.	0.	0.	0.	0.

180/070

S	S	*	TOTAL IONOSPHERIC ABSORPTION LOSS (DECIBELS)							
O A	I A	*	*****							
L M	G M	*	AVERAGE SUNSPOT NUMBER (R12) 180.							
G	H G	*	ELECTRON GYRO-FREQUENCY (MHZ) 1.120							
P L	A L	*	TOTAL GEOMAGNETIC FIELD (GAUSS) 0.400							
E	L F	*	*****							
		*	SIGNAL FREQUENCY (MHZ)							
(DEG)	(DEG)	*	2.00	3.00	4.00	6.00	8.00	12.00	16.00	24.00 32.00
*****										
0	0	*	327.	241.	181.	109.	72.	37.	22.	11. 6.
	10	*	234.	173.	130.	78.	51.	27.	16.	8. 4.
	20	*	151.	111.	84.	50.	33.	17.	10.	5. 3.
	30	*	110.	81.	61.	37.	24.	12.	8.	4. 2.
	45	*	80.	59.	44.	27.	18.	9.	5.	3. 2.
	65	*	63.	46.	35.	21.	14.	7.	4.	2. 1.
	90	*	57.	42.	32.	19.	13.	6.	4.	2. 1.
*****										
20	0	*	307.	237.	170.	103.	67.	35.	21.	10. 6.
	10	*	230.	162.	122.	73.	48.	25.	15.	7. 4.
	20	*	142.	105.	79.	47.	31.	16.	10.	5. 3.
	30	*	103.	76.	57.	34.	23.	12.	7.	3. 2.
	45	*	75.	55.	42.	25.	16.	9.	5.	2. 1.
	65	*	59.	44.	33.	20.	13.	7.	4.	2. 1.
	90	*	54.	40.	30.	18.	12.	6.	4.	2. 1.
*****										
40	0	*	251.	185.	139.	84.	55.	29.	17.	8. 5.
	10	*	180.	133.	100.	60.	39.	20.	12.	6. 3.
	20	*	116.	86.	64.	39.	25.	13.	8.	4. 2.
	30	*	84.	62.	47.	28.	18.	10.	6.	3. 2.
	45	*	61.	45.	34.	20.	13.	7.	4.	2. 1.
	65	*	48.	36.	27.	16.	11.	5.	3.	2. 1.
	90	*	44.	32.	24.	15.	10.	5.	3.	1. 1.
*****										
60	0	*	170.	125.	94.	57.	37.	19.	12.	6. 3.
	10	*	121.	90.	67.	41.	27.	14.	8.	4. 2.
	20	*	78.	58.	43.	26.	17.	9.	5.	3. 1.
	30	*	57.	42.	32.	19.	12.	6.	4.	2. 1.
	45	*	41.	31.	23.	14.	9.	5.	3.	1. 1.
	65	*	33.	24.	18.	11.	7.	4.	2.	1. 1.
	90	*	30.	22.	16.	10.	7.	3.	2.	1. 1.
*****										
80	0	*	79.	58.	44.	26.	17.	9.	5.	3. 1.
	10	*	56.	42.	31.	19.	12.	6.	4.	2. 1.
	20	*	36.	27.	20.	12.	8.	4.	2.	1. 1.
	30	*	26.	19.	15.	9.	6.	3.	2.	1. 1.
	45	*	19.	14.	11.	6.	4.	2.	1.	1. 0.
	65	*	15.	11.	8.	5.	3.	2.	1.	0. 0.
	90	*	14.	10.	8.	5.	3.	2.	1.	0. 0.
*****										
100	0	*	4.	3.	2.	1.	1.	0.	0.	0. 0.
70	10	*	3.	2.	2.	1.	1.	0.	0.	0. 0.
180	20	*	2.	1.	1.	1.	0.	0.	0.	0. 0.
	30	*	1.	1.	1.	0.	0.	0.	0.	0. 0.
	45	*	1.	1.	1.	0.	0.	0.	0.	0. 0.
	65	*	1.	1.	0.	0.	0.	0.	0.	0. 0.
	90	*	1.	1.	0.	0.	0.	0.	0.	0. 0.

S	S	TOTAL IONOSPHERIC ABSORPTION LOSS (DECIBELS)									
O A	I A	*****									
L N	G N	AVERAGE SUNSPOT NUMBER (R12) 180.									
A G	N G	ELECTRON GYRO-FREQUENCY (MHZ) 1.400									
R L	A L	TOTAL GEOMAGNETIC FIELD (GAUSS) 0.500									
E	L E	*****									
		* SIGNAL FREQUENCY (MHZ)									
(DFG)	(DEG)	* 2.00	3.00	4.00	6.00	8.00	12.00	16.00	24.00	32.00	
*****											
0	0	*	300.	222.	168.	103.	68.	36.	22.	10.	6.
	10	*	215.	159.	120.	73.	49.	26.	16.	7.	4.
	20	*	138.	103.	77.	47.	31.	16.	10.	5.	3.
	30	*	101.	74.	56.	34.	23.	12.	7.	4.	2.
	45	*	73.	54.	41.	25.	17.	9.	5.	3.	1.
	65	*	58.	43.	32.	20.	13.	7.	4.	2.	1.
90	*	53.	39.	29.	18.	12.	6.	4.	2.	1.	
*****											
20	0	*	282.	204.	158.	96.	64.	33.	20.	10.	6.
	10	*	202.	149.	113.	69.	46.	24.	15.	7.	4.
	20	*	130.	96.	73.	44.	29.	15.	9.	5.	3.
	30	*	94.	70.	53.	32.	21.	11.	7.	3.	2.
	45	*	69.	51.	38.	24.	16.	8.	5.	2.	1.
	65	*	54.	40.	30.	19.	12.	6.	4.	2.	1.
90	*	49.	37.	28.	17.	11.	6.	4.	2.	1.	
*****											
40	0	*	231.	171.	129.	79.	52.	27.	17.	8.	5.
	10	*	165.	122.	92.	56.	37.	20.	12.	6.	3.
	20	*	106.	79.	60.	36.	24.	13.	8.	4.	2.
	30	*	77.	57.	43.	26.	18.	9.	6.	3.	2.
	45	*	56.	42.	31.	19.	13.	7.	4.	2.	1.
	65	*	44.	33.	25.	15.	10.	5.	3.	2.	1.
90	*	40.	30.	23.	14.	9.	5.	3.	1.	1.	
*****											
60	0	*	156.	115.	87.	53.	35.	19.	11.	5.	3.
	10	*	111.	83.	62.	38.	25.	13.	8.	4.	2.
	20	*	72.	53.	40.	25.	16.	9.	5.	3.	1.
	30	*	52.	39.	29.	18.	12.	6.	4.	2.	1.
	45	*	38.	28.	21.	13.	9.	5.	3.	1.	1.
	65	*	30.	22.	17.	10.	7.	4.	2.	1.	1.
90	*	27.	20.	15.	9.	6.	3.	2.	1.	1.	
*****											
80	0	*	72.	53.	40.	25.	16.	9.	5.	3.	1.
	10	*	52.	38.	29.	18.	12.	6.	4.	2.	1.
	20	*	33.	25.	19.	11.	8.	4.	2.	1.	1.
	30	*	24.	18.	14.	8.	5.	3.	2.	1.	0.
	45	*	18.	13.	10.	6.	4.	2.	1.	1.	0.
	65	*	14.	10.	8.	5.	3.	2.	1.	0.	0.
90	*	13.	9.	7.	4.	3.	2.	1.	0.	0.	
*****											
100	0	*	4.	3.	2.	1.	1.	0.	0.	0.	0.
TO	10	*	3.	2.	1.	1.	1.	0.	0.	0.	0.
180	20	*	2.	1.	1.	1.	0.	0.	0.	0.	0.
	30	*	1.	1.	1.	0.	0.	0.	0.	0.	0.
	45	*	1.	1.	0.	0.	0.	0.	0.	0.	0.
	65	*	1.	1.	0.	0.	0.	0.	0.	0.	0.
	90	*	1.	0.	0.	0.	0.	0.	0.	0.	0.

180/140



S S \* TOTAL IONOSPHERIC ABSORPTION LOSS (DECIBELS)  
 O A I A \*  
 L N G H \* AVERAGE SUNSPOT NUMBER (R12) 180.  
 A G N G \* ELECTRON GYRO-FREQUENCY (MHZ) 1.820  
 P L A I \* TOTAL GEOMAGNETIC FIELD (GAUSS) 0.650  
 E L F \*

		* SIGNAL FREQUENCY (MHZ)								
(DEG)	(DEG)	* 2.00	3.00	4.00	6.00	8.00	12.00	16.00	24.00	32.00
*****										
0	0	* 264.	197.	150.	94.	63.	34.	21.	10.	6.
	10	* 189.	141.	107.	67.	45.	24.	15.	7.	4.
	20	* 122.	91.	69.	43.	29.	16.	10.	5.	3.
	30	* 88.	66.	50.	31.	21.	11.	7.	3.	2.
	45	* 64.	48.	37.	23.	15.	8.	5.	2.	1.
	65	* 51.	38.	29.	18.	12.	6.	4.	2.	1.
20	90	* 46.	34.	26.	16.	11.	6.	4.	2.	1.
	0	* 248.	185.	141.	89.	59.	32.	20.	10.	6.
	10	* 177.	132.	101.	63.	42.	23.	14.	7.	4.
	20	* 114.	85.	65.	41.	27.	15.	9.	4.	3.
	30	* 83.	62.	47.	29.	20.	11.	7.	3.	2.
	45	* 60.	45.	34.	21.	14.	8.	5.	2.	1.
40	65	* 48.	36.	27.	17.	11.	6.	4.	2.	1.
	90	* 43.	32.	25.	15.	10.	6.	3.	2.	1.
	0	* 203.	151.	115.	72.	48.	26.	16.	8.	5.
	10	* 145.	108.	83.	51.	35.	19.	11.	6.	3.
	20	* 94.	70.	53.	33.	22.	12.	7.	4.	2.
	30	* 68.	51.	39.	24.	16.	9.	5.	3.	2.
60	45	* 49.	37.	28.	18.	12.	6.	4.	2.	1.
	65	* 39.	29.	22.	14.	9.	5.	3.	2.	1.
	90	* 36.	27.	20.	13.	8.	5.	3.	1.	1.
	0	* 137.	102.	78.	49.	33.	17.	11.	5.	3.
	10	* 98.	73.	56.	35.	23.	12.	8.	4.	2.
	20	* 63.	47.	36.	22.	15.	8.	5.	2.	1.
80	30	* 46.	34.	26.	16.	11.	6.	4.	2.	1.
	45	* 33.	25.	19.	12.	8.	4.	3.	1.	1.
	65	* 26.	20.	15.	9.	6.	3.	2.	1.	1.
	90	* 24.	18.	14.	8.	6.	3.	2.	1.	1.
	0	* 63.	47.	36.	22.	15.	8.	5.	2.	1.
	10	* 45.	34.	26.	16.	11.	6.	4.	2.	1.
100	20	* 29.	22.	17.	10.	7.	4.	2.	1.	1.
	30	* 21.	16.	12.	8.	5.	3.	2.	1.	0.
	45	* 15.	12.	9.	5.	4.	2.	1.	1.	0.
	65	* 12.	9.	7.	4.	3.	2.	1.	0.	0.
	90	* 11.	8.	6.	4.	3.	1.	1.	0.	0.
	0	* 3.	2.	2.	1.	1.	0.	0.	0.	0.
180	10	* 2.	2.	1.	1.	1.	0.	0.	0.	0.
	20	* 1.	1.	1.	1.	0.	0.	0.	0.	0.
	30	* 1.	1.	1.	0.	0.	0.	0.	0.	0.
	45	* 1.	1.	0.	0.	0.	0.	0.	0.	0.
	65	* 1.	0.	0.	0.	0.	0.	0.	0.	0.
	90	* 1.	0.	0.	0.	0.	0.	0.	0.	0.

180/182

S	S	*	TOTAL IONOSPHERIC ABSORPTION LOSS (DECIBELS)							
O A	I A	*								
L N	G N	*	AVERAGE SUNSPOT NUMBER (R12) 210.							
A G	N G	*	ELECTRON GYRO-FREQUENCY (MHZ) 0.700							
R L	A L	*	TOTAL GEOMAGNETIC FIELD (GAUSS) 0.250							
F	L E	*								
		*	SIGNAL FREQUENCY (MHZ)							
(DEG)	(DEG)	*	2.00	3.00	4.00	6.00	8.00	12.00	16.00	24.00 32.00
*****										
0	0	*	396.	292.	217.	129.	83.	42.	25.	12. 7.
	10	*	283.	209.	156.	92.	59.	30.	18.	8. 5.
	20	*	183.	135.	100.	59.	38.	19.	12.	5. 3.
	30	*	133.	98.	73.	43.	28.	14.	8.	4. 2.
	45	*	97.	71.	53.	31.	20.	10.	6.	3. 2.
	65	*	76.	56.	42.	25.	16.	8.	5.	2. 1.
	90	*	69.	51.	38.	23.	15.	7.	4.	2. 1.
*****										
20	0	*	372.	274.	204.	121.	78.	39.	24.	11. 6.
	10	*	266.	196.	146.	86.	56.	28.	17.	8. 5.
	20	*	172.	127.	94.	56.	36.	18.	11.	5. 3.
	30	*	125.	92.	68.	41.	26.	13.	8.	4. 2.
	45	*	91.	67.	50.	29.	19.	10.	6.	3. 2.
	65	*	72.	53.	39.	23.	15.	8.	5.	2. 1.
	90	*	65.	48.	36.	21.	14.	7.	4.	2. 1.
*****										
40	0	*	304.	234.	167.	99.	64.	32.	19.	9. 5.
	10	*	218.	161.	120.	71.	46.	23.	14.	6. 4.
	20	*	140.	104.	77.	46.	29.	15.	9.	4. 2.
	30	*	102.	75.	56.	33.	21.	11.	6.	3. 2.
	45	*	74.	55.	41.	24.	16.	8.	5.	2. 1.
	65	*	59.	43.	32.	19.	12.	6.	4.	2. 1.
	90	*	53.	39.	29.	17.	11.	6.	3.	2. 1.
*****										
60	0	*	206.	152.	113.	67.	43.	21.	13.	6. 4.
	10	*	147.	108.	81.	48.	31.	16.	9.	4. 3.
	20	*	95.	70.	52.	31.	20.	10.	6.	3. 2.
	30	*	69.	51.	38.	22.	14.	7.	4.	2. 1.
	45	*	50.	37.	28.	16.	11.	5.	3.	1. 1.
	65	*	40.	29.	22.	13.	8.	4.	3.	1. 1.
	90	*	36.	27.	20.	12.	8.	4.	2.	1. 1.
*****										
80	0	*	95.	70.	52.	31.	20.	10.	6.	3. 2.
	10	*	68.	50.	37.	22.	14.	7.	4.	2. 1.
	20	*	44.	32.	24.	14.	9.	5.	3.	1. 1.
	30	*	32.	24.	18.	10.	7.	3.	2.	1. 1.
	45	*	23.	17.	13.	8.	5.	2.	1.	1. 0.
	65	*	18.	14.	10.	6.	4.	2.	1.	1. 0.
	90	*	17.	12.	9.	5.	4.	2.	1.	0. 0.
*****										
100	0	*	5.	3.	3.	2.	1.	1.	0.	0. 0.
10	10	*	3.	2.	2.	1.	1.	0.	0.	0. 0.
180	20	*	2.	2.	1.	1.	0.	0.	0.	0. 0.
	30	*	2.	1.	1.	1.	0.	0.	0.	0. 0.
	45	*	1.	1.	1.	0.	0.	0.	0.	0. 0.
	65	*	1.	1.	0.	0.	0.	0.	0.	0. 0.
	90	*	1.	1.	0.	0.	0.	0.	0.	0. 0.

S S \* TOTAL IONOSPHERIC ABSORPTION LOSS (DECIBELS)  
 O A I A \*  
 L N G H \* AVERAGE SUNSPOT NUMBER (P12) 210.  
 A G H G \* ELECTRON GYRO-FREQUENCY (MHZ) 1.120  
 R L A L \* TOTAL GEOMAGNETIC FIELD (GAUSS) 0.400  
 E L F \*

\* SIGNAL FREQUENCY (MHZ)

(DFG)	(DFG) *	2.00	3.00	4.00	6.00	8.00	12.00	16.00	24.00	32.00
*****										
0	0 *	349.	257.	193.	117.	77.	40.	24.	11.	7.
	10 *	249.	184.	138.	83.	55.	28.	17.	8.	5.
	20 *	161.	119.	89.	54.	35.	18.	11.	5.	3.
	30 *	117.	86.	65.	39.	26.	13.	8.	4.	2.
	45 *	85.	63.	47.	28.	19.	10.	6.	3.	2.
	65 *	67.	50.	37.	22.	15.	8.	5.	2.	1.
20	90 *	61.	45.	34.	20.	13.	7.	4.	2.	1.
	0 *	327.	242.	181.	110.	72.	37.	22.	11.	6.
	10 *	234.	173.	130.	78.	51.	27.	16.	8.	4.
	20 *	151.	112.	84.	51.	33.	17.	10.	5.	3.
	30 *	110.	81.	61.	37.	24.	12.	8.	4.	2.
	45 *	80.	59.	44.	27.	18.	9.	5.	3.	2.
40	65 *	63.	47.	35.	21.	14.	7.	4.	2.	1.
	90 *	57.	42.	32.	19.	13.	7.	4.	2.	1.
	0 *	268.	198.	148.	90.	59.	30.	18.	9.	5.
	10 *	192.	142.	106.	64.	42.	22.	13.	6.	4.
	20 *	124.	91.	69.	41.	27.	14.	8.	4.	2.
	30 *	90.	66.	50.	30.	20.	10.	6.	3.	2.
60	45 *	65.	48.	36.	22.	14.	7.	4.	2.	1.
	65 *	52.	38.	29.	17.	11.	6.	4.	2.	1.
	90 *	47.	35.	26.	16.	10.	5.	3.	2.	1.
	0 *	181.	134.	100.	60.	40.	21.	12.	6.	3.
	10 *	129.	96.	72.	43.	28.	15.	9.	4.	2.
	20 *	83.	62.	46.	28.	18.	9.	6.	3.	2.
80	30 *	61.	45.	34.	20.	13.	7.	4.	2.	1.
	45 *	44.	33.	24.	15.	10.	5.	3.	1.	1.
	65 *	35.	26.	19.	12.	8.	4.	2.	1.	1.
	90 *	32.	23.	18.	11.	7.	4.	2.	1.	1.
	0 *	84.	62.	46.	28.	18.	10.	6.	3.	2.
	10 *	60.	44.	33.	20.	13.	7.	4.	2.	1.
100	20 *	39.	29.	21.	13.	8.	4.	3.	1.	1.
	30 *	28.	21.	16.	9.	6.	3.	2.	1.	1.
	45 *	20.	15.	11.	7.	4.	2.	1.	1.	0.
	65 *	16.	12.	9.	5.	4.	2.	1.	1.	0.
	90 *	15.	11.	8.	5.	3.	2.	1.	0.	0.
	0 *	4.	3.	2.	1.	1.	0.	0.	0.	0.
120	10 *	3.	2.	2.	1.	1.	0.	0.	0.	0.
	20 *	2.	1.	1.	1.	0.	0.	0.	0.	0.
	30 *	1.	1.	1.	0.	0.	0.	0.	0.	0.
	45 *	1.	1.	1.	0.	0.	0.	0.	0.	0.
	65 *	1.	1.	0.	0.	0.	0.	0.	0.	0.
	90 *	1.	1.	0.	0.	0.	0.	0.	0.	0.

210/112

S S \* TOTAL IONOSPHERIC ABSORPTION LOSS (DECIBELS)  
 O A I A \*  
 L N G M \* AVERAGE SUNSPOT NUMBER (R12) 210.  
 A G N G \* ELECTRON GYRO-FREQUENCY (MHZ) 1.400  
 R L A L \* TOTAL GEOMAGNETIC FIELD (GAUSS) 0.500  
 E L F \*

		* SIGNAL FREQUENCY (MHZ)								
(DEG)	(DEG)*	2.00	3.00	4.00	6.00	8.00	12.00	16.00	24.00	32.00
0	0 *	320.	237.	179.	109.	73.	38.	23.	11.	7.
	10 *	229.	170.	128.	78.	52.	27.	17.	8.	5.
	20 *	148.	109.	83.	50.	33.	18.	11.	5.	3.
	30 *	107.	79.	60.	37.	24.	13.	8.	4.	2.
	45 *	78.	58.	44.	27.	18.	9.	6.	3.	2.
	65 *	62.	46.	34.	21.	14.	7.	4.	2.	1.
20	0 *	56.	42.	31.	19.	13.	7.	4.	2.	1.
	10 *	301.	223.	168.	103.	68.	36.	22.	10.	6.
	10 *	215.	159.	120.	74.	49.	26.	16.	8.	4.
	20 *	139.	103.	78.	47.	31.	16.	10.	5.	3.
	30 *	101.	75.	56.	34.	23.	12.	7.	4.	2.
	45 *	73.	54.	41.	25.	17.	9.	5.	3.	1.
40	65 *	58.	43.	32.	20.	13.	7.	4.	2.	1.
	90 *	53.	39.	29.	18.	12.	6.	4.	2.	1.
	0 *	246.	182.	138.	84.	56.	29.	18.	9.	5.
	10 *	176.	130.	98.	60.	40.	21.	13.	6.	4.
	20 *	113.	84.	63.	39.	26.	13.	8.	4.	2.
	30 *	82.	61.	46.	28.	19.	10.	6.	3.	2.
60	45 *	60.	44.	34.	21.	14.	7.	4.	2.	1.
	65 *	47.	35.	26.	16.	11.	6.	3.	2.	1.
	90 *	43.	32.	24.	15.	10.	5.	3.	2.	1.
	0 *	166.	123.	93.	57.	38.	20.	12.	6.	3.
	10 *	119.	88.	66.	41.	27.	14.	9.	4.	2.
	20 *	77.	57.	43.	26.	17.	9.	6.	3.	2.
80	30 *	56.	41.	31.	19.	13.	7.	4.	2.	1.
	45 *	40.	30.	23.	14.	9.	5.	3.	1.	1.
	65 *	32.	24.	18.	11.	7.	4.	2.	1.	1.
	90 *	29.	21.	16.	10.	7.	3.	2.	1.	1.
	0 *	77.	57.	43.	26.	17.	9.	6.	3.	2.
	10 *	55.	41.	31.	19.	12.	7.	4.	2.	1.
100	20 *	35.	26.	20.	12.	8.	4.	3.	1.	1.
	30 *	26.	19.	14.	9.	6.	3.	2.	1.	1.
	45 *	19.	14.	11.	6.	4.	2.	1.	1.	0.
	65 *	15.	11.	8.	5.	3.	2.	1.	1.	0.
	90 *	13.	10.	8.	5.	3.	2.	1.	0.	0.
	0 *	4.	3.	2.	1.	1.	0.	0.	0.	0.
120	10 *	3.	2.	2.	1.	1.	0.	0.	0.	0.
	20 *	2.	1.	1.	1.	0.	0.	0.	0.	0.
	30 *	1.	1.	1.	0.	0.	0.	0.	0.	0.
	45 *	1.	1.	1.	0.	0.	0.	0.	0.	0.
	65 *	1.	1.	0.	0.	0.	0.	0.	0.	0.
	90 *	1.	0.	0.	0.	0.	0.	0.	0.	0.

210/140

S S \* TOTAL IONOSPHERIC ABSORPTION LOSS (DECIBELS)  
 O A I A \*\*\*\*\*  
 L N G N \* AVERAGE SUNSPOT NUMBER (R12) 210.  
 A G N G \* ELECTRON GYRO-FREQUENCY (MHZ) 1.820  
 R L A L \* TOTAL GEOMAGNETIC FIELD (GAUSS) 0.650  
 E L E \*\*\*\*\*

		* SIGNAL FREQUENCY (MHZ)									
(DEG)	(DEG)	2.00	3.00	4.00	6.00	8.00	12.00	16.00	24.00	32.00	
0	0	282.	210.	160.	100.	67.	36.	22.	11.	6.	
	10	201.	150.	115.	71.	48.	26.	16.	8.	5.	
	20	130.	97.	74.	46.	31.	17.	10.	5.	3.	
	30	94.	70.	54.	33.	23.	12.	7.	4.	2.	
	45	64.	51.	39.	24.	16.	9.	5.	3.	2.	
	65	54.	40.	31.	19.	13.	7.	4.	2.	1.	
20	0	49.	37.	28.	17.	12.	6.	4.	2.	1.	
	10	264.	197.	150.	94.	63.	34.	21.	10.	6.	
	10	189.	141.	108.	67.	45.	24.	15.	7.	4.	
	20	122.	91.	69.	43.	29.	16.	10.	5.	3.	
	30	89.	66.	50.	31.	21.	11.	7.	3.	2.	
	45	65.	48.	37.	23.	15.	8.	5.	2.	1.	
40	0	51.	38.	29.	18.	12.	6.	4.	2.	1.	
	10	46.	35.	26.	16.	11.	6.	4.	2.	1.	
	10	216.	161.	123.	77.	52.	28.	17.	8.	5.	
	10	155.	116.	88.	55.	37.	20.	12.	6.	4.	
	20	100.	74.	57.	35.	24.	13.	8.	4.	2.	
	30	73.	54.	41.	26.	17.	9.	6.	3.	2.	
60	0	53.	39.	30.	19.	13.	7.	4.	2.	1.	
	10	42.	31.	24.	15.	10.	5.	3.	2.	1.	
	20	38.	28.	22.	13.	9.	5.	3.	1.	1.	
	10	146.	109.	83.	52.	35.	19.	12.	6.	3.	
	10	105.	78.	59.	37.	25.	13.	8.	4.	2.	
	20	67.	50.	38.	24.	16.	9.	5.	3.	2.	
80	0	49.	37.	28.	17.	12.	6.	4.	2.	1.	
	10	36.	27.	20.	13.	9.	5.	3.	1.	1.	
	20	28.	21.	16.	10.	7.	4.	2.	1.	1.	
	30	26.	19.	15.	9.	6.	3.	2.	1.	1.	
	10	68.	51.	39.	24.	16.	9.	5.	3.	2.	
	10	48.	36.	28.	17.	12.	6.	4.	2.	1.	
100	0	31.	23.	18.	11.	7.	4.	2.	1.	1.	
	10	23.	17.	13.	8.	5.	3.	2.	1.	1.	
	20	17.	12.	9.	6.	4.	2.	1.	1.	0.	
	30	13.	10.	7.	5.	3.	2.	1.	1.	0.	
	45	12.	9.	7.	4.	3.	2.	1.	0.	0.	
	65	12.	9.	7.	4.	3.	2.	1.	0.	0.	
180	0	3.	3.	2.	1.	1.	0.	0.	0.	0.	
	10	2.	2.	1.	1.	1.	0.	0.	0.	0.	
	20	2.	1.	1.	1.	0.	0.	0.	0.	0.	
	30	1.	1.	1.	0.	0.	0.	0.	0.	0.	
	45	1.	1.	0.	0.	0.	0.	0.	0.	0.	
	65	1.	0.	0.	0.	0.	0.	0.	0.	0.	

S	S	*	TOTAL IONOSPHERIC ABSORPTION LOSS (DECIBELS)							
O A	I A	*	*****							
L N	G U	*	AVERAGE SUNSPOT NUMBER (R12) 240.							
A G	N G	*	ELECTRON CYRO-FREQUENCY (MHZ) 0.700							
R L	A L	*	TOTAL GEOMAGNETIC FIELD (GAUSS) 0.250							
F	L E	*	*****							
		*	* SIGNAL FREQUENCY (MHZ)							
(DEG)	(DEG)	*	2.00	3.00	4.00	6.00	8.00	12.00	16.00	24.00 32.00
*****										
0	0	*	421.	310.	231.	137.	88.	45.	27.	13. 7.
	10	*	301.	222.	165.	98.	63.	32.	19.	9. 5.
	20	*	194.	143.	107.	63.	41.	21.	12.	6. 3.
	30	*	141.	104.	77.	46.	30.	15.	9.	4. 2.
	45	*	103.	76.	56.	33.	22.	11.	7.	3. 2.
	65	*	81.	60.	44.	26.	17.	9.	5.	2. 1.
	90	*	74.	54.	40.	24.	15.	8.	5.	2. 1.
*****										
20	0	*	395.	291.	217.	128.	83.	42.	25.	12. 7.
	10	*	283.	209.	154.	92.	59.	30.	18.	8. 5.
	20	*	182.	134.	100.	59.	38.	19.	12.	5. 3.
	30	*	134.	98.	73.	43.	28.	14.	8.	4. 2.
	45	*	96.	71.	53.	31.	20.	10.	6.	3. 2.
	65	*	76.	56.	42.	25.	16.	8.	5.	2. 1.
	90	*	69.	51.	38.	22.	15.	7.	4.	2. 1.
*****										
40	0	*	323.	238.	177.	105.	68.	34.	20.	10. 6.
	10	*	231.	171.	127.	75.	49.	25.	15.	7. 4.
	20	*	149.	110.	82.	48.	31.	16.	9.	4. 3.
	30	*	108.	80.	59.	35.	23.	12.	7.	3. 2.
	45	*	79.	58.	43.	26.	17.	8.	5.	2. 1.
	65	*	62.	46.	34.	20.	13.	7.	4.	2. 1.
	90	*	57.	42.	31.	18.	12.	6.	4.	2. 1.
*****										
60	0	*	218.	161.	120.	71.	46.	23.	14.	7. 4.
	10	*	156.	115.	86.	51.	33.	17.	10.	5. 3.
	20	*	101.	74.	54.	34.	21.	11.	6.	3. 2.
	30	*	73.	54.	40.	24.	15.	8.	5.	2. 1.
	45	*	53.	39.	29.	17.	11.	6.	3.	2. 1.
	65	*	42.	31.	23.	14.	9.	4.	3.	1. 1.
	90	*	38.	28.	21.	12.	8.	4.	2.	1. 1.
*****										
80	0	*	101.	75.	56.	34.	21.	11.	6.	3. 2.
	10	*	72.	53.	40.	24.	15.	8.	5.	2. 1.
	20	*	47.	34.	26.	15.	10.	5.	3.	1. 1.
	30	*	34.	25.	19.	11.	7.	4.	2.	1. 1.
	45	*	25.	18.	14.	8.	5.	3.	2.	1. 0.
	65	*	19.	14.	11.	6.	4.	2.	1.	1. 0.
	90	*	18.	13.	10.	6.	4.	2.	1.	1. 0.
*****										
100	0	*	5.	4.	3.	2.	1.	1.	0.	0. 0.
70	10	*	4.	3.	2.	1.	1.	0.	0.	0. 0.
180	20	*	2.	2.	1.	1.	0.	0.	0.	0. 0.
	30	*	2.	1.	1.	1.	0.	0.	0.	0. 0.
	45	*	1.	1.	1.	0.	0.	0.	0.	0. 0.
	65	*	1.	1.	1.	0.	0.	0.	0.	0. 0.
	90	*	1.	1.	0.	0.	0.	0.	0.	0. 0.

240/070

S S \* TOTAL IONOSPHERIC ABSORPTION LOSS (DECIBELS)  
 O A I A \*  
 I N G H \* AVERAGE SUNSPOT NUMBER (R12) 240.  
 A G N G \* ELECTRON GYRO-FREQUENCY (MHZ) 1.120  
 R L A L \* TOTAL GEOMAGNETIC FIELD (GAUSS) 0.400  
 E L F \*

		* SIGNAL FREQUENCY (MHZ)									
(DFG)	(DEG)	*	2.00	3.00	4.00	6.00	8.00	12.00	16.00	24.00	32.00
*****											
0	0	*	370.	273.	205.	124.	81.	42.	25.	12.	7.
	10	*	265.	196.	147.	89.	58.	30.	18.	9.	5.
	20	*	171.	126.	95.	57.	38.	19.	12.	6.	3.
	30	*	124.	92.	69.	42.	27.	14.	9.	4.	2.
	45	*	90.	67.	50.	30.	20.	10.	6.	3.	2.
	65	*	71.	53.	40.	24.	16.	8.	5.	2.	1.
20	0	*	348.	257.	193.	116.	76.	39.	24.	11.	7.
	10	*	249.	184.	138.	83.	55.	28.	17.	8.	5.
	20	*	161.	119.	89.	54.	35.	18.	11.	5.	3.
	30	*	117.	86.	65.	39.	26.	13.	8.	4.	2.
	45	*	85.	63.	47.	28.	19.	10.	6.	3.	2.
	65	*	67.	49.	37.	22.	15.	8.	5.	2.	1.
40	0	*	314.	237.	183.	110.	72.	37.	23.	10.	6.
	10	*	224.	171.	130.	80.	52.	27.	16.	8.	5.
	20	*	151.	114.	87.	53.	34.	18.	11.	5.	3.
	30	*	112.	85.	64.	38.	25.	13.	8.	4.	2.
	45	*	84.	62.	46.	27.	18.	10.	6.	3.	2.
	65	*	66.	48.	36.	21.	14.	7.	5.	2.	1.
60	0	*	285.	210.	165.	100.	66.	34.	21.	9.	5.
	10	*	204.	150.	113.	68.	45.	23.	14.	7.	4.
	20	*	131.	97.	73.	44.	29.	15.	9.	4.	3.
	30	*	95.	70.	53.	32.	21.	11.	7.	3.	2.
	45	*	69.	51.	38.	23.	15.	8.	5.	2.	1.
	65	*	55.	40.	30.	18.	12.	6.	4.	2.	1.
80	0	*	255.	190.	145.	88.	58.	30.	18.	9.	5.
	10	*	184.	138.	104.	64.	42.	22.	13.	6.	4.
	20	*	126.	95.	71.	44.	29.	15.	9.	4.	3.
	30	*	92.	69.	51.	32.	21.	11.	7.	3.	2.
	45	*	67.	50.	38.	23.	15.	8.	5.	2.	1.
	65	*	53.	40.	30.	18.	12.	6.	4.	2.	1.
100	0	*	224.	171.	130.	79.	52.	27.	16.	8.	5.
	10	*	161.	119.	89.	54.	35.	18.	11.	5.	3.
	20	*	117.	86.	65.	39.	26.	13.	8.	4.	2.
	30	*	86.	63.	47.	28.	19.	10.	6.	3.	2.
	45	*	63.	47.	35.	22.	14.	7.	5.	2.	1.
	65	*	50.	37.	28.	17.	11.	6.	3.	2.	1.
120	0	*	193.	145.	107.	66.	42.	22.	13.	6.	4.
	10	*	138.	102.	76.	46.	30.	16.	9.	5.	3.
	20	*	89.	65.	49.	30.	19.	10.	6.	3.	2.
	30	*	64.	48.	36.	22.	14.	7.	4.	2.	1.
	45	*	47.	35.	26.	16.	10.	5.	3.	2.	1.
	65	*	37.	27.	21.	12.	8.	4.	3.	1.	1.
140	0	*	161.	126.	95.	57.	38.	19.	12.	6.	3.
	10	*	124.	92.	69.	42.	27.	14.	9.	4.	2.
	20	*	90.	67.	50.	30.	20.	10.	6.	3.	2.
	30	*	67.	49.	37.	22.	15.	8.	5.	2.	1.
	45	*	50.	37.	28.	17.	11.	6.	3.	2.	1.
	65	*	37.	27.	21.	12.	8.	4.	3.	1.	1.
160	0	*	124.	92.	69.	42.	27.	14.	9.	4.	2.
	10	*	90.	67.	50.	30.	20.	10.	6.	3.	2.
	20	*	67.	49.	37.	22.	15.	8.	5.	2.	1.
	30	*	50.	37.	28.	17.	11.	6.	3.	2.	1.
	45	*	37.	27.	21.	12.	8.	4.	3.	1.	1.
	65	*	27.	21.	15.	9.	5.	3.	1.	1.	0.
180	0	*	90.	67.	50.	30.	20.	10.	6.	3.	2.
	10	*	64.	47.	35.	21.	14.	7.	4.	2.	1.
	20	*	41.	30.	23.	14.	9.	5.	3.	1.	1.
	30	*	30.	22.	17.	10.	7.	3.	2.	1.	1.
	45	*	22.	16.	12.	7.	5.	2.	1.	1.	0.
	65	*	17.	13.	10.	6.	4.	2.	1.	1.	0.
200	0	*	67.	49.	37.	22.	15.	8.	5.	2.	1.
	10	*	50.	37.	28.	17.	11.	6.	3.	2.	1.
	20	*	37.	27.	21.	12.	8.	4.	3.	1.	1.
	30	*	27.	21.	15.	9.	5.	3.	1.	1.	0.
	45	*	21.	15.	11.	7.	4.	2.	1.	1.	0.
	65	*	16.	12.	9.	5.	3.	2.	1.	1.	0.
220	0	*	42.	30.	23.	14.	9.	5.	3.	1.	1.
	10	*	30.	22.	17.	10.	7.	3.	2.	1.	1.
	20	*	22.	16.	12.	7.	5.	2.	1.	1.	0.
	30	*	16.	12.	9.	5.	3.	2.	1.	1.	0.
	45	*	12.	9.	6.	4.	2.	1.	1.	0.	0.
	65	*	9.	6.	4.	2.	1.	1.	0.	0.	0.
240	0	*	27.	21.	15.	9.	5.	3.	1.	1.	0.
	10	*	21.	15.	11.	7.	4.	2.	1.	1.	0.
	20	*	15.	11.	8.	5.	3.	1.	1.	0.	0.
	30	*	11.	8.	6.	4.	2.	1.	1.	0.	0.
	45	*	8.	6.	4.	2.	1.	1.	0.	0.	0.
	65	*	6.	4.	2.	1.	1.	0.	0.	0.	0.

S S \* TOTAL IONOSPHERIC ABSORPTION LOSS (DECIBELS)  
 O A I A \*  
 I N G M \* AVERAGE SUNSPOT NUMBER (R12) 240.  
 A G N G \* ELECTRON GYRO-FREQUENCY (MHZ) 1.400  
 R L A L \* TOTAL GEOMAGNETIC FIELD (GAUSS) 0.500  
 E L E \*

		* SIGNAL FREQUENCY (MHZ)								
(DEG)	(DEG)	* 2.00	3.00	4.00	6.00	8.00	12.00	16.00	24.00	32.00
0	0	* 340.	252.	190.	116.	77.	40.	25.	12.	7.
	10	* 243.	180.	136.	83.	55.	29.	18.	8.	5.
	20	* 157.	116.	88.	54.	36.	19.	11.	5.	3.
	30	* 114.	84.	64.	39.	26.	14.	8.	4.	2.
	45	* 83.	61.	46.	28.	19.	10.	6.	3.	2.
	65	* 65.	48.	37.	23.	15.	8.	5.	2.	1.
20	0	* 340.	252.	190.	116.	77.	40.	25.	12.	7.
	10	* 243.	180.	136.	83.	55.	29.	18.	8.	5.
	20	* 157.	116.	88.	54.	36.	19.	11.	5.	3.
	30	* 114.	84.	64.	39.	26.	14.	8.	4.	2.
	45	* 83.	61.	46.	28.	19.	10.	6.	3.	2.
	65	* 65.	48.	37.	23.	15.	8.	5.	2.	1.
40	0	* 314.	237.	179.	109.	72.	38.	23.	11.	7.
	10	* 228.	169.	128.	78.	52.	27.	17.	8.	5.
	20	* 147.	109.	82.	50.	34.	18.	11.	5.	3.
	30	* 107.	79.	60.	37.	24.	13.	8.	4.	2.
	45	* 78.	58.	44.	27.	18.	9.	6.	3.	2.
	65	* 61.	46.	34.	21.	14.	7.	4.	2.	1.
60	0	* 261.	194.	146.	89.	59.	31.	19.	9.	5.
	10	* 187.	138.	105.	64.	42.	22.	14.	7.	4.
	20	* 121.	89.	67.	41.	27.	14.	9.	4.	2.
	30	* 88.	65.	49.	30.	20.	10.	6.	3.	2.
	45	* 64.	47.	36.	22.	14.	8.	5.	2.	1.
	65	* 50.	37.	28.	17.	11.	6.	4.	2.	1.
80	0	* 176.	131.	99.	60.	40.	21.	13.	6.	4.
	10	* 126.	93.	71.	43.	29.	15.	9.	4.	3.
	20	* 81.	60.	46.	28.	18.	10.	6.	3.	2.
	30	* 59.	44.	33.	20.	13.	7.	4.	2.	1.
	45	* 43.	32.	24.	15.	10.	5.	3.	2.	1.
	65	* 34.	25.	19.	12.	8.	4.	2.	1.	1.
100	0	* 14.	11.	8.	5.	3.	2.	1.	1.	0.
	10	* 82.	61.	46.	28.	19.	10.	6.	3.	2.
	20	* 58.	43.	33.	20.	13.	7.	4.	2.	1.
	30	* 38.	28.	21.	13.	9.	4.	3.	1.	1.
	45	* 27.	20.	15.	9.	6.	3.	2.	1.	1.
	65	* 20.	15.	11.	7.	5.	2.	1.	1.	0.
180	0	* 4.	3.	2.	1.	1.	0.	0.	0.	0.
	10	* 3.	2.	2.	1.	1.	0.	0.	0.	0.
	20	* 2.	1.	1.	1.	0.	0.	0.	0.	0.
	30	* 1.	1.	1.	0.	0.	0.	0.	0.	0.
	45	* 1.	1.	1.	0.	0.	0.	0.	0.	0.
	65	* 1.	1.	0.	0.	0.	0.	0.	0.	0.

240/140

240



S S *		TOTAL IONOSPHERIC ABSORPTION LOSS (DECIBELS)									
O A I A *		*****									
I N G N *		AVERAGE SUNSPOT NUMBER (R12) 240.									
A G N G *		ELECTRON GYRO-FREQUENCY (MHZ) 1.820									
R L A L *		TOTAL GEOMAGNETIC FIELD (GAUSS) 0.650									
F L E *		*****									
		* SIGNAL FREQUENCY (MHZ)									
(DEG)	(DEG)	*	2.00	3.00	4.00	6.00	8.00	12.00	16.00	24.00	32.00
*****											
0	0	*	299.	223.	170.	106.	71.	38.	24.	11.	7.
	10	*	214.	160.	122.	76.	51.	27.	17.	8.	5.
	20	*	138.	103.	79.	49.	33.	18.	11.	5.	3.
	30	*	100.	75.	57.	36.	24.	13.	8.	4.	2.
	45	*	73.	54.	42.	26.	17.	9.	6.	3.	2.
	65	*	58.	43.	33.	20.	14.	7.	5.	2.	1.
90	*	52.	39.	30.	19.	12.	7.	4.	2.	1.	
*****											
20	0	*	281.	210.	160.	100.	67.	36.	22.	11.	6.
	10	*	201.	150.	114.	71.	48.	26.	16.	8.	5.
	20	*	130.	97.	74.	46.	31.	17.	10.	5.	3.
	30	*	94.	70.	54.	33.	22.	12.	7.	4.	2.
	45	*	69.	51.	39.	24.	16.	9.	5.	3.	2.
	65	*	54.	40.	31.	19.	13.	7.	4.	2.	1.
90	*	49.	37.	28.	17.	12.	6.	4.	2.	1.	
*****											
40	0	*	230.	172.	131.	81.	55.	29.	18.	9.	5.
	10	*	165.	123.	94.	58.	39.	21.	13.	6.	4.
	20	*	106.	79.	60.	38.	25.	14.	8.	4.	2.
	30	*	77.	57.	44.	27.	18.	10.	6.	3.	2.
	45	*	56.	42.	32.	20.	13.	7.	4.	2.	1.
	65	*	44.	33.	25.	16.	11.	6.	3.	2.	1.
90	*	40.	30.	23.	14.	10.	5.	3.	2.	1.	
*****											
60	0	*	155.	116.	88.	55.	37.	20.	12.	6.	4.
	10	*	111.	83.	63.	39.	26.	14.	9.	4.	3.
	20	*	72.	53.	41.	25.	17.	9.	6.	3.	2.
	30	*	52.	39.	30.	18.	12.	7.	4.	2.	1.
	45	*	38.	28.	22.	13.	9.	5.	3.	1.	1.
	65	*	30.	22.	17.	11.	7.	4.	2.	1.	1.
90	*	27.	20.	15.	10.	6.	3.	2.	1.	1.	
*****											
80	0	*	72.	54.	41.	25.	17.	9.	6.	3.	2.
	10	*	51.	38.	29.	18.	12.	7.	4.	2.	1.
	20	*	33.	25.	19.	12.	8.	4.	3.	1.	1.
	30	*	24.	18.	14.	9.	6.	3.	2.	1.	1.
	45	*	18.	13.	10.	6.	4.	2.	1.	1.	0.
	65	*	14.	10.	8.	5.	3.	2.	1.	1.	0.
90	*	13.	9.	7.	4.	3.	2.	1.	0.	0.	
*****											
100	0	*	4.	3.	2.	1.	1.	0.	0.	0.	0.
	10	*	3.	2.	1.	1.	1.	0.	0.	0.	0.
	20	*	2.	1.	1.	1.	0.	0.	0.	0.	0.
	30	*	1.	1.	1.	0.	0.	0.	0.	0.	0.
	45	*	1.	1.	0.	0.	0.	0.	0.	0.	0.
	65	*	1.	1.	0.	0.	0.	0.	0.	0.	0.
90	*	1.	0.	0.	0.	0.	0.	0.	0.	0.	
*****											
180	0	*	4.	3.	2.	1.	1.	0.	0.	0.	0.
	10	*	3.	2.	1.	1.	1.	0.	0.	0.	0.
	20	*	2.	1.	1.	1.	0.	0.	0.	0.	0.
	30	*	1.	1.	1.	0.	0.	0.	0.	0.	0.
	45	*	1.	1.	0.	0.	0.	0.	0.	0.	0.
	65	*	1.	1.	0.	0.	0.	0.	0.	0.	0.
90	*	1.	0.	0.	0.	0.	0.	0.	0.	0.	

240/182

## 2.6 REFERENCES FOR SKY WAVE MECHANISMS

1. Radio Ray Propagation in the Ionosphere  
John M. Kelso  
McGraw-Hill, New York, 1964
2. Radio Waves in the Ionosphere  
K. G. Budden  
Cambridge, University Press, 1961
3. The Magneto-Ionic Theory and Its Applications to the Ionosphere  
J. A. Ratcliffe  
Cambridge, University Press, 1959
4. Ionospheric Radio Waves  
Kenneth Davies  
Blaisdell, Waltham, Massachusetts, 1969
5. Principles of Optics, 3rd Edition  
M. Born and E. Wolf  
Pergamon Press, 1965
6. Sun, Earth and Radio  
J. A. Ratcliffe  
World University Library Series (Paperback)  
McGraw-Hill, 1970  

This is a broad-brush treatment of the material by one of the acknowledged masters of the subject. Though the presentation is non-mathematical, the insight and experience of the author allow a treatment which is highly lucid and far from superficial.
7. Physics of the Upper Atmosphere  
J. A. Ratcliffe (Ed.)  
Academic Press, New York, 1960

8. Physics of the Earth's Upper Atmosphere  
C. O. Hines, I. Paghis, T. R. Hartz, and J. A. Fejer (Eds.)  
Prentice-Hall, Englewood Cliffs, NJ, 1965
9. C.C.I.R. Atlas of Ionospheric Characteristics  
Report 340-1, Geneva, 1967/1971  
C.C.I.R. of the  
International Telecommunications Union  
Geneva, Switzerland, 1967/1971
10. Ionospheric Radio Propagation  
Kenneth Davis  
Monograph 80, 1 April 1965  
National Bureau of Standards, U.S. Department of Commerce  
U.S. Government Printing Office, Washington, DC, 1965  
  
This monograph is a progenitor of Reference 4. Reference 4 provides a better theoretical treatment of propagation mechanics, but this reference is of value for the synoptic data on geophysical phenomena which it contains.
11. C.C.I.R. Interim Method for Estimating Sky-Wave Field Strength and Transmission Loss at Frequencies Between the Approximate Limits of 2 and 30 MHz  
Report 252-2, New Delhi, 1970  
C.C.I.R. of the  
International Telecommunications Union  
Geneva, Switzerland, 1970
12. "International Geomagnetic Reference Field 1975," Transactions American Geophysical Union, Vol. 57, No. 3, March 1976, pp. 120-121.

The specific references cited above, especially [1-4, 6-8] offer ample and excellent bibliographical resources. Through them, access to the source literature in the field can be gained.

### 3.0 THE GROUND WAVE

In this chapter the properties of the ground wave as a signal delivery mechanism will be developed and displayed. The objective, as in the case of the sky wave, is to elucidate principles by which the transmission loss associated with this mode of signal delivery can be estimated.

To serve as an intermediate stage in the estimation of transmission loss, the concept of propagation loss is introduced. The working definition of propagation loss used in this chapter (Section 3.3) differs from, but is equivalent to, the formal definition given in Chapter 1.0 (Section 1.2). Forewarned, the reader should experience no real difficulty in reconciling the two.

There is included at the end of the chapter an atlas of propagation loss data for the ground wave. It is specialized for parameter values expected in a marine environment.

PRECEDING PAGE BLANK-NOT FILMED

### 3.1 DEFINITION OF GROUND WAVE

The term "ground wave" denotes an electromagnetic wave propagated in the close neighborhood of the surface of the earth. It is assumed to originate from a source also in the immediate vicinity of the surface of the earth. The configuration of the wave is intimately related to the physical properties of the earth and of the lower atmosphere, as well as to the character and geometrical disposition of the source of the wave.

One way to approach the problem of defining the ground wave is to specify mechanisms excluded from its propagation--definition by exception. Not included are the normal, or anomalous, geometrical optical mechanisms involving the ionosphere as a medium. Also excluded are the iono-scatter and tropo-scatter mechanisms of propagation which depend on turbulence of the medium.\* The ground wave, then, is that electromagnetic wave originating at a source in the immediate vicinity\*\* of the surface of the earth, and propagated in the close neighborhood of the surface of the earth under control of mechanisms involving the physical and geometrical properties of the earth and of the non-turbulent lower atmosphere.

It is not intended to imply by this definition that the wave therein denoted does not extend to regions remote from the surface of the earth. Clearly it may. However, the character of the wave tends to lose its dependence on the details of interaction with the earth and lower atmosphere by the time it has reached more remote regions. Behavior of the wave becomes much simplified in the remote regions. Thus, confining the "ground wave" to a region in the close neighborhood of the surface of the earth more nearly reflects a restriction of attention to that region than it does a physical confinement of the wave thereto.

---

\*These mechanisms have been largely ignored in this treatment. While they have legitimate areas of application, they are not of significant value for jamming in the HF range of frequencies. Their transmission loss in that frequency range is too high for them to merit consideration in other than very exceptional circumstances. They form a category of mechanisms best treated separately from both the sky wave and the ground wave categories.

\*\*Terms like "close neighborhood" and "immediate vicinity" clearly impose no precisely quantitative boundary to the region in question and, indeed, there is no intent to do so. They really mean "close enough that the presence of the earth is a significant factor." Generally this condition will be true for path terminal heights in the range less than 10 kilometers, unless the two terminals are too close together.

Description of the ground wave, though straightforward in concept, is very complex in its full detail. Because of the complexity, it is common practice to attempt to break the most general case down into a set of sub-cases, in each member of which one propagation mechanism or another is dominant. The ground wave is then thought of as an aggregation\* of sub-waves, each of which is described in terms of one of the mechanisms.

The approach leaves some nagging doubts in the mind because the component waves may not, strictly speaking, separately satisfy Maxwell's equations and the physical boundary conditions. Thus, they are in some sense mathematical fictions. The individual mechanisms may represent dependent pieces of a total solution, or alternative representations of a partial or total solution. A single mechanism can stand alone only by virtue of a set of circumstances which causes it to dominate. This situation is in contrast to, say, modes in a waveguide in which case the modes are separately complete solutions, which may or may not co-exist. Nevertheless, the approach does lead to computational techniques which are reasonably tractable, which correctly exhibit most of the observed phenomena and which afford accuracy adequate for most purposes.

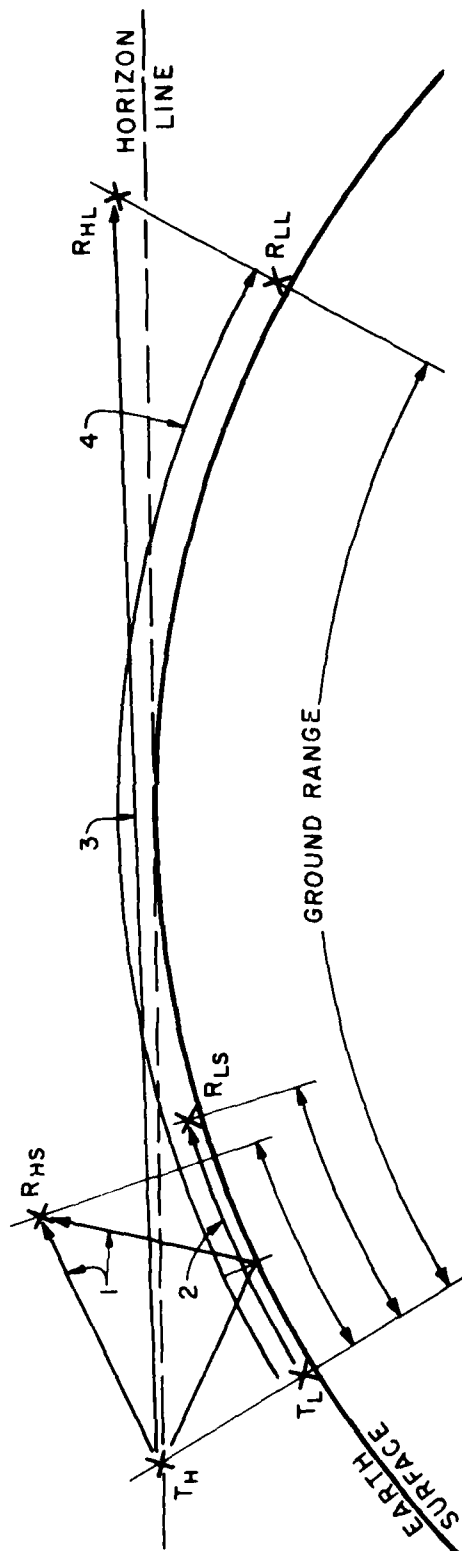
The ground wave propagation mechanisms fall easily into two categories: a) those which can be described in terms of the principles of geometrical optics, and b) those which require description in terms of physical optics or full wave principles. In Figure 3-1, these mechanisms are illustrated in terms of four regimes which are differentiated by the locations of the path terminals relative to each other and relative to the surface of the earth.

The regime numbered "1" in the figure comprises two ray paths,\*\* a "direct" ray and a "ground reflected" ray. It is differentiated by the fact

---

\*But not necessarily a simple sum.

\*\*The terms "ray path" and "wave path"--or, in some cases, just "path"--are used to denote a route between path terminals. The meaning of "ray path" (or just "ray") should be fairly clear. It is, simply, the ray trajectory of geometrical optics. The meaning of "wave path" may be less evident because it is used when geometrical optical principles fail. It is defined to be the geodesic curve connecting path terminals. The time of transit of a signal between terminals is related to the length of the "wave path." Additional significance can be attached to it with the aid of the discipline called "geometrical theory of diffraction." In this discussion "wave path" is used simply to designate a route that cannot be called a ray.



$T_H$  - TRANSMITTER: HIGH  
 $T_L$  - TRANSMITTER: LOW  
 $R_{HS}$  - RECEIVER: HIGH, SHORT RANGE  
 $R_{LS}$  - RECEIVER: LOW, SHORT RANGE  
 $R_{HL}$  - RECEIVER: HIGH, LONG RANGE  
 $R_{LL}$  - RECEIVER: LOW, LONG RANGE

Figure 3-1. The four regimes (wave paths numbered 1-4) by which propagation mechanisms are differentiated.

that the path terminal points are "high"\* above the earth and "close" to each other. The point is that the path terminals are well within sight of each other along the direct ray path and that the direct ray path does not come too close to, or "graze," the surface of the earth. In calling the two routes "ray paths" the implication is clearly that geometrical optical principles are applicable to the description of propagation under this regime. In fact, this regime comprises the geometrical optical category.

The regime numbered "2" is differentiated by the fact that the path terminals are "low,"\*\* but not too "distant" from each other. This regime is associated with a plane earth surface wave mechanism. It falls into the physical optical, or full wave, category, but does admit the simplifications attendant on the plane earth approximation.

The regime numbered "3" in Figure 3-1 is an elaboration of the first. It differs from the first in the fact that the wave path lies so close to the horizon line that ray principles begin to fail and diffraction effects are important. This regime also belongs to the physical optical, or full wave, category.

The regime numbered "4" is an elaboration of the second, differing from the latter in the fact that the distance between path terminals is too great to neglect the spherical shape of the surface of the earth. It too falls in the physical optical, or full wave, category.

Note that each of the four regimes is characterized by some sort of simplifying or limiting situation in the disposition of the path terminals. Each of the regimes requires a different method of calculation, appropriate to the particular kind of simplicity or limit involved. It is evident that the boundaries separating the regimes are not sharp and distinct. Their location is a matter of degree. The locations are, moreover, dependent on the values of the variables (to be discussed shortly) specifying physical (or geophysical) properties of the earth and atmosphere. The category into which a given situation falls is determined by tests on the distinguishing variables. To a degree, the boundaries established by the tests are arbitrary, but they have been set to avoid the occurrence of excessive error in application of any of the calculation methods. An appropriate set of categorizing parameter tests is, then, an essential element of the computer program by means of which loss data are calculated.

---

\* "High" and "low," "close" and "distant" are here indefinite measures which, when expressed quantitatively, ought to be stated in wavelength units.

\*\* Not necessarily at the surface of the earth.



### 3.2 VARIABLE QUANTITIES

Like the sky wave, the ground wave is a function of a goodly number of variables. These variables classify neatly into three categories:

1. Variables specifying geophysical\* properties along the wave path.
2. Variables specifying disposition of the path terminals.
3. Variables specifying essential properties of the source of the electromagnetic wave.

The members of each category will be enumerated and discussed in turn.

#### 3.2.1 Geophysical Property Variables

In Figure 3-2 the surface of the earth is shown as the boundary between two media, "earth" and "atmosphere," in which an electromagnetic wave may propagate. Consider the earth medium first. As suggested in the figure, the properties of the earth can be characterized by two quantities, the permittivity,  $\epsilon$ , and the conductivity,  $\sigma$ .

For frequencies within the HF range, the permittivity of earth materials, as a function of material type, varies over a range from about 5 to about 81. For sea water, the value of  $\epsilon$  is confined to the top few units

---

\*The term "geophysical" here connotes the "physical" properties--specifically, the electrical properties--of earth and atmosphere constituents.

\*\*Throughout this chapter use of the symbol  $\epsilon$  differs, in part, from the practice followed in Chapter 2.0. In the MKSA rationalized system of units, the permittivity of a medium,  $\epsilon_m$ , is composed of two factors, the absolute permittivity of free space,  $\epsilon_0$  ( $8.8542 \times 10^{-12}$  farads/meter), and the relative permittivity of the medium,  $\epsilon$  (a variable dimensionless numeric). Thus,  $\epsilon_m = \epsilon \epsilon_0$ . As a matter of convenience in discussion, the factor  $\epsilon_0 = 8.8542 \times 10^{-12}$  farads/meter will be dropped. The term "permittivity" and the symbol " $\epsilon$ " (as well as quantitative values associated with them) henceforth will be construed to signify (and evaluate) the "relative permittivity," a dimensionless numeric.

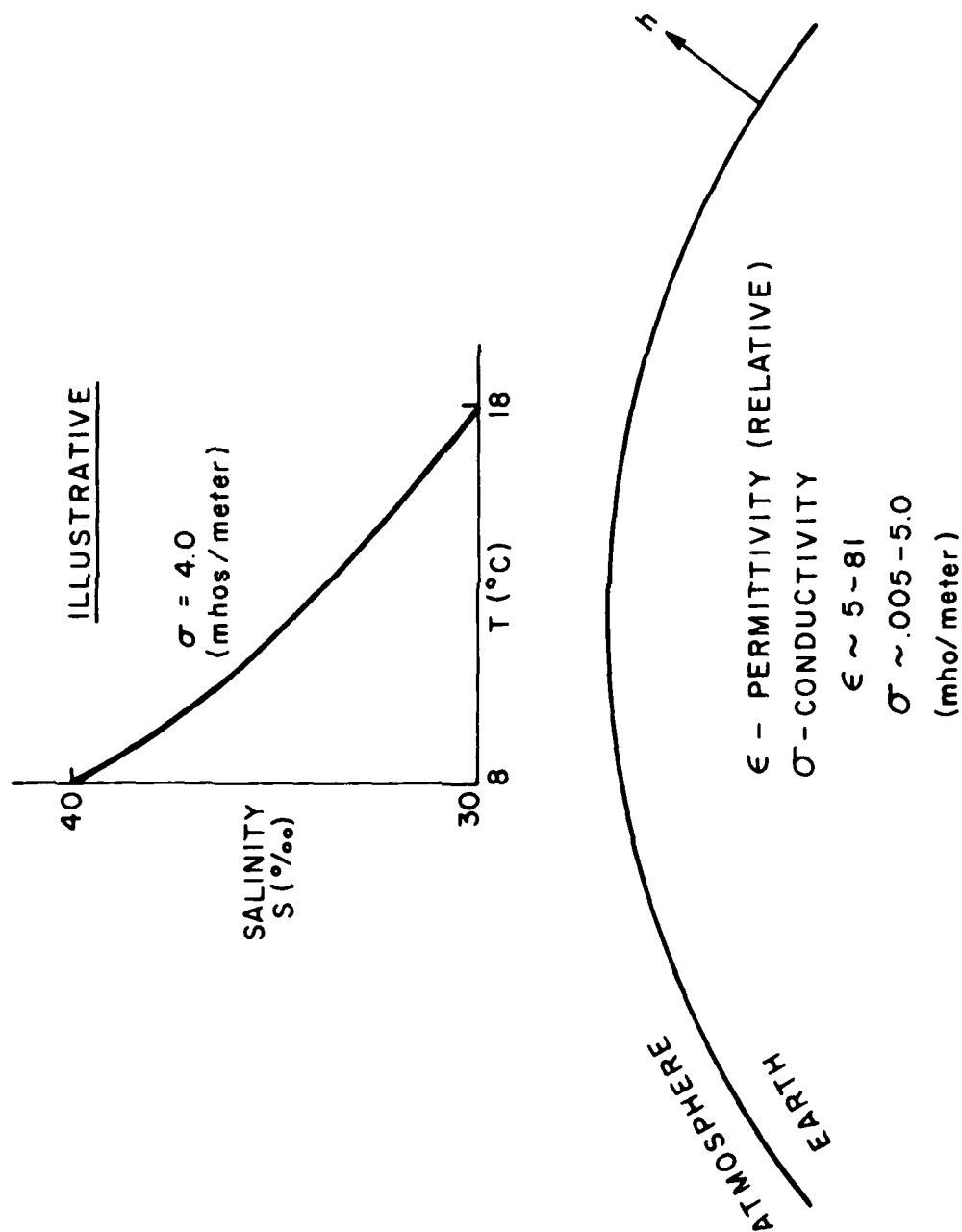


Figure 3-2. Geophysical factors related to the earth ( $\epsilon$  and  $\sigma$ ) which affect ground wave propagation.

of this (relative) permittivity range. Within the HF range,\* the variation of  $\epsilon$  with frequency is small and, for our purpose, may be neglected. Variations with temperature and salinity also are small and may be neglected. In this document the value 80.0 will be used for the permittivity,  $\epsilon$ , of sea water.

The conductivity of earth materials, as a function of material type, varies over a range from about 0.005 mho/meter to about 5.0 mhos/meter. For "solid" materials, at the low end of the range, the most important single factor in the variation of conductivity is moisture content. For water, salinity is the important factor. The conductivity of "fresh" water is of the order of 0.001 mho/meter; that of sea water lies at the top of the range. For sea water, conductivity is a function of temperature, T ( $^{\circ}$ Celsius), and of salinity, S ( $^{\circ}$ /oo),\*\* as illustrated at the top of Figure 3-2.

Information about the geographical and temporal variation of surface temperature of the ocean areas of the world is given in considerable detail in one of the references [1]. Examination of the charts in this reference leads to the conclusion that  $-2^{\circ}$  C to  $+30^{\circ}$  C is an adequate range for the surface temperature of sea water for our purpose.

Information about surface salinity can be found in another of the references [2]. For this variable, the data are rather more limited than for temperature. From the data provided in the reference, a range is derived for surface salinity that extends from 30  $^{\circ}$ /oo to 40  $^{\circ}$ /oo.

Note that it is the surface values of T and S--within the first few meters--which count, rather than the values at great depth. The reason is that sea water is such a good conductor at frequencies in the HF range that the wave penetrates only a short distance (depending on the frequency) below the surface.

In a third reference [3] tables are presented giving conductivity as a function of temperature and salinity. Within the ranges for T and S derived above, data in those tables can be represented by the formula

$$\begin{aligned} \sigma = & [ 4.58 + 0.1164 (S-35) ] \\ & + [ 0.10 + 0.0025 (S-35) ] (T-18) \\ & + [ 0.00035 + 0.000011 (S-35) ] (T-18)^2 \end{aligned} \quad 3-1a$$

\*Above 1 or 2 GHz, the value of  $\epsilon$  for sea water begins to diminish significantly as the frequency increases.

\*\*The symbol " $^{\circ}$ /oo" denotes "parts per thousand."

or,

$$\begin{aligned}\sigma = & [0.265 + 0.0750 S] \\ & + [0.01376 + 0.002104 S] T \\ & + [-0.000035 + 0.000011 S] T^2\end{aligned}\tag{3-1b}$$

where T is in degrees Celsius (centigrade) and S is in parts per thousand (‰). Based on this formula, a chart of conductivity contours on a (T, S) grid has been prepared and is presented in Figure 3-3.

When the distribution of sea surface temperature and salinity are correlated, it appears that values of conductivity,  $\sigma$ , between 3.0 and 5.0 mhos/meter will cover most of the situations of interest.

As a sidelight, it is interesting to note that the most common method for determining salinity is to measure conductivity and compute salinity, compensating for temperature.

In Figure 3-4, as in Figure 3-2, the surface of the earth is shown as an inter-medium boundary. In Figure 3-4, in contrast to Figure 3-2, attention is focused on the atmosphere as a medium. Again, two variables are used to characterize the relevant properties of the medium. They are derived from the refractive index,  $n$  (a dimensionless numeric), of the atmosphere. The refractive index of the atmosphere differs only a little from unity. However, it is the difference which counts. Thus, it is convenient to subtract unity from the refractive index and multiply the (positive) remainder by  $10^6$  to scale it to a convenient numerical range. This modification gives the refractivity,  $N$ .

The quantities  $n$  and  $N$  are functions of the height,  $h$  (meters), \* above the surface of the earth. The symbol  $N_s$  signifies the value of  $N$  at the surface of the earth (not necessarily sea level). The symbol  $N_0$  signifies the value of  $N$  at sea level, or the value of  $N_s$  "reduced to sea level" by an appropriate rule. Since this discussion is concerned with propagation over sea water, the relevant values of  $N_0$  and  $N_s$  are equal. The surface refractivity ( $N_s = N_0$ ) is the first of the variables to be used for specifying properties of the atmosphere.

The second atmospheric property variable is the average gradient of refractivity measured over the first kilometer of height,  $\Delta N/\Delta h$  ( $\Delta h = 1$  km). At the bottom of Figure 3-4 the relation between  $n$  and  $N$ , a possible mode of variation with height and the significance of  $\Delta N/\Delta h$  are illustrated. In this example  $N_s = N_0 = 350$ ,  $\Delta N/\Delta h = -50$  and the decrease of  $N$  with height is exponential (similar to that of a "standard atmosphere"). In an actual atmosphere the shape of the  $N(h)$  curve near the bottom ( $h = 0$ ) can differ significantly from that shown in the illustration.

---

\*In some places kilometers, where noted.

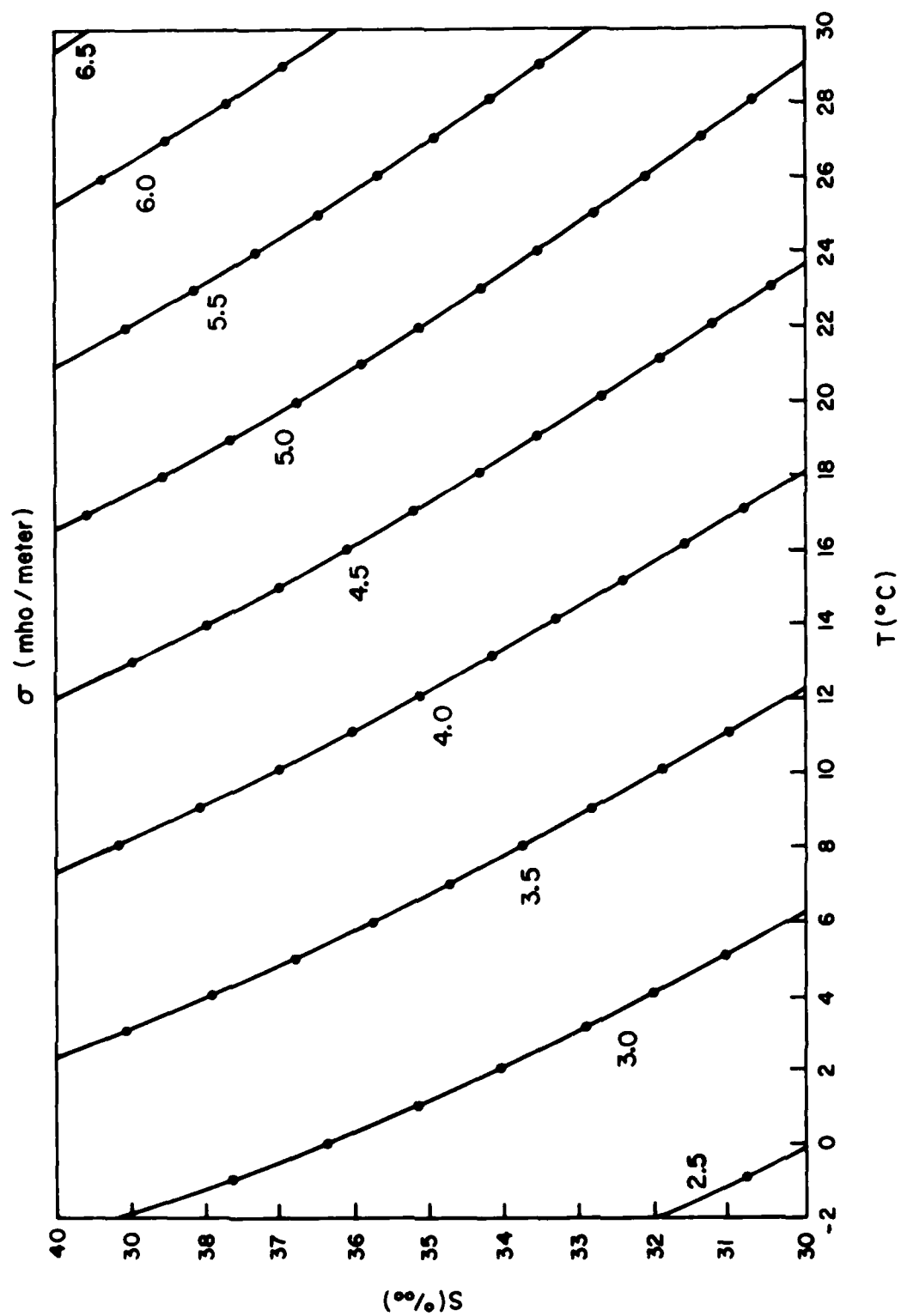


Figure 3-3. Conductivity ( $\sigma$ ) contour chart for sea water as a function of temperature ( $T$ ) and salinity ( $S$ ).

$$n \sim 1.000350$$

$$N = (n - 1) \times 10^6$$

$$N_0 = N_s = \text{SURFACE REFRACTIVITY (280-400)}$$

$$\frac{\Delta N}{\Delta h} = \text{REFRACTIVITY GRADIENT (-35 TO -70)}$$

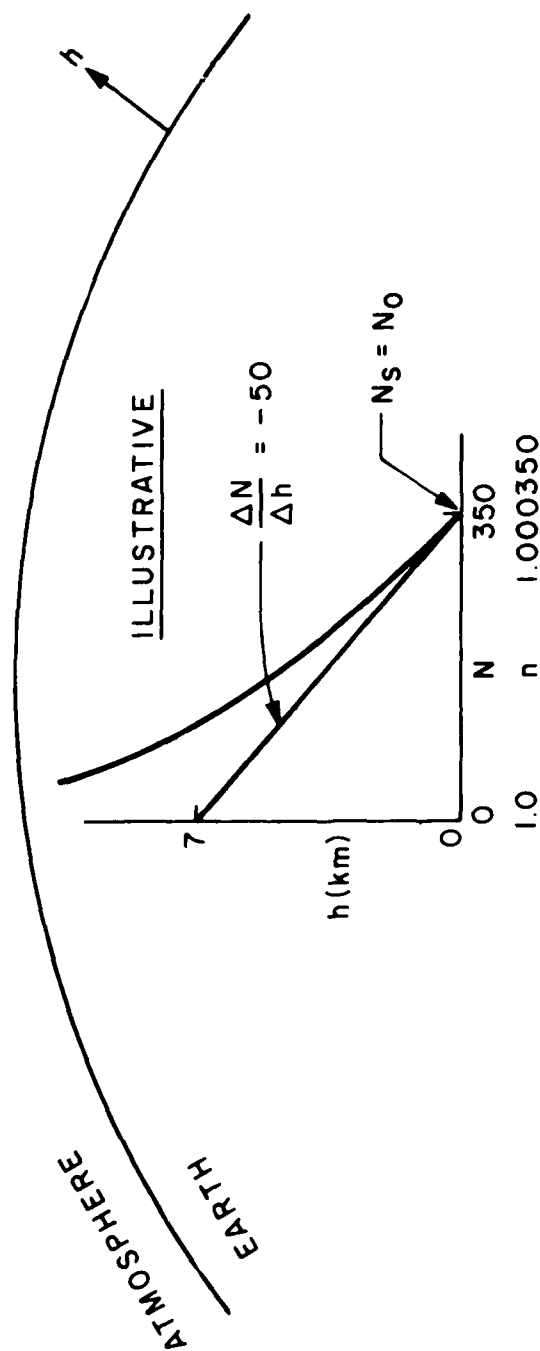


Figure 3-4. Geophysical factors related to the lower atmosphere ( $N_0$ ,  $N_s$  and  $\Delta N/\Delta h$ ) which affect ground wave propagation.

In a pragmatic sense it turns out that the variables  $N_s$  and  $\Delta N/\Delta h$  are not entirely independent. From empirical studies of the climatology of refractivity, a relationship between them has been found that can be represented by a rather simple functional statement [ 4, 5]. \*

$$\overline{\Delta N}/\Delta h = -7.32 \exp (0.005577 \overline{N}_s)$$

3-2

$$(\Delta h = 1 \text{ km})$$

The "bar" over  $\Delta N$  and  $N_s$  in the above expression signifies that these values are means--specifically, monthly means averaged over six to eight years from 45 locations. With this statement, an estimate of  $\overline{\Delta N}/\Delta h$  can be made, given the value of  $\overline{N}_s$ . Several such pairs of values are listed in the first two columns of Table 3-1.

\*The geographical range of validity of this expression seems not to be firmly established. The relationship appears to vary somewhat with climate. The expression given above (Equation 3-2) represents data acquired in the continental United States. Though the form of the expression appears to be satisfactory for several geographic regions from which data are available, the values of the constants obtained for other regions differ from those for the United States. For example:

- a. In Germany, the following expression has been found [ 10 ].

$$\overline{\Delta N}/\Delta h = -9.30 \exp (0.004565 \overline{N}_s)$$

$$(\Delta h = 1 \text{ km})$$

- b. For data acquired in the British Isles [ 11 ], the following is a possible representation.

$$\overline{\Delta N}/\Delta h = -3.65 \exp (0.0074 \overline{N}_s)$$

$$(320 \leq \overline{N}_s \leq 350, \Delta h = 1 \text{ km})$$

For values of  $\overline{N}_s$  between 300 and 400, the divergence among the values of  $\overline{\Delta N}/\Delta h$  yielded by the three expressions is not catastrophically great, as can be seen by plotting the three on a semi-log grid. Begging the availability of data from a more widespread selection of regions, and considering the day-to-day variability in any region (remember; the above expressions involve monthly means of  $N_s$  and  $\Delta N/\Delta h$ ), it seems not unreasonable to use the expression given in the text. It is, of course, possible to use currently measured values of  $\Delta N/\Delta h$  when appropriate data are available.

A need is indicated for additional research on the correlation of  $\Delta N/\Delta h$  and  $N_s$ , especially for the maritime regions.

Table 3-1. Relationship between  $N_s$  and  $\alpha$ .

$\bar{N}_s$	$\Delta\bar{N}/\Delta h$	$dn/dh$	$\alpha$	Comment
240	-27.91	$-27.91 \times 10^{-9}$	1.216	
260	-31.21	$-31.21 \times 10^{-9}$	1.248	
280	-34.89	$-34.89 \times 10^{-9}$	1.286	
300	-39.01	$-39.01 \times 10^{-9}$	1.331	Close to 4/3
320	-43.61	$-43.61 \times 10^{-9}$	1.385	
340	-48.75	$-48.75 \times 10^{-9}$	1.450	
355	-53.01	$-53.01 \times 10^{-9}$	1.510	Close to 3/2
360	-54.51	$-54.51 \times 10^{-9}$	1.532	
380	-60.94	$-60.94 \times 10^{-9}$	1.634	
400	-68.13	$-68.13 \times 10^{-9}$	1.767	Close to 7/4

Contour charts giving values of  $\bar{N}_0$  on a worldwide range are presented in two of the references [4, 5]. Charts are given for two seasonal periods, winter (February) and summer (August). An examination of these charts leads to the observation that, for ocean areas, the value of  $\bar{N}_0 = \bar{N}_s$  varies from 300 to 400. With the aid of Table 3-1 (or Equation 3-2) corresponding values of  $\Delta\bar{N}/\Delta h$  can be estimated.

It will be useful, at this point, to define another variable, the "earth radius factor,"  $\alpha$ , and to relate it to  $\Delta\bar{N}/\Delta h$ . Though the name, "earth radius factor," may suggest that  $\alpha$  has something to do with earth properties, it really is introduced as an aid in accounting for the refractive properties of the atmosphere.

In standard mathematics texts (calculus) the local "radius of curvature,"  $\rho$ , of a curve is defined to be the reciprocal of the magnitude of the "curvature vector,"  $\bar{C}$ . If the radius of the earth is denoted by  $a$ , then the curve which is



the intersection with the surface of the earth of a plane through the center of the earth has a radius of curvature  $\rho = a$ . The curvature,  $C$ , of the curve has the magnitude  $C = 1/\rho = 1/a$ . These relationships are shown at the left in Figure 3-5.

Assume, as suggested at the upper center of Figure 3-5, that the refractive index of the atmosphere is a function only of height above the surface of the earth, i. e.,  $n = n(h)$ . An atmosphere satisfying this condition is said to be "spherically stratified." This is the "normal" condition of the undisturbed atmosphere. In some treatises on ray optics, it is shown that ray paths in a spherically stratified medium are plane curves having a radius of curvature given by\*

$$\rho = \frac{n}{(dn/dh) \cos \beta} \quad 3-3$$

and, hence, a curvature given by

$$C = \frac{1}{n} \frac{dn}{dh} \cos \beta \quad 3-4$$

For the choice of positive sense of the curvature vector on which Equations 3-3 and 3-4 are based, positive values of  $\rho$  and  $C$  imply concavity of the ray path toward the center of the earth. The value of  $dn/dh$  is expected to be negative in a normal atmosphere, yielding a positive value of ray curvature.

These relationships are shown at the right in Figure 3-5. The angle,  $\beta$ , is defined (center of Figure 3-5) as the angle between the local ray direction and the local horizontal direction (which is perpendicular to the local radial direction).

If the ray direction is nearly "horizontal" along its path, the height of the ray above the surface of the earth depends on the difference in curvature,  $\Delta C$ , between the ray path and the surface of the earth. If this difference is zero, then a ray traveling horizontally at the surface at one point will remain at the surface. Suppose that from both the curvature of the ray path and the curvature of the surface of the earth an amount equal to the curvature of the ray path is subtracted. The effect is to straighten the curvature of the ray path and to reduce the curvature of the surface of the earth, without markedly disturbing the separation of ray path and earth. Straight ray paths are characteristic

---

\*For example: Max Born and Emil Wolf, Principles of Optics, Third (Revised) Edition, Pergamon Press, 1965; Section 3.1.4, p. 119. The desired relationships can be derived from Equation (14) by appropriate specialization, if due care is exercised in defining the positive sense of the curvature vector.

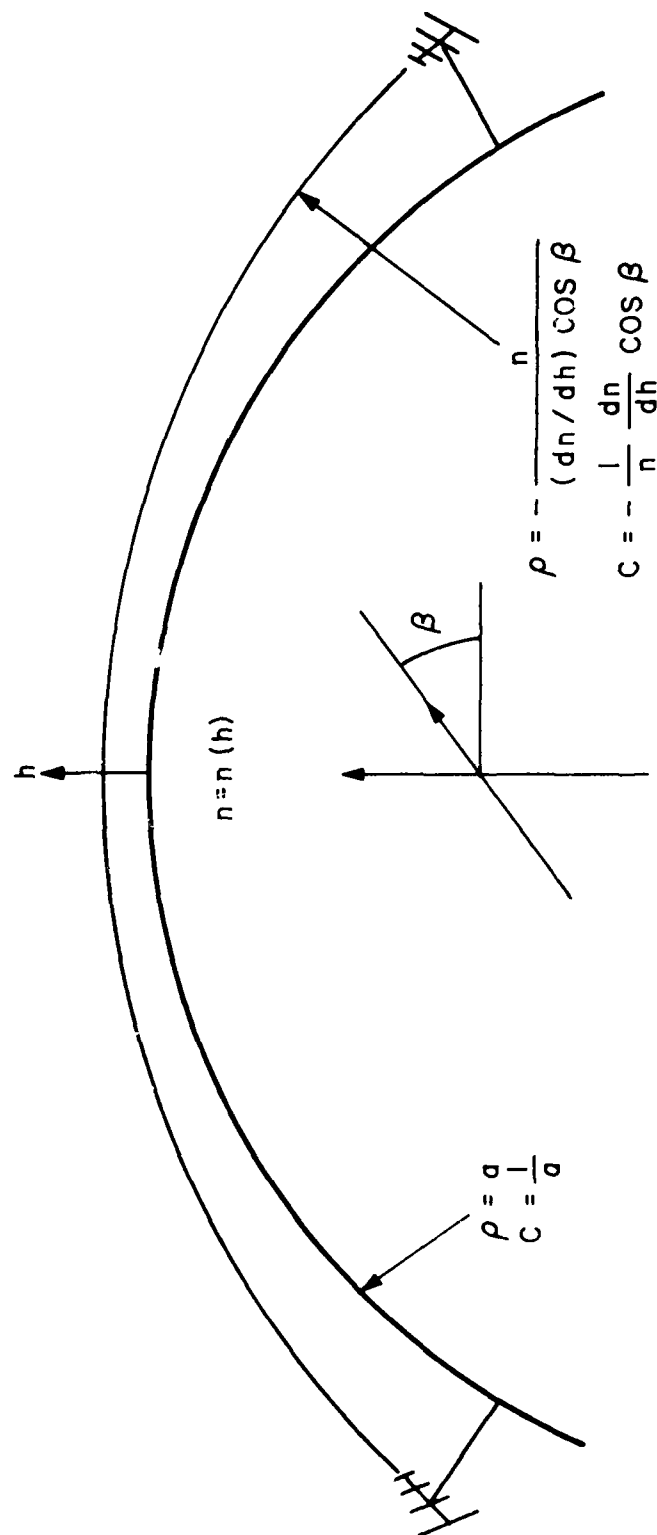


Figure 3-5. Relative curvature of ray path and surface of the earth.

of homogeneous (non-stratified) media. Thus the effect of atmospheric refractivity can be accounted for, at least approximately, in the ground wave case by an adjustment of the curvature of the surface of the earth.

Quantitatively, subtraction of the ray curvature from the surface curvature modifies the surface curvature to an "effective" value,  $C_e$ .

$$C_e = \Delta C = \frac{1}{a} - \left(-\frac{1}{n} \frac{dn}{dh} \cos \beta\right) \quad 3-5$$

From the effective curvature,  $C_e$ , an effective radius for the surface of the earth,  $a_e$ , can be defined.

$$\frac{1}{a_e} = C_e = \frac{1}{a} + \frac{1}{n} \frac{dn}{dh} \cos \beta \quad 3-6$$

It is convenient to define from this expression the earth radius factor,  $x$

$$x = \frac{a_e}{a} = \frac{1}{1 + (a/n)(dn/dh) \cos \beta} \quad 3-7$$

If, now, the value of  $\Delta N/\Delta h$  is associated with  $dn/dh$  as follows:

$$(\Delta N/\Delta h) \approx 10^{-9} = dn/dh \quad (\text{refractive index units/meter}) \quad 3-8$$

then a value of  $x = a_e/a$  can be found as a function of  $N_s$ . This relationship is given numerically in columns 1 and 4 of Table 1 and graphically in Figure 3-6.

Since, for the ocean areas,  $N_s = N_0$  lies between 300 and 400, the earth radius factor for propagation over sea water will lie between 1.331 and 1.767, insofar as Equation 3-2 is valid. Note that the commonly quoted value,  $4/3$ , lies at the bottom of this range. It appears that, for ocean areas, the value  $3/2$  for the earth radius factor might be more nearly appropriate than  $4/3$ .

In computations of ground wave propagation it is  $\alpha$ , rather than  $N_s = N_0$  and  $\Delta N/\Delta h$ , which is used directly. It is evident that the use of  $x$ , derived in the manner outlined above, implies the imposition of a restrictive model for the refractivity of the atmosphere. That model is one in which the gradient of refractive index is a constant (i. e., not dependent on height) and is quantitatively equal to  $\Delta N/\Delta h \approx 10^{-9}$ . With this model, the refractivity of the atmosphere is constrained to decrease linearly with height above the surface. The model is realistic, on the average, only in the immediate vicinity of the surface of the earth, perhaps within the first 2 or 3 kilometers.

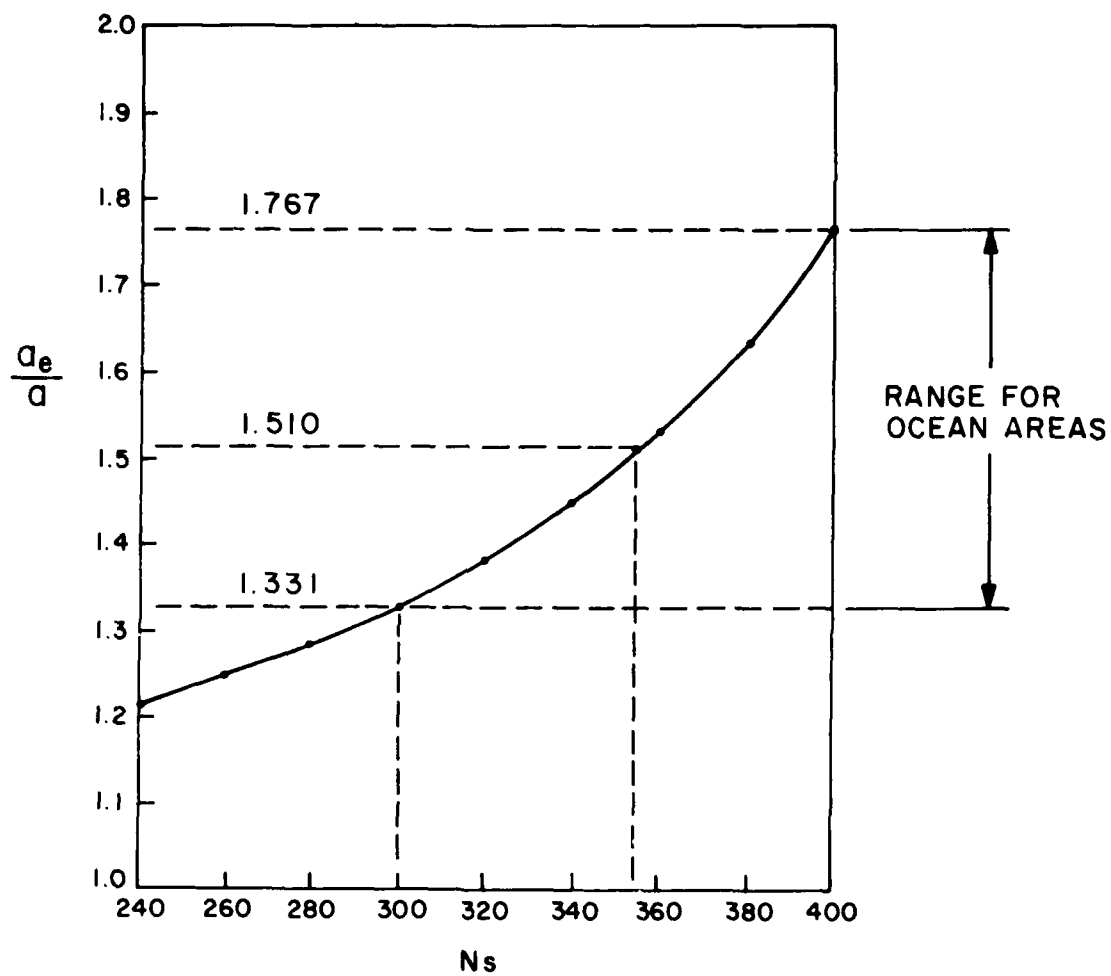


Figure 3-6. Earth radius factor ( $\alpha = a_e/a$ ) as a function of surface refractivity ( $N_s$ ).

To recapitulate, the variables in the geophysical property group are earth permittivity, earth conductivity, atmosphere surface refractivity and atmosphere refractivity gradient at the surface. In contrast to the sky wave, the geophysical variables affecting the ground wave have relatively stable values as functions of time. The range of variation is limited and the effects on wave propagation are ones of limited degree rather than of gross kind. In this treatment, we shall require that the variables exhibit the property of homogeneity along the wave path. The so-called "mixed path"\* problem will not be treated. A limited form of nonhomogeneity transverse to the path will be permitted in the case of atmospheric refractivity. Values for the variables appropriate to wave propagation over sea water have been delineated and, in the computations, the ranges of the variables will be confined to such values.

### 3. 2. 2 Path Terminal Disposition Variables

The disposition of the path terminals is specified by the three quantities illustrated in Figure 3-7. One variable is the ground range, or distance, between the points on the surface of the earth directly "below" the terminal points. The other two variables are the heights above the surface of the earth at which the two path terminals are located.

Ground range was assigned the role of primary independent variable in the computations. Two sets of loss data, as a function of range, were computed. For the first, the maximum range was restricted to 90 km to give good curve readability at the shorter ranges. For the second, the range was extended until the computed loss exceeded 200 dB in order to determine the greatest useful range in each case.

If the path terminals are both assumed to be on board ships, then the range of possible terminal heights is quite restricted. To limit the volume of computation which had to be done and to allow greater opportunity for exploration of the effects of other variables, a single value--15.0 meters--was assigned to both of the terminal height variables. This value ought to be satisfactory for most HF antennas installed on board ships except, perhaps, when calculating fields at closest distances, generally at distances shorter than the range of principal interest for the purpose of this document.

### 3. 2. 3 Source Property Variables

The source of the electromagnetic wave--the ground wave--is assumed to be an elemental dipole with its axis radially (vertically) oriented. Three

A "mixed path" can be exemplified by one which has one terminal on land and the other at sea, a significant portion of the path traversing each medium.

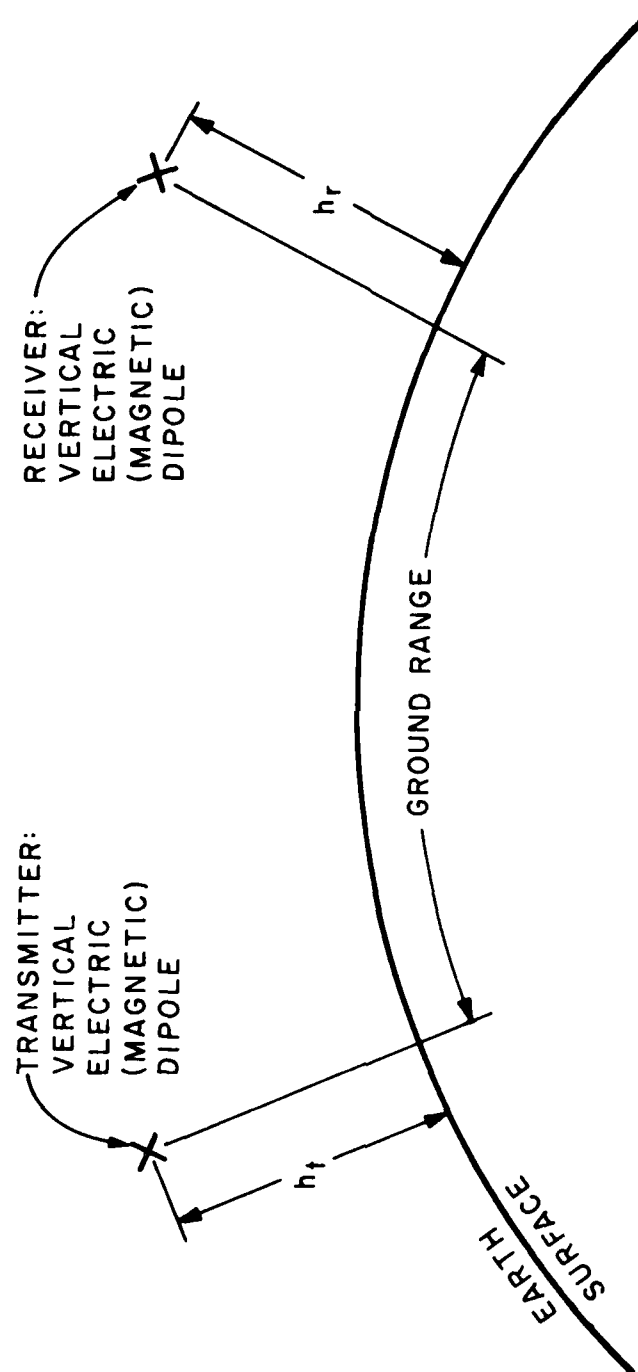


Figure 3-7. Disposition of transmitter and receiver relative to the surface of the earth.

variables are required to specify the essential properties of the source, the wave frequency, the dipole type and the source strength.

Five values of wave frequency, spanning the HF band, were selected for loss computations. They were 2.0, 4.0, 8.0, 16.0 and 32.0 MHz.

Two dipole types are permitted in the computations. If an electric dipole is specified, the associated electromagnetic field will be "vertically" polarized. If a magnetic dipole is specified, the associated wave will be "horizontally" polarized.

The third variable is the strength of the source. To make the computation procedure tractable, the source strength must be specified in terms of dipole moment. The details of the problems surrounding specification of source strength will be treated at length in Section 3.3.

### 3.3 PROPAGATION LOSS CONCEPTS

The concept of "transmission loss" was exercised in connection with the sky wave case. It was a useful concept because it approximated  $\Gamma_{0a}$ , the value of which was needed for engineering and operational uses. The nature of the approximation was known and the value of the defect\* could be estimated when necessary. In any event, the defect generally was a small part of the entire quantity.

In the sky wave case, transmission loss was a convenient concept because it was amenable to quantitative evaluation both by physical and mathematical procedures. The mathematical procedure had particular convenience because of the possibility of breaking it up into six separable pieces, two associated, respectively, with properties of the two terminal devices and the other four associated with the mechanisms of wave propagation between path terminals.

The transmission loss concept is equally useful in connection with the ground wave case. However, it is there less convenient for quantitative evaluation, especially by mathematical procedures. The reason is that the mathematical procedure does not fall apart into pieces as convenient to evaluate or use as those in the sky wave case. If only measured, rather than calculated, loss values were to be considered the same loss definition -- that of transmission loss -- would serve equally well for both ground wave and sky wave cases.

For the ground wave case it will be expedient to define an alternate loss concept which will be called "propagation loss."\*\* Propagation loss differs from transmission loss principally in the handling of antenna gain concepts. The latter subject will be accorded some specific attention, subsequently, with the intent of showing how propagation loss values can be modified to approximate transmission loss.

\*The "defect" in the approximation is just the dissipative losses in the transmitting terminal device (antenna system), e.g.,  $\Gamma_{tt}$ .

\*\*Don't worry too much about the exact literal meanings of the names assigned to the two loss concepts. In some senses they would seem to possess more logic and be more truly descriptive of the respective concepts if interchanged. It seems better, at this point, to bow to history than to stand on principle, if for no reason other than to avoid confusion in perusal of the literature on the subject.



The situation is illustrated in Figure 3-8 for a special case, the short-range flat-earth regime. The path terminal symbols, 1 and 2, represent dipoles (electric or magnetic) with their axes radially\* oriented, located at different heights above the surface of the earth. The symbols 1' and 2' below the surface of the earth represent image dipoles, which are appropriate to this special case.

The problem of quantitative evaluation of propagation loss by mathematical procedures tends to be computation bound. The limits are set not so much by what is possible as by what is affordable. Some compromises are necessary to keep the computational work within reasonable bounds. In the discussions which follows, every effort will be made to lay open to view the areas of compromise so that judgment can be rendered about the consequences thereof in applications of the computed data to specific situations.

### 3.3.1 Definition of Propagation Loss

The concept of "propagation loss" which is to be used in connection with the ground wave is very similar to that of "transmission loss" which was used in connection with the sky wave. It is, however, not identical. The differences have rather subtle consequences which need to be examined carefully.

Propagation loss,  $\Gamma_{pn}$ , is defined as the ratio of the total power radiated,  $P_{t,d}$ , from the transmitter (source) located at one path terminal to the power available,  $P_{r,d}$ , from the receiver (sink) located at the other path terminal. The terminal devices are defined to be lossless elemental (i.e., small) dipoles of the same kind (either electric or magnetic). The dipole axes are oriented radially. The situation is suggested in Figures 3-7 and 3-8. Thus,

$$\Gamma_{pn} = P_{t,d} / P_{r,d} \quad 3-9$$

If the corresponding quantities in decibel form are used, this expression becomes

$$\gamma_{pn} = P_{t,d} - P_{r,d} \quad 3-10$$

---

\*By "radially," it is meant that the dipole axis passes through the center of the earth. The term "vertically" also would be appropriate.

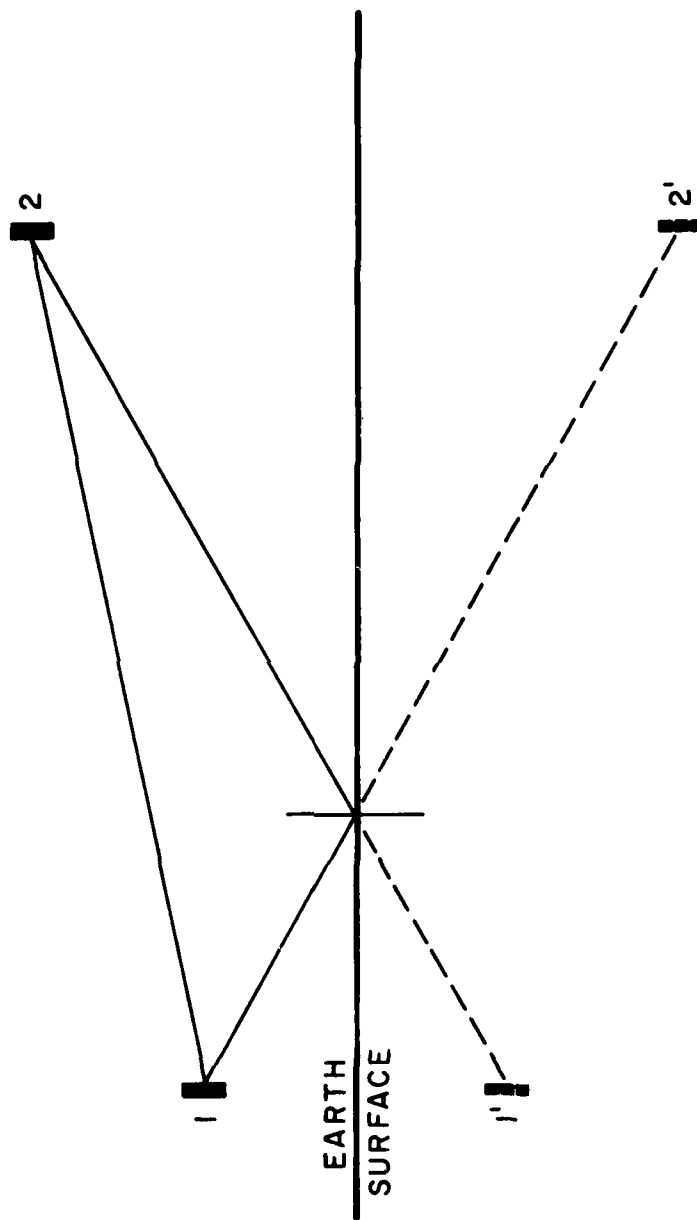


Figure 3-8. Path terminals (1 and 2) and their images (1' and 2') relative to the surface of the earth.

The difference between this definition of propagation loss and the previously stated definition of transmission loss lies in the specific restriction of the terminal devices to elemental dipoles. The definition of transmission loss allowed a greater degree of generality. However, the definition of propagation loss of itself involves no conceptual compromises.

Acceptance of a modified loss definition for the ground wave is forced on us by the solutions to the ground wave problem which are available for use. The alternate loss definition is not without problems of its own. Though conceptually straight forward, in practice difficulty arises in attempting to calculate the two power levels on which the definition is based. The reasons will become evident as the discussion proceeds.

### 3.3.2 Calculation of Electromagnetic Fields

The fundamental problem in electromagnetics on which the treatment of ground wave transmission is based is calculation of the electric and magnetic fields in the neighborhood of the surface of the earth, which fields arise from an electric or magnetic dipole, also in the neighborhood of the surface of the earth and having its dipole axis oriented radially thereto. The strength of the fields is directly proportional to the strength of the dipole source, which is specified (implicitly, if not explicitly) in terms of its dipole moment. This task of calculation may be considered the basic ground wave problem.

Excellent solutions to this basic problem are available in the literature [7, 8, 9]. While the solutions in most general form involve no significant conceptual compromise, some of the specializations are infinite in form. For computational purposes, these must be bounded, leading to numerical approximations. Carefully done, little need be lost in the process of numerical evaluation. The loss in accuracy involved should not be a matter for concern in the applications which this document is intended to address.

The solution to the basic problem is complex and the computation of field strength is exacting and tedious. The intrusion into the problem by the earth as a third party produces much more profound effects on the ground wave than it does on the sky wave. In the sky wave case, the earth is involved only in the wave launching and retrieval processes and not in the propagation process, except as it dictates the spherical geometry of the region in which the action takes place. In the ground wave case, the wave is intimately involved with the earth throughout the entire process from launch to retrieval.

The differences between the two cases arise, principally, because geometrical optical (ray) theory generally fails in the ground wave case.\* The delineation of power density flux tubes of small cross section connecting the path terminal regions is not generally justifiable. Hence, it is not possible to express the effects of propagation mechanisms in terms of power density flux values influent and effluent at the ends of flux tubes. The fields generated by the source in the presence of the earth generally lack (in regions near the earth) essential properties which characterize the ordinary far field of an antenna.\*\* Hence, the use of path terminal device properties such as antenna gain is less easily, if at all, justifiable.

To state the case in another manner, though the path terminals may be sufficiently distant from each other for each ordinarily to be considered in the far field of the other, neither may be sufficiently distant from the surface of the earth to be considered in its far field as a scatterer. The conceptual consequences of this state of affairs are profound. Some of them will be examined in the next three subsections.

### 3.3.3 Application of Reciprocity Principles

The transmission system under discussion is linear in source dipole moment (excitation) and in electric and magnetic field strength (response). The truth of this statement does not depend on the values of the geophysical property variables. These variables are assumed to be (and, in practice, are) independent of the strength of the electrical excitation and response quantities. The reciprocity principle is, therefore, applicable.

By invoking the reciprocity principle in the form of an appropriate theorem, it can be established that the field produced at one path terminal point by a dipole of given moment at the other path terminal is independent

\*A possible exception occurs in the case of regime number 1 discussed in Section 3.1 and used as an illustration in Figure 3-8. If the dipoles in Figure 3-7 are high enough above the surface of the earth and close enough together that the "surface wave" component of the field can be neglected, then ray principles may be applicable. The situation might then be handled in a manner similar to the multimode sky wave if the effects of the presence of the ground on the path terminal devices are properly accounted for.

\*\*For example, the surface wave component of the field, which predominates in regimes number 2 and 4 of Figure 3-1, does not have an inverse square diminution of power density with distance.

of which of the terminals is designated "transmitter." This statement holds even though the terminal disposition is not symmetrical, as suggested by Figure 3-8 in which terminal 2 is at a greater height than is terminal 1.

It follows that the power loss in transmission between 1 and 2 has the same value for transmission in either direction.

The radiation resistance of an elemental dipole above earth is known to depend on its height above the surface of the earth. Thus, for a dipole source of given fixed moment, the power radiated will vary as a function of its height. The power radiated from a dipole of fixed moment will not, in general, be the same if the dipole is located at position 2 as it would if located at position 1 (Figure 3-8).

Since the power loss must have the same value for either direction of transmission, the absorption aperture of the dipole designated "receiver" also will not, in general, be the same for both directions of transmission. It too will vary with height above the surface of the earth. As a matter of fact, equality of power loss in the two directions requires only that ( $G_1$  and  $G_2$  are radiation gains and  $A_1$  and  $A_2$  are absorption apertures at, respectively, path terminals 1 and 2)

$$G_1 A_2 = G_2 A_1 \quad 3-11a$$

or:

$$\frac{A_1}{G_1} = \frac{A_2}{G_2} \quad 3-11b$$

This relation says, simply, that it is the product of radiative and absorptive properties at, respectively, the two path terminals which must be independent of the direction of transmission.

Thus, while the reciprocity principle provides assurance that a calculated loss value ought not to depend on the direction of transmission over the path, it does not give assurance that the radiative and absorptive processes individually will be the same for both directions of transmission. This ambiguity engenders difficulties which will be discussed in subsection 3.3.4.

This second form of the condition should not be too surprising since, for any antenna, the gain,  $G$ , and absorption aperture,  $A$ , have the following relationship.

$$A = (\lambda^2/4\pi)G \text{ or } A/G = \lambda^2/4\pi$$

#### 3.3.4 Evaluation of Radiated and Available Power

An essential concomitant of the procedure for computing field strength is specification of the strength of the source by its dipole moment. This constraint is inherent in the nature of the basic problem. For system engineering or operational purposes, specification of source strength in terms of power radiated would be more convenient. Furthermore, the definition of propagation loss involves the power radiated rather than the dipole moment. If we propose to calculate propagation loss directly from the definition, then the power radiated by the source must be calculated.

It is therefore necessary to establish a relationship between power radiated and dipole moment. The difficulty with which we are faced is that, for a given dipole moment, the power radiated depends on the type of dipole involved and on its height above the surface of the earth. Thus, it is not possible to specify correctly such a relationship independently of terminal type and disposition.

It is possible to calculate the power radiated from a dipole of specified type and dipole moment, situated at a specified height above the surface of the earth. The first step in the calculation is to evaluate, using solutions to the basic problem, the field strength at a sufficiently large number of points on a closed surface which encloses the source. The second step is to integrate over the closed surface the time-averaged normal component of the poynting vector, which vector is derived from the calculated field values.

Thus, calculation of the radiated power involves, firstly, a large number of iterations of the same procedure by means of which the field at the receiving terminal is to be calculated. It involves, secondly, a large numerical double integration. The result is the relationship between radiated power and dipole moment for a single combination of dipole type and disposition. The absorptive properties of a receiving dipole having the same type and disposition could be derived from the radiative properties.

The computational task just outlined, though possible, is formidable. It is at this point that one of the conceptual compromises is called for.

There are two situations in which the power radiated by an electric dipole of specified moment can easily be determined as a function of dipole moment only. The first of these is when the dipole is at the surface of the earth, which is assumed to be plane, and when the value of earth conductivity,  $\sigma$ , is made infinite. The second is when the height above the surface is so great that the dipole can be considered to be in free space.

The power radiated from an elemental electric dipole placed at the surface of the earth (plane, perfectly conducting) can be derived from the expression for its radiation resistance,  $R_E$  ( $\Delta L$  denotes the elemental length of the dipole).

$$R_E = 160\pi^2 \left( \frac{\Delta L}{\lambda} \right)^2 \quad 3-12$$

The power,  $P$ , radiated when the dipole excitation current is  $I$  (rms) is given by the expression

$$P = I^2 R_E = 160\pi^2 \left( \frac{I\Delta L}{\lambda} \right)^2 \quad 3-13$$

Solving for the dipole moment ( $I\Delta L$ ) in terms of the power gives

$$(I\Delta L) = \frac{\lambda \sqrt{P}}{4\pi \sqrt{10}} \quad 3-14$$

It is this situation (dipole at the surface) and this relationship (Equation 3-14) which has been used to specify the dipole moment in terms of the "power radiated." The same expression will be used without regard to actual dipole height in any specific case. This configuration and relationship may be called the "reference transmitter" for the calculation of power loss.

If the same electric dipole\* is removed to a point distant from the earth, i.e., into free space, then the expression for the radiation resistance,  $R'_E$ , becomes

$$R'_E = 80\pi^2 \left( \frac{\Delta L}{\lambda} \right)^2 \quad 3-15$$

The power,  $P'$ , radiated becomes

$$P' = I^2 R'_E = 80\pi^2 \left( \frac{I\Delta L}{\lambda} \right)^2 = \frac{P}{2}$$

---

\*That is to say, one of the same moment.

SOUTHWEST RESEARCH INST SAN ANTONIO TX

DELINEATION OF CONSTRAINTS IMPOSED BY PROPAGATION FACTORS AT HF--ETC(U)  
APR 76 E C HAYDEN N00039-75-C-0481

N00039-75-C-0481

NL

4.5 4

$$\frac{d}{dt} \left( \frac{1}{2} \dot{\theta}^2 \right) = \dot{\theta} \ddot{\theta}$$

FND

Page 11

FILME:  
0.82

DTIC



Before proceeding to calculation of magnetic dipole moment in terms of power radiated, it will be convenient to digress a bit to derive the condition for equal radiation of power from an electric and a magnetic dipole in free space. The magnetic dipole is envisioned as a closed ring of current of strength  $I$  (rms) about the edge of an elemental surface of area  $\Delta A$ . The magnetic dipole moment is specified by  $I\Delta A$ . If  $\theta$  denotes angle measured with respect to dipole axis and  $r$  denotes radial distance from dipole center, then the amplitudes of the far fields of an electric dipole are

$$E_{\theta} = \frac{60\pi (I\Delta L)}{\lambda r} \sin \theta \quad 3-17a$$

$$H_{\phi} = \frac{(I\Delta L)}{2\lambda r} \sin \theta \quad 3-17b$$

Similarly, the amplitudes of the far fields of a magnetic dipole are

$$H_{\theta} = \frac{2\pi}{\lambda} * \frac{(I\Delta A)}{2\lambda r} \sin \theta \quad 3-18a$$

$$E_{\phi} = \frac{2\pi}{\lambda} * \frac{60\pi (I\Delta A)}{\lambda r} \sin \theta \quad 3-18b$$

Thus, excepting the factor  $2\pi/\lambda$ , the corresponding fields of the electric and magnetic dipoles are given by the same expressions, but are orthogonal in polarization. For equal fields, the dipole moments ought to bear the following relationship

$$\frac{2\pi}{\lambda} (I\Delta A) = (I\Delta L) \quad 3-19a$$

$$\text{or} \quad (I\Delta A) = \frac{\lambda}{2\pi} (I\Delta L) \quad 3-19b$$

Since, in both cases, the electric and magnetic fields are everywhere in phase and orthogonal, the amplitude of the poynting vector will everywhere be, simply,  $E_{\theta}H_{\phi}$  or  $E_{\phi}H_{\theta}$  as the case may be. The direction will everywhere be radial. The power radiated will, therefore, be the same in both cases if the dipole moments satisfy Equation 3-19.

Returning from the digression and using the result derived therein, it is now possible to specify the moment of a magnetic dipole which will be the "equivalent" of the previously specified electric dipole. From Equations 3-14 and 3-19.

$$(I\Delta A) = \frac{\lambda}{2\pi} (I\Delta L) = \frac{\lambda^2 \sqrt{P}}{8\pi^2 \sqrt{10}} \quad 3-20$$

The magnetic and electric dipoles so defined are equivalent in the sense that in free space they will radiate the same amount of power, namely  $P/2$ .

To digress again very briefly, it is possible to parlay this result into an expression for the value of a radiation resistance,  $R'_M$ , for the magnetic dipole in free space. Remembering that the power radiated in this situation really is  $P' = P/2$ , Equation 3-20 yields

$$R'_M = \frac{P'}{I^2} = \frac{P/2}{I^2} = 320\pi^4 \left( \frac{\Delta A}{\lambda^2} \right)^2 \quad 3-21$$

This result is in accord with that obtained by other methods.

If the magnetic dipole source defined above (Equation 3-20) is placed at the surface (plane, perfectly conducting) trouble ensues. One view of the situation is that the source is exactly cancelled by its image. In any event, the radiation resistance is zero; no power is radiated.\* Clearly, in this situation electric/magnetic dipole equivalence does not hold.

At this point, it is useful to recapitulate. In order to avoid a formidable computational task, a convention has been established by which source dipole moment (electric or magnetic) is specified as a function of a power level,  $P$ . The convention is defined in terms of a special case, namely, an electric dipole at the surface (plane, perfectly conducting).

---

\*If the conductivity of the earth is finite, the source is not totally cancelled; power is radiated, the amount depending on the conductivity value.

This configuration is called the "reference transmitter"\* and the power radiated in the reference situation is to be used as the value of  $P_{t,d}$  in the definition of propagation loss (Equation 3-9).

However, the value of  $P_{t,d}$  is known to be in error in situations other than the reference situation. Two other discrete points on the error function are known. When the dipole (electric or magnetic) is sufficiently high above the earth, the power actually radiated is one-half of the reference value. If the dipole is of the magnetic type and is at the surface, the power radiated tends to zero as the conductivity becomes larger.

Most of the transition between the value of power radiated with the dipole at the surface and the value with the dipole distant from the surface takes place within about the first  $0.35\lambda$  above the surface for the electric dipole and  $0.25\lambda$  above the surface for the magnetic dipole. Above these heights, the power radiated oscillates about the final (free space) value in a manner decreasing with height. The transition is essentially complete at a dipole height of  $3\lambda$  or  $4\lambda$ .

The value of dipole moment, given as a function of power radiated, in the convention just defined has been used as the source strength in calculating the electromagnetic field at the receiving path terminal point. It is useful to know -- as a landmark case -- the value of electric field,  $E$ , which would be produced at the surface (plane, perfectly conducting) at a distance,  $D$ , from the reference radiator (in the expression  $E_{mV/m}$  is in millivolts/meter,  $P_{kw}$  is in kilowatts and  $D_{km}$  is in kilometers).

$$E_{mV/m} = 300 \sqrt{P_{kw}} / D_{km} \quad 3-22$$

\*The convention used in this document agrees with that used by Bremmer [9]. Some authors and agencies have used other definitions of the reference transmitter. In reading the literature one must be aware of this hazard. One such agency is the C.C.I.R. of the International Telecommunications Union. This agency has used dipole moment and power radiated in the free space situation to define the reference transmitter. Furthermore, the calculated field strength (propagation loss is not given) has been multiplied by the factor 1.047 to simulate a  $\lambda/2$  dipole, rather than an elemental dipole, transmitter. This factor is the square root of the ratio of gains of the  $\lambda/2$  and elemental dipoles referred to isotropic, i.e.,

$$\left[ \frac{60/36.5}{1.5} \right]^{1/2} = \left[ \frac{1.6438}{1.5000} \right]^{1/2} = [1.0959]^{1/2} = 1.047$$

The field in free space of a dipole source of the same moment, measured in the equatorial plane ( $\theta = 90^\circ$ ), would be (the primed quantities denote actual "in free space" counterparts of the unprimed "at the surface" values)

$$\begin{aligned} E'_{mV/m} &= 150 \sqrt{P_{kw}} / D_{km} \\ &= 150 \sqrt{2P'_{kw}} / D_{km} \\ &= 212 \sqrt{P'_{kw}} / D_{km} \end{aligned} \quad 3-23$$

in which  $P/2 = P'$  is the power actually radiated in the free space situation.\*

To complete the calculation of propagation loss, it is yet necessary to calculate the power available from the dipole at the receiving path terminal. The power available,  $P_r$ , is the product of the absorption aperture,  $A$ , of the terminal device and the incident power density flux,  $S$ .

$$P_r = A S = A \frac{E^2}{\eta} = A \frac{E^2}{120\pi} \quad 3-24$$

\*Under the C.C.I.R. definition of reference radiator described in a previous footnote, this expression would become

$$E'_{mV/m} \Big|_{CCIR} = 222 \sqrt{P'_{kw}} / D_{km}$$

For the same dipole removed to the surface, the field,  $E$ , would be

$$\begin{aligned} E_{mV/m} \Big|_{CCIR} &= 444 \sqrt{P'_{kw}} / D_{km} \\ &= 444 \sqrt{P_{kw}/2} / D_{km} \\ &= 314 \sqrt{P_{kw}} / D_{km} \end{aligned}$$

For the same radiated power, the C. C. I. R. reference transmitter will yield field strength values which are 3.41 dB higher than those yielded by the reference transmitter defined in this document. Of this, 3.01 dB is a consequence of the 2:1 relationship of  $P$  to  $P'$  and 0.40 dB is due to the factor 1.047 used by C. C. I. R. to simulate a  $\lambda/2$  dipole.

As has previously been noted, the absorption cross section of the dipole is a function of its type and height above the surface. The problem is closely related to that of calculating power radiated by the source.

Again, a conceptual compromise is indicated. The convention which has been adopted for use in this document is the counterpart of the one adopted for the reference transmitter. The absorption aperture to be used for specifying power available at the receiving path terminal in terms of the field strength at that terminal is that of an electric dipole receiver at the surface (plane, perfectly conducting).

$$A_{d,i} = (3/2) (2) (\lambda^2/4\pi) = 3\lambda^2/4\pi \quad 3-25$$

This expression defines the "reference receiver." This value of  $A_{d,i}$  will be used for converting field strength at the receiver to available power, regardless of the actual receiving terminal disposition in any specific case. The expression defining this conversion is found by inserting the value of  $A_{d,i}$  from Equation 3-25 into Equation 3-24.

$$P_{r,d} = A_{d,i} E^2 / 120\pi = \frac{3\lambda^2}{4\pi} * \frac{E^2}{120\pi} = \frac{\lambda^2 E^2}{160\pi^2} \quad 3-26$$

The actual absorption aperture of a dipole, electric or magnetic, in free space is

$$A'_{d,i} = (3/2) (\lambda^2/4\pi) = 3\lambda^2/8\pi \quad 3-27$$

That of a magnetic dipole at the surface (plane, perfectly conducting) is zero.

It is useful to know the value of propagation loss which would occur in two landmark cases, both dipoles at the surface and both dipoles in free space. These cases can serve as examples of application of the principles which have been discussed.

For both (electric) dipoles at the surface, the field strength given by Equation 3-22 (with proper adjustment of units) can be substituted into Equation 3-26 to yield

$$P_{r,d} = \frac{\lambda^2}{160\pi^2} * \frac{(300)^2 P_{kw}}{D_{km}^2} * 10^{-6} = \frac{\lambda^2}{160\pi^2} * \frac{(300)^2 P_{t,d} * 10^{-3}}{D^2 * 10^{-6}} * 10^{-6} \quad 3-28$$

This expression can be rearranged to yield one for the propagation loss (Equation 3-9).

$$\Gamma_{pn} = \frac{P_{t,d}}{P_{r,d}} = \left[ \left( \frac{2}{3} \right)^2 \left( \frac{1}{2} \right)^2 \right] \left[ \left( \frac{4\pi D}{\lambda} \right)^2 \right] = \left( \frac{1}{2G_{d,i}} \right)^2 \Gamma_b \quad 3-29$$

The quantity  $G_{d,i}$  is the gain over isotropic of a dipole in free space and the quantity  $\Gamma_b$  is the propagation loss (or transmission loss) between an isotropic transmitter and receiver in free space. The quantity  $\Gamma_b$  is, in the literature, commonly called "basic transmission loss."

For both (electric) dipoles distant from the surface, Equations 3-23 and 3-27 may be combined with Equation 3-24 to yield

$$\begin{aligned} P'_{r,d} = A'_{d,i} E'^2 / 120\pi &= \frac{\lambda^2}{320\pi^2} * \frac{(150)^2 (2) P'_{kw}}{D_{km}} * 10^{-6} \\ &= \frac{\lambda^2}{320\pi^2} * \frac{(150)^2 (2) P'_{t,d} * 10^{-3}}{D^2 * 10^{-6}} * 10^{-6} \end{aligned} \quad 3-30$$

Rearranging this expression produces one for the loss  $\Gamma'_{pn}$ .\*

$$\Gamma'_{pn} = \frac{P'_{t,d}}{P'_{r,d}} = \left( \frac{2}{3} \right)^2 \left( \frac{4\pi D}{\lambda} \right)^2 = \left( \frac{1}{G_{d,i}} \right)^2 \Gamma_b \quad 3-31$$

\*If the C. C. I. R. reference transmitter discussed in previous footnotes were complemented with a comparable reference receiver (i. e. a  $\lambda/2$  dipole in free space) the resulting expression for loss in the free space situation would be

$$\Gamma'_{tn} \Big|_{CCIR} = \left[ \frac{1}{1.0959G_d} \right]^2 \Gamma_b$$

The loss thus defined would more properly be called "transmission loss" than "propagation loss" because the path terminal antenna gains are included. The loss so defined would be related to that defined in this document as follows

$$\frac{\Gamma'_{tn} \Big|_{CCIR}}{\Gamma_{pn}} = \frac{(2)^2}{(1.0959)^2} = 3.33$$

This ratio corresponds to  $6.02 - 0.80 = 5.22$  dB. The 6.02 dB arises because of the choice of the free space, rather than the surface, situation for reference. The 0.80 dB arises from the gain excess of the  $\lambda/2$  dipoles above the elemental dipoles.

For the case of the electric dipoles at the surface, the propagation loss given by Equation 3-29 is both exactly correct and consonant with the conventions specified for calculation of power radiated from the transmitter and power available from the receiver. In contrast, for the case of the dipoles distant from the surface, the propagation loss given by Equation 3-31 is exactly correct but not consonant with the conventions for the reference transmitter and receiver. For this case it has been possible to calculate correctly the power radiated from the transmitter and available from the receiver. If, in this case, the conventions had been followed the second expression (Equation 3-31) would not have differed from the first (Equation 3-29). The consequence would have been a value for the propagation loss,  $\Gamma_{pn}$ , which was less than the actual loss  $\Gamma'_{pn}$  by a factor of 4.0 (6.02 dB).

It is incumbent on the user of the computed propagation loss data to make judicious use of knowledge about the nature of these two conceptual compromises in any application of the loss data to specific situations.

### 3.3.5 Treatment of Antenna Gain

The definition of propagation loss is based on elemental dipole radiative and absorptive devices. This was done because a tractable solution was available to the ground wave transmission problem stated in terms of such devices. In general, path terminal devices will be more complex in configuration and performance than an elemental dipole.

In the sky wave problem the added complexity was treated in terms of a "far field" property, the "directivity" or "gain," which was defined as a function of direction relative to device references. Being a far-field property, the gain concept is the perfect complement to the geometrical optical power density flux tube concept of propagation, which was there applicable. Since the latter is not generally applicable to the ground wave problem, an alternative treatment, or counterpart, of the gain concept is required which is applicable to the ground wave case.

Rigorously speaking, calculation of the field at a path terminal such as 2 in Figure 3-8, produced by an extended source\* in the neighborhood of 1 in the same figure, requires that the extended source be represented as a distribution of elemental dipoles. The linearity property of the system

\*That is to say, an antenna or antenna array, in contrast to an elemental dipole.

guarantees applicability of the superposition principle. Thus, the total field at 2 can be found as the sum of elemental fields, each of which is produced by one of the elemental dipoles utilized in the source representation.

A similar complication exists in calculation of the response of an extended sink (receiver) in the neighborhood of 2 to the field produced by a source (extended or not) in the neighborhood of 1.

Thus, the concept of antenna gain becomes inextricably intertwined with the concept of propagation mechanism. Rigorously speaking, the concepts of antenna pattern and, hence, of antenna gain are not generally applicable in the case of ground wave transmission. The reason is that the several components of the ground wave do not all diminish with distance in accord with the inverse square law, even in regions which might otherwise be considered the far field of the source.

Practically speaking, a judicious retreat can be made from the rigorous forward position espoused in the preceding few paragraphs. A third conceptual compromise is indicated at this point. The basis for retreat can be stated in the following way. If the extended source (or sink) is sufficiently "compact," then the concept of antenna pattern and gain may be carefully applied. "Sufficiently compact" means, roughly, that extension in the radial direction is small enough that the height gain functions of the dipole source may be considered constant and that extension in tangential (horizontal) directions is small enough that the surface wave attenuation functions may be considered constant. These two conditions correspond, roughly, to the far field criteria applied in defining conventional antenna gain.

For shipboard antenna installations designed for use in the HF band, the compactness condition generally will be satisfied.

If the compactness condition is satisfied, the extended terminal device can be replaced by an equivalent elemental dipole for the purpose of making the propagation loss calculation. The problem, then, is to define the dipole equivalent heights of the two path terminals and to specify how the values of power radiated and available should be modified.

For a source extended in height, but sufficiently compact, a weighted mean height,  $h_{wm}$ , can be defined. If the extended source is represented by a distribution of elemental dipoles, the weighted mean height can be



defined by the following expression ( $h_i$  is the height of the  $i$ th dipole and  $M_i$  is the dipole moment of the  $i$ th dipole).

$$h_{wm} \sum_i M_i = \sum_i h_i M_i \quad 3-32$$

Rearrangement yields an expression for the desired quantity.

$$h_{wm} = \frac{\sum_i h_i M_i}{\sum_i M_i} \quad 3-33$$

The gains of the transmitting and receiving antennas,  $G_{t,d}$  and  $G_{r,d}$ , respectively, can be used to modify the power radiated and power available in the definition of propagation loss (Equation 3-9). The result is an estimate of the transmission loss.

$$\Gamma_{tn} = \frac{P_{t,d}/G_{t,d}}{P_{r,d} * G_{r,d}} = \Gamma_{pn}(1/G_{t,d}G_{r,d}) \quad 3-34a$$

or, in terms of the corresponding quantities in decibel form,

$$\gamma_{tn} = \gamma_{pn} - g_{t,d} - g_{r,d} \quad 3-34b$$

Note that the gain values in Equations 3-34 must be values referred to an elemental dipole reference, rather than an isotropic reference. These references differ by a factor of 1.5 (the gain of an elemental dipole referred to isotropic), which is equivalent to 1.76 dB. It is useful to keep in mind the fact that the gain of a  $\lambda/2$  dipole relative to an elemental dipole is the factor  $1.6438/1.5000 = 1.0959$ , which is equivalent to 0.40 dB.

It yet remains to state rules by which the gain values to be inserted into Equations 3-34 can be determined from the physical structure and disposition of the antennas. The point to keep in mind when formulating the rules is the fact that the effect of the surface of the earth on the propagation mechanism already is included in the propagation loss calculation. Two cases can be identified.

Case 1. Antenna isolated from (i. e., not connected to) the ground.

Rule: Determine the gain as if the antenna were in free space. The gain should be evaluated for a direction lying in a plane perpendicular to the vertical through the antenna and along the wave path.

Case 2. Antenna fed against (i. e., connected to) the ground.

Rule: Supplement the physical antenna by its image structure, formed as if by a perfectly conducting plane ground surface. Determine the gain as if the antenna-plus-image were in free space. The gain should be evaluated for a direction lying in a plane perpendicular to the vertical through the antenna and along the wave path.

The procedure for determining the gain can be illustrated with an elevated half-wave dipole and a quarter-wave monopole fed at the base against ground. The former is an example of Case 1 and the latter of Case 2. When the appropriate rules are applied, both examples reduce to the case of a half-wave dipole in free space. The gain values to be used in Equations 3-34 are

$$G_{t,d} = G_{r,d} = 1.6438/1.5000 = 1.0959 \quad 3-35a$$

or, in a corresponding expression in decibel form,

$$g_{t,d} = g_{r,d} = 0.40 \text{ dB} \quad 3-35b$$

### 3.3.6 Wave and Antenna Polarization

In contrast to the sky wave, there is no significant depolarization mechanism associated with the ground wave. The media (sea water or earth, and lower atmosphere) are not birefringent; they do not exhibit characteristic wave polarizations as does a magneto-plasma. There is, however, a large disparity between the attenuation rates of vertically and horizontally polarized field components. This is a consequence of wave boundary geometry, rather than of medium properties.

In general, a transmitting antenna--especially one mounted on a ship--will radiate some power in both (i. e., horizontal and vertical) polarizations. Because these polarizations are orthogonal, and because no significant depolarization mechanism is active, the fields propagated in the two polarizations can be treated separately.

A receiving antenna mounted on a ship is likely to have some response to incident fields of either polarization. If the field incident on a receiving antenna has power in both polarizations, the total antenna response can be found by combining the separate responses to the two orthogonally polarized components. This possibility is assured by the superposition theorem. However, because of the stability of the ground wave mechanisms, the combination

must be done by a deterministic phasor addition procedure, rather than by a random phasor addition procedure (i. e., by simple addition of the separate power responses. The phase to use in making the deterministic combination depends on the polarization characteristic of the antenna for the direction of the wavefront normal of the incident field and on the relative phases of the two field components.

At the transmitting end of a path, judgment must be exercised in assigning a value to the ratio of the power densities radiated in the two polarizations. At the receiving end of the path, corresponding judgment must be exercised in assigning a value to the ratio of the responses to the two polarizations. If the polarization characteristic of one or both of the antennas is not purely vertical or horizontal, the total field power gain value must be appropriately divided between the two polarizations. To illustrate the principle, consider an antenna radiating in a specified direction, a circularly polarized field at a total field power gain\* of 8 (9.03 dB). If the field is resolved into two equal orthogonal linearly polarized components, the power gain for each component would be half that of the total field power gain, or 4 (6.02 dB).

---

\*Power gain relative to an elemental dipole,  $G_{x,d}$ .

### 3.4 ATLAS OF PROPAGATION LOSS CHARTS

In the charts presented at the end of this section, propagation loss is shown graphically as a function of the principal independent variable, ground range. A directory to the charts, Table 3-2, will be found immediately before the charts.\* The charts are arranged into two groups, each with two sub-groups. In the first group, the ground range is limited to 90 km to afford good chart readability for the short ranges at which signal delivery via ground wave is most likely to be useful. In the second group, ground range is limited to values for which the propagation loss does not exceed 200 dB. In each group, the first sub-group is for a vertically polarized wave and the second for a horizontally polarized wave.

Certain of the potential variables were held at fixed values, the same for all charts. The (relative) permittivity of sea water was set at the value 80.0. The value 15.0 meters was selected for the height of both path terminals. This value is representative of the mean height of various shipboard mounted HF antennas.

The remaining three variables, conductivity ( $\sigma$ ), earth radius factor ( $\alpha$ ) and frequency ( $f$ ) were used parametrically. This problem organization is portrayed graphically in Figure 3-9. It applies to each of the four sub-groups. Each chart in a sub-group (excepting the one entitled "Summary") corresponds to a pair of values of  $\sigma$  and  $\alpha$ . On each chart, frequency ( $f$ ) is represented parametrically by five individual curves.\*\* Thus, each chart corresponds to one of the vertical stacks, or columns, of blocks portrayed in Figure 3-9.

Calculations were done for all of the nine possible stacks. Examples of the computer-printed tables prepared from the calculations are given in Figures 3-10 and 3-11. The tables in Figure 3-10 each represent one curve from the central combination of  $\sigma$  and  $\alpha$  for each of the sub-groups (A and B) of group I of the charts. Those in Figure 3-11 are corresponding examples from group II. A total of 180 tables, each representing an individual case (curve) was produced.

When the results were examined, it became clear that the variation of propagation loss with  $\sigma$  and  $\alpha$ , over the sets of values appropriate for

---

\*Table 3-2 is on page 289.

\*\*In a few instances in which the curves fell very close together, the curve for 4 MHz has been omitted.

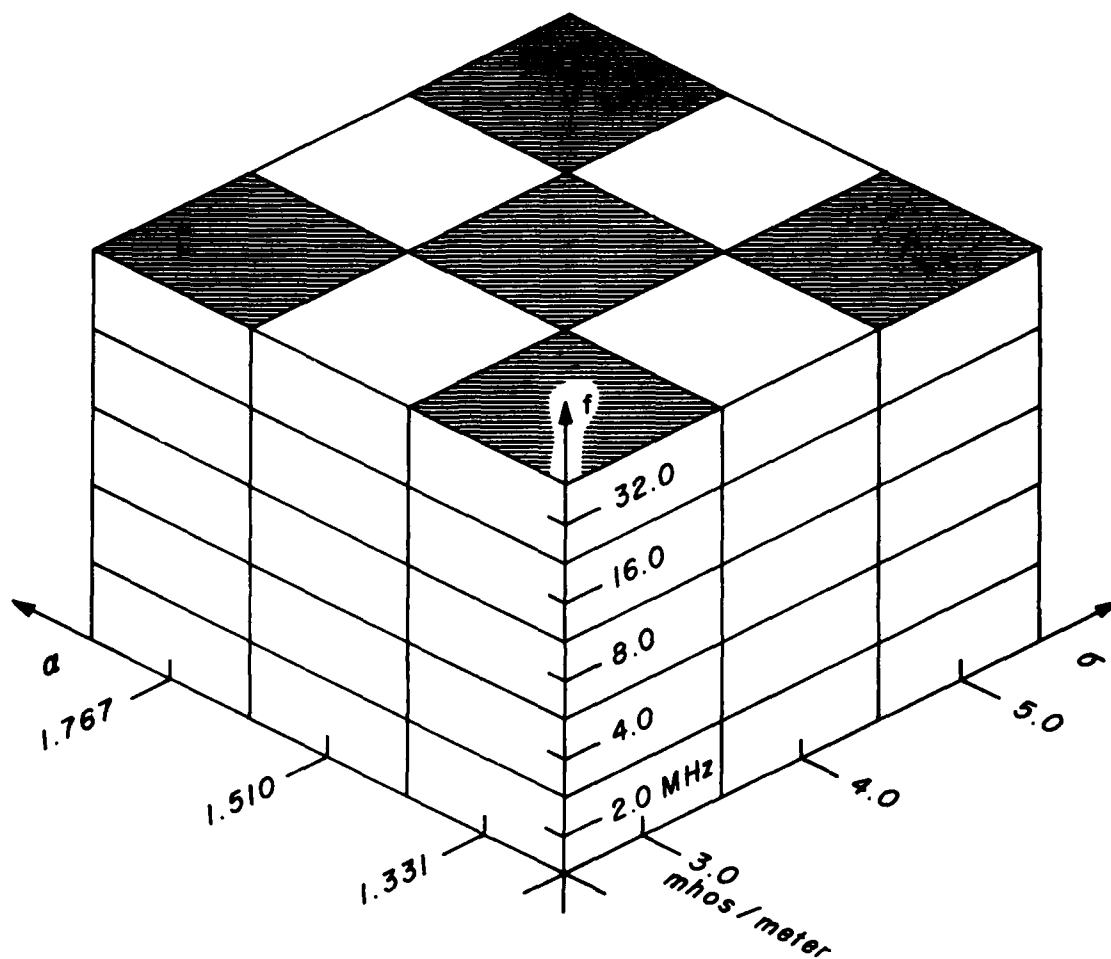


Figure 3-9. Coordinate structure showing values of three variables, conductivity ( $\sigma$ ), earth radius factor ( $\alpha$ ) and frequency ( $f$ ). The five stacks of "boxes" topped by a shaded area represent combinations of the three variables for which charts of propagation loss versus ground range are presented in the chart section.

GROUND WAVE PROPAGATION LOSS AND PHASE LAG  
 VERTICAL POLARIZATION, FREQUENCY = 4000 KHZ  
 EARTH CONSTANTS, CONDUCTIVITY = 4.0000 MHUS/M, PERMITTIVITY = 80.00  
 HEIGHT OF THE FIRST TERMINAL = 15.0 M  
 HEIGHT OF THE SECOND TERMINAL = 15.0 M  
 (EFFECTIVE RADIUS)/(TRUE RADIUS) = 1.510

DISTANCE KILOMETERS	PROP LOSS DECIBELS	PHASE RADIAN	DISTANCE KILOMETERS	PROP LOSS DECIBELS	PHASE RADIAN
2.00	41.09	-1.11	32.00	65.56	-1.51
4.00	47.13	-1.16	34.00	66.12	-1.53
6.00	50.67	-1.20	36.00	66.66	-1.55
8.00	53.19	-1.23	38.00	67.18	-1.56
10.00	55.15	-1.26	40.00	67.67	-1.58
12.00	56.75	-1.28	42.00	68.15	-1.60
14.00	58.11	-1.31	44.00	68.60	-1.62
16.00	59.28	-1.33	46.00	69.04	-1.63
18.00	60.33	-1.35	48.00	69.46	-1.65
20.00	61.24	-1.37	50.00	69.87	-1.67
22.00	62.04	-1.41	52.00	70.26	-1.69
24.00	62.84	-1.43	54.00	70.64	-1.70
26.00	63.62	-1.45	56.00	71.01	-1.72
28.00	64.31	-1.47	58.00	71.37	-1.73
30.00	64.95	-1.49	60.00	71.72	-1.75

GROUND WAVE PROPAGATION LOSS AND PHASE LAG  
 HORIZONTAL POLARIZATION, FREQUENCY = 4000 KHZ  
 EARTH CONSTANTS, CONDUCTIVITY = 4.0000 MHUS/M, PERMITTIVITY = 80.00  
 HEIGHT OF THE FIRST TERMINAL = 15.0 M  
 HEIGHT OF THE SECOND TERMINAL = 15.0 M  
 (EFFECTIVE RADIUS)/(TRUE RADIUS) = 1.510

DISTANCE KILOMETERS	PROP LOSS DECIBELS	PHASE RADIAN	DISTANCE KILOMETERS	PROP LOSS DECIBELS	PHASE RADIAN
2.00	73.50	1.00	32.00	130.04	1.49
4.00	92.16	1.51	34.00	131.13	1.48
6.00	101.00	1.67	36.00	132.17	1.47
8.00	105.16	1.56	38.00	133.20	1.46
10.00	109.24	1.54	40.00	134.16	1.45
12.00	112.48	1.54	42.00	135.08	1.45
14.00	115.20	1.54	44.00	135.97	1.44
16.00	117.57	1.53	46.00	136.81	1.43
18.00	119.66	1.53	48.00	137.53	1.42
20.00	121.54	1.52	50.00	138.11	1.41
22.00	123.24	1.52	52.00	138.17	1.40
24.00	124.81	1.51	54.00	138.41	1.40
26.00	126.25	1.51	56.00	140.62	1.39
28.00	127.60	1.50	58.00	141.32	1.38
30.00	128.86	1.49	60.00	141.99	1.37

Figure 3-10. Example of computer printout for a short range case.  
 Range limit set at 90 km.  
 Top: Vertical polarization; Bottom: Horizontal polarization

GROUND WAVE PROPAGATION LOSS AND PHASE LAG  
 VERTICAL POLARIZATION, FREQUENCY = 4000 KHZ  
 EARTH CONSTANTS, CONDUCTIVITY = 4.000 MHOS/M, PERMITTIVITY = 80.00  
 HEIGHT OF THE FIRST TERMINAL = 15.0 M  
 HEIGHT OF THE SECOND TERMINAL = 15.0 M  
 (EFFECTIVE RADIUS)/(TRUE RADIUS) = 1.510

* DISTANCE KILOMETERS	* PROP LOSS DECIBELS	* PHASE RADIAN	* DISTANCE KILOMETERS	* PROP LOSS DECIBELS	* PHASE RADIAN	* DISTANCE KILOMETERS	* PROP LOSS DECIBELS	* PHASE RADIAN
50.00	69.87	-0.67	850.00	131.56	-0.56	1650.00	181.40	-0.48
100.00	77.35	-1.06	900.00	134.74	-0.95	1700.00	184.46	-0.87
150.00	82.59	-1.44	950.00	137.91	-1.34	1750.00	187.52	-1.26
200.00	86.98	-1.82	1000.00	141.07	-1.73	1800.00	190.58	-1.65
250.00	90.97	-2.20	1050.00	144.21	-2.11	1850.00	193.63	-2.03
300.00	94.73	-2.58	1100.00	147.35	-2.50	1900.00	196.68	-2.42
350.00	98.35	-2.97	1150.00	150.48	-2.89	1950.00	199.73	-2.81
400.00	101.86	-2.93	1200.00	153.60	3.01	2000.00	202.78	3.09
450.00	105.31	2.54	1250.00	156.71	2.62	2050.00	205.82	2.70
500.00	108.70	2.15	1300.00	159.82	2.23	2100.00	208.86	2.31
550.00	112.05	1.76	1350.00	162.92	1.84	2150.00	211.89	1.92
600.00	115.37	1.38	1400.00	166.01	1.46	2200.00	214.93	1.53
650.00	118.65	.99	1450.00	169.10	1.07	2250.00	217.96	1.15
700.00	121.91	.60	1500.00	172.18	.68	2300.00	220.99	.76
750.00	125.14	.21	1550.00	175.26	.29	2350.00	224.02	.37
800.00	128.36	-.17	1600.00	178.33	-.10	2400.00	227.04	-.02

GROUND WAVE PROPAGATION LOSS AND PHASE LAG  
 HORIZONTAL POLARIZATION, FREQUENCY = 4000 KHZ  
 EARTH CONSTANTS, CONDUCTIVITY = 4.000 MHOS/M, PERMITTIVITY = 80.00  
 HEIGHT OF THE FIRST TERMINAL = 15.0 M  
 HEIGHT OF THE SECOND TERMINAL = 15.0 M  
 (EFFECTIVE RADIUS)/(TRUE RADIUS) = 1.510

* DISTANCE KILOMETERS	* PROP LOSS DECIBELS	* PHASE RADIAN	* DISTANCE KILOMETERS	* PROP LOSS DECIBELS	* PHASE RADIAN	* DISTANCE KILOMETERS	* PROP LOSS DECIBELS	* PHASE RADIAN
20.00	121.73	1.55	220.00	174.75	.29	420.00	204.65	-1.43
40.00	134.46	1.45	240.00	177.90	.13	440.00	207.59	-1.60
60.00	141.49	1.37	260.00	180.99	-.04	460.00	210.42	-1.78
80.00	147.91	1.27	280.00	184.03	-.20	480.00	213.30	-1.96
100.00	152.83	1.15	300.00	187.03	-.37	500.00	216.17	-2.14
120.00	157.14	1.03	320.00	190.01	-.55	520.00	219.04	-2.32
140.00	161.07	.89	340.00	192.97	-.72	540.00	221.90	-2.50
160.00	164.73	.75	360.00	195.91	-.90	560.00	224.76	-2.68
180.00	168.20	.60	380.00	198.84	-1.07	580.00	227.61	-2.86
200.00	171.52	.45	400.00	201.74	-1.25	600.00	230.46	-3.04

Figure 3-11. Example of computer printout for a long range case.  
 Propagation loss limit set at 200 dB.  
 Top: Vertical polarization; Bottom: Horizontal polarization

ocean areas, was small enough to obviate the necessity for providing charts for all possible combinations. Five of the nine possible combinations were selected for presentation, comprising the four extreme cases and the central case. These are denoted by the columns topped by shaded areas in Figure 3-9.

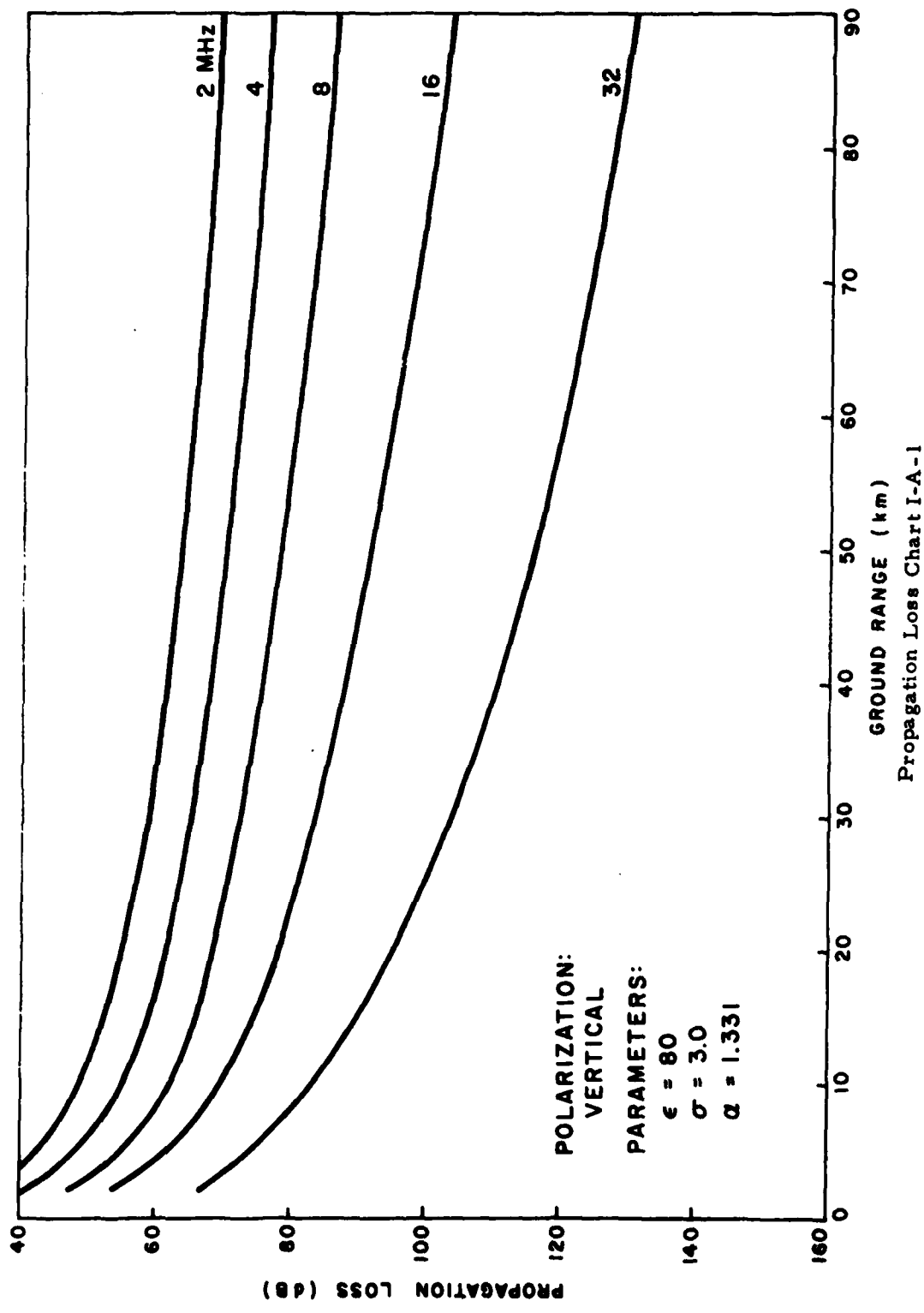
The last chart in each sub-group, the one entitled "Summary," is included to aid visualization of the total range of variation of propagation loss with  $\sigma$  and  $\alpha$  in each of the sub-groups. Curves for the low and high limits of loss as a function of  $\sigma$  and  $\alpha$  are given for the lowest and highest frequencies.

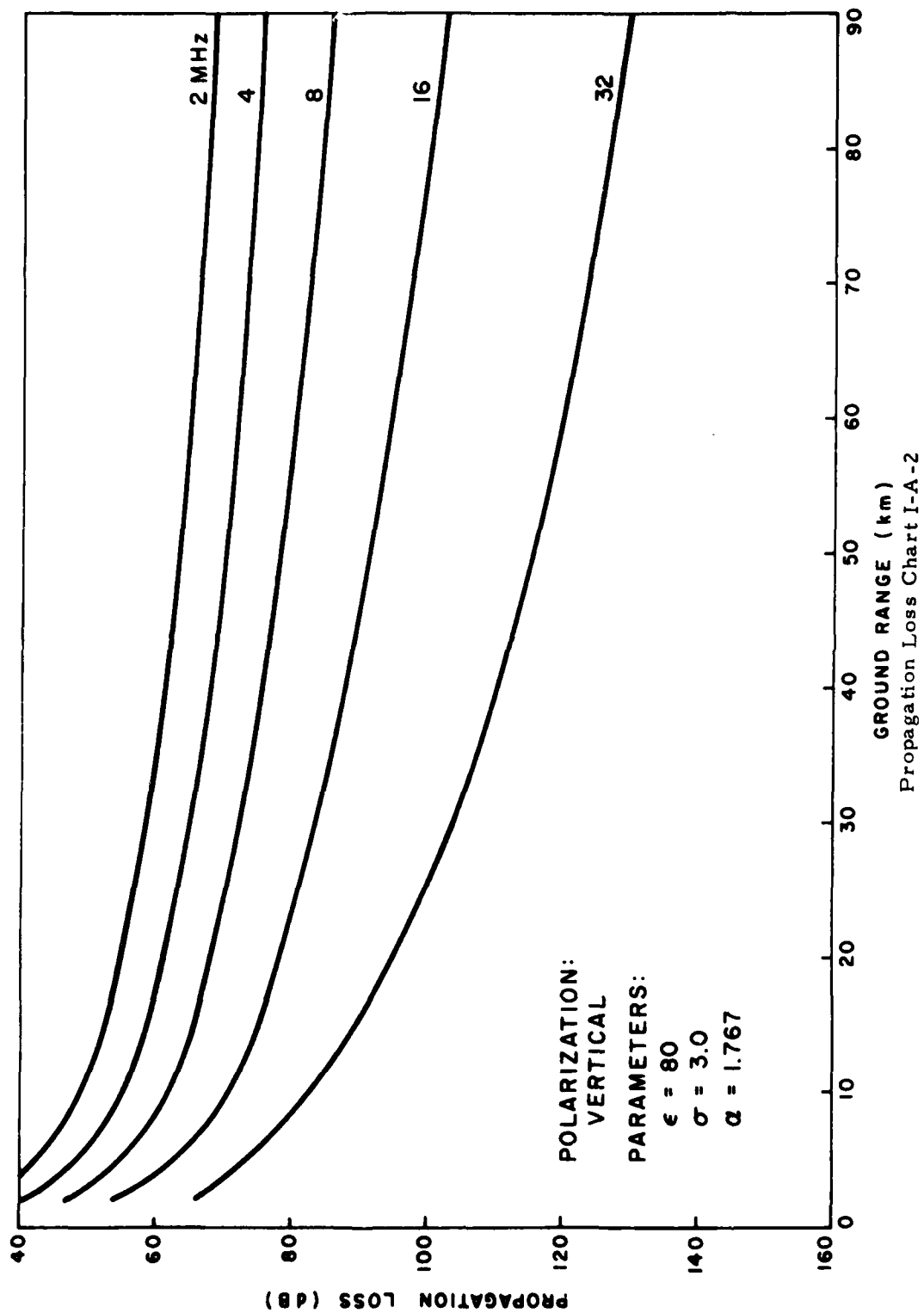
When propagation information is presented in the form of curves for which distance is the independent variable, there frequently is included a curve for a special reference case, perhaps a "free space" or "flat earth" curve. If the propagation data are expressed in terms of field strength, this is easily done. Equation 3-22 provides a suitable basis for such a curve. However, when the data are given in terms of loss, the situation is more complex. Equation 3-29 shows why this is so. The propagation loss,  $\Gamma_{pn}$ , given by this expression is a function of frequency (via  $\lambda$ ) as well as of distance. Thus, if reference curves of loss were to be plotted, a separate one would be required for each frequency. If, for any reason, such comparisons are desired, data can be generated for any specific situation from Equation 3-29.

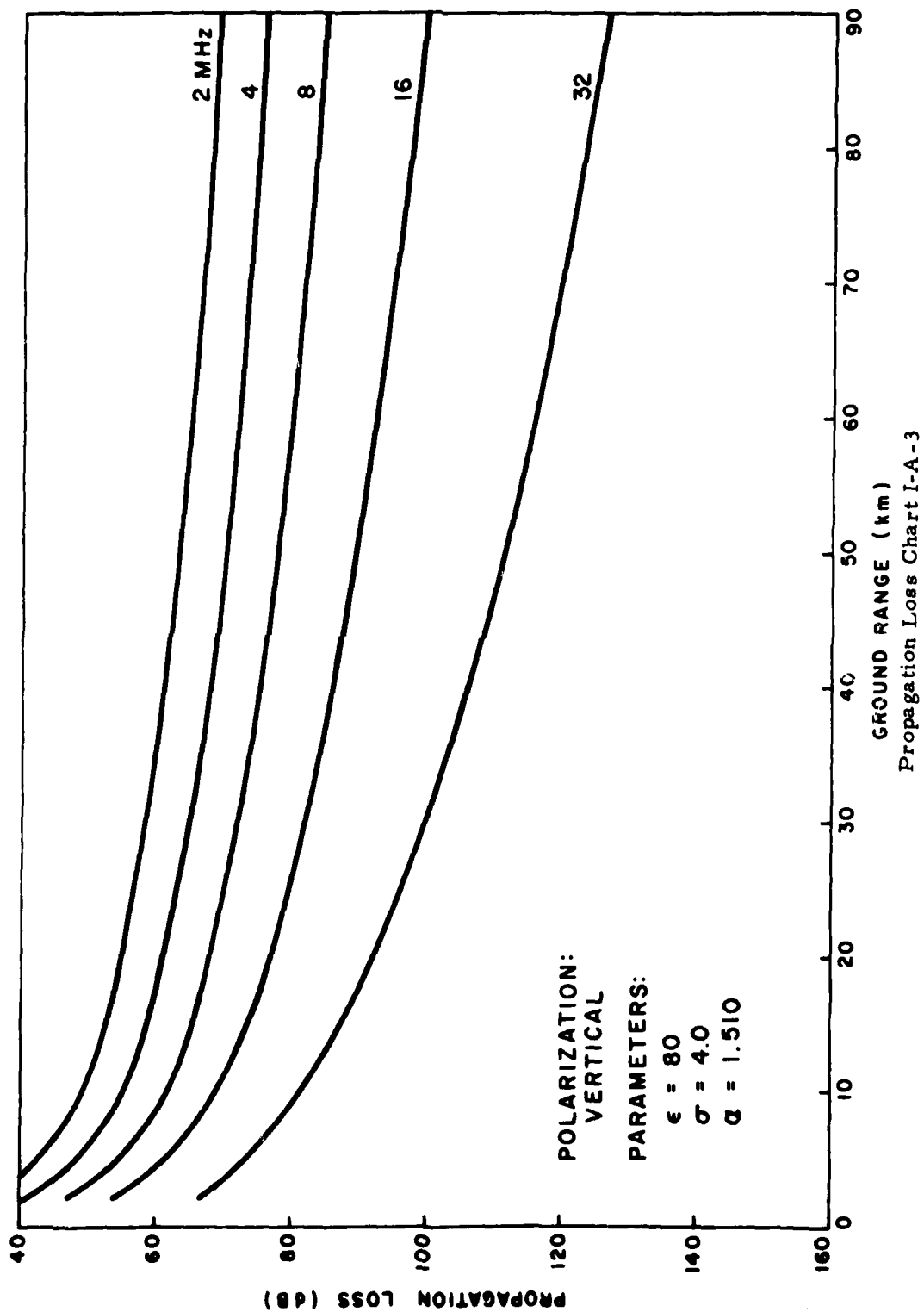


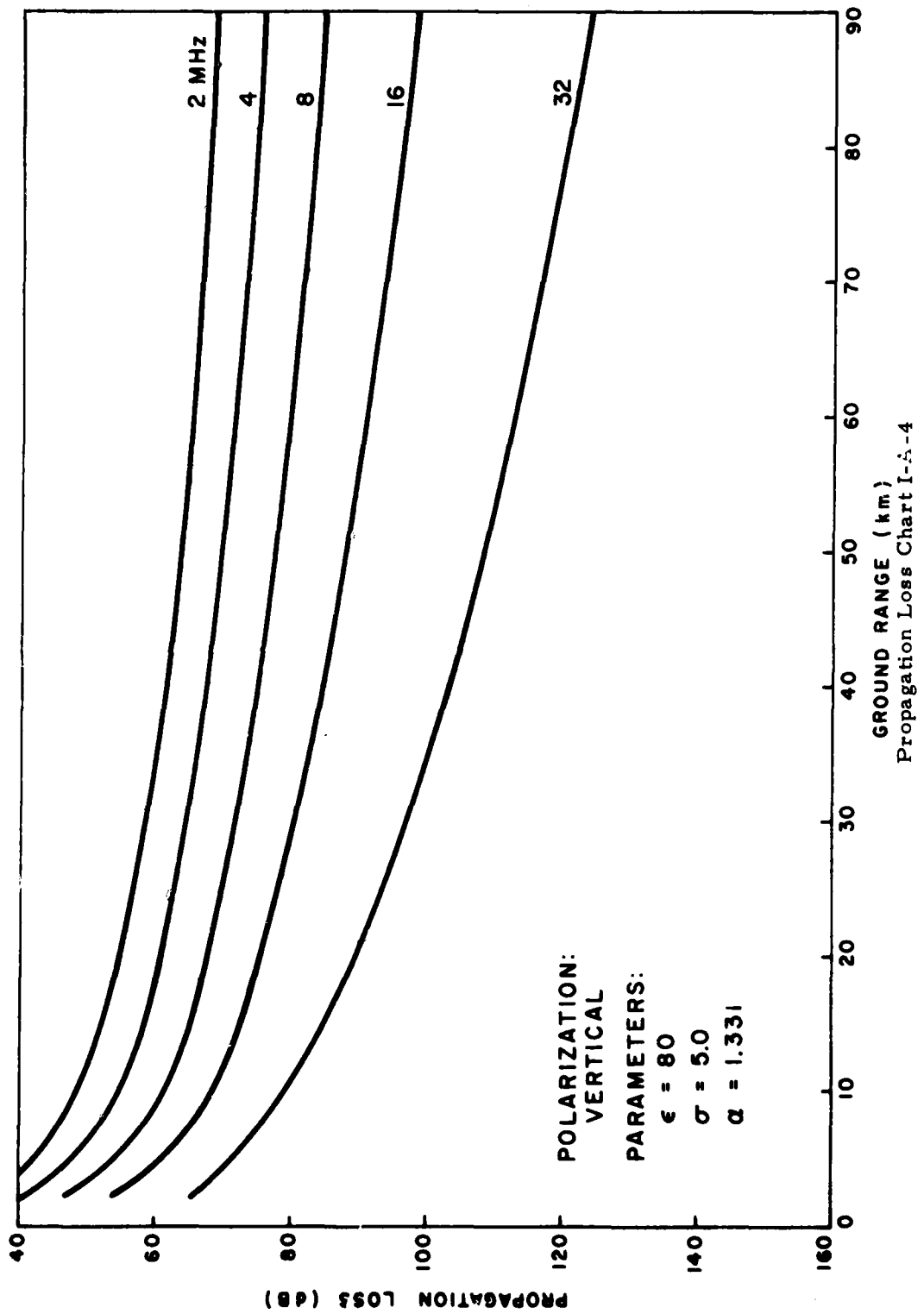
Table 3-2. Directory to propagation loss charts.

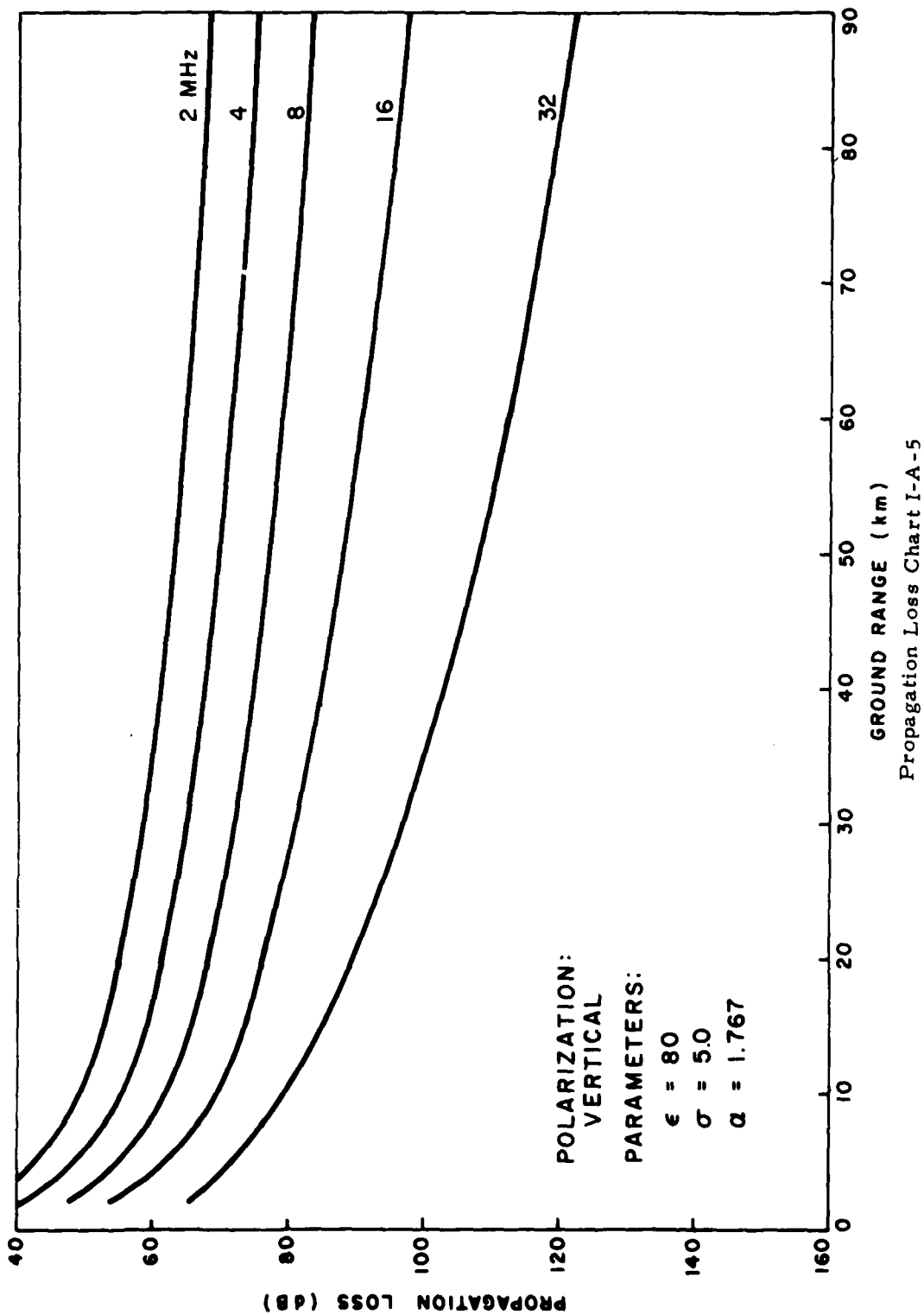
<u>Case</u>			<u>Chart</u>
I.	Short Range ( $\leq 90$ km):		
A.	Vertical Polarization		
	1.	$\sigma = 3.0$ $\alpha = 1.331$	I-A-1
	2.	$\sigma = 3.0$ $\alpha = 1.767$	I-A-2
	3.	$\sigma = 4.0$ $\alpha = 1.510$	I-A-3
	4.	$\sigma = 5.0$ $\alpha = 1.331$	I-A-4
	5.	$\sigma = 5.0$ $\alpha = 1.767$	I-A-5
	6.	Summary	I-A-6
B.	Horizontal Polarization		
	1.	$\sigma = 3.0$ $\alpha = 1.331$	I-B-1
	2.	$\sigma = 3.0$ $\alpha = 1.767$	I-B-2
	3.	$\sigma = 4.0$ $\alpha = 1.510$	I-B-3
	4.	$\sigma = 5.0$ $\alpha = 1.331$	I-B-4
	5.	$\sigma = 5.0$ $\alpha = 1.767$	I-B-5
	6.	Summary	I-B-6
II.	Long Range (Loss $\leq 200$ dB):		
A.	Vertical Polarization		
	1.	$\sigma = 3.0$ $\alpha = 1.331$	II-A-1
	2.	$\sigma = 3.0$ $\alpha = 1.767$	II-A-2
	3.	$\sigma = 4.0$ $\alpha = 1.510$	II-A-3
	4.	$\sigma = 5.0$ $\alpha = 1.331$	II-A-4
	5.	$\sigma = 5.0$ $\alpha = 1.767$	II-A-5
	6.	Summary	II-A-6
B.	Horizontal Polarization		
	1.	$\sigma = 3.0$ $\alpha = 1.331$	II-B-1
	2.	$\sigma = 3.0$ $\alpha = 1.767$	II-B-2
	3.	$\sigma = 4.0$ $\alpha = 1.510$	II-B-3
	4.	$\sigma = 5.0$ $\alpha = 1.331$	II-B-4
	5.	$\sigma = 5.0$ $\alpha = 1.767$	II-B-5
	6.	Summary	II-B-6

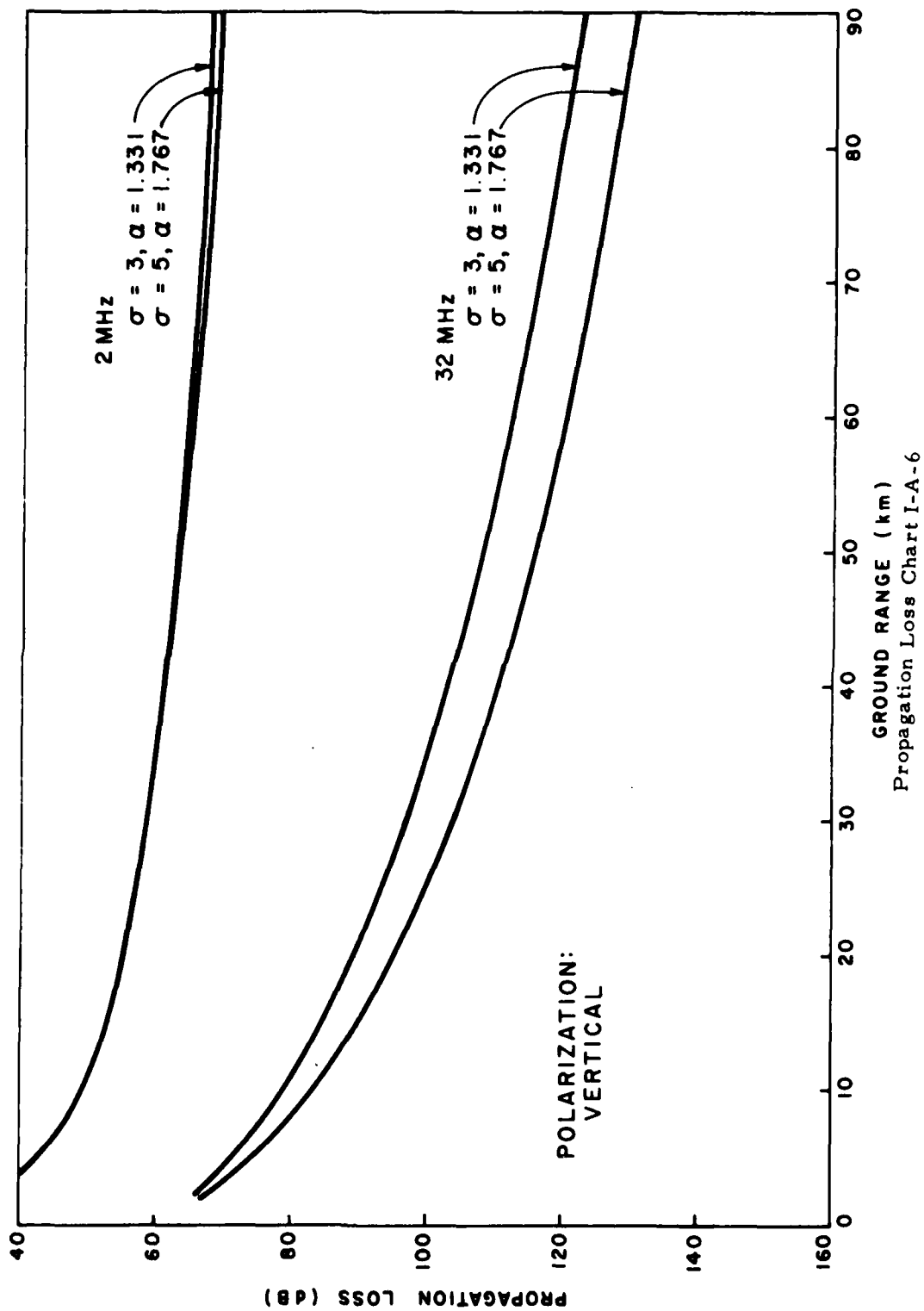


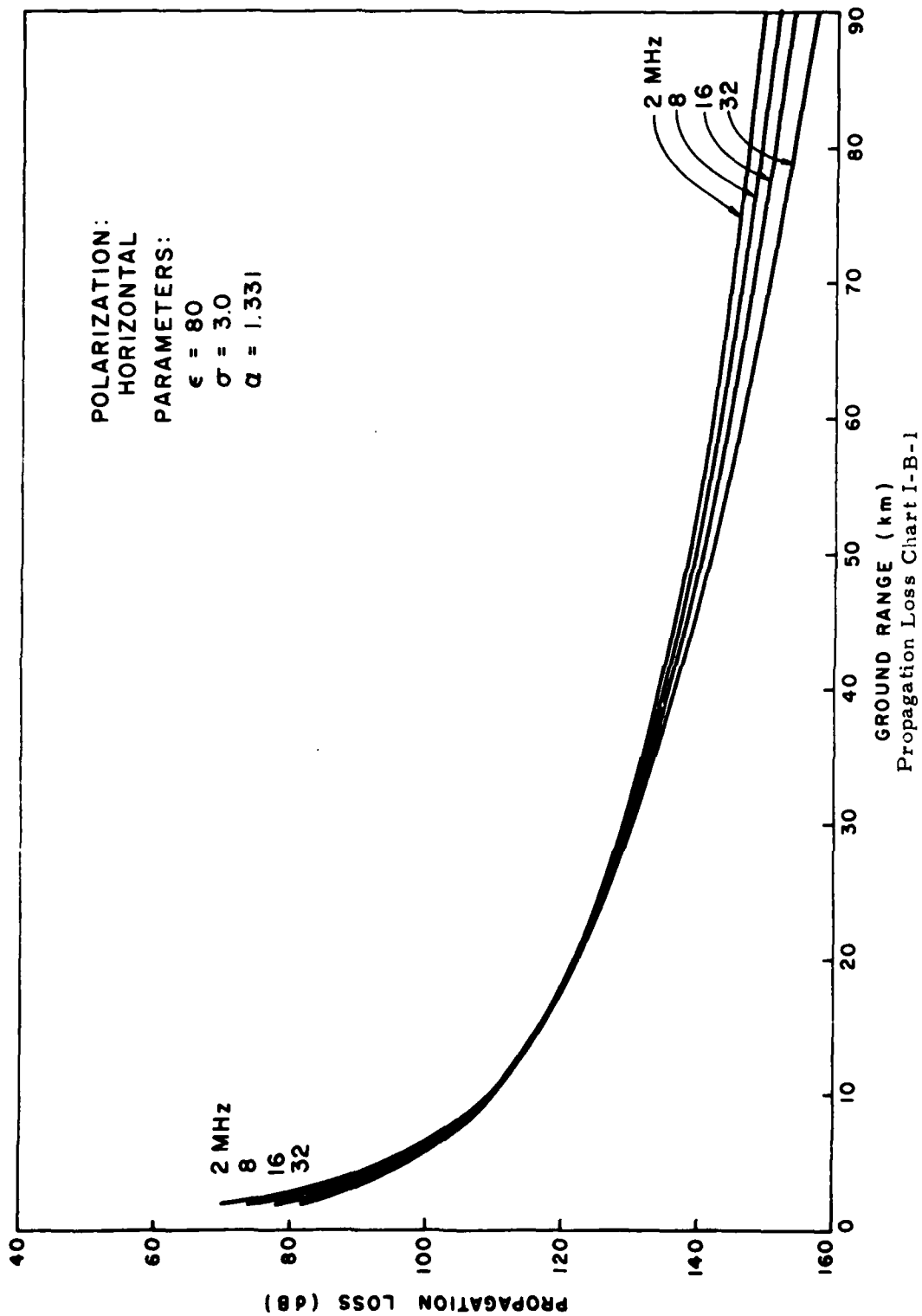




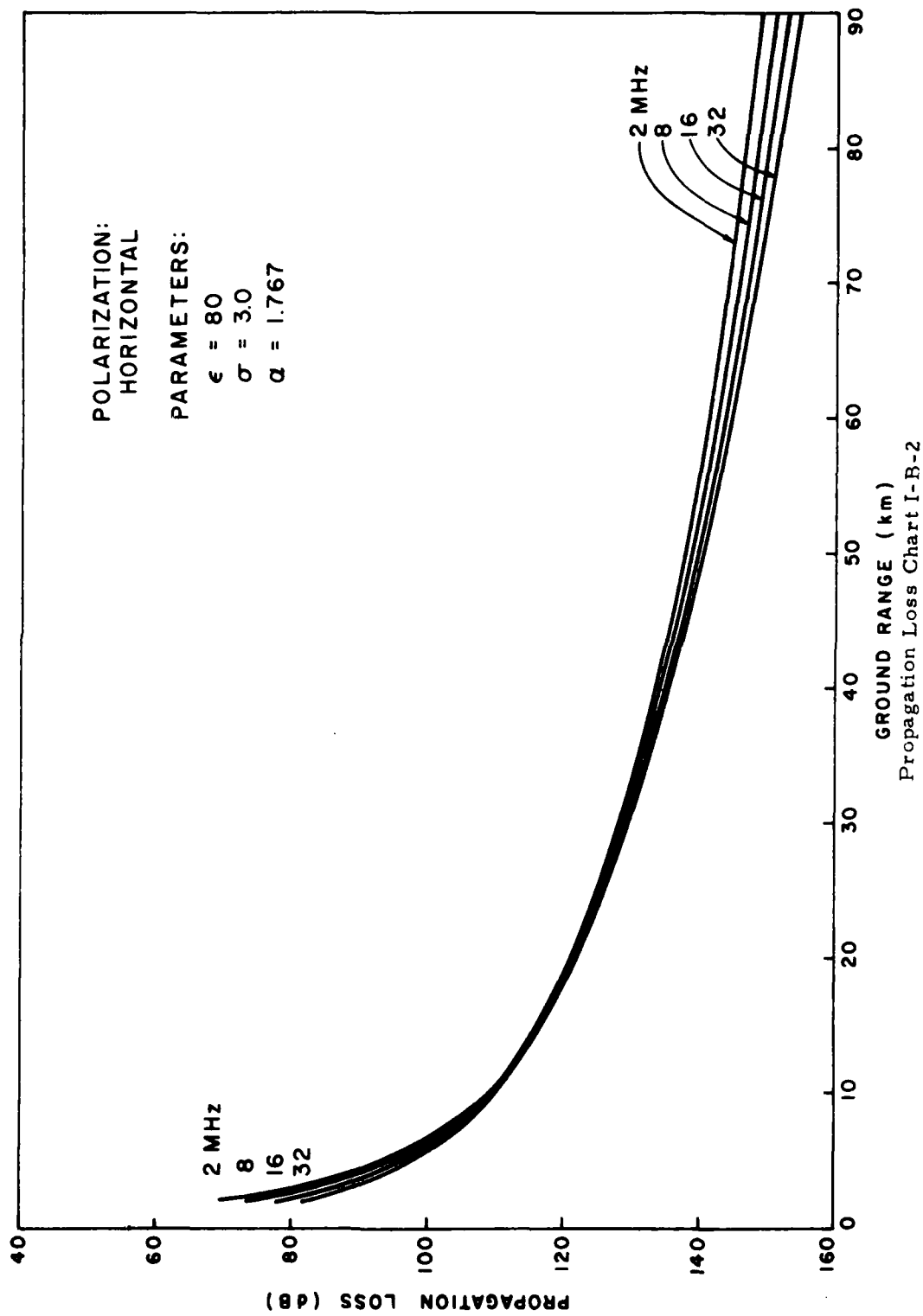


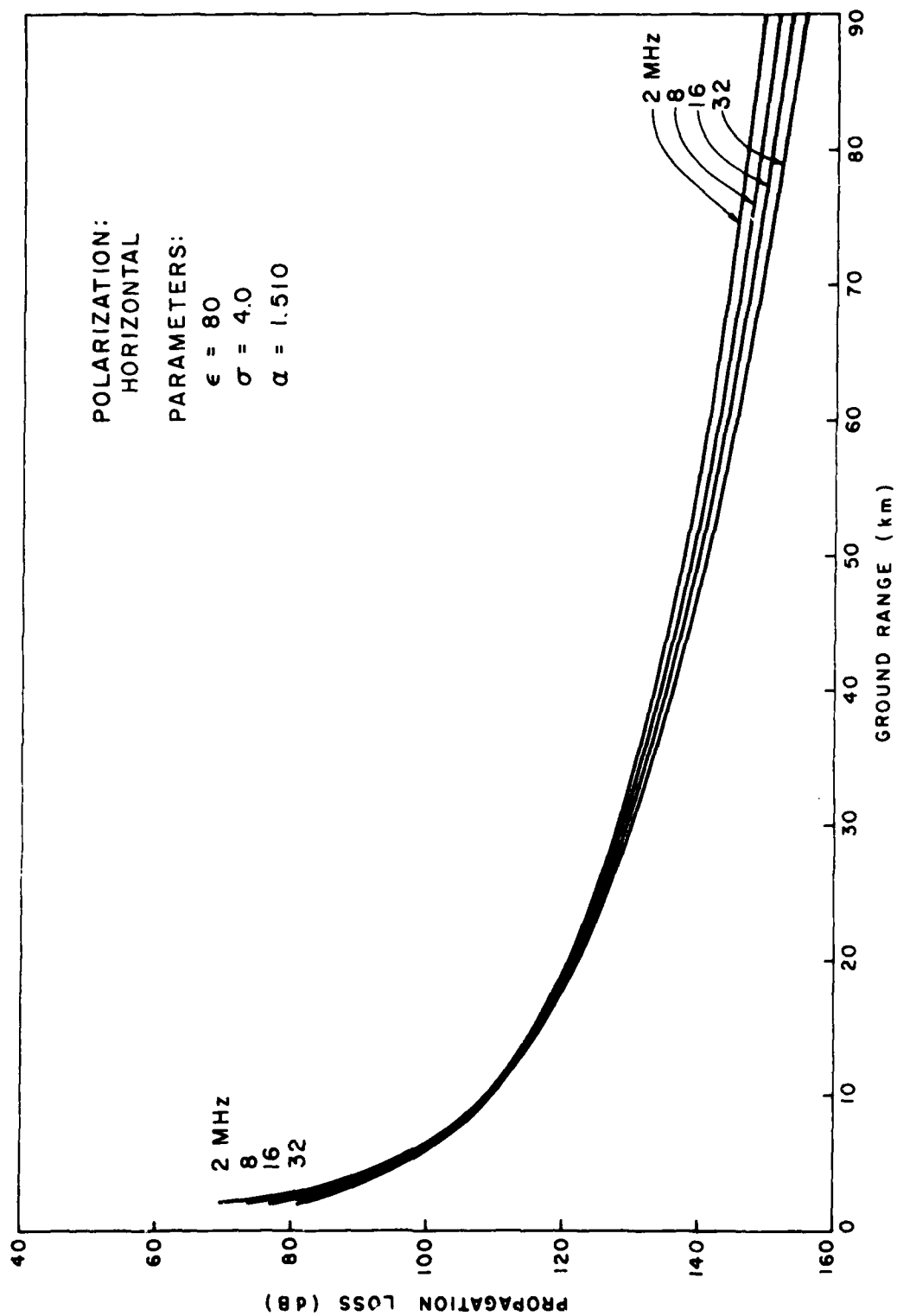




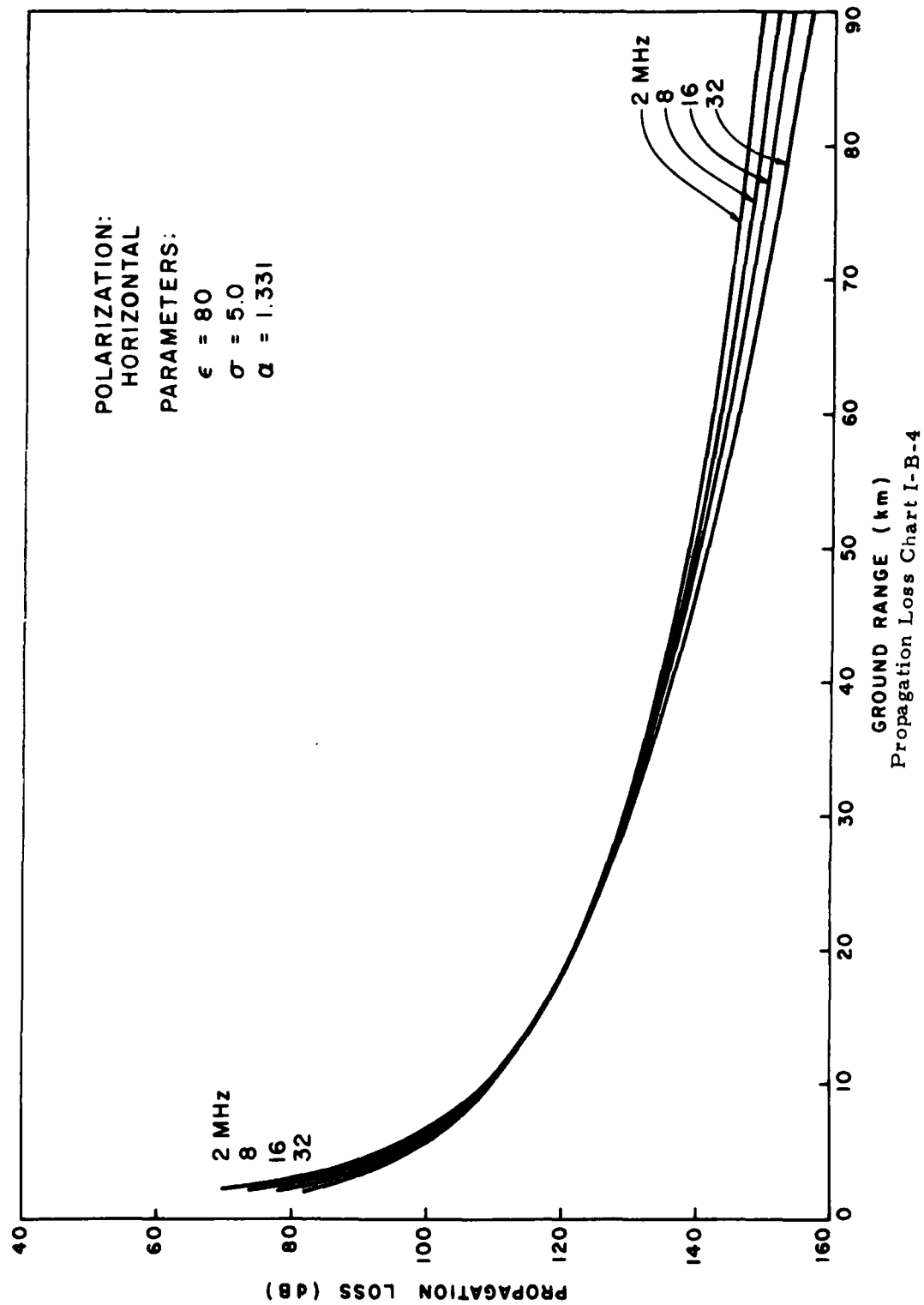


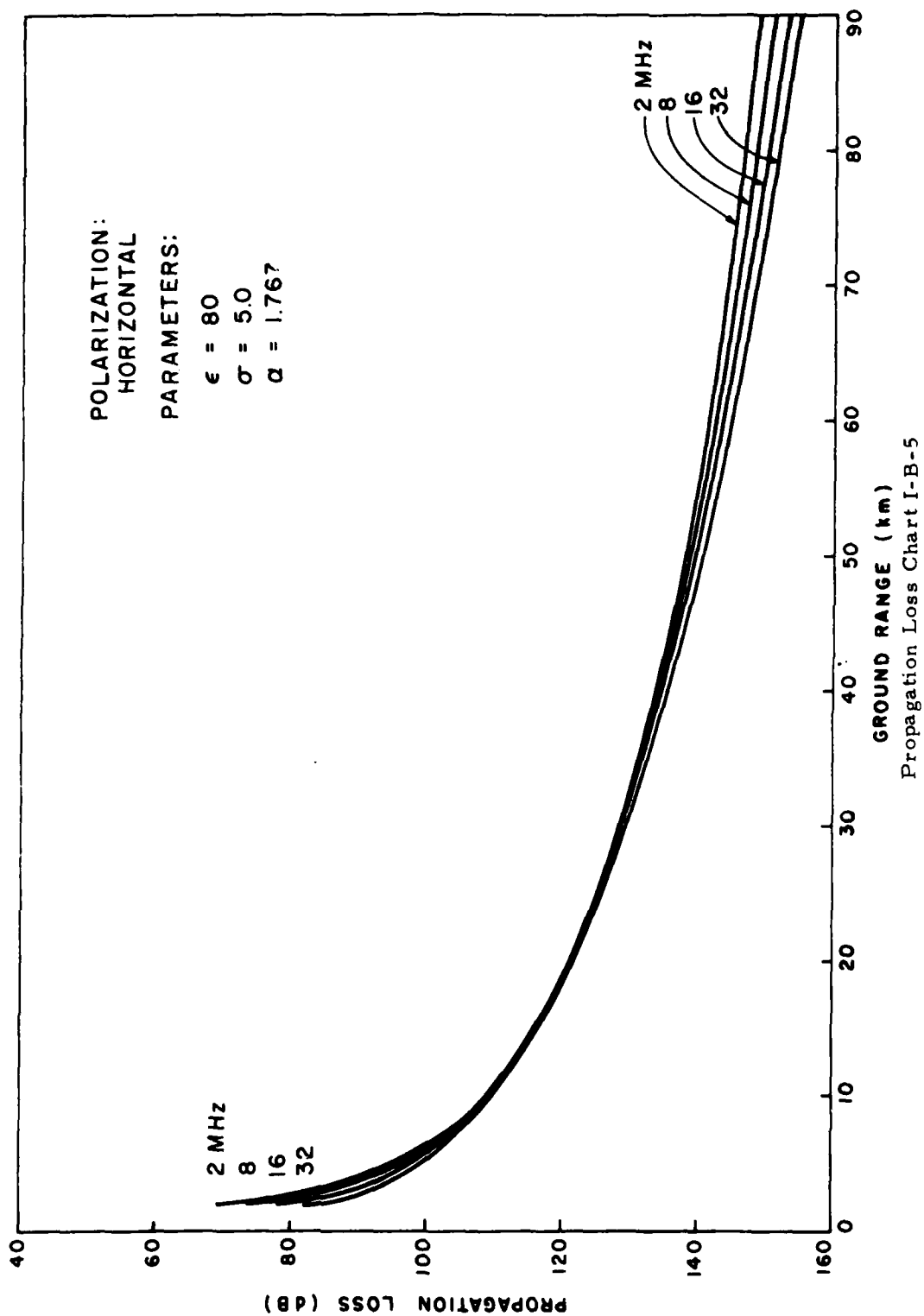


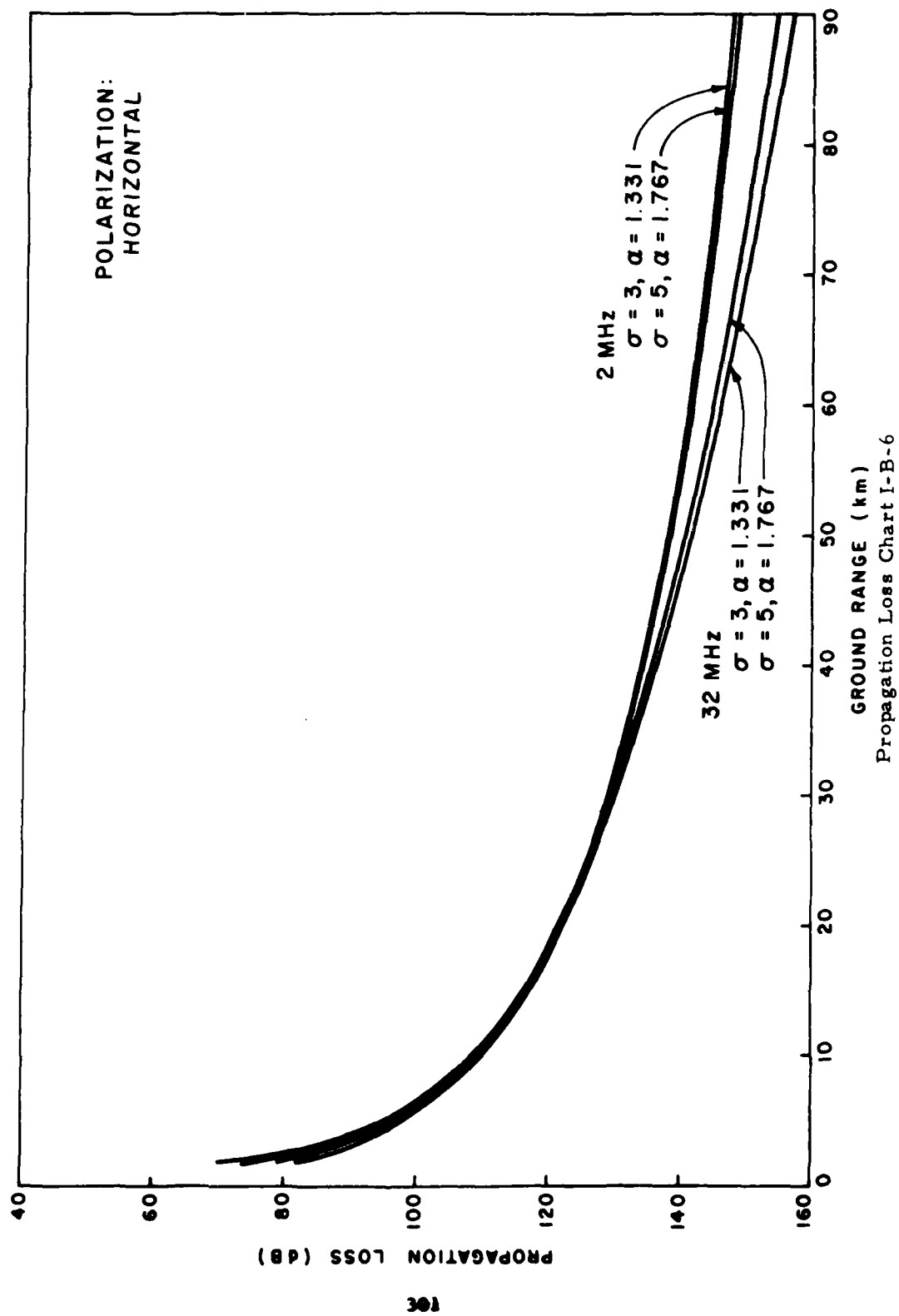


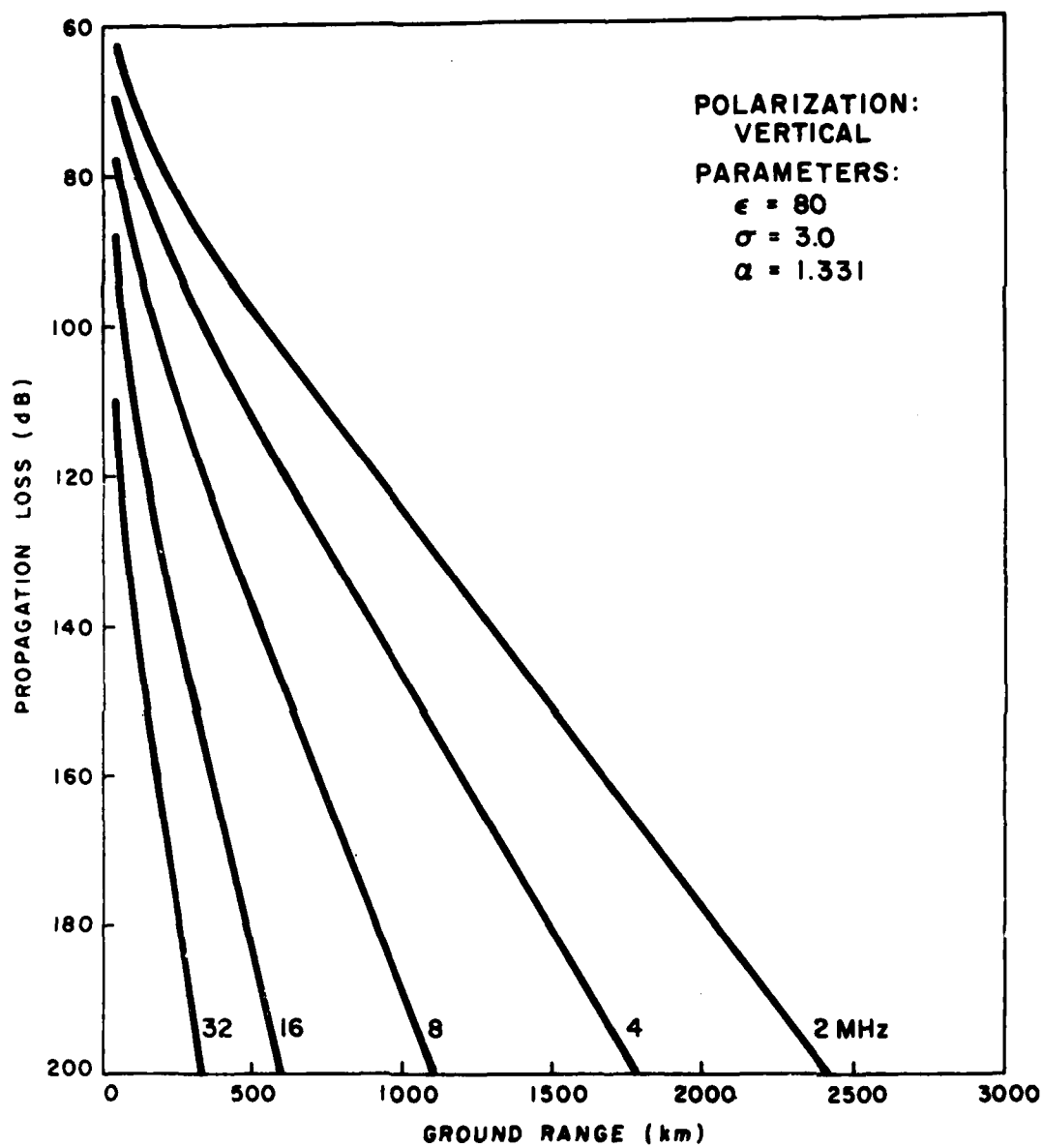


Propagation Loss Chart I-B-3

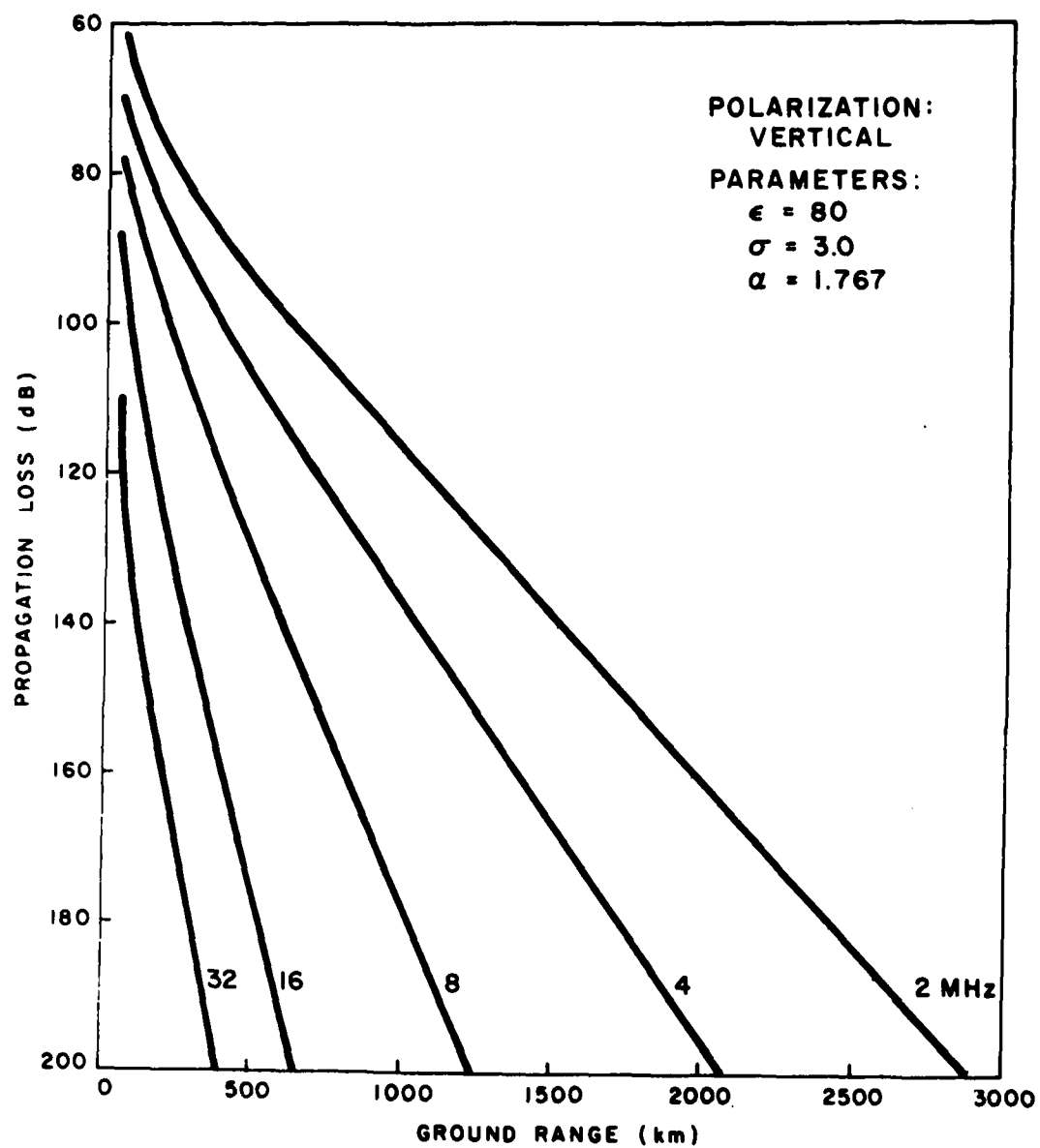




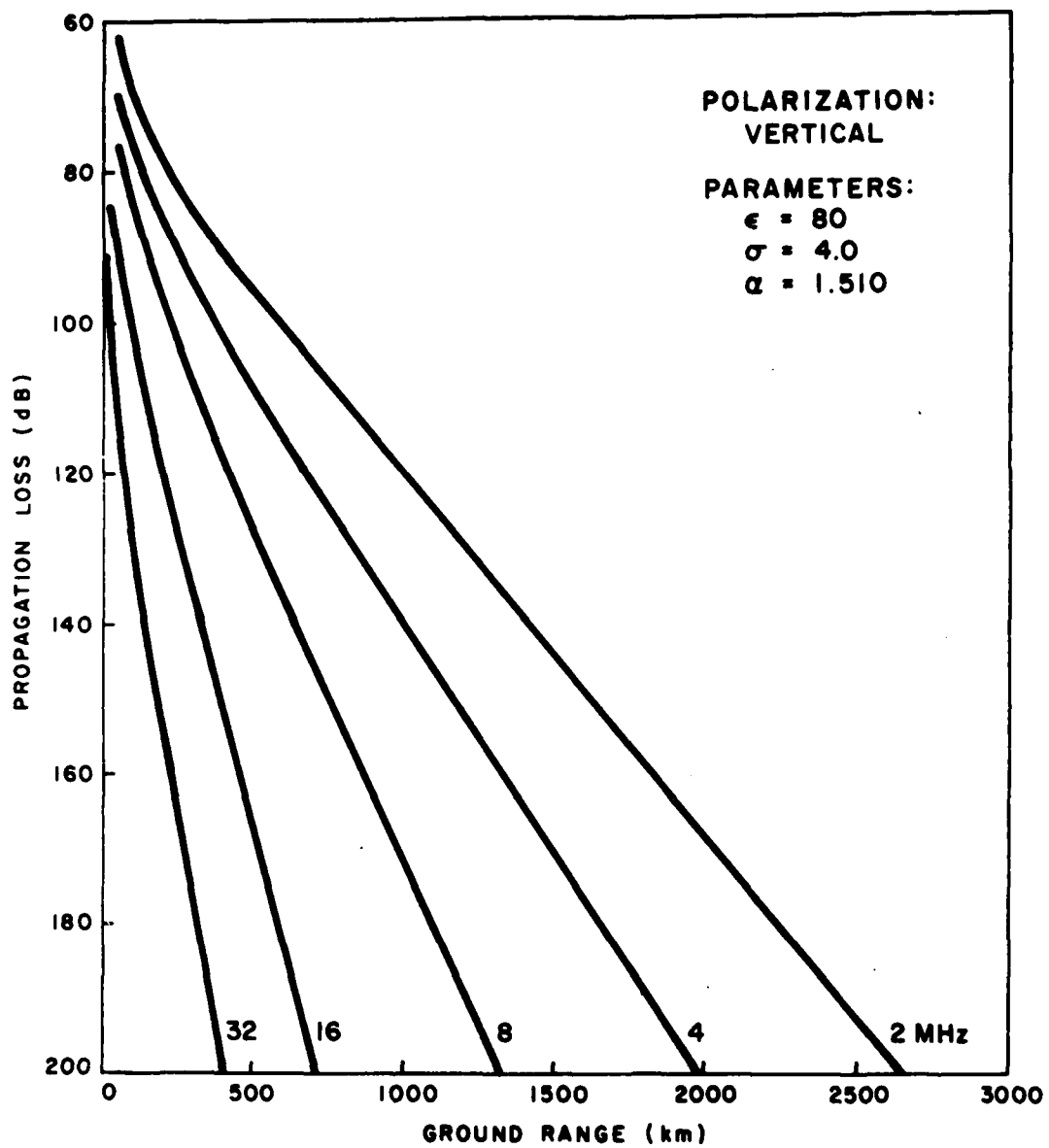




Propagation Loss Chart II-A-1

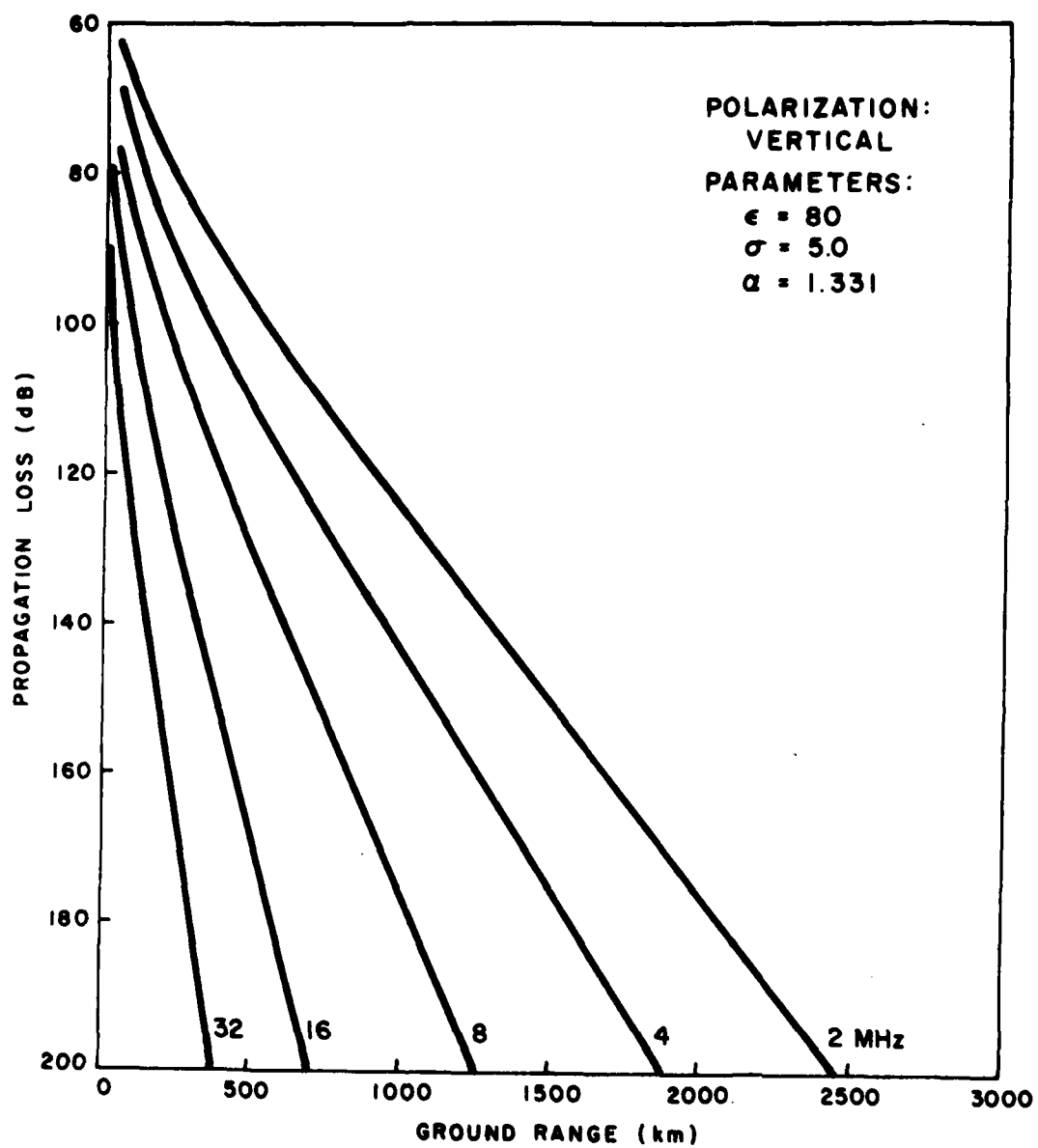


Propagation Loss Chart II-A-2

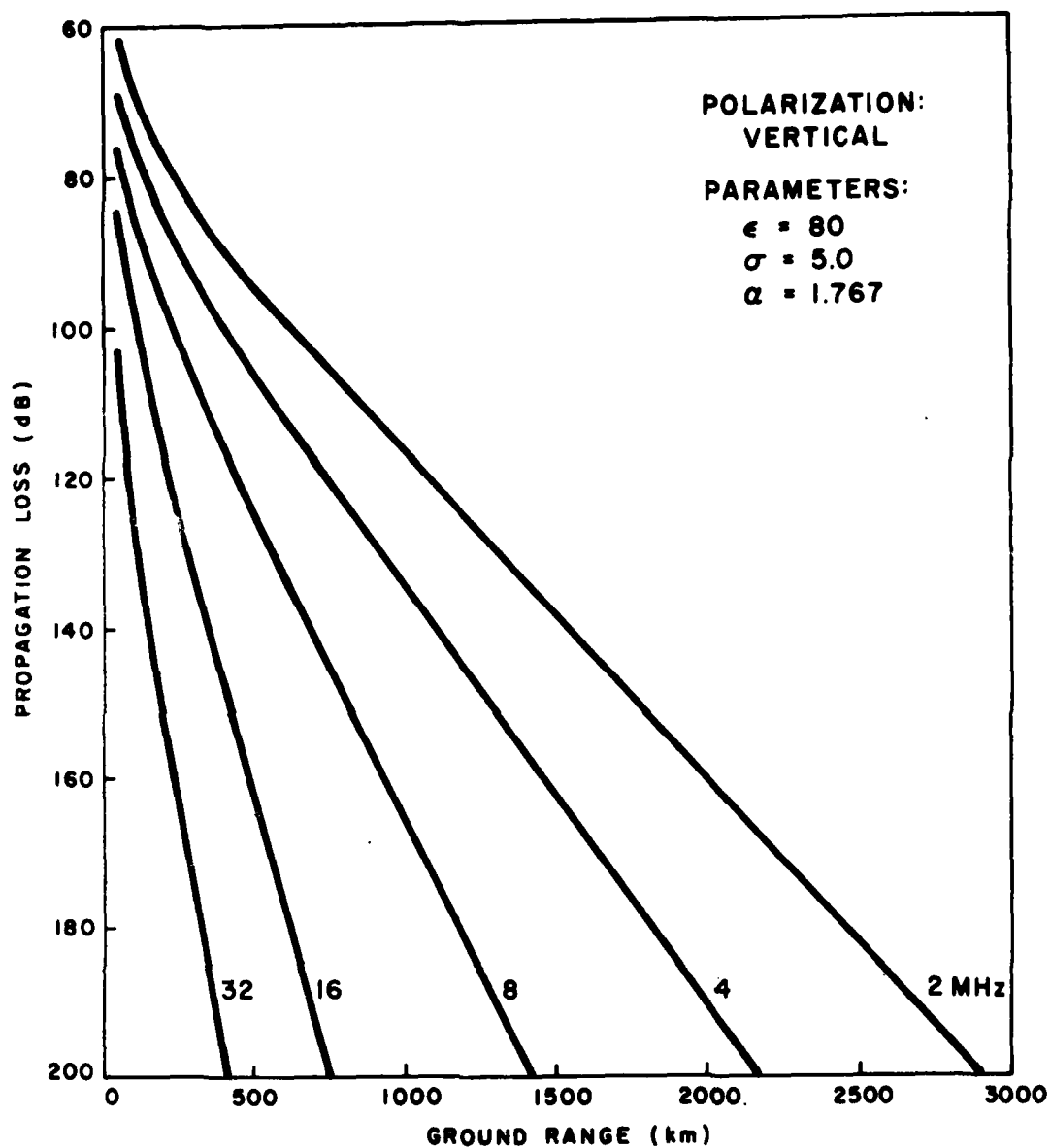


Propagation Loss Chart II-A-3

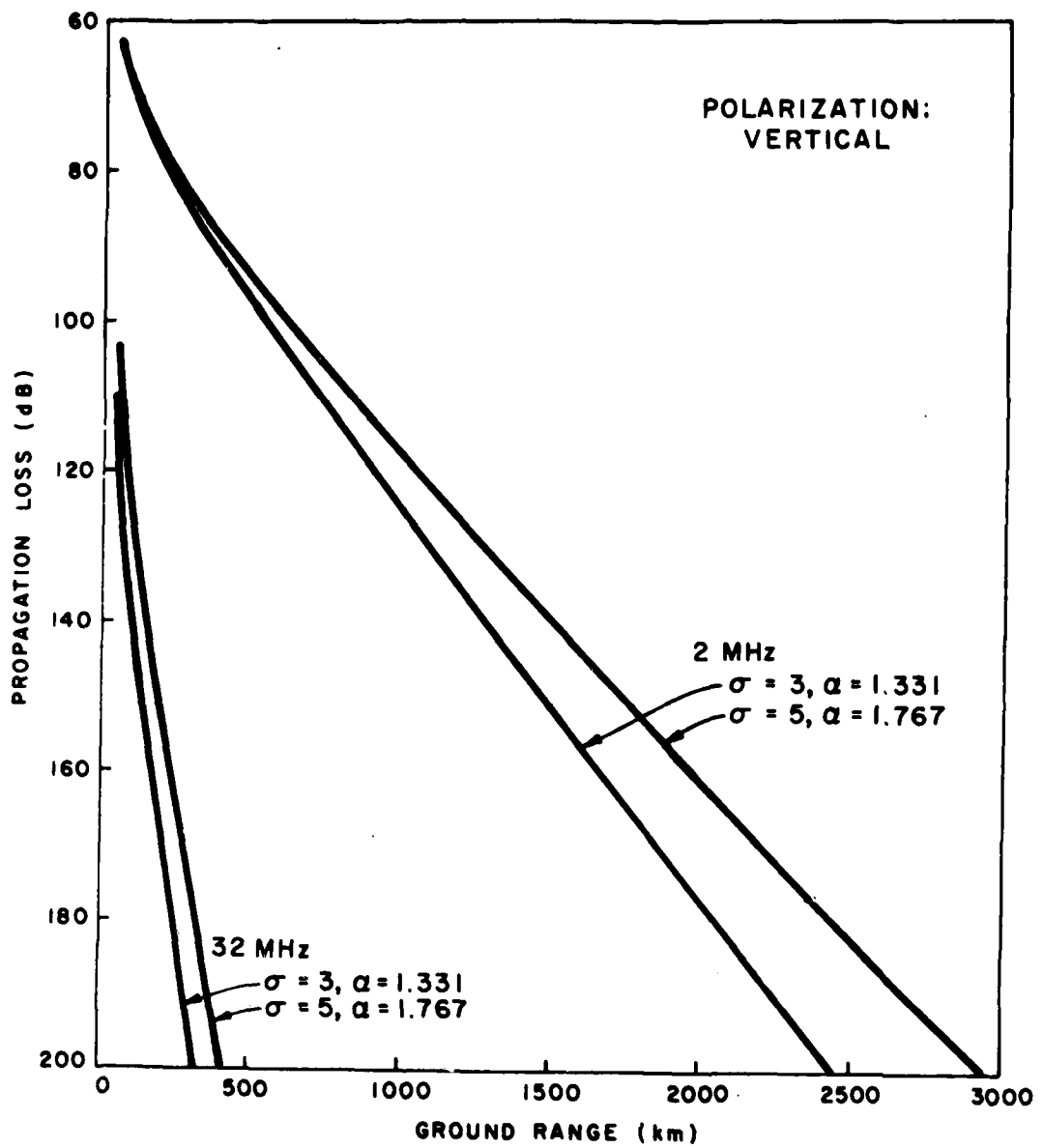




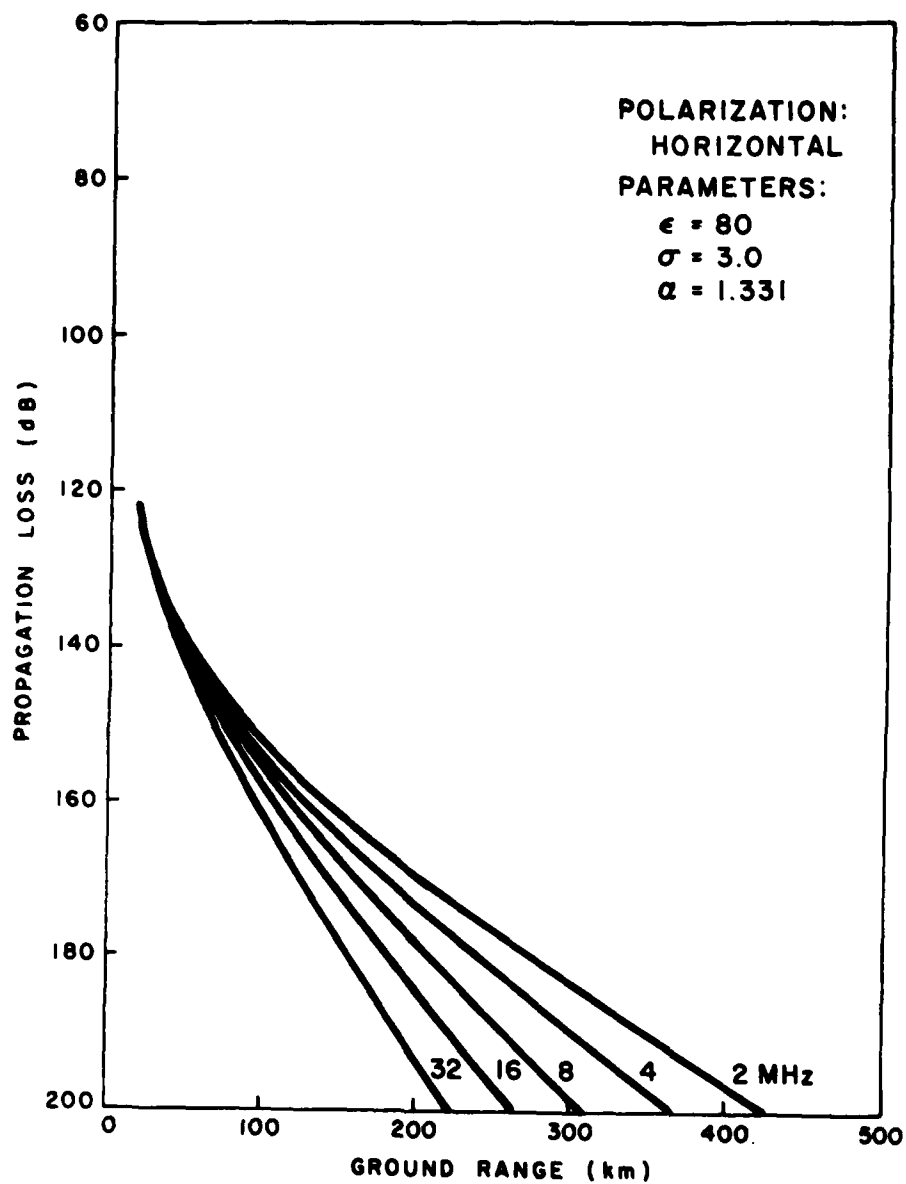
Propagation Loss Chart II-A-4



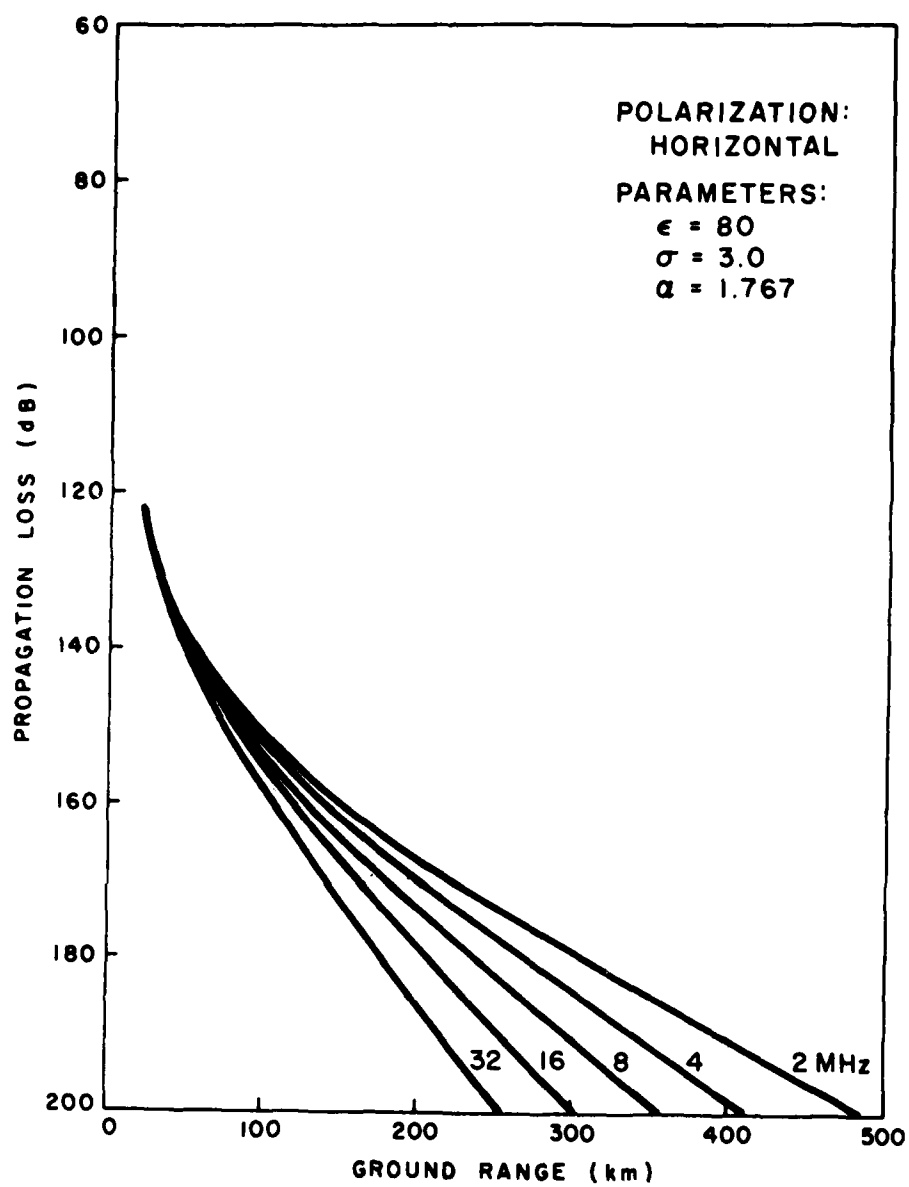
Propagation Loss Chart II-A-5



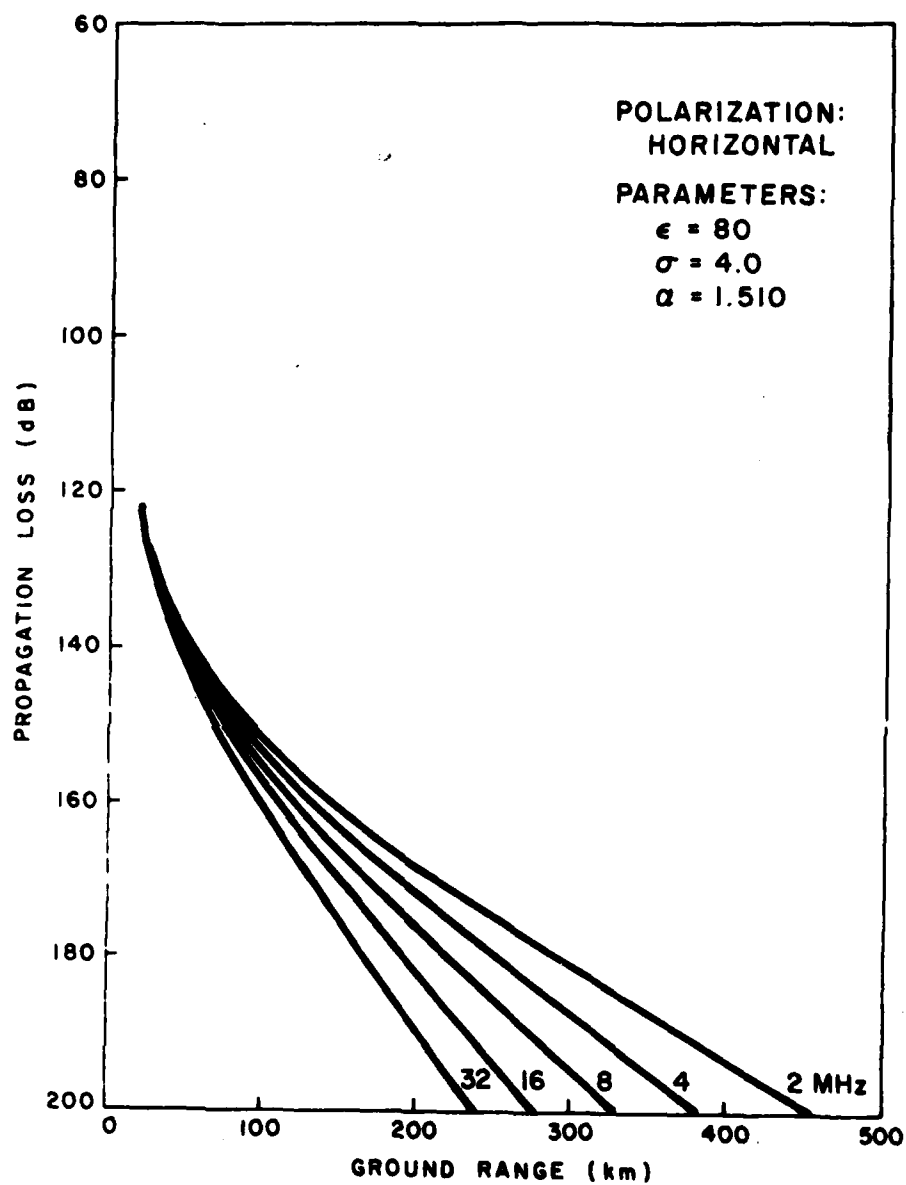
Propagation Loss Chart II-A-6



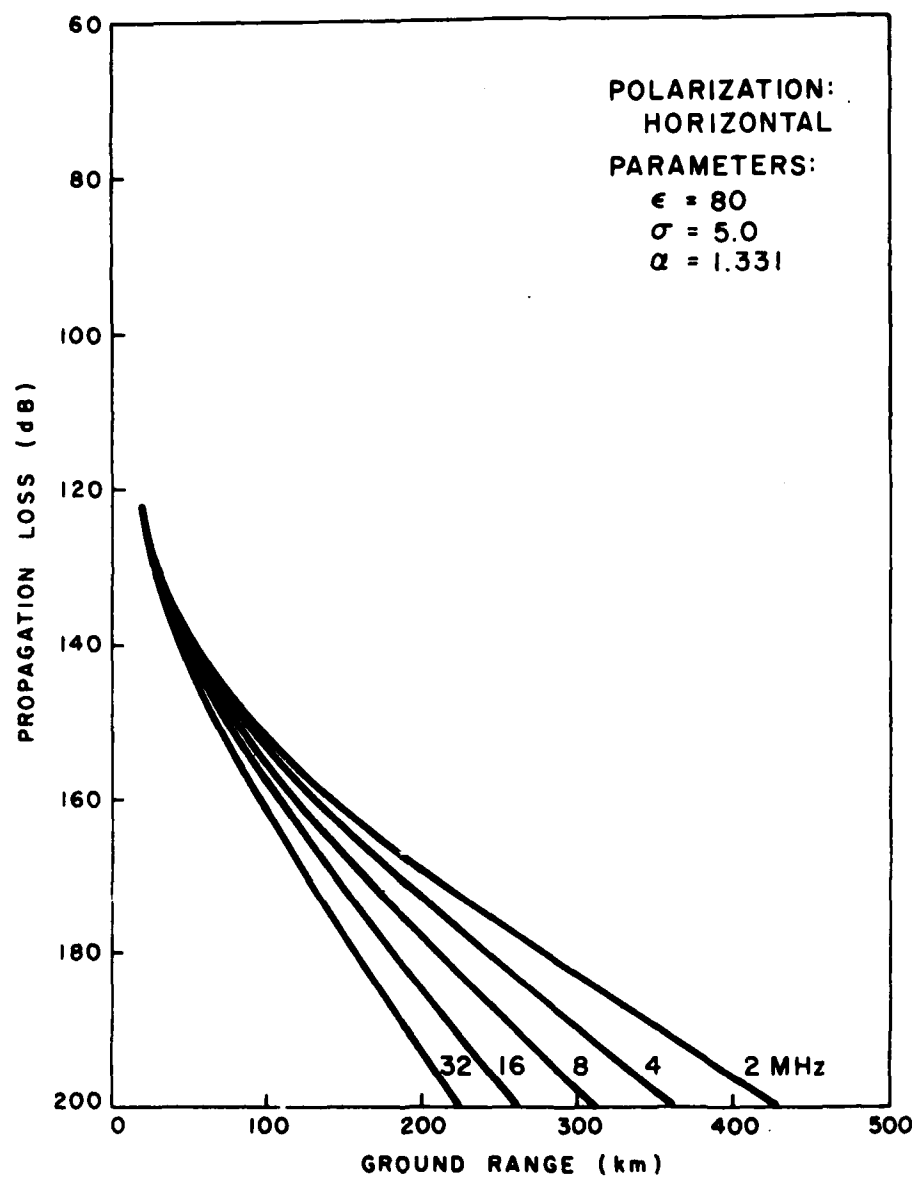
Propagation Loss Chart II-B-1



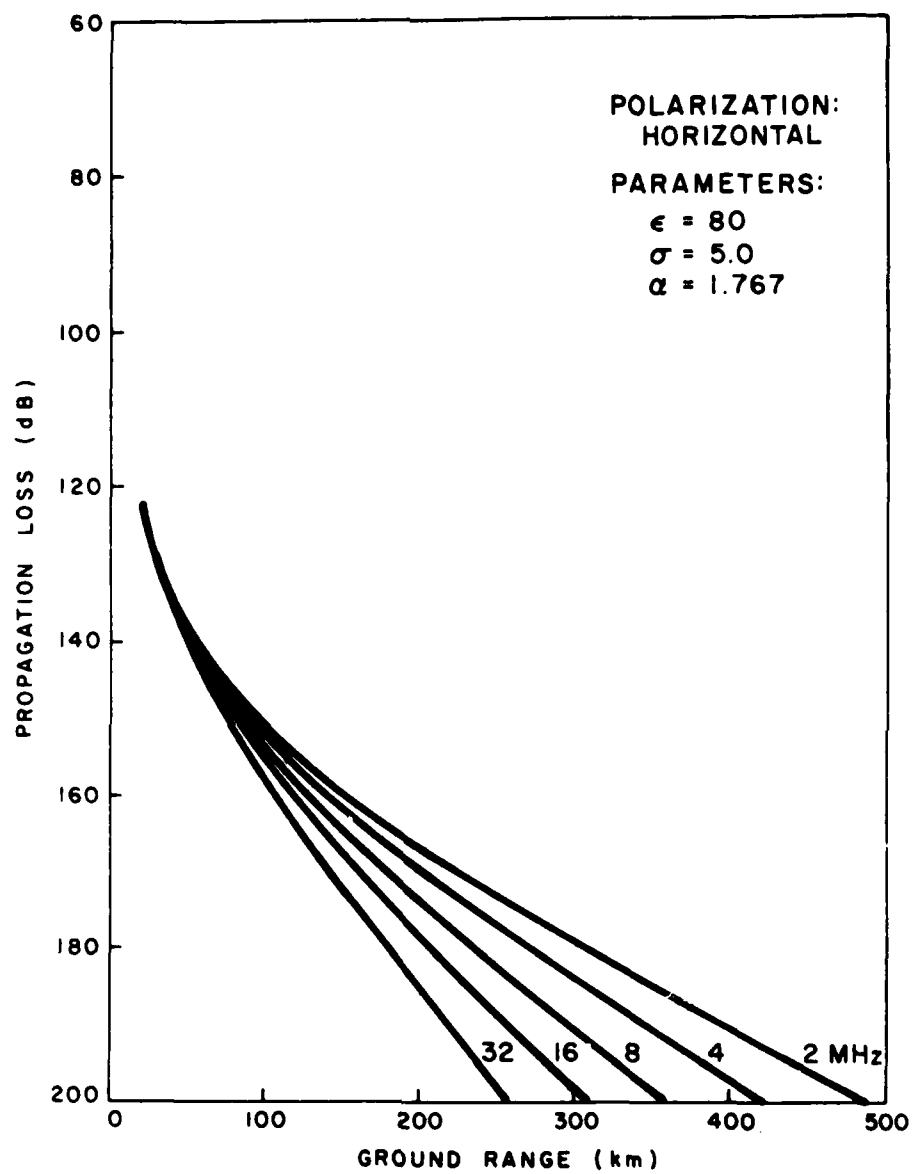
Propagation Loss Chart II-B-2



Propagation Loss Chart II-B-3

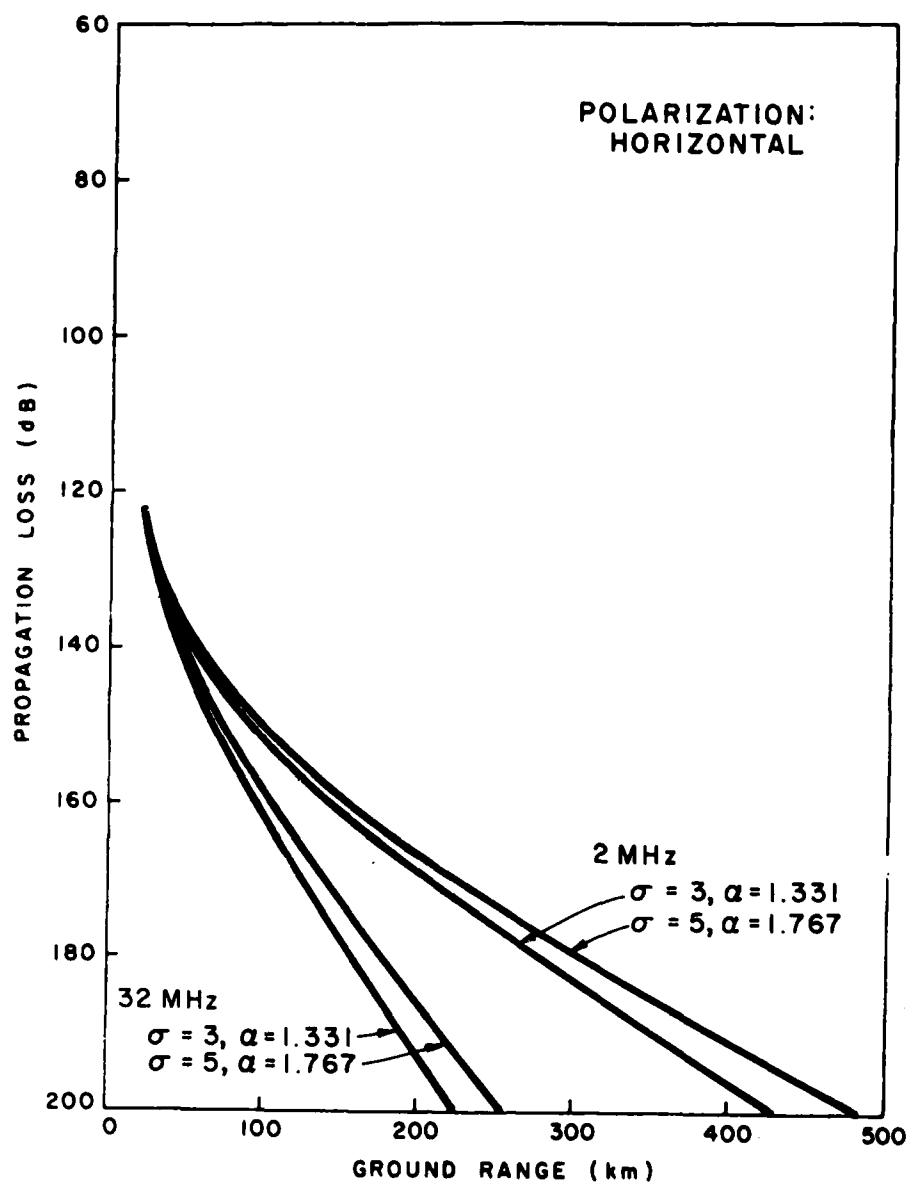


Propagation Loss Chart II-B-4



Propagation Loss Chart II-B-5





Propagation Loss Chart II-B-6

### 3.5 REFERENCES FOR GROUND WAVE MECHANISMS

1. World Atlas of Sea Surface Temperatures

Publication No. 225, Second Edition-1944

1973 Reprint

U. S. Naval Oceanographic Office

Washington, D. C. 20390

2. Handbook of Oceanographic Tables

Special Publication SP-68, 1966

Compiled by Eugene L. Bialek

U.S. Naval Oceanographic Office

Washington, D.C. 20390

3. Tables for Rapid Computation of Density and Electrical Conductivity of Sea Water

Special Publication SP-11 (Formerly H.O. Pub. No. 619)

May 1956

U.S. Navy Hydrographic Office

Washington, D.C.

4. Climatic Charts and Data of the Radio Refractive Index for the United States and the World

B. R. Bean, J. D. Horn and A. M. Ozanich, Jr.

National Bureau of Standards Monograph 22

November 25, 1960

Washington, D.C.

5. Radio Meteorology

B. R. Bean and E. R. Dutton

National Bureau of Standards Monograph 92

March 1, 1966

Washington, D.C.

6. Private Communication

Leslie A. Berry, March 31, 1975

Institute for Telecommunication Sciences

U.S. Department of Commerce

Boulder, Colorado 80302

7. Electromagnetic Diffraction and Propagation Problems  
V. A. Fock, Pergamon Press (London), 1965
8. Advances in Radio Research, Volume 1  
J. A. Saxton, Editor  
"Electromagnetic Surface Waves," J. R. Wait  
Academic Press (London), 1964
9. Terrestrial Radio Waves  
H. Bremmer, Elsevier Publishing Co., 1949 (1962 Reprint)
10. Die Radiometeorologie und ihre Bedeutung fur die  
Ausbreitung der m-, dm-, und cm-Wellen auf grosse  
Entfernung," B. R. Bean, L. Fehlhaber and J. Grosskopf  
Nachrichtentechnische Zeitschrift, Vol. 15, pp. 9-10  
  
Result is quoted in reference 5, p. 16, Equation 1.37.
11. "The Radio Refractive Index Gradient over the British Isles"  
J. Atmospheric and Terrestrial Physics, Vol. 21, Nos. 2/3,  
pp. 157-166

#### ACKNOWLEDGEMENT

The basic FORTRAN program with which the ground wave calculations were done was written by Leslie A. Berry and colleagues [6]. The program has been modified in certain ways to serve our purposes and convenience--as well as to run on the CDC CYBER 74 computer system which was used for the ground wave calculations.

The mathematical principles and techniques on which the calculations are based have been exposted by Fock [7], Wait [8] and Bremmer [9] in recent times. The roots of the methods date back at least to Arnold Sommerfeld (1909). Other contributors to development of the relevant propagation theory and solution techniques include H. Weyl, Balth. van der Pol, K. N. Niessen, W. H. Wise and K. A. Norton. A wealth of specific reference information to this literature can be found in [7], [8], and [9].

FILM  
0-8